The Ordovician Exposed:
Short Papers, Abstracts, and Field Guides

for the

12th International Symposium on the Ordovician System

June 3-17, 2015 at James Madison University

Harrisonburg, Virginia USA

Central Appalachian Mountains

The Ordovician Exposed:
Short Papers, Abstracts, And Field Guides

for the

12th International Symposium on the Ordovician System

June 3-17, 2015 at James Madison University

Harrisonburg, Virginia USA

Central Appalachian Mountains

Edited by

Stephen A. Leslie, Daniel Goldman, and Randall C. Orndorff

Cover Photo: Sandbian carbonate succession of the uppermost Big Valley, McGlone, McGraw and lowermost Nealmont formations exposed in the North Fork Quarry near Riverton, West Virginia Germany Valley. Field stop of the conference field trip. Photo by John Haynes

The Ordovician Exposed: Short Papers, Abstracts, and Field Guides for the 12th International Symposium on the Ordovician System

June 3-17, 2015

James Madison University
Harrisonburg, Virginia USA
Central Appalachian Mountains

<u>Organizing Committee:</u>

Stephen A. Leslie, James Madison University (Chair)
Daniel Goldman, University of Dayton (Co-Chair)
Randall C. Orndorff, United States Geological Survey (Co-Chair)
John T. Haynes, James Madison University
Matthew R. Saltzman, The Ohio State University
John F. Taylor, Indiana University Pennsylvania
Achim Herrmann, Louisiana State University
Charles E. Mitchell, University of Buffalo
John E. Repetski, United States Geological Survey
Stig M. Bergström, The Ohio State University
Jesse Carlucci, Midwestern State University
Stephen R. Westrop, University of Oklahoma
Carlton Brett, University of Cincinnati

Suggested Reference Format:
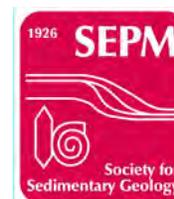
Preface

   For nearly two centuries some of the world's most notable geologists and paleontologists have intensively studied the Ordovician rocks of North America. The "layer cake" sedimentary strata deposited in the vast epicontinental seas of the interior and the flanking folded and thrusted mountain belts provided both complex problems and fertile ground for new theories and methods. The problem of correlating between regions in the large cratonic interior and between disparate biofacies gave rise to exciting new studies in sequence, event, quantitative, and chemo-stratigraphy. Distinctive and traceable marker beds, geochemically fingerprinted K-bentonites, and carbon isotope excursions allow for correlation with unprecedented precision, which led to new questions (and answers) about Ordovician climate and oceanography, global carbon cycling, and the timing of tectonic events. Recent innovations in using geochemistry to study the ancient environment has greatly increased our understanding of Ordovician climate cyclicity and its effects on Earth's biota. Advances in geochronology have given the geologic community amazingly precise dates on Ordovician K-bentonites, increasing the precision and usefulness of our most fundamental tool – the geologic time scale.

   It is an exciting time in Ordovician research and the highlights of this work are presented here at the 12th International Symposium on the Ordovician System. The conference includes fifty-nine talks and 18 posters presentations given by over 80 delegates representing 14 different countries. Its overall theme is ***Integrated Stratigraphy***, and as noted above comprises the latest research in sedimentary geochemistry, geochronology, sequence stratigraphy, event stratigraphy, and quantitative stratigraphic methods. These studies provide the stratigraphic framework and paleoenvironmental context for examining the evolution, diversification, and extinction of Ordovician life. ISOS 2015 offers 4 field trips - 3 to the southern, central, and northern Appalachian Mountains, and one to eastern and central Oklahoma - to examine classic exposures of Ordovician rocks and the only Ordovician GSSP in the United States.

   Finally, we would like to thank the presenters, field trip leaders, and manuscript reviewers, all of whom are essential to a successful symposium.

On behalf of the entire Organizing Committee,

Stephen A. Leslie, Daniel Goldman, and Randall C. Ordorff

Table of Contents

Short Papers

Abstracts

Field Trip Guides

Pre-meeting Trips

Mid-Conference Trip

CONFERENCE PROGRAM

Oral Presentation Schedule

Monday, June 8

8:50 AM - **Opening Remarks-** *Stephen A. Leslie*

ISOTOPE STRATIGRAPHY/CLIMATE
Session Chairs: Stephen A. Leslie and Daniel Goldman

9:00 AM
Deciphering the movement of the Argentine Precordillera from tropical to higher latitudes, Late Cambrian–Late Ordovician, through conodont $\delta^{18}O$ paleothermometry

> *Guillermo L. Albanesi, Christopher R. Barnes, Julie A. Trotter, Ian S. Williams, and Stig M. Bergström*

9:15 AM
An integrated scheme for $\delta^{13}C$ chemostratigraphy and conodont biostratigraphy in the Ordovician of Sweden and useful tie-points for global correlation

> *Mikael Calner, Oliver Lehnert, Rongchang Wu and Michael M. Joachimski*

9:30 AM
Lower-Middle Ordovician carbon and sulfur isotope stratigraphy at Shingle Pass, Nevada, USA: changes in the carbon and sulfur cycles and a link between oxygen levels and biodiversity

> *Cole Edwards and Matthew R. Saltzman and David A. Fike*

9:45 AM
Upper Ordovician carbon isotope chemostratigraphy on the Yangtze Platform, South China: Implications for the correlation of the Guttenberg $\delta^{13}C$ excursion (GICE)

> *Ru Fan, Stig M. Bergström, Yuanzheng Lu, Xuelei Zhang, Shiben Zhang, Xin Li, and Shenghui Deng*

10:00 AM
Paired $\delta^{13}C_{carb}$-$\delta^{13}C_{org}$ records from the Laurentian margins during late Katian glaciation

> *David Jones, Seth Finnegan, Mark Hellmer*

10:15-10:45 AM   *Break*

10:45 AM
Neodymium isotopes and the Late Ordovician evolution of the North American Mid-continental Seaway

> *Ken MacLeod and Kelsey Putman Hughes*

11:00 AM

Evidence of warming during the early Katian- Conodont apatite $\delta^{18}O$ and bulk carbonate $\delta^{13}C$ records from the Upper Mississippi Valley, US

Page Quinton, *Achim D. Herrmann, Stephen A. Leslie, Kenneth G. MacLeod*

11:15 AM

Ordovician temperature trends: constraints from $\delta^{18}O$ analysis of conodonts from New South Wales, Australia (Short paper)

Page Quinton, *Ian G. Percival, Yong-Yi Zhen, and Kenneth G. MacLeod,*

11:30 AM

Coupled carbon and strontium isotope stratigraphy of a Middle Ordovician Bahamian-type carbonate platform at Clear Spring, Maryland

Matthew Saltzman, *Cole Edwards, and Stephen A. Leslie*

11:45 AM

Middle–Late Ordovician (Darriwilian–Sandbian) paired $\delta^{34}S$ and $\delta^{13}C$ records reveal dynamic cycling through the Great Ordovician Biodiversification Event

Seth A. Young, *Benjamin C. Gill, Cole T. Edwards, Matthew R. Saltzman, and Stephen A. Leslie*

12:00 PM - 1:30 PM *Lunch*

BIOSTRATIGRAPHY
Session Chairs: Achim Herrmann and John Haynes

1:30 PM

Proposed Auxiliary Stratigraphic Section and Point (ASSP) for the base of the Ordovician System at Lawson Cove, Utah, USA

James Miller, *Ethington, Raymond L., Repetski, John E., Ripperdan, R.L., and Taylor, John F.*

1:45 PM

A biostratigraphic reappraisal of Tremadocian graptolites from SW Europe and NW Africa

Juan Carlos Gutiérrez-Marco, *Gian Luigi Pillola, Artur A. Sá and Emmanuel L.O. Martin*

2:00 PM

Early Ordovician (Tremadocian) faunas and biostratigraphy of the Gerd-Kuh section, eastern Alborz, Iran (Short Paper)

Mansoureh Ghobadi Pour, Leonid E. Popov, ***Lars E. Holmer****, Mahmud Hosseini-Nezhad, Rahimeh Rasulic, Khadijeh Fallah, Arash Amini and Hadi Jahangir*

2:15 PM

The Cambrian-Ordovician boundary in the Cordillera Oriental, NW Argentina (Short Paper)

Guillermo L. Albanesi, *M. Eugenia Giuliano, Fernanda E. Pacheco, Gladys Ortega and C. Rubén Monaldi*

2:30 PM
Iberian Ordovician and its international correlation

Juan Carlos Gutiérrez-Marco, *Artur A. Sá , Isabel Rábano, Graciela N. Sarmiento, Diego C. García-Bellido, Enrique Bernárdez, Saturnino Lorenzo, Enrique Villas, Andrea Jiménez-Sánchez, Jorge Colmenar and Samuel Zamora*

2:45 PM
The *Pygodus serra* Zone in Cuyania, Argentina (Short Paper)

Susana Heredia, *Ana Mestre, Tatiana Soria, and Cintia Kaufmann*

2:45-3:15 PM   *Break*

3:15 PM
Biostratigraphy and paleoecology of Late Ordovician (Ka2) conodonts and microbrachiopods from north Queensland, Australia (Short Paper)

*Yong Yi Zhen and **Ian Percival***

3:30 PM
Latest Ordovician-earliest Silurian chitinozoans from Puna, western Gondwana

G. Susana de la Puente, *Claudia V. Rubinstein, N. Emilio Vaccari, and Florentin Paris*

4:00 PM
A revised biostratigraphic framework for the near-field Hirnantian deposits of the Central Anti-Atlas (southern Morocco) and their correlation to the Wangjiawan GSSP (Yichang, China)

Lorena Tessitore, *This R. A. Vandenbroucke, Jean-François Ghienne, Marie-Pierre Dabard, Alfredo Loi, Florentin Paris, and Philippe Razin*

4:15 - 5:30 PM   **POSTER SESSION**
                          Authors present at posters

– –

Tuesday, June 9

INTEGRATED APPROACHES IN STRATIGRAPHY
Session Chairs: Matt Saltzman and John Taylor

9:00 AM
Correlation of Upper Ordovician K-bentonites in the East Baltic – A combined approach of chitinozoan biostratigraphy and sanidine geochemistry

Heikki Bauert, *Garmen Bauert, Jaak Nõlvak, and Tarmo Kiipli*

9:15 AM

Chronostratigraphic correlation of the North American Upper Ordovician Standard: the 2015 Edition

Charles Mitchell, Bryan K. Sell, Stephen A. Leslie, and Daniel Goldman

9:30 AM

The more the merrier? Reconciling sequence stratigraphy, chemostratigraphy and multiple biostratigraphic indices in the correlation of the Katian Reference Section, central Oklahoma.

Stephen Westrop, Lisa Amati, Carlton E. Brett, Robert E. Swisher, Jesse R. Carlucci, Daniel Goldman, Stephen A. Leslie, and Roger Burkhalter

9:45 AM

A CONOP9 quantitative stratigraphic model of Baltic Ordovician and Silurian chitinozoan distribution and K-bentonites

Liina Antonovitš, Viiu Nestor, Jaak Nõlvak, Garmen Bauert, Olle Hints, and Tarmo Kiipli

10:00 AM

High-Resolution Stratigraphic Correlation and Biodiversity Dynamics of Middle and Late Ordovician Marine Fossils from Baltoscandia and Poland

Daniel Goldman, David H. Sheets, Stig M. Bergström, Jaak Nõlvak, and Teresa Podhalanska

10:15-10:45 AM   ***Break***

10:45 AM

Ordovician sequence stratigraphy of the Siberian Platform revised

Andrei Dronov, Kanygin, A.V., Timokhin, and T.V. Gonta

11:00 AM

Trilobite biofacies and sequence stratigraphy: an example from the Upper Ordovician of Oklahoma

Jesse Carlucci

11:15 AM

Milankovitch cycles in the Juniata Formation, Late Ordovician, Central Appalachian Basin, USA

Linda Hinnov and Richard J. Diecchio

11:30 AM

Traces of explosive volcanic eruptions in the Upper Ordovician of the Siberian Platform

Warren Huff, A.V. Dronov, B. Sell, A.V. Kanygin, & T.V. Gonta

11:45 AM

Early-middle Darriwilian graptolite and conodont faunas from the central Precordillera of San Juan Province, Argentina (Short paper)

Fernanda Serra, Nicolás A. Feltes, Gladys Ortega and **Guillermo L. Albanesi**

12:00 PM - 1:30 PM   *Lunch*

<u>**ORDOVICIAN OF THE WORLD**</u>
Session Chairs: John Repetski and Charles Mitchell

1:30 PM
Characterization of a platform to basin transition in a mixed siliclastic-carbonate basin: Upper Ordovician of central, KY and Cincinnati, Ohio

  Allison Young*, Carlton E. Brett, and Patrick I. McLaughlin*

1:45 PM
Recurring Taphofacies in the Upper Ordovician (Katian) of the Cincinnati Arch: A Predictive Model Based on Sequence Stratigraphy

  Christopher Aucoin*, Carlton E Brett, James R Thomka, Benjamin F Dattilo,*

2:00 PM
Taphonomic comparisons of two Laurentian Upper Ordovician epeiric sea "small shelly faunas"

  *Benjamin F. Dattilo, **Rebecca L. Freeman**, Jessie L. Reeder, Amanda Straw, Christopher Aucoin, Carlton Brett, and Anne Argast*

2:15 PM
Lithofacies differentiation of the Late Ordovician Lianglitag Formation limestones on the central part of the Central Tarim Uplift, Tarim Block, NW China

  Yuanyuan Zhang*, Yue Li, Axel Munnecke, and Wang Guan*

2:30 PM
Geographic differentiation of the Middle and Upper Ordovician strata in South China

  Linna Zhang*, Junxuan Fan and Yuandong Zhang*

2:45 - 3:15 PM   *Break*

3:15 PM
In search of the elusive Hirnantian Stage in the High Arctic: a preliminary report from North Greenland

  *Christian Rasmussen, Jan Rasmussen, Svend Stouge, Jisuo Jin, and Axel Munnecke, and **David Harper***

3:30 PM
Clast Research in northern Germany – How erratics contribute to the Ordovician picture

  Adrian Popp

3:45 PM
A new type of cool-water carbonate buildups: Middle Ordovician Moyeronia-Angarella "reefs" of the Siberian platform

  Andrei Dronov*, Axel Munnecke, and Veronica B. Kushlin*

4:00 PM

Middle Ordovician strata of western Inner Mongolia: depositional and tectonic history

Paul Myrow, Jitao Chen, Anne Hakim, Zachary Snyder, Stephen A. Leslie, David A. Fike, and Peng Tang

4:15 PM

Ordovician of the Anarak Region: implications in understanding Early Palaeozoic history of Central Iran (Short Paper)

*Vachik Hairapetian, Mansoureh Ghobadi Pour, Leonid E. Popov, S. Hassan Hejazi, **Lars E. Holmer**, David Evans and Ali Sharafi*

4:30 PM

Field and petrographic evidence for late diagenetic silicification of Cambrian and Ordovician carbonates of the Shenandoah Valley, Virginia

Daniel Doctor

4:45 PM

Early Ordovician lithistid sponge-Calathium reefs on the Yangtze Platform and their paleoceanographic implications

Qi-jian Li, Yue Li, Jianpo Wang, and Wolfgang Kiessling

- -

Thursday, June 11

PALEOBIOLOGY/PALEOGEOGRAPHY/PALEOECOLOGY
Session Chairs: Randall Orndorff and Stig Bergström

9:00 AM
Risk and resilience during and after the Late Ordovician extinctions

*Seth Finnegan, **David Harper**, and Christian Rasmussen*

9:15 AM
Immigration, speciation, and biodiversity in Ordovician seas of Laurentia

Alycia Stigall, Jennifer E. Bauer, Hannah-Maria R. Brame, Adriane R. Lam, and David F. Wright

9:30 AM
Biogeographic origins and dispersal pathways of invasive taxa: the Late Ordovician (Katian) Richmondian Invasion, Cincinnati area, Ohio

Adriane Lam and Alycia Stigall

9:45 AM
Palaeobiogeographic distribution of Lituitidae cephalopods in late Dapingian to early Katian (Ordovician) and its implications

Xiang Fang, Yunbai Zhang, Chen Tingen, Zhang Yuandong, Song Yanyan, and Ma Xuan

10:00 AM

Preferential extinction of mesopelagic species and disruption of graptolite community structure during the Late Ordovician mass extinction

> ***Charles Mitchell***, *H. David Sheets, Michael J. Melchin, Jason Loxton, and Petr Štorch*

10:15-10:45 AM   ***Break***

10:45 AM

Brachiopod Community Response to the Ordovician Mass Extinction on Anticosti Island

> ***Amelinda Webb*** *and Lindsey Leighton*

11:00 AM

Foreland basin formation, environmental change and trilobite paleoecology, Late Ordovician of eastern Laurentia

> ***Stephen Westrop***, *Lisa Amati, Jesse R. Carlucci, Carlton E. Brett, Robert E. Swisher*

11:15 AM

Evolution of the Darriwilian to Katian graptolites from NW China

> ***Junxuan Fan***, *Daniel Goldman, Qing Chen, Xu Chen, and Yuandong Zhang*

11:30 AM

Early-Middle Ordovician chitinozoan biodiversification of Upper Yangtze Platform, South China

> ***Yan Liang***, *Peng Tang, and Renbin Zhan*

11:45 AM

The onset of the 'Ordovician Plankton Revolution' in the late Cambrian

> ***Thomas Servais***, *Taniel Danelian, Ronald Martin, Axel Munnecke, Hendrik Nowak, Alexander Nützel, Vincent Perrier, Thijs Vandenbroucke, and Mark Williams*

12:00 - 1:30 PM   ***Lunch***

Systematic Paleontology: Session Chairs: Jesse Carlucci and Stephen Westrop

1:30 PM

Late Ordovician, deep-water Foliomena brachiopod fauna from the island of Bornholm, Denmark

> ***David Harper*** *and Arne Nielsen*

1:45 PM

Ordovician (Darriwilian-Sandbian) linguliform brachiopods from the southern Cuyania Terrane of west-central Argentina

> ***Lars E. Holmer***, *Leonid E. Popov, Oliver Lehnert, and Mansoureh Ghobadi Pour*

2:00 PM
New Cryptostome Prophyllodictya (Bryozoa) from the Nantzinkuan Formation (Early Tremadocian, Lower Ordovician) of Liujiachang Section, Western Hubei, China and Its Phylogenetic Implications

Junye Ma, Paul D. Taylor, and Fengsheng Xia

2:15 PM
A new tube-like enigmatic animal and its burrows from the Upper Ordovician of the Siberian platform

*Veronica Kushlina, **Andrei V. Dronov,** and David A.T. Harper*

2:30 PM
The Early-Middle Ordovician acritarch assemblage from eastern Yunnan

Yan Kui, Li Jun, and Thomas Servais

2:45 - 3:15 PM   ***Break***

2:45 PM
Graptolite faunas and biostratigraphy from the Hulo Formation (Ordovician) in the Anji area, SE China

Xuan Ma, and Yuandong Zhang

3:00 PM
The Sandbian (Upper Ordovician) Raphiophorid trilobite Ampyxina powelli: new insights on its description and taphonomy

Michael Meyer, Edward Fowler, Aaron Howard, and William Fleming

3:15 PM
Life on the edge in eastern Alaska: basal Ordovician (Tremadocian), platform margin faunas of the Jones Ridge Limestone (Short Paper)

John F. Taylor, Tyler J. Allen, John E. Repetski, Justin V. Strauss, and Savannah J. Irwin

3:30 PM
Agglutinated benthic foraminifera in Upper Ordovician black shales from the northern Holy Cross Mountains (Poland)

Wieslaw Trela and Sylwester Salwa

3:45 – 5:30 PM   ***WORKSHOPS***

People are encouraged to bring specimens for other specialists to examine and discuss.
Microscopes will be available to examine fossil specimens.

Poster Presentations

Lithologies, ages, and provenance of clasts in the Ordovician Fincastle Conglomerate, Botetourt County, Virginia, USA

Harvey Belkin, *John E. Repetski and Randall C. Orndorff*

Carbon isotope stratigraphy of the Ordovician-Silurian boundary interval and associated oolites in southern Norway

Hanna Calner, *Mikael Calner, and Oliver Lehnert*

Geographic distribution and dynamics of the graptolite biodiversity during the end-Ordovician mass extinction in South China

Qing Chen *and Junxuan Fan*

Was the Great Ordovician Biodiversification Event (GOBE) caused by increased atmospheric oxygen?: Evidence from paired carbon isotopes from bulk carbonate ($\delta^{13}C_{carb}$) and organic matter ($\delta^{13}C_{org}$) from North America

Cole Edwards *and Matthew R. Saltzman*

The presence of the Lower-Middle Ordovician genus *Baltoniodus* in the central Andean Basin, Argentina: the stratigraphic significance (Short paper)

Susana Heredia, *Josefina Carlorosi, and Graciela Sarmiento*

The balognathiid apparatuses of *Eoplacognathus robustus* Bergström and *E. lindstroemi* Hamar (Short Paper)

Susana Heredia *and Ana Mestre*

New data on the Late Ordovician acritarchs and cryptospores from the Moyero and Moyerokan River sections, northeast of the Siberian Platform

Elena Raevskaya *and Andrei Dronov*

Biostratigraphy of the Cambrian–Ordovician boundary beds and the position of the lower Ordovician boundary at Kopet-Dagh, Iran (Short Paper)

Hadi Jahangir, Mansoureh Ghobadi Pour, **Lars E. Holmer**, *Leonid E. Popov, Ali-Reza Ashuri, Adrian Rushton, Tatiana Yu. Tolmacheva and Arash Amini*

The first sphinctozoan-bearing reef from an Ordovician back-arc basin

Qi-jian Li, Yue Li, and Wolfgang Kiessling

A taxonomic restudy of *Ningxiagraptus* Geh, 2002

Xuan Ma, *Xu Chen, and Daniel Goldman*

The Stairsian-Jeffersonian Stage boundary in southern New Mexico and westernmost Texas, USA

James Loch, *J. F. Taylor, R. L. Ripperdan, P. M. Myrow, and S. J. Irwin,*

A long-overdue systematic revision of Ordovician graptolite faunas from New South Wales, Australia (Short Paper)

Ian Percival, *Petr Kraft, Zhang Yuandong, and Lawrence Sherwin*

Lower Silurian "hot shales" in Poland as a response to Late Ordovician climatic changes

Teresa Podhalańska and Wieslaw Trela

Chitinozoan biodiversity in the Ordovician of Gondwana using the quantitative stratigraphic correlation program CONOP9

Rachael Kathleen Sales, **Daniel Goldman***, Florentin Paris and H. David Sheets*

Determining absolute depths of Ordovician (Katian) benthic assemblages in the upper Cincinnatian (Maysvillian to Richmondian) of the Cincinnati Arch region, USA

Cameron E. Schwalbach, Carlton E. Brett, **Christopher D. Aucoin***, and James R. Thomka*

Ordovician Chronostratigraphy Changes through Time as Recorded in the USGS Geologic Names Lexicon

Nancy Stamm and **Randall C. Orndorff**

New conodont records from the Rinconada Formation, eastern margin of the Argentine Precordillera: tectono-stratigraphic implications (Short Paper)

Gustavo G. Voldman, **Guillermo L. Albanesi***, Juan L. Alonso, Luis P. Fernández, Aldo L. Banchig, Raúl Cardó, Gladys Ortega and Alberto M. Vallaure*

Carbonate microfacies analysis of the Middle-Upper Ordovician succession of the Moyero River section, NE of Siberian Platform

Alexey Zaitsev, Inna Ziyatdinova, Evdokiya Kozhevnikova, and **Andrei Dronov**

The Cambrian-Ordovician boundary in the Cordillera Oriental, NW Argentina

Guillermo L. Albanesi[1, 2], M. Eugenia Giuliano[1, 2], Fernanda E. Pacheco[3], Gladys Ortega[1], and C. Rubén Monaldi[4]

[1] *CICTERRA (CONICET-UNC), Córdoba, Argentina. galbanes@com.uncor.edu, megiuliano@efn.uncor edu*
[2] *Museo de Paleontología, Facultad de Ciencias Exactas, Físicas y Naturales, Universidad Nacional de Córdoba, Casilla de Correo 1598, 5000 Córdoba, Argentina.*
[3] *Gestión Ambiental, Secretaría de Estado de Minería de la Provincia de Santa Cruz.*
[4] *CONICET, Facultad de Ciencias Naturales, Universidad Nacional de Salta, Argentina.*

THE CAMBRIAN/ORDOVICIAN BOUNDARY

The global Cambrian/Ordovician inter-systemic boundary was a controversial problem regarding the fossil record and reference stratigraphic section. The Cambrian/Ordovician Boundary Working Group of the International Subcommission on Ordovician Stratigraphy (ICS-IUGS) selected the conodont species *Iapetognathus fluctivagus* as the index fossil for establishing the boundary after comprehensive taxonomic studies. Nicoll *et al.* (1999) monographed *I. fluctivagus* and other species of *Iapetognathus* as well as its purported ancestor *Iapetonudus ibexensis,* and they documented their known occurrences, ranges and correlations with other fossils considered significant to define the base of the Tremadocian. Cooper *et al.* (2001) proposed the section of Green Point, western Newfoundland, Canada, for the GSSP for the Cambrian/Ordovician (C/O) boundary determined there by the first appearance of *I. fluctivagus*, which was later approved by the IUGS executive.

Terfelt *et al.* (2012) revisited the taxonomy, stratigraphic ranges and lineage of *Iapetognathus*, with interpretations that were refuted by Miller *et al.* (2014). The latter authors concluded that the homotaxial succession of *Iapetognathus* species, as defined by Nicoll *et al.* (1999), should be maintained for determining the base of the Ordovician System globally. The definition of the C/O boundary in Argentina was evaluated following the newly conodont biostratigraphic concepts (Nicoll *et al*. 1999; Cooper *et al*. 2001) in the Volcancito Formation at the Famatina Range of western Argentina (Albanesi *et al.* 2005). Previous studies about this boundary by means of conodonts were carried out in the Cajas Range of the Cordillera Oriental, northwestern Argentina, by Rao (1999) according to the definition of the C/O boundary by Barnes (1988) on the base of the *Cordylodus lindstromi* Zone. Recently, other study areas, such as Lari in the Puna region (Giuliano et al. 2013) or new localities in the Cordillera Oriental; e. g., Santa Victoria, Nazareno, El Moreno, Alfarcito (e. g., Zeballo and Albanesi 2009), were surveyed as potential sites for the location of the C/O boundary (Figure 1). Albanesi and Pacheco (2010) recorded *I. fluctivagus* in the Amarilla Creek section of the Cajas Range, close to the base of the upper Cardonal Formation. This stratigraphic interval (44. 5 m thick) consists of grey-greenish shales interbedded with calcareous sandstones that represent an upper off-shore environment. The present contribution attempts a better approximation of the C/O boundary considering a resampling for conodonts through the critical interval, with the definition of successive conodont zones and the record of the FAD of *I. fluctivagus*.

THE *IAPETOGNATHUS* ZONE

At the Amarilla Creek section the *Iapetognathus* Zone (26. 5 m thick) records the greater number and diversity of conodonts. This biozone is recognized in the lower-upper part of the Cardonal Formation,*

where the basal exposed strata of the upper part of the section represent the mid to upper *Cordylodus lindstromi* Zone recognized in previous studies. The index species *I. fluctivagus* is recorded few meters below the record of *Rhabdinopora* sp., which are considered the global guide fossils of the referred horizon (Nicoll et al. 1999; Cooper et al. 2001). Most associated species continue their records from the underlying zone, adding the appearance of *Iapetognathus fluctivagus*, *I. jilinensis*, *I. aengensis*, C*ordylodus prolindstromi*, *C.* cf. *andresi*, C. cf. *viruanus*, *Phakelodus elongatus*, *Fryxellodontus* sp., *Eoconodontus notchpeakensis*, *Problematoconites perforatus*, *Furnishina furnishi*, *Acanthodus uncinatus* and *A. lineatus*. Several of these species continue their occurrences in the following *Cordylodus angulatus* Zone. The *Iapetognathus* Zone was recognized in the United States, China, Canada, Kazakhstan, and it is identified in the Cajas Range, Argentina, in the present study. The record of *I. jilinensis* expands the recognition of the zone to Sweden, Estonia and Alaska, and is particularly described in China, where it verifies a stratigraphic range similar to that of *I. fluctivagus* (Nicoll et al. 1999).
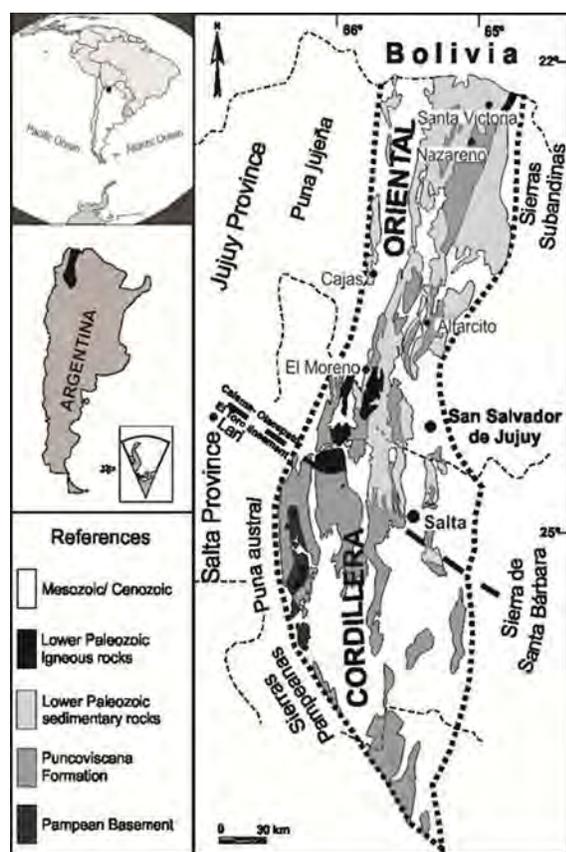
Figure 1. —Index map of sample sites in north - western Argentina (after Zeballo and Albanesi 2009).

Figure 2. —Biostratigraphic chart of the Upper Cambrian - Lower Ordovician (after Zeballo and Albanesi 2009)

DISCUSSION AND CONCLUSIONS

The biostratigraphic record through the Amarilla Creek section displays a continuous succession of biozones that spans the Furongian upper Stage 10 to the lower Tremadocian Stage in Cardonal Formation, which is truncated and contacts by fault with the Floian Acoite Formation. In the upper Cardonal Formation the *Cordylodus lindstromi*, *Iapetognathus* and *Cordylodus angulatus* zones are recognized (Figure 2). Although *I. fluctivagus* is scarce, its FAD confirms the C/O boundary in the lower upper part

of the studied section. The abundance of cosmopolitan species in this ancient basin of the Gondwanan margin reflects the important faunal exchange during the late Cambrian and early Ordovician across the Iapetus Ocean in middle to high latitudes (Zeballo and Albanesi 2009).

The conodont elements exhibit a black color alteration (CAI 5 = 300º and 480º), probably related to the influence of the nearby granite that intruded the Paleozoic rocks during the Jurassic-Cretaceous boundary interval.

ACKNOWLEDGMENTS

REFERENCES

ALBANESI, G. L., ESTEBAN, S. B., ORTEGA, G., HÜNICKEN, M. A. and BARNES, C. R., 2005. Bioestratigrafía y ambientes sedimentarios de las Formaciones Volcancito y Bordo Atravesado (Cámbrico Superior–Ordovícico Inferior), Sistema de Famatina, provincia de La Rioja. *Asociación Geológica Argentina, Serie D: Publicación Especial,* 8: 41–64.

ALBANESI, G. L. and PACHECO, F. E., 2010. Conodont Biostratigraphy and Paleoenvironments of the Cardonal Formation (Cambrian–Ordovician) from the Cajas Range, Cordillera Oriental, Northwestern Argentina and Paleobiogeographic Interpretation. GeoCAnada, Calgary. http:/ /www. geocanada2010. ca/

BARNES, C. R., 1988. The proposed Cambrian–Ordovician global Boundary stratotype and point (GSSP) in Western Newfoundland, Canada. *Geological Magazine,* 125 (4): 381–414.

COOPER, R. A., NOWLAN, G. S. and WILLIAMS, S. H., 2001. Global stratotype section and point for the base of the Ordovician System. *Episodes,* 24: 19–28.

GIULIANO, M. E., ORTEGA, G., ALBANESI, G. and MONALDI, R., 2013. Late Cambrian–Early Tremadocian conodont and graptolite records from the El Médano section, Salar del Rincón, Puna of Salta, Argentina. *Proceedings of the 3rd International Conodont Symposium, Argentina. Publicación Especial APA,* 13: 33–37.

MILLER, J. F., REPETSKI, J. E., NICOLL, R. S., NOWLAN, G. S. and ETHINGTON, R. L., 2014. The conodont *Iapetognathus* and its value for defining the base of the Ordovician System, *GFF*, 136 (1): 185–188.

NICOLL, R. S., MILLER, J. F., NOWLAN, G. S., REPETSKI, J. E. and ETHINGTON, R. L., 1999. *Iapetonudus* (new genus) and *Iapetognathus* Landing, unusual earliest Ordovician multielemnt condont taxa and their utility for biostratigraphy. *Brigham Young University Geology Studies,* 44: 27–101.

RAO, R. I., 1999. Los conodontes Cambro–Ordovícicos de la sierra de Cajas y del Espinazo del Diablo, Cordillera Oriental, República Argentina. *Revista Española de Micropaleontología,* 31 (1): 23–51.

TERFELT, F., BAGNOLI, G. and STOUGE, S., 2012. Re-evaluation of the conodont *Iapetognathus* and implications for the base of the Ordovican System GSSP. *Lethaia,* 45: 227–237.

ZEBALLO, F. J. and ALBANESI, G. L., 2009. Conodontes cámbricos y *Jujuyaspis keideli* Kobayashi (Trilobita) en el Miembro Alfarcito de la Formación Santa Rosita, quebrada de Humahuaca, Cordillera Oriental de Jujuy. *Ameghiniana*, 46 (3): 537–556.

Ordovician of the Anarak Region: implications in understanding Early Palaeozoic history of Central Iran

Vachik Hairapetian[1], Mansoureh Ghobadi Pour[2,3], Leonid E. Popov[3], S. Hassan Hejazi[1], Lars E. Holmer[4], David Evans[5] and Ali Sharafi[1]

[1] *Department of Geology, Khorasgan (Isfahan) Branch, Islamic Azad University, PO Box 81595−158, Isfahan, Iranl: vachik@khuisf.ac ir*
[2] *Department of Geology, Faculty of Sciences, Golestan University, Gorgan, Iran mghobadipour@yahoo.co.uk*
[3] *Department of Geology, National Museum of Wales, Cardiff CF10 3NP, Wales, United Kingdom leonid.popov@museumwales.ac.uk*
[4] *Institute of Earth Sciences, Palaeobiology, Uppsala University, SE-752 36 Uppsala, Sweden Lars.Holmer@pal.uu.se*
[5]*Natural England, Suite D, Unex House, Bourges Boulevard, Peterborough PE1 1NG, England, United Kingdom david.evans@naturalengland.org.uk*

ABSTRACT: The Pol-e Khavand area south-east of the town of Anarak preserves important clues for understanding geological evolution of Central Iran during the Palaeozoic. New observations confirm the non-conformable relationship between Doshakh metamorphites and overlying unmetamorphosed Lower Palaeozoic sediments, suggesting accretion of the volcanic arc in front of the Yazd block sometime in the late Cambrian to early Ordovician. The newly introduced volcano-sedimentary Polekhavand Formation preserves evidence of a ?Late Cambrian to Early Ordovician post-collisional bimodal volcanism and related extensional regime in the Pol-e Khavand area during that time. The Middle to Upper Ordovician interval of the studied succession is assigned to the newly introduced Chahgonbad Formation. The Darriwilian age of the base of this lithostratigraphical unit is demonstrated by the brachiopods *Tritoechia* and *Yangtzeella* which co-occur with a diverse a cephalopod assemblage. The low diversity fauna including brachiopods *Hibernodonta* sp., *Hindella* sp., *Rostricellula* cf. *ambigena* and trilobites *Vietnamia* cf. *teichmulleri* suggest a Katian age for the upper part of the unit. There is insufficient evidence for the existence of the hypothetical Palaeo-Tethys suture zone south of the Pol-e Khavand area.

INTRODUCTION

The presence of the Ordovician sediments along the northern margin of the Yazd block south-east of Anarak in Central Iran (Fig. 1) was first established during geological mapping of the area about thirty years ago by Sharkovski et al. (1984). For a lithostratigraphical subdivision of the Lower Palaeozoic part of the sedimentary succession the authors of the report applied the formal units (Shirgesht and Niur formations) earlier established by Ruttner et al. (1968) in the adjacent Tabas Block, eastern Central Iran. Sharkovski et al. (1984) also provided the first detailed description of the Anarak Metamorphic Complex and suggested stratigraphical relationships between the Ordovician sediments and metamorphic rocks of the Doshakh Unit. They assigned a Lower Cambrian age to the Lakh Marble within the Anarak Metamorphic Complex on the basis of the occurrence of Lower Cambrian archaeocyathids. In 2004 the area was visited by a team of Italian geologists to sample biostratigraphically constrained sites for palaeomagnetic studies. Results of these studies were published recently by Muttoni et al. (2009). They also collected an abundant ostracod assemblage described by Schallreuter et al. (2006), who inferred an Upper Ordovician (Katian) age for the fossiliferous horizon. More recently significant contradictions in the understanding of the geology of the area are revealed in publications by Bagheri and Stampfi (2008)

and by Buchs et al. (2013). These authors consider the Anarak Metamorphic Complex to comprise Palaeozoic to Triassic meta-sediments, meta-igneous rocks and serpentinized ultramafic rocks which were onlapped or tectonically interfingered with Jurassic to Neogene sediments. They also postulated that the Anarak Metamorphic Complex was thrusted onto Palaeozoic sedimentary cover of the Yazd (Cimmerian) block, whilst discussion of the stratigraphical contacts between the Doshakh metamorphites and Ordovician volcano-sedimentary succession was omitted.

Recent discoveries and continuing reviews of the Ordovician faunas and lithostratigraphy in the Anarak area put a new light on the geological history of the northern margin of the Yazd block. This is potentially important for re-evaluating the existing models of the tectonic evolution of Central Iran through the Palaeozoic.

GENERAL OUTLINE OF THE ORDOVICIAN SUCCESSION
The Ordovician deposits are exposed in two isolated localities south-east of the town of Anarak. The studied transect is situated in the Pol-e Khavand area at 21 km south-east of the town of Anarak (Fig. 1a-c). This is the same section as described by Sharkovski et al. (1984). New field observations convincingly confirmed previous reports by these researches of the existence of the sharp non-conformity between Doshakh metamorphites and overlying unmetamorphosed siliciclastic Lower Palaeozoic sediments (unit 1 Sharkovski et al. 1984), which contain channels, infilled with pebbly conglomerates. Reworked clasts of greenschists characteristic of the Doshakh metamorphites are common in these conglomerates, while some characteristic minerals, like muscovite and chlorite occur in the matrix. These stratigraphical contacts have been traced for over 1000 m west of the studied section and have also been observed in several excavations.

Notwithstanding existing claims regarding the 'great similarities' between the Ordovician successions observed in the Pol-e Khavand area and those of the the Derenjal Mountains in the Tabas Block (Schallreuter et al. 2006), there are important differences. The Shirgesht Formation of the Tabas Block ranges continuously from the Cambrian (Furongian) to the Middle Ordovician (Darriwilian), while a presumably Upper Ordovician interval at the top of the unit is barren (Ghobadi Pour et al. 2006; Ghobadi Pour and Popov 2009; Popov et al. 2011). Unlike the Lower Palaeozoic succession of the Tabas Block, the ?Late Cambrian to Ordovician deposits in the Pol-e Khavand area rest with non-conformity on the Doshakh metamorphites. There is a distinct disconformity at the base of the fossiliferous part of the succession, and there is a good evidence of ?Late Cambrian to Early Ordovician bimodal volcanism. Both are unknown in the Derenjal Mountains. To overcome the problems addressed above we propose two new lithostratigraphical units namely the Polekhavand and Chahgonbad formations with the type sections located in the Pol-e Khavand area south-east of Anarak.

Polekhavand Formation (?Cambrian, Furongian to Lower Ordovician)
Type section is located at about 1. 5 km south-west of the eastern foothills of the Pol-e Khavand Mountains (N33°10′58″; E 53°53′39″, altitude 1383 m). Total thickness is about 180 m.

Distribution: The unit has a restricted distribution in the northern part of the Yazd block south-east of the town of Anarak.
Lower boundary: The Polekhavand Formation rests with non-conformity on Doshakh metamorphites.

Upper boundary: In the type section the unit is overlain disconformably by the Chahgonbad Formation.
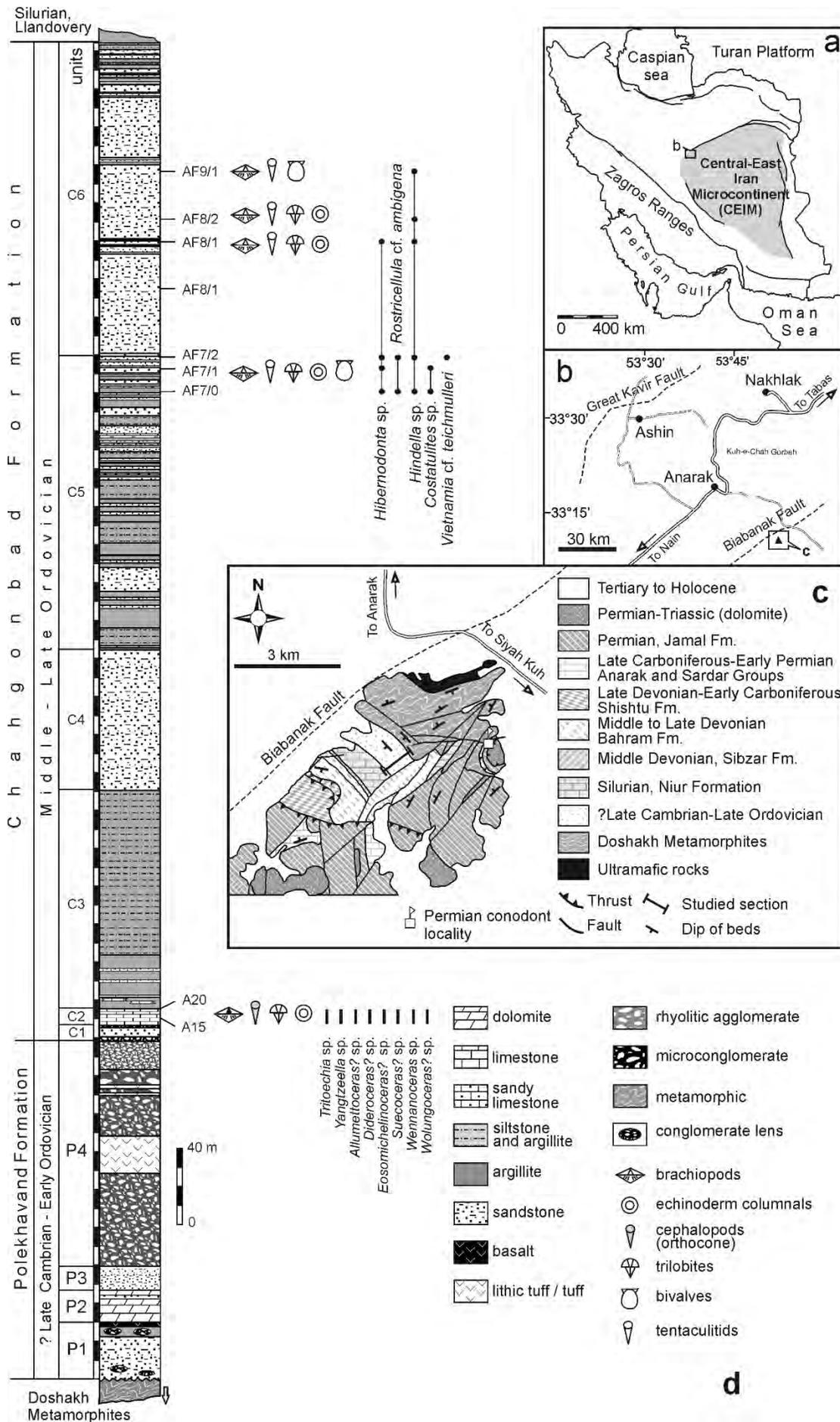
Fig. 1. a, simplified map of Iran showing location of the Anarak area; b, sketch map of the vicinity of Anarak showing geographical position of the Pol-e Khavand area; c, simplified geological map (slightly modified after Sharkovski et al. 1984) of the Pol-e Khavand area south-east of Anarak, showing the position of the studied section and approximate location of the Permian conodont sample after Bagheri and Stampfli (2008); d, stratigraphical column of the Ordovician deposits exposed in the Pol-e Khavand area, showing lithostratigraphical subdivision, position of sampled fossiliferous horizons and stratigraphical distribution of brachiopods cephalopods, trilobites and tentaculitids.

Subdivision: In the type section the Polekhavand Formation can be subdivided into four informal units (Fig. 1d), including: (P1) up to 28. 5 m of greenish-grey, fine-grained sandstones with conglomerate lenses and a bed of amygdaloidal basalts in the upper part; (P2) up to 17. 3 m of yellowish-brown dolomite with a bed of medium- to coarse-grained sandstone in the upper part; (P3) up to 15. 7 m of poorly sorted, fine-grained sandstone; (P4) up to 117 m purplish-brown, poorly sorted agglomerates with numerous rhyolite lithic clasts up to 90 cm across, intercalated with lithic tuffs and tuffs.

Biostratigraphy and chronostratigraphical age: The rocks assigned to the Polekhavand Formation are barren and its age is defined by stratigraphical position between the Doshakh metamorphites accreted to the Yazd block sometime in the ?late Cambrian–early Ordovician and the Darriwilian to Katian Chahgonbad Formation.

Depositional environments and lithofacies: The lower unit comprises alluvial fan deposits with channels infilled with debris of metamorphic rocks suggesting erosion of uplifted rocks of the Doshakh Metamorphic Complex. The presence of amygdaloidal basalts also suggests that the lower part of the Polekhavand Formation formed in a terrestrial environment, while the dolomites suggest a brief restricted marine incursion. The upper unit was probably formed on the flanks of the volcanic build-up. It shows several packages, including individual units of agglomerates, separated by tuff horizons. The former probably represent multiple rhyolite mass flows (probably lahars) caused by the collapse and fragmentation of growing rhyolite domes. Each flow horizon probably represented an individual eruption. Laterally there are a few small packages of red jasper most likely derived from a hot rhyolite flow, as a result of hot water leaching silica and subsequently re-precipitating in cool cavities, as it is common at the outer margins of the flow.

Chahgonbad Formation (Middle Ordovician, Darriwilian to Upper Ordovician, Katian)
Type section: is located in the Pol-e Khavand area at about 1. 5-2 km south-west of the eastern foothills of the Pol-e Khavand Mountains and about 4 km north of the Chahgonbad well (N33°10′50″; E 53°53′40″, altitude 1384 m). Total thickness is about 505 m.

Distribution: The unit has a restricted distribution in the northern part of the Yazd block south-east of the town of Anarak.

Lower boundary: The Chahgonbad Formation is separated by disconformity from the Polekhavand Formation.

Upper boundary: In the type section the unit is separated by a paraconformity from the Sillurian (Llandovery, Rhuddanian to Aeronian) transgressive black shales (so-called 'hot shales'). Formal lithostratigraphical subdivision for the Silurian is not established for the Anarak area.

Subdivision: In the type section the Chahgonbad Formation can be subdivided into six informal units (Fig. 1d), including: (C1) up to 10. 5 m of oligomict microconglomerate and coarse-grained sandstone; (C2) up to 8. 7 m of brownish-purple argillaceous bioclastic limestones with a bed of oolitic ironstones up to 0. 4 m thick at the base; (C3) up to 115 m of intercalating grey argillites and sandstones with several tuff horizons; (C4) up to 73. 6 m of violet-red sandstone sandstone with a few beds of argillites and siltstones, cross-bedded sandstones in the upper 15 m; (C5) up to 136 m of violet-red and greenish red argillites, siltstones and sandstones; (C6) up to 161 m of violet-red and greenish-red sandstones with siltstone and argillite intercalations in the middle and upper part.

Biostratigraphy and chronostratigraphical age: The only fossils previously reported from the Chahgonbad Formation are ostracods recovered from the unit C1 and described by Schallreuter et al. (2006). However, the mid Katian age of the ostracod fauna assessed in the cited publication is put in question by its co-occurrence with the brachiopods *Tritoechia* sp. and a new species of *Yangtzeella*, which suggests a Darriwilian age for the unit. Other components of the brachiopod assemblage include *Camerella* sp., *Phragmorthis* sp. and an orthide similar to *Lomatorthis*. Cephalopods, including *Allumettoceras*? sp., *Dideroceras*? sp., *Eosomichelinoceras*? sp., *Suecoceras*? sp., *Wennanoceras* sp. and *Wolungoceras*? sp. represent the most distinctive component of the faunal assemblage of Unit C1. Preliminary results of the study of this cephalopod fauna suggest that it is somewhat different from the Dariwillian assemblages of the Alborz Mountains (Evans et al. 2013) and may show some affinity with North China and South Korea. Other components of the fauna are the poorly preserved trilobites *Nilleus* sp. and unidentified asaphids, as well as echinoderms, which are currently under study. The two uppermost units (Fig. 1d; units C5 and C6) contain a low diversity fauna of brachiopods, trilobites and tentaculitids. The most common taxa are *Hibernodonta* sp. and *Hindella* sp. In the unit C5 they overlap with the rhynchonellide *Rostricellula* cf. *ambigena* (Barrande, 1847), characteristic of the lower Katian in Bohemia and Morocco (Havlíček 1961; Villas 1985; Colmenar and Álvaro 2014), and the tentaculitid *Costalulites* sp. Another biostratigraphically informative taxon is the trilobite *Vietnamia* cf. *teichmulleri* (Hamman and Leone, 1997) which was previously known from the Punta Serpeddi Formation of Sardinia. In unit C6, the brachiopod *Hindella* sp. tends to form a monotaxic association and the age of this interval is probably mid to late Katian.

Depositional environments and lithofacies: The moderately diverse fauna from Unit C1 inhabited offshore substrates while the presence of oolitic ironstones within the unit may suggest low rates of sedimentation. Low diversity faunal associations from units C8 and C9 inhabited nearshore siliciclastic shoals.

DISCUSSION

The non-conformity between Doshakh metamorphites and the overlying volcano-sedimentary Polekhavand Formation suggests that a Late Permian to Triassic age for the 'Doshakh accretionary wedge' inferred by Bagheri and Stampfli (2008) is extremely unlikely. Instead Doshakh metamorphites most probably represent remnants of the Late Precambrian to Late Cambrian volcanic arc accreted in front of Central Iran sometime in the Late Cambrian to Early Ordovician, while the unmetamorphosed Ordovician succession represents an onlap assemblage sealing the Late Cambrian to Early Ordovician

suture. Exhumation and erosion of the Doshakh metamorphites resulted in the deposition of the terrigenous sediments of the Polekhavand Formation during the Late Cambrian to Early Ordovician, while post-collisional bimodal volcanism occurred in the area, suggesting an extensional regime at that time. Deposition of the Chahgonbad Formation coincided with marine transgression in the Pol-e Khavand area, which occurred in the Darriwilian time.

An important aspect for evaluation of the age of the Doshakh metamorphic complex is the age of the Lakh Marbles. Notwithstanding recent claims to the contrary in recent publications by Bagheri and Stampfli (2008) and Buchs et al. (2013), reports of so-called 'archaeocyathids' were indeed published, including illustrations of a few specimens in a short note by Mel'nikov et al. (1986). Subsequently Kruse and Zhuravlev (2008, p. 636) restudied the specimens, which were housed in the Paleontological Institute Moscow, and came to the conclusion that specimens identified as *Dictocyathus*, *Paranacyathus* and *Agastrocyathus* are in reality naturally etched specimens of the desmosponge *Rankenella*, whereas a specimen identified as *Coscinocyathus* represents an eocrinoid oscicle. *Rankenella* is well known from the middle to upper Cambrian Mila Formation of eastern Alborz, where it can be found as an important reef-builder in the metazoan build-ups of the Mila Formation Member 3 (Kruse and Zhuravlev 2008, p. 636). Thus the mid to late Cambrian age of the Lakh Marbles is sufficiently proved in present. Thus the supposed 'late Palaeozoic corals' illustrated by Bagheri and Stampfli (2008, pl. 2, fig. H) are in reality desmosponge the *Rankenella*, while the echinoderm ossicles (Bagheri and Stampfli 2008, pl. 2, figs F, G) probably belong to eocrinoids.

Some authors of the present manuscript (Hairapetian, Holmer and Popov) recently revisited the supposed locality of the Permian (Kungurian–Roadian) conodonts, associated with the Doshakh metamorphic complex, in the eastern margin of the Pol-e Khavand area (Bagheri and Stampfli 2008, fig. 2; pl. 1, fig. A). There are indeed unmetamorphosed Permian carbonates exposed in proximity to the outcrop area of brecciated quartzites assigned to the Doshakh metamorphites. Nevertheless, stratigraphical contacts between these two units are not evident. The surrounding area is strongly tectonized. Keeping in mind strong differences in the degree of metamorphism of the rocks, contacts between limestones and brecciated quartzites are most probably faulted. Conodonts extracted from the limestones cannot be used for biostratigraphical dating of the adjacent quartzites. The data presented shows that there is insufficient proof of the late Palaeozoic age of the metamorphic rocks exposed in the Anarak area and in particular of the Doshakh metamorphites and the Lakh Marbles.

CONCLUSIONS

Restudy of the Ordovician succession in the Pol-e Khavand south-east of the town of Anarak reveals significant differences between the Lower Palaeozoic sedimentary successions of the northern part of the Yazd block and the Tabas block. As a consequence a substantial revision of the Ordovician lithostratigraphy of the area is proposed with the introduction of the Polekhavand and Chahgonbad formations. New observations convincingly establishes the existence of the sharp non-conformity between the Doshakh metamorphic complex and the overlying volcano-sedimentary Polekhavand Formation reported earlier by Sharkovski et al. (1984), while the ?late Cambrian to early Ordovician post-collisional bimodal volcanism suggests an extensional regime in the area during that interval. The ?late Cambrian–early Ordovician Polekhavand Formation was deposited mainly in the terrestrial environment, while a marine transgression in the Pol-e Khavand area occurred only in the Darriwilian. In the absence of sufficient proof of the late Palaeozoic age for the metamorphic rocks, the Doshakh metamorphic complex

most probably represents a remnant of a late Precambrian-Cambrian volcanic arc accreted to Central Iran during the Early Palaeozoic, and the position of the hypothetical Palaeo-Tethys suture zone south of the Pol-e Khavand area inferred by Bagheri and Stampfi (2008, fig. 2) and Buchs et al. (2013, fig. 2) is doubtful. The new geological data provided here does not fit into existing models of the tectonic development of the Anarak region and the northern margin of Central Iran during the Palaeozoic. These latter models require careful reconsideration and improvement.

ACKNOWLEDGMENTS

REFERENCES

BAGHERI, S. and STAMPFLI, G., 2008. The Anarak, Jandaq and Posht-e-Badam metamorphic complexes in central Iran: new geological data, relationships and tectonic implications. T*ectonophysics*, 451: 123–155.

BARRANDE, J., 1847. Über die Brachiopoden der silurischen Schichten von Böhmen, I. *Naturwissenschaftliche Abhandlungen (Haidingers)*, 1: 1–154.

BRUTON, D. L., WRIGHT, A. J. and HAMEDI, M. A., 2004. Ordovician trilobites of Iran. *Palaeontographica*, A271: 111–149.

BUCHS, D. M., BAGHERI, S., MARTIN, L., HERMANN, J. and ARCULUS, R., 2013. Paleozoic to Triassic ocean opening and closure preserved in Central Iran: Constraints from the geochemistry of meta-igneous rocks of the Anarak area. *Lithos*, 172–173: 267–287.

COLMENAR, J. and ÁLVARO, J. J., 2014. Integrated brachiopod-based bioevents and sequence-stratigraphic framework for a Late Ordovician subpolar platform, eastern Anti-Atlas, Morocco. *Geological Magazine*, DOI: http:/ /dx.doi.org/10.1017/S0016756814000533.

EVANS, D. H., GHOBADI POUR, M. and POPOV, L. E., 2013. Review of the Early to Mid Ordovician orthoconic cephalopods from Iran. *Bulletin of Geosciences*, 88: 21–44.

GHOBADI POUR, M., WILLIAMS, M., VANNIER, J., MEIDLA, T. and POPOV, L. E., 2006. Ordovician ostracods from east Central Iran. *Acta Palaeontologica Polonica*, 51: 551–560.

GHOBADI POUR, M. and POPOV, L. E., 2009. First report on the occurrence of *Neseuretinus* and Ovalocephalus in the Middle Ordovician of Iran. *Acta Palaeontologica Polonica*, 54: 125–133.

HAMMANN, W. and LEONE, F., 1997. Trilobites of the post–Sardic (Upper Ordovician) sequence of southern Sardinia. Part 1. *Beringeria*, 20: 1–217.

HAVLÍČEK, V. 1961. Rhynchonelloidea des böhmischenälteren Paläozoikums (Brachiopoda). *Rozpravy Ústredního ústavu geologického*, 27: 1–211, 27 pl.

KRUSE, P. D. and ZHURAVLEV, A. Yu., 2008. Middle-Late Cambrian *Rankenella-Girvanella* reefs of the Mila Formation, northern Iran. *Canadian Journal of Earth Sciences*, 45: 619–639.

MEL'NIKOV, B. N., ROZANOV, A. Yu., SUSLOV, M. V. and FONIN, V. D., 1986. First archaeocyathids from the Lower Cambrian of Central Iran. *Izvestiya Akademii Nauk SSSR*, 1986(7): 134–138.

MUTTONI, G., MATTEI, M., BALINI, M., ZANCHI, A., GAETANI, M. and BERRA, F., 2009. The drift history of Iran from the Ordovician to the Triassic. In: Brunet, M. -F., Granath, J. W. and

Wilmsen, M., Eds., *South Caspian to Central Iran basins,* 7–29.*. London: The Geological Society. Special Publication 312:

POPOV, L. E., BASSETT, M. G., HOLMER, L. E. and GHOBADI Pour, M. 2009. Early ontogeny and soft tissue preservation of siphonotretide brachiopods: new data from the Cambrian - Lower Ordovician of Iran. *Gondwana Research*, 16: 151–161.

RUTTNER, A., NABAVI, M. and HAJIAN, J., 1968. Geology of the Shirgesht area (Tabas area, East Iran). *Reports of the Geological Survey of Iran*, 4: 1–133.

SCHALLREUTER, R., HINZ-SCHALLREUTER, I., BALINI, M. and FERRETTI, A. 2006. Late Ordovician Ostracoda from Iran and their significance for palaeogeographical reconstructions. *Zeitschrift für Geologische Wissenschaften*, 34(5–6): 293–345.

SHARKOVSKI, M., SUSOV, M. and KRIVYAKIN, B., Eds., 1984. *Geology of the Anarak area (Central Iran), Explanatory text of the Anarak quadrangle map, 1: 250. 000, V/O Technoexport Report*, 19. Tehran: Geological Survey of Iran, 143 pp.

VILLAS, E., 1985. Braquiópodos del Ordovícico medio y superior de las Cadenas Ibéricas Orientales. *Memorias del Museo Paleontológico de la Universidad de Zaragoza*, 1: 1–223.

ZANCHI, A., S. ZANCHETTA, E. GARZANTI, M. BALINI, F. BERRA, M. MATTEI and MUTTONI, G., 2009. The Cimmerian evolution of the Nakhlak–Anarak area, central Iran, and its bearing for the reconstruction of the history of the Eurasian margin. In M. -F. Brunet, M. Wilmsen and J. W. Granath (Eds.), *South Caspian to Central Iran Basins,* 261–286. London: The Geological Society. Special Publication 312.

The Balognathiid Ordovician conodonts *Eoplacognathus robustus* Bergström and *E. lindstroemi* Hamar

Susana Heredia[1] and Ana Mestre[1]

[1]*CONICET- Instituto de Investigaciones Mineras (UNSJ). Libertador 1109, San Juan (5400), Argentina.*
sheredia@unsj.//edu.ar

INTRODUCTION

The *Eoplacognathus* apparatus was first described, and their species defined as key zonal and subzonal conodonts by Bergström (1971), based on only P elements. This original description is only based on the oral shape of the P elements. The key conodonts *E. robustus* and *E. lindstroemi* document accurately the homonymous subzones for the conodont-bearing strata.

The Middle-Upper Ordovician strata of the Ponón Trehué outcrops, exposed in the San Rafael Block (Fig. 1), provided a large collection of conodonts. Previous work on this conodont fauna was carried out by Heredia (1982, 1998, 2001, and 2002). A recent revision of this collection allowed us to reinterpret S and M elements previously assigned to the *Baltoniodus* species as belonging to the *E. robustus* and *E. lindstroemi* apparatuses.
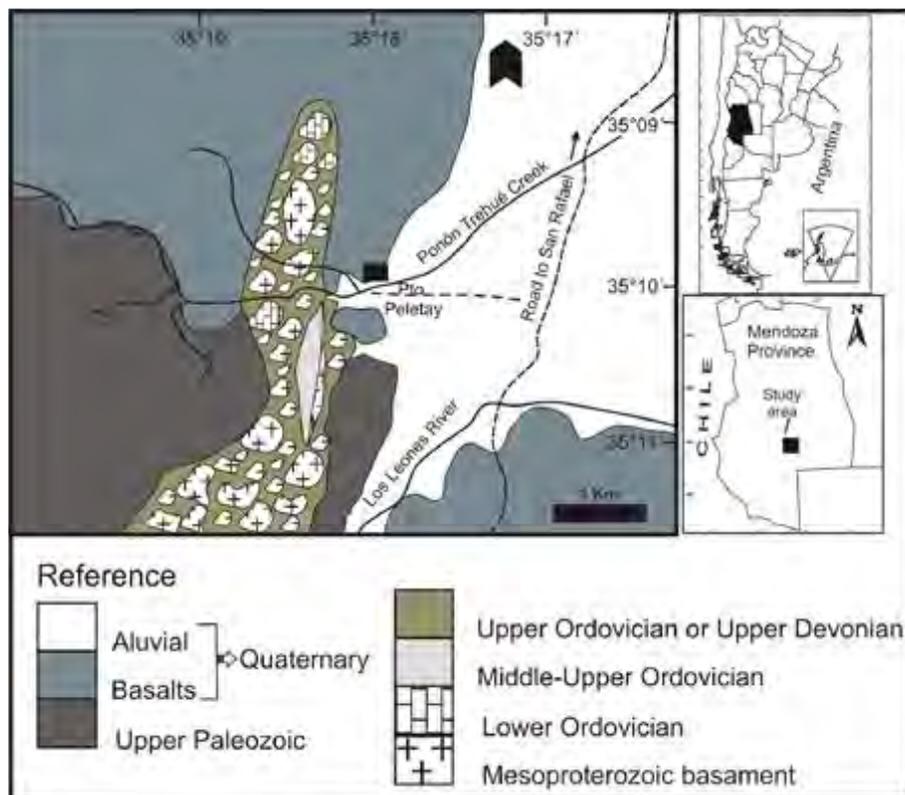
FIGURE 1. —Geologic map of the Ponón Trehué Ordovician outcrops. Arrow points to location of the La Tortuga type section.

The main goal of this contribution is to analyze morphological characters of P elements, including S and M elements as part of the *Eoplacognathus* apparatus proposing a new reconstruction of it, and finally to make a focus on the inclusion of these conodont species in the family Balognathidae.

BRIEF CONSIDERATIONS ON TAXONOMY

The family Polyplacognathidae Bergström included three genera, *Polyplacognathus* Stauffer; *Eoplacognathus* Hamar, and *Cahabagnathus* Bergström. All these genera are characterized exclusively by bimembrate apparatuses. Stouge and Bagnoli (1990) reported for the first time S and M elements in the apparatus of *Eoplacognathus pseudoplanus* and proposed a change in this genus name to *Lenodus pseudoplanus*, including the genus *Lenodus* to the Family Balognathidae. These authors kept the genus *Eoplacognathus* in the Polyplacognathidae. However, Löfgren and Zhang (2003) continued using the designation *Eoplacognathus pseudoplanus,* and they recognized S and M elements for this species. Mellgren et al. (2012) recognized S elements in the *E. foliaceous* apparatuses.
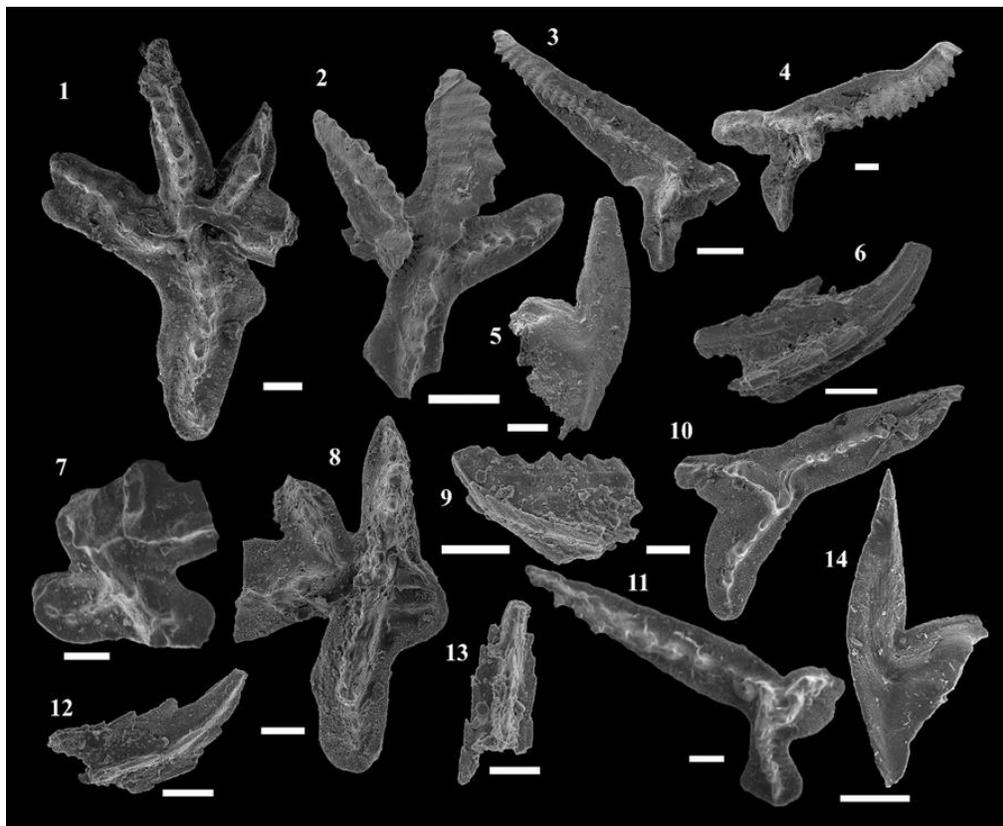
PLATE 1: Index conodonts from La Tortuga section, Upper Darriwilian, Ponón Trehué Formation (Sierra Pintada, Mendoza). Scanning electron microscope photomicrographs, scale bar 0. 1 mm. 1-6, *Eoplacognathus lindstroemi* Hamar, all the elements from PT11'. 1, dextral Pa elements CORD MP 2364(1-2). 2, sinistral Pa element, CORD MP 2364(3). 3, dextral Pb element CORD MP 2362(2). 4, sinistral Pb element CORD MP 2361(2). 5, M element, CORD MP 2290(6). 6, Sd element, CORD MP 2290(2). 7-14. *Eoplacognathus robustus* Bergström. 7, dextral Pa element CORD MP 2228(1), PT 8. 8, sinistral Pa element CORD MP 2225 (1), PT 9. 9, Sb element CORD MP 2292 (2) PT9. 10, sinistral Pb element CORD MP 2223(5), PT 9. 11, dexral Pb, CORD MP 2229(1) PT9. 12, Sd element, CORD MP 2292(4), PT9. 13, Sa element, CORD MP 2292(3), PT9. 14, M element, CORD MP 2292(1), PT9.

REFERENCES

BERGSTRÖM, S., 1971. Conodont biostratigraphy of the Middle and Upper Ordovician of Europe and Eastern North America. In: Sweet, W. C. and Bergström, S., (eds.) *Symposium on Conodont Biostratigraphy,* 83-161. Boulder: Geological Society of America. Memoir 127.

HAMAR, G. 1966. The Middle Ordovician of the Oslo Region, Norway. 22. Preliminary report on conodonts from the Oslo-Asker and Ringerike districts. *Norsk Geol. Tidsskr*., 46:27-83.

HEREDIA, S., 1982. *Pygodus anserinus* Lamont et Lindström (Conodonte) en el Llandeillano de la Formación Ponón Trehué, Provincia de Mendoza, Argentina. *Ameghiniana*, 19 (3-4): 229-233.

-----, 1998. *Eoplacognathus robustus* (Conodonta) en la Formación Ponón Trehué, Sierra Pintada, provincia de Mendoza, Argentina. *Ameghiniana*, 35(3): 337-344.

-----. 2001. Late Llanvirn conodonts from Ponón Trehué Formation, Mendoza, Argentina. *GAIA*, 16: 101-117.

-----, S. 2002. Upper Llanvirn–Lower Caradoc Conodont biostratigraphy, southern Mendoza, Argentina. In: Aceñolaza, F. G., (Ed.): *Aspects of the Ordovician System in Argentina,* 167–176, Buenos Aires: Instituto Superior de Correlación Geológica (INSUGEO). Serie Correlación Geológica 16

LÖFGREN, A. and ZHANG, J. H. 2003. Element association and morphology in some Middle Ordovician platform-equipped conodonts. *Journal of Paleontology*, 77: 723–739.

MELLGREN, J., SCHMITZ, B., AINSAAR, L., KIRSIMÄE, K. and ERIKSSON, M. 2012. Conodont dating of the Middle Ordovician breccia cap-rock limestone on Osmusaar Island, northwestern Estonia. *Estonian Journal of Earth Sciences*, 61(3): 133-148.

STOUGE, S. and BAGNOLI, G. 1999. The suprageneric classification of some Ordovician prioniodontid conodonts. *Bolletino della Società Paleontológica Italiana*, 37: 145-158.

The presence of the middle Ordovician genus *Baltoniodus* (Lindström, 1955) in the Central Andean Basin, Argentina: The stratigraphic significance

Susana Heredia[1], J. Carlorosi[2] and G. Sarmiento[3]

[1]CONICET- Instituto de Investigaciones Mineras (UNSJ). Libertador 1109, San Juan (5400), Argentina. sheredia@unsj.edu.ar
[2]CONICET- INSUGEO (UNT). Miguel Lillo 205, Tucumán (4000), Argentina.
[3] Departamento de Paleontología, Universidad Complutense de Madrid, José Antonio Novais, Madrid (28040), Spain.

ABSTRACT: Lower Palaeozoic sedimentary rocks of the central Andean basin of Argentina are concentrated in northwestern Argentina and the Famatina basins. Since the pioneering works on conodonts (Monaldi and Monaldi 1978; Rao *et al.* 1991, among others) there have been numerous contributions on this subject. The Ordovician sections of Chaschuil (Suri Formation, Famatinian basin), Gallinato Creek (Santa Gertrudis Formation, Mojotoro Range), Los Colorados, Lipán and Zenta (Eastern Cordillera and Subandean Range) were sampled and several conodont collections were obtained (Aceñolaza et al. 2008; Carlorosi et al. 2013)(Fig. 1). The discovery of the conodont key species *Baltoniodus triangularis* Lindström in these sections allowed us to recognize a global scheme that pointed out the basal Dapingian (Wang *et al*. 2009; Carlorosi *et al*. 2013). Also many elements of the genus *Baltoniodus* were recovered from the Santa Gertrudis Formation, which were studied for this contribution. Our main aims are to present a new species of the multielement genus *Baltoniodus* that has been recovered from the studied area and to establish the stratigraphical relation between *B. triangularis* and this species.
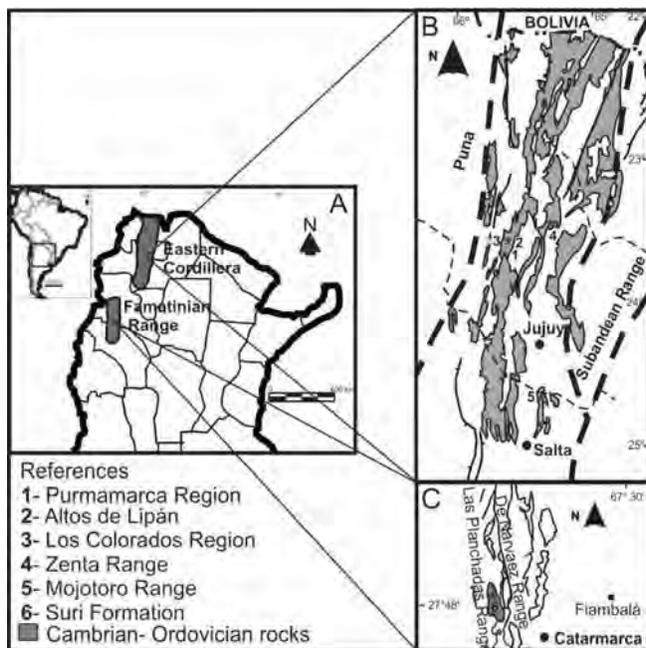
FIGURE 1- Map showing the location of the studied areas. Each area is indicated by a number.

STRATIGRAPHY

The areas of study are: 1 - Quebrada de Chamarra (Los Colorados Region, Fig. 1-B3) . The section is located at 23°31'56. 4'' S and 65°40'04. 3'' W. A 2500 m thick succession constituted by two formations, Acoite and Alto del Cóndor, but only the uppermost Alto del Cóndor Formation have been taken in consideration. 2 - Altos de Lipán (Fig. 1-B2): A section cropping out in the eastern flank of the Altos de Lipán, Purmamarca (Jujuy), at 23°41'50'' S, 65°40'35'' W. 3 –Mojotoro Range of the Salta province (Fig. 1-B5). Ordovician sandstones and siltstones of the Santa Gertrudis Formation yield conodonts (24°41'10. 96'' S and 65°17'18. 79'' W.). 4 - The last area is the Suri Formation which is outcropping in the Chaschuil area, Famatinian Basin (27°47'57. 40'' S and 68°3'20. 92'' W. Fig. 1- C6).

CONODONTS AND STRATIGRAPHY

The conodont associations recovered from each study area are comparable in respect to the presence of significant species, the fauna consists of: *Baltoniodus triangularis* (Lindström), *Baltoniodus* sp. nov. A, *Drepanodus arcuatus* Pander, *Drepanoistodus basiovalis* (Sergeeva), *Drepanoistodus forceps* Lindström, *Erraticodon patu* Cooper, *Gothodus costulatus* Lindström, *Oistodus* sp., *Trapezognathus diprion* (Lindström), *Trapezognathus quadrangulum* Lindström and *Triangulodus* sp, among others. This conodont association can be assigned to an interval that spans the lowermost to lower Dapingian (*Baltoniodus triangularis* Zone) (Wang *et al*. 2009; Carlorosi *et al*. 2013).

The *Baltoniodus triangularis* apparatus was described for the Baltoscandia area, South China and the Central Andean Basin (Lindström, 1955; Stouge and Bagnoli, 1990; Wang *et al*., 2009 among others). The morphological characters used for the definition of this new species (*B*. sp. nov. A) are primarily based on P elements (Pl. 1) that had been compared to the P elements of *B. triangularis*. This new species is defined on those elements shown by Cooper (1981) and Albanesi and Vaccari (1994) and assigned as *Baltoniodus navis* (*sensu* Cooper). Moreover, the association of advanced forms of *B. triangularis*, *B*. sp. nov. *A* and *Erraticodon patu* in the Santa Gertrudis and Suri formations allows to propose the upper part of the *B. triangularis* Zone and establish a closer affinity for northwestern Argentina with the Australian faunal province.

REFERENCES

ACEÑOLAZA, F. G., HEREDIA, S. and CARLOROSI, J. M. T., 2008. La "Sepulturas Limestone" (Harrington en Harrington y Leanza, 1957) en su área tipo, fósiles y edad. Provincia de Jujuy, Argentina. *Acta Geológica Lilloana*, 20 (2): 147 – 158.

ALBANESI, G. L. and VACCARI, E. N., 1994. Conodontos del Arenig en la Formación Suri, Sistema del Famatina, Argentina. *Revista Española de Paleontología*, 26: 125‑146.

CARLOROSI, J., HEREDIA, S. and ACEÑOLAZA, G., 2013. Middle Ordovician (early Dapingian) conodonts in the Central Andean Basin of NW Argentina. *Alcheringa*, 37: 1 – 13.

COOPER, B. J., 1981. Early Ordovician conodonts from the Horn Valley Siltstone, Central Australia. *Palaeontology*, 24: 147‑183.

LINDSTRÖM, M., 1955. Conodonts from the lowermost Ordovician strata of south-central Sweden. *Geologiska Föreningens i Stockholm Förhandlingar*, 76 - 4(21): 517-604.

MONALDI, C. R. and MONALDI, O. H., 1978. Hallazgo de una nueva fauna en la Formación Santa Gertrudis (Ordovícico), Provincia de Salta, República Argentina. *Revista de la Asociación Geológica Argentina*, 33: 245-246.

RAO, I. R., HUNICKEN, M. A. and ORTEGA, G., 1991**.** Conodontes y graptolitos ordovícicos en la quebrada de Los Colorados (Departamento de Tumbaya), Cordillera Oriental, Provincia de Jujuy, Argentina. *Anais de la Academia Brasilera de Ciencias,* 63: 185-192.

STOUGE, S., and BAGNOLI, G., 1990. Lower Ordovician (Volkhovian-Kunda) conodonts from Hagudden, northern Öland, Sweden: *Palaeontographia Italica*, 77: 1-54.

WANG, X., STOUGE, S., CHEN, X., LI, Z., WANG, C., FINNEY, S., ZENG, Q., ZHOU, Z., CHEN, H. and ERDTMANN, B., 2009. The global stratotype section and point for the base of the Middle Ordovician Series and the Third Stage (Dapingian). *Episodes,* 32: 96‑113.
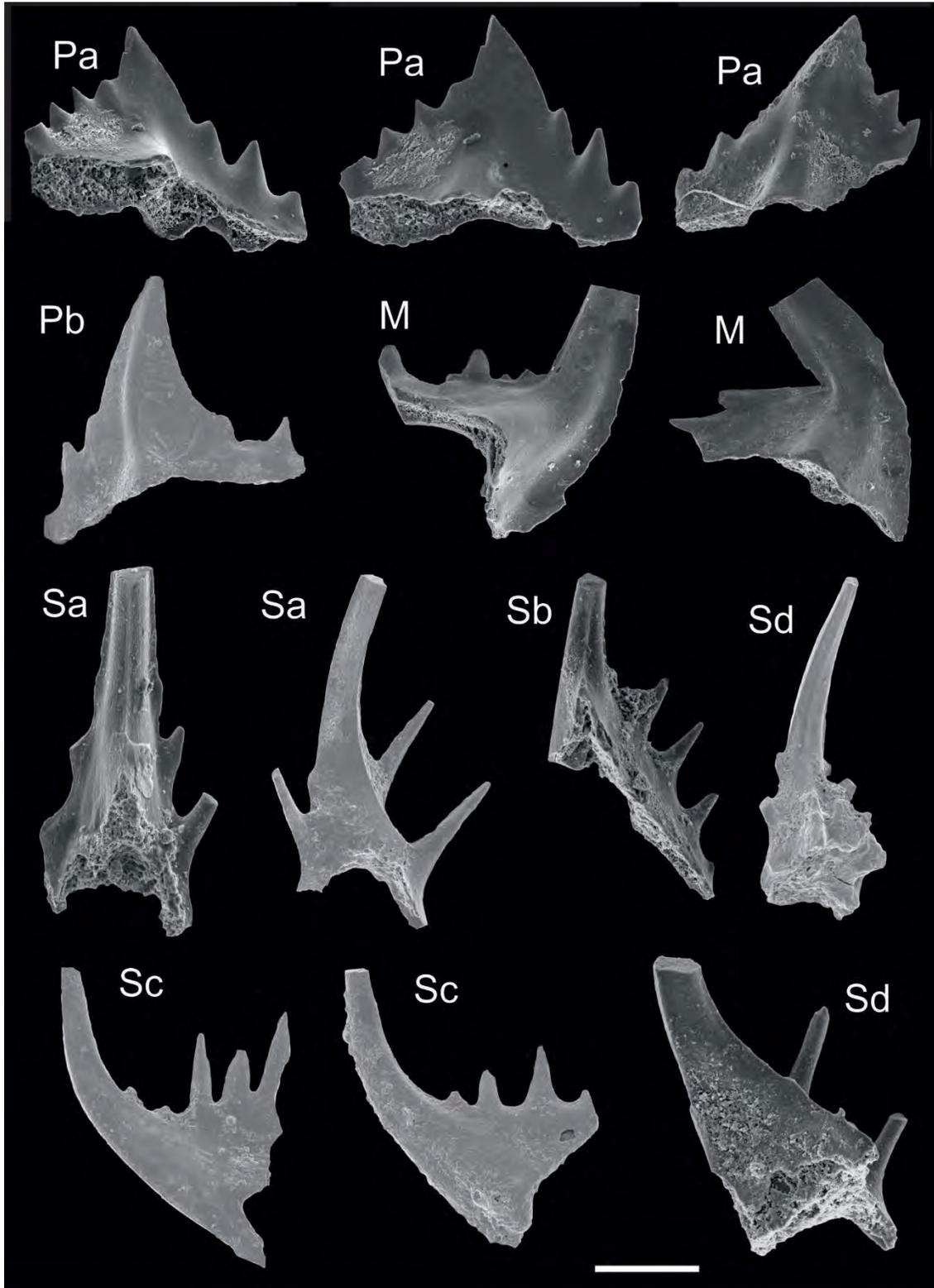
PLATE 1- Apparatus of the species *Baltoniodus* sp. nov. A. Elements recovered from de Santa Gertrudis Formation in the Mojotoro Range. Scale bar: 10 μm.

The *Pygodus Serra* Zone in Cuyania, Argentina

Susana Heredia[1], Ana Mestre[1], Tatiana Soria[1], Cintia Kaufmann[1]

[1] CONICET- IIM, Facultad de Ingeniería, Universidad Nacional de San Juan. Libertador San Martin 1109, 5500, San Juan, Argentina, sheredia@unsj.edu.ar

INTRODUCTION

Middle Ordovician outcrops of the Cuyania terrane extend from latitude 29º S to 33º S, and correlative rocks appear near San Rafael City (35º S) in the south of Mendoza Province, Western Argentina (Fig. 1) (Keller et al. 1996). These upper Darriwilian deposits are known as Ponón Trehué Formation which has been studied from different scopes (see Heredia 2006). Also, upper Darriwilian deposits have been recognized in the Villicum range and Cauquenes Dam (Fig. 1).

A Greenville-type basement (Cingolani and Varela 1999) is present in the Ponón Trehué region and is partially covered by Ordovician carbonate-siliciclastic sedimentary rocks (complete references in Heredia 2006). The biostratigraphy of these deposits is based on conodonts, and constrained by *Pygodus serra* (Hadding), *Pygodus anserinus* Lamont et Lindström, *Eoplacognathus robustus* Bergström and *Eoplacognathus lindstroemi* Bergström. These latter two species have been also recovered in Los Azules Formation and the first one in La Cantera Formation in the Precordillera basin (Fig. 1). The main goal of this contribution is to record the *Pygodus serra* Zone, and the *E. robustus* and *E. lindstroemi* subzones in Cuyania. Additionally, we also briefly compare the sedimentary successions that bear such key conodonts.
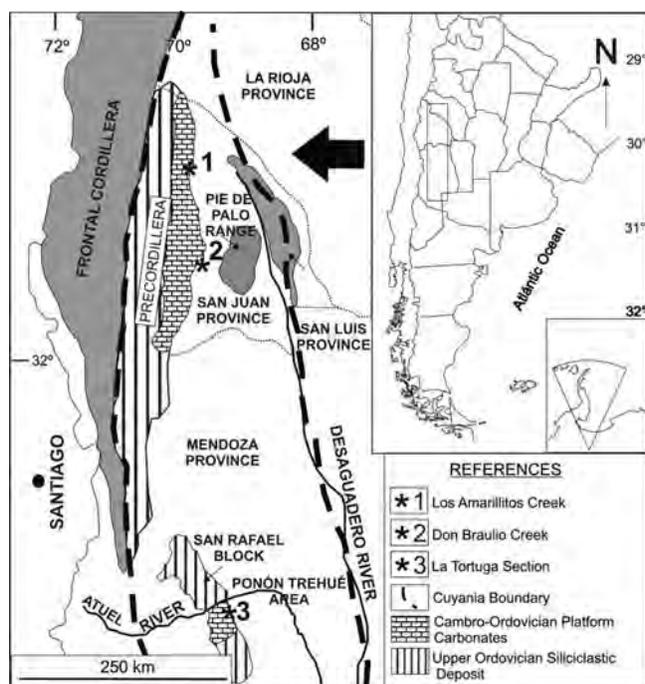
Figure 1. —Location map of sections mentioned in text.

The Ponón Trehué Formation (upper Darriwilian to lower Sandbian) in the La Tortuga section (Fig. 1) is composed of granite conglomerate, sandstone and thin-bedded, fossiliferous limestone, which represents a depositional cycle from shallower to deeper environments (complete references in Heredia 2006). The Don Braulio (Villicum range) and Los Amarillitos (Los Cauquenes Dam) sections: The siliciclastic units examined in this paper are the Los Azules and La Cantera formations that crop out in the Central and Eastern Precordillera.

These formations both represent the clastic input to the basin over the Cambrian- Middle Ordovician carbonate facies. The Ordovician siliciclastic rocks in the Cerro Viejo region (Los Azules Formation) is composed by dark claystone and siltstone, black shale, and yellowish calcareous siltstone and marly mudstone. A rich Darriwilian-Sandbian graptolite fauna occurs in the Los Azules Formation (complete references in Ortega et al. 2007). The Los Amarillitos section (Fig. 1) is located on the western flank of the Cauquenes Range. It is composed by black mudstone, chert and black shale beds alternating in the lower part; followed by folded black shale in the middle part which is covered in turn by black coarse massive siltstone with disperse carbonate nodules. To the top the succession is composed by yellowish calcareous siltstone.

The La Cantera Formation is a siliciclastic unit that outcrops at eastern flank of Villicum Range. This succession in Don Braulio section (Fig. 1) overlies the Los Azules Formation by an erosive surface and it is unconformably overlain by Hirnantian diamictites of Don Braulio Formation. The base of the La Cantera Formation is composed mainly of greenish, coarse siliciclastic deposits. The record of graptolites assemblages (Peralta 1993) indicates a Middle-Upper Ordovician age.

System	Series	Stage	Bergström (1971, 1983)	Cuyania Heredia et al. (2014)	3	2	1
Ordovician	Middle	upper Darriwilian	*Pygodus serra* — *E. lindstr.*	*Pygodus serra* — *E. lindstr.*			
			E. robustus	*E. robustus*			
			E. reclinat.	*?*			
			E. foliaceus				
		E. suec.	*P. anitae*	*E. suec.* — *P. anitae*			

Figure 2. —**Biostratigraphic chart comparing upper Darriwilian *Pygodus serra* Zone and subzonal key conodonts of Bergström (1971) and those recorded in Cuyania, Argentina.**

CONODONTS

Numerous specimens of the conodont apparatuses of *Pygodus serra*, *Eoplacognathus robustus* and *E. lindstroemi* were recovered from the PonónTrehué Formation. The *E. robustus* was found in fossiliferous sandstone beds at the base of the conglomerates of La Cantera Formation (Heredia et al. 2014). Few and well preserved elements of *E. robustus* together with early forms of *E. lindstroemi* were recovered from Los Azules Formation in Los Amarillitos section from carbonate nodules.

CONCLUSIONS

The conodont species *E. robustus* and *E. lindstroemi* recovered from sections mentioned above are recording the *E. robustus* and *E. lindstroemi* subzones of the *Pygodus serra* Zone (Fig. 2). The upper part of the *Pygodus serra* Zone in Cuyania is recorded in La Cantera and Ponón Trehué formations by coarse clastic deposition followed by finer siliciclastic deposits. The first conclusion is that this coarse sedimentary change in the history of Cuyania occurs in the *E. robustus* subzone, followed by fine rich carbonate sedimentation during the *E. lindstroemi* subzone recording a rise of the sea level. Therefore, comparing the facies of these three studied sections allowed us to interpret them as controlled mainly by eustasy.

REFERENCES

BERGSTRÖM, S., 1983. Biogeography, evolutionary relationships and biostratigraphic significance of Ordovician platform conodonts. *Fossils and Strata,* 15: 35-58.

CINGOLANI, C. and VARELA, R., 1999. The San Rafael Block, Mendoza (Argentina): Rb – Sr Isotopic age of basement rocks. *II South American Symposiumon Isotope Geology, Actas*: 23- 26.

HEREDIA, S., 2006. Revisión estratigráfica de la Formación Ponón Trehué (Ordovícico), Bloque de San Rafael, Mendoza. *Serie Correlación Geológica*, 21: 59- 74.

HEREDIA, S., KAUFMANN, C., MESTRE, A., SORIA T., and ORTEGA, G., 2014. La edad de la base de la Formación La Cantera (Ordovícico) en la Precordillera Oriental, Sierra de Villicum, San Juan. *XIX Congreso Geológico Argentino*, Córdoba. S2-13.

KELLER, M., LEHNERT, O. AND BORDONARO, O. 1996. The Ordovician of San Rafael: Its significance for the history of the Precordillera. *The Geological Society of America South–Central Section, Abstract with Programs*. University of Texas, Austin. 28, (1): 38748.

ORTEGA, G., ALBANESI, G. L. and FRIGERIO, S. E., 2007. Early Darriwilian graptolite and conodont biofacies in the Los Azules Formation, Cerro Viejo section, Central Precordillera, Argentina. In: Munnecke, A. and Servais, T. Eds. Early Palaeozoic Palaeogeography and Palaeoclimate, *Palaeogeography, Palaeoclimatology Palaeoecology*, 245 (1-2): 245-263.

PERALTA, S. H., 1993. Estratigrafía y consideraciones paleoambientales de los depósitos marino clásticos eopaleozoicos de la Precordillera Oriental de San Juan. *12° Congreso Geológico Argentino y 2° Congreso de Exploración de Hidrocarburos, Actas* 1: 128-137.

SATO, A. M., TICKY, J. H., LLAMBIAS, E. J. and SATO, K. 2000. The Las Matras Tonalitic-Trondhjemitic pluton, central Argentina: Greenvillian age constraints, geochemical characteristics and regional implications. *Journal of South American Earth Sciences*, 13: 587-610.

Biostratigraphy of the Cambrian–Ordovician boundary beds at Kopet-Dagh, Iran

Hadi Jahangir[1], Mansoureh Ghobadi Pour[2, 4], Lars E. Holmer[3], Leonid E. Popov[4], Ali-Reza Ashuri[1], Adrian Rushton[5], Tatiana Yu. Tolmacheva[6] and Arash Amini[2]

[1] *Department of Geology, Faculty of Sciences, Ferdowsi University, Mashhad 917751436, Iran, jahangir. hadi@gmail.com*

[2] *Department of Geology, Faculty of Sciences, Golestan University, Gorgan, Iran, mghobadipour@yahoo.co.uk*

[3] *Institute of Earth Sciences, Palaeobiology, Uppsala University, SE-752 36 Uppsala, Sweden Lars. Holmer@pal.uu.se*

[4] *Department of Geology, National Museum of Wales, Cardiff CF10 3NP, Wales, UK: leonid.popov@museumwales.ac.uk*

[5] *The Natural History Museum, Cromwell Road, London SW7 5BD, UK: a.rushton@nhm.ac.uk*

[6] *A. P. Karpinskii, Russian Geological Research Institute, Srednii pr. 74, 199106 St. Petersburg, Russia: Tatiana_Tolma heva@vsegei.ru*

ABSTRACT: A continuous succession comprising upper Cambrian (Furongian) to Lower Ordovician (Tremadocian) conodont biozones is reported for the first time from the Kopet-Dagh Region of northeastern Iran. Seven biostratigraphical units are recognized, including the *Proconodontus tenuiserratus* and *Proconodontus posterocostatus* zones; these two lowermost biostratigraphical units are defined by euconodont species which have not been previously reported from Iran and temperate latitude peri-Gondwana. The conodont diversity and abundance decreased significantly above the *Eoconodontus notchpeakensis* Zone; the conodont faunas of the succeeding *Cordylodus proavus*, *Cordylodus lindstromi* (*sensu lato*) and *Cordylodus angulatus* zones are characterised by oligotaxic to monotaxic associations dominated by species of *Cordylodus*. In the absence of diagnostic conodont species, the position of the lower boundary of the Ordovician System in the Kalat Valley Section can be placed somewhat below the first occurrence of the early planktonic graptolite *Rhabdinopora flabelliformis*, which approximately coincides with the onset of black shale deposition.

INTRODUCTION

The main objective of this paper is to review the available information on the conodont biostratigraphy of the Cambrian–Ordovician boundary beds in the Kuh-e Saluk Mountains, south of the city of Bojnurd, in the North Khorosan Province, northeastern Iran (Fig. 1a, b). This area was mapped (1: 250000) by Bolourchi and Mehr Parto (1987); however, the coverage of the Lower Palaeozoic rocks in this map is not adequately shown. Ahmadzadeh-Heravi (1983) proved the existence of the continuous succession from the Upper Cambrian to the Silurian exposed along the road connecting Bojnurd and Esfaraen, south of the Pelmis Pass and also presented the first and only published report on the occurrence of the Cambrian and Early Ordovician conodonts in the area.

The studied section, which is here referred as the Kalat Valley is situated on the western side of the Kalat stream, about 39 km south of Bojnurd. Geographical coordinates of the zero point at the base of the first limestone bed are 37°13′36″N; 57°23′2″E, altitude 1620 m. The underlying beds are covered by allochthonous, strongly weathered argillite and therefore cannot be observed. No formal lithostratigraphical subdivision can be applied to the Cambrian (Furongian) and Lower Ordovician deposits of Kopet-Dagh at present. Ghavidel-Syooki (2001) assigned this part of the succession to the
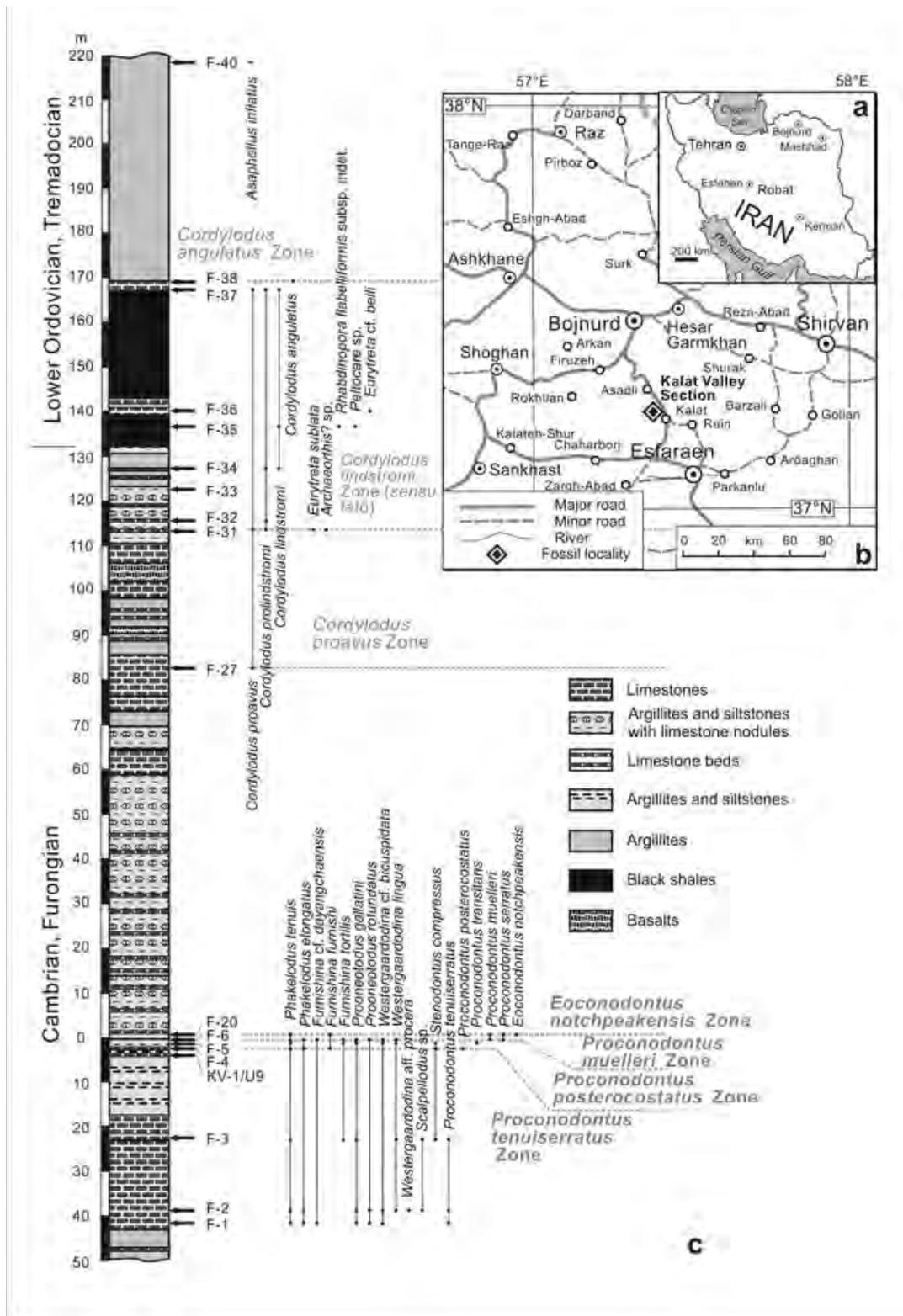
Figure 1. —a, simplified map of Iran showing location of Bojnurd situated north of the Kalat Valley Section; b, geographical map of the vicinity of Bojnurd showing geographical position of the Kalat Valley Section west of the road connecting Bojnurd and Esfaraen; c, stratigraphic column of the terminal Cambrian and Lower Ordovician (Tremadocian) deposits exposed in the Kalat Valley Section, showing position of sampled fossiliferous horizons and stratigraphic distribution of conodonts and selected species of brachiopods, trilobites and graptolites.

Lashkarak Formation; however, this formation was defined in Central Alborz within a completely different tectonostratigraphical unit. Moreover, as demonstrated by Ghobadi Pour et al. (2011), the Lashkarak Formation, as originally defined by Gansser & Huber (1962), is confined to Middle and Upper Ordovician deposits.

The Cambrian–Ordovician boundary beds in the Kalat Valley section comprise a monotonous succession of mostly siliciclastic sediments, which were deposited in the outer shelf environment, with some limestone units representing mostly shell beds formed by bioclasts transported across the shelf during occasional strong storm events. Carbonate nodules in argillites are relatively common in the Cambrian part of the observed succession, but completely disappear in the Tremadocian. Only the lowermost part of the studied section, corresponding to the *Proconodontus tenuiserratus* Zone, contains a significant amount of carbonates. The autochthonous benthic faunas are dominated by low diversity trilobite associations, while disarticulated shells of the rhynchonelliform brachiopods usually are displaced offshore. The lingulate brachiopods are relatively common and moderately diverse within the interval from the *Proconodontus tenuiserratus* to *Eoconodontus notchpeakensis* Zone, but decrease markedly in abundance and diversity up sequence.

CONODONT BIOSTRATIGRAPHY

The conodont yield in the studied samples is very low. Among 17 productive samples the content of conodont elements usually does not exceed 20 specimens per standard 1. 5 kg sample, and fewer than half of the sampled limestone horizons were productive for conodonts. Nevertheless, it is still possible to build conodont based biostratigraphical framework for the late Furongian to Tremadocian of the Kopet-Dagh Region, which is comparable to the conodont zonal schemes of the Cold Domain *sensu* Zhen and Percival (2003), and in particular, to the Baltoscandian province (Kaljo et al. 1986; Szaniawski and Bengtson 1998; Bagnoli and Stouge 2014). Seven successive conodont zonal assemblages can be recognised in the terminal Cambrian to Early Ordovician (lower Tremadocian) sedimentary succession of the Kalat Valley section. These include the *Proconodontus tenuiserratus* and *Proconodontus posterocostatus* zones, two lowermost biostratigraphical units defined by euconodont species, which have not been previously reported from Iran.

Proconodontus tenuiserratus Zone
The zone spans a 30. 6 m thick interval in the lowermost part of the measured section. In addition to the eponymous species, *Stenodontus compressus* Chen and Gong, 1986 is the only other euconodont in the assemblage, which is otherwise dominated by proto- and paraconodonts, including *Phakelodus tenuis* Müller, 1959, *Phakelodus elongatus* Müller, 1959, *Furnishina dayangchaensis* Chen & Gong, 1986, *Furnishina tortilis* Müller, 1959, *Furnishina furnishi* Müller, 1959, *Prooneotodus gallatini* Müller, 1959, *Prooneotodus rotundatus* (Druce and Jones, 1971), *Scalpellodus* sp., *Westergaardodina* cf. *bicuspidata* Müller, 1959, *Westergaardodina ligula* Müller, 1959, *Westergaardodina procera* Müller and Hinz, 1991.

Proconodontus posterocostatus Zone
Conodonts of this zone recovered from a condensed interval, which is only 2. 75 m thick. In addition, eponymous species of the associated assemblage includes *Proconodontus transitans* Szaniawski and Bengtson, 1998, which appears in the upper part of the unit (Fig. 1c), and proto- and paraconodonts *Phakelodus tenuis*, *Phakelodus elongatus*, *Furnishina tortilis*, *Furnishina*

furnishi, *Prooneotodus gallatini*, *Westergaardodina* cf. *bicuspidata* and *Westergaardodina ligula*, all of which are transitional from the *Proconodontus tenuiserratus* Zone.

***Proconodontus muelleri* Zone**
This zone is only 0. 15 m thick in the studied transect. It is defined by the first appearance of eponymous taxon and *Proconodontus serratus* Miller, 1969, while taxonomic composition of the proto- and paraconodont taxa ranges unchanged from the underlying unit. A condensed interval, corresponding to the *Proconodontus posterocostatus* and *Proconodontus muelleri* zones, is closely followed by the termination of more or less continuous carbonate sedimentation, while influx of fine siliciclastic sediments significantly increased since the beginning of *Eoconodontus notchpeakensis* Zone. These together with basalt volcanism, which is evident from the overlying deposits, may suggest a development of extensional tectonic regime in the area and related subsidence of the basin about that time.

***Eoconodontus notchpeakensis* Zone**
This zone is defined by the first appearance of the eponymous species, which co-occurs with transitional eoconodont taxa, including *Proconodontus muelleri* Miller, 1969 and *Proconodontus serratus.* The diversity and abundance of proto- and paraconodonts, which are represented by only two species (Fig. 1c) decreased considerably.

Conodont diversity and abundance decreased significantly up sequence. In the middle and upper parts of the Kalat Valley section, the conodont elements occur in a few horizons separated by thick barren intervals, yet successive appearance of *Cordylodus proavus* Müller, 1959, *Cordylodus lindstromi* Druce and Jones, 1971 and *Cordylodus angulatus* Pander, 1856, have been documented. All these species are the index-taxa of globally recognised conodont zones. Species of *Cordylodus* are the only common conodonts within that stratigraphical interval. They tend to form oligotaxic to monotaxic associations. A similar decline in diversity of the conodont fauna at the time of proliferation of *Cordylodus* species is also evident in the terminal Cambrian–early Ordovician (Tremadocian) conodont successions of other parts of Iran, and in particular from the Alborz Region (Müller 1973; Jahangir 2014) and the Tabas Region of Central Iran (Ghaderi et al. 2009).

THE CAMBRIAN–ORDOVICIAN BOUNDARY IN THE KALAT VALLEY SECTION

Only two conodont species, *Cordylodus lindstromi* and *Cordylodus prolindstromi* Nicoll, 1991, occur within transitional Cambrian–Ordovician boundary interval in the Kalat Valley section; however, their application for precise definition of the system boundary in the studied section is rather limited. Nevertheless, black shales just below the first documented occurrence of *Cordylodus lindstromi* (Fig. 1c; sample F-36) contain the biostratigraphically informative early planktonic graptolites. These graptolites occur in association with a few obolid brachiopods and the olenid trilobite *Peltocare* sp. probably representing a new species. Although the graptolite material from Kalat is not identified with certainty[, the regularity of the mesh is more suggestive of a subspecies close to *Rhabdinopora flabelliformis flabelliformis* (Eichwald, 1840) rather than *R. f. parabola* (Bulman 1954) or *R. f. canadensis* (Lapworth 1898), in which the mesh is less regular. If this is accepted, the age of these graptolites is likely to be close to that of "Assemblage 2" of Cooper *et al.* (1998 fig. 3) that is early but not earliest Tremadocian. Thus the lower boundary of the Ordovician System in the Kalat section may be close or somewhat below the first unit of the black graptolitic argillites, which contain the early planktonic graptolite *Rhabdinopora flabelliformis* subsp. indet. It is probably the best approximation in definition of the system boundary

presently achievable in Iran. Occurrence of *Rhabdinopora flabelliformis* subsp. indet. in the Kalat Section allows direct correlation with the GSSP section in Green Point, Newfoundland, where this graptolite appears just above the Cambrian – Ordovician boundary defined by FAD of *Iapetognathus fluctivagus*. A worldwide graptolite and conodont based correlation of the Green Point section was discussed in great details in the publication by Cooper et al. (2001) and there is no reason to repeat it here. In Baltica, Avalonia (Britain), western North America, North China and parts of Gondwana (Erdtmann, 1986, 1988; Buatois et al. 2006) the beginning of the Tremadocian Stage (upper *Cordylodus lindstromi* to *Cordylodus angulatus* zones) coincided with the extensive deposition of black shales and substantial sea-level rise.

In spite of a low diversity, the micromorphic acrotretide brachiopods also are of some value for biostratigraphical subdivision and correlation of the Cambrian–Ordovician boundary beds due to scarcity of other fossils. The members of *Quadrisonia→Eurytreta* lineage are particularly illustrative in that respect. Shells of *Quadrisonia* occur on the Kalat Valley section in the *Proconodontus tenuiserratus* Zone, but they require further study. *Eurytreta sublata* Popov, in Koneva and Popov 1988, is a geographically widespread taxon, which in Malyi Karatau (Karatau-Naryn terrane, Kazakhstan) is confined to the *Cordylodus proavus* Zone (Holmer et al. 2001), and in Laurentia (Utah) it ranges from the *Cordylodus proavus* to *Cordylodus intermedius* Zone (Popov et al. 2002). In Kopet-Dagh (Fig. 1c; sample F-31) this species co-occurs with *Cordylodus prolindstromi* at the base of the *Cordylodus lindstromi* Zone (*sensu lato*). *Eurytreta* cf. *belli* (Davidson, 1868) as revised by Sutton et al. (2000) appears in the Kalat Valley section together with *Cordylodus lindstromi* just above the black shale unit with *Rhabdinopora* (Fig. 1c). This brachiopod taxon is widespread globally within *Cordylodus lindstromi* and *Cordylodus angulatus* zones (Popov and Holmer 1994; Holmer et al. 2001, 2005; Popov et al. 2002).

The continuous character of sedimentation across the Cambrian–Ordovician boundary in the Kopet-Dagh Region is in sharp contrast with the sedimentary succession of the Alborz Region in northern Iran, where this interval corresponds to a widespread hiatus on top of '*Cruziana*' sandstones originally deposited in shoal complexes (Kebria-ee Zadeh et al. 2015), while the conodont record between the *Cordylodus proavus* and *Paltodus deltifer* zones is missing (Müller 1973; Jahangir et al. 2014). The trilobite species *Asaphellus inflatus* Lu, 1962, which usually occurs at the base of the Ordovician succession in Eastern Alborz (Ghobadi Pour 2006), appears in the Kalat Valley Section within the *Cordylodus angulatus* Zone, well above the base of the Ordovician System (Fig. 1c, sample F-40).

DISCUSSION AND CONCLUSIONS

The Kalat Valey section shows the most complete succession of conodont biozones, and includes the earliest euconodont species yet documented in Iran. The earliest euconodont taxa yet known in Alborz Region and in Central Iran are *Proconodontus muelleri* and *Proconodontus serratus* (Müller, 1973; Ghaderi et al. 2009; Jahangir 2014). Both appear in the middle part of the Furongian euconodont biostratigraphical succession of the Tropical Domain, e. g., Laurentia and Australasian segment of Gondwana (Druce and Jones 1971; Miller 1980; Miller et al. 2003). The early Furongian euconodont record is poor and incomplete in the faunas of the Cold Domain confined to the peri-Gondwanan Oaxaquia terrane (Landing 2007), Alborz and Central Iran (Jahangir 2014) and Baltica (Müller and Hinz 1991; Szaniawski and Bengtson 1998; Bagnoli and Stouge 2014). The Furongian conodont succession of Kopet-Dagh where *Proconodontus muelleri* and *Proconodontus serratus* zone are now documented represents a noticeable exception. Yet the Furongian faunas of Kopet-Dagh are characterised by a proliferation of paraconodont taxa, while a few cosmopolitan euconodont species are of low diversity and

abundance; these can be taken to indicate cold water faunas, and taken as the evidence that the region was located deep within temperate latitudes already in the Furongian. The first signs of a possible extensional tectonic regime in the Kopet-Dagh, as indicated by basin subsidence and associated volcanism, were already evident in the late Furongian, but if it was the first sign of rifting, or if the Kopet-Dagh remained an integral part of Gondwana Domain later through the Ordovician is not yet clear.

ACKNOWLEDGEMENTS

REFERENCES

AHMADZADEH-HERAVI, M., 1983. Brachiopods and conodonts from the Lower Palaeozoic sediments at southern Bojnurd city. *Journal of Technology and Science, Tehran University*, 45: 1–24. [In Persian.]

BAGNOLI, G. and STOUGE, S., 2014. Upper Furongian (Cambrian) conodonts from the Degerhamn quarry road section, southern Öland, Sweden. *GFF*, 136: 436–458.

BLOURCHI, M. H. and MEHR PARTO, M., 1987, Geological map of Bojnurd. *Geological survey of Iran, Quadrangle map of Iran 1: 250. 000 Series*, No. J-3.

BUATOIS, L. A., ZEBALLO, F. J., ALBANESI, G. L., ORTEGA, G., VACCARI, E. and MÁNGANO, M. G. 2006. Depositional Environments and Stratigraphy of the Upper Cambrian-Lower Ordovician Santa Rosita Formation at the Alfarcito area, Cordillera Oriental, Argentina: Integration of biostratigraphic data within a sequence stratigraphic framework. *Latin American Journal of Sedimentology and Basin Analysis*, 13: 65–95.

BULMAN, O. M. B., 1954. The graptolite fauna of the Dictyonema shales of the Oslo region. *Norsk Geologisk Tidsskrift*, 33: 1–40.

CHEN, J. and GONG, W., 1986. Conodonts. In Chen, J., Ed., *Contributions to Dayangcha International Conference Camibrian/Ordovician Boundary*, 93–223. Beijing, China Prospect Publishing House.

COOPER, R. A., MALETZ, J., WANG, H. and ERDTMANN, B. –D., 1998, Taxonomy and evolution of earliest Ordovician graptolites: Norsk Geologisk Tiddskrift, 78: 3–32.

COOPER, R. A., NOWLAN, G. S. and WILLIAMS, S. H., 2001. Global Stratotype Section and Point for base of the Ordovician System. *Episodes*, 24: 19–28.

DAVIDSON, T. 1868. On the earliest forms of Brachiopoda hitherto discovered in the British Palaeozoic rocks. *Geological Magazine*, **5**: 303–316. DRUCE, E. C. and JONES, P. J., 1971. Cambro–Ordovician conodonts from the Burke River Structural Belt, Queensland. *Bureau of Mineral Resources, Geology and Geophysics, Bulletin*, 110: 1–159.

EICHWALD, E. 1840. *Ueber das silurische Schichtensysstem in Esthland*. Akademie der St. Petersburg, 240 pp.

ERDTMANN, B. -D. 1986, Early Ordovician eustatic cycles and their bearing on punctuations in early nematophorid (planktic) graptolite evolution. In Walliser, O. H., Ed., *Lecture Notes in Earth Sciences, Volume 8: Global Bioevent*s: 139–152.

ERDTMANN, B. -D. 1988. The earliest Ordovician nematophorid graptolites: taxonomy and correlation. *Geological Magazine*, 125: 327-348.

GANSSER, A. and HUBER, H. 1962. Geological observations in the Central Elburz, Iran. *Schweizerische Mineralogische und Petrographische Mitteilungen*, 42: 593–630.

GHADERI, A., AGHANABATIL, A., HAMDI, B. and MILLER, J. F., 2009. Biostratigraphy of the first and second member of type section of the Shirgesht Formation in north of Tabas with special emphasis on conodonts. *Journal of Earth Scinces Iran*, 67: 150–163. [In Persian.]

GHAVIDEL-SYOOKI, M. 2001. Palynostratigraphy and Paleobiogeography of the Lower Paleozoic sequence in the northeastern Alborz Range (Kopet-Dagh Region) of Iran. In: Goodman, D. K. and Clarke, R. T., Eds., *Proceedings of the IX International Palynological Congress, Houston, Texas, U. S. A, 1996,* 17–35. American Association of Stratigraphic Palynologists Foundation.

GHOBADI POUR, M. 2006. Early Ordovician (Tremadocian) trilobites from Simeh-Kuh, Eastern Alborz, Iran. In Bassett, M. G. and Deisler, V. K. (eds). *Studies in Palaeozoic palaeontology*. *National Museum of Wales Geological Series*, 25, 93–118.

GHOBADI POUR, M., POPOV, L. E., KEBRIA-EE ZADEH, M. R. and BAARS, C., 2011c. Middle Ordovician (Darriwilian) brachiopods associated with the *Neseuretus* biofacies, eastern Alborz Mountains, Iran. *Memoirs of the Association of Australasian Palaeontologists*, 42: 263–283.

HOLMER, L. E., POPOV, L. E., KONEVA S. P. and BASSETT, M. G. 2001. Cambrian – early Ordovician brachiopods from Malyi Karatau, the western Balkhash Region, and northern Tien Shan, Central Asia. *Special Papers in Palaeontology*, 65: 1–180.

HOLMER, L. E., POPOV, L. E., STRENG, M. and MILLER, J. F. 2005. Lower Ordovician (Tremadocian) lingulate brachiopods from the House and Fillmore Formations, Ibex Area, Western Utah, USA. *Journal of Palaeontology*, 79: 884–906.

JAHANGIR, H., GHOBADI POUR, M. and ASHOURI, A. -R., 2014 (1392). Palaeobiogeography of conodonts from the Alborz Mountains through Cambrian–Ordovician transition. *Paleontology (Iran)*, 1(2): 137–148. [In Persian.]

KALJO, D., BOROVKO, N., HEINSALU, H., KHAZANOVICH, K., MENS, K., POPOV, L., SERGEYEVA, S., SOBOLEVSKAYA, R. & VIIRA, V., 1986. The Cambrian-Ordovician boundary in the Baltic–Ladoga clint area. *Eesti NSV Teaduste Akadeemia Toimetised. Geoloogia*, 35: 97–108.

KEBRIA-EE ZADEH, M. -R., GHOBADI POUR, M, POPOV, L. E., BAARS, C., and JAHANGIR, H., 2015. First record of the Ordovician fauna in Mila-Kuh, eastern Alborz, northern Iran. Estonian Journal of Earth Sciences. *Estonian Journal of Earth Sciences*, 64. [In press.]

KONEVA, S. P. and POPOV, L. E., 1988. Acrotretides (inarticulate brachiopods) from the Cambrian–Ordovician boundary beds of the Malyi Karatau Range (south Kazakhstan). *Ezhegodnik Vsesoiuznogo Paleontologicheskogo Obshchestva*, 31: 52–72. [In Russian.]

LANDING, E., WESTROP, S. R. and KEPPIE, J. D., 2007. Terminal Cambrian and lowest Ordovician succession of Mexican West Gondwana: biotas and sequence stratigraphy Of the Tinu Formation. *Geological Magazine*, 144: 909–936.

LAPWORTH, C., 1898. *An Intermediate Textbook of Geology. 13th edition*. Edinburgh and London.

LU, Y., 1962. Early Ordovician trilobites. *In*: Wang Yu, Ed., *A handbook of index fossils of Yangtze District,* 42–47, Beijing: Science Press. [In Chinese.]

MATTHEW, G. F., 1901. New species of Cambrian fossils from Cape Breton. *New Brunswick Natural History Society, Bulletin*, 4: 269–286.

MILLER, J. F., 1969. Conodont fauna of the Notch Peak Limestone (Cambro-Ordovician) House Range, Utah. *Journal of Paleontology*, 43: 413–439.

-----, 1980. Taxonomic revisions of some Upper Cambrian and Lower Ordovician conodonts with comments on their evolution. The University of Kansas, *Paleontological Contribution*, 99: 1–44.

MILLER, J. F., EVANS, J. D., LOCH, R. L., ETHINGTON, J. H., HOLMER, L. E. and POPOV, L. E., 2003. Stratigraphy of the Sauk III interval (Cambrian-Ordovician), western Millard County, Utah, and Central Texas. *BVU Geology Studies*, 47, 23–118.

MÜLLER, K., 1959. Kambrische Conodonten. *Zeitschrift Deutschen Geologische Gesellschaft*, 111: 434–485.

-----, Late Cambrian and Early Ordovician conodonts from northern Iran. *Reports of Geological Survey of Iran*, 30: 1–77.

MÜLLER, K. J. and HINZ, I., 1991. Upper Cambrian conodonts from Sweden. *Fossils and Strata*, 28: 1–153.

NICOLL, R. S., 1991. Differentiation of Late Cambrian–Early Ordovician species of *Cordylodus* with biapical basal cavities. *BMR Journal of Australian Geology and Geophysics*, 12: 223–244.

-----, 1994. Seximembrate apparatus structure of the Late Cambrian coniform conodont *Teridontus nakamurai* from the Chatsworth Limestone, Georgina Basin, Queensland. *AGSO Journal of Australian Geology and Geophysics*, 15: 367–379.

PANDER, C. H., 1856. *Monographie der fossilen Fische des silurischen Systems der russisch–baltischen Gouvernments*. St Petersburg: Akademie der Wissenschaft, 91 pp.

POPOV, L. E., and L. E. HOLMER. 1994. Cambrian-Ordovician lingulate brachiopods from Scandinavia, Kazakhstan, and South Ural Mountains. *Fossils and Strata*, 35: 1–156.

POPOV, L. E., HOLMER, L. E. and MILLER, J. F., 2002. Lingulate brachiopods from the Cambrian-Ordovician boundary beds of Utah. *Journal of Paleontology*, 76: 211–228.

SUTTON, M. D., BASSETT, M. G. and CHERNS, L., 2000. Lingulate brachiopods from the Lower Ordovician of the Anglo-Welsh basin. Part 2. *Monographs of the Palaeontographical Society, London*, 154, 61–114.

SZANIAWSKI, H. and BENGTSON, S. 1998. Late Cambrian euconodonts from Sweden. [In: Szaniawski, H., Ed., Proceedings of the Sixth European Conodont Symposium (ECOS VI)], *Palaeontologia Polonica*, 58: 7–29.

ZHEN, Y. Y., and PERCIVAL, I. G., 2003. Ordovician conodont biogeography–reconsidered. *Lethaia*, 36: 357–369.

A long-overdue systematic revision of Ordovician graptolite faunas from New South Wales, Australia

Ian G. Percival[1], Petr Kraft[2], Zhang Yuandong[3] and Lawrence Sherwin[4]

[1]*Geological Survey of New South Wales, 947-953 Londonderry Road, Londonderry, N. S. W. 2753, Australia*
ian.percival@trade.nsw.gov.au
[2]*Faculty of Science, Institute of Geology and Palaeontology, Charles University, Albertov 6, 128 43 Praha 2, Czech Republic*
kraft@natur.uni.cz
[3]*Nanjing Institute of Geology and Palaeontology, 39 East Beijing Road, Nanjing 210008, China ydzhang@nigpas.ac.cn*
[4]*Geological Survey of New South Wales, Locked Bag 21, Orange, N. S. W. 2800, Australia lawrence. sherwin@trade.nsw.gov.au*

ABSTRACT: A review of the history of systematic taxonomic and biostratigraphic studies of Ordovician graptolites from New South Wales demonstrates that these faunas have been neglected relative to those from Victoria which form the basis for the Pacific Province zonation. Research projects currently underway will alleviate this deficiency, with initial focus on (a) three localities yielding early Floian faunas, and (b) earliest Bolindian (late Katian) faunas from two areas. Many of these graptolites are illustrated for the first time from New South Wales in this interim report.

HISTORIC OVERVIEW

Ordovician graptolites of the Pacific Province have an extensive though discontinuous record in NSW (New South Wales). They are not nearly as well known as contemporaneous faunas from Victoria, which have benefitted from much more sustained scientific interest, due initially to their occurrence in siltstones and black shales associated with gold deposits and subsequently by providing the basis for biostratigraphic zonation of the Ordovician in Australasia (VandenBerg and Cooper 1992). Specimens from NSW were first described by T. S. Hall (1900, 1902) from the Junction Reefs area south of Orange, and from Tallong in the Shoalhaven River gorge west of Goulburn (Hall 1909, 1920). Further systematic study of Late Ordovician graptolites was carried out by Naylor (1936) in the Goulburn region, and by Sherrard (1943, 1949, 1954, 1962) who undertook an extensive documentation of graptolites from many parts of the Lachlan Orogen, concentrating on the Yass and Tallong areas. These publications unfortunately were poorly illustrated compared to today's standards, and the material is generally badly preserved, so that many of the species described are unrecognizable. A third phase of graptolite documentation commenced in the late 1960s and was focussed on the Macquarie Volcanic Province in the central west of the state, with papers by Moors (1969, 1970) on the Late Ordovician graptolite fauna of the Malongulli Formation. The first graptolites of definite Early Ordovician age from NSW were illustrated by Sherwin (1979, 1990) from west of Parkes. The Early Ordovician age postulated by Keble and Macpherson (1941) for graptolites in hornfels near Narrandera has not been confirmed by subsequent collecting which indicates this is a Darriwilian assemblage. Middle Ordovician (Darriwilian) graptolites from elsewhere in NSW had been widely reported (e. g. Sherrard 1954, Smith 1966) but it wasn't until the early 1980s that detailed systematic work (e. g. Jenkins 1982) and acceptable images (Sherwin 1983) were published. Subsequent studies have focussed on Late Ordovician forms, commencing with Jenkins et al. (1982) who described Eastonian (Katian) graptolites from Narooma on the NSW south coast. Identifications and age implications of a supposed Gisbornian (i. e. Sandbian) fauna from west of Orange (Rickards et al. 2001; Sherwin and Rickards 2000) were contested and corrected by VandenBerg (2003) who determined the age as early Bolindian. The most recent publications on NSW graptolites involved documentation of a fauna of mid-Katian age from north of Canberra (Williamson and Rickards 2006), and description of near-contemporaneous dendroids
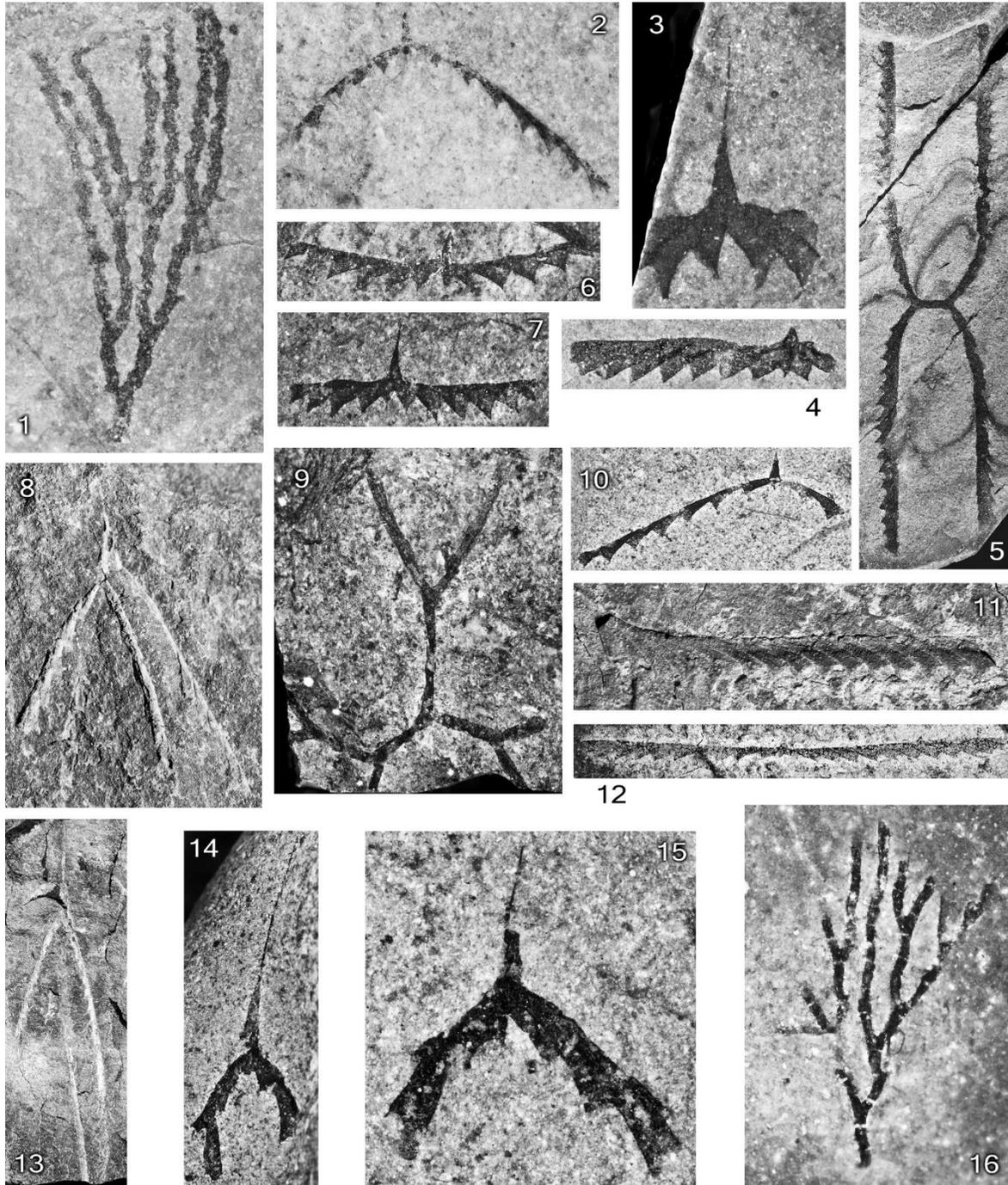
Figure 1. —Early Ordovician (Floian) graptolites from central NSW. 1. *Callograptus* sp., X10. 2, *Paradelograptus pritchardi* (T. S. Hall), X6. 3. *Cymatograptus* cf. *undulatus* (Törnquist), X10. 4. *Didymograptus* (*Expansograptus*) cf. *similis* (J. Hall), X6. 5. *Tetragraptus approximatus* Nicholson, X2. 5. 6. *Didymograptus*? sp., X8. 7. *Didymograptus* (*Expansograptus*) cf. *asperus* (Harris and Thomas), X8. 8. *Pendeograptus pendens* (Elles), X4. 9. *Clonograptus* sp., X8. 10. *Acrograptus*? sp., X6. 11. wide ?tetragraptid stipe, X4. 12. *Expansograptus elongatus* (Harris and Thomas), X4. 13. *Pendeograptus* cf. *pendens* (Elles), X2. 14. *Aorograptus victoriae* (T. S. Hall), X8. 15. *Aorograptus* sp., X15. 16. *Dendrograptus* sp., X15. 1-5 from Yarrimbah Formation; 6-14 from Hensleigh Siltstone; 15-16 from "Trelawney Beds" (now Drik Drik Formation).

from west of Wellington (Percival and Quinn 2012). Current research projects, discussed below, aim to remedy the lack of up-to-date knowledge of Ordovician graptolites from NSW by providing systematic descriptions of several key faunas, including some of the oldest and youngest known Ordovician assemblages in the state.

EARLY ORDOVICIAN FAUNAS

Yarrimbah Formation
The oldest known NSW graptolites, of late Lancefieldian age (*approximatus* Zone), occur in Yarrimbah Formation cherty siltstones in a quarry about 16 km west of Parkes in central NSW (Sherwin 1979). The fauna includes *Callograptus* sp., *Cymatograptus* cf. *undulatus* (Törnquist), *Didymograptus (Expansograptus)* cf. *similis* (J. Hall), *Paradelograptus pritchardi* (T. S. Hall) and *Tetragraptus approximatus* Nicholson (Fig. 1. 1-5). Associated with the graptolites are deep water lingulate brachiopods, described by Percival and Engelbretsen (2007), and fragmentary caryocarids.

Hensleigh Siltstone
A slightly younger (Bendigonian) graptolite fauna is known from the upper Hensleigh Siltstone at Bakers Swamp, 26 km south of Wellington. This fauna comprises *Acrograptus*? sp., *Aorograptus victoriae* (T. S. Hall), *Clonograptus* sp., *Didymograptus (Expansograptus)* cf. *asperus* (Harris and Thomas), *Didymograptus* (*Expansograptus*) *elongatus* (Harris and Thomas), *Didymograptus*? sp. and *Pendeograptus pendens* (Elles) (Fig. 1. 6-14). None of these forms has previously been described or illustrated from this locality. Conodonts from autochthonous and allochthonous limestones lower in the formation indicate the *Prioniodus elegans* Zone (Zhen et al. 2003), consistent with the age of the graptolite fauna.

Drik Drik Formation
Formerly known as the "Trelawney Beds" (Packham 1969), the locality (about 20 km southeast of Tamworth in the New England region of NSW) is now known to include allochthonous blocks of late Ordovician limestone, and an Early Ordovician siltstone clast rarely yielding graptolites such as *Aorograptus* sp. and *Dendrograptus* sp. (Fig. 1. 15, 16), all reworked into an Early Devonian sedimentary unit called the Drik Drik Formation (Furey-Greig 2000). Age of the siltstone clast is imprecise, probably Bendigonian (early to middle Floian).

LATE ORDOVICIAN (LATE KATIAN) FAUNAS

Malachis Hill Formation
Outcrops of Malachis Hill Formation on the densely forested southern flanks of Mount Canobolas, southwest of Orange, contain an early Bolindian graptolite fauna (Fig. 2) that includes *Anticostia macgregorae* Stewart and Mitchell, *Anticostia tenuissima* (Ross and Berry), *Anticostia thorsteinssoni* (Melchin), *Dicellograptus* ex gr. *ornatus* (Elles and Wood), *Styracograptus* cf. *tubuliferus* (Lapworth) and *Styracograptus*? sp., associated with rare specimens of the trilobite *Triarthrus*. This fauna, comparable with that described from the Keenans Bridge locality west of Orange NSW (VandenBerg 2003), is roughly equivalent to the *Dicellograptus ornatus* Biozone in Nevada (Štorch et al. 2011), Zone 13 (*Rectograptus truncatus intermedius* Zone) in the Marathon region of Texas (Goldman et al. 1995), the *Amplexograptus prominens* Biozone of Anticosti, Quebec (Stewart and Mitchell 1997), the *Dicellograptus complanatus* Biozone to lower *Dicellograptus complexus* Biozone in South China (Mu et

al. 1993, Chen et al. 2000), and the *Dicellograptus complanatus* Biozone of Britain (Zalasiewicz et al. 2009).
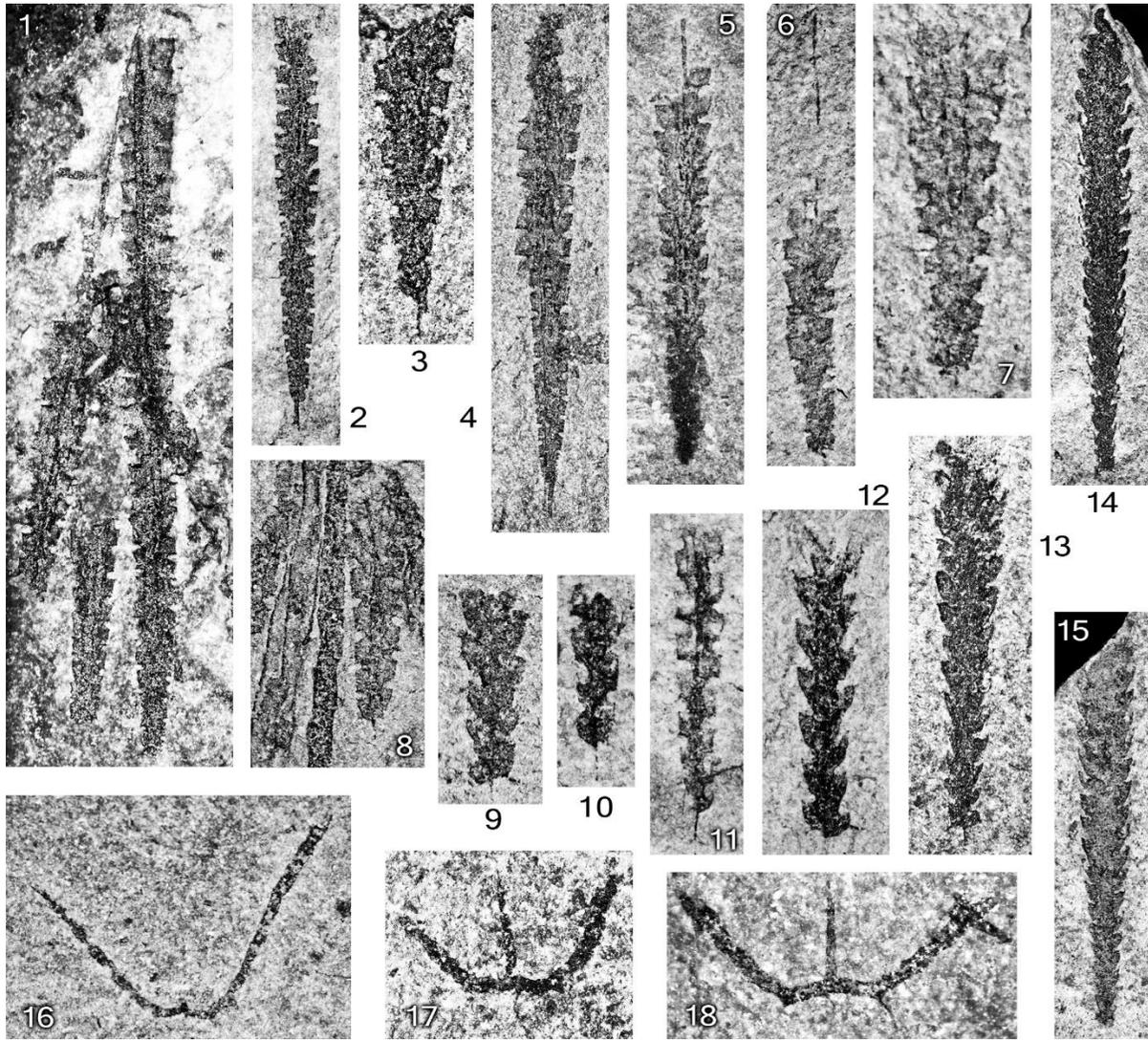
Figure 2. —Late Katian graptolites from Malachis Hill Formation, Charleville Road locality, Canobolas State Forest, south of Orange, NSW. 1-7, *Styracograptus* cf. *tubuliferus* (Lapworth), 1. Several specimens, possibly current-aligned, X4. 2. X4, 3. X8, 4. X4, 5. X4, 6. X6. 7. X8. 8. Partial stipe of *Dicellograptus* (left-hand specimen) and *Normalograptus* (right-hand specimen), X8. 9. *Anticostia tenuissima* (Ross and Berry), X10. 10, 11. *Styracograptus*? sp., 10. X10, 11. X8. 12. *Anticostia macgregorae* Stewart and Mitchell, X10. 13-15, *Anticostia thorsteinssoni* (Melchin), 13. X6, 14. X4, 15. X4. 16-18. *Dicellograptus* ex gr. *ornatus* (Elles and Wood), 16. X6, 17, 18. Juvenile specimens, both X10.

Uppermost Malongulli Formation, Malongulli Trig

Black shale of the uppermost Malongulli Formation on the NE flank of Malongulli Trig (Percival 1976) is similar in age to the Malachis Hill Formation, being assigned to the earliest Bolindian (Bo1) *uncinatus* Zone (late Katian age) based on the presence of *Styracograptus uncinatus* (Keble and Harris), together with *Styracograptus tubuliferus* (Lapworth), *Acanthograptus* sp., *Anticostia thorsteinssoni* (Melchin), *Anticostia uniformis* (Mu and Lin, in Mu et al.), *Dicellograptus flexuosus* Lapworth, *Leptograptus*? sp.,

Normalograptus sp., *Phormograptus* cf. *connectus* (Mu in Wang), *Pleurograptus* cf. *linearis* (Carruthers), *Rectograptus abbreviatus* (Elles and Wood) and *Sinoretiograptus mirabilis* Mu et al. (Fig. 3).
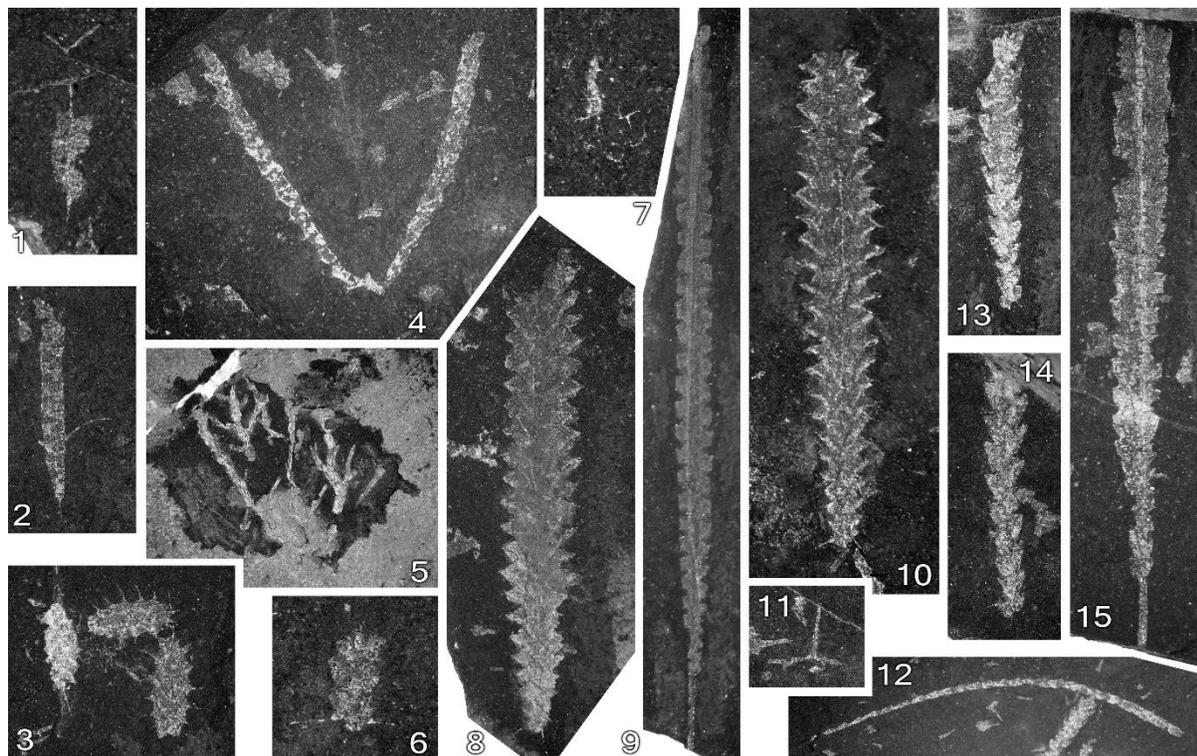
Figure 3. —Late Katian graptolites from uppermost Malongulli Formation, tributary of Sugarloaf Creek, NE flank of Malongulli Trig, NSW. 1, 2, *Styracograptus uncinatus* (Keble and Harris), 1. juvenile colony, X12, 2. X4. 3. *Sinoretiograptus mirabilis* Mu et al., X4. 4. *Dicellograptus flexuosus* Lapworth, X4. 5. *Acanthograptus* sp., X4. 6. *Anticostia thorsteinssoni* (Melchin), X8. 7. *Phormograptus* cf. *connectus* (Mu in Wang), X12. 8, 10. *Rectograptus abbreviatus* (Elles and Wood), both X4. 9, 15. *Styracograptus tubuliferus* (Lapworth), 9. X3, 15. X4. 11, 12. *Pleurograptus* cf. *linearis* (Carruthers), 11. X4, 12. X2. 13, 14, *Anticostia uniformis* (Mu and Lin, in Mu et al.), both X4.

ACKNOWLEDGMENTS

REFERENCES

CHEN, X., RONG, J. Y., MITCHELL, C. E., HARPER, D. A. T., FAN, J. X., ZHAN, R. B., ZHANG, Y. D., LI, R. Y. and WANG, Y., 2000. Latest Ordovician to earliest Silurian graptolite and brachiopod

biozonation from the Yangtze region, South China with a global correlation. *Geological Magazine* 137: 623-650.

FUREY-GREIG, T. M., 2000. Late Ordovician (Eastonian) conodonts from the Early Devonian Drik Drik Formation, Woolomin area, eastern Australia. *Records of the Western Australian Museum Supplement* 58: 133-143.

GOLDMAN, D., BERGSTRÖM, S. M. and MITCHELL, C. E., 1995. Revision of the Zone 13 graptolite biostratigraphy in the Marathon, Texas, standard succession and its bearing on Upper Ordovician graptolite biogeography. *Lethaia* 28: 115-128.

HALL, T. S., 1900. On a collection of graptolites from Mandurama. *Records of the Geological Survey of New South Wales* 7: 16-17.

-----, 1902. The graptolites of New South Wales, in the collection of the Geological Survey. *Records of the Geological Survey of New South Wales* 7: 49-59.

-----, 1909. Notes on a collection of graptolites from Tallong, New South Wales. *Records of the Geological Survey of New South Wales* 8: 339-341.

-----, 1920. On a further collection of graptolites from Tolwong, New South Wales. *Records of the Geological Survey of New South Wales* 9: 63-66.

JENKINS, C. J.. 1982. Darriwilian (Middle Ordovician) graptolites from the Monaro Trough sequence east of Braidwood, New South Wales. *Proceedings of the Linnean Society of New South Wales* 106: 173-179.

JENKINS, C. J., KIDD, P. K. and MILLS, K. J., 1982. Upper Ordovician graptolites from the Wagonga Beds near Batemans Bay, New South Wales. *Journal of the Geological Society of Australia* 29: 367-373.

KEBLE, R. A. and MACPHERSON, J. H., 1941. Lower Ordovician graptolites in New South Wales. *Records of the Australian Museum* 21: 57-58.

MOORS, H. T., 1969. On the first occurrence of a *Climacograptus bicornis* with a modified basal assemblage, in Australia. *Proceedings of the Linnean Society of New South Wales* 93: 227-231.

-----. 1970. Ordovician graptolites from the Cliefden Caves area, Mandurama, N. S. W., with a re-appraisal of their stratigraphic significance. *Proceedings of the Royal Society of Victoria* 83: 253-288.

MU, E. Z., LI, J. J., GE, M. Y. CHEN, X., LIN, Y. K. and NI, Y. N. 1993. Upper Ordovician Graptolites of Central China region. *Palaeontologia Sinica* B29: 1-393.

NAYLOR, G. F. K. 1936. The Palaeozoic sediments near Bungonia: their field relations and graptolite fauna. *Journal and Proceedings of the Royal Society of New South Wales* 69: 123-134.

PACKHAM, G. H., 1969. Tamworth area, pp. 230-231. In Packham, G. H., ed., The Geology of New South Wales. *Journal of the Geological Society of Australia* 16(1).

PERCIVAL, I. G., 1976. The geology of the Licking Hole Creek area, near Walli, central western New South Wales. *Journal and Proceedings of the Royal Society of New South Wales* 109: 7-23.

PERCIVAL, I. G. and ENGELBRETSEN, M. J., 2007. Early Ordovician lingulate brachiopods from New South Wales. *Proceedings of the Linnean Society of New South Wales* 128: 223-241.

PERCIVAL, I. G. and QUINN, C. D., 2012. Reassessment of Ordovician stratigraphy west of the Catombal Range, Wellington region, central New South Wales. *Proceedings of the Linnean Society of New South Wales* 132: 221-235.

RICKARDS, B., SHERWIN, L. and WILLIAMSON, P., 2001. Gisbornian (Caradoc) graptolites from New South Wales, Australia: systematics, biostratigraphy and evolution. *Geological Journal* 36: 59-86.

SHERRARD, K., 1943. Upper Ordovician graptolite horizons in the Yass–Jerrawa district, N. S. W. *Journal and Proceedings of the Royal Society of New South Wales* 76: 252-257.

-----, 1949. Graptolites from Tallong and the Shoalhaven Gorge, New South Wales. *Proceedings of the Linnean Society of New South Wales* 74: 62-82.

-----, 1954. The assemblages of Ordovician graptolites in New South Wales. *Journal and Proceedings of the Royal Society of New South Wales* 87: 73-101.

-----, 1962. Further notes on assemblages of graptolites in New South Wales. *Journal and Proceedings of the Royal Society of New South Wales* 95: 167-178.

SHERWIN, L., 1979. Age of the Nelungaloo Volcanics, near Parkes. *Quarterly Notes of the Geological Survey of New South Wales* 35: 15-18.

-----, 1983. New occurrences of Ordovician graptolites from central New South Wales. *Quarterly Notes of the Geological Survey of New South Wales* 53: 1-4.

-----, 1990. Early Ordovician graptolite from the Peak Hill District. *Quarterly Notes of the Geological Survey of New South Wales* 90: 1-4.

SHERWIN, L and RICKARDS, B., 2000. *Rogercooperia*, a new genus of Ordovician glossograptid graptolite from southern Scotland and New South Wales, Australia. *Scottish Journal of Geology* 36: 159-164.

SMITH, R. E., 1966. The geology of Mandurama-Panuara. *Journal and Proceedings of the Royal Society of New South Wales* 98: 239-262.

STEWART, S. and MITCHELL, C. E., 1997. *Anticostia*, a distinctive new Late Ordovician "glyptograptid" (Diplograptacea, Graptoloidea) based on three-dimensionally preserved specimens from Anticosti Island, Quebec. *Canadian Journal of Earth Sciences* 34: 215-228.

ŠTORCH, P., MITCHELL, C. E., FINNEY, S. C. and MELCHIN, M. J., 2011. Uppermost Ordovician (upper Katian-Hirnantian) graptolites of north-central Nevada, U. S. A. *Bulletin of Geosciences* 86: 301-386.

VANDENBERG, A. H. M., 2003. Discussion of 'Gisbornian (Caradoc) graptolites from New South Wales, Australia: systematics, biostratigraphy and evolution' by B. Rickards, L. Sherwin and P. Williamson. *Geological Journal* 38: 175-179.

VANDENBERG, A. H. M. and COOPER, R. A., 1992. The Ordovician graptolite sequence of Australasia. *Alcheringa* 16: 33-85.

WILLIAMSON, P. L. and RICKARDS, R. B., 2006. Eastonian (Upper Ordovician) graptolites from Michelago, near Canberra. *Proceedings of the Linnean Society of New South Wales* 127: 133-156.

ZALASIEWICZ, J. A., TAYLOR, L. S., RUSHTON, A. W. A., LOYDELL, D. K., RICKARDS, R. B. and WILLIAMS, M., 2009. Graptolites in British Stratigraphy. *Geological Magazine* 146: 785-850.

ZHEN, Y. Y., PERCIVAL, I. G. and WEBBY, B. D., 2003. Early Ordovician (Bendigonian) conodonts from central New South Wales, Australia. *Courier Forschungsinstitut Senckenberg* 245: 39-73.

Early Ordovician (Tremadocian) faunas and biostratigraphy of the Gerd-Kuh section, eastern Alborz, Iran

Mansoureh Ghobadi Pour[1,2], Leonid E. Popov[2], Lars E. Holmer[3], Mahmud Hosseini-Nezhad[4], Rahimeh Rasuli[4], Khadijeh Fallah[4], Arash Amini[1] and Hadi Jahangir[5]

[1]*Department of Geology, Faculty of Sciences, Golestan University, Gorgan, Iran, e-mail: mghobadipour@yahoo.co.uk*
[2]*Department of Geology, National Museum of Wales, Cardiff CF10 3NP, Wales, United Kingdom, e-mail: leonid.popov@museumwales.ac.uk*
[3]*Lars E. Holmer, Institute of Earth Sciences, Palaeobiology, Uppsala University, SE-752 36 Uppsala, Sweden, e-mail: Lars.Holmer@pal.uu.se*
[4]*Department of Geology, Damghan University of Sciences, Damghan, Iran, e-mail: hoseininezhad@yahoo.com*
[5]*Hadi Jahangir, Department of Geology, Faculty of Sciences, Ferdowsi University, Azadi Square, Mashhad 91775-1436, Iran, e-mail: jahangir.hadi@gmail.com*

ABSTRACT: The Tremadocian of the East Alborz Region is dominated by condensed fine clastic sediments. These beds have yielded low to medium diversity trilobite associations, which belong to the olenid, nileid and raphiophorid biofacies, characteristic of an outer shelf environment. Five successive trilobite biozones can be recognised in the Tremadocian succession of Alborz. The lower Tremadocian *Asaphellus inflatus–Dactylocephalus* and *Psilocephalina lubrica* zones are characterised by medium diversity trilobite associations with strong links to contemporaneous faunas of South China. Three upper zones are documented in the section at Gerd-Kuh, the successive *Vachikaspis insueta* and *Kayseraspis* zones represent a low diversity interval during a time of rapid changes in the sea level changes; the medium diversity fauna of the *Asaphellus fecundus–Taihungshania miqueli* zone shows strong links to the faunas of Mediterranean segment of Gondwana. Brachiopods in Gerd-Kuh are represented by the monotaxic *Tarfaya* Association and the low diversity *Paralenorthis–Xinanorthis* Association. The recurrent oligotaxic *Protambonites* Association invaded the area in the late Tremadocian during short term regressive episodes.

INTRODUCTION

The Gerd-Kuh area in the southern foothills of eastern Alborz, northern Iran (geographical coordinates N 36° 09′ 46″, E 54° 9′ 56″) is an isolated rocky mound, raised more than 200 m above its base The Cambrian and Ordovician deposits had not previously been reported from the area and on existing geological maps the exposed sedimentary rocks were referred to the Devonian. Nevertheless the exposures at Gerd-Kuh represent one of the most complete and easily accessible fossiliferous Lower Ordovician sections in the Alborz Mountains. The Tremadocian trilobites and brachiopods from Gerd-Kuh have not been previously a subject of detailed studies, although most of the taxa were documented by Ghobadi Pour (2006) from the Simeh-Kuh section, north-west of Damghan.

The Cambrian–Ordovician boundary in the Gerde-Kuh section is placed provisionally at the base of the monotonous unit of olive-green to dark grey mudstones. In the absence of diagnostic fossils it is made by comparison with the Simeh-Kuh and Deh-Molla sections situated eastwards, where the characteristic *Asaphellus inflatus–Dactylocephalus* trilobite association was reported at the lower part of the mudstone unit (Ghobadi Pour 2006, 2011a, 2011b).

Based on superficial similarities, in previous studies the Lower Ordovician deposits were usually assigned to the Lashkarak Formation; however, Ghobadi Pour *et al*. (2011c) recently demonstrated that

the Lashkarak Formation, as it was originally defined by Gansser and Huber (1962), is confined only to the Middle (Darriwilian) and Upper Ordovician and it is separated by the widespread disconformity from the underlying Ordovician sediments. The Ordovician age was inferred by some researchers for the Mila Formation Member 5 (Peng *et al*. 1999; Bruton *et al*. 2004); however, it remains informal unit, which has no defined boundaries. Therefore, pending a general revision of the early Palaeozoic lithostratigraphy of the Alborz Region, we presently do not refer the Lower Ordovician sediments exposed in Gerd-Kuh to any existing formal lithostratigraphical unit.

The Ordovician part of the studied succession is underlain by characteristic '*Cruziana* sandstones', which is the unit of horizontal and cross-laminated fine to medium grained quartzose and arkosic sandstones, up to 32 m thick, with a few beds of silty argillites in the lower part and billingsellid shell beds in the middle and upper part. The upper 10 m of the unit contain *Skolithos* and *Cruziana* trace fossils. The overlying Tremadocian succession comprises 93.3 m of dark-grey argillites and siltstones.

The faunal succession within the unit is represented by three distinct trilobite associations that define, in ascending order, the *Vachikaspis insueta*, *Kayseraspis* sp. and *Asaphellus fecundus—Taihungshania miqueli* zones. Brachiopods are represented by the monotaxic *Tarfaya* Association, which co-occurs with trilobites indicative of the *Vachikaspis insueta* and *Kayseraspis* sp. zones, and by the low diversity *Paralenorthis–Xinanorthis* Association, which occurs with trilobites that are characteristic of the *Asaphellus fecundus–Taihungshania miqueli* Zone. The recurrent *Protambonites* Association re-appears three times through the studied sequence (Fig. 1; 50.1–51.23 m, 63.3–64.8 m and 66.2–68.6 m above the top of *Cruziana* sandstones'). It occurs in sandstone units representing shoal complexes, which were deposited during episodes of the maximum shallowing of the basin. The Tremadocian argillites are overlain with a sharp, uneven boundary by quartzose sandstones with shell beds comprised broken, disarticulated valves of the organophosphatic brachiopod *Thysanotos multispinulosus* Popov *et al*., 2008, suggesting the Floian age (Figs. 1, 2).

BIOSTRATIGRAPHY AND CORRELATION

The biostratigraphical study of the Tremadocian trilobite succession in the eastern Alborz enables us to develop formal biostratigraphic framework with five successive trilobite zones. The trilobite zones proposed below are based on the regional occurrences of well-characterised taxa, with the base of each zone defined by the first documented occurrence of the eponymous species and with the top placed at the base of the overlying zone (Fig. 2). Two lowermost trilobite biostratigraphic subdivisions, namely *Asaphellus inflatus–Dactylocephalus* and *Psilocephalina lubrica–Asaphopsis elhameae* zones, are not represented in the Gerd-Kuh section and they are characterised from the previously studied trilobite successions in Simeh-Kuh and Deh-Molla (Ghobadi Pour 2006, 2011a, 2011b).

The *Asaphellus inflatus–Dactylocephalus* Zone. This is the lowermost Ordovician biostratigraphical unit defined in the eastern Alborz. In the Deh-Molla and Simeh-Kuh sections *Asaphellus inflatus* Lu, 1962 appears in the lower part of the argillite unit, somewhat above the boundary with cross-bedded '*Cruziana* sandstones'. The characteristic trilobite assemblage includes also *Chashania chashanensis* Lu and Shu in Zhou et al., 1977; *Chungkingaspis sinensis* (Sheng, 1958); *Conophrys simehensis* (Ghobadi Pour, 2006); *Dactylocephalus mehriae* Ghobadi Pour, 2006 and *Geragnostus* cf. *yangtzeensis* Lu, 1975. Remarkably, except *Conophrys simehensis* (Ghobadi Pour, 2006) and *Dactylocephalus mehriae* Ghobadi Pour, 2006, which are endemic for Alborz, all other taxa also occur in South China where they are confined to the *Asaphellus inflatus—Dactylocephalus* Zone (Peng 1990a, Zhou and Zhen 2009).
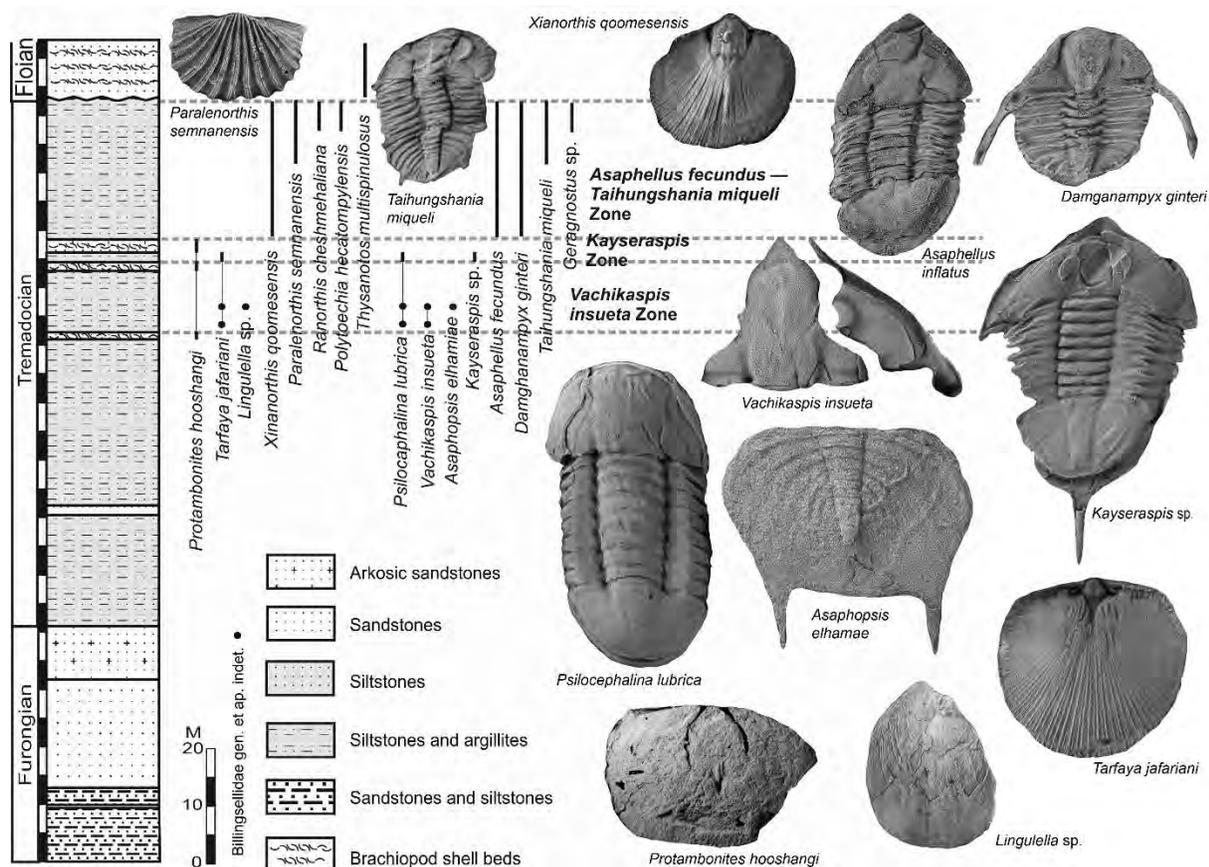
Figure 1. Stratigraphic column showing the Cambrian–Ordovician boundary beds in the Gerd-Kuh section, with sampled fossiliferous horizons, stratigraphic ranges of selected trilobite and brachiopod species and photographic images of characteristic trilobite and brachiopods species.

The *Psilocephalina lubrica* Zone. This zone contains the richest and most diverse trilobite fauna within studied stratigraphical interval. In addition to the eponymous taxa it includes *Geragnostus sidenbladhi jafari* Ghobadi Pour, 2006, *Apatokephalus* sp., *Asaphellus* sp., *Conophrys simehensis*, *Kayseraspis ghavideli* Ghobadi Pour, 2006 and *Presbynileus*? *biroonii* Ghobadi Pour, 2006. Only *Conophrys simehensis* is a holdover from the *Asaphellus inflatus—Dactylocephalus* Zone, whereas all other species are newcomers. *Psilocephalina lubrica* and species of *Asaphopsis* are common in the *Tungzuella* Zone of South China (Peng 1990b), where they are also associated with species of *Apatokephalus* and *Geragnostus*, while species endemic to the Alborz Region constitute a core of the assemblage. In the Deh-Molla section, *Asaphopsis elhamae* is present in abundance in the tempestite shell beds. Here it occurs together with conodonts characteristic of the *Paltodus deltifer* Zone (Ghobadi Pour 2011a, 2011b).

The *Vachikaspis insueta* Zone. This is the lowermost biostratigraphical unit recognised in the Tremadocian of the Gerd-Kuh section (Fig. 1; 54.1–65.8 m above the top of the '*Cruziana* sandstones'). In Gerd-Kuh, the eponymous species form an oligotaxic association with *Asaphopsis elhamae* and *Psilocephalina lubrica*, of which extend down into the *Psilocephalina lubrica–Asaphopsis elhamae* Zone. The zone is marked by a substantial decrease in trilobite diversity, with *Vachikaspis insuetis* forming a monotaxic association in the Simeh-Kuh section. The interval of the *Vachikaspis insueta* Zone coincides

also with proliferation of the brachiopod *Tarfaya jafariani* Popov *et al*., 2009, which occurs in abundance through the whole interval and is also present in the succeeding *Kayseraspis* Zone.
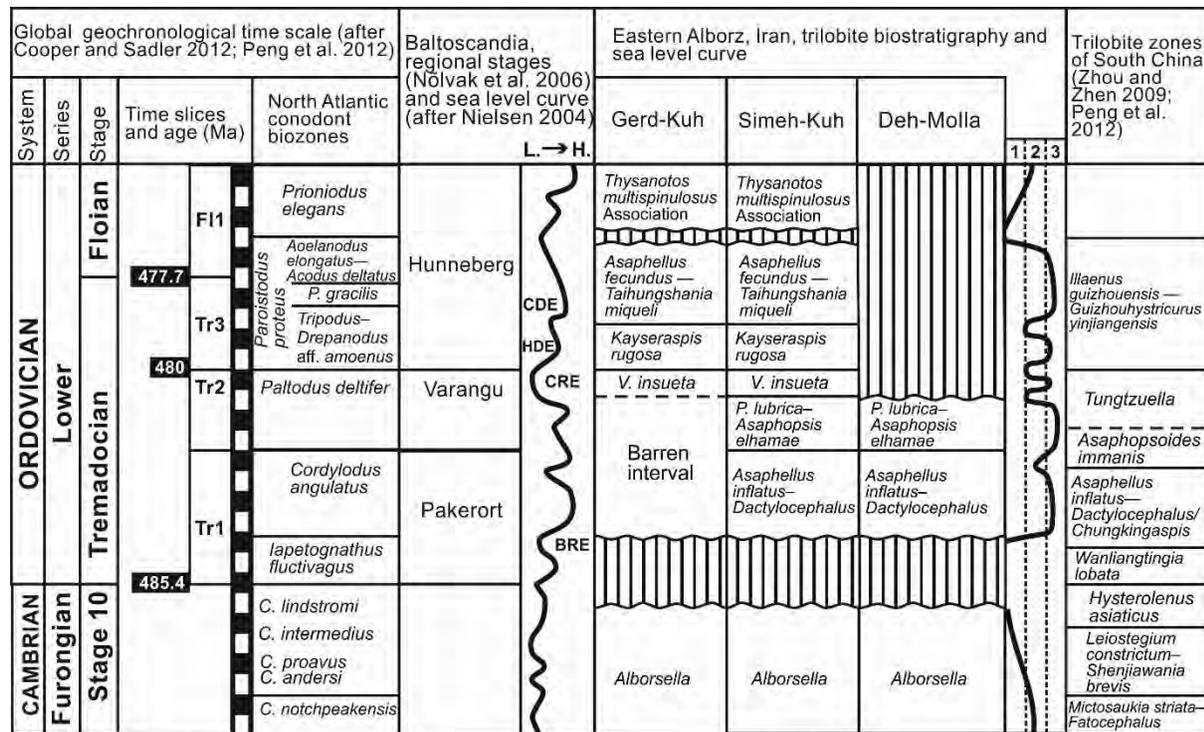
Figure 2. Chrono- and biostratigraphical chart of the uppermost Cambrian to Lower Ordovician (Tremadocian) strata of Eastern Alborz showing correlation with biostratigraphical trilobite succession of South China and North Atlantic conodont biozones. BRE, Black Mountain Regressive Event; CRE, Ceratopyge Regressive Event; HDE, Hagastrand Drowning Event; CDE, Copiosus Drowning Event; 1, peritidal zone; 2, inner shelf; 3, outer shelf.

The *Kayseraspis* Zone (65.8-69.6 above the top of the '*Cruziana* sandstones'). This zone coincides with the entire range of a new species of *Kayseraspis*, which is characterised by transverse ridges on the anterior part of the glabella. The assemblage also includes two holdovers from the underlying zone, *Psilocephalina lubrica* and *Vachikaspis insueta*. In Gerd-Kuh and Simeh-Kuh a substantial sea level drop resulted in formation of a shoal complex. In Simeh-Kuh the shell beds within this interval contain conodonts of the lowermost *Drepanoistodus* aff. *amoenus* Subzone of the *Paroistodus proteus* Zone (Ghobadi Pour *et al*. 2007).

The *Asaphellus fecundus–Taihungshania miqueli* Zone (69.6–93.3 m above the top of the '*Cruziana* sandstones'). In addition to the eponymous taxa, the characteristic zonal assemblage includes *Geragnostus* (*Geragnostella*) *lycaonicus*, *Damghanmpyx ginteri*, *Apatokephalus* sp. and *Euloma* sp. In Gerd Kuh, raphiophorid trilobite *Damghanmpyx ginteri* occurs in abundance and forms accumulations of isolated sclerites on the bedding surfaces. The uppermost Tremadocian age of the lower part of the *Asaphellus fecundus –Taihungshania miqueli* Zone is confirmed by the occurrence of the conodonts of the *Drepanoistodus* aff. *amoenus* Subzone of the *Paroistodus proteus* Zone (Ghobadi Pour *et al*. 2007) in its lower part. However, it is likely that the upper part of the zone is of the Floian age. Outside Iran

Taihungshania miqueli (Bergeron, 1894) was reported from the lower Floian of the Montagne Noire (Bergeron, 1894; Courtessole *et al*., 1981), the Seydişehir Formation of the eastern Taurus Mountains in central Turkey (Dean and Monod 1990) and the Rann Formation Lower Member of United Arab Emirates (Fortey *et al*. 2011). It seems that the first appearance of *Taihungshania miqueli* is slightly diachronous in various regions with the earliest documented occurrence in Iran (Ghobadi Pour *et al*. 2007).

TREMADOCIAN SUCCESSION OF GERD-KUH IN RELATION TO BASIN HISTORY

The latest Cambrian in the East Alborz Region was the time of a lowstand, characterised by deposition of cross-laminated quartzose sands with *Cruziana* and *Skolithos* trace fossils, as well as billingsellide brachiopod shell beds, within a nearshore shoal system. This sandstone unit can be widely recognised in eastern Alborz. The transition to the Ordovician coincided with a significant drowning event. In the absence of conodonts and graptolites, the precise timing of the initial flooding of the region cannot be defined, although correlation with the *Asaphellus inflatus–Dactylocephalus* Zone of the Tremadocian succession in South China suggests that it occurred during the *Cordylodus angulatus* Zone and was probably synchronous with the transgressive phase of the Black Mountain Eustatic Event of Miller (1984). In Gerd-Kuh, the background deposits through the entire Tremadocian interval are represented by dark-grey to olive-grey finely laminated mudstones and siltstones that were deposited with a net sedimentation rate c. 10 mm per millennium. No progradational or retrogradational patterns can be recognised, probably due to the extremely low supply of siliciclastic sediment. It is likely that in Gerd-Kuh, depositional sequences were controlled mainly by eustasy through the Tremadocian.

The magnitude of sea level rise at the beginning of the Tremadocian Age cannot be estimated based on the available data from the Gerd-Kuh section; however, it can be inferred from the occurrence of olenides and agnostides in the *Asaphellus inflatus–Dactylocephalus* Trilobite Association documented from the Deh-Molla and Simeh-Kuh sections. This association can be compared with the Olenid–*Asaphellus* biofacies as defined by Balseiro *et al*. (2011). In the Lower Ordovician of Cordillera Oriental, this biofacies occurs in the upper offshore to offshore-transition environments.

The succeeding trilobite associations of the *Psilocephalina lubrica—Asaphopsis elhamae*, *Vachikaspis*, *Kayseraspis* zones are dominated by nileid taxa and can be considered to be part of the open-shelf nileid biofacies (Ghobadi Pour 2006). A trilobite association of the *Asaphellus fecundus–Taihungshania miqueli* Zone was assigned to the raphiophorid biofacies (Ghobadi Pour *et al*. 2007), which were confined to an outer shelf environment between the distal part of the upper offshore and the proximal part of the lower offshore (Vidal 1998). Outer shelf background sedimentation was interrupted four times by increased influx of coarser clastics. These resulted in deposition of four distinct sandstone units about 1.5-2 m thick. The first unit is situated within the barren interval and does not contain indicative fossils, whereas three upper sandstone beds comprise medium to coarse, calcareous sandstones with a parallel and low angle cross-bedding, and with brachiopod shell beds formed mainly by disarticulated valves of *Protambonites*. Deposition of these sandstones took place in a turbulent environment near-shore, above the fair-weather wave base, probably within shoal systems.

Sedimentary facies and associated biofacies in Gerd-Kuh suggest that outer shelf environments well below the fair-weather wave base prevailed in the area during the Tremadocian Epoch. Three regressive episodes with possible amplitudes of a few tens metres occurred in the late Tremadocian within a

relatively short time interval from the base of the *Vachikaspis insueta* Zone to the base of the *Asaphellus fecundus–Taihungshania miqueli* Zone. The trilobite based correlation suggests that successive regressions occurred within the uppermost part of the *Paltodus deltifer* Conodont Zone and the lower part of the *Drepanoistodus* aff. *amoenus* Subzone of the *Paroistodus proteus* Conodont Zone. It is probable that deposition on the seafloor was inhibited for considerable time during lowstand intervals, which is supported by sharp and sometime erosional contacts with overlying argillites, while there is no evidence of aerial exposure of sediments.

REFERENCES

BALSEIRO, D., WAISFELD, B.G. and BUATOIS, L.A., 2011. Unusual trilobite biofacies from the Lower Ordovician of the Argentine Cordillera Oriental: new insights into olenid palaeoecology. *Lethaia*, 44:58–75.

BERGERON, J., 1894. Notes paléontologiques I. Crustacés. *Bulletin de la Sociétége´ologique de France*, 21 (for 1893):333–346.

BRUTON, D.L., WRIGHT, A.J. and HAMEDI, M.A., 2004. Ordovician trilobites of Iran. *Palaeontographica*, Abteilung A271:111–149.

COOPER. R.A. and SADLER, P. M., 2012. The Ordovician Period. In: Gradstein, F. M., Ogg, J. G., Schmitz, M. and Ogg, G., Eds., *The Geologic Time Scale 2012*. Elsevier, 489–523.

COURTESSOLE, R., PILLET, J., VIZCAÏNO, D. and ESCHARD, R., 1985. Étude biostratigraphique et se´dimentologique des formations arénacées de l'Arénigien du Saint-Chinianais oriental (Hérault), versant sud de la Montagne Noire (France méridionale). *Mémoires de la Société d'Études Scientifiques de l'Aude*, 1985:1–99.

DEAN, W.T. and MONOD, O., 1990. Revised stratigraphy and relationships of Lower Palaeozoic rocks, eastern Taurus Mountains, south central Turkey. *Geological Magazine*, 127:333–347.

GANSSER, A. and HUBER, H., 1962. Geological observations in the Central Elburz, Iran. *Schweizerische Mineralogische und Petrographische Mitteilungen*, 42:593–630.

FORTEY, R.A., HEWARD, A.P and MILLER, C.G., 2011. Sedimentary facies and trilobite and conodont faunas of the Ordovician Rann Formation, Ras Al Khaimah, United Arab Emirates. *GeoArabia*, 16: 127–152.

GHOBADI POUR, M., 2006. Early Ordovician (Tremadocian) trilobites from Simeh-Kuh, Eastern Alborz, Iran. In: M.G. Bassett, & V.K. Deisler, Eds., Studies in Palaeozoic palaeontology, *National Museum of Wales Geological Series*, 25: 93–118.

GHOBADI POUR, M., KEBRIAEE-ZADEH, M.-R. and POPOV, L.E., 2011a. Early Ordovician (Tremadocian) brachiopods from Eastern Alborz Mountains, Iran. *Estonian Journal of Earth Sciences*, 60:65–82.

GHOBADI POUR, M., MOHIBULLAH, M., WILLIAMS, M., POPOV, L.E. and TOLMACHEVA, T.Yu., 2011b. New, early ostracods from the Ordovician (Tremadocian) of Iran: systematic, biogeographical and palaeoecological significance. *Alcheringa*, 35:517–529,

GHOBADI POUR, M., POPOV, L.E., KEBRIA-EE ZADEH, M.R. and BAARS, C. 2011c. Middle Ordovician (Darriwilian) brachiopods associated with the *Neseuretus* biofacies, eastern Alborz Mountains, Iran. *Memoirs of the Association of Australasian Palaeontologists*, 42:263–283.

GHOBADI POUR, M., VIDAL, M. and HOSSEINI-NEZHAD, M., 2007. An Early Ordovician trilobite assemblage from the Lashkarak Formation, Damghan area, northern Iran. *Geobios*, 40:489–500.

LU, Y., 1962. Early Ordovician trilobites. In: Wang Yu, Ed., *A handbook of index fossils of Yangtze District, Science Press*, 42–47, Beijing. [In Chinese.]

LU, Y. 1975. Ordovician trilobite faunas of central and southwestern China. *Palaeontologica Sinica, New Series B*, 11, 1–463. [In Chinese and English.]

MILLER, J.F., 1984. Cambrian and earliest Ordovician conodont biofacies and provincialism. In: Clark, D.L., Ed., Conodont Biofacies and Provincialism. *Geological Society of America Special Paper*, 196:43–68.

NIELSEN, A.T., 2004. Ordovician sea level changes: A Baltoscandian Perspective. In: Webby, B. D., Paris, F., Droser, M. L. and Percival, I. G., Eds., *The Great Ordovician Biodiversification Event*. New York: Columbia University Press, 84–93.

NÕLVAK, J., HINTS, O. and MÄNNIK, P., 2006. Ordovician timescale in Estonia: recent developments. *Proceedings of the Estonian Academy of Sciences, Geology*, 55:95–108.

PENG, S., 1990a. Trilobites from the Nantsinkwan Formation of the Yangtze Platform. Beringeria, 2, 3-53.

PENG, S., 1990b. Trilobites from the Panjiazui Formation and Madaoyu Formation in Jiangnan Slope Belt. *Beringeria*, 2:55–171.

PENG, S., GEYER, G. and HAMDI, B., 1999. Trilobites from the Shahmirzad section, Alborz Mountains, Iran: Their taxonomy, biostratigraphy and bearing for international correlation. *Beringeria*, 25:3–66.

PENG, S., BABCOCK, L.E. and COOPER. R.A., 2012. The Cambrian Period. In: GRADSTEIN, F.M., OGG, J.G., SCHMITZ, M., and OGG, G., Eds. *The Geologic Time Scale 2012*, Elsevier, 438–488 pp.

POPOV, L.E., GHOBADI POUR, M., BASSETT, M.G. and KEBRIAEE-ZADEH, M.R., 2009. Billingsellide and orthide brachiopods: New insights into earliest Ordovician evolution and biogeography from Northern Iran. *Palaeontology*, 52:35–52.

POPOV, L.E., GHOBADI POUR, M. & HOSSEINI, M., 2008. Early to Middle Ordovician lingulate brachiopods from the Lashkarak Formation, Eastern Alborz Mountains, Iran. *Alcheringa*, 32:1–35.

SHENG, X., 1958. Ordovician trilobites of southwestern China. *Acta Palaeontologica Sinica*, 6:169–204 [In Chinese with English summary.]

VIDAL, M., 1998. Le modéle des biofaciés à Trilobites: un test dans l'Ordovicien inférieur de l'Anti-Atlas, Maroc. Comptes Rendus de l'Académie des Sciences. *Earth and Planetary Sciences*. 327:327–333.

ZHOU, Z., LIU, Y., MENG, X. and SUN, Z., 1977. Trilobita, In *Palaeontological Atlas of Central and South China. (1)*. Beijing: Geological Publishing House, 104–266. [In Chinese.]

ZHOU Z. and ZHEN Y., 2009. *Trilobite record of China*. Beijing: Science Press, 402 pp.

Ordovician temperature trends: constraints from $\delta^{18}O$ analysis of conodonts from New South Wales, Australia

Page C. Quinton[1], Ian G. Percival[2], Yong-Yi Zhen[2] and Kenneth G. Macleod[1]

[1] *Department of Geological Sciences, University of Missouri, Columbia, Missouri 65211, USA, pcq6y5@mail.missouri.edu, MacLeodK@mail.missouri.edu*
[2] *Geological Survey of New South Wales, 947-953 Londonderry Road, N. S. W. 2753, Australia, ian.percival@trade.nsw.gov.au, Yong-Yi. zhen@trade.nsw.gov.au*

ABSTRACT: The argument that temperature change and biological change during the Ordovician are correlated and, perhaps, causally related has been advanced by measurements of $\delta^{18}O_{phos}$ values on conodont apatite, a phase more resistant to diagenetic alteration than carbonates. However, the available conodont $\delta^{18}O_{phos}$ records are discontinuous and are biased towards North American samples. To test the generality of global patterns and to expand the geographical range of studied regions, we document $\delta^{18}O_{phos}$ values from conodont apatite as well as $\delta^{13}C$ and $\delta^{18}O_{calcite}$ values from bulk carbonate from New South Wales, Australia. New results span most of the Ordovician and include the first Late Ordovician phosphate $\delta^{18}O$ values from the Australian continent. The data from New South Wales show an ~1. 5‰$_{VSMOW}$ increase in $\delta^{18}O_{phos}$ values during the Early and Middle Ordovician. This pattern matches previously documented trends from Laurentia and central Australia, but values in New South Wales are consistently ~2. 5‰$_{VSMOW}$ lower than those from other regions. We attribute these low $\delta^{18}O_{phos}$ values to local paleoceanographic effects on the seawater $\delta^{18}O$ value.

INTRODUCTION

Critical to recent advances in documentation of the history of Ordovician sea water surface temperatures is the fact that $\delta^{18}O_{phos}$ values in conodont apatite are more resistant to diagenetic overprinting than are carbonate $\delta^{18}O$ values. Currently available $\delta^{18}O_{phos}$ data for the Ordovician are strongly biased towards North American studies, with only limited research conducted in Gondwana (e. g. Trotter et al. 2008). Data from both northern Gondwana and Laurentia, which were located in similar tropical to lower temperate zones but widely separated by the Paleo-Pacific Ocean, are important to recognizing and confirming global climatic trends. This study, for the first time, reports oxygen isotopic results for conodonts from Ordovician limestones in New South Wales. These limestones are part of the Tasmanides and form part of the eastern third of Australia, encompassing Paleozoic rocks accreted to the Precambrian cratons and overlying Early to Middle Paleozoic intracratonic basins of the Australian Plate. The dataset includes analyses of 25 samples ranging in age from Tremadoc limestones of the Delamerian continental margin in the far west of the state through Floian, Darriwilian, Sandbian and Katian limestones of the Macquarie Volcanic Province in the central west of New South Wales (Fig. 1A). The latter are the youngest Ordovician limestones sampled for conodont apatite in Australia and provide temperature constraints for an interval of proposed climatic cooling and glaciation.

SAMPLING AND ANALYTICAL PROCEDURES

The oldest (mid-Tremadocian) sample and two samples from the Floian Stage are limestones from the Koonenberry Belt in far western New South Wales, between the city of Broken Hill and the town of Wilcannia. The Koonenberry Belt consists of latest Precambrian and early Paleozoic sedimentary rocks

onlapping the Proterozoic cratonic margin of Australia in the vicinity of Broken Hill. The other 22 limestone samples are from the Macquarie Volcanic Province in the central part of New South Wales in the vicinity of the cities of Orange, Parkes, Wellington, and Cowra. These limestones represent flanking carbonate deposits around contemporaneous emergent and semi-emergent volcanic islands; most are in situ, but some are allochthonous blocks that were reworked from the shelf edge into deeper water slope sediments.

Oxygen isotope analyses were performed on monospecific samples of ~40 conodont elements (with a CAI ranging from 2- 4) while bulk carbonate carbon and oxygen isotopic ratios were measured from the limestones yielding these conodont elements. The ten conodont species analyzed include; *Belodina confluens, Bergstroemognathus extensus, Erraticodon patu, Juanognathus variabilis, Panderodus gracilis, Periodon macrodentatus, Phragmodus undatus, Protopanderodus? nogamii, Triangulodus emanuelensis,* and *Yaoxianognathus ani*. Conodont samples were prepared for oxygen isotopic analysis by isolating the PO_4^{3-} anion using techniques modified from O'Neil et al. (1994) and LaPorte et al. (2009) as described by Quinton and MacLeod (2014). Samples were analyzed on a continuous flow Thermo-Finnigan Delta Plus XL gas source mass spectrometer connected to a Thermo-Finnigan TC-EA high-temperature conversion-elemental analyzer set to 1400°C during analytical runs. Values for each run were corrected using the international NBS-120c standard. Corrected values correspond to a value of 22. 6‰$_{VSMOW}$ for NBS-120C and external precision is ±0. 3‰$_{VSMOW}$ (1 standard deviation) based on results for this standard. All values are reported on the VSMOW-scale.

Bulk carbonate carbon and oxygen isotopic ratios were measured from 24 micritic rock chips selected from 2-3 kg limestone samples collected in the field. Samples were analyzed on a Kiel III Carbonate device connected to a Thermo-Finnigan Delta Plus isotope ratio mass spectrometer. Bulk carbonate carbon and oxygen results are reported in standard δ–notation as per mil (‰) values on the VPDB-scale and are corrected to a nominal value of 1. 95‰ ($\delta^{13}C$) and -2. 20‰ ($\delta^{18}O_{calcite}$) for the within-run average of replicates of the NBS-19 standard run with the samples. External precision based on 1 standard deviation of the uncorrected values for NBS-19 run throughout the course of the study is ±0. 04‰$_{VPDB}$ for carbon and ±0. 06‰$_{VPDB}$ for oxygen.

RESULTS

Measured oxygen isotopic values from conodonts range from 13. 6‰$_{VSMOW}$ to 16. 5‰$_{VSMOW}$ with an average of 15. 1‰$_{VSMOW}$ and show an increase of ~1. 5‰$_{VSMOW}$ from the Early to Middle Ordovician, whereas $\delta^{18}O_{phos}$ values for the Late Ordovician range from 15. 4‰$_{VSMOW}$ to 17. 5‰$_{VSMOW}$ with an average of 16. 8‰$_{VSMOW}$ (Fig. 1B). No trends are evident in either the carbon or oxygen isotopic results from bulk carbonates (Table 1). Measured $\delta^{13}C$ values range from −6. 6‰$_{VPDB}$ to 1. 6‰$_{VPDB}$ with an average of −0. 4‰$_{VPDB}$. The $\delta^{18}O_{calcite}$ values range from −18. 3‰$_{VPDB}$ to −6. 1‰$_{VPDB}$ with an average of -10. 3‰$_{VPDB}$. As is common in early Paleozoic samples, oxygen isotope measurements from the bulk carbonate are quite low with wide fluctuations and likely reflect diagenetic overprinting. This concern about the fidelity of the $\delta^{18}O_{calcite}$ values is a primary justification for measuring phosphate $\delta^{18}O$ values.

DISCUSSION

Conodont apatite $\delta^{18}O_{phos}$ values from New South Wales record an increase of ~1. 5‰ through the Early to Middle Ordovician (Fig. 1B). Our results expand the Australian conodont $\delta^{18}O_{phos}$ dataset considerably, not only in the much greater number of samples analyzed, but also in their age range. New samples analyzed range in age from the mid-Tremadocian to the late Katian. Additionally, our samples are from a paleogeographic location removed from Laurentia and allow for a global comparison of Ordovician $\delta^{18}O$ trends.

Table 1. —Bulk carbonate $\delta^{13}C$ and $\delta^{18}O_{calcite}$ values from New South Wales, Australia.

Sample ID	Zone	Age (Ma)	$\delta^{13}C$	$\delta^{18}O_{calcite}$
MH23	Ea 4	448. 5	-6. 6	-11. 4
B4. 10	Ea 3 (Upper)	449. 0	1. 5	-8. 0
B4. 7	Ea 3	449. 6	1. 6	-7. 4
B4. 8	Ea 3	449. 6	1. 3	-7. 0
C861	Ea 3	450. 0	-0. 7	-6. 8
CH296. 7	Ea 2 (Upper)	450. 0	0. 0	-11. 6
CH299. 2	Ea 2 (Upper)	450. 0	-1. 8	-10. 7
CH269. 2	Ea 2 (Middle)	451. 0	-0. 1	-18. 3
TH2-1	Ea 2 (Middle)	451. 0	0. 0	-8. 6
CH57. 5	Ea 2	452. 0	-0. 3	-10. 3
DB42. 8	Ea 1 (Middle)	452. 5	1. 1	-7. 7
DB 45. 1	Ea 1 (Middle)	452. 5	-1. 9	-6. 7
DB 54. 1	Ea 1 (Middle)	452. 5	-1. 8	-7. 0
Top DB	Ea 1 (Middle)	452. 5	-4. 3	-6. 1
DB 16. 1	Ea 1 (Middle)	453. 5	1. 2	-7. 8
FH50. 5	Ea 1 (Lower)	454. 5	0. 7	-12. 4
FH115. 7	Ea 1 (Lower)	454. 5	1. 6	-10. 5
C1472	Gi 1	457. 0	0. 8	-11. 3
C1450	Gi 1	460. 0	1. 1	-12. 7
C1456	Gi 1	460. 0	-0. 4	-12. 4
C1458	Da 4	460. 5	-0. 7	-11. 7
C2346	Da 2	469. 0	-1. 5	-14. 1
C1481	Be 1	479. 0	-0. 3	-14. 7
C1481	Be 1	479. 0	-0. 3	-13. 3
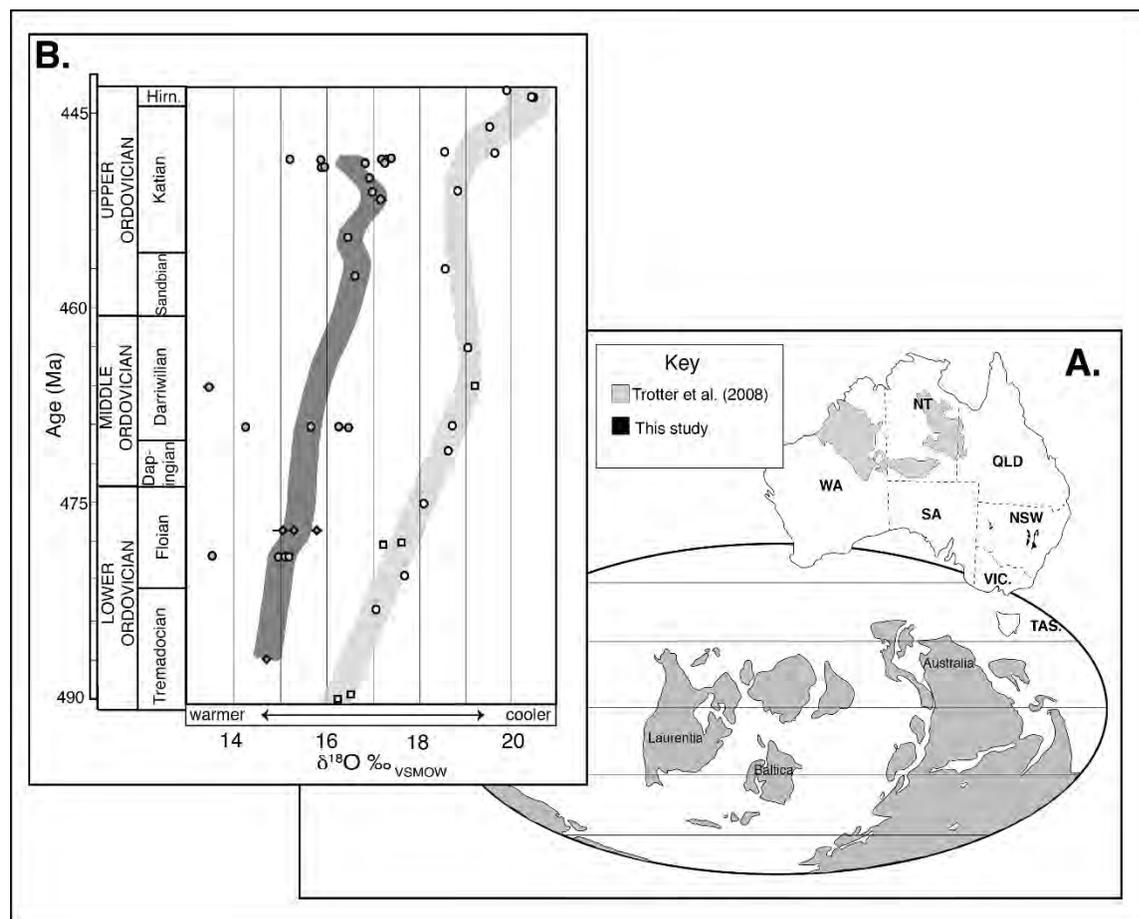
Figure 1. —A. Global paleogeography of the Middle to Late Ordovician with a map of Australia showing sample locations from this study and Trotter et al. (2008). Australian state abbreviations are as follows; NSW= New South Wales, NT= Northern Territory, QLD= Queensland, SA= South Australia, TAS= Tasmania, VIC= Victoria, WA= Western Australia. B. New monospecific conodont apatite oxygen isotope ratios from the Koonenberry Belt (diamonds) and the Macquarie Volcanic Province (circles) and an average $\delta^{18}O_{phos}$ curve for this study (dark gray) are plotted with previous single species and mixed conodont $\delta^{18}O_{phos}$ results (light gray) from Newfoundland (open circles) and central Australia (open squares) from Trotter et al. (2008). Data from Trotter et al. (2008) renormalized to NBS 120c = 22. 6‰VSMOW.

Although our sampling resolution is relatively coarse through the Lower and Middle Ordovician (due to the discontinuity of limestones within a volcanic-dominated succession, and the scarcity of conodonts), the size and direction of the shift towards higher average $\delta^{18}O_{phos}$ values agrees with the trends observed by Trotter et al. (2008). Those authors measured $\delta^{18}O_{phos}$ values using SIMS (secondary ion mass spectrometry) on single species and mixed conodont assemblages from three intracratonic basins in northern and central Australia (Georgina Basin – two samples, Canning Basin – two samples, and Amadeus Basin – one sample) spanning the Early to Middle Ordovician. That study, also incorporating analyses of younger Ordovician samples from Canada, revealed a progressive increase in $\delta^{18}O_{phos}$ values through the Early to Middle Ordovician which was interpreted as indicating cooling associated with, and possibly contributing to, the Great Ordovician Biodiversification Event. That similar patterns are observed on separate continental blocks (Laurentia and Australia) and in distinct paleoceanographic settings: the epicontinental shallow carbonate platform of central Australia (Trotter et al. 2008) and in

fringing carbonates associated with volcanic islands of eastern Australia (this study), strengthens arguments that increasing $\delta^{18}O$ values through the Early and Middle Ordovician are global patterns.

There is significant scatter in $\delta^{18}O_{phos}$ values from New South Wales. For example, in the Katian where sampling density is highest, $\delta^{18}O_{phos}$ values fluctuate by up to 2. 1‰. The scatter could, in part, be a function of paleoecological differences among the conodont taxa analyzed, potentially due to depth partitioning within the water column. Paleoecological differences, however, cannot account for all of the scatter in the data as up to ~1. 5‰ differences are observed in $\delta^{18}O_{phos}$ values of conodont taxa within the same interval. A portion of the scatter among samples could reflect environmental differences (e. g. precipitation/evaporation rates) among sample localities or even intra- and interannual variability in temperature and/or salinity (Quinton and MacLeod, 2014). Alternatively, this variability could represent relatively rapid climatic fluctuations due to glacial and interglacial episodes (e. g. Elrick et al. 2013) though testing this possibility is beyond the resolution of samples available from the sections studied. The fact that up to ~2‰ variability around a relatively stable $\delta^{18}O_{phos}$ average seems to be a common feature of high resolution $\delta^{18}O_{phos}$ records from the Katian, even in studies where smaller scale climatic fluctuations could be resolvable (e. g. Buggisch et al. 2010; Quinton and MacLeod 2014), suggests that glacial influences on temperature and seawater $\delta^{18}O$ values is not the only explanation possible for scatter in results.

The $\delta^{18}O_{phos}$ values from New South Wales are consistently ~2. 5‰ lower than those reported for correlative samples from elsewhere (Bassett et al. 2007; Trotter et al. 2008, Buggisch et al. 2010; Herrmann et al. 2011; Elrick et al. 2013; Quinton and MacLeod 2014). All these samples represent carbonate deposition in tropical to subtropical latitudes, but those from New South Wales (except that from the Koonenberry Belt) differ in that they were deposited in an oceanic back-arc basin setting rather than from intracratonic basins. The reason for the offset in $\delta^{18}O_{phos}$ values is unclear. One possible explanation involves locality-specific differences in the balance of evaporation, precipitation, and runoff from adjacent land areas which would influence the $\delta^{18}O$ values of local seawater and, thus, the $\delta^{18}O_{phos}$ values of conodonts living in these waters. Specifically, either excess evaporation in the epicontinental seas covering Laurentia and central Australia would increase seawater $\delta^{18}O$ values resulting in higher conodont $\delta^{18}O_{phos}$ values or freshwater input from the emergent islands of the Macquarie Volcanic Province could have resulted in seawater $\delta^{18}O$ values of this region being lower than open ocean values.

CONCLUSIONS

Oxygen isotopic ratios analyzed from conodont apatite from Ordovician limestones in New South Wales confirm trends obtained from other Ordovician conodont isotopic studies over the same chronostratigraphic intervals in central and northern Australia and Laurentia (Trotter et al. 2008; Quinton and MacLeod 2014). The New South Wales dataset shows an ~1. 5‰$_{VSMOW}$ increase in $\delta^{18}O_{phos}$ through the Early and Middle Ordovician consistent with decrease in average sea surface temperatures. These results strengthen the argument that biodiversification in the first half of the Ordovician was associated with cooling. Katian $\delta^{18}O_{phos}$ averages are relatively stable but values from different separates from the same sample can differ by up to 2‰. Similar within sample differences in $\delta^{18}O_{phos}$ values are observed in Darriwilian and Floian aged samples. The cause of this variability cannot be determined at the resolution of this study, but possible explanations include rapid climatic shifts, paleoceanographic differences, environmental variability, paleobiological factors relating to the conodont taxa analyzed. Finally, the

consistent ~2. 5‰ offset between the new data and previous studies from other regions suggests paleoceanographic effects led to large differences in seawater $\delta^{18}O$ values among regions.

ACKNOWLEDGMENTS

REFERENCES

BASSETT, D., MACLEOD, K. G., MILLER, J. F. and ETHINGTON, R. L., 2007. Oxygen isotopic composition of biogenic phosphate and temperature of Early Ordovician seawater. *Palaios*, 22: 98-103.

BUGGISCH, W., JOACHIMSKI, M. M., LEHNERT, O., BERGSTRÖM, S. M., REPETSKI, J. E. and WEBERS, G. F., 2010. Did intense volcanism trigger the first Late Ordovician icehouse? *Geology*, 38: 327-330.

ELRICK, M., REARDON, D., LABOR, W., MARTIN, J., DESROCHERS, A. and POPE, M., 2013. Orbital-scale climate change and glacioeustasy during the early Late Ordovician (pre-Hirnantian) determined from $\delta^{18}O$ values in marine apatite. *Geology*, 41: 775-778.

HERRMANN, A. D., MACLEOD, K. G. and LESLIE, S. A., 2010. Did a volcanic mega-eruption cause global cooling during the Late Ordovician? *Palaios*, 25: 831-836.

LAPORTE, D. F., HOLMDEN, C., PATTERSON, W. P., PROKOPIUK, T. and EGLINGTON, B. M., 2009. Oxygen isotope analysis of phosphate: Improved precision using TC/EA CF-IRMS. *Journal of Mass Spectrometry*, 44: 879-890.

O'NEIL, J. R., ROE, L. J., REINHARD, E. and BLAKE, R. E. 1994. A rapid and precise method of oxygen isotope analysis of biogenic phosphate. *Israel Journal of Earth Sciences*, 43: 203-212.

QUINTON, P. C. and MACLEOD, K. G., 2014. Oxygen isotopes from conodont apatite of the midcontinent US: Implications for Late Ordovician climate evolution. *Palaeogeography, Palaeoclimatology, Palaeoecology*, 404: 57-66.

TROTTER, J. A., WILLIAMS, I. S., BARNES, C. R., LÉCUYER, C. and NICOLL, R. S., 2008. Did cooling oceans trigger Ordovician biodiversification? Evidence from conodont thermometry. *Science*, 321: 550-554.

Early-Middle Darriwilian graptolite and conodont faunas from the Central Precordillera of San Juan Province, Argentina

Fernanda Serra[1], Nicolás A. Feltes[1], Gladys Ortega[2] and Guillermo L. Albanesi[1]

[1]CICTERRA (CONICET-UNC), Av. Vélez Sarsfield 1611, X5016GCA, Argentina. fserra@efn.uncor.edu
[2]CONICET-Museo de Paleontología, FCEFyN, UNC, Av. Vélez Sarsfield 297, X5016GCA.

INTRODUCTION

The Precordillera of western Argentina is characterized by lower Paleozoic carbonate rocks, which includes conspicuous Lower-Middle Ordovician deposits overlain by Middle-Upper Ordovician black shales involving a hiatus related to the global Sandbian transgressive event. The relative dating of the units indicate a diachronous deposition of the succession, which begins in the upper Dapingian (*Isograptus maximus* Zone) in the north and ranges to the lower Darriwilian (*Levisograptus dentatus* Zone) in the south. The study sections from the Central Precordillera of San Juan Province, located to the south west and north east of Jáchal City, involve the Las Aguaditas Creek, Las Chacritas River, Oculta Creek, Potrerillo Hill and La Chilca Hill (Figure 1A). In the Jáchal area, the Ordovician System is extensively represented and has been the subject of many paleontological and geological studies (references in Albanesi et al. 2013).

The present contribution deals with early Darriwilian graptolites and index conodonts recorded from units that overlie the calcareous San Juan Formation (upper Tremadocian-lower Darriwilian), spanning the lower part of the Las Aguaditas, Gualcamayo and Los Azules formations, and the Las Chacritas Formation in their respective areas.

GRAPTOLITE FAUNA

At the Las Aguaditas Creek section graptolites were recorded from the basal strata of the lower member (*ca*. 23 m) of the Las Aguaditas Formation. Incomplete specimens of *Levisograptus* sp., *Xiphograptus* sp., *Acrograptus* sp. and *Holmograptus* sp. were recovered from the base of the formation. Few meters above this level, the richness increases with a graptolite association that includes *Tetragraptus bigsbyi*, *T.* cf. *serra*, *T. quadribrachiatus*, *Pseudophyllograptus* sp., *Xiphograptus* sp., *Acrograptus* sp., *Holmograptus bovis*, *Jiangshanites* sp., *Arienigraptus angulatus*, *Paraglossograptus tentaculatus*, *Cryptograptus antennarius*, *Levisograptus primus* and *Levisograptus* sp. Although the specimens of *Levisograptus* do not show much detail for a specific identification, this fauna can be referred to as the upper *Levisograptus dentatus* Zone considering the presence of *A. angulatus*. Moreover, conodonts from the *Yangtzeplacongathus crassus* Zone were recorded in these strata. *Paraglossograptus* and *Tetragraptus* are the most abundant taxa in the lower part of this formation. In the calcareous Las Chacritas Formation at Las Chacritas River section, a scarce graptolite fauna was recorded in association with conodonts of the *Y. crassus* and *E. pseudoplanus* zones, suggesting an early-middle Darriwilian age.

A diverse graptolite fauna was collected from the Gualcamayo Formation exposed in the La Chilca Hill. *Pseudobryograptus parellelus* is abundant in the lower calcareous unit and decreases upwards to the top strata, where *Levisograptus* becomes dominant. Graptolites and conodonts correspond to the *L. dentatus*
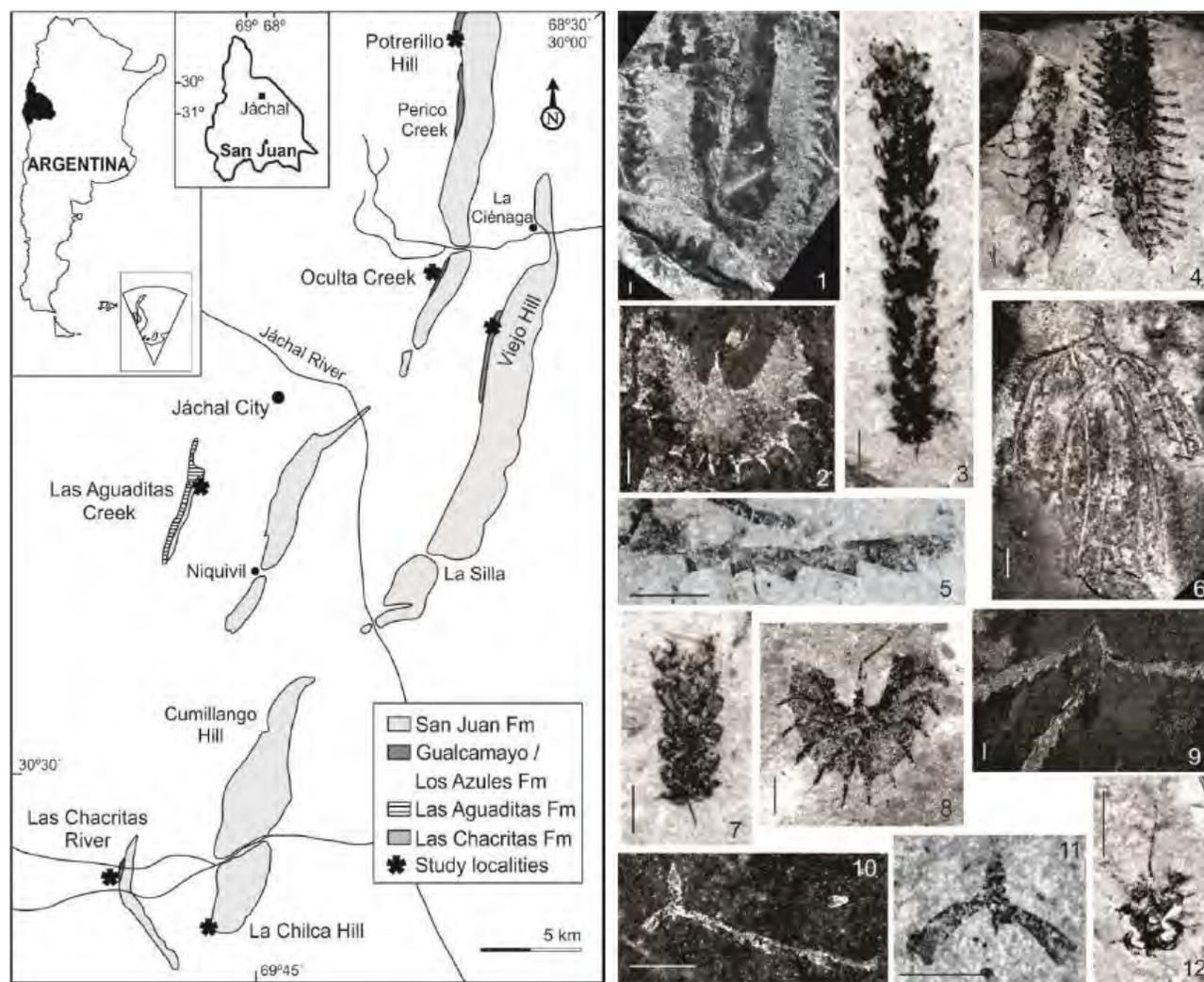
FIGURE 1. —A) Location map of the study areas. B) Early-Middle Darriwilian Graptolites. 1. *Tetragraptus bigsbyi* (Hall), CORD-PZ 34533, Las Aguaditas Creek; 2. *Arienigraptus angulatus* Mu, CORD-PZ 25502, Las Aguaditas Creek; 3, 7. *Levisograptus dentatus* (Brongniart). 3. CORD-PZ 22347, La Chilca Hill, 7. CORD-PZ 22350, La Chilca Hill. 4. *Paraglossograptus tentaculatus* (Hall), CORD-PZ 22272, La Chilca Hill. 5. *Xiphograptus* sp., CORD-PZ 22292, La Chilca Hill. 6, 11 *Pseudobryograptus parallelus* Mu. 6. CORD-PZ 14468, Potrerillo Hill, 11. CORD-PZ 22194, La Chilca Hill. 8. *Parisograptus* sp. CORD-PZ 22316, La Chilca Hill. 9. *Tetragraptus acanthonotus* (Gurley), CORD-PZ 23163, Potrerillo Hill. 10. *Holmograptus bovis* Williams and Stevens, CORD-PZ 25503, Las Aguaditas Creek. 12. *Levisograptus sinicus* (Mu and Lee), CORD-PZ 25664, Oculta Creek.

and *Y. crassus* zones. In the lower Gualcamayo Formation at the Potrerillo Hill, a relatively poor graptolite assemblage of the *L. austrodentatus* Zone is followed by shales with abundant and diverse graptolites from the *L. dentatus* Zone (Ortega and Albanesi 2000). Conodonts from the *Y. crassus* Zone were also recovered; particularly, the presence of *Tetragraptus acanthonotus*, *P. parallelus*, and *Zygograptus* cf. *abnormis* suggests the lower *L. dentatus* Zone.

The lower member of the Los Azules Formation in the Oculta Creek contains a diverse graptolite assemblage that includes *T. quadribrachiatus*, *T. acanthonotus*, *Pseudotrigonograptus ensiformis*, *Acrograptus* sp., *H. bovis*, *Xiphograptus lofuensis*, *Pseudobryograptus* sp., *Isograptus* cf. *divergens*,

Arienigraptus sp., *Parisograptus caduceus, P. tentaculatus*, *L. sinicus*, *L. primus*, *L. austrodentatus*, and *L. dentatus*. This fauna could be referred to the lower *L. dentatus* Zone, early-middle Darriwilian in age. Typical conodonts of the *Y. crassus* Zone were recorded at the top of the San Juan Formation, immediately underlying the Los Azules Formation (Voldman, Albanesi, and Ortega 2013). In the Viejo Hill, the lower member of the Los Azules Formation contains a rich graptolite assemblage referred to the upper part of the *L. dentatus* Zone according to the presence of *A. angulatus* and *L. pungens*. Selected graptolites are illustrated in Figure 1B. The mentioned graptolite faunas are related with transgressive events that correspond to outer-platform facies, which suggests that these units represent a deep-outer shelf depositional environment.

CONCLUSIONS

According to the graptolite-conodont records, the black shales at different study areas can be referred to the early-middle Darriwilian *L. austrodentatus-L. dentatus* zones and the *Y. crassus* Zone. The occurrence of particular taxa, such as *P. parallelus*, *T. acanthonothus*, and *Z.* cf. *abnormis* suggests that the lower *L. dentatus* Zone is present in some localities of the Central Precordillera; e. g., the Oculta Creek, La Chilca Hill, and Potrerillo Hill. At the Las Aguaditas section, the upper *L. dentatus* Zone is identified by *A. angulatus*.

ACKNOWLEDGMENTS

REFERENCES

ALBANESI, G. L., BERGSTRÖM, S. M., SCHMITZ, B., SERRA, F., FELTES, N. A., VOLDMAN, G. G. and ORTEGA, G., 2013. Darriwilian (Middle Ordovician) $\delta^{13}C_{carb}$ chemostratigraphy in the Precordillera of Argentina: Documentation of the middle Darriwilian Isotope Carbon Excursion (MDICE) and its use for intercontinental correlation. *Palaeogeography, Palaeoclimatology, Palaeoecology*, 389: 48–63.

ORTEGA, G. and ALBANESI, G. L., 2000. Graptolitos de la Formación Gualcamayo (Ordovícico Medio) en el cerro Potrerillo, Precordillera Central de San Juan, Argentina. *Boletín Academia Nacional de Ciencias*, 64: 27-59.

VOLDMAN, G. G., ALBANESI, G. L. and ORTEGA, G., 2013. Middle Ordovician conodonts and graptolites at Los Cauquenes Range, Central Precordillera of San Juan, Argentina. In: ALBANESI, G. L. and ORTEGA, G., Eds., *Conodonts from the Andes, 3rd International Conodont Symposium*, 117-121. Buenos Aires: Asociación Paleontológica Argentina, no. 13.

Life on the edge in eastern Alaska: basal Ordovician (Tremadocian), platform-margin faunas of the Jones Ridge Formation

John F. Taylor[1], Tyler J. Allen[1], John E. Repetski[2], Justin V. Strauss[3], and Savannah J. Irwin[1]

[1] *Geoscience Department, Indiana University of Pennsylvania, Indiana, PA 15705, USA*
[2] *U. S. Geological Survey, Reston, VA 22092, USA*
[3] *Department of Earth Sciences, Dartmouth College, Hanover, NH 03750, USA*

INTRODUCTION

As the most fossiliferous and least deformed succession of unequivocally Laurentian lower Paleozoic strata in Alaska, the Jones Ridge Limestone has provided critical data for numerous stratigraphic studies (e. g. Palmer 1968; Harris et al. 1995; Dumoulin et al. 2002; Dumoulin and Harris 2012) focused on the Cambrian and Ordovician of northwestern North America/northeastern Laurentia (Figure 1). The Jones Ridge faunas are also significant in having provided the type material for some of the widespread and biostratigraphically useful latest Furongian and (perhaps) earliest Tremadocian species described by Kobayashi (1936) and Palmer (1968). Unfortunately, some of those taxa were based on very limited material for which, in the earlier study in particular, no detailed information regarding locality or stratigraphic horizon was provided. The limited amount of information and material available for study from Jones Ridge results largely from its remote location on the Yukon-Alaska boundary approximately 25km north of Eagle, Alaska, which renders it accessible only by helicopter. Parts of three field seasons (2010, 2011, and 2014) were invested in re-description and intensive sampling of the type section of the Jones Ridge Formation in order to produce an integrated and greatly refined set of biostratigraphic, chemostratigraphic, and sedimentological data. The new data support the interpretation offered by Palmer (1968) of the Jones Ridge strata as the product of deposition in outermost platform to upper slope environments offered by Palmer (1968) on the basis of taxonomic content of the faunas and close proximity of deep water units of equivalent age a very short distance to the southwest.

PREVIOUS WORK

Brabb (1967), in naming the formation, divided the Jones Ridge Limestone into two informal members of greatly unequal thickness. His lower member comprises nearly 900m of Cambrian to Lower Ordovician limestone and dolomite; the upper member consists of less than 20m of Upper Ordovician bioclastic grainstone. The unconformity at the base of the upper member, which omits the entire Middle Ordovician and at least some part of the Lower Ordovician, marks the top of the Sauk Megasequence (Harris et al. 1995; Dumoulin and Harris 2012). Palmer (1968) dealt almost exclusively with the Cambrian trilobite faunas, but his stratigraphic columns for the Jones Ridge Limestone also include the Lower Ordovician strata at the top of the lower member, and show at least the approximate stratigraphic position of all collections archived by the U. S. Geological Survey and Canadian Geological Survey at the time of his study.

In his correlation diagram, Palmer (1968, figure 2) shows more than 90m of Lower Ordovician strata. At that time, however, the top of the *Saukia* trilobite Zone served as the Cambrian-Ordovician boundary in Laurentian North America (Winston and Nicolls 1967). The faunas assigned to the Lower Ordovician at
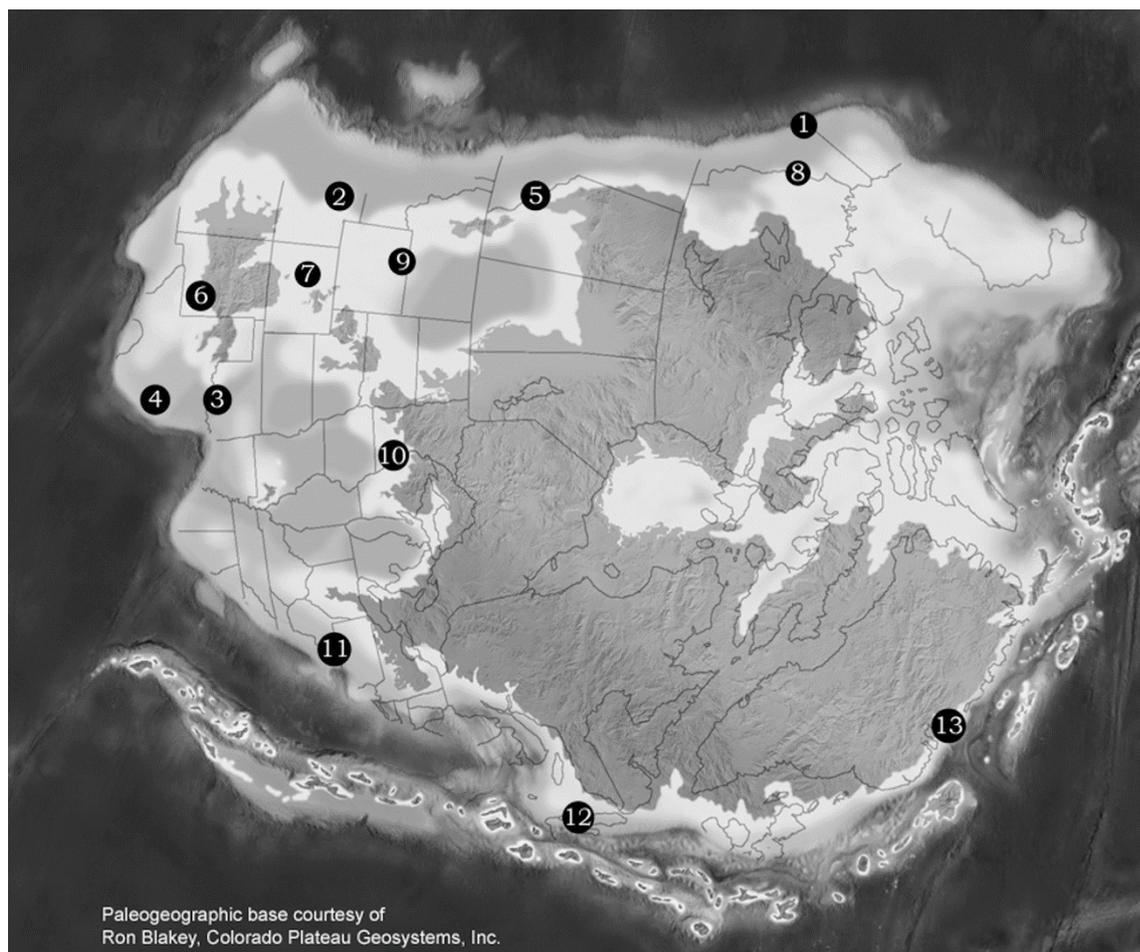
Figure 1. —Paleogeographic map showing locations in Laurentian North America where faunas of the Lower Ordovician *Symphysurina* Zone have been reported. 1 – Jones Ridge Formation, eastern Alaska, 2 – House Formation, Ibex area, western Utah, 3 – Mckenzie Hill Formation, southern Oklahoma, 4 –Wilberns Formation, central Texas, 5 – Survey Peak Formation, southern Alberta, 6 – Bliss Formation, New Mexico, 7 – Manitou Formation, Colorado, 8- Rabbitkettle Formation, District of Mackenzie, 9- Snowy Range Formation, northern Wyoming, 10- Oneota Dolomite, southern Minnesota, 11 – Stonehenge Formation, Maryland, 12 – Shallow Bay Formation, western Newfoundland, 13 – Antiklinalbugt Formation, northeast Greenland.

Jones Ridge represented the overlying *Missisquoia* and *Symphsurina* Zones. Relocation of the systemic boundary to the base of the *Iapetognathus* conodont Zone with ratification of the GSSP at Green Point Newfoundland (Cooper et al. 2001) raised the base of the Ordovician to the middle of the *Symphysurina* Zone, rendering the lower part of that zone and all of the underlying *Missisquoia* Zone as Cambrian. At that point, even the strata from which Kobayashi and Palmer reported *Symphysurina* could not confidently be assigned to the Ordovician. Harris et al. (1995) provided the first conclusive evidence of Lower Ordovician strata in the Jones Ridge Formation, reporting conodont faunas at least as young as the *Cordylodus angulatus* conodont Zone. The Jones Ridge column in their correlation chart, replicated in Dumoulin and Harris (2012), showed the Lower Ordovician part of the formation spanning the entire Tremadocian Stage and extending up into the basal Arenig, although no faunal collections were shown to support that broad a temporal range. Consequently, one of the primary objectives of the current project

was to establish the thickness and age range of the Lower Ordovician strata preserved at the top of the lower member.

LITHOSTRATIGRAPHY

Detailed lithologic information recovered in recent years allows delineation of several new members within the original lower member of the Jones Ridge Formation. Although formal description of these new units falls outside the scope of this paper, three are introduced and treated briefly herein to provide context for the new faunal data. We propose the name Nimrod member for the package of Upper Ordovician limestone previously referred to only as the upper member of the Jones Ridge Limestone (Brabb, 1967; Rigby et al., 1988). These strata consist of medium- to thick-bedded, locally silicified, coarse-grained bioclastic grainstone. The contact between these strata and the overlying Road River Formation is poorly exposed and consists of a sharp transition from bioclastic limestone of the Nimrod member into mid-Wenlock interbedded chert, siltstone, and graptolitic shale (Blodgett et al., 1984). . The uppermost 200m of Cambrian and lowermost Ordovician strata that directly underlie the Nimrod member consist largely of fine-grained, nodular lime mudstone and wackestone that was deposited at, or just seaward of the platform margin. This interval is herein set apart as the Hi-Yu member. An interval roughly 125 meters thick, with abundant microbial reefs directly underlies the Hi-Yu member and is designated the Harrington Creek member. The Harrington Creek member consists of interbedded wackestone and minor packstone with m-scale microbial reefs that locally host *Girvanella* and *Epiphyton* fabrics. We propose the name Squaw Mountain member for the next subjacent package, which comprises approximately 120 meters of barren, burrow-mottled dolomicrite and massive recrystallized dolomite. The Squaw Mountain member is separated from an underlying ~400 m thick package of massive, thick-bedded dolostone by a profound paleokarst horizon. We tentatively refer to these underlying strata as the Funnel Creek Formation and separate them from the lower Jones Ridge Formation.

CONODONT BIOSTRATIGRAPHY

Conodonts were recovered from more than 15 horizons (Figure 2), 8 of them within the uppermost part of the Hi-Yu member that yields *Symphysurina*. So far, more than 500 elements have been recovered, documenting the presence at least part of three Furongian and two Tremadocian conodont zones. These collections, combined with the trilobite data, constrain the position of the Cambrian-Ordovician boundary to within less than 1. 5m and confirm that nearly 70m of Lower Ordovician strata are preserved below the unconformity that separates the Hi-Yu and Nimrod members. All of the recovered faunas thus far are dominated numerically by cosmopolitan taxa, most notably the species of *Cordylodus* and *Proconodontus*, as well as *Teridontus nakamurai* and *Eoconodontus notchpeakensis*.

 The recovery of a single element of *Granatadontus ani* 244m above the base of the section confirms an age at least as young as the *Proconodontus posterocostatus* Zone for that horizon. Four specimens of *Proconodontus muelleri* at 262. 5m and a single element of *Eoconodontus notchpeakensis* from 291m placed the bases of the *P. muelleri* and *Eoconodontus* Zones at least as low as shown in Figure 2. Perhaps significantly, 291m is also the lowest documented occurrence of Palmer's "Trempealeauan-2" trilobite fauna suggesting that the appearance of *E. notchpeakensis* coincided with the replacement of the "Trempealeauan-1" fauna with the "Trempealeauan-2" fauna. If this is the true FAD of *E. notchpeakensis* (which is far from certain given the recovery only 13 elements from lower horizons),
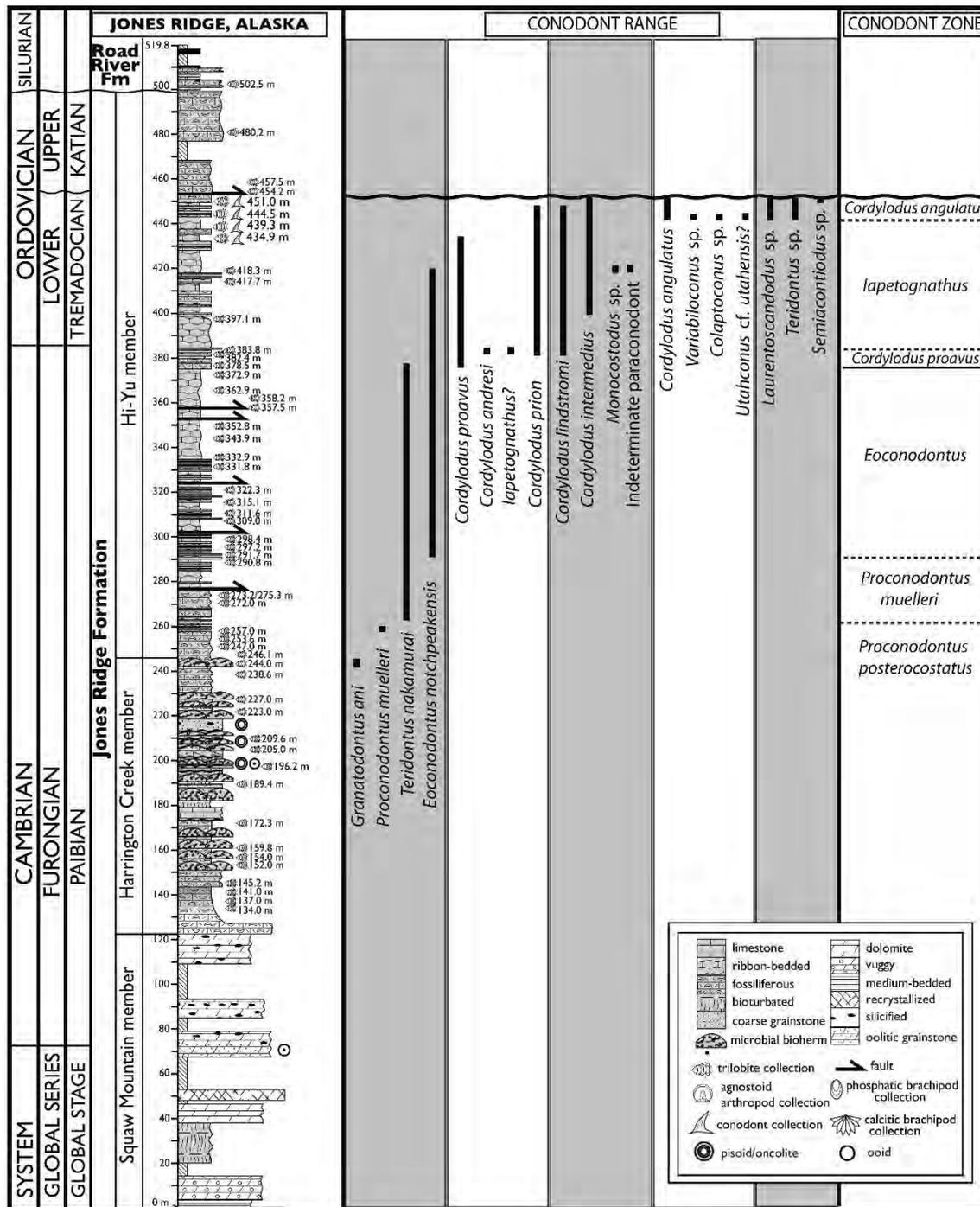
Figure 2. —Stratigraphic column and range chart showing new, informal member stratigraphy proposed for the uppermost 500m of the Jones Ridge Formation, the stratigraphic distribution of conodont species recovered, and conodont zones documented. *C. = Cordylodus. Procono. = Proconodontus.*

then the situation on the northern Laurentian slope is similar to that reported from the southern (Appalachian) slope by Miller et al. (2011) in advocating designation of the base of the *Eoconodontus* Zone for the base of the uppermost global stage (Stage 10) of the Cambrian System. There the FAD of *E. notchpeakensis* appears to coincide with the turnover between the *Kiethiella subclavata* and *Kiethiella schucherti* trilobite Faunas of Ludvigsen et al. (1989).

Conodont collections from the upper 70m of the Hi-Yu member (Figure 2) represent three Ibexian conodont zones and reveal a significant gap in the zonal succession. A large (more than 100 element) collection from 383.8m is provisionally assigned to the *Iapetognathus* Zone on the basis of two small specimens identified here as *Iapetognathus?* sp. The presence of several specimens of *Cordylodus lindstromi* confirms that the collection is no older than the underlying *C. lindstromi* Zone. The trilobite genus *Ptychopleurites* dominates the fauna from 382.4, assigning that horizon to the uppermost Cambrian *Tangshanaspis* trilobite Zone (formerly known as the *Missisquoia depressa* Subzone of the *Missisquoia* Zone), a unit that lies entirely within the basal, *Hirsutodontus hirsutus* Subzone of the *Cordylodus proavus* Zone. Consequently, the upper two zones of the *C. proavus* Zone, the entire *C. intermedius* Zone, and (most likely) the *C. lindstromi* Zone are not represented in the Jones Ridge succession. The two highest collections from the Hi-Yu member (444.5m and 451 m) contain *Cordylodus angulatus* and are assigned to the *C. angulatus* Zone, apparently the youngest Tremadocian biozone at Jones Ridge.

TRILOBITE BIOSTRATIGRAPHY

Spacing of macrofossil collections through the Furongian was improved nearly an order of magnitude over the reconnaissance-level resolution of earlier studies, reducing the spacing of productive horizons from every 50-60 meters on average (Palmer 1968) to approximately every 6-7 meters (Figure 3). All Furongian faunas identified by Palmer (1968) were recovered and supplemented with additional taxa that were not present in his collections. The refined sampling also documented a fauna that Palmer did not report from Jones Ridge in the interval between his "Dresbachian-2" (Paibian) and "Trempealeauan-1" (Jiangshanian?) faunas. The focus of this paper, however, is the Ibexian faunas assigned to the Ordovician in earlier work. As previously noted, the *Ptychopleurites*-bearing, *Tangshanaspis* Zone fauna of Kobayashi (1936) was resampled and its range established (Figure 3). All younger collections from the Hi-Yu member are assigned to the *Symphysurina* Zone and are dominated by the eponymous genus. Some collections also contain a few specimens of other taxa known from the *Symphysurina* Zone elsewhere, including *Highgatella* and at least two hystricurine genera.

The new collections reveal a much higher species diversity for *Symphysurina* than reported by Kobahayashi (1936), who reported only two species: *S. spicata* and *S.* cf. *S. woosteri*, two of the many species within this genus that display a prominent pygidial spine. At least five different species of *Symphysurina* with spinose pygidia are represented in the new collections. One strongly resembles *S, spicata,* but is more likely to represent a somewhat younger species. None compare favorably with *S. woosteri.* At least three other species of the genus without a pygidial spine are also present , two of which are very similar to (although probably not conspecific with) *S. elegans* and *S. porifera* from basal Ordovician strata in northeast Greenland (McCobb et al. 2014). Although no conodont data have been recovered from the interval where *S. elegans* occurs, its association with such very basal Ordovician trilobite genera as *Tulepyge* and *Chasbellus* indicates close age equivalence with *S.* cf. *S. elegans* from the Jones Ridge. Conodonts were recovered from the beds that yield *S. porifera* in northeast Greenland and confirm that, like *S.* cf. *S. porifera* at Jones Ridge, it occurs in the *Cordylodus angulatus* Zone. The striking morphologic similarity and stratigraphic position of the two species from Jones Ridge and the two Greenland species suggests that a distinct sub-province of the Laurentian faunal province existed at the easternmost margin of that paleocontinent during deposition of the upper part of the *Symphysurina* Zone. Continued work on the Jones Ridge *Syphysurina* Zone collections may provide a rigorous test of that hypothesis, particularly as the associated hystricurine taxa are described and compared with the unique hystricurines of the Greenland succession.
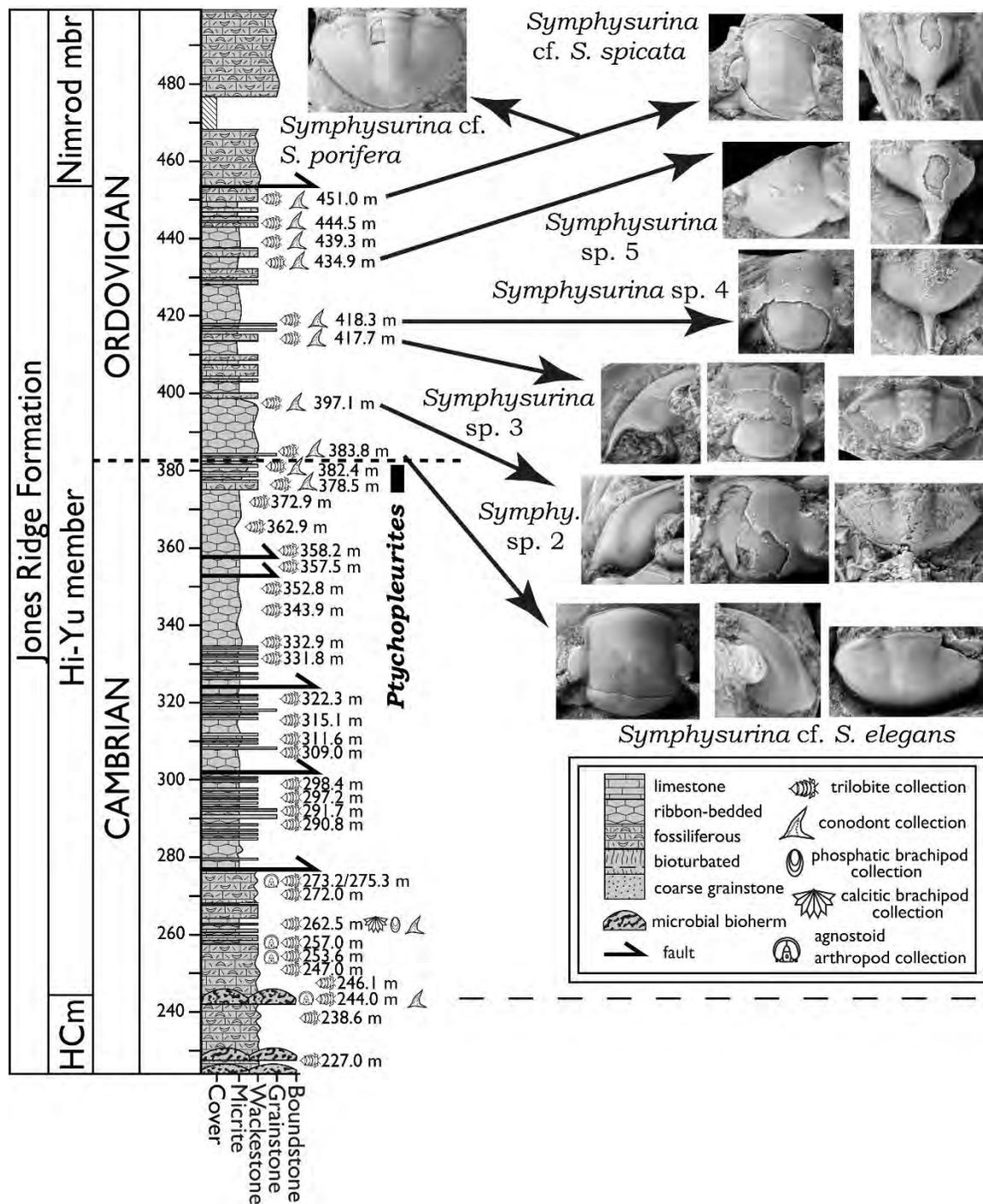
Figure 3. —Stratigraphic column showing lithologies and selected horizons from which new faunal collections were recovered in the uppermost Harrington Creek and Hi-Yu members of the Jones Ridge Formation. HCm identifies uppermost beds of Harrington Creek member. Black bar denotes vertical range established for uppermost Cambrian trilobite genus *Ptychopleurites*. Large arrows link photos of the six species of *Symphysurina* recovered from Tremadocian strata at the top of the Hi-Yu member with the specific horizons where they occur.

ACKNOWLEDGMENTS

REFERENCES

BRABB, E. E., 1967. Stratigraphy of the Cambrian and Ordovician rocks of east-central Alaska: *U. S. Geological Survey, Professional Paper 559-A*, A1–A30.

BLODGETT, R. B., POTTER, A. W. and CLOUGH, J. G., 1984, Upper Ordovician-Lower Devonian biostratigraphy and paleoecology of the Jones Ridge-Squaw Mountain area, east-central Alaska. *Geological Society of America, Abstracts with Programs.* 16, p. 270.

COOPER, R. A., NOWLAN, G. S. and WILLIAMS, S. H., 2001. Global stratotype section and point for the base of the Ordovician System. *Episodes* 24: 19–28.

DUMOULIN, J. A., HARRIS, A. G., GAGIEV, M., BRADLEY, D. C. and REPETSKI, J. E., 2002. Lithostratigraphic, conodont, and other faunal links between lower Paleozoic strata in northern and central Alaska and northeastern Russia. In: Miller, E. L., Grantz, A., and Klemperer, S. L., Eds., *Tectonic Evolution of the Bering Shelf–Chukchi Sea–Arctic Margin and Adjacent Landmasses*, 291–312. Boulder, CO: *Geological Society of America* Special Paper 360.

DUMOULIN, J. A. and HARRIS, A. G., 2012. Cambrian–Ordovician sedimentary rocks of Alaska. In: Derby, J. R., Fritz, R. D., Longacre, S. A., Morgan, W. A., and Sternbach, C. A., Eds., *The Great American Carbonate Bank: The geology and economic resources of the Cambrian – Ordovician Sauk megasequence of Laurentia*, 649–673. Tulsa, OK: American Association of Petroleum Geologists. Memoir 98.

HARRIS, A. G., DUMOULIN, J. A., REPETSKI, J. E. and CARTER, C., 1995. Correlation of Ordovician rocks of northern Alaska. In: Cooper, J. D., Droser, M. L., and Finney, S. C., Eds., *Ordovician Odyssey: Short papers for the Seventh International Symposium on the Ordovician System*, 21–26. Fullerton, CA: Pacific Section, Society for Sedimentary Geology (SEPM). Book 70

KOBAYASHI, T., 1936. Cambrian and Lower Ordovician trilobites from northwestern Canada. *Journal of Paleontology*, 10: 157–167.

LUDVIGSEN, R., WESTROP, S. R. and KINDLE, C., 1989, Sunwaptan (Upper Cambrian) trilobites of the Cow Head Group, western Newfoundland, Canada: *Palaeontographica Canadiana,* 6: 1–175.

MCCOBB, L. M. E., BOYCE, D., KNIGHT, I. and STOUGE, S., 2014. Early Ordovician (Skullrockian) trilobites of the Antiklinalbugt Formation, northeast Greenland, and their biostratigraphic significance. *Journal of Paleontology*, 88: 982–1018.

MILLER, J. F., EVANS, K. R., FREEMAN, R. L., RIPPERDAN, R. L. and TAYLOR, J. F., 2011. Proposed stratotype for the base of the Lawsonian Stage (Cambrian Stage 10) at the first appearance datum of *Eoconodontus notchpeakensis* (Miller) in the House Range, Utah, USA. *Bulletin of Geosciences*, 86: 595–620.

PALMER, A. R., 1968. *Cambrian trilobites of east-central Alaska.* Washington, DC: U. S. Geological Survey. Professional Paper 559-B, 115 pp..

RIGBY, J. K., POTTER, A. W. and BLODGETT, R. B., 1988, Ordovician sphinctozoan sponges of Alaska and Yukon Territory. *Journal of Paleontology,* 62:, 731–746.

WINSTON, D. and NICHOLLS, H., 1967. Late Cambrian and Early Ordovician faunas from the Wilberns Formation of central Texas. *Journal of Paleontology*, 41: 66–96.

New conodont records from the Rinconada Formation, eastern margin of the Argentine Precordillera: Tectono-stratigraphic implications

Gustavo G. Voldman[1,2], Guillermo L. Albanesi[1,2], Juan L. Alonso[3], Luis P. Fernández[3], Aldo L. Banchig[4], Raul Cardó[4,5], Gladys Ortega[1] and Alberto M. Vallaure[3]

[1]*Museo de Paleontología, CIGEA, Facultad de Ciencias Exactas, Físicas y Naturales, Universidad Nacional de Córdoba, X5000JJC, Córdoba, Argentina. gvoldman@efn.uncor.edu*
[2]*CICTERRA-CONICET, Argentina.*
[3]*Departamento de Geología, Universidad de Oviedo, c/ Arias de Velasco s/n, 33005 Oviedo, Spain.*
[4]*Departamento de Geología, Universidad Nacional de San Juan, c/ Ignacio de La Rosa y Meglioli s/n, 5400, San Juan, Argentina.*
[5]*SEGEMAR (Servicio Geológico y Minero Argentino), Sargento Cabral 685 (oeste), San Juan, Argentina.*

INTRODUCTION

The Rinconada Formation is a *ca*. 3750 m-thick mélange that records a period of instability in the Lower Paleozoic basin of the Argentine Precordillera; nevertheless, its origin and geological setting are a matter of debate (Heim, 1948; Amos, 1954; Peralta, 1993; Gosen *et al.,* 1995; Peralta, 2013a). The mélange crops out along the eastern flank of the Villicum, Zonda and Pedernal ranges (Fig. 1) and is mainly made of mudstones, locally containing sandstone-mudstone alternations, conglomerates and up to km-scale blocks. The age of the formation is controversial because of the inherent reworked character of its components and the difficulty to detect autochthonous (coeval) fossils amongst the reworked material. In order to improve the understanding of the sedimentary history and the provenance of the mélange, we conducted an integrated study of the Rinconada Formation consisting of a systematic conodont sampling coupled with detailed structural and sedimentological studies. Twenty-four conodont samples obtained from carbonate-cemented sandstones, conglomerates and olistoliths were processed following standard laboratory techniques. All the conodont samples present a CAI around 3, which corresponds to burial temperatures of about 110-200 °C (Epstein *et al.,* 1977), and commonly display sugary textures with scarce mineral overgrowths and common fractures. For the conodont zonation of the Precordillera and its global correlation, we followed the recent biostratigraphic schemes of Benedetto *et al.* (2007), Cooper and Sadler (2012), Albanesi *et al.* (2013) and Serra *et al.* (2015) (Fig. 2).

PREVIOUS WORK

On the basis of the Potrerillos section, Peralta and Medina (1986) distinguished three members in the Rinconada Formation: a late Darriwilian - early Sandbian lower pelitic (mudstone dominated) member which includes carbonate blocks, a Silurian psammitic (sandy) middle member and an Early Devonian upper siltstone member. Cuerda (1981) described a graptolitic association composed of *Climacograptus* cf. *minutus*, *Diplograptus* sp. and *Monograptus* sp., whose referred age, Early Silurian age (Llandovery), is consistent with previous reports. Benedetto and Franciosi (1998) described from the upper levels of the Rinconada Formation Wenlock brachiopods, which correlated with specimens recovered from the Tambolar Formation at Pachaco. Peralta (1993) and Gosen *et al.* (1995) assigned a Silurian age to the Rinconada Formation, although the latter authors did not rule out an Ordovician age for parts of the unit. In the El Martillo Creek section (Rinconada area), Dorn (1993) obtained a total thickness of 2100 m for the Rinconada Formation, and distinguished a lower olistostromic unit, 1600 m in thickness, of uncertain age, and an upper 500 m-thick interval of alternations of greenish and purplish sandstones, mudstones,
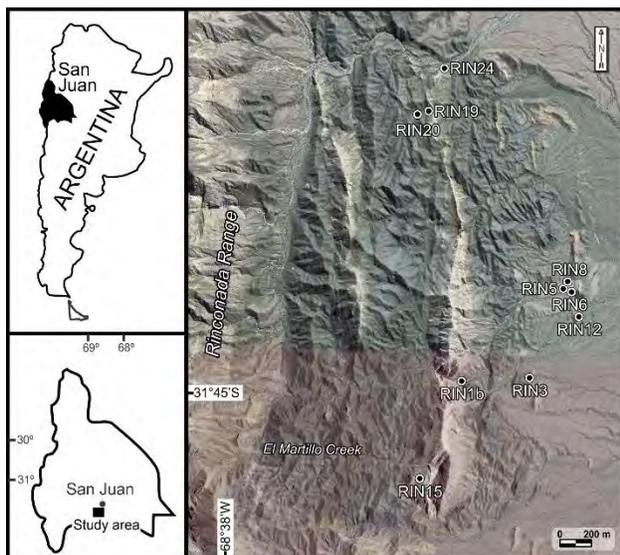
Figure 1: Location map and Google Earth satellite image of the study area.

ferruginous intervals and olistoliths, which would correspond to middle member of Peralta and Medina (1986). Sarmiento *et al.* (1986) studied a conodont fauna from the top of the San Juan Formation and the base of the Rinconada Formation, which they attributed to the middle Darriwilian (early Llanvirn). Peralta and Uliarte (1986) supported this age with graptolites from the base of the Rinconada Formation and interpreted that a gradual transition exists with the underlying San Juan Limestones, yet those carbonates correspond to allochthonous blocks.

Also, in the Rinconada area, Lehnert (1995) obtained an early Darriwilian conodont assemblage (*Histiodella sinuosa* Zone) from the top of the San Juan Formation. This author also reported early-middle Darriwilian conodonts from the limestone pebbles of carbonate conglomerate olistoliths, and less biostratigraphycally constrained, early to middle Darriwilian conodont specimens from three limestone olistoliths, with younger ages to the east. Following these data, Gosen *et al.* (1995) interpreted that the Rinconada Formation is a sedimentary mélange, whose internal stratigraphy mirrors the stratigraphic sequence of the source area located to the west after its progressive erosion.

RESULTS

At the Rinconada type locality (Fig. 1), isolated carbonate blocks of decametric size yielded conodont assemblages of variable ages. The sample RIN24 beared *Bestroemognathus extensus, Oelandodus costatus, Periodon flabellum, Tropodus australis, Tropodus comptus, Reutterodus andinus, Rossodus barnesi,* which probably represent the *Prioniodus elegans* Zone of early Floian age. The major carbonate slice (sample RIN1b) produced a conodont fauna from the *Oepikodus evae* Zone of late Floian age, which includes its zonal marker. The samples RIN6 and RIN8 that include a conodont fauna referable to the early Darriwilian were taken from two closely located blocks. In particular, RIN6 yielded *R. barnesi*, *Semiacontiodus potrerillensis*, *Scolopodus rex*, *Protopanderodus* sp., *P. flabellum,* and *Histiodella sinuosa*, which is an index species according to the North American biostratigraphic zonations (*e. g.,* Bauer, 2010; Stouge, 2012). The sample RIN8 produced *Ansella jemtlandica, Drepanodus arcuatus, Paltodus*? *jemtlandicus, Parapaltodus simplicissimus* and *S. potrerillensis*, without well-known key species. The southernmost productive sample (RIN15) comes from a limestone block that contains a slightly younger conodont fauna, integrated by *Drepanoistodus* sp., *Histiodella holodentata*, *H. sinuosa*, *Erraticodon alternans*, *Juanognathus serpaglii*, *Paltodus*? *jemtlandicus*, *Paroistodus horridus*, *P. macrodentatus*, *R. barnesi* and *S. potrerillensis*. This species association can be referred to the *Yangtzeplacognathus crassus* Zone from the middle Darriwilian.

Another type of block is represented by giant slabs up to tens of meters in size of grey, quartzitic sandstones, some of them with carbonate cement, with their internal bedding mostly parallel to the

System	Series	Stage	Precordillera conodont zonation
Ordovician	Middle	Darriwilian	Eoplacognathus pseudoplanus
			Yangtzeplacognathus crassus
			Lenodus variabilis / P. horridus / P. gladysae
			Microzarkodina parva
		Daping.	Paroistodus originalis
			Baltoniodus navis
			Tripodus laevis
	Lower	Floian	O. intermedius
			Scolcolop. oldstock.
			Oepikodus evae / Juanog. variabilis
			Oepik. communis
			Prioniodus elegans / Tropodus sweeti
			Oelandodus elongatus - Acodus deltatus
		Tremad.	Paroistodus proteus / Stiptognathus borealis
			Paltodus deltifer

Figure 2: **Conodont biostratigraphic chart of the Lower-Middle Ordovician of the Argentine Precordillera. The gray intervals correspond to the analyzed conodont samples.**

regional bedding (Gosen *et al.,* 1995). From these blocks, sample RIN20 provided *H. minutiserrata*, *R. barnesi*, *P. macrodentatus* and *S. potrerillensis*, which are representative of the *L. variabilis* Zone.This way, we record for the first time thick sandstone packages in the lower Darriwilian strata of the Precordillera. Instead, this time interval is represented in the platform by diachronous black shales, which overlie the limestones of the San Juan Formation.

Limestone clasts incorporated in polymyct conglomerates provided valuable information as well. For instance, sample RIN3 produced a conodont association consisting of *A. jemtlandica*, *Baltoniodus* sp., *Costiconus costatus*, *Periodon macrodentatus*, *Pteracontiodus cryptodens* and *Scolopodus rex*, which is typical of the *Lenodus variabilis* Zone (early Darriwilian). A limestone boulder (RIN19) from a conglomerate olistolith yielded a conodont fauna consisting of *Drepanodus arcuatus, Gothodus* sp., *S. krummi, T. sweeti, Paltodus deltifer, P. primus, Variabiloconus variabilis*. This conodont association represents the *Acodus deltatus* Subzone from the basal Floian.

The upper part of the Rinconada Formation displays lenticular reddish calcareous sandstones with iron oolites that alternate with debris-flow deposits. Two conodont samples RIN5 and RIN12 provided specimens ranging through the early Pridoli, such as *Dapsilodus obliquicostatus, Decoriconus fragilis*, *Pseudooneotodus beckmani*, *P. bicornis* and *Zieglerodina*? cf. *zellmeri*. A contemporaneous association was recognized by Mestre (2009), who also reported conodonts from coquinas of the Tambolar Formation (the Pachaco facies) near the San Juan River (*cf.,* Peralta 2013b).

DISCUSSION AND CONCLUSIONS

The conodont data here presented suggest that the Rinconada Formation mélange comprises deposits that range in age from Early Ordovician to late Silurian. The limestone blocks appear to have derived from Floian and Darriwilian levels of the San Juan Formation. Noticeably, this is also the age yielded by the limestone clasts of the conglomerate blocks that form some olistoliths (no Dapingian conodonts were recovered so far). This indicates that the Rinconada mélange was also fed from some conglomerate deposits that, in turn, had been fed from the erosion of the San Juan Formation. It is also interesting to

note that the blocks of Ordovician quartzitic sandstones immersed in the Rinconada mélange reveal a kind of deposit not reported in the Argentine Precordillera so far, as were laid down in this basin.

ACKNOWLEDGMENTS

REFERENCES

ALBANESI, G. G., BERGSTRÖM, S. M., SCHMITZ, B., SERRA, F., FELTES, N. A., VOLDMAN, G. G. and ORTEGA, G., 2013. Darriwilian (Middle Ordovician) $\delta^{13}C$ chemostratigraphy in the Precordillera of Argentina: Documentation of the middle Darriwilian Isotope Carbon Excursion (MDICE) and its use for intercontinental correlation. *Palaeogeography, Palaeoclimatology, Palaeoecology,* 389: 48–63.

AMOS, A. J., 1954. Estructura de las formaciones paleozoicas de La Rinconada, pie oriental de la Sierra Chica de Zonda, San Juan. *Revista de la Asociación Geológica Argentina*, 9: 5–38

BAUER, J. A., 2010. Conodonts and Conodont Biostratigraphy of the Joins and Oil Creek Formations, Arbuckle Mountains, South-central Oklahoma. *Oklahoma Geological Survey Bulletin*, 1–39.

BENEDETTO, J. L. and FRANCIOSI, M., 1998. Braquiópodos silúricos de las Formaciones Tambolar y Rinconada en la Precordillera de San Juan, Argentina. *Ameghiniana*, 35 (2): 115–132.

BENEDETTO, J. L., ACEÑOLAZA, G. F., ALBANESI, G. L., *et al.,* 2007. Los fósiles del Proterozoico Superior y Paleozoico Inferior de Argentina. *Asociación Paleontológica Argentina, Publicación Especial*, 11: 9–32.

COOPER, R. A. and SADLER, P. M., 2012. The Ordovician Period. In: Gradstein, F. M., Ogg, J. G., Schimtz, M. D. and Ogg, G. M., Eds., *The Geologic Time Scale 2012*, 489–523. Amsterdam: Elsevier.

CUERDA, A. J., 1981. Graptolites del Silúrico inferior de la Formación Rinconada, Precordillera de San Juan. *Ameghiniana*, 18: 241–247.

DORN, G. A., 1993. "Estudio estratigráfico de la Formación Rinconada en su localidad tipo, Sierra Chica de Zonda, Precordillera de San Juan". Universidad Nacional de Córdoba, unpubl. Thesis, 75 pp.

EPSTEIN, A. G., EPSTEIN, J. B. and HARRIS, L. D., 1977. *Conodont color alteration – An index to organic metamorphism*. Washington, DC: U. S. Geological Survey. Professional Paper 995, 27 pp.

GOSEN, W. VON, BUGGISCH, W. and LEHNERT, O., 1995. Evolution of the Early Paleozoic mélange at the eastern margin of the Argentine Precordillera. *Journal of South America Earth Sciences*, 8: 405–424

HEIM, A., 1948. *Observaciones tectónicas en la Rinconada, Precordillera de San Juan*. Buenos Aires: Secretaria de Industria y Comercio de la Nación, Dirección de Minas y Geología. Boletín 64: 44 pp.

LEHNERT, O., 1995. Ordovizische Conodonten aus der Präkordillere Westargentiniens: Ihre Bedeutung für Stratigraphie und Paläogeographie. *Erlanger Geologische Abhandlungen*, 125: 1–193.

MESTRE, A., 2009. Primeros conodontes de la Formación Tambolar (Facies Pachaco), Silúrico de la Precordillera Argentina, y sus implicancias bioestratigráficas. *Ameghiniana*, 46: 469–479.

PERALTA, S. H., 1993. Estratigrafía y consideraciones paleoambientales de los depósitos marino–clásticos eopaleozoicos de la Precordillera Oriental de San Juan. *Actas 12° Congreso Geológico Argentino*, *Mendoza*, 1: 128–137.

-----, 2013a. Devónico de la sierra de La Invernada, Precordillera de San Juan, Argentina: revisión estratigráfica e implicancias paleogeográficas. *Revista de la Asociación Geológica Argentina*, 70: 202–215.

-----, 2013b. El Silúrico de la sierra de La Invernada, Precordillera de San Juan: implicancias estratigráficas y paleogeográficas. *Revista de la Asociación Geológica Argentina*, 70: 477–487.

PERALTA, S. H. and MEDINA, E., 1986. Estratigrafía de la Formación Rinconada en el borde oriental del Cerro Pedernal, Precordillera Oriental de San Juan. *Actas Primeras Jornadas sobre Geología de la Precordillera, San Juan. Asociación Geológica Argentina, serie A*, 2: 157–162.

PERALTA, S. H. and ULIARTE, E., 1986. Estructura de la Formación Rinconada (Eopaleozoico) en su localidad tipo, Precordillera de San Juan. *Actas Primeras Jornadas sobre Geología de la Precordillera, San Juan. Asociación Geológica Argentina, serie A*, 2: 237–242.

SARMIENTO, G., VACCARI, N. and PERALTA, S. H., 1986, Conodontes ordovícicos de la Rinconada, Precordillera de San Juan, Argentina. *Actas IV Congreso Argentino de Paleontología y Bioestratigrafía*, *Mendoza*, 3: 219–224.

SERRA, F., ALBANESI, G. L., ORTEGA, G. and BERGSTRÖM, S. M., 2015. Biostratigraphy and palaeoecology of Middle–Late Ordovician conodont and graptolite faunas of the Las Chacritas River section, Precordillera of San Juan, Argentina. *Geological Magazine*, DOI: 10.1017/S0016756814000752.

STOUGE, S. 2012. Middle Ordovician (late Dapingian–Darriwilian) conodonts from the Cow Head Group and Lower Head Formation, western Newfoundland, Canada. *Canadian Journal of Earth Sciences*, 49: 59–90.

Biostratigraphy and paleoecology of Late Ordovician (Ka2) conodonts and microbrachiopods from north Queensland, Australia

Yong Yi Zhen and Ian G. Percival

Geological Survey of New South Wales, 947-953 Londonderry Road, Londonderry, N. S. W. 2753, Australia
yong-yi.zhen@trade.nsw.gov.au; ian.percival@trade.nsw.gov.au)

ABSTRACT: Late Ordovician conodont fauna from allochthonous limestones in the Wairuna Formation of the Broken River Province, north Queensland, contains 23 species typical of the deeper water *Protopanderodus* biofacies. Many of these species also occur in allochthonous limestones in the Malongulli Formation and correlative units of the Macquarie Volcanic Province in central New South Wales, and are also recognized in North and South China, which supports assignment of the Wairuna Formation conodont fauna to the *Taoqupognathus tumidus-Protopanderodus insculptus* Biozone of middle Katian age. Associated linguliformean brachiopods include species of *Acrosaccus*, *Atansoria*, *Biernatia*, *Conotreta*, *Elliptoglossa*, *Hisingerella*, *Nushbiella*, *Paterula* and *Scaphelasma*, which are identical to those known from the Malongulli Formation. Subtle paleoecological differences between faunas of the Malongulli Formation limestones (interpreted as forming in a deeper water peri-platform and upper slope environment) and those of the Wairuna Formation limestones imply that the latter were likely originally deposited on the shelf edge and subsequently reworked downslope. This study provides compelling paleontological evidence of strong affinity between Late Ordovician limestones of the Macquarie Volcanic Province and the Broken River Province, suggesting these regions (today separated by 1600 km) were linked by a volcanic island chain characterized by identical geochemical signatures in volcanic rocks associated with the limestones.

INTRODUCTION

Late Ordovician faunas are known from just two localities in eastern Queensland. Palmieri (1978) described conodonts from the Fork Lagoons beds of the Anakie Inlier in central Queensland. The second locality is within the Wairuna Formation of the Broken River Province of north Queensland, about 200 km west of Townsville (Fig. 1), from which heliolitine corals were described by Dixon and Jell (2012) and a few conodonts have been illustrated (Talent et al. 2002, 2003). Our contribution documents the diverse conodont and linguliformean microbrachiopod fauna recovered from allochthonous limestone within the Wairuna Formation exposed along Kaos Gully (Fig. 1). Conodont species include *Aphelognathus* sp., *Belodina confluens*, *Belodina* sp., *Besselodus* sp. nov., *Coelocerodontus trigonius*, *Drepanodus arcuatus*, *Drepanoistodus suberectus*, Gen. et sp. nov., *Panderodus gracilis*, *Panderodus nodus*, *Panderodus* sp., *Paroistodus*? *nowlani*, *Paroistodus* sp., *Periodon grandis*, *Phragmodus undatus*, *Pseudooneotodus mitratus*, *Protopanderodus insculptus*, *Protopanderodus liripipus*, *Scabbardella altipes*, *Strachanognathus parvus*, *Spinodus spinatus*, *Taoqupognathus tumidus* and *Yaoxianognathus* sp. (Fig. 2). This fauna is typical of the *Protopanderodus* biofacies found in shelf margin to slope settings, and is dated as middle Katian (Fig. 3). Associated brachiopods include species of *Acrosaccus*, *Atansoria*, *Biernatia*, *Conotreta*, *Elliptoglossa*, *Glossella*, *Hisingerella*, *Nushbiella*, *Paterula* and *Scaphelasma* (Fig. 4). The fauna is highly significant in demonstrating strong paleoecological affinity to contemporaneous deeper water assemblages flanking volcanic islands of the Macquarie Volcanic Province of central NSW (New South Wales), separated today by more than 1600 km from the Broken River Province.
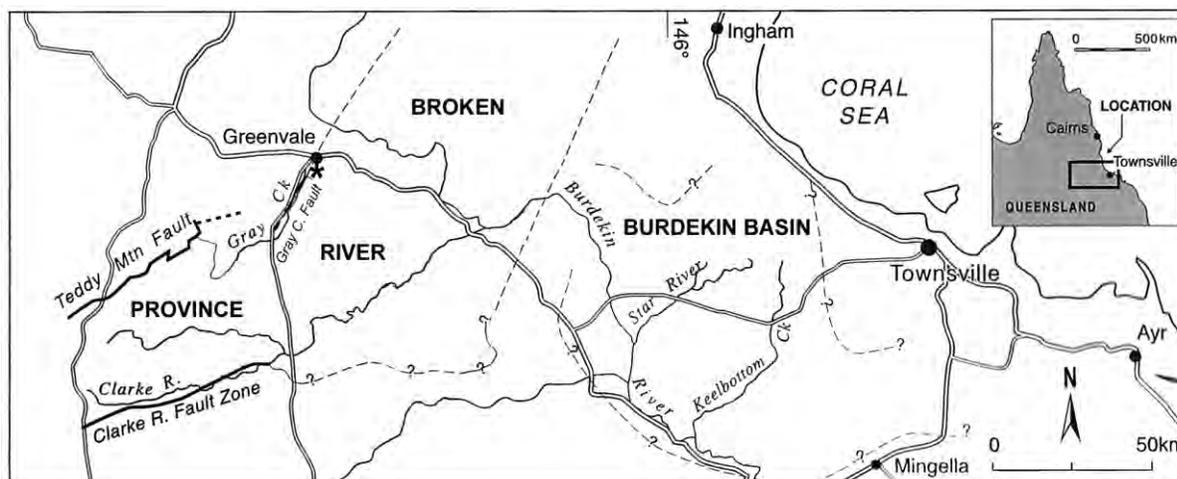
Figure 1. —Map showing the study area in the Townsville hinterland, north Queensland (modified from Talent et al., 2003). Locality of the Kaos Gully section, just south of Greenvale, is indicated by a star. Major tectonic elements of the region are shown, including the Broken River Province and the Burdekin Basin.

BIOSTRATIGRAPHY

Zhen (2001) established three successive Late Ordovician conodont zones in eastern Australia and China based on species of *Taoqupognathus*, from oldest to youngest *T. philipi*, *T. blandus*, and *T. tumidus*. Biostratigraphically important conodonts recognized in the Wairuna Formation include *T. tumidus* (Fig. 2. 19)*, Protopanderodus insculptus* (Fig. 2. 9)*, P. liripipus* (Fig. 2. 8)*, Periodon grandis* (Fig. 2. 5), *Belodina confluens* (Fig. 2. 1) and *Phragmodus undatus* (Fig. 2. 10). This fauna correlates with the *T. tumidus* fauna, widely reported from the Macquarie Volcanic Province of NSW and elsewhere in eastern Gondwana and peri-Gondwana (Fig. 3). More specifically, the north Queensland fauna is almost identical at species level with that previously documented from allochthonous limestone clasts in the lower part of the Malongulli Formation in central NSW (Trotter and Webby 1995). Its middle Katian age (Eastonian 3, possibly extending into Eastonian 4) is further constrained by graptolites of late Katian (earliest Bolindian) age occurring higher in the Malongulli Formation (Percival et al. this volume).

In the Ordos Basin of North China, *T. tumidus* was reported from the top of the Taoqupo Formation (Zhen et al. 2003), which is considered to be of middle Katian age and correlated with the *pygmaeus* to *complexus* graptolite Biozones (Chen et al. 1995). *Taoqupognathus blandus* first appears in the upper part of the Yaoxian Formation (which underlies the Taoqupo Formation), hence the *T. blandus* Biozone recognized in eastern Australia can be correlated with the uppermost *Tasmanognathus gracilis-Tas. multidentatus* Biozone (upper part of the Yaoxian Formation) and the *Y. neimengguensis* Biozone (spanning the lower part of the Taoqupo Formation) of the Ordos Basin in North China. The succeeding *T. tumidus* Biozone of eastern Australia correlates with the *Y. yaoxianensis* Biozone of North China (Zhen 2001) and with the *Protopanderodus insculptus* Biozone in South China (Fig. 3). In eastern Australia, *P. insculptus* was reported only in the *T. tumidus* Biozone in association with *P. liripipus*, and it is absent from the underlying *T. blandus* Biozone. Similarly in South China, *P. liripipus* is common in the entire Pagoda Formation (both *H. europaeus* and *P. insculptus* biozones) and its time equivalent units, but only occurs in association with *P. insculptus* at the top of the Pagoda Formation and the Linhsiang Formation in the *P. insculptus* Biozone.

83
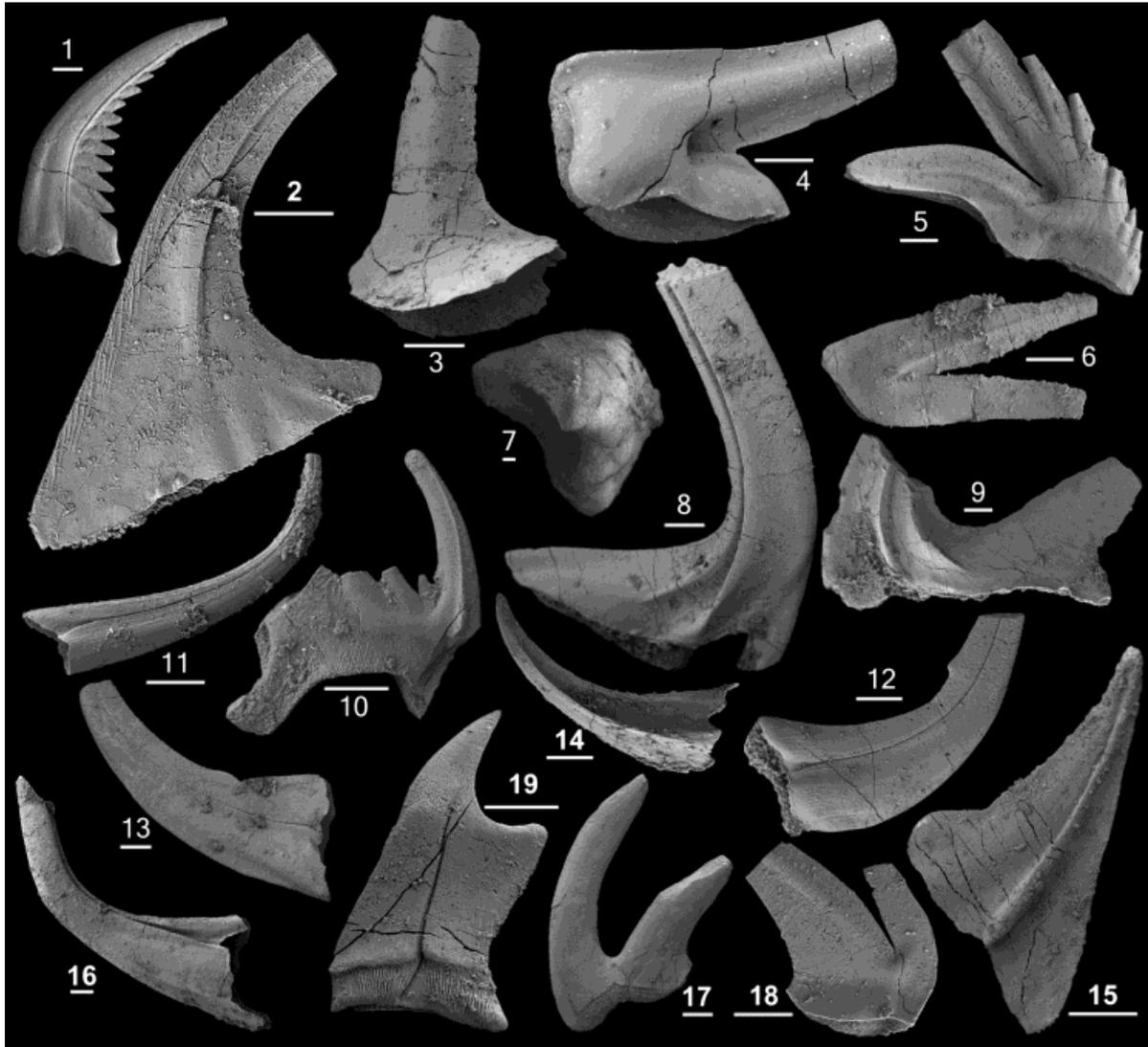
Figure 2. —Late Ordovician (Ka2) conodonts from allochthonous limestone within the Wairuna Formation. 1, *Belodina confluens* **Sweet, S2 (grandiform) element, view of furrowed side. 2,** *Besselodus* **sp. nov. Sc element, inner-lateral view. 3,** *Drepanoistodus suberectus* **(Branson and Mehl), Sa element, lateral view. 4,** *Paroistodus* **sp. M element, posterior view. 5,** *Periodon grandis* **(Ethington), M element, posterior view. 6,** *Paroistodus?* ***nowlani*** **Zhen, Webby and Barnes, M element, anterior view. 7,** *Pseudooneotodus mitratus* **(Moskalenko), upper view. 8,** *Protopanderodus liripipus* **Kennedy, Barnes and Uyeno, Sb element, outer-lateral view. 9,** *Protopanderodus insculptus* **(Branson and Mehl), Sc element, inner-lateral view. 10,** *Phragmodus undatus* **Branson and Mehl, Sb element, outer-lateral view. 11,** *Panderodus gracilis* **(Branson and Mehl), similiform element, outer-lateral view. 12,** *Panderodus nodus* **Zhen, Webby and Barnes, long-based element, outer-lateral view. 13,** *Panderodus* **sp. outer-lateral view. 14,** *Coelocerodontus trigonius* **Ethington, asymmetrical tetragoniform element, outer-lateral view. 15, Gen. et sp. nov. Pa element, inner-lateral view. 16,** *Scabbardella altipes* **(Henningsmoen), Sb (long-based acodiform) element, outer-lateral view. 17,** *Spinodus spinatus* **(Hadding) Sc element, outer-lateral view. 18,** *Strachanognathus parvus* **Rhodes. short-based element, inner-lateral view. 19,** *Taoqupognathus tumidus* **Trotter and Webby, Sb3 element, outer-lateral view. Scale bars 100 µm.**

Series	Stage	Conodont zones North American Midcontinent	Conodont zones Baltoscandia		Conodont zones Australia	Conodont zones North China	Conodont zones South China
Late Ordovician	Hirnantian	Aphelognathus shatzeri	O. hassi (lower part)		?	?	Aphelognathus ordovicicus
			Noixodontus fauna				
			Amorphognathus ordovicicus			Aph. zuoquensis	
	Ka4	Aph. divergens				Aph. divergens	
	Ka3	Aph. grandis				Aph. grandis	
	Ka2	Oulodus robustus	Amorphognathus superbus		Tao. tumidus - Pro. insculptus *	Yaoxianognathus yaoxianensis	Protopanderodus insculptus
		O. velicuspis					
	Ka1	Belodina confluens			Tao. blandus	Yaoxianognathus neimengguensis	Hamar. europaeus
		Plectodina tenus	Baltoniodus alobatus		Tao. philipi	Tas. multidentatus	Baltoniodus alobatus
	Sandb.	Ph. undatus			Tas. careyi	Tas. gracilis	

Figure 3. —Conodont-based correlation of the allochthonous limestone (indicated by *) within the Wairuna Formation with other Late Ordovician conodont successions established in Australia, North China (An and Zheng 1990; Wang et al. 2011), South China (Wang et al. 2011), Baltoscandia and North American Midcontinent.

PALEOECOLOGY

The Kaos Gully conodont assemblage is quantitatively dominated by four species – *Scabbardella altipes* (Fig. 2. 16)*, Besselodus* sp. nov. (Fig. 2. 2), *Protopanderodus liripipus* (Fig. 2. 8) and *P. insculptus* (Fig. 2. 9) – which together constitute over three-quarters of all specimens recovered. This assemblage represents a typical *Protopanderodus* biofacies found in shelf margin to slope settings, and supports interpretation of an allochthonous origin for the limestone in the Wairuna Formation (Talent et al. 2002, 2003) which probably formed on the shelf edge before being redeposited downslope. Associated linguliformean microbrachiopods in the limestone include *Elliptoglossa adela*, *Paterula malongulliensis* and *Hisingerella hetera* together with new species of *Acrosaccus*, *Atansoria*, *Biernatia*, *Nushbiella* and *Scaphelasma* which also occur in allochthonous limestones of the Macquarie Volcanic Province in central NSW (Percival et al. in review). The fauna of those limestones from NSW, characterized by a distinctive siliceous sponge component not seen in the Broken River Province, is interpreted to indicate original deposition in an outer shelf edge to upper slope periplatformal setting (Webby 1992; Percival and Webby 1996), probably in deeper water than the limestones in the Wairuna Formation.

CONCLUSIONS

Late Ordovician deeper water limestones preserved as allochthonous clasts in the Wairuna Formation of the Broken River Province represent the last known vestige of a probable chain of volcanic islands that stretched for 1600 km or more (present day) offshore to the eastern margin of Gondwana. The conodont and microbrachiopod fauna comprises identical species to those in the contemporaneous Malongulli Formation of the Macquarie Volcanic Province in central NSW. This paleontological evidence provides additional and independent support for linkages previously recognised between the two regions, based on significant similarities in the geochemical signature of volcanic rocks associated with the Ordovician limestones in both provinces (Henderson et al. 2011).
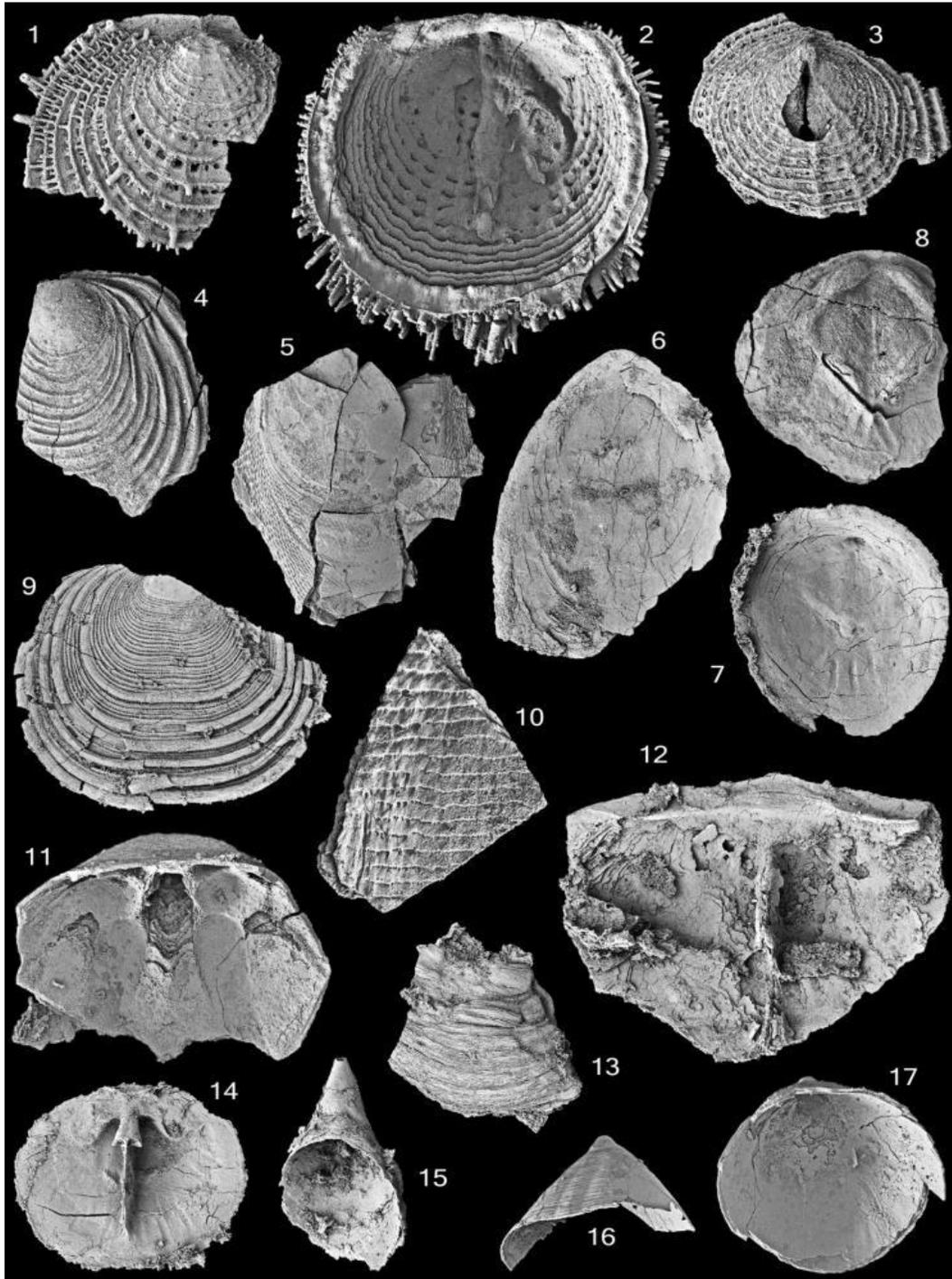
Figure 4. —Late Ordovician (Ka2) linguliformean microbrachiopods from allochthonous limestone within the Wairuna Formation. 1-3, *Nushbiella* sp. nov., 1, exterior of dorsal valve, x30; 2, interior of dorsal valve, 20; 3, exterior of ventral valve, x30. 4, *Acrosaccus* sp. nov., exterior of dorsal valve, x30. 5. *Glossella* sp., indeterminate valve exterior, x15. 6, *Elliptoglossa adela* Percival, interior of ventral valve, x25. 7, *Paterula malongulliensis* Percival, interior of dorsal valve, x50. 8, *Atansoria* sp. nov., interior of dorsal valve, x30. 9, *Scaphelasma* sp., exterior of dorsal valve, x40. 10, *Westonia*? sp., fragment of shell exterior showing distinctive ornament, x15. 11, 12, *Conotreta*? sp., 11, interior of ventral valve, x30; 12, interior of dorsal valve, x30. 13, *Undiferina* sp., fragment of shell exterior, x30. 14, 15, *Biernatia* sp. nov., 14, interior of dorsal valve, x40; 15, oblique view of ventral valve showing partial interior, x40. 16, 17, *Hisingerella hetera* (Percival), 16, posterior view of ventral valve to show pseudointerarea, x30; 17, interior of ventral valve, x30.

ACKNOWLEDGMENTS

REFERENCES

AN, T. X. and ZHENG, S. C., 1990. *The conodonts of the marginal areas around the Ordos Basin, North China*. Beijing: Science Press, 199 pp. (in Chinese with English abstract).

CHEN, X., RONG, J. Y., WANG, X. F., WANG, Z. H., ZHANG, Y. D. and ZHAN, R. B., 1995. *Correlation of the Ordovician rocks of China: charts and explanatory notes.* International Union of Geological Sciences, Publication 31, 104 pp.

DIXON, O. A. and JELL, J. S., 2012. Heliolitine tabulate corals from Late Ordovician and possibly early Silurian allochthonous limestones in the Broken River Province, Queensland, Australia. *Alcheringa*, 36, 69-98.

HENDERSON, R. A., INNES, B. M., FERGUSSON, C. L., CRAWFORD, A. J. and WITHNALL, I. W., 2011. Collisional accretion of a Late Ordovician oceanic island arc, northern Tasman Orogenic Zone, Australia. *Australian Journal of Earth Sciences*, 58: 1-19.

PALMIERI, V., 1978. *Late Ordovician conodonts from the Fork Lagoons Beds, Emerald area, central Queensland.* Geological Survey of Queensland Publication 369, Palaeontological Paper 43, 55 pp.

PERCIVAL, I. G., KRAFT, P., ZHANG, Y. D. and SHERWIN, L. 2015. A long-overdue systematic revision of Ordovician graptolite faunas from New South Wales, Australia. *Stratigraphy*, 12: (this issue.)

PERCIVAL, I. G. and WEBBY, B. D., 1996. Island benthic assemblages: with examples from the Late Ordovician of Eastern Australia. *Historical Biology*, 11: 171-185.

TALENT, J. A., MAWSON, R. and SIMPSON, A., 2003. The "lost" Early Ordovician-Devonian Georgetown Carbonate Platform of northeastern Australia. *Courier Forschungsinstitut Senckenberg*, 242: 71-80.

TALENT, J. A., MAWSON, R., SIMPSON, A. and BROCK, G. A., 2002. *Palaeozoics of NE Queensland: Broken River Region: Ordovician-Carboniferous of the Townsville hinterland: Broken River and Camel Creek regions, Burdekin and Clarke River basins*. Sydney: Macquarie University Centre for Ecostratigraphy and Palaeobiology. Special Publication No. 1: International Palaeontological Congress Post-5, Field Excursion Guidebook.

TROTTER, J. A. and WEBBY, B. D., 1995. Upper Ordovician conodonts from the Malongulli Formation, Cliefden Caves area, central New South Wales. *AGSO Journal of Australian Geology and Geophysics*, 15(4): 475-499.

WANG, Z. H., QI, Y. P. and WU, R. C., 2011. *Cambrian and Ordovician conodonts in China*. Hefei: China University of Science and Technology Press, 388 pp. (in Chinese with English summary).

WEBBY, B. D. 1992. Ordovician island biotas: New South Wales record and global implications. *Journal and Proceedings of the Royal Society of New South Wales*, 125: 51-77.

ZHEN, Y. Y., 2001. Distribution of the Late Ordovician conodont genus *Taoqupognathus* in eastern Australia and China. *Acta Palaeontologica Sinica*, 40(3): 351-361.

ZHEN, Y. Y., PERCIVAL, I. G. and FARRELL, J. R., 2003. Late Ordovician allochthonous limestones in Late Silurian Barnby Hills Shale, central western New South Wales. *Proceedings of the Linnean Society of New South Wales*, 124: 29-51.

ABSTRACTS
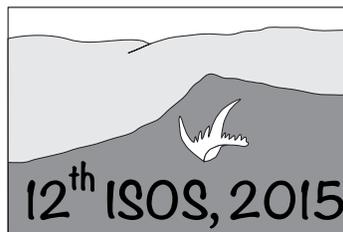
Deciphering the movement of the Argentine Precordillera from tropical to higher latitudes, Late Cambrian–Late Ordovician, through conodont $\delta^{18}O$ paleothermometry

Guillermo L. Albanesi[1], Christopher R. Barnes[2], Julie A. Trotter[3], Ian S. Williams[4], and Stig M. Bergström[5]

[1]*CICTERRA-CONICET – Facultad de Ciencias Exactas, Físicas y Naturales, Universidad Nacional de Córdoba, Av. Vélez Sarsfield 1611, Córdoba, X5016GCA, Argentina, galbanes@com.uncor.edu.*
[2]*School of Earth and Ocean Sciences, University of Victoria, P.O. Box 1700, Victoria, V8W 2Y2, B.C., Canada.*
[3]*School of Earth and Environment, University of Western Australia, Perth, WA 6009, Australia.*
[4]*Research School of Earth Sciences, Australian National University, Canberra, ACT 0200, Australia.*
[5]*School of Earth Sciences, Division of Earth History, The Ohio State University, 125 S. Oval Mall, Columbus, Ohio 43210.*

The Cambrian-Middle Ordovician succession in the Precordillera of north-central Argentina is in several respects unique in South America. It is largely composed of richly fossiliferous carbonates whose lithology and diverse shelly and conodont faunas differ conspicuously from those of coeval poorly fossiliferous clastic successions in adjacent parts of Gondwana. Because of these differences, the Precordillera has during recent decades been regarded as an allochthonous tectonic unit of the exotic Cuyania Terrane whose geographic origin has been controversial. Hence, in some models, the Precordillera has been interpreted to be originally derived from a low-latitude segment of Gondwana and later in the Ordovician moved southward toward higher latitudes during periods of major faulting. In another, and perhaps more common model, the Precordillera is interpreted to have moved during the Late Cambrian-Early Ordovician from the southern margin of Laurentia across the Iapetus Ocean to finally dock at higher latitudes with Gondwana as suggested by the end of carbonate deposition and the presence of Late Ordovician glaciogenic sediments. However, many details in the Precordilleran drift history remain unclear.

The Late Cambrian-Early Ordovician shelly faunas in the Precordillera are of general Laurentian type but stratigraphically slightly younger faunas have a paleogeographically mixed character where during the Dapingian-Darriwilian there is a gradually increasing number of colder-water taxa typical of the Avalonian and Baltic Provinces. This faunal change is exhibited in several fossil groups.

Obviously, changes in ocean temperature are likely to reflect latitudinal changes of a moving microcontinent such as the Precordillera. In order to test if such temperature changes could be used for tracing the drift of the Precordillera, we used the oxygen composition ($\delta^{18}O_{phos}$) from well-preserved conodonts from Precordilleran and Laurentian successions. The objective was to test the possibility of a general temperature trend toward colder ocean water during the late Furongian (Late Cambrian)-early Sandbian (Late Ordovician) time that could reflect a latitudinal drift of the Precordillera. We used biostratigraphically well-dated samples from the Precordillera and two Laurentian control sites in Texas and Alberta. The $\delta^{18}O$ composition in conodonts was measured *in situ* at high spatial resolution (30μ spots) using the sensitive high resolution ion microprobe (SHRIMP II) at the Australian National University. The conodont $\delta^{18}O$ values range from 16.9 in the Tremadocian to 19.5 in the Sandbian for the Precordillera, whereas this degree of change is not seen in the values obtained from the conodonts of Texas and Alberta representing Laurentia.

The resulting data show that there is a progressive change toward colder sea water temperatures in the Precordilleran samples after the early Darriwilian. This change can be correlated with the period of increased influx of colder-water faunal elements. Unfortunately, the virtual absence of conodont-bearing carbonates in the Upper Ordovician of the Precordillera makes it impossible to continue these studies into the Late Ordovician. However, we conclude that the new isotope data support the model of a drift of the Precordillera from tropical to higher latitudes across the Iapetus but further detailed studies in the Precordilleran and North American successions are needed to clarify unequivocally whether or not the Precordillera originated from southern Laurentia (Ouachita Embayment) as advocated by many authors.

A CONOP9 quantitative stratigraphic model of Baltic Ordovician and Silurian chitinozoan distribution and K-bentonites

Liina Antonovitš, Viiu Nestor, Jaak Nõlvak, Garmen Bauert, Olle Hints, and Tarmo Kiipli

Institute of Geology at Tallinn University of Technology, Ehitajate 5, 19086, Tallinn, Estonia; liina.paluveer@ttu.ee.

The Baltic Ordovician-Silurian sedimentary succession is rich in well-preserved microfossils and contains numerous altered volcanic ash beds, both of which are valuable tools for regional stratigraphy. Over decades large amounts of data on the distribution of chitinozoans and conodonts have been collected in the Baltic region, and the corresponding biozonations are well established. Also, new methods have allowed much improved fingerprinting of individual K-bentonite layers. Such large integrated data sets can be efficiently analyzed and interpreted by the help of quantitative stratigraphic tools. One of these, CONOP9, has proved especially useful for automatic correlation as well as for high-resolution biodiversity analysis (Sadler 2012). We have previously applied CONOP9 to analyze diversification history of Ordovician and Silurian chitinozoans (Hints et al. 2011 and Paluveer et al. 2014). Here we extend these approaches by combing the Ordovician and Silurian data sets, including data from additional sections and incorporating the K-bentonite database in order to provide independent test for biostratigraphy and examine possible links between volcanic activity and chitinozoan diversity. The combined Ordovician-Silurian data set includes 80 sections from Baltoscandia, and 319 chitinozoan species and 50 geochemically fingerprinted K-bentonites (Kiipli et al. 2013). The composite model was created after several consecutive runs of CONOP9; good results were achieved using level penalty with ca 1200 steps and 6000 trials. Secondary penalty of TEASER and STACKER were applied to avoid placing an event in a section where it was not observed and to penalize taxon ranges from extending too far.

The CONOP9-derived diversity curve shows that chitinozoans thrived during the Darriwillian and Sandbian with standing diversity reaching 40 species in Baltoscandia. A small crisis coincided with the basal Katian, followed by a major late Katian-Hirnantian decline and extinction, with ca 10 species crossing the system boundary. The Silurian diversity peaks in the Telychian and late Sheinwoodian – early Homerian reached standing diversity of ca 30 species. The main Silurian biotic crises for chitinozoans correspond to the Ireviken and Mulde events and associated environmental changes. However, the Lau Event is not clearly expressed in the model suggesting that it might have been less severe for chitinozoans compared to the Hirnantian, Ireviken and Mulde events. A best-fit CONOP9 composite has strong local range support in the Ordovician, where the model revealed excellent or above-average fit of most conventional index species. In the Silurian the zonal taxa generally showed larger misfit values. Incorporation of K-bentonites did not alter chitinozoan succession, but helped to more precisely correlate the CONOP9 composite with regional stages.

REFERENCES

HINTS, O., NÕLVAK, J., PALUVEER, L. and TAMMEKÄND, M., 2011. Conventional and CONOP9 approaches to biodiversity of Baltic Ordovician chitinozoans. In: Gutiérrez-Marco, J.C., Rábano, I. and García-Bellido, D., Eds., *Ordovician of the World*, 243-249. Madrid: *Instituto Geológico y Minero de España. Cuadernos del Museo Geominero*, no. 14.

KIIPLI, T., KALLASTE, T., KIIPLI, E. and RADZEVICIUS, S., 2013. Correlation of Silurian bentonites based on the immobile elements in the East Baltic and Scandinavia. *GFF*, 135(2):152-161.

PALUVEER, L., NESTOR, V. and HINTS, O., 2014. Chitinozoan diversity in the East Baltic Silurian: first results of a quantitative stratigraphic approach with CONOP. *GFF*, 136(1):198-202.

SADLER, P. M., 2012. Integrating carbon isotope excursions into automated stratigraphic correlation: an example from the Silurian of Baltica. *Bulletin of Geosciences,* 87:681-694.

Recurring taphofacies in the Upper Ordovician (Katian) of the Cincinnati Arch: A predictive model based on sequence stratigraphy

Christopher D. Aucoin[1], Carlton E. Brett[1], James R. Thomka[1], and Benjamin F. Dattilo[2]

[1]500 Geology-Physics Building, University of Cincinnati, Cincinnati OH 45221, aucoincd@mail.uc.edu.
[2]Department of Geosciences, Indiana University-Purdue University-Fort Wayne, 2101 East Coliseum Blvd, Fort Wayne, Indiana, 46805.

The Upper Ordovician (Katian: Cincinnatian Series) in the Ohio-Kentucky-Indiana tristate is known for its diverse fossil assemblages. These include several distinct recurring tapho- and biofacies, including: A) shell-rich, often slightly phosphatic, fossil fragmental packstones and grainstones; B) nodular shaly packstones rich in relatively well preserved bryozoans and brachiopods; C) blue-gray claystone deposits commonly referred to as 'butter shales', generally with few interbeds; these are typically rich in bivalves and may contain articulated trilobites. These facies form meter to decameter scale cycles, some of which have been traced for over 150 km, indicating that these do not represent simple localized events, but rather broad scale depositional intervals. Type B shelly mudstones appear to reflect somewhat less storm reworked, fully oxic facies with higher input of terrigenous sediment. Finally, Type C taphofacies also referred to as 'trilobite shales' contain relatively abundant, articulated trilobites and well-preserved mollusks, including uncrushed and commonly *in situ* bivalves. These beds may pass upramp into sparse greenish gray mudstones that contain a mixture of mollusks and opportunistic bryozoans.

Here we present the occurrence of these facies in the context of eustatic fluctuations at multiple scales, resulting in a predictive model for development of such bodies based on the coincidence of specific systems tracts of different orders. Type A shelly limestones are composed of disarticulated and/or fragmented brachiopod, crinoid, and bryozoan debris, frequently with minor impregnation of grains by phosphate. These deposits record prolonged reworking of shelly debris and probably time averaging during intervals of low sedimentation, which promoted shell build-up by reworking and taphonomic feedback. Such facies are widespread during times of early transgression when nearshore sequestering was coupled to offshore sediment starvation. Storm winnowing further concentrated skeletal accumulations. They are probably best developed when short-term transgressions were superimposed on overall deepening trends. Under conditions of somewhat greater sediment input, mixed mud and shell accumulations of Type B developed; largely in the highstands of small scale cycles superimposed on longer term stable to slightly falling sea level trends. In contrast Type C butter shales represent low-energy environments with a moderate background influx of mud-dominated sediment, which favored vagrant trilobites and infaunal deposit- and suspension-feeding annelids and mollusks. Rapidly deposited mud layers up to several centimeters thick episodically smothered benthic communities. These conditions generally occur in the late transgressive to early highstand systems tracts (HSTs) of certain sedimentary cycles. We suggest that the most persistent trilobite-bearing butter shales form preferentially where the HST of a higher-order sequence is superimposed upon a longer-term HST to falling state systems tract, amplifying offshore mud sedimentation.

A model combining the effects of offshore sediment starvation during base level rise, and offshore mud sedimentation during highstands provides the basis for understanding three tapho- and biofacies of skeletal accumulation. Superimposition of the different phases of small and larger scale cycles can produce weakening or amplification of these effects yielding mixed shelly mudrocks, or the more extreme end members: TST-TST pairings produce especially sediment starved conditions and condensed beds; HST-HST pairings produce distinctive thicker mudstone intervals. This generalized model explains many of the features of the classic Cincinnatian and similar mixed siliciclastic-carbonate systems.

Correlation of Upper Ordovician K-bentonites in the East Baltic – A combined approach of chitinozoan biostratigraphy and sanidine geochemistry

Heikki Bauert, Garmen Bauert, Jaak Nõlvak, and Tarmo Kiipli

Institute of Geology at Tallinn University of Technology, Ehitajate tee 5, Tallinn 19086; heikki.bauert@ttu.ee.

Ordovician K-bentonite beds have a long history of investigation and by now have been reported on most major paleocontinents. As the corresponding volcanic eruptions represent instantaneous events in the geological record, the K-bentonites are invaluable for local and regional correlations as well as for radiometric dating and for building up a global numeric time scale. About a hundred K-bentonites have been identified in the Upper Ordovician mudstones in Scania, southern Sweden. However a vast majority of these are thin (less than 1 cm) and are difficult to identify in the coeval carbonate-dominated successions of the Baltoscandian basin, which obviously limits the usage of K-bentonites in regional chronostratigraphy. In this study we analyse the potential of chitinozoan biostratigraphy combined with fingerprinting sanidine phenocryst composition to aid correlation of Sandbian and Katian K-bentonites in the Paleobaltic basin. The high evolution rate of chitinozoans and their planktic behavior makes them a valuable correlation tool for Lower Paleozoic rocks. They are among the most useful microfossils in the Upper Ordovician strata of Baltoscandia, providing biostratigraphic resolution which far exceeds of that of conodonts.

The Kukruse K-bentonite (more appropriately termed as a feldspathic tuff) is encountered in drillcores of Central Estonia can be confidently traced outside of oil shale accumulation area in the Paleobaltic basin by the presence of *Conochitina tigrina*. Up to 17 thin K-bentonites (Grefsen and Sinsen K-bentonite complexes) have been recorded in the variably argillaceous wackestones of the Haljala Stage, although the usual number encountered in a single drill core is three to seven ones. The Grefsen and Sinsen K-bentonite complexes, erected in Norway, can not be reliably separated in the East Baltic sections neither by chitinozoans nor by conodonts. The Kinnekulle K-bentonite at the base of the Keila Stage is the thickest and the most widely studied Upper Ordovician K-bentonite in Baltoscandia. As for chitinozoan biostratigraphy, this bed is located just below the findings of extremely short-ranged *Angochitina multiplex* encountered at least in 10 East Baltic and 2 Swedish drillcore sections. Five Katian K-bentonites of Pirgu age have been distinguished in the East Baltic sections. The lower two occur in the *Tanuchitina bergstroemi* Zone, while three others can be found in the overlying *Conochitina rugata* Zone. *Bursachitina umbilicata* is another chitinozoan key species which occurrence is strictly restricted to the *Conochitina rugata* Zone.

The Institute of Geology at Tallinn University of Technology has successfully applied a little used XRD method to determine the (Na+Ca) component in sanidine phenocrysts that can be useful for discriminating individual K-bentonite beds. The Na+Ca content in sanidine $(K,Na,Ca)AlSi_3O_8$ solid solution was calculated using a linear relationship between K-sanidine (d = 4.233 Å) and albite (d = 4.033 Å). In favourable cases (a sharp sanidine 201 reflection and a low content of authigenic potassium feldspar) the precision of the method is ± 1%, in less favourable cases – the precision is ± 2%. The studies accomplished in recent years have shown a good potential of this method for discriminating the Katian K-bentonites of Pirgu age in the East Baltic with the following results: BIV – 47–48; BIII – 34-36; BII – 42–44, BI – 37–38, BI – 25 mol%. The corresponding values for the Kinnekulle K-bentonite of Sandbian age range between 24–26 mol%. The same method has been successfully applied for discrimination of Silurian K-bentonites in the East Baltic sections.

Detailed chitinozoan biostratigraphic studies, combined with XRD fingerprinting of sanidine composition, could be a promising cost-effective and time-wise supplementary method in discriminating individual K-bentonite beds in other Lower Paleozoic paleobasins as well.

Lithologies, ages, and provenance of clasts in the Ordovician Fincastle Conglomerate, Botetourt County, Virginia, USA

Harvey E. Belkin, John E. Repetski, and Randall C. Orndorff

U.S. Geological Survey, 12201 Sunrise Valley Drive, Reston, Virginia 20192, hbelkin@usgs.gov.

The Fincastle Conglomerate is a Middle or early Late Ordovician polymictic, poorly sorted, matrix- and clast-supported cobble-rich conglomerate that has limited outcrop in the overturned Pine Hills syncline

just north of Fincastle, VA. The Fincastle has been treated as a member of the Liberty Hall, Bays, or the Martinsburg Formation, and this controversy is not solved, to date, by this study. The Fincastle Conglomerate is the most northeastern of at least six coarse conglomerates located in a similar stratigraphic position that extend to Georgia from Virginia west of the Blue Ridge structural front. All except the Fincastle are dominated (>95%) by carbonate clasts; Fincastle clasts are much more varied and siliceous. It is this clast diversity that provides increased value for provenance and related studies. We have used a multidisciplinary approach that involves conodont analysis, sandstone petrography, *in-situ* outcrop clast characterization, optical and electron-beam petrography, and X-ray diffraction to provide data on lithologies, ages, and provenance.

   We examined samples from three Fincastle localities, the Dixon construction site along US Route 220, and east and west of Big Gulch, a ravine northeast along strike. The size, roundness, and lithology of 1,656 clasts (> 1 cm) were measured in the field. Average clast size was 4.4 cm; the largest clast found in this study was 21 cm and all were well- to sub-rounded. Although, the clast lithology varies among the different localities, the average lithology is sandstone and siltstone 12%, vein quartz 17%, limestone 31%, quartzite and meta-sandstone 31%, chert 6%, and others 3%. Neither dolomite, igneous, nor high-grade metamorphic clasts were identified either in field study or in detailed laboratory analysis.

   The lithologies, textures, and sedimentary structures of the Fincastle conglomerate indicate deposition in a submarine channel fan near the outer shelf edge of a foreland basin. Variability and relatively small-scale, discontinuous coarse conglomerate lenses suggest lateral migration of the channel. The roundness of the cobble-sized clasts indicates that they were re-deposited from another environment rather than eroded during canyon formation. The coarse, well-rounded clasts suggest a relatively near but, high relief source area.

   Quantitative estimates of framework constituents in 23 sandstones and 6 matrix samples were made using the point-counting technique (1000 counts) and petrographic modes were plotted on the ternary QFL diagram of Dickinson et al. (1983). Data for the Fincastle sandstones plot close to the Q-rich Q-F side and indicate tectonic environments from passive margin to transitional continental uplift. Matrix modes have considerably less feldspar and plot in the foreland basin tectonic environment region. The Fincastle sandstone modes are similar to those described from the Chilhowee suite by Simpson and Eriksson (1989, 1990).

   Paleogeographic and tectonic reconstruction, and facies distribution suggest that the Fincastle conglomerate was sourced from Taconic orogeny highlands to the southeast. The lack of dolomite clasts is curious even though the Upper Cambrian and Lower Ordovician succession in the vicinity is dominantly dolomite. This may suggest that the source of the carbonate clasts was to the east of the dolomitic shelfal carbonate facies of, e.g, the Upper Cambrian to Lower Ordovician Knox Group. Furthermore, the erosional level sampled by the Fincastle did not reach down to the underlying basement of igneous or high-grade metamorphic rocks. Several limestone clasts yielded sparse numbers of proto- and paraconodonts, indicating a most likely age of Late Cambrian or, less likely, earliest Early Ordovician for those clasts. Bits of matrix adhering onto those clasts produced a few euconodont fragments of taxa that range from Middle through Upper Ordovician; but do not confirm the identity of the host formation.

An integrated scheme for δ^{13}C chemostratigraphy and conodont biostratigraphy in the Ordovician of Sweden and useful tie-points for global correlation

Mikael Calner[1], Oliver Lehnert[1,2] , Rongchang WU[3], and Michael M. Joachimski[2]

[1]*Department of Geology, Lund University, Sölvegatan 12, SE-223 62 Lund, Sweden, Mikael.Calner@geol.lu.se.*
[2]*GeoZentrum Nordbayern, Lithosphere Dynamics, University of Erlangen-Nürnberg, Schloßgarten 5, D-91054, Erlangen, Germany.*

[3]Key Laboratory of Economic Stratigraphy and Palaeogeography, Nanjing Institute of Geology and Palaeontology, Chinese Academy of Sciences, 39 East Beijing Road, Nanjing 210008, China.

The Ordovician strata of Sweden and adjacent areas form a thin veneer of a cool-water type of limestone with subordinate fine-grained siliciclastic strata. Deeper subtidal mud mounds are locally important but true, shallow subtidal reefs with wave-resistant frameworks are absent. Carbonate skeletal grains and facies indicating tropical conditions first appear in the Hirnantian when Baltica has drifted northwards from middle latitudes into the southern hemisphere tropics. In the Early and Middle Ordovician the basin subsidence was extremely slow and adjacent relief was very small due to widespread peneplanation of the underlying basement rocks in the latest Precambrian. This lack of higher relief source areas and the cool climate result in exceptionally low carbonate sedimentation rates and the upper Tremadocian through Hirnantian succession is only slightly more than 100 metres thick in the Swedish parts of the Baltoscandian Basin. The evolving Caledonian Orogeny changed this pattern along the margins of the basin from about Mid Ordovician times during continental collision of Baltica with Laurentia-Greenland and Avalonia and emplacement of thrust sheets resulted in the development of foreland basins along the western and southern margins of Baltica, respectively. Over the last few years we have performed a series of detailed studies on Ordovician δ^{13}C chemostratigraphy and conodont biostratigraphy of core sections from southern and central Sweden (Bergström et al. 2011; 2012; Calner et al. 2014; Lehnert et al. 2014; Wu et al. 2015). These studies now provide a means of correlation of the Swedish Ordovician on regional and global scales. Most of the important tie-points for global chemostratigraphic correlation are identified (MDICE, GICE, KOPE, WHITEWATER, and HICE), suggesting that the stratigraphic completeness of the preserved Ordovician is surprisingly high and that the very minor thickness of strata is due to stratigraphic condensation rather than erosion. Of particular importance is the identification and characterization of several minor δ^{13}C excursions in the Floian, Dapingian and Darriwilian. Among these are both positive (BFICE) and negative excursions (BDNICE, LDNICE), which seem to be reliable correlation tools for the Baltoscandian Basin. Their potential for intercontinental correlation, however, has to be verified by future chemostratigraphic studies.

REFERENCES

BERGSTRÖM, S. M., CALNER, M., LEHNERT, O. and NOOR, A., 2011. A new Upper Ordovician-Lower Silurian drillcore standard succession from Borenshult in Östergötland, southern Sweden: 1. Stratigraphical review with regional comparisons. *GFF,* 133:149-171.

BERGSTRÖM, S. M., LEHNERT, O., CALNER, M. and JOACHIMSKI, M. M., 2012. A new Upper Ordovician-Lower Silurian drillcore standard succession from Borenshult in Östergötland, southern Sweden: 2. Significance of δ^{13}C chemostratigraphy. *GFF,* 134:39-63.

CALNER, M., LEHNERT, O., WU, R., DAHLQVIST, P. and JOACHIMSKI, M. M., 2014. δ^{13}C chemostratigraphy in the Lower-Middle Ordovician succession of Öland (Sweden) and the global significance of the MDICE. *GFF,* 136:48-54.

LEHNERT, O., MEINHOLD, G., WU, R., CALNER, M. and JOACHIMSKI, M. M., 2014. δ^{13}C chemostratigraphy in the late Tremadocian through early Katian carbonate succession of the Siljan district (Central Sweden). *Estonian Journal of Earth Sciences,* 63:277-286

WU, R., CALNER, M., LEHNERT, O., PETERFFY, O. and JOACHIMSKI, M. M., 2015. Lower-Middle Ordovician δ^{13}C chemostratigraphy of western Baltica (Jämtland, Sweden). *Palaeoworld.* doi:10.1016/j.palwor.2015.01.003.

Carbon isotope stratigraphy of the Ordovician-Silurian boundary interval and associated oolites in southern Norway

Hanna Calner[1], Mikael Calner[1], Oliver Lehnert[1, 2, 3]

[1]Department of Geology, Lund University, Sölvegatan 12, SE-223 62 Lund, Sweden; Hanna.Calner@geol.lu.se.
[2]GeoZentrum Nordbayern, Lithosphere Dynamics, University of Erlangen-Nürnberg, Schloßgarten 5, D-91054, Erlangen, Germany.
[3]Institute of Geology, Tallinn University of Technology, Ehitajate tee 5, Tallinn 19086, Estonia.

Oolitic limestone appears to form a time-specific sedimentary facies across Baltoscandia and much of the North American continent during a brief time interval in the latest Hirnantian. The North American oolites are known from e.g., Oklahoma and Texas panhandle (Keel/Pettit oolites), Arkansas (Cason oolite), and from Missouri and Illinois (Leemon oolite; all names following Amsden and Barrick 1986). In Baltoscandia, a similar, few metres thin suite of oolites is known from outcrops and core sections over a distance of at least 800 km across southern Norway (top of Langøyene Formation), southern Sweden (Skultorp Member of the Loka Formation) and Estonia (Saldus Formation). In China, the Kuanyinchiao oolitic bed appears to be of the same age. This circum-tropical distribution of Hirnantian oolites is of major significance in respect to environmental and biotic changes associated with the latest Ordovician mass-extinction. In a first step it is necessary to constrain the stratigraphic position of these oolites in order to evaluate their synchroneity in time. New and previously published $\delta^{13}C$ records across the stratigraphic range of several of the oolites show that they correspond in time with the late peak interval and early falling limb of the Hirnantian Isotope Carbon Excursion (HICE), i.e. in the late *extraordinarius* Zone (cf. Harper et al. 2014). We present the first $\delta^{13}C$ records from sections exposing the Ordovician-Silurian boundary interval in the Oslo-Asker district of southern Norway (see Calner et al. 2013 for a recent summary of the local geology). Here, oolites that are 2-9 m thick occurs at several localities; for instance quartz-rich oolitic limestone at Hovedøya (the Norwegian type locality for the Ordovician-Silurian boundary), and limestone conglomerates and oolites at Brønnøya, Konglungen, and at Vettre road-cut. At all localities the $\delta^{13}C$ values of the oolites scatters around 5‰ with a peak value of 5.90‰ recorded in a reworked clast in a conglomerate on southern Brønnøya, proving their Hirnantian age. At most localities the oolites are overlain by black shales of the Early Silurian Solvik Formation, marking the post-Hirnantian transgression. At the Ordovician-Silurian type locality at Hovedøya, however, the quartz-rich oolitic limestone and the black shales of the Solvik Formation are interlayered by a 0.6 m thick brown siltstone followed by a 0.6 m thick limestone-marl alternation. The $\delta^{13}C$ data scatter between 2-3‰ in the limestone-marl alternation confirming its Hirnantian age and the position of the Ordovician-Silurian boundary as defined by Worsley (1982).

REFERENCES

AMSDEN, T. W. and BARRICK, J., 1986. Late Ordovician-Early Silurian strata in the Cantral United States and the Hirnantian Stage. *Oklahoma Geological Survey Bulletin,* 139:95 pp.
CALNER, M., AHLBERG, P., LEHNERT, O. and ERLSTRÖM, M. (eds.) 2013. The Lower Palaeozoic of southern Sweden and the Oslo Region, Norway. Field Guide for the 3rd Annual Meeting of the IGCP project 591. *Sveriges geologiska undersökning, Rapporter och Meddelanden,* 133:96 pp. [available online at http://igcp591.org/]
HARPER, D. A. T., HAMMARLUND, E. U. and RASMUSSEN, C. M. Ø., 2014. End Ordovician extinctions: A coincidence of causes. *Gondwana Research,* 25:1294-1307.
WORSLEY, D. (ed.), 1982. International Union of Geological Sciences, Subcommission on Silurian Stratigraphy. Field Meeting Oslo Region 1982. *Paleontological Contributions from the University of Oslo,* 278:1–175.

Trilobite biofacies and sequence stratigraphy: an example from the Upper Ordovician of Oklahoma

Jesse R. Carlucci[1] and Stephen R. Westrop[2]

[1]*Kimbell School of Geosciences, Midwestern State University, Wichita Falls, TX 76308.*
[2]*Oklahoma Museum of Natural History and School of Geology & Geophysics, University of Oklahoma, Norman, OK 73072, swestrop@ou.ed.*

There have been surprisingly few empirical investigations of the fundamental principle that the architecture of depositional sequences exerts considerable control on observed patterns of faunal distribution and replacement. We examined trilobite associations in two sequences of the Upper Ordovician (Sandbian) Bromide Formation of southern Oklahoma. Cluster analysis and ordination of genus abundance data identified five lithofacies-related biofacies that are also differentiated by diversity

patterns. Biofacies of the transgressive system tract (TST) of successive sequences are more similar to each other than they are to biofacies in the highstand systems tract (HST) of the same sequence. This similarity likely records dominance of large, robust convex sclerites in taphonomically degraded samples from condensed, strongly winnowed grainstone and rudstone. Horizons with articulated exoskeletons of isoteline trilobites preserved by obrution deposits occur most commonly in the early HST and record behavioral aggregations. Grainstone and rudstone of the later HST are less winnowed than those of the TST, and show less fragmentation and sorting of sclerites. These changes in taphonomic conditions preserve ecological patterns more clearly. In most biofacies, rarefied alpha diversity (samples) and gamma diversity (biofacies) of middle and outer ramp HST deposits are greater than in the TSTs, and biofacies replace each other downramp. Diversity patterns do not agree with model predictions and other data sets that indicate low beta and high alpha diversity in the TST, likely because of taphonomic degradation. Vertical replacement of biofacies is expressed by the appearance of peritidal facies in which trilobites are rare. Biofacies shifts also characterize sequence boundaries, and are most profound in the inner ramp successions characterized by sharp facies offsets. Comparison with bathymetrically similar deposits in the Taconic Foreland Basin showed similar diversity trends along environmental gradients, with some differences in shallow water settings attributed to taphonomic differences.

Geographic distribution and dynamics of the graptolite biodiversity during the end-Ordovician mass extinction in South China

Qing Chen[1], Junxuan Fan[2]

[1]*Key Laboratory of Economic Stratigraphy and Palaeogeography, Nanjing Institute of Geology and Palaeontology, Chinese Academy of Sciences, Nanjing 210008, China; qchen@nigpas.ac.cn*
[2]*State Key Laboratory of Palaeobiology and Stratigraphy, Nanjing Institute of Geology and Palaeontology, Chinese Academy of Sciences, Nanjing 210008, China; fanjunxuan@gmail.com*

As part of palaeobiodiversity study, the research on geographic dynamics of fossil biodiversity goes a further step than the traditional cataloguing work based on fossil occurrences, because the former can reveal not only the temporal patterns but also the spatial dynamics of macroevolution. In the present study we focused on the geographic distribution and dynamics of graptolite biodiversity in South China during the end-Ordovician mass extinction.

The study area lies between latitude 24°-34° north, longitude 101°-121° east in South China, and the study time interval ranges from the *Dicellograptus complexus* Biozone (late Katian) to the *Akidograptus ascensus* Biozone (earliest Rhuddanian). Forty-nine sections with precise biostratigraphic classification and detailed fossil lists were collected from the Geobiodiversity Database. The taxonomic classifications of the graptolites were revised based on a unified systematic classification scheme. Those species found in only one section, or with open nomenclature were omitted from the dataset.

First we divided the study area into two regions, the shallow-water region and the deeper-water region. We calculated the total diversity of the graptolite fauna in each graptolite biozone in each region, and found that the duration and intensity of the extinction event were considerably different between these two environmental regions. The mass extinction event influenced the graptolite fauna in the shallow-water region first and then the deeper-water region. Second, we divided the study area into 2°×2° geographical cells and measured the similarity of graptolite fauna between any two cells by using Cluster Analysis with Jaccard Index. It can be found that the graptolite fauna showed moderate geographic differentiation from near-shore to off-shore before the extinction event. However, during and after the extinction event, most of those stenotropic species were eliminated, and only those eurytopic species survived and occupied most of the preferred habitat.

Taphonomic comparisons of two Laurentian Upper Ordovician epeiric sea "small shelly faunas"

Benjamin F. Dattilo[1], Rebecca L. Freeman[2], Jessie L. Reeder[1], Amanda Straw[1], Christopher Aucoin[3], Carlton Brett[3], and Anne Argast[1]

[1]*Geosciences, Indiana University Purdue University Fort Wayne, 212 Coliseum Boulevard, Fort Wayne, IN 46805-1499, dattilob@ipfw.edu.*
[2]*Department of Earth and Environmental Science, University of Kentucky, Lexington, KY 40506.*
[3]*Department of Geology, University of Cincinnati, Cincinnati, OH 45221-0013.*

The Elgin Member of the Upper Ordovician (Katian) Maquoketa Formation of Iowa contains phosphorite beds consisting of millimeter-scale phosphatic fossils, primarily steinkerns. Similar beds occur in the coeval strata of the classic Cincinnatian Series around the Cincinnati, Ohio area. Initial sampling of the phosphate-rich beds of the Maquoketa allows comparison between the faunal composition and taphonomy of these beds and collections from the more extensively sampled Cincinnatian strata. We isolated these fossils by dissolution of bulk samples in acetic acid and examined the same strata in thin section to study the fossils in context.

The Maquoketa diminutive phosphatized fossils have been interpreted as evidence of dwarfed faunas indicative of environmental stress, such as anoxia, which may have also contributed to phosphogenesis. An alternative explanation for the small size is that phosphogenesis was size-selective and that phosphatic particles were concentrated by reworking as less-durable shell material was destroyed. These hypotheses can be tested by examining the fauna for "normal" sized elements.

Insoluble residue from sampled phosphate-rich strata in both field areas yields abundant molluscan steinkerns, as well as crinoid columnals, conodonts, scolecodonts, bryozoan zooecia steinkerns and other fossils associated with a normal marine fauna. In Cincinnatian occurrences, the composition of the phosphatic assemblages is variable but is a reflection of the variability of faunal composition seen in these strata rather than an indication of an unusual fauna associated with extreme conditions; most are associated with diverse marine assemblages. Insoluble residues from both areas yield steinkerns that precipitated in small pores within larger skeletons. This phenomenon can be seen in thin section, where phosphate is present within certain parts of the larger preserved skeletons. The maximum size of the steinkerns of the Maquoketa is larger than those of most Cincinnatian occurrences, although size is variable in Cincinnatian occurrences. In Cincinnatian strata the abundance of small phosphatic fossils correlates with evidence for reworking; heavily reworked beds yield the most residue. Examined in thin section, the sampled strata of the Maquoketa appear to be heavily reworked and represent an extreme end-member of this concentration of durable phosphatic material.

Detailed examination using an SEM and associated XRF elemental mapping reveals that the phosphatic steinkerns of both localities are very similar in their taphonomy. Both consist of botryoidal growths of carbonate fluorapatite (CFA). The botryoidal growth appears to have nucleated on the walls of the original shell, first forming a lining of variable thickness. Some steinkerns have secondary botryoidal growths on the outside of the steinkern indicating continued precipitation of CFA after destruction of the original shell. This secondary precipitation suggests that reworking played a role not only in concentrating the phosphatic material but also in encouraging continued precipitation of CFA.

The size of the available pore space appears to have played a role in encouraging the precipitation of CFA. In thin section the CFA is limited to smaller parts of larger shells, such as the apices of gastropods and did not precipitate on the inside of the larger, more open spaces within the shell. Many of the phosphate-filled spaces are also sediment-filled, suggesting that subdivision of the larger space into smaller pores enhanced the precipitation of CFA. The difference in the maximum size of the steinkern achieved in the different assemblages suggests that geochemical factors affected size limits.

The most distinctive aspect of phosphate-rich Ordovician strata of mid-Laurentia is the degree of reworking that concentrated the durable small fossils. Details of taphonomy also suggest that phosphate precipitation was an iterative process enhanced by reworking, and that small pore spaces enhanced this mineralization, thus selectively preserving certain sizes and parts of the larger fauna.

Field and petrographic evidence for late diagenetic silicification of Cambrian and Ordovician carbonates of the Shenandoah Valley, Virginia

Daniel H. Doctor

U.S. Geological Survey, 12201 Sunrise Valley Drive, Reston, Virginia 20192, dhdoctor@usgs.gov.

A number of isolated hills and ridges of erosionally-resistant Cambrian-Ordovician carbonate bedrock are evident throughout the Shenandoah Valley. A common feature of many of these hills is the local abundance of silicified carbonate rock residuum that is derived from and mantles the overlying the bedrock. Occasionally, outcrops of silicified bedrock provide an opportunity to sample the rock *in situ*. These "cherts", and other silica-rich rocks reveal several common factors of silica replacement of original carbonate rock. While most models of chert formation in carbonates favor early (eogenetic) diagenesis within the sedimentary environment, the model proposed here is one of late (mesogenetic) diagenesis associated with hydrothermal fluid migration induced by tectonic deformation, or associated with the intrusion of igneous dikes and plugs of Mesozoic or Eocene age, or both. Several lines of commonly observed petrographic evidence favoring mesogenetic silicification of these carbonate rocks include: 1) progressive replacement of anhedral to subhedral dolomite grains with microcrystalline quartz and growth of authigenic K-feldspars; 2) zoned quartz overgrowths on euhedral quartz grains that likely formed as primary chemical precipitates, possibly within voids; 3) clasts of brecciated chalcedony- bearing chert floating in a matrix of dolomite that has been altered to microcrystalline quartz; 4) co- occurrence of iron oxides accompanying silica precipitation. Field evidence also supports a model of late diagenetic silicification associated with deformation or hydrothermal alteration. Nodular siliceous masses in carbonates more commonly occur in isolated zones found along or adjacent to faults rather than as stratigraphically-bedded chert. In these zones, silica replacement of carbonate is often associated with outcrops showing evidence of intense local deformation, and the replacement likely results from localized pressure solution of siliceous minerals in the carbonate matrix being re- precipitated as microcrystalline quartz, or as replacement due to migration of hydrothermal fluids. Further geochemical characterization of these samples may shed light on the compositions of diagenetic fluids that resulted in the silicification of the original carbonate rocks.

A New Type of Cool-water Carbonate Buildups: Middle Ordovician *Moyeronia-Angarella* "Reefs" of the Siberian Platform

Andrei V. Dronov[1], Axel Munnecke[2], and Veronica B. Kushlina[3]

[1]*Geological Institute, Russian Academy of Sciences. Pyzhevsky per.7, 119017, Moscow, Russia, dronov@ginras.ru.*
[2]*GeoZentrum Nordbayern, University Erlangen-Nuremberg, Loewenichstr. 28, D-91054 Erlangen, Germany.*
[3]*Boryssiak Paleontological Institute of Russian Academy of Sciences, Profsouznaya ul. 123, 117997, Moscow, Russia*

   Stromatolite bioherms and biostromes are typical organic buildups for the Lower and the lowermost Middle Ordovician of the Siberian platform. However, closer to the end of the Middle Ordovician for a very short time a new and very specific type of organic buildups appears in the succession. The buildups are so far known only from a single locality on the right bank of the Moyero River about 0,5 km upstream of the mouth of its right tributary Bugarikta River on the northeastern part of the Tungus basin near the Anabar Land. The buildups are represented by 8 individual bioherms up to 2-2.5 m high and about 5-12m in diameter, forming a kind of a barrier system. Surrounding rocks are well-bedded marls and bioclastic wackestones of the Moyero Formation (Mukteian Regional Stage that corresponds roughly to the Late Darriwilian). The main reef-building organisms are *Moyeronia*, *Angarella,* and solenoporacean algae. Calcareous green algae have not been found. *Moyeronia* is a problematic fossil of an up to a few cm size with a complex shell structure and is interpreted as a mollusk. *Angarella* is also a problematic endemic

fossil of Siberia of up to 1 dm size that usually is assigned to inarticulate brachiopods. Fragments of trilobites, ostracods, brachiopods, echinoderms, and algae rhodoliths represent the main bioclasts in the surrounding rocks. Both, small-scale, symmetrical wave ripple marks in the surrounding rocks as well as the high abundance of solenoporacean algae point to very shallow-water conditions.

   The bioherm-containing rocks of the Mukteian regional stage form a single depositional sequence. It is underlain by pure quartz sandstones that correspond to the Baykit depositional sequence, and is overlain by bioclastic limestone of the Volgino depositional sequence with a regional unconformity at the base. Pattern of long-term lithological changes in the Ordovician of the Siberian Tungus basin demonstrates striking similarities with contemporaneous basins of Laurentia. The Ordovician succession of the Tungus basin starts with the Lower and the lower part of the Middle Ordovician represented by warm-water tropical carbonates. These carbonates are overlain by the upper Middle Ordovician unit of well-washed siliciclastic sandstones (Baykit Sandstone) similar to the Eureka quartzite of Laurentia. The Upper Ordovician carbonates in this area have been interpreted as temperate-water carbonates, and thus the Late Middle Ordovician *Moyeronia*/*Angarella* bioherms can be considered as the very beginning of the temperate-water carbonate series. Together with the Hecker-type mud mounds of Baltoscandia they probably represent a second type an unusual Middle Ordovician cool-water reefs.

Ordovician sequence stratigraphy of the Siberian Platform revised

Andrei V. Dronov[1], A.V. Kanygin[2], A.V. Timokhin[2], and T.V. Gonta[2]

> [1]*Geological Institute, Russian Academy of Sciences. Pyzhevsky per.7, 119017, Moscow, Russia, dronov@ginras.ru.*
> [2]*Trofimuk Institute of Petroleum Geology and Geophysics, Siberian Branch of Russian Academy of Sciences. Acad. Koptyug 3, 630090, Novosibirsk, Russia.*

   Ordovician succession of the Siberian Platform was previously subdivided into nine depositional sequences based mainly on analysis of regional unconformities developed in the Irkutsk basin and in the southern and western margins of the Tungus basin (Dronov et al., 2009; Kanygin et al., 2010). Recent investigations in the central part of the Tungus basin and in its northeastern margin in a proximity of the Anabar Land allow introducing some corrections into the scheme. 1) The former Baykit sequence that correspond to the Baykitian and Mukteian regional stages could be subdivided into Baykit *s.stricto* and Muktey depositional sequences. Muktey sequence is well represented in the outcrops along the Moyero River valley where it bounded by well-developed erosional surfaces and contain *Moyeronia*/*Angarella* bioherms. 2) The former Kirensk-Kudrino depositional sequence also turned out to be compiled of two cycles of deposition separated by an unconformity. The unconformity and the two cycles could be observed on the left bank of the Moyero River in the outcrop No 70. The lower cycle (Kirensk depositional sequence) is represented by intercalation of limestone and marl beds while the upper cycle (Kudrino depositional sequence) consists of pure quartz sandstone with phosphate conglomerate at the base. 3) The former Kety sequence composed of the Nirundian and the Burian regional stages should be subdivided into two depositional sequences corresponding to the Nirundian and to the Burian stages respectively. In the outcrops along the Nizhaya Chunku River valley, the unconformity between these two sequences stressed by conglomerate with limestone and siltstone pebbles.

   The revised sequence stratigraphic scheme of the Ordovician of the Siberian platform consists of 12 depositional sequences. From the base to the top they are as follows: (1) Nya; (2) Ugor; (3) Kimai; (4) Baykit; (5) Muktey; (6) Volgino; (7) Kirensk; (8) Kudrino; (9) Mangazea; (10) Dolbor; (11) Nirunda; (12) Bur. Having in mind that two Hirnantian depositional sequences are not represented in the Siberian succession the number of the Siberian Ordovician sequences coincides with the number of the Baltoscandian ones (Dronov et al., 2011). That could be regarded as an indicator for eustatic origin of sea-level fluctuations responsible for developments of these sequences. Precise correlation of some of the

individual sequences however remains obscure due to lack of reliable biostratigraphic, chemostratigraphic and absolute age data.

Lower-Middle Ordovician carbon and sulfur isotope stratigraphy at Shingle Pass, Nevada, USA: Changes in the carbon and sulfur cycles and a link between oxygen levels and biodiversity

Cole T. Edwards[1,2], Matthew R. Saltzman[1], and David A. Fike[2]

[1]School of Earth Sciences, 275 Mendenhall Ave., 125 South Oval Mall, The Ohio State University, Columbus, Ohio 43210, cole.edwards@wustl.edu.
[2]Department of Earth and Planetary Sciences CB 1169, 1 Brookings Dr., Washington University, St. Louis, MO 63130.

The Ordovician seawater sulfur isotopic record (δ^{34}S) remains relatively poorly known compared to the well-studied carbon isotopic record (δ^{13}C). Primary seawater δ^{13}C and δ^{34}S trends measured from carbonate rocks are used as proxies for changes in organic and pyrite burial, respectively, and provide a proxy for redox conditions. Here we report paired carbon and sulfur isotopic data from well-preserved carbonate rocks from the Great Basin region of North America measured from the Lower-Middle Ordovician carbonate strata of the Pogonip Group at Shingle Pass, NV, USA. Preserved near the base of the North American Stairsian Stage (Tremadocian global Stage) are positive isotope excursions in the δ^{13}C (1.5‰) and δ^{34}S (10‰) records. These excursions have been interpreted as having been caused by the expansion of anoxic waters into shallow environments with increased burial rates of organic matter and pyrite with concomitant oxygenation of the atmosphere. The onset of these excursions appears to be coincident, but the recovery to baseline values for δ^{13}C is more rapid compared to δ^{34}S and suggests that the seawater sulfate reservoir was larger than previously thought. High-resolution sampling throughout this interval using methods thought to ensure the measurement of the most pristine seawater isotopic value confirms that these excursions are coincident and coupled, but that the methods used to extract carbonate-associated sulfate (CAS) can impart up to an 8‰ shift in the overall δ^{34}S trend.

The timing of these excursions and interpreted anoxic event corresponds to a major extinction of a group of trilobites (Symphysurinid "biomere") and represents a major biogeochemical event. After the extinction and excursion events the strong coupling between δ^{13}C and δ^{34}S trends weakened, indicating that oxygen levels may have increased enough to prevent major expansion of ocean anoxia globally compared to similar episodes thought to have occurred during the late Cambrian and earliest Ordovician. The suppression of recurrent anoxic conditions into nearshore environments is interpreted here to be a central cause in fostering the increase of biodiversity rates locally and globally that makes up the earliest pulses of biodiversity associated with the Great Ordovician Biodiversification Event (GOBE).

Was the Great Ordovician Biodiversification Event (GOBE) caused by increased atmospheric oxygen?: Evidence from paired carbon isotopes from bulk carbonate (δ^{13}C$_{carb}$) and organic matter (δ^{13}C$_{org}$) from North America

Cole T. Edwards[1,2] and Matthew R. Saltzman[2]

[1]School of Earth Sciences, 275 Mendenhall Ave., 125 South Oval Mall, The Ohio State University, Columbus, Ohio 43210, cole.edwards@wustl.edu.
[2]Department of Earth and Planetary Sciences CB 1169, 1 Brookings Dr., Washington University, St. Louis, MO 63130.

The Great Ordovician Biodiversification Event (GOBE) represents one of the greatest radiations of marine faunas in the Phanerozoic, but identifying the causes of this diversification event remains unknown but actively pursued. Recent studies focused on identifying a causal link between the first pulses of biodiversity and increasing oxygen levels from organic/pyrite burial have shown promise that such a relationship exists but fail to explain long-term trends. A recent compilation of paired measurements from bulk carbonate ($\delta^{13}C_{carb}$) and organic matter ($\delta^{13}C_{org}$) from published reports from North America shows an overall increase of 3‰ in the isotopic difference ($\delta^{13}C$) of these paired measurements throughout the Ordovician, which we use here to test whether this could be caused by increased atmospheric oxygen levels. The measured $\delta^{13}C$ value is controlled in part by the isotopic depletion associated with dissolved CO_2 and the formation of carbonate minerals (Δ_{carb}), the summation of secondary biological and geological processes (Δ_2), but mostly by the biological fractionation effect (ε_p) imparted during the formation of biomass. Experimental work has shown that ε_p is also a function of both biological processes (growth rate and cell surface area/volume), the amount of dissolved CO_2 ($[CO_2]$), or the partial pressure of O_2 (pO_2). Using estimates from modern and ancient environments for Δ_2 and Δ_{carb} (in place of any fossil or geologic evidence that suggests otherwise) we use the long-term $\delta^{13}C$ trend as a proxy for ε_p. Mass-balance isotope model estimates for $[CO_2]$ broadly constrain the atmospheric CO_2 control on ε_p, which we can then use to calculate a pO_2 trend throughout the Ordovician assuming there were not fundamental changes in the dominant biomass producing phytoplankton. pO_2 levels were low during the Early Ordovician (~10%), but increased steadily throughout the late Early and Middle Ordovician to near-modern levels (19-23%). The timing and rate of this increase matches the major pulses of global biodiversity up until the end Ordovician mass extinction. This relationship may indicate that there was a strong relationship between atmospheric oxygen levels and global biodiversity levels during the early Paleozoic. Once atmospheric oxygen levels reached high enough levels that were near modern levels (21%), global biodiversity levels appear to have peaked and plateaued at relatively high levels for nearly 200 million years throughout the Paleozoic prior to the end Permian mass extinction.

Evolution of the Darriwilian to Katian graptolites from NW China

Junxuan Fan[1], Daniel Goldman[2], Qing Chen[3], Xu Chen[3], Yuandong Zhang[3]

[1]*State Key Laboratory of Palaeobiology and Stratigraphy, Nanjing Institute of Geology and Palaeontology, Chinese Academy of Sciences, Nanjing 210008, China; fanjunxuan@gmail.com*
[2]*Department of Geology, University of Dayton, 300 College Park, Dayton, OH 45469, USA; dgoldman1@udayton.edu*
[3]*Key Laboratory of Economic Stratigraphy and Palaeogeography, Nanjing Institute of Geology and Palaeontology, Chinese Academy of Sciences, Nanjing 210008, China; qchen@nigpas.ac.cn, xuchen@nigpas.ac.cn, ydzhang@nigpas.ac.cn*

The Darriwilian to Katian graptolite fauna from northwestern China has been systematically studied by the present authors and their colleagues, which provides a unified taxonomic framework for the evolutionary analysis. All the range data of the seven available sections, the Dawangou (Kalpin, Xinjiang, taken as the reference section), Sishichang (Aksu, Xinjiang), and Subashigou (Kalpin, Xinjiang), Guanzhuang (Pingliang, Gansu), Longmendong (Longxian, Shaanxi), Dashimen (Wuhai, Inner Mongolia), and Gongwusu (Wuhai, Inner Mongolia) were compiled into the Geobiodiversity Database and reformatted for quantitative biostratigraphy. After removing those names of open nomenclature, a total of 121 species or subspecies from seven sections were ready for graphic correlation analysis. An updated version of the graphic correlation program – SinoCor 4.0 was used to produce the composite sequence (CS). The CS spans a duration from early Darriwilian to early Katian in age, including eight graptolite biozones, the *Cryptograptus gracilicornis*, *Pterograptus elegans*, *Didymograptus murchisoni*, *Jiangxigraptus vagus*, *Nemagraptus gracilis*, *Climacograptus bicornis*, *Diplacanthograptus caudatus*, *and Diplacanthograptus spiniferus* biozones, in ascending order. The precise graptolite richness curve based on the counting of boundary-crossers demonstrates two major diversity peaks during the study interval, one in the basal *D. murchisoni* Biozone and the other in the basal *N. gracilis* Biozone (Fig. 1).
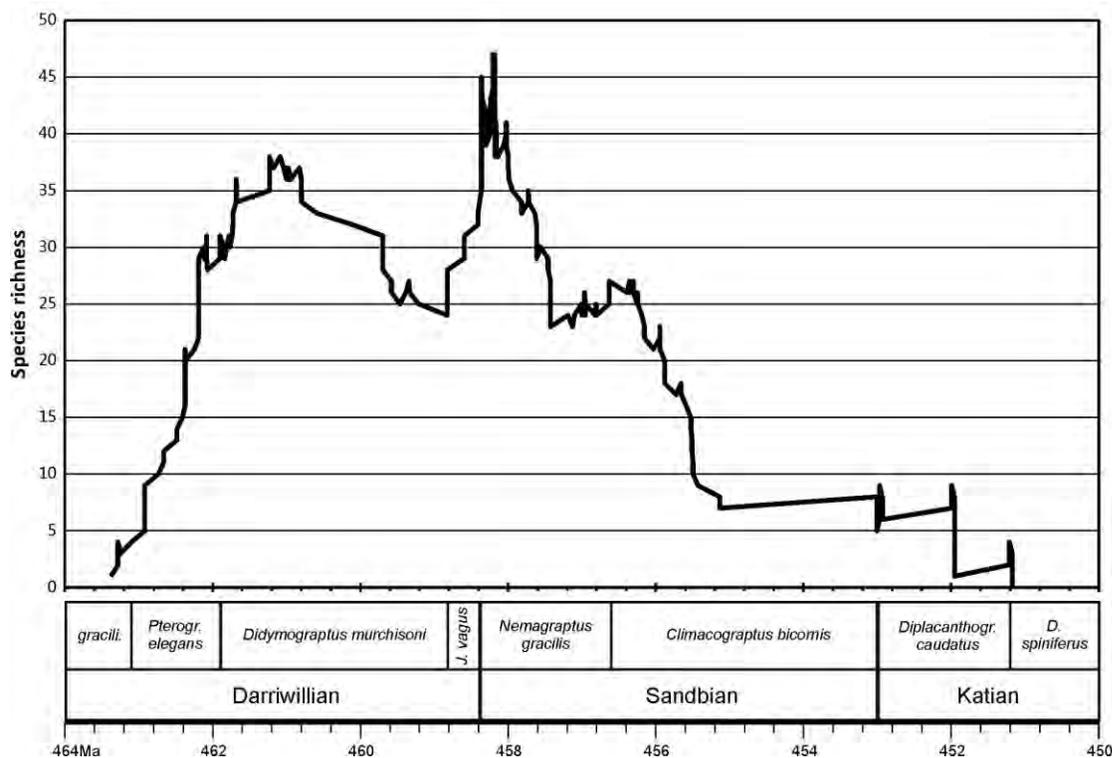
Fig. 1.—Richness curve of graptolites from Darriwilian to Katian

Upper Ordovician carbon isotope chemostratigraphy on the Yangtze Platform, South China: Implications for the correlation of the Guttenberg δ¹³C Excursion (GICE)

Ru Fan[1,2,3,4], Stig M. Bergström[5], Yuanzheng Lu[1,2,3], Xuelei Zhang[1], Shiben Zhang[1,2,3], Xin Li[1,2,3], and Shenghui Deng[1,2,3]

[1]*Research Institute of Petroleum Exploration & Development, Beijing 100083, PRC, rufan@petrochina.com.cn.*
[2]*State Key Laboratory for Enhanced Oil Recovery of China, Beijing 100083, PRC.*
[3]*Key Laboratory for Oil and Gas Reservoirs of PetroChina, Beijing 100083, PRC.*
[4]*Nanjing Institute of Geology and Palaeontology, Chinese Academy of Sciences, Nanjing, Jiangsu Province 210008, PRC.*
[5]*School of Earth Sciences, Division of Geological History, The Ohio State University, Columbus, Ohio 43210, USA.*

Samples of Upper Ordovician marine carbonates from four sections on the Yangtze Platform (1, the Liangcun section northeast of Xishui County Town, Guizhou Province; 2, the Zhuazhuayan section southwest of Leibo County Town, Sichuan Province; 3, the Xiaogangwan section east of Wulong County Town, Chongqing Municipality; 4, the Shatan section north of Nanjiang County Town, Sichuan Province) have been analyzed for carbon isotope ($\delta^{13}C$) chemostratigraphy. A distinct positive $\delta^{13}C$ excursion ($\delta^{13}C_{max}$ >2) is observed in all sections which ranges through the *Hamarodus brevirameus* Conodont Zone, and locally into slightly younger strata. The base of this zone is the First Appearance Datum (FAD) of *H. brevirameus* and its top coincides with the FAD of the conodont *Protopanderodus insculptus*. Based on its position in the *H. brevirameus* Zone, this excursion is identified as the well-known Guttenberg Excursion (GICE) confirming the global significance of this paleoceanographic event. The fact that in the Black Knob Ridge section in the USA, the GSSP of the base of the global Katian Stage, the beginning of

the GICE is just below the base of the Katian makes it possible to locate this key level in our study sections even in the absence of the diagnostic graptolite *D. caudatus*. Our carbon curves through the GICE interval show three minor secondary peaks reflecting paleoceanographic changes or selective preservation of the isotope signal. However, because a global review of the GICE shows that such minor peaks, which are often based on a single elevated δ^{13}C value, are of irregular occurrence, they are interpreted as local, rather than global, phenomena. The suggested global cooling in the early Katian might have favored the generation of methane hydrates and hence the reduction of the amount of ^{12}C in the marine carbonates.

Palaeobiogeographic distribution of Lituitidae cephalopods in late Dapingian to early Katian (Ordovician) and its implications

Fang Xiang, Zhang Yunbai, Chen Tingen, Zhang Yuandong, Song Yanyan, and Ma Xuan

Nanjing Institute of Geology and Palaeontology, CAS, Nanjing 210008, China, royfangxiang@gmail.com.

Lituitidae cephalopods are among the most significant fossil groups in late Dapingian to early Katian globally, which were extensively distributed in South China, North China, Sibumasu, Tarim, Tibet, Baltica and Laurentia, etc. Based on latest taxonomic studies, the family comprises nine genera, including *Lituites*, *Trilacinoceras*, *Ancistroceras*, *Sinoceras*, *Holmiceras*, *Angelinoceras*, *Rhynchorthoceras*, *Cyclolituites* and *Tyrioceras*, which appear to fall into four groups. Herein we present the global palaeobiogeographic distribution of the Lituitidae cephalopods through Dapingian to early Katian, which display a progressively-reducing distribution with time, and become restricted in the northeastern peri-Gondwana region in early Katian with a low diversity, until the group became extinct suddenly in mid Katian globally. In South China, Lituitidae cephalopods displays a continuous biofacies gradient from Yangtze Region (platform) to Jiangnan Region (slope), and a progressive expansion of its ecological habitats with time from shallow water into deeper waters until mid Katian. The palaeobiogeographic distribution and biofacies gradient pattern of lituitids may be related with worldwide sea-level changes during the Ordovician.

Risk and resilience during and after the Late Ordovician extinctions

Seth Finnegan[1], Christian M. Ø. Rasmussen[2] and David A.T. Harper[3]

[1]*Department of Integrative Biology, University of California, Berkeley CA 94720-3140, seth.finnegan@gmail.com.*
[2]*Natural History Museum of Denmark (Geological Museum), University of Copenhagen, Copenhagen, DK-1350 Denmark.*
[3]*Palaeoecosystems Group, Department of Earth Sciences, Durham University, Durham DH1 3LE, UK.*

The Late Ordovician Mass Extinction (LOME) coincided with major global climate changes, but there are numerous mechanisms that could have caused marine invertebrate extinctions. Determining which were most important requires dissecting extinction patterns across time, space, environments, and taxa. Here we use a large and taxonomically standardized global database of the local stratigraphic ranges of rhynchonelliform brachiopods to examine extinction selectivity patterns through the Late Ordovician-Early Silurian interval and to evaluate which potential extinction mechanisms are best supported by these data. During the first pulse of the Late Ordovician Mass Extinction predictors with the greatest marginal influence on extinction risk were paleolatitudinal range and paleobathymetric distribution: genera with absolute paleolatitudinal ranges < 25° or bathymetric ranges limited to deeper waters suffered most. Neither of these predictors are associated with extinction risk during other intervals, suggesting that they are indicative of extinction mechanisms unique to the latest Katian interval. Preferential extinction of exclusively deep-water genera suggests that changes in the vertical distribution of water mass quality such as dissolved oxygen content were important drivers. The importance of paleolatitudinal range suggests

that interactions between changing seawater temperature and paleogeography also played a prominent role in driving extinctions. To test this latter hypothesis, we estimated thermal tolerance ranges of latest Ordovician species based on their known occurrences and temperature gradients extracted from paleoclimatic models. We extracted estimates for two distinct climate modes: a 'greenhouse' state with high sea levels and high CO_2 and an 'icehouse' state with relatively low sea levels and low CO_2. We then estimated whether each genus would have been expected to survive a cooling (greenhouse-icehouse) scenario or a warming (icehouse-greenhouse) scenario based on whether any of its constituent species would have been able to access water temperatures within their tolerance range. Models that include expected survival under a cooling scenario are strongly favored, advocating a direct role for ocean cooling in driving the first pulse of the mass extinction. We argue that the LOME, long regarded as relatively nonselective, is in fact strongly selective with respect to biogeographic and bathymetric parameters that themselves are not closely correlated with taxonomic identity.

High-resolution stratigraphic correlation and biodiversity dynamics of Middle and Late Ordovician marine fossils from Baltoscandia and Poland

Daniel Goldman[1], H. David Sheets[2], Stig M. Bergström[3], Jaak Nõlvak[4], and Teresa Podhalańska[5]

[1]*Department of Geology, University of Dayton, 300 College Park, Dayton, OH 45469, dgoldman1@udayton.edu.*
[2]*Dept. of Physics, Canisius College, 2001 Main Street, Buffalo NY 14208.*
[3]*School of Earth Sciences, The Ohio State University, Columbus, OH 43210.*
[4]*Institute of Geology at Tallinn University of Technology, Ehitajate tee 5, Tallinn, 19086, Estonia.*
[5]*Polish Geological Institute-National Research Institute, 4, Rakowiecka Street, 00-975 Warsaw, Poland.*

The Middle and Upper Ordovician rocks of Baltoscandia have been divided into spatially distinct, composite litho- and biofacies units called confacies belts. A precise regional correlation of outcrops and boreholes located in different confacies belts has always been problematic due to the pronounced biogeographical and lithofacies differentiation. Correlation between sections in the graptolite-rich black shales of the Scanian confacies and the carbonate-rich North Estonian confacies belts has been particularly difficult. To overcome these problems we used Constrained Optimization (CONOP9, Sadler et al., 2003) and Horizon Annealing (HA, Sheets et al., 2012) to construct a high resolution correlation model and composite range chart compiled from the stratigraphic range data of 554 chitinozoan, conodont, ostracod, and graptolite species from 38 drill cores and outcrops in Poland and Baltoscandia. We also used the CONOP composite as a timescale in which to calculate biodiversity, extinction, and origination rates through the Middle and Late Ordovician. Our data show that overall biodiversity forms a broad but uneven plateau from the base of the Uhaku to the late Kukruse Baltic stages, followed by a distinct drop in the Haljala Stage mainly due to a steep decline in conodont diversity. Two distinct diversity peaks occur in the Keila and Rakvere Baltic stages, with a dramatic decline at the basal Oandu Stage associated with the $\delta13C$ isotope excursion that correlates with the North American GICE event. Fossil diversity declines from the Nabala through Vormsi stages, with a slight rebound in the middle Pirgu. The main Late Ordovician extinction begins in the mid – late Pirgu Stage. Chitinozoan diversity exhibits peaks in the Lasnamagi and lower Keila stages, drops through the Oandu, and then gradually declines across the rest of the Ordovician. Conodonts have a main diversity peak in the lower Uhaku, a smaller peak Kukruse, and then decline gradually through the Late Ordovician with a slight rebound in the Mid to Late Katian global Stage. Graptoloid diversity exhibits a main peak in the Kukruse (Sandbian) followed by decline, a smaller peak in the late Keila, a decline thereafter. Our ostracod data indicate an uneven climb in diversity through the mid Pirgu followed by a very steep decline. These patterns are similar to other published diversity curves but also differ in some important aspects.

REFERENCES

SADLER, P.M., KEMPLE, W.G. and KOOSER, M.A., 2003, Contents of the compact disk—CONOP9 programs for solving the stratigraphic correlation and seriation problems as constrained optimization. *In* P.J. Harries (ed.), *High resolution approaches in stratigraphic paleontology*. Dordrecht, Topics in Geobiology, v. 21, Kluwer Academic Publishers, 461–465.

SHEETS, H.D., MITCHELL, C.E., IZARD, Z.T., WILLIS, J.M., MELCHIN, M.J. and HOLMDEN, C. 2012: Horizon annealing: a collection-based approach to automated sequencing of the fossil record. *Lethaia*, v. 45, pp. 532–547.

A biostratigraphic reappraisal of Tremadocian graptolites from SW Europe and NW Africa

Juan Carlos Gutiérrez-Marco[1], Gian Luigi Pillola[2], Artur A. Sá[3] and Emmanuel L.O. Martin[4]

[1] *Instituto de Geociencias (CSIC, UCM), José Antonio Novais 12, E-28040 Madrid, Spain. jcgrapto@ucm.es*
[2] *Dipartimento di Scienze Chimiche e Geologiche, Università di Cagliari, Via Trentino 51, 09127 Cagliary, Italy. pillolag@unica.it*
[3] *Departamento de Geologia, Universidade de Trás-os-Montes e Alto Douro, PO Box 1013, 5001-801 Vila Real, Portugal; and Geosciences Center, University of Coimbra, 3000-272 Coimbra, Portugal. asa@utad.pt.*
[4] *UMR CNRS 5276 Laboratoire de Géologie de Lyon, Terre, Planètes, Environnement (LGLTPE), Géode - campus de la Doua, Université Lyon 1, 2 rue Dubois, 69622 Villeurbanne cedex, France. emmanuel.martin@univ-lyon1.fr*

Tremadocian graptolites are rare fossils in the whole peri-Gondwanan Europe, northwestern Africa and the Near and Middle East. This is in part due to the absence of suitable marine facies, which are largely dominated by shallow-water siliciclastic sediments such as green shales and coarse sandstones, but also owing to the general lack of a distinctive sedimentary record. The Cambrian/Ordovician boundary involves, regionally, major erosive unconformities (excepted in SW Sardinia) and diachronic stratigraphic gaps, mainly associated to the denudation of rift shoulders during a multistage rifting through the Furongian and the Lower Ordovician epochs. This rifting was connected to the opening of the Rheic Ocean, which also generated thick volcano-sedimentay sequences and plutonism related to the long-lived Ollo de Sapo Magmatic Event, ranging in age between *ca*. 490 and 465 Ma, with a maximum at about 477 Ma and a youngest age of approximately 479 Ma for the massive metavolcanic sequences.

Early Tremadocian (Tr1) graptolites are represented in North Africa (Morocco, Algeria) and in scattered localities in Sardinia, southeastern France and northern Turkey. They compose a low-diversity assemblage of quadriradiate pendent *Rhabdinopora* (*R. flabelliformis* and its ecological subspecies *R. f. socialis, R. f. anglica* or *R. f. norvegica*, adapted to shallow and mid-shelf environments), without *Staurograptus* and with very few *Anisograptus*? (a triradiate genus). Representatives of the early biradiate development (*Adelograptus* or *Aorograptus* Zone) have been rarely recognized in the Algerian Sahara and in northern Mauritania, with the extremely rare occurrence of *Adelograptus* "*tenellus*" and remains of other branched species (*Paradelograptus*?, *Aorograptus*? spp.). Slightly above these beds, a single Saharan borehole yielded the enigmatic anisograptid *Choristograptus louai*, a graptolite recently recorded also in the Fezouata Formation of Morocco, probably from a horizon of middle Tremadocian (Tr 2) age. In the same unit the occurrence of *Bryograptus* has been cited from one locality, but is pending revision.

In contrast with the few graptolite records from early to middle Tremadocian beds, late Tremadocian green shales, with locally abundant graptolites, are widely distributed over the entire area, but with little lateral continuity. This is the case of the *Araneograptus murrayi* Zone that has been recognized in NW Africa (Mauritania, Morocco, Algeria), as well as in the Ossa Morena Zone of the Iberian Massif, SW Sardinia (Fluminese area), SE France (Montagne Noire), and Germany (Thuringia). Besides the large conical rhabdosomes of *A. murrayi*, that locally occur in massive monospecific concentrations (maybe reflecting mass mortality caused by toxic events?), the zonal assemblage yielded other anisograptids (*Kiaerograptus, Paratemnograptus*), sigmagraptids (*Paradelograptus*) and early dichograptines (*Clonograptus, Tetragraptus* s.l., *Didymograptus* s.l.). Finally, the latest Tremadocian *Hunnegraptus copiosus* graptolite Zone has been identified in SW Spain, the Moroccan Anti-Atlas and in a single

locality in the Central Taurus (Turkey). Apart of the rare record of its nominal form, most of the associated graptolites may range from the previous biozone into the earliest Floian strata. The assemblage includes multiramous horizontal forms (*Clonograptus, Paradelograptus*) and two- to four-stiped rhabdosomes (*Kiaerograptus*, *Didymograptus* s.l., *Tetragraptus* s.l.). These two late Tremadocian (Tr3) graptolite zones bear not only planktic graptolites, but also remains of benthic dendroids of the genera *Dictyonema, Callograptus, Aspidograptus, Desmograptus* and *Ptilograptus*, most of them occurring as transported elements.

Iberian Ordovician and its International Correlation

Juan Carlos Gutiérrez-Marco[1], Artur A. Sá[2], Isabel Rábano[3], Graciela N. Sarmiento[4], Diego C. García-Bellido[5], Enrique Bernárdez[6], Saturnino Lorenzo[7], Enrique Villas[8], Andrea Jiménez-Sánchez[8,9], Jorge Colmenar[8], and Samuel Zamora[10]

[1]*Instituto de Geociencias (CSIC, UCM), José Antonio Novais 12, 28040 Madrid, Spain, jcgrapto@ucm.es.*
[2]*Departamento de Geologia, Universidade de Trás-os-Montes e Alto Douro, PO Box 1013, 5001-801. Vila Real, Portugal; and Geosciences Center, University of Coimbra, 3000-272 Coimbra, Portugal.*
[3]*Museo Geominero, Instituto Geológico y Minero de España, Ríos Rosas 23, 28003 Madrid, Spain.*
[4]*Departamento de Paleontología, Facultad de Ciencias Geológicas, Universidad Complutense de Madrid, 28040 Madrid, Spain.*
[5]*The Environment Institute, Department of Biological Sciences, University of Adelaide, SA 5005, Australia.*
[6]*Departamento de Geología, Universidad de Atacama, Av. Copayapu 485, Copiapó (Atacama), República de Chile.*
[7]*Departamento de Ingeniería Geológica y Minera, Universidad de Castilla-La Mancha, Plaza Manuel Meca 1, 13400 Almadén (Ciudad Real), Spain.*
[8]*Departamento de Ciencias de la Tierra, Universidad de Zaragoza, Pedro Cerbuna 10, 50009 Zaragoza, Spain.*
[9]*Center of Biology, Geosciences and Environmental Education, University of West Bohemia, Klatovska 51, 306-19 Plzen, Czech Republic.*
[10]*Instituto Geológico y Minero de España, Manuel Lasala 44 -9ºB, 50006 Zaragoza, Spain.*

The regional chronostratigraphy of the British Ordovician, established mainly for shelly facies, is hard to correlate in the Iberian Peninsula, especially after the separation and drift of Avalonia from Gondwana by the early Middle Ordovician. The same applies to the Ordovician global scale, whose stratotypes involve deeper-water facies and faunas not recorded in the high-paleolatitudinal settings of southern peri-Gondwana. In order to solve the problem, an alternative regional scheme for the "Mediterranean" Ordovician was proposed in the 1970s. This comprises five regional stages plus the global Tremadocian and Hirnantian, which are largely based on the distribution of endemic shelly fossils combined with some graptolites and a good palynological record. This Ordovician scale presents precise correlation potential for southwestern and central Europe (Ibero-Armorica, Sardinia, Bohemia, Bulgaria) and the vast area from northern Africa to Saudi Arabia and part of the Middle East. Sporadic occurrences of graptolites and shelly faunas of Baltic or Avalonian affinities allow for indirect correlation with the global stages through their own regional scales. Despite the advantages of such a regional "Mediterranean" scale, the terms "Ordovician Oddyssey" and "*Quo vadis* Ordovician?", used as titles for the books that arose from the Ordovician symposia of 1985 (Las Vegas) and 1990 (Prague), are still applicable to the Iberian Ordovician chronostratigraphy. Some authors prefer to use the global scale directly, without valid references to precise correlation, whereas others use the old British scale without acknowledging the redefinition by British authors between 1972 and 2010.

In Iberia, as well as in other peri-Gondwanan areas lying in high paleolatitudes close to the Ordovician South Pole, the general scarcity of graptolites and conodonts in the Lower and Middle Ordovician, and the largely endemic nature of the shelly faunas, impose serious difficulties for correlating the successions in this region with the new global chronostratigraphy. This is illustrated by the fact that only two of the taxa used for the definition of the global stages and series have been recorded in paleogeographically southern

peri-Gondwana (*Levisograptus austrodentatus* in Turkey and *Metabolograptus extraordinarius* in Bohemia). The situation is similar with the taxa defining the base of the *stage slices*, were only Dw2's (*Didymograptus artus*) and Ka3's (*Amorphognathus ordovicicus*) diagnostic species are recognizable where appropriate litho- and biofacies are developed, and may be distant from their respective FADs. Single records of the graptolites *Tetragraptus azkharensis* (a form closely allied to *T. approximatus*, Fl1) and *Dicellograptus complanatus* (Ka4) are known from France, but come from Ordovician olistoliths within Carboniferous mélanges in Montagne Noire and south Armorican Massif.

The paleontological record from the Iberian Ordovician includes low diversity benthic assemblages of trilobites, ostracods, brachiopods, echinoderms, molluscs, etc., regarded as cold-water faunas, later shifting to more temperate types, and even relatively warm-water faunas due to the Boda event that preceeded the Hirnantian glaciation. Faunal affinities suggest strong links within a single paleogeographical realm (equivalent to the "Mediterranean", "*Selenopeltis*" or "Calymenacean-Dalmanitacean" provinces of previous authors). Within this common scenario, faunal differences are strongly conditioned by the development of different biofacies defined by the type of substrate, inshore-offshore gradients and even paleocurrents.

The Ibero-Bohemian Ordovician scheme allows regional correlations within the southern peri-Gondwanan areas and can be regarded of similar rank and suitability as other regional scales used in Australasia, Baltoscandia, Avalonia, North America or China. According to the current policy of the International Ordovician Subcommission, a fundamental contribution to the development of a global chronostratigraphy will be the detailed cataloguing of as many as possible of these commonly distinctive regional Ordovician sections.

Late Ordovician, deep-water *Foliomena* brachiopod fauna from the island of Bornholm, Denmark

David A.T. Harper[1] and Arne T. Nielsen[2]

[1]*Palaeoecosystems Group, Department of Earth Sciences, Lower Mountjoy, Durham University, Durham DH1 3LE, UK, david.harper@durham.ac.uk*
[2] *Natural History Museum of Denmark (Geological Museum), University of Copenhagen, Øster Voldgade 5-7, DK-1350 Copenhagen, Denmark.*

The deep-water brachiopod *Foliomena* fauna is one of the most widespread, Phanerozoic marine assemblages. Distributional data for the *Foliomena* and related biotas from over 30 localities, globally, through the early Sandbian to late Katian interval, are now available from deeper-water, marginal biofacies. The fauna was first described in detail from the Lindegård Mudstone in Scania, southernmost Sweden, in the early 1970s and this association of small, thin-shelled brachiopods has since then been recorded from the Avalonian, Gondwanan and Laurentian margins together with its most diverse and extensive development in South China. A hitherto unpublished assemblage collected in the 1800s from the upper Katian Lindegård Mudstone of Bornholm, Denmark, including *Christiania*, *Cyclospira*, *Dedzetina* and *Foliomena* itself together with species of *Glyptorthis*, *Leptestiina*, *Nubialba*, *Proboscisambon* and *Sowerbyella* confirms the persistence of this deep-water biofacies in southern Scandinavia and develops further the evolutionary and geographical patterns of the *Foliomena* fauna around the margins of Baltica, prior to its extinction at the end of the Katian. Deep-water facies persisted into the Hirnantian on Bornholm where the shelly fauna is characterised by sparse *Aegiromena,* indicative of the deepest-water associations of the terminal Ordovician *Hirnantia* fauna.

Milankovitch cycles in the Juniata Formation, Late Ordovician, central Appalachian basin, USA

Linda A. Hinnov and Richard J. Diecchio

Department of Atmospheric, Oceanic and Earth Sciences, George Mason University, Fairfax, VA 22030, lhinnov@gmu.ed.

The Juniata Formation is a thick succession of prevalently red, cyclically bedded arenites, wackes, and mudrocks found in the Upper Ordovician of the Central Appalachian Basin, USA. Its thickness exceeds 1600 ft in western Maryland, and is thicker in Pennsylvania. The typical cycle ranges from less than 1 to more than 15 feet in thickness, and has three facies: (1) a lower cross-bedded arenite with a channeled basal contact and upper burrowed surface, (2) interbedded mudstone and vertically burrowed arenite to wacke, and (3) an upper bioturbated mudstone to shale with occasional pedogenic structures. In some outcrops, the cycles predominantly have the characteristics of regressive tidal flat deposits, however elsewhere the Juniata cycles have been described as fluvial. Regionally, the Juniata was probably deposited in various environments.

Long and continuous well logs of the subsurface Juniata provide an unparalleled opportunity to investigate Milankovitch controls on the cyclic deposition. In the Preston 119 well, northern West Virginia, a particularly long 2700 ft gamma-ray log provides a high-resolution proxy of terrigenous siliciclastic flux to the northern Central Appalachian Basin shoreline, from the early Maysvillian (Reedsville Shale) to the Ordovician/Silurian transition (Tuscarora Sandstone). This log records multiple-scale gamma-ray cycles with spectrally determined thicknesses of 316 ft, 70 ft, 23 ft, 12.2 ft, 11.5 ft and 8.4 ft. After the 316 ft cycle, the 23 ft cycle has the highest magnitude. Adopting GTS2012 as a preliminary timescale indicates that the log is approximately 4 million years long (from ~448 Ma in the early Maysvillian to 443.8 Ma at the Ordovican/Silurian boundary). This indicates an average accumulation rate for the logged section of 2700 ft/4 myr = 675 ft/myr. The 316 ft cycle therefore calibrates to a periodicity of 316 ft/(675 ft/myr) = 0.468 myr, which is close to the Earth's long eccentricity cycle period of 405 kyr. Readjusting gives an average accumulation rate of 316 ft/405 kyr = 0.78 ft/kyr; from this the shorter cycles calibrate to: 90 kyr (short eccentricity?), 30 kyr (obliquity), 15.6 kyr, 14.7 kyr and 10.8 kyr (precession index). Tuning to control for variable accumulation rates leads to further adjustments that can be compared with theoretical predictions for Ordovician-age obliquity and precession index periodicities. In sum, the gamma-ray cycles provide strong evidence for sea level oscillations forced by Milankovitch cycles with a dominant obliquity component.

The strong obliquity signal captured by the Preston 119 log is reminiscent of the obliquity forcing of Oligocene climate and sea level following the glaciation of Antarctica. The Late Ordovician world analogously experienced glaciation of Gondwana, which straddled the South Pole; this may have led to ice sheet dynamics that generated obliquity-paced sea level oscillations that affected Late Ordovician shorelines. This Milankovitch-forced glacio-eustatic record from eastern North America joins other suspected Milankovitch-forced coeval successions reported in northern Africa and northwestern Australia.

Ordovician (Darriwilian-Sandbian) linguliform brachiopods from the southern Cuyania Terrane of West-central Argentina

Lars E. Holmer[1], Leonid E. Popov[2], Oliver Lehnert[3,4,5], and Mansoureh Ghobadipour[6]

[1]*Department of Earth Sciences, Palaeobiology, SE-752 36 Uppsala, Sweden; Lars.Holmer@pal.uu.se.*
[2]*Department of Geology, National Museum of Wales, Cathays Park, Cardiff CF10 3NP, Wales, UK.*
[3]*GeoZentrum Nordbayern, University of Erlangen-Nürnberg, Schloßgarten 5, D-91054, Erlangen, Germany.*
[4]*Department of Geology, Lund University, Sölvegatan 12, SE-223 62 Lund, Sweden.*
[5]*Institute of Geology, Tallinn University of Technology, Ehitajate tee 5, Tallinn 19086, Estonia.*
[6]*Department of Geology, Faculty of Sciences, Golestan University, Gorgan, Iran.*

The first Ordovician micromorphic linguliform brachiopods are described from the southern part of the Cuyania Terrane in the Province of Mendoza of west-central Argentina. The focus of the study is on

carbonate successions exposed in Block of San Rafael, south of the famous Precordillera of San Juan, La Rioja and Mendoza representing the largest area of the so-called Cuyania terrane. Because of its origin which is exotic to this part of western Gondwana based on sedimentological, paleontological, and geochemistry evidence as well as the regional geological development, this terrane became over more than two decades one of the most discussed regions in South America. As summarized by Keller (1999, 2012), many aspects of the Precordillera and, therefore also of the thin carbonate cover resting on the Grenvillian San Rafael basement, point to an origin of this large crustal segment from Ouachita Basin of west-central Texas, even when there are controversial discussions and models favouring a par-autochthonous origin in some tropical peri-Gondwana area. The common record of major Cambrian through Lower/Middle Ordovician sedimentary events with this southern part of the Laurentian margin displays that the tropical platform carbonates exposed in this extensive Cuyania Terrane could be interpreted to represent a part of the "Great American Carbonate Bank" (Keller 2012).

In the San Rafael region to the south, the lingulate brachiopod faunas occur in two successive assemblages. The older assemblage was recovered from the uppermost part of the Ponon Trehue Formation (*Lenodus variabilis* Biozone; Darriwilian), and is dominated by *Numericoma rowelli* sp. nov. It shows affinity to contemporaneous faunas from Whiterockian, Antelope Valley Limestone at Meiklejohn Peak in central Nevada. The second, and younger assemblage was recovered from the lower Lindero Formation (Peletay and lower Los Leones Members; upper Darriwilian-basal Sandbian; *Pygodus serra* and *P. anserinus* Biozones; Lehnert et al. 1999) and is mainly dominated by the new genus *Mendozotreta*, with its type species *M. devota* (Krause & Rowell), *Conotreta* cf. *multisinuata* Cooper, *Rhysotreta corrugata* Cooper, *Scaphelasma septatum* Cooper, *Ephippelasma minutum* Cooper, and *Biernatia minor* Cooper. In addition, the fauna includes also *Elliptoglossa sylvanica* Cooper, *Rowellella margarita* Krause & Rowell, and *Paterula* cf. *perfecta* Cooper. This second lingulate microbrachiopod assemblage is closely comparable to the coeval microbrachiopod fauna from the Pratt Ferry Formation of Alabama.

REFERENCES

BORDONARO, O., KELLER, M., and LEHNERT, O., 1996. El Ordovícico de Ponón Trehue en la Provincia de Mendoza (Argentina): Redefiniciones estratigráficas. *XIII Congreso Geológico Argentino y III Congreso de Exploración de Hidrocarburo*s, Actas, 1:541-550; Buenos Aires.

KELLER, M., 1999. Argentine Precordillera: Sedimentary and plate tectonic history of a Laurentian crustal fragment in South America: *Geological Society of America Special Paper* 341:131 pp.

KELLER, M., 2012, The Argentine Precordillera: A little American carbonate bank. *AAPG Memoir* 98:985-1000.

LEHNERT, O., KELLER, M., and BORDONARO, O. (1998): Early Ordovician conodonts from the southern Cuyania terrane (Mendoza Province, Argentina. *Palaeontologia Polonica* 58:45-63.

LEHNERT, O., BERGSTRÖM, S., KELLER, M., and BORDONARO, O., 1999. Middle Ordovician (Darriwilian – Caradocian) conodonts from the San Rafael region, west-central Argentina: Biostratigraphic, paleoecologic and paleogeographic implications. *Bolletino della Societá Paleontologica Italiana* 37:199-214.

Traces of explosive volcanic eruptions in the Upper Ordovician of the Siberian Platform

Warren D. Huff[1], A.V. Dronov[2], B. Sell[3], A.V. Kanygin[4], and T.V. Gonta[4]

[1]*Department of Geology, University of Cincinnati, OH 45221-0013, huffwd@ucmail.uc.edu.*
[2]*Geological Institute, Russian Academy of Sciences. Pyzhevsky per.7, 119017, Moscow, Russia.*
[3] *Earth and Environmental Sciences, University of Michigan, Ann Arbor, Michigan 48109.*
[4]*Trofimuk Institute of Petroleum Geology and Geophysics, Siberian Branch of Russian Academy of Sciences. Acad. Koptyug 3, 630090, Novosibirsk, Russia.*

In recent years more than a dozen K-bentonite beds have been discovered in the Upper Ordovician of the Tungus basin on the Siberian Platform. All the beds were identified in the outcrops of the Baksian, Dolborian and Burian regional stages, which correspond roughly to the Upper Sandbian, Katian and probably lowermost Hirnantian Global Stages (Bergström et al., 2009). The 4 lowermost beds from the

Baksian and Dolborian Regional Stages were studied in detail. They are represented by thin beds (1-2 cm) of soapy light gray or yellowish plastic clays and usually easily identifiable in the outcrops. The beds were traced in the outcrops over a distance of more than 60 km along the Podkamennaya Tunguska River valley.

All K-bentonite beds have been found within the Upper Ordovician cool-water carbonate succession. The four lowermost K-bentonite beds, which were sampled, have been studied by powder X-ray diffraction (XRD) and scanning electron microscopy (ESEM) together with energy dispersive X-ray analysis. Modeling of the XRD tracings using NEWMOD showed the samples consist of R3 ordered illite-smectite with 80% illite and 20% smectite plus a small amount of corrensite, which is a regularly interstratified chlorite-smectite. A minor amount of quartz is indicated by peaks at 4.21Å and 3.33Å. The presence of a chlorite phase indicates a primary magma rich in Fe & Mg. And the low percent of smectite in both mixed-layer phases reflects a high degree of burial metamorphism since the time of their origin. The K-bentonites provide evidence of intensive explosive volcanism on or near the western (in present day orientation) margin of the Siberian craton in Late Ordovician time.

The K-bentonite beds from the Baksian and Dolborian regional stages (Katian) of the southwestern part of the Tungus basin in Siberia are thus derived from the alteration of volcanic ash falls. All four beds contain volcanogenic euhedral zircon and apatite phenocrysts. Zircon crystals from the uppermost K-bentonite bed within the Baksian regional stage provides a $^{206}Pb/^{238}U$ age of 450.58±0.27 Ma. The timing of volcanism is surprisingly close to the period of volcanic activity of the Taconic arc near the eastern margin of Laurentia. It looks like Taconic arc has its continuation along the western continental margin of Siberia and both of them constitute a single Taconic-Yenisei volcanic arc. Field studies of the Upper Ordovician succession along the Moyero River in the vicinity of the Anabar shield demonstrate an absence of K-bentonite beds along the eastern margin (in present day orientation) of the Siberian Platform. This contradicts popular palaeogeographic interpretations (www.scotese.com) and points to the position of a subduction zone along the western but not the eastern margin of the Siberian palaeocontinent at this time.

Paired $\delta^{13}C_{carb}$ - $\delta^{13}C_{org}$ records from the Laurentian margins during late Katian glaciation

David S. Jones[1], Seth Finnegan[2], and Mark C. Hellmer[1,3]

[1]*Amherst College, Geology Department, 11 Barrett Hill Rd, Amherst, MA 01002, djones@amherst.edu.*
[2]*University of California, Berkeley, Department of Integrative Biology, 1005 Valley Life Sciences Bldg #3140, Berkeley, CA 94720-3140.*
[3]*Imperial College London, Department of Civil and Environmental Engineering, South Kensington Campus, London, SW7 2AZ UK.*

A growing body of evidence suggests that continental ice sheets existed on Gondwana during a prolonged Ordovician-Silurian icehouse, with peak glacial conditions in the Hirnantian Stage. Here we use paired inorganic ($\delta^{13}C_{carb}$) and organic ($\delta^{13}C_{org}$) carbon isotope stratigraphy to investigate potential oceanographic and climatic changes during the late Katian phase of the icehouse. The lower Beaverfoot Formation in the Canadian Rocky Mountains (Pedley Pass, British Columbia) and the Pabos Formation in the Gaspé Peninsula (Percé, Quebec) each host a pronounced negative $\delta^{13}C_{carb}$ excursion in uppermost Katian strata, with isotope ratios declining ~2‰ below baseline values before rising beneath the Katian-Hirnantian boundary. At Percé, the ~35 m thick Côte de la Surprise Member of the White Head Formation contains a Hirnantian fauna; a positive $\delta^{13}C_{carb}$ excursion in this unit reaches +1.5‰. We tentatively correlate the Côte de la Surprise excursion to the earliest Hirnantian excursion in the lowermost Ellis Bay Formation on Anticosti Island. Exposure of the Côte de la Surprise Member at Percé is truncated by faulting above this excursion.

The late Katian negative $\delta^{13}C_{carb}$ excursion is broadly paralleled by a negative excursion in $\delta^{13}C_{org}$ at Pedley Pass, but not at Percé. The covariant isotope data from Pedley Pass suggest that both $\delta^{13}C_{carb}$ and $\delta^{13}C_{org}$ record primary changes in ocean chemistry. Cyclical $\delta^{13}C_{carb}$ oscillations with magnitudes < 1.0‰

are superimposed on the rise below the Katian-Hirnantian boundary, during a time when independent evidence suggests the presence of continental ice on Gondwana. In this context, we speculate that the $\delta^{13}C_{carb}$ cycles in the Beaverfoot may be a manifestation of Milankovitch type forcing of the climate during the Ordovician-Silurian icehouse, although the absence of cycles in the parallel $\delta^{13}C_{org}$ record may point to a diagenetic origin of the $\delta^{13}C_{carb}$ cycles. The lack of $\delta^{13}C_{carb}$ - $\delta^{13}C_{org}$ covariation at Percé may be explained by several factors, including contamination of $\delta^{13}C_{org}$ by exogenous organic matter shed from the Taconic Mountains.

The Early-Middle Ordovician acritarch assemblage from eastern Yunnan

Yan Kui[1], Li Jun[1], and Thomas Servais[2]

[1]*Nanjing Institute of Geology and Palaeontology, Chinese Academy of Sciences, East Beijing Road, 210008 Nanjing, China, kuiyan@nigpas.ac.cn.*
[2]*UMR 8198 Evo-Eco-Paléo CNRS, Université de Lille1, SN5, USTL, F-59655 Villeneuve d'Ascq, France*

Since 1926, Zhu first studied Ordovician rocks from eastern Yunnan, the Ordovician stratigraphic sequence of eastern Yunnan have been set up progressively, which is the Tangchi, Hungshihyen, Qiaojia and Daqing formations in ascending order (Zhang and Zhang, 2013). Several studies on Ordovician acritarch assemblages in eastern Yunnan have been carried out since 1980s, such as Fang (1986), Gao (1991), Li (1991), Li and Yuan (1995, 1997), and Li et al. (2004). Their studies show variety in diversity and systematic of the acritarch assemblage from eastern Yunnan. Recently Zhang and Zhang (2013) restudied graptolite from this area, which give us more stratigraphic information.

The samples were collected from the Tangchi and Hungshihyen formations of the Liujiang section and the Qiaojia Formation of the Guihuaqing Reservoir Bank section in the Luquan for acritarch analysis.

A total of 31 species assigned to 25 genera have been recognized from the Tangchi Formation and 33 species attributed to 27 genera from the Hungshihyen Formation in the Liujiang section, and 25 species assigned to 19 genera from the Qiaojia Formation in the Guihuaqing Reservoir Bank section. The acritarch assemblage is dominated by *Leiosphaeridia*, *Dactylofusa velifera*, *Rhopaliophora* and *Pterospermella* from the Tangchi Formation, *Ploygonium*, *Cymatiogalea/Stelliferidium*, *Coryphidium* and *Striatotheca* from the Hungshihyen Formation, and *Polygonium*, *Cymatiogalea*, and *Leiosphaeridia* from the Qiaojia Formation.

Zhang and Zhang (2013) identified the *Baltograptus varicosus* graptolite Zone in the Hungshihyen Formation, which referred to the interval of the middle Floian. The present of *Arbusculidium filamentosum*, *Aureotesta clathrata* var. *simplex*, *Coryphidium* cf. *elegans*, *Cristallinium cambriense*?, *Dactylofusa velifera*, *Dasydorus cirritus* and *Rhopaliophora* indicate that the Tangchi Formation probably represent the sediment of the Upper Tremadocian (1d)-Middle Floian (2b). The Hungshihyen Formation represents the middle-upper Floian strata because of the present of *Ampullula erchunensis*, *Barakella felix*, and *Coryphidium bohemicum*. Most acritarch taxa identified from the Qiaojia Formation in the Guihuaqing Reservoir Bank Section are widely distributed in the Floian-Darriwilian South China, so that the Qiaojia Formation probably represents the sediments of the Dapingian or Darriwilian age. More detailed studies are need on the Ordovician biostratigraphy, palaeoenvironment, and palaeogeography in eastern Yunnan.

REFERENCES

FANG X., 1986. Ordovician micropaleoflora in Kunming-Luquan region, Yunnan Province and its stratigraphical significance. *Professional Papers of Stratigraphy and Palaeontology*, 16: 125–172 (in Chinese with English abstract).

GAO L., 1991. Acritarchs from the Lower Ordovician Hongshiya Formation of Wuding, Yunnan. *Geological Review*, 37: 445-455 (in Chinese with English abstract).

LI J., 1991. The Early Ordovician acritarchs from Southwest China. Unpublished Ph. D. Thesis, Nanjing Institute of

geology and palaeontology, Academia Sinica, Nanjing, 88pp (in Chinese with English summary).

LI J. and YUAN X., 1995. Early Ordovician Armorican quartzite facies from eastern Yunnan, China. *Journal of Stratigraphy*, 19: 58-61 (in Chinese with English abstract).

_____, 1997. Arenigian acritarchs from the Upper Yangtze Region, Southern China. *Journal of Stratigraphy*, 21: 281-288 (in Chinese with English abstract).

LI J., SERVAIS, T., YAN K., ZHU H., 2004. A nearshore-offshore trend in the acritarch distribution of the Early-Middle Ordovician of the Yangtze Platform, South China. *Review of Palaeonbotany and Palynology*, 130: 141-161.

ZHANG J. and ZHANG Y., 2014. Graptolite fauna of the Hungshihyen Formation (Early Ordovician), eastern Yunnan, China. *Alcheringa*, 38: 434-449.

A new tube-like enigmatic animal and its burrows from the Upper Ordovician of the Siberian Platform

Veronica B. Kushlina[1], Andrei V. Dronov[2] and David A.T. Harper[3]

[1]*Boryssiak Paleontological Institute of Russian Academy of Sciences, Profsouznaya ul. 123, 117997, Moscow, Russia, vkush@paleo.ru.*
[2]*Geological Institute, Russian Academy of Sciences. Pyzhevsky per.7, 119017, Moscow, Russia.*
[3]*Palaeoecosystems Group, Department of Earth Sciences, Durham University DH1 3LE, UK.*

Numerous conical-shaped, trace fossils similar to "Jõhvilites" from the Jõhvi regional stage of Estonia and northwestern Russia were found, during 2013, in the Upper Ordovician (Katian) cool-water carbonate succession of the Dzherom Formation (Dolborian regional stage) in northeastern part of the Tungus basin on the Siberian platform (Moyerokan and Moyero River valleys). The fossils are represented by vertically oriented conical or bulbous accumulations of bioclastic material (bioclastic packstone) surrounded by carbonate rocks with much lower concentrations of bioclasts (mudstone or wackestone). The dominant bioclasts are fragments of trilobite carapaces, brachiopod and ostracods shells. The regular conical shape of the trace fossils is similar to *Conichnus conicus* Männil, 1966 from the Upper Ordovician of Baltoscandia but is usually larger (10-15 cm high and about 7-12 cm in diameter). Closely spaced conical or bulbous burrows sometimes overlap each other. In several conical detrital accumulations, calcite tubes of about 1-2 cm in diameter were found in an axial or slightly tilted position in the cones.

During 2014, outcrops of the Dolbor Formation (Dolborian regional stage) along the Nizhnaya Chunku River in the southern part of the Tungus basin yielded numerous large (up to 1,5 m long and up to 5 cm in diameter) tube-like organisms of unknown affinity were studied. Where *in situ* the lower end of the tube is vertically oriented (perpendicular to bedding planes) and surrounded by a detritic envelope of conical shape. Detritic cones are thus closely connected with the calcite tubes and represent trace fossils for which the tube-like animals were trace-makers. It seems that the sessile animal burrowed into the sediment and accumulated bioclastic debris around its lower end in order to construct a kind of anchor preventing it from being plucked out by storm events. The tube-like animal has a uniform skeleton consisting of fibrous calcite. It appears to represent an undescribed cnidarian, probably similar to *Sphenothallus*. The tube-like animals and their traces are abundant in the Dolborian regional stage deposits of the Tungus basin.

Biogeographic origins and dispersal pathways of invasive taxa: The Late Ordovician (Katian) Richmondian invasion, Cincinnati area, Ohio

Adriane R. Lam[1] and Alycia L. Stigall[2]

[1]*Department of Geological Sciences, Ohio University, Athens, OH 45701, lam2ar@dukes.jmu.edu.*

²OHIO Center for Ecology and Evolutionary Studies and Department of Geological Sciences, Ohio University, Athens, OH 45701.

   The Late Ordovician Richmondian Invasion involved the immigration of over 60 genera into the Cincinnati Basin. Multiple competing hypotheses about the geographic origin of the invaders and the processes that facilitated the faunal migration event have been articulated over the past century. To clarify pathways and processes of the invasion, a suite of quantitative biogeographic methods were employed. These analyses compared biogeographic patterns using either all invader genera (Parsimony Analysis of Endemicity [PAE]) or brachiopod and trilobite clades with resolved species-level phylogenetic hypotheses (Fitch Parsimony, Lieberman-modified Brooks Parsimony Analysis [LBPA], and BioGeoBEARS) during two timeslices—the T1 (Cincinnati depositional sequences M5-C3) and T2 (C4-C6 sequences).

   Biogeographic patterns recovered from BioGeoBEARS analysis and Fitch optimization of four brachiopod and trilobite clades that speciated during the focal intervals produced congruent results. During the T1 timeslice, several dispersal paths operated among interior Laurentian basins as well as cool-water marginal basins. During the T2 timeslice, dispersal occurred among the Upper Mississippi Valley, Northern and Southern Laurentia, the Southern Appalachian Basin, and the Cincinnati Basin. Furthermore, BioGeoBEARS analysis indicated a prominent role for founder event speciation in the evolution of these clades.

   General area cladograms of geodispersal and vicariance patterns produced via LBPA were identical for the T1 timeslice, indicating that cyclical processes controlled speciation processes during this time. Both areagrams indicate that the Upper Mississippi Valley, Western Midcontinent, Southern Laurentia and areas north of the Transcontinental Arch share a close area relationship. The Scoto-Appalachian Basin and Cincinnati Basin also share a close area relationship. The T2 time slice vicariance and geodisperal areagrams are incongruent and indicate that non-cyclical events primarily structured biogeographic patterns during this interval. Notably, Baltica became separated from the Southern Appalachian Basin and connected to Northern Laurentia during this time interval. The Western Midcontinent, Upper Mississippi Valley, and areas North of the Transcontinental Arch also exhibit close area relationships within both vicariance and geodispersal areagrams during this interval.

   Results of PAE based on occurrence data for over 60 genera of Richmondian invaders across the C1 to C5 depositional sequences indicates that several dispersal paths operated during the invasion interval. Three separate dispersal events were hypothesized to occur from Baltica into Laurentia. In addition, several of the paths uncovered using parsimony and maximum likelihood methods are echoed in the PAE analysis, such as the close area relationship between the Upper Mississippi Valley, Western Midcontinent, and areas north of the Transcontinental Arch.

   The equatorial Iapetus current would have facilitated dispersal between Laurentia and Baltica with volcanic island arcs providing stepping-stones between paleocontinents. Dispersal among Laurentian basins, particularly midcontinent basins, during the T1 timeslice was aided by counter-clockwise circulation patterns created by the influx of cool water into the Laurentian craton via the Sebree Trough. In addition, upwelling zones within the western midcontinent region facilitated dispersal of planktic larvae into surrounding basins. Dispersal among Laurentian basins during the T2 timeslice was likely influenced by a major transgression which took place at the C5 sequence boundary, hypothesized to have broken down preexisting physical barriers and allowing dispersal across deep-water areas acting as thermal barriers. Strong storm activity and surface currents aided in dispersal of larvae among western and eastern basins.

   When combined, these results indicate that several multidirectional dispersal paths were operational before and during the Late Ordovician Richmondian Invasion, thus supporting several prior hypotheses about the biogeographic origin and immigration pathways used by invasive taxa. Maximum likelihood analyses reveal that founder-event speciation was an important speciation type among benthic Paleozoic taxa.

The first sphinctozoan-bearing reef from an Ordovician back-arc basin

Qijian Li[1], Yue Li[2], and Wolfgang Kiessling[1,3]

[1]GeoZentrum Nordbayern, University of Erlangen-Nürnberg, Erlangen 91054, Germany,
qijianli@hotmail.com.
[2]Nanjing Institute of Geology and Palaeontology, Chinese Academy of Sciences, Nanjing 210008, China.
[3]Museum für Naturkunde, Invalidenstr. 43, 10115 Berlin, Germany.

Compared to the Permian and Triassic, there were just sporadic and limited reports of reef-building sphinctozoans (multi-chambered sponges) in the Early Paleozoic. Here we document the oldest sphinctozoan-coral-microbial reef from the Upper Sanqushan Formation (late Katian) of southeast China, which is also the first report of Ordovician sphinctozoans from South China. The studied site (29° 00'15"N, 118°32'17"E) is located next to Wu'ai village, some 11 km to the north of the Changshan. Paleogeographically, this site belongs to the north margin of Zhe-Gan platform. The sponges occur in a >120m thick reef that is mainly constructed by calcimicrobes (*Kordephyton*, *Renalcis* and *Epiphyton*) with a low abundance of *in situ* metazoans, predominantly sphinctozoan sponges (*Corymbospongia*) and rugose corals (mostly *Palaeophyllum* and *Streptelasma*). Only a few centimeter-scale fragments of massive tabulate corals and stromatoporoids are found in thin sections. *Tetradium* is the only genus of tabulate corals which is preserved in growth position. Crinoids and brachiopods are common reef dwellers. Stromatactis is abundant. Bio- and litho-facies in this area as well as the characteristics of the microbialite show that the reef developed in a deeper subtidal setting that was unfavorable for most metazoan reef builders. In contrast to the high-energy stromatolite-sphinctozoan reefs from the Late Silurian, our case represents a low-energy community, indicating that the first reef-building sphinctozoan (*Corymbospongia*) might have originated in a relatively deep environment on seamounts of a back-arc basin during the Late Ordovician.

Early Ordovician lithistid sponge-*Calathium* reefs on the Yangtze Platform and their paleoceanographic implications

Qijian Li[1], Yue Li[2], Jianpo Wang[3], and Wolfgang Kiessling[1,4]

[1]GeoZentrum Nordbayern, University of Erlangen-Nürnberg, Erlangen 91054, Germany,
qijianli@hotmail.com.
[2]Nanjing Institute of Geology and Palaeontology, Chinese Academy of Sciences, Nanjing 210008, China.
[3]Wuhan Center of Geological Survey, Wuhan 430205, China.
[4]Museum für Naturkunde, Invalidenstr. 43, 10115 Berlin, Germany.

Lithistid sponge-*Calathium*-microbial reefs were widespread on the Yangtze Platform during the Early Ordovician and are well studied. However, the biological affinity and the role of *Calathium* in these reefs have remained unclear up to now. We document lithistid sponge-*Calathium* reefs from the Upper Hunghuayuan Formation (early Floian) at Huanghuachang in Hubei, South China. These reefs have a three-dimensional skeletal framework that is mostly produced by *Calathium* and lithistid sponges. *Calathium* had a critical role in reef construction, as demonstrated by well-developed lateral outgrowths, which connected individuals of the same species and with lithistid sponges. Bryozoans, stromatoporoids and microbial components were secondary reef builders.

Morphological, constructional and functional analyses provide evidence that *Calathium* was a sponge-grade metazoan rather than a receptaculitid alga as previously thought. Lithistid sponge-*Calathium* reefs of early Floian achieved a comparable ecological complexity as Cambrian archaeocyathan-dominated reefs. At the dawn of the Ordovician Radiation, these lithistid sponge-*Calathium* reefs as well as the oldest bryozoan reefs in the same area show that a suite of calcifying metazoans began to take control over reefs individually or in concert, indicating an initial rebound for metazoan-dominated reefs after the late-Early Cambrian metazoan reef crisis.

Distributional data of *Calathium* were extracted from the Paleobiology Database (PaleobioDB, http://paleobiodb.org). After sampling standardization, an equatorward shrinkage of the latitudinal range has been found from the Early through Middle Ordovician. And we compiled body size data of *Calathium*

based on our own material and the literature. A significant increase of body size from the Early to the Middle Ordovician is evident (W=3.5, p=0.01005, two-tailed Wilcoxon test). Both latitudinal distribution and body-size trend of *Calathium* supported that gradual global cooling through the Early Ordovician may have been a key driver for the return of metazoan reefs.

Early-Middle Ordovician chitinozoan biodiversification of Upper Yangtze Platform, South China

Yan Liang, Peng Tang and Ren-bin Zhan

State Key Laboratory of Palaeobiology and Stratigraphy, Nanjing Institute of Geology and Palaeontology, Chinese Academy of Science, Nanjing 210008, China, liangyan@nigpas.ac.cn.

As an extinct group of organic-walled, planktonic microfossils, chitinozoans are widely preserved in many types of marine deposits from Early Ordovician (late Tremadocian) to Late Devonian (latest Famennian). Recently, chitinozoans are becoming more and more important in biostratigraphy and the stratigraphic correlation because of the short stratigraphical range and the wide distribution of their species. For more than 10 years, paleontologists in China have conducted many case studies particularly on the Great Ordovician Biodiversification event (GOBE), i.e. the Ordovician radiation, and many of their preliminary achievements on the macroevolution of graptolites, trilobites, brachiopods and conodonts have obtained a lot of attention from their international colleagues. But, up to now, there are very few studies particularly on the Ordovician chitinozoan radiation in China, which becomes the main theme of our investigation.

Altogether, 264 samples from 5 Lower-Middle Ordovician sections in the Upper Yangtze Platform have been collected and processed for the study of chitinozoans. The rocks yielding these samples include the Cambrian-Ordovician boundary strata to the lower Darriwilian at the Xiangshuidong section (Songzi, southwestern Hubei, central China), the uppermost Darriwilian to the lower Sandbian at the Jieling section (northern Yichang, western Hubei, central China), the Cambrian-Ordovician boundary strata to the lower Floian at the Xishui section (northern Guizhou, SW China), the upper Tremadocian to the lower Sandbian at the Tongzi section (northern Guizhou, SW China), and the Darriwilian at the Shizipu section (Zunyi, northern Guizhou, SW China), representing different paleogeographic settings on the Upper Yangtzer Platform.

According to our preliminary systematic study, about 112 species of 21 genera have been identified, indicating a significantly higher chitinozoan diversity than that of those previous data, such as the diversity curve of Paris et al. (2004), the only reference revealing the Ordovician chitinozoan diversity of China. Unfortunately, data are far from enough to investigate the chitinozoan macroevolution in China about ten years ago. For example, the taxonomic diversity of early Sandbian indicated by Paris et al. (2004) is only 15 species including taxa of open nomenclature. Our preliminary investigation shows that there are 21 species of chitinozoans could be recognized from the Miaopo Formation (lower Sandbian) of Jieling, northern Yichang, while those taxa of open nomenclature, about 22 species, are excluded (Liang et al., 2014, 2015). Some more material has also obtained from the Saergan Formation (lower Sandbian) of Dawagou, northern Tarim (Hennissen et al., 2010), and the materials documented by Zhang and Chen (2005) for this particular period. Besides, our investigation shows an apparent taxonomic diversity acme for the first time during late Tremadocian and early Floian, representing the first pulse of the Ordovician chitinozoan radiation in South China, which coincides with that of graptolites (Chen et al., 2006).

Further systematic study and related macroevolutionary analyses are in progress.

REFERENCES

CHEN, X., ZHANG, Y. D. and FAN, J. X., 2006. Ordovician graptolite evolutionary radiation: a review. *Geological journal*, 41: 289-301.
HENNISSEN, J., VANDENBROUCKE, T. R. A., CHEN, X., TANG, P. and VERNIERS, J., 2010. The Dawangou auxiliary GSSP (Xinjiang autonomous region, China) of the base of the Upper Ordovician Series: putting global chitinozoan biostratigraphy to the test. *Journal of Micropalaeontology*, 29: 93-113.

LIANG, Y., TANG, P., WU, R. C., LUAN, X.C. and ZHAN, R. B., 2015. Chitinozoan biostratigraphy of the Middle-Upper Ordovician Miaopo Formation of Yichang, Hubei Province. *Journal of Stratigraphy*, in press. (In Chinese with English Abstract)

LIANG, Y., TANG, P., ZHAN, R. B. and WU, R. C., 2014. New data of early Late Ordovician chitinozoans from the Miaopo Formation at Jieling, Yichang, Central China. *GFF*, 136(1): 162-166.

PARIS, F., ACHAB, A., ASSELIN, A., CHEN, X. H., GRAHN, Y., NÕLVAK, J., OBUT, O., SAMUELSSON, J., SENNIKOV, N., VECOLI, M. and VERNIERS, J., 2004. Chitinozoans. In: WEBBY, B. D., DROSER, M. L., PARIS, F. and PERCIVAL, I. (ed.): *The Great Ordovician Biodiversification Event*, 294-311. New York: Columbia University Press, 466 pp.

ZHANG, M. and CHEN, X. H., 2005. Chitinozoans from the Upper Ordovician of the graptolite *Nemagraptus gracilis* Zone of the central Yangtze Region. *Acata Micropalaeontologica Sinica*, 22(4): 383-391. (In Chinese with English Abstract)

The Stairsian-Jeffersonian Stage boundary in southern New Mexico and westernmost Texas, USA

James Loch[1], J. F. Taylor[2], R. L. Ripperdan[3], P. M. Myrow[4], and S. J. Irwin[2]

[1]*University of Central Missouri, loch@ucmo.edu.*
[2]*Geoscience Department, Indiana University of Pennsylvania, Indiana, PA 15705.*
[3]*947 Curran Ave., Kirkwood, MO, 63122.*
[4]*Department of Geology, Colorado College, Colorado Springs, CO 80903.*

The Hitt Canyon Formation (El Paso Group) in the southwestern USA contains trilobite faunas that tightly constrain the position of the Stairsian – Jeffersonian Stage boundary in close association with a marked negative carbon isotope (δ13C) excursion referred to as the 'José Event.' This conjunction of stratigraphic markers facilitates detailed correlation to contemporaneous successions.

The informal middle member of the Hitt Canyon, referred to as the "Cookes member," is characterized by numerous microbial bioherms interstratified with nodular lime mudstone and bioclastic rudstone. The overlying Jose' Member comprises dark, oolitic limestone with locally coquinoid concentrations of trilobite sclerites. The succeeding McKelligon Formation marks a return to lighter gray interstratified lime mudstone with bioherms that include Calathium and Archaeoscyphia.

Sparse trilobite faunas from the Cookes and lower part of the Jose include Hyperbolocheilus, Hystricurus, Flectihystricurus, Pseudoclelandia and other genera restricted to the Stairsian Stage in the standard Ibexian succession of western Utah. The Stairsian collections from the El Paso Group include some species with restricted stratigraphic ranges in Utah and southern Idaho, allowing recognition of several of the eleven new trilobite-based biozones recently delineated within the Stairsian Stage in the Great Basin. The uppermost collection in the Cookes Member at Cable Canyon in southern New Mexico is assigned to the Bearriverops loganensis Zone, while the next higher collection in that section, from the lower third of the Jose, represents the Pseudohystricurus obesus Zone. Four other zones that lie between these units in the new zonation are likely absent due to an unconformity at the Cookes-Jose member contact in this area.

The appearance in the upper part of the Jose member of multiple species of the asaphid Aulacoparia, and the less abundant bathyurid Cullisonia (formerly Jeffersonia), marks the transition into the overlying stage. Although Aulacoparia characterizes the base of the Tulean Stage in Utah, we assign the strata in the upper Jose and overlying McKelligon Formation to the eastern Laurentian Jeffersonian Stage on the basis of the abundance of bathyurids and the absence of hystricurids from these units -- a faunal composition more similar to the trilobite faunas of the North American mid-continent.

Carbon isotope profiles through the preserved Sauk Sequence carbonates of the El Paso Group reach their maximum negative value immediately below the Cookes – Jose' member boundary. The 'José Event' punctuates a distinctive pattern of δ13C variation through the Cookes and José members extending into the lower McKelligon Formation and allows detailed correlation of the Stairsian-Jeffersonian stadial boundary into the Ibexian rocks of Utah and the sparsely fossiliferous Jefferson City Formation of Missouri. The characteristic sharp fall in δ13C values, within the Macerodus dianae conodont Zone, is

easily recognized in the uppermost units of the lowest informal member of the Fillmore Formation in the Ibex region, just above the informal 'Hintze's Reef' unit.

New cryptostome *Prophyllodictya* (bryozoa) from the Nantzinkuan Formation (early Tremadocian, Lower Ordovician) of Liujiachang section, western Hubei, China and its phylogenetic implications

Junye Ma[1], Paul D. Taylor[2], and Fengsheng Xia[1]

[1]*Department of Micropalaeontology and State Key Laboratory of Palaeobiology and Stratigraphy (SKLPS), Nanjing Institute of Geology and Palaeontology, Chinese Academy of Sciences(CAS), Nanjing 210008, China, jyma@nigpas.ac.cn.*
[2]*Department of Earth Sciences, Natural History Museum, London SW7 5BD, UK.*

Bryozoa is the only phylum having a biomineralized skeleton that is lacking in the Cambrian, their fossil record goes back to the early Ordovician (Hu and Spjeldnaes, 1991; Taylor and Ernst, 2004; Xia *et al*. 2007). New cryptostome *Prophyllodictya* has been identified from the Nantzinkuan Formation (Early Tremadocian, Lower Ordovician) of Liujiachang, central China. Colony morphology and the phylogenetic position of *Prophyllodictya* within Cryptostomata are explored. And the results of phylogenetic analysis suggest that *Prophyllodictya* appears at a basal position in the cryptostome tree, which accords with the simplicity of its morphology and chronostratigraphical occurrence among early bryozoans. This new *Prophyllodictya* bryozoa from the Nantzinkuan Formation antedates the previously oldest known bryozoan from Fenghsiang Formation by several million years and shed light on the origination of bryozoa.

REFERENCES

HU Z., SPJELDNAES, N., 1991. Early Ordovician bryozoans from China. In: Bigey, F. P.& J.-L. d'Hondt., Eds., *Bryozoa Living and Fossil*. Bulletin de la Societe des Sciences Naturelles de l'Ouest de la France. Mémoire Hors Serie 1. pp. 179-85
TAYLOR, P.T., ERNST, A., 2004. Bryozoans, p. 147-156. *In* Webby, B. D., Paris, F., Droser, M. L., and Percival, I. G., Eds., *The Great Ordovician Biodiversification Event*. Columbia University Press, New York. pp. 99-119.
XIA F., ZHANG S, WANG Z., 2007. The oldest bryozoans: new evidence from the late Tremadocian (Early Ordovician) of East Yangtze Gorges. *Journal of Paleontology*, 81: 1308-1326.

Graptolite faunas and biostratigraphy of the Hulo Formation (Ordovician) in the Anji area, SE China

Xuan Ma[1] and Yuandong Zhang[2]

[1]*Nanjing Institute of Geology & Palaeontology, University of Chinese Academy of Sciences, 39 East Beijing Road, P.R. China, mxnjues1990@126.com*
[2]*Key Laboratory of Economic Stratigraphy & Palaeogeography, Nanjing Institute of Geology & Palaeontology, Chinese Academy of Sciences, 39 East Beijing Road, P.R. China.*

The Jiangnan Region is located to the southeast of Yangtze Region, and is generally regarded as representing a slope environment of South China Plate during the Ordovician (Zhang et al., 2007). Anji area is located in the northeastern Jiangnan Region and adjacent to northwestern Majin-Wuzhen Fault. In this region, graptolite sequences are complete or nearly complete, providing a good case for studying the graptolite diversification in Ordovician geographically and temporally (Zhang et al., 2006, 2007, 2008). Some 1100 samples were collected from the Hulo Formation of the Jiumulong section in Anji area, SE

China. A total of 32 species assigned to 19 genera have been recognized from the Hulo Formation and can be divided into three graptolite biozones : the *Acrograptus ellsae* Biozone, the *Nicholsonograptus fasciculatus* Biozone and the *Pterograptus elegans* Biozone. The graptolite assemblage is dominated by three zone fossils above as well as *Tylograptus geniculatus*, *Tylograptus intermedius*, *Cryptograptus tricornis, Phyllograptus uniformis, Xiphograptus norvegicus, Kalpinograptus ovatus, Archiclimacograptus angulatus* etc.

   In the Early to Middle Ordovician in the Jiangnan Region, the graptolite diversification is prominent and can be divided into three stages and one peak based on the trajectory and the faunal composition, and the third stage ranges from the early Darriwilian to the end of Middle Ordovician. During this stage, graptolites' ecosphere dominated in large-scale expansion, and graptolite diversity fluctuated in high level, and significant replacements of graptolite faunas took place (Chen et al., 2006; Zhang et al., 2008, 2010). Evolutionary-radiation study is based on three aspects: taxonomic diversity, ecologic diversity and disparity or morphological diversity (Chen et al., 2006). The graptolite fauna of the Hulo Formation in Anji area can provide excellent evidence to explore the relationship of the environment changes and the graptolite evolutionary-radiation.

REFERENCES

CHEN, X., ZHANG, Y. D., FAN, J. X., 2006. Ordovician graptolite evolutionary radiation: a review. *Geological Journal*, 41: 289-301.
ZHANG, Y. D., CHEN, X., 2006. Evolutionary radiation of the Early-Mid Ordovician graptolites in South China. *In*: J.Y. Rong (ed.), *Originations, Radiations and Biodiversity Changes-Evidences from the Chinese Fossil Record*. Science Press, Beijing, 285-316.
ZHANG, Y. D., CHEN, X., YU, G. H., GOLDMAN, D., LIU, X., 2007. *Ordovician and Silurian rocks of northwaet Zhejiang and northeast Jiangxi Provinces, SE. China*. University of Sciences and Technology of China Press, Hefei, 5-15
ZHANG, Y. D., CHEN, X., 2008. Diversity history of Ordovician graptolites and its relationship with environmental change. *Science in China Series D - Earth Science,* 51: 161-171
ZHANG, Y. D., CHEN, X., GOLDMAN, D., ZHANG, J. CHENG, J.F., SONG, Y.Y., 2010. Diversity and paleobiogeographic distribution patterns of Early and Middle Ordovician graptolites in distinct depositional environments of South China. *Science in China Series D - Earth Science,* 53: 1811–1827.

A taxonomic restudy of *Ningxiagraptus* Geh, 2002

Xuan Ma[1], Xu Chen[1], and Dan Goldman[2]

[1]*Key Laboratory of Economic Stratigraphy & Palaeogeography, Nanjing Institute of Geology & Palaeontology, Chinese Academy of Sciences, 39 East Beijing Road, P.R. China, mxnjues1990@126.com.*
[2]*Department of Geology, University of Dayton, 300 College Park, Dayton, OH 45469.*

   Yang Jingzhi and Mu Enzhi (1954) first reported the graptolite fauna from the black shale of Miaopo Formation (Sandbian, Upper Ordovician) in Yichang, South China, in which they identified a peculiar species, *Leptograptus* sp. nov. The specimens of this species were later studied and identified by Geh (1963a) as a known species, *Leptograptus yangtzensis* Mu.

   However, Ge (in Mu et al., 2002) later regarded that the species did not belong to *Leptograptus*, and assigned it to *Ningxiagraptus* Ge, a new genus he erected in the same publication and designated *Janograptus reclinatus* Ge, 1990 as its type species. The new genus included three species: *Ningxiagraptus reclinatus* (Ge), *Ningxiagraptus yangtzensis* (Mu) and *Ningxiagraptus*? *yuani* (Sun). Based on our restudy of the type specimens of *Janograptus reclinatus* stored in NIGPAS and new specimens of *Ningxiagraptus yangtzensis* (Mu) collected in recent years by some of the present authors, herein we regard *Ningxiagraptus reclinatus* (Ge) (=*Janograptus reclinatus* Ge, 1990) as a junior synonym of *Ningxiagraptus yangtzensis* Mu (in Geh, 1963a) (=*Leptograptus yangtzensis* Mu (in Geh, 1963a)). Thus, the type species of the genus *Ningxiagraptus* should be changed to *Ningxiagraptus yangtzensis* (Mu), and accordingly we revise the diagnoses of the genus *Ningxiagraptus* as follows:

1. Two stipes are reclined with simple, straight thecae. 2. The sicula is commonly inclined towards and pressed tightly against th2[1], with a noteworthy bend. 3. Virgella and mesial spines on the first thecal pair are present in the proximal end. 4. The proximal development resembles that of *Dicellograptus* except for the origination of the second theca, which turns upward at the sicular aperture and tends to be "U"-shaped in the former (v. "L"-shaped in the latter). Despite of the different theca types from that of *Dicellograptus*, *Ningxiagraptus* is very similar to *Dicellograptus* in the development and the morphology of the proximal end, especially to the coeval *Dicellograptus rectus* (Ruedemann, 1947), and accordingly we put *Ningxiagraptus* also under the Superfamily Dicranograptoidea.

Neodymium isotopes and the Late Ordovician evolution of the North American mid-continental seaway

Kenneth G. MacLeod[1] and Kelsey P. Hughes[2]

[1]*Dept. of Geological Sciences, University of Missouri, Columbia, MO 65211, macleodk@missouri.edu.*
[2]*506 E. Winston Cir., Broken Arrow, OK 74011.*

Study of neodymium isotopic ratios in Late Ordovician samples has good potential to advance understanding of interactions among climate, paleoceanography, and patterns of sedimentation in the North American mid-continental seaway. Well documented Late Ordovician events include loss of tropical character in limestones after the Turinian, changes in facies distribution within the seaway, large carbon isotopic excursions, and a Period-culminating glaciation and mass extinction. However, an increasingly well resolved dataset of conodont oxygen isotopic measurements provides no evidence for progressive regional cooling over the last 10 million years of Ordovician. Attempts to integrate these different observations into coherent paleoenvironmental scenarios often result in explicit or implicit predictions about the source and circulation of water in the seaway. Neodymium isotopic studies could be used to test these predictions as neodymium isotopes are a quasi-conservative water mass tracer and an indicator of the age of source regions contributing sediment to the basin.

Possible insights from and challenges for neodymium studies will be discussed relative to data from the Richmondian-aged Dubuque/Maquoketa transition in NE Iowa and SE Minnesota. In much of the upper Mississippi Valley, the limestone-rich Dubuque Formation is disconformably overlain by the shalely Maquoketa Formation. The contact coincides with one or more phosphatic hardgrounds, and the lower Maquoketa is phosphate-rich. This lithologic progression has been explained by invoking upwelling of cool, nutrient-rich waters from the Sebree Trough during a time of sea level rise resulting in enhanced local productivity and the deposition of phosphatic, low oxygen Maquoketa Shales over the Dubuque Limestones. Conodont oxygen isotopic ratios at several locations do not support contemporary cooling, and the values are similar to Late Ordovician conodont oxygen isotopic values across the mid-continent. However, neodymium isotopes measured on phosphatic brachiopod shells collected at the Webber Quarry in Dubuque, IA do support a paleoceanographic change across the Dubuque/Maquoketa contact. The lowest neodymium isotopic values are at the base of the measured section. These values are ~4 units higher than values measured in older (Turinian/Chatfieldian) samples from the same area indicating significant change between the Turinian and the Richmondian. Across the lower 8 m of the Webber Quarry section, values increase by an additional 3 to 4 units. Couched relative to previous Nd studies, all Webber Quarry neodymium isotopic values are too high to be considered part of the Mid-continent aquafacies, and data do not exist to determine the timing or rate of the Turinian to Richmondian increase. During the Dubuque/Maquoketa transition, values increase from those similar to the low end of Taconic aquafacies to values transitional between Taconic aquafacies and the Open Ocean aquafacies. Such a shift is consistent with an increased influence of waters from the south and/or the east as invoked in the upwelling model. Alternatively, the shift could be explained by an increased input of young Taconic volcanics and subsequent boundary exchange. Parallel measurement of detrital material and phosphatic fossils are needed to distinguish between these possibilities, and better geographic and stratigraphic coverage will be required to maximize the contribution of Nd-based constraints on circulation and source regions to the development of paleoceanographic models spanning the Late Ordovician.

The Sandbian (Upper Ordovician) raphiophorid trilobite Ampyxina powelli: New insights on its description and taphonomy

Mike Meyer[1], Edward Fowler[2], Aaron Howard[3], and William Fleming[4]

[1]*Penn State Harrisburg.*
[2]*Agua Dulce, California, efowler3093@att.net.*
[3]*Western Carolina University.*
[4]*East Carolina University.*

Ampyxina powelli is a small (~1 cm long) trilobite commonly found in Upper Ordovician (Sandbian) deep-water shales and limestones in the Liberty Hall facies (lower Edinburg Formation) of southwest Virginia. Though this trilobite has been used as a biostratigraphic index fossil for the region, due to its relative sparseness and limited range, A. powelli has been subject to very few studies in the last half-century. Recently one of the few active localities where A. powelli has been found, the Tucker Farmhouse locality in southwest-most Roanoke County, VA, is again being sampled with A. powelli specimens sampled. To better understand the evolutionary placement of A. powelli within the greater Raphiophorid group, its developmental history, and taphonomy, these newly collected specimens have been analyzed using modern techniques. These include an updated description, new information on its biostratigraphic correlation, taphonomy, and geometric morphometric, statistical, and micro-beam analyses. New data on the stratigraphic relationships of A. powelli, graptolite faunas, and recent GSSP data allow for a better constraint on the age of the supporting shales. The updated description includes new insights into its morphology and phylogenetic relationships. Geometric morphometric analysis does not show any sub-groups present in the newly collected specimens. The presence or absence of cephalic spines does not seem to correspond to any dimorphic or ontogenetic groups. The taphonomy of A. powelli is simple, there is rarely any organic material associated with the fossils, which supports a molt-based origin for the concentration of trilobite carapaces at this locality. Where there is evidence for organic remains it is mostly in the form of relatively small Pyrite framboids attached or within the calcitic carapace. Overall, this is an intriguing species that requires further investigation and will continue to contribute to the understanding of this region's Ordovician paleoecology.

Proposed auxiliary stratigraphic section and point (ASSP) for the base of the Ordovician System at Lawson Cove, Utah, USA

James F. Miller[1], Raymond L. Ethington[2], John E. Repetski[3], R.L. Ripperdan[4], and John F. Taylor[5]

[1]*Geography, Geology & Planning, Missouri State University, Springfield, MO 65897, jimmiller@missouristate.edu.*
[2]*Geological Sciences Department, University of Missouri, Columbia, MO 65211.*
[3]*U.S. Geological Survey, 12201 Sunrise Valley Drive, Reston, Virginia 20192.*
[4]*1417 Fairbrook Drive, Des Peres, MO 63131.*
[5]*Geoscience Department, Indiana University of Pennsylvania, Indiana, PA 15705.*

   The base of the Ordovician System was defined to coincide with the lowest occurrence of the conodont *Iapetognathus fluctivagus* in Bed 23 of the Green Point section in the Cow Head Group of western Newfoundland. That horizon was intended to provide a reliable marker for a wide range of depositional environments, in recognition of strong differences between high-latitude Acado-Baltic and tropical environments such as in western Laurentia. However, intercontinental correlations based on associated taxa and non-biological stratigraphic markers at Green Point have proven to be problematic, in part because the depositional environment of the Cow Head Group is so different from shallow-water carbonates in western Laurentia and elsewhere.
   We propose establishing an Auxiliary Stratotype Section and Point (ASSP) at the lowest occurrence of *Iapetognathus fluctivagus* in the Lawson Cove section in the Ibex Area, Utah, USA to provide a more robust framework for a variety of stratigraphic markers that are poorly constrained in the existing GSSP. Lawson Cove was the alternative section considered for the base of the Ordovician GSSP.

Three papers in *Ordovician Odyssey*, the proceedings volume of the 1995 Ordovician Symposium, reported close associations of *Iapetognathus* n. sp. 1 with the basal Tremadocian trilobite *Jujuyaspis* in Texas, New Mexico, and Utah. In the Utah paper, Miller and Taylor summarized known occurrences of *Iapetognathus* n. sp. 1 in various sections. Nicoll et al. (1999 BYU Geology Studies) named *I*. n. sp. 1 as *I. fluctivagus* and listed 21 occurrences of that species globally (their Table 2).

The Ibex Area is an ideal location for a basal Ordovician ASSP. Cambrian–Ordovician strata in the region are ~5300 m thick and were deposited on a shallow carbonate platform. The Lawson Cove section comprises 243 m of limestone that is without known unconformities. The section is on public land that is administered by a U.S. government agency and is always accessible. An ordinary passenger car can be driven to the base of the section. These strata have yielded many kinds of data that provide a broad context within which the system boundary can be correlated.

Faunal relationships at Lawson Cove and nearby sections provide the basis for precise global correlation using several fossil groups. Nearly 65,000 identified conodont elements have been used to delineate ten conodont zones or subzones below the proposed ASSP, and four above, that are recognized throughout Laurentia and on other paleo-continents. Important species level ancestor–descendant relationships have been identified. *Iapetonudus ibexensis*, the ancestor of *Iapetognathus fluctivagus*, occurs at the base of the 4.9-m *Iapetognathus* Zone. *Iapognathus sprakersi* and *Iapetognathus aengensis* occur higher in the section. Calcareous and phosphatic brachiopods have been documented in the Ibex sections. Tightly spaced trilobite collections through the boundary interval at Lawson Cove document rapid turnover in species of such biostratigraphically useful Laurentian genera as *Symphysurina*, *Chasbellus*, *Highgatella*, *Clelandia*, and *Millardicurus*. The cosmopolitan genus *Jujuyaspis* occurs less than one meter above the proposed ASSP. *Jujuyaspis* also occurs ~30 cm above the base of the *Iapetognathus* Zone at the nearby Lava Dam North section, where the zone is 4.3 m thick and contains a 15-cm shale band that yielded *Anisograptus matanensis*, a widespread lower Tremadocian planktic graptolite.

Carbon-isotope stratigraphy and sequence stratigraphy are non-biological tools that are useful for characterizing the proposed ASSP. The most prominent positive excursion peak on the carbon-isotope profile is only ~15 cm below the proposed ASSP. Miller et al. (2003 BYU Geology Studies) documented detailed sequence-stratigraphic and biostratigraphic frameworks at Lawson Cove, and one of their sequence boundaries coincides with the occurrence of *Jujuyaspis*. These diverse correlation tools would make the Lawson Cove section a useful ASSP.

Preferential extinction of mesopelagic species and disruption of graptolite community structure during the Late Ordovician mass extinction

Charles E. Mitchell[1], H. David Sheets[2], Michael J. Melchin[3], Jason Loxton[3] and Petr Štorch[4]

[1]*Department of Geology, University at Buffalo, SUNY, Buffalo, New York 14260, cem@buffalo.edu.*
[2]*Department of Physics, Canisius College, Buffalo, New York 14208.*
[3]*Department of Earth Sciences, St. Francis Xavier University, Antigonish, Nova Scotia B2G 2W5, Canada.*
[4]*Institute of Geology v.v.i., Academy of Sciences of the Czech Republic, 165 00 Praha 6, Czech Republic.*

Pelagic graptolites provide a unique window into the habitat changes and ecological disruptions that accompanied the Late Ordovician mass extinction (LOME). Although climate changes are a source of stress in ecological communities, few paleobiological studies have systematically addressed the impact of global climate changes on the fine details of community structure. We present here a detailed study of habitat selectivity and changes in the within-community species abundance distribution patterns of the late Katian and Hirnantian graptolite faunas during the LOME.

Using a Bayesian likelihood model, we employ the distribution of graptolite species among a set of well-studied localities of known depositional setting to infer whether those species were most likely members of the near-surface, epipelagic biotope or the deeper and exclusively oceanic, mesopelagic biotope. Deep sites: Dob's Linn, Vinini Creek (NV) and Trail Creek (ID). Shallow sites: Mirny Creek (Siberia) and three sites in the Canadian Arctic (Eleanor Lake, Truro Island and Cape Manning). Among the 40 species present in the *P. pacificus* Zone at these sites, 10 had posterior probabilities of being

epipelagic > 0.9, 14 appear to have been mesopelagic (p{mesopelagic} > 0.9) and 16 remained indeterminate (p's < 0.9). We then used these biofacies affiliations to assess the biofacies composition of a set of 303 samples from 15 sections from Laurentia (5), South China (5), Siberia (4) and Kazakhstan (1) that span the late Katian to early Hirnantian. Eleven of these sections were not part of the original Bayesian biofacies inference process and consequently provide a cross validation test – a test that strongly supports the biofacies model. Shallow shelf sites were dominated by epipelagic species (average proportion of mesopelagic species was 20-30%), whereas at mid to outer shelf sites 40-50% of species were mesopelagic. Slope to ocean floor sites were dominated by mesopelagic species (50-60% mesopelagic). Differences were even more pronounced in the species relative abundances at ocean floor (Vinini Creek) and outer shelf (Blackstone River, Yukon) sites.

Structural changes within graptolite communities Vinini Creek and Blackstone River exhibit significant decreases in community complexity and evenness as a consequence of the preferential decline in abundance of mesopelagic species. At both sites, the decline of mesopelagics took place during an interval of eustatic sea-level rise. The observed changes in community complexity and evenness commenced well before the dramatic loss in species diversity and population depletions that mark the tipping point of the extinction event. Environmental isotope and biomarker data suggest that the extent of the oxygen minimum zone in the paleotropical oceans, upon which these species relied, decreased sharply during the latest Katian time, with a consequent change in phytoplankton community composition. Most deep-water species became rare as populations were depleted in step with this habitat loss and extinction risks rose correspondingly.

Similar preferential loss of mesopelagic species occurred during the latest Katian in China, Siberia and Kazakhstan – i.e., throughout the paleotropics. Although many of the affected species persisted in ephemeral populations for hundreds of thousands of years, the toll of enhanced extinction risk depleted the diversity of paleotropical (diplograptine) graptolite species during the latest Katian and early Hirnantian. Our results support previous interpretations of the depth-related biotope structure of graptolite communities. In contrast these results contradict both the hemispheric asymmetry and depth susceptibility predictions of the gamma ray burst hypothesis of LOME causation. Finally, and most significantly, these results indicate that the effects of long-term climate change on habitats can degrade populations in ways that cascade through communities, with effects that persist for geologically significant intervals of time and culminate in mass extinction.

Chronostratigraphic correlation of the North American Upper Ordovician standard: The 2015 edition

Charles E. Mitchell[1], Bryan K. Sell[2], Stephen A. Leslie[3] and Daniel Goldman[4]

[1]*University at Buffalo, Department of Geology, 411 Cooke Hall, Buffalo, NY 14260-3050, cem@buffalo.edu.*
[2]*Independent Contractor, 221 Ridge Hill Road, Mechanicsburg, PA 17050.*
[3]*James Madison University, Department of Geology & Environmental Science, MSC 6903, Harrisonburg, VA 22807.*
[4]*University at Buffalo, Department of Geology, Science Center Room 179 300 College Park, Dayton, OH 45469-2364.*

Regionally endemic faunas and complex facies relations in the Late Ordovician succession of the Black River to Utica Group succession in New York State (NY) and the Tyrone to Fairview Formation succession in the Cincinnati region (type areas of the Mohawkian and Cincinnatian series, respectively) have impeded correlation of these rocks – both with one another and globally. Recent biostratigraphic work tied to geochemically correlated K-bentonites offer some new insights.

First, graptolite faunas from Core 75NY2 (Ballston Spa area) provide new details about the age of the base of the Utica Shale. A K-bentonite in the uppermost Glens Falls Limestone within the core corresponds to a bed in the lower Martinsburg Shale in West Virginia above the widespread Millbrig K-bentonite, within the upper part of the *Climacograptus bicornis* Zone and at the top of the falling limb of the GICE. The lower 7 m of the Utica Shale in 75NY2 contains a fauna dominated by *Diplograptus?*

rugosus. This fauna, although not previously recorded in the region, is also present in the basal Utica Shale in the central Mohawk Valley. It is followed by the incoming of the *C. americanus* Zone assemblage, and two meters higher in the core, by the FAD of *Diplacanthograptus caudatus*. This succession closely matches that at the Katian Stage GSSP. The Sherman Falls K-bentonite occurs at 26.1 m above the base of the Utica Shale in 75NY2. Thus, the base of the Katian Stage lies slightly above the base of the Utica Group and is likely approximately equivalent to the age of the base of the Sugar River Limestone.

   The standard correlation from NY into the Cincinnatian succession requires substantial revision. The Millbrig K-bentonite is present in the uppermost Black River Group, Selby Limestone in NY and the M4 sequence, Tyrone Limestone in Kentucky (KY). The overlying M5-M6 Lexington Limestone to Point Pleasant Formation succession has typically been equated to the entire Trenton Group, with the basal Cincinnatian Kope Formation, highstand of the C1 sequence, as the midcontinent expression of the upper Utica Group, Indian Castle Shale. The presence of a *D. spiniferus* Zone graptolite fauna in both units supported this correlation, but relations of the graptolites to the *Amorphognathus tvaerensis-A. superbus* conodont zone boundary was remarkably different in the two regions. In the KY the FAD of *A. superbus* within the lower part of the M6, mid-Lexington Limestone succession lies above the FAD of *D. spiniferus* (based on occurrences in the Stamping Grounds Member and the Middletown Core). In the NY succession the FAD of *A. superbus* can be traced via K-bentonite correlations to a level in the lower Utica Shale (lower part of the *C. americanus* Zone, between the Sherman Falls and Kayohoura-1 K-bentonites). This is a similar graptolite/conodont zonal tie position as occurs at Black Knob Ridge. The recent discovery that the Brannon K-bentonite (highstand of M6A sequence) is a geochemical match for the Paradise K-bentonite of lower-most Indian Castle Shale in NY (Sell et al., *in press,* GSA Bulletin), suggests that the graptolite FAD's are of similar age in both regions and that *A. superbus* appears at a markedly younger level in KY than it does in NY. Accordingly, the Indian Castle highstand is M6A rather than C1, and the base of the Cincinnatian Series in NY must lie in the upper part of the Utica Shale succession, likely that overlying the "Honey Hill Discontinuity" of Baird and others. The Brannon-Paradise K-bentonite correlation is supported by a prominent episode of fault-induced soft-sediment deformation that can be traced from core 75NY2 to the Thruway Discontinuity that caps the Dolgeville Formation and through the upper Rust Formation in NY to the Brannon Member seismites in KY.

Middle Ordovician strata of western Inner Mongolia: Depositional and tectonic history

Paul M. Myrow[1], Jitao Chen[2], Anne Hakim[1], Zachary Snyder[1], Stephen Leslie[3], David A. Fike[4], and Peng Tang[2]

[1]*Colorado College, pmyrow@coloradocollege.edu.*
[2]*Nanjing Institute of Geology and Palaeontology.*
[3]*James Madison University.*
[4]*Washington University.*

   Ordovician strata in the western margin of the North China Block (NCB), one of China's main tectonic provinces, make up a thick succession of mixed carbonate and siliciclastic sedimentary rocks. The oldest strata, Middle Ordovician rocks of the lower Sandaokan Formation, are transgressive systems tract deposits with retrogradationally stacked parasequences that include lowstand shoreline quartz sandstone deposits and shallow marine carbonate facies dominated by bioturbated wackestone. Chemostratigraphic data indicate that the lower part of the Sandaokan Formation records the rising limb of MDICE, the middle Darriwilian positive isotopic excursion, recognized for the first time in the western North China Block. The contact between the Sandaokan and the thick massive-weathering carbonate of the overlying Zhuozishan Formation may represent the Sauk–Tippecanoe megasequence boundary. The Zhuozishan and overlying Kelimoli Formation may represent a megasequence with the Kelimoli representing highstand deposits with deep-marine facies. The Kelimoli, which contains abundant slumps and slides, consists primarily of fine-grained carbonate turbidites and graptolite-bearing black shale. It is capped by a

sequence boundary marked by meters-thick beds of coarse breccia, which might be linked to a eustatic lowstand associated with the Middle–Upper Ordovician boundary interval. The Kelimoli may record the falling limb of MDICE.

The Sandaokan Formation rests unconformably on the Cambrian Series 3 Abuqiehai Formation, a mixed siliciclastic–carbonate deposits similar in character to those of the Laurentian inner detrital belt. The unconformity in our section in Inner Mongolia records a hiatus of similar timing and duration to a regionally extensive unconformity recorded along the ancient northern Indian continental margin in the Cambrian–Ordovician boundary interval. We interpret the western margin of the NCB to have been affected by a regionally significant tectonic event at this time that occurred on the northern margin of east Gondwana, the Kurgiakh or Bhimphedian orogeny. The Inner Mongolian region was, therefore, likely an along-strike continuation of northern Indian margin, in contrast to most recent paleogeographic reconstructions.

Lower Silurian "hot shales" in Poland as a response to Late Ordovician climatic changes

Teresa Podhalańska[1], Wieslaw Trela[2]

[1]*Polish Geological Institute-National Research Institute, Rakowiecka 4, 00-975 Warsaw, Poland, teresa.podhalanska@pgi.gov.pl.*
[2]*Polish Geological Institute-National Research Institute, Zgoda 21, 25-953 Kielce, Poland.*

Late Ordovician to early Silurian was time interval of significant paleogeographic, palaeoclimatic and sea-level changes reported in marine ecosystems. The switch from the icehouse to greenhouse climate during this time is easily readable in the East European Platform – EEP (NE Poland) and the Holy Cross Mountains – HCM (SE Poland). In Late Ordovician and early Silurian time both regions as a part of Baltica were positioned in 30°S at the northern margin of the Rheic Ocean (Nawrocki et al., 2007).

Sedimentary record of the Ordovician/Silurian boundary in the EEP is represented by regressive succession made up of the upper Katian mixed siliciclastic-carbonate facies grading upwards into sandy mudstones, sandstones and marls developed during the early Hirnantian sea-level fall (Podhalańska, 2009). Their correlation with Late Ordovician icehouse climate is supported by C isotope data and the Hirnantian fauna (*op.cit*). The post-glacial transgression initiated in the latest Ordovician *persculptus* Chron facilitated deposition of black graptolite shales predominating in the Lower Llandovery sedimentary record. They are represented by the Jantar Bituminous Claystone Member, which refers to as organic-rich and condensed "hot shale" unit. The TOC values, increased amounts of radioactive elements and trace metals indicate on deposition of this shales beneath anoxic bottom waters due to increased export of organic matter and sediment starvation during the post-glacial transgression (Podhalańska, 2009). Numerous graptolites recognized in the Jantar Member are indicative for the Rhuddanian *ascensus–acuminatus–cyphus* Biozones. These rocks – marked on wireline logs by increased gamma ray records (PG) – are the most perspective hydrocarbon source rocks and shale gas resources in the Llandovery succession of the EEP. They are coeval to "hot shales" deposited on the Gondwana shelf, which are the most important petroleum source rocks in N African and Arabian Peninsula (Lüning et al., 2000).

The sedimentary succession across the Ordovician/Silurian boundary in the HCM can also be interpreted in relation to climate and sea-level changes. The uppermost Ordovician is made up of mudstones and sandstones of the Zalesie Formation interpreted as regressive deposits related to Hirnantian glacioeustatic event (Trela and Szczepanik, 2009). They yielded acritarch assemblage predominated by species of *Veryhachium* accompanied by exotic peri-Gondwanian species of *Frankea* redeposited from zone of collision between Avalonia and Baltica located westward of the HCM (*op. cit*). The overlying Rhuddanian black shales and radiolarian cherts of the Bardo Formation are interpreted as transgressive deposits documenting marine flooding initiated in the late Hirnantian. The starvation of coarse-grained siliciclastics during the early Silurian post-glacial flooding increased organic carbon burial and facilitated development of suboxic bottom waters produced by short-lived anoxic events.

Sedimentary environment in the southern HCM was strongly influenced by upwelling driven by the SE trade winds responsible for increase of primary productivity and massive appearance of radiolarians recorded in chert-rich unit of the Bardo Formation.

REFERENCES

LÜNING, S., CRAIG, J., LOYDELL, D.K., ŠTORCH, P.P., FITCHES, B., 2000. Lower Silurian hot shales in North Africa and Arabia: regional distribution and depositional model. *Earth Science Review* 49: 121-200.

NAWROCKI, J., DUNLAP, J., PECSKAY, Z., KRZEMIŃSKI, L., ŻYLIŃSKA, A., FANNING, M., KOZŁOWSKI, W., SALWA, S., SZCZEPANIK, Z., TRELA, W., 2007. Late Neoproterozoic to Early Palaeozoic palaoegeography of the Holy Cross Mountains (Central Poland): an integrated approach. *Journal of the Geological Society, London*, 164: 405–423.

PODHALAŃSKA, T., 2009. The Late Ordovician Gondwana glaciation – a record of environmental changes in the depositional succession of the Baltic Depression (Northern Poland) (in Polish with English summary). *Pr. Państw. Inst. Geol.*, 193, 132 p.

TRELA, W. and SZCZEPANIK. Z., 2009. Litologia i zespół akritarchowy formacji z Zalesia w Górach Świętokrzyskich na tle zmian poziomu morza i paleogeografii późnego ordowiku. *Przegląd Geologiczny,* 57: 147–157.

Clast research in northern Germany – How erratics contribute to the Ordovician picture

Adrian Popp

Gerstenfeldweg2, 49716 Meppen, Germany Adrian.Popp@t-online.de.

Clast research as defined by Schallreuter (1998) also encompasses the research on geschiebes (glacial erratic boulders). The geschiebes have been transported from Baltoscandia (mainly Sweden, Norway, Denmark, and Estonia) during one of the three major glaciations (Elster, Saale, Weichsel) in Northern Europe. Collecting geschiebes has a long history and tradition in the northern part of Germany and the neighboring countries. Current research on clasts (e.g. geschiebes and other erratic boulders) is carried out in northern Germany with the main goal to trace back the clasts to their source area but also to provide information about the geology of Baltoscandia from these scattered 'archives'. But sometimes these clasts are the only remains of strata, which had been eroded completely in the source area.

Despite the Rhenish Slate Mountains and the Harz, northern Germany is lacking outcrops of Ordovician strata. But Ordovician geschiebes found in this part of the country show a great variety of lithologies and (stratigraphic) units. The most important lithologies are limestones and (graptolite) shales, but also the 'brick limestone' (or 'Backstein limestone', mid Sandbian age), a silicified and later de-calcified limestone is a common geschiebe in northern Germany.

While the classical geschiebes are known to be transported during one of the glaciations, there are other clasts believed to be transported much earlier (during late Paleogene – early Quarternary) by the 'Baltic river system'. The latter clasts are today concentrated in spots, scattered over the northern and eastern parts of Germany, the Netherlands and Poland. One of these 'hot spots' of occurrence is found in the border area between the Netherlands and Germany. Here not only a high concentration of isolated Ordovician sponges can be found but also a variety of silicified and also de-calcified limestones, similar to the 'brick limestone' (late Sandbian), and cherts (so called 'Lavender Blue Hornsteins') of late Katian age. These erratic boulders cannot yet be easily linked to their source area, which is suspected to lie in the eastern part of the Baltic area or beyond.

The limitation from the clasts' dimensions can be advantageous, because the investigation is more focused on all its information, such as lithology and faunal content. New genera and species and other palaeontologic information (palaeobiology, palaeoecology, palaeobiogeography) were derived from clasts in northern Germany and provided valuable insights to the Ordovician world of Baltica.

Unfortunately, today the scientific research on this topic decreases and is mainly carried out by amateurs, being rarely recognized by professional scientists.

REFERENCES

SCHALLREUTER, R., 1998. Klastenforschung unter besonderer Berücksichtigung der Geschiebeforschung. [Clast Research with Special Regard to the Geschiebe (Glacial Erratic Boulder) Research] – *Archiv für Geschiebekunde* 2 (5): 265-322, 2 plts., 28 figs., 1 tab., Hamburg.

Latest Ordovician-earliest Silurian chitinozoans from Puna, western Gondwana

G. Susana de la Puente[1], Claudia V. Rubinstein[2], N. Emilio Vaccari[3], and Florentin Paris[4,5]

[1]*CONICET-Departamento de Geología y Petróleo, Universidad Nacional del Comahue, Buenos Aires 1400 (Q8300IBX), Neuquén, Argentina, sudelapuente@gmail.com.*
[2]*Paleopalinología, IANIGLA-CCT CONICET, Av. Ruiz Leal s/n°, Parque General San Martín, 5500 Mendoza, Argentina.*
[3]*CICTERRA-CONICET, Universidad Nacional de Córdoba. Av. Vélez Sarsfield 1611. X5016 GSA. Córdoba, Argentina.*
[4]*Rue des Jonquilles, 35235 Thorigné-Fouillard, France.*
[5]*Géosciences-Rennes, CNRS UMR 6118, Université de Rennes 1, 35042 Rennes, France.*

Chitinozoans from Late Ordovician-early Silurian Upper Member of the Salar del Rincón Formation from Puna of northwestern Argentina are analyzed. This area belongs to the Central Andean Basin situated on the western Gondwanan margin during the early Palaeozoic. The Upper Member of the Salar del Rincón Formation could include the postglacial stage of the late Hirnantian glaciation, even when direct evidence of the glacially-related deposits are not recorded in this part of the basin. Although its contact with the Lower Member has been considered transitional, the marine to mixed Upper Member deposits could represent a transgressive event developed on conglomerate and cross-beded sandstones of the Lower Member deposits that involves an erosive contact. Strongly bioturbated grey to greenish-grey shales characterize the lower and middle part of the Upper Member of the unit. This part of the section (around 20 m thick) contains a chitinozoan association, mainly composed of *Spinachitina verniersi* Vandenbroucke in Vandenbroucke et al., 2009, *Cyathochitina kuckersiana* (Eisenack, 1934) and *Cyathochitina latipatagium* (Jenkins, 1969). *Spinachitina oulebsiri* Paris et al., 2000, *Eisenackitina* sp. cf. *ripae* Soufiane & Achab, 2000, *Ancyrochitina corniculans* Jenkins,

1969, *Angochitina* spp. and *Ancyrochitina* spp. are present in a lower proportion. The chitinozoan association indicates a late Hirnantian age for these deposits. A different chitinozoan association is observed in the base of a lenticular coarse-grained sandstone bed (15 m thick) upward in the section (around 20 m above the preceding chitinozoan-bearing sample), which is deposited over the shaley to silty part of the member. *Spinachitina* is practically absent in this level. A single incomplete specimen bearing comparatively longer processes is observed. *Cyatochitina caputoi* group Da Costa, 1971, *Belonechitina pseudarabiensis* Butcher, 2009, *Angochitina hansonica* Soufiane and Achab, 2000, *Ordochitina* sp. cf. *nevadensis* Soufiane and Achab, 2000 and *Plectochitina* spp. are the main components. *Cy. caputoi* and *B. pseudarabiensis* indicate the earliest Rhuddanian age. The last chitinozoan-bearing sample is from a shaley level deposited above the coarse- grained sandstone bed. These specimens are poorly-preserved. *Cy. kuckersiana* group, *Cy. caputoi* group, *O.* sp. cf. *nevadensis*, *A. hansonica*?, *Angochitina* spp. and *Ancyrochitina* spp. are observed. The upper part of this section shows an increasing sediment grain size and finishes with a ferruginous and chitinozoan-barren level. All chitinozoan-bearing levels also contain acritarchs and cryptospores. The Salar del Rincón Formation is succeeded by Late Carboniferous deposits (Cerro Oscuro Formation) through an angular discordance. According to palynomorphs the Upper Member of the Salar del Rincón unit records latest Ordovician-earliest Silurian deposits, which are usually absent in other parts of the Central Andean Basin. Latest Hirnantian-earliest Rhuddanian chitinozoan associations from western Puna allow correlating these western Gondwanan deposits with other glacially- related regions of northern Gondwana, such as North Africa and Arabian Peninsula, where the records of the glacial and postglacial events, which occurred in the Ordovician-Silurian boundary, are well-known.

Evidence of warming during the early Katian conodont apatite δ^{18}O and bulk carbonate δ^{13}C records from the Upper Mississippi Valley, US

Page C. Quinton[1], Achim D. Herrmann[2], Stephen A. Leslie[3], and Kenneth G. MacLeod[1]

[1]*Department of Geological Sciences, University of Missouri, Columbia, Missouri 65211, pcq6y5@mail.missouri.edu,*
[2]*Department of Geology and Geophysics, Coastal Studies Institute E301/302 Howe-Russell Geoscience Complex, Louisiana State University Baton Rouge LA 70803.*
[3]*Geology and Environmental Science, James Madison University, 395 South High St., MSC 6903, Harrisonburg, VA 22807.*

The Sandbian-Katian boundary is marked by major environmental changes in Laurentia's epicontinental seaway that are often related to the onset of Late Ordovician cooling culminating in the Hirnantian glaciation. Early Katian cooling is supported by a shift from warm-water to cool-water carbonate deposition coinciding with the M4/M5 sequence boundary, an ~3‰ positive δ^{13}C excursion (GICE), and an increase in phosphate and chert deposition. Whereas these lithological and geochemical observations do indicate environmental change, they are not uniquely associated with cooling. To further examine the nature of the environmental changes at the Sandbian - Katian boundary, especially the temperature history, we measured δ^{18}O values from conodont apatite and bulk carbonate δ^{13}C values from two sections in the Upper Mississippi Valley, US. The sections at Decorah, IA and Rochester, MN are ideal for this study because they are well exposed, contain the Deicke and Millbrig K-bentonites, and yield high abundances of excellently preserved conodonts.

Results from Decorah show an ~1‰ positive excursion in δ^{13}C values confined to the Guttenberg Member; δ^{18}O$_{phos}$ values show an ~0.5‰ decrease above the Guttenburg Member. Bulk carbonate δ^{13}C values range from -3.9‰ to 1.0‰ with an average of -0.4‰. Average δ^{18}O$_{phos}$ values for conodont apatite range from 17.7‰ to 19.8‰ with an average of 19.0‰. Preliminary results from Rochester, MN suggest that bulk carbonate δ^{13}C values and δ^{18}O$_{phos}$ values are on average ~1‰ lower than those at Decorah. The δ^{13}C excursion observed at Decorah is small in magnitude but occurs within the correct interval and is likely the local manifestation of the GICE.

Contrary to predictions of early Katian cooling, the slight decrease in δ^{18}O values at Decorah suggest that, if anything, temperatures increased following the GICE. This result is consistent with previous results from the Upper Mississippi Valley and Kentucky and further support the proposition that early Katian environmental changes in Laurentia's epicontinental seaway are more complicated than previously appreciated.

New data on the Late Ordovician acritarchs and cryptospores from the Moyero and Moyerokan River sections, northeast of the Siberian Platform

Elena Raevskaya[1] and Andrei Dronov[2]

[1]*FGUNPP "Geologorazvedka", Knipovich str., 11, block 2, Saint-Petersburg, 191019, Russia, lena.raevskaya@mail.ru.*
[2]*Institute of Geology, Russian Academy of Sciences, Pyzhevsky per.7, Moscow, 119017, Russia.*

In the year 2013 two Upper Ordovician sections in the Moyero and its right tributary Moyerokan River valleys were sampled for acritarchs for the first time. The sections are located in a remote place in northeastern part of the Siberian Platform in a close proximity of the Anabar Land. The studied sedimentary succession is represented by rhythmic intercalation of greenish-grey and cherry-red siltstones and bioclastic limestone related to the Dzherom Formation. The formation embraces two regional stages (the Baksian and the Dolborian) which correspond to the upper Sandbian and Katian stages of the Global Scale.

   Almost all of the 65 processed palynological samples contain acritarchs and cryptospores of moderate preservation. The lower part of the Dzherom Formation, correlated to the Baksian stage, contain abundant *Dicommopalla macadamii, Gorgonisphaeridium* sp*., Buedingisphaeridium* sp*.,* and less numerous *Peteinosphaeridium accinctulum, Peteinosphaeridium septuosum, Peteinosphaeridium* aff. *P. indianaense, Sacculidium tenuibarbatum*, *Sacculidium inornatum, Sacculidium* spp, *Multiplicisphaeridium irregulare*, *Solisphaeridium* spp. and others. In the upper part of the formation, corresponding to the Dolborian regional stage, some additional taxa such as *Veryhachium lairdii, ?Petaloferidium* sp*.,* Gen. indet. A, sp.1, 2 and Gen. indet. B, sp. 1, 2, 3 occur. The latter two taxa were recently discovered in the Dolbor Formation cropping out along the Nirunda River located far to the southwest of the Siberian Platform (Raevskaya, Dronov, 2014).

   The cryptospores are relatively abundant at several levels of the studied interval in both regional stages. They are represented by different morphotypes including naked and enveloped monads, dyads and tetrads. Among the most common taxa *Sphaerasaccus glabellus, Tetrahedraletes medinensis, Velatitetras laevigata, Segestrespora laevigata, Abditusdyadus laevigata, Dyadospora murusdensa, Pseudodyadospora laevigata* have been identified.

   Comparison of the new data with those from the type Upper Ordovican Kulumber River section (Raevskaya, 2006) and recently obtained from the Nirunda River section (Raevskaya, Dronov, 2014) show uniformity of late Ordovician acritarch and cryptospore assemblages within the large epicontinental Tungus basin of the Siberian Platform. This supports inner-regional correlations.

   Future taxonomic investigations are required to estimate the variety of the discovered acritarchs and cryptospores. The remarkable percentage of the widespread acritarchs in Siberian assemblages as *Dicommopalla, Peteinophaeridium, Sacculidium,* etc. supplies the obtained palynological material with a good potential for possible improvement of interregional biostratigraphic correlations and for possible biogeographic implications.

In search of the elusive Hirnantian Stage in the High Arctic: A preliminary report from North Greenland

Christian M. Ø. Rasmussen[1], Jan A. Rasmussen[1], Svend Stouge[1], Jisuo Jin[2], Axel Munnecke[3], and David A.T. Harper[4]

[1]*Natural History Museum of Denmark (Geological Museum), University of Copenhagen, Øster Voldgade 5-7, DK-1350 Copenhagen, Denmark, christian@snm.ku.dk.*
[2]*Department of Earth Sciences, University of Western Ontario, London, Ontario N6A 5B7, Canada.*
[3]*GeoZentrum Nordbayern, Fachgruppe Paläoumwelt, Friedrich-Alexander-Universität Erlangen- Nürnberg, D - 91054 Erlangen, Germany.*
[4]*Palaeoecosystems Group, Department of Earth Sciences, Lower Mountjoy, Durham University, Durham DH1 3LE, UK.*

   Sedimentary rocks along the North Greenland coastline can, almost exclusively, be ascribed to the evolution of the Lower Palaeozoic Franklinian Basin. Within an approximately 200 kilometer wide, predominately ice free zone between the Inland Ice and the coastline of the Arctic Ocean, a shallow-water carbonate facies is exposed in the southern part of the basin but clearly separated from turbiditic siliciclastics to the north. The carbonates are near horizontal, often yielding abundant fossils. Systematic reconnaissance along this coastline was first conducted during the last century. Since the pioneering expeditions of Dr. Lauge Koch, who single-handedly completed the first cartographical and geological surveys of the region, from dog sledge, several mapping campaigns have been conducted in the region. Spanning the late 1970s to early 1990s systematic mapping was conducted by the Geological Survey of Greenland. However, as the strata belonging to the Franklinian Basin are exposed along a 850 kilometers transect in one of the most remote and least accessible regions on the planet, focus has primarily been on identifying lithological units that can be mapped at broad scales in order to produce maps covering a

1:500,000 scale.

   Almost two kilometers of Ordovician – Silurian strata are exposed along the entire transect, mostly in carbonate facies. During the Late Ordovician – early Silurian interval, North Greenland was positioned within the tropical belt, on the north-facing margin of Laurentia. Extensive carbonate deposition had already commenced by the Mid-Late Ordovician with the formation of small mud-mounds on the platform, towards the end of the Ordovician. Silurian strata are characterized by large reef complexes.

   The Upper Ordovician – lower Silurian strata is assigned to the Morris Bugt Group; more specifically the Ordovician – Silurian boundary lies within the Turesø Formation, which crops out in the central and eastern part of North Greenland and within the Alegatsiaq Fjord Formation which crops out in the western part. Thus, potentially, Hirnantian strata are well exposed. Recognition of the terminal Ordovician stage has though proved elusive as previous research, based primarily on conodonts, has highlighted a barren interval spanning the boundary. The most detailed studies have been conducted in the Børglum Elv region in central North Greenland and near Centrum Sø in eastern North Greenland. Here the ranges of biostratigraphically important conodonts of Late Ordovician and early Silurian age are separated by an approximately 30 meter barren interval.

   In recent years focus has been on macrofossils, notably the pentamerid brachiopods, which are unusually abundant and diverse in North Greenland. Commonly they occur in easily-recognizable coquinas which can be tracked over vast distances ranging from the Franklinian Basin in North Greenland to the great interior basins of North America. These macrofossil studies have allowed for easy recognition of the Upper Ordovician – lower Silurian interval in the field which again has facilitated more focused studies through the boundary succession. In the Børglum Elv region, identification of key pentamerid coquinas in the field has informed further sedimentological studies which now reveal a succession of repeated shallowing-upwards sequences within the barren interval. In order to further shed light on the possible occurrence of Hirnantian strata we present the first δ^{13}C curve based on bulk rock data through this interval. This does not yet show unequivocal evidence of the occurrence of the Hirnantian Stage in central North Greenland. However, it does indicate that at least part of this elusive terminal Ordovician stage occurs within the extensive carbonate deposits of central North Greenland.

Chitinozoan biodiversity in the Ordovician of Gondwana using the quantitative stratigraphic correlation program CONOP9

Rachel K. Sales[1], Daniel Goldman[2], Florentin Paris[3], and H. David Sheets[4]

[1]*Department of Biology, University of Dayton, 300 College Park, Dayton, OH 45469.*
[2]*Department of Geology, University of Dayton, 300 College Park, Dayton, OH 45469,*
dgoldman1@udayton.edu.
[3]*Géosciences Rennes, Université de Rennes1, UMR 6118 du CNRS, Rennes, 35042, France.*
[4]*Dept. of Physics, Canisius College, 2001 Main Street, Buffalo NY 14208.*

   The regional and global biodiversity patterns of Ordovician chitinozoans have been examined in detail, but typically within the traditional biostratigraphic temporal frameworks of unequal duration biozones or time slices (e.g., Paris et al., 2004). Recently, Goldman et al. (2008, 2013) and Hints et al. (2011) used the quantitative stratigraphic correlation program CONOP9 (Sadler et al., 2003) to examine Ordovician Baltoscandian chitinozoan biodiversity with both equal duration bins and interval-free approaches to temporal standardization. In this study we used CONOP9 to construct an Ordovician composite range chart from the stratigraphic range data of 167 chitinozoan species from 65 boreholes and outcrops across Gondwana. These data were gathered from the published ranges of species in sections from Argentina, North Africa, the Middle East, Australia, and southern Europe. The CONOP9-derived results differ from previously published results in some significant and interesting ways. The global and N. Gondwana curves of Paris et al. (2004) exhibit two peaks, in the upper Darriwilian and the mid Katian, with a Sandbian decline in between (the trough and second peak are slightly younger in the N. Gondawana curve than in the global pattern). The CONOP9-derived pattern lacks the very pronounced upper Darriwilian

peak in the Paris et al. (2004) curves, instead exhibiting climbing diversity straight through the mid Sandbian. After a mid Sandbian peak there is a distinct decline followed by a strong lower Katian rebound. Additionally, unlike the global pattern the youngest peak in the CONOP9-derived curve is uppermost Katian to early Hirnantian, not mid Katian. Chitinozoan diversity curves from Baltoscandia tend to have an upper Darriwilian to lower Sandbian diversity plateau followed by a long upper Sandbian to Hirnantian decline, a decline which is delayed and steeper in the CONOP9 Gondwana curve. These differences, particularly with the previous N. Gondwana curve could be attributable, in part, to CONOP-produced range extensions or perhaps from the substantial amount of post-2004 data in our analyses that tended to focus on the late Katian - Hirnantian interval.

   We also compared the CONOP9 Gondwana chitinozoan diversity curve to changes in sea level (Dronov et al. 2011) and a generalized carbon isotope curve (Bergström et al. 2009). Our diversity curve matches the Dronov et al. (2011) sea level curve remarkably well with diversity peaks matching sea level highs and extinctions corresponding to regressions. With respect to the Ordovician carbon isotope record, the sharp decline in upper Sandbian chitinozoan diversity is approximately coincident with the globally recognized GICE excursion, and the very steep Hirnantian decline is coincident with the HICE (with the admittedly coarse precision of comparing curve inflections within stages). The climbing chitinozoan diversity through the Darriwilian appears unaffected by the MDICE excursion.

REFERENCES

BERGSTRÖM, S.M., CHEN, X., GUTIÉRREZ-MARCO, J-C., and DRONOV, A. 2009. The new chronostratigraphic classification of the Ordovician System and its relations to major regional series and stages and to δ^{13}C chemostratigraphy. *Lethaia* v. 42, 97–107.
DRONOV, A.V., AINSAAR, L., KALJO, D., MEIDLA, T., SAADRE, T. and EINASTO, R. 2011. Ordovician of Baltoscandia: Facies, sequences and sea-Level changes. *In*, J.C. Gutiérrez-Marco, I. Rábano and D. García-Bellido (eds.), *Ordovician of the World*. Cuadernos del Museo Geominero, 14. Instituto Geológico y Minero de España, p. 143-150. Madrid.
GOLDMAN, D., SHEETS, H.D., BERGSTRÖM, S.M., NÕLVAK, J., PODHALAŃSKA, T., MITCHELL, C.E., and VANDENBROUKE, T.R.A. 2013. High-resolution stratigraphic correlation and biodiversity dynamics of Middle and Late Ordovician marine fossils from Baltoscandia and Poland. *Geological Society of America Abstracts with Programs. Vol. 45, No. 7, p. 236*.
GOLDMAN, D., SHEETS, H. DAVID, BERGSTROM, S. M., and NÕLVAK, J. 2008. Middle and Late Ordovician Biodiversity Dynamics in Marine Microfossils from Baltoscandia. *Geological Society of America Abstracts with Programs 40(5): 4*.
HINTS, O., NÕLVAK, J., PALUVEER, L. and TAMMEKÄND, M. 2011. Conventional and Conop9 approaches to biodiversity of Baltic Ordovician chitinozoans. *In*, J.C. Gutiérrez-Marco, I. Rábano and D. García-Bellido (eds.), *Ordovician of the World*. Cuadernos del Museo Geominero, 14. Instituto Geológico y Minero de España, p. 243-249. Madrid.
PARIS, F., ACHAB, A., ASSELIN, E., XIAO-HONG, C., GRAHN, Y., NÕLVAK, J., OBUT, O., SAMUELSSON, J., SENNIKOV, N., VECOLI, M., VERNIERS, J., XIAO-FENG, W. and SEETO, T. W. 2004. Chitinozoans. *In* B.D. Webby, M. Droser, F. Paris and I.G. Percival (eds.), *The Great Ordovician Biodiversification Event*. Columbia University Press, New York, 294-311.

Coupled carbon and strontium isotope stratigraphy of a Middle Ordovician Bahamian-type carbonate platform at Clear Spring, Maryland

Matthew Saltzman[1], Cole Edwards[2], and Stephen Leslie[3]

[1]*Ohio State University, saltzman.11@gmail.com.*
[2]*Washington University, St. Louis, MO.*
[3]*James Madison University, Harrisonburg, VA.*

   Carbon isotope stratigraphy has a unique role in the interpretation of Earth history as one of the few geochemical proxies that have been widely applied throughout the geologic time scale. However, in addition to consideration of the role of diagenesis, numerous studies have raised awareness of the fact that

C-isotope trends derived from ancient carbonate platforms may not be representative of dissolved inorganic carbon from a well-mixed global ocean reservoir. Both of these variables (diagenesis, water mass residence time) may change in response to sea level, producing trends in C-isotopes on ancient carbonate platforms that are unrelated to the global carbon cycle.

Studies of C-isotopes in modern carbonate platform settings such as the Great Bahama Bank (GBB) provide important analogues. Carbonate sediments of the GBB may have elevated C-isotopes relative to open ocean waters reflecting differential photosynthetic fractionation and precipitation of calcium carbonate (which lowers pH and converts bicarbonate into 12-C enriched carbon dioxide, leaving residual bicarbonate heavier). Few studies of ancient carbonates have attempted to explicitly compare C-isotope trends in both restricted platform settings and open marine settings. We studied a restricted Bahamian-type carbonate platform of Middle-Late Ordovician (Darriwilian-early Sandbian) age included in the St. Paul Group of Maryland, notable for sedimentologic evidence of severe restriction and a general lack of open marine macrofauna.

We are able to correlate the C-isotope curve from the St. Paul Group to other sections globally by using a combination of conodont microfossils and measurement of Sr isotopes on conodont apatite. Coeval C-isotope trends from open marine settings in the western United States and Estonia are comparable to the restricted platform in Maryland. In our Ordovician example, local factors appear to have modified the magnitude of the global trends, but not the timing and direction. A remaining question is whether magnitude differences are a function of sedimentation rate and completeness. We continue to test hypotheses of global correlations of C-isotope trends in the Middle-Late Ordovician by utilizing the rapidly changing Sr isotope curve at that time. Ongoing studies not yet completed involve collaboration with Olle Hints and Stig Bergstrom to study conodont Sr isotopes in Estonia and Sweden, respectively.

Determining absolute depths of Ordovician (Katian) benthic assemblages in the upper Cincinnatian (Maysvillian to Richmondian) of the Cincinnati Arch region, USA

Cameron E. Schwalbach, Carlton E. Brett, Christopher D. Aucoin, and James R. Thomka

University of Cincinnati, 500 Geology-Physics Building, schwalce@mail.uc.edu.

Recent correlations of Upper Ordovician (upper Cincinnatian: Maysvillian to Richmondian) strata using a combination of marker beds, faunal epiboles, and carbon isotope stratigraphy has revealed consistent patterns of changes in facies and biotic composition along a gently south sloping ramp in the Cincinnati Arch region. The Rowland Member of the Drakes Formation in Kentucky, Ohio, and Indiana provides an excellent opportunity to quantify biotic gradients in relation to absolute depth zones along a gently dipping carbonate ramp. Recent correlations permit recognition of transects that range from deep subtidal (30 to 40 m depth range) to shallow subtidal and shoal settings (5 to 15 m depth range) to supratidal (~ 0 to 2 m above sea level) within single small-scale cycles, and have a gradient of only a few cm per km [Brett et al., 2014]. Cycles within the Rowland Member display four well-defined lithofacies, each containing a distinct biofacies. Distal to proximal facies include: (A) offshore mudstones rich in brachiopods and bryozoans; (B) shoal carbonates containing corals and stromatoporoid sponges; (C) shallow subtidal mollusk-rich carbonate mudstones (micrites) interbedded with dark algal-rich shales; and (D) inter- to supratidal shaly lime mudstones with glauconite-filled burrows, sparse ostracode and lingulid faunas and scattered desiccation cracks.

The distinct facies present within this depositional system provide a rich temporal and environmental framework in which to study ecological-evolutionary patterns. Marine benthic assemblages arrayed gradationally along these environmental gradients were quantified using ordination techniques to provide proxies of ecological parameters, particularly those related to water depth. While it is commonly possible to determine the relative position of a given facies or fossil community, it is far more difficult to assign absolute depths in terms of meters below sea level. Absolute depth estimates were made using a variety of exposure-related sedimentary structures,

including indicators of shoreline, normal wave base, and storm wave base, as well as biologic evidence of light-related zones. The configuration of depth-related facies and biotic gradients within this interval thus provides a unique opportunity to assign fossil assemblages to quantitatively defined depth zones along a gently dipping carbonate ramp.

The onset of the 'Ordovician plankton revolution' in the Late Cambrian

Thomas Servais[1], Taniel Danelian[1], Ronald Martin[2], Axel Munnecke[3], Hendrik Nowak[1], Alexander Nützel[4], Vincent Perrier[5], Thijs Vandenbroucke[1], and Mark Williams[5]

[1]*CNRS-Université de Lille, France, thomas.servais@univ-lille1.fr.*
[2]*University of Delaware.*
[3]*Universität Erlangen-Nürnberg, Germany.*
[4]*Universität München, Germany.*
[5]*University of Leicester, UK.*

The Great Ordovician Biodiversification Event (GOBE) comprises the diversifications of all groups of marine organisms during the Ordovician Period. It is now clear that this adaptive radiation was initiated by some fossil groups earlier in the Cambrian and continued for others beyond the end of the Ordovician, making the GOBE part of a long-term early Palaeozoic radiation that also includes the Cambrian Explosion. It is likely that environmental changes triggered the diversification of the phyto- and zooplankton during the late Cambrian, permitting an increase in diversity and abundance of plankton-feeding groups during the Ordovician. In addition, molecular clock and fossil data indicate evidence for a late Cambrian to Ordovician switch to planktotrophy in invertebrate larvae. Here we analyse in detail the onset of the diversification of the different groups of the plankton in the late Cambrian - Early Ordovician interval leading up to the subsequent 'Ordovician Plankton Revolution'. Our analyses include the changing diversities of the phytoplankton (acritarchs), diverse groups of zooplankton (e.g. chitinozoa, graptolites, radiolarians, etc.) and the switch to a planktonic mode of life of metazoan fossil groups (e.g. arthropods, etc.) that were part of the Cambrian benthos. The possible causes of the 'plankton revolution' are discussed. They include changes in palaeoclimate, palaeogeography or tectonic and volcanic activity, sea-water chemistry, as well as increased nutrient supply.

Ordovician chronostratigraphy changes through time as recorded in the USGS Geologic Names Lexicon

Nancy R. Stamm and Randall C. Orndorff

U.S. Geological Survey, 12201 Sunrise Valley Drive, Reston, Virginia 20192, nstamm@usgs.gov.

Modifications to the geologic time scale have been significant, particularly in recent decades owing in part to more precise biostratigraphic zonations and advances in isotopic dating techniques. Because the definitions of geologic time intervals have been modified as more information is gathered, interpreted, and published, the geologic age of a unit as stated in a report published, for example in 1950, may be different according to today's time scale. Many changes have occurred to chronostratigraphic units throughout the geologic column, and particularly in the Ordovician, Carboniferous, Permian, and Quaternary. The U.S. Geologic Names Lexicon ("Geolex", http://ngmdb.usgs.gov/Geolex/), is a standard reference for the Nation's stratigraphic nomenclature. Geolex's content is built from literature published from the late 1800's to today.

Geolex uses the modern time scale and age estimates. This has required updating the age estimates for many geologic units. These updated age estimates are shown in Geolex's "Unit Summary" pages; the ages as originally determined are preserved in the synopsis for each publication.

The Ordovician System has seen many changes over the last several decades. For example, the Upper Cambrian to Middle Ordovician Beekmantown Group, of wide areal extent in the central and northern

Appalachians, is subdivided into 39 formations. Many of the formations have been the subject of recent studies, but several have not. The general ages of many of the "not-recently-studied" formations can be updated to today's time scale by using the fossils identified in reports published long ago. We tested our methodology on the Axemann Limestone of the Beekmantown Group.

   Until recently the Axemann Limestone of the Beekmantown Group in central Pennsylvania was considered simply as Lower Ordovician (Canadian), based on fossils reported in previous (e.g., between 1911 and 1967) publications. The Axemann includes the gastropod *Ophileta* and trilobite *Jeffersonia* (Butts and Moore, 1936, USGS Bulletin 855, p. 29), brachiopods *Diparelasma* and *Tritoechia* (Lees, 1967, Pennsylvania Geological Survey, 4th Series, General Geology Report, no. 52, p. 26), and conodonts of the upper *Acodus deltatus-Oneotodus costatus* to lower *Oepikodus communis* zones (Collamer, 1985, University of Maryland, unpublished M.S. thesis, 257 p.). Applying today's chronostratigraphy, these fossils indicate the Axemann is Tulean (upper Tremadocian to lower Floian), which is in agreement with recently published studies (e.g., AAPG Memoir 98, chapters 4 and 15, 2012). Examples like this demonstrate how Geolex can be used to not only correlate current chronostratigraphic units from North America to Great Britain, and even globally, but can also be used as a history of changes to the chronostratigraphy of a system.

Immigration, speciation, and biodiversity in Ordovician seas of Laurentia

Alycia L. Stigall[1], Jennifer E. Bauer[2], Hannah-Maria R. Brame[3], Adriane R. Lam[1], and David F. Wright[4]

[1]*316 Clippinger Lab Department of Geological Sciences and OHIO Center for Ecology and Evolutionary Studies, Ohio University, Athens, Ohio 45701, stigall@ohio.edu.*
[2]*1412 Circle Drive, 306 Department of Earth and Planetary Sciences, University of Tennessee, Knoxville, Tennessee 37996.*
[3]*Petroleum Underground Storage Tank Release Compensation Board, 50 West Broad Street Suite 1500, Columbus Ohio, 43215.*
[4]*155 South Oval Mall, School of Earth Sciences, The Ohio State University, Columbus, Ohio, 43210.*

   Biotic immigration events (BIMEs), the dispersal of taxa from one biogeographic area to another, facilitate changes in biodiversity dynamics both today and throughout geologic time. Whether biotic immigration has a long-term positive or negative effect on ecosystem structure is context dependent. For example, BIMEs have been associated with biodiversity increases linked to ecologic and evolutionary processes such as niche partitioning, species packing, and higher speciation rates. Yet substantial biodiversity decline has also been documented following introductions of extrabasinal taxa within ecosystems due to elevated extinction and/or reduced speciation rates. In these instances, greater competition/predation from ecologically dominant invasive species may have acted to suppress the process of species formation and/or increase extinction rates among incumbents.

   In this contribution, we explore the relationships among BIMEs, the rate and biogeographic mode of speciation events, and overall patterns of biodiversity change during the Middle through Late Ordovician interval in the epicontinental seas of Laurentia. The focal interval spans the Dapingian to Katian Stages, beginning with the Great Ordovician Biodiversification Event (GOBE) and ending after the Richmondian Invasion. Substantial tectonic, oceanographic, and paleoclimatic events occurred during this interval including the Blountian and Taconic tectophases of the Taconian Orogeny, the Guttenberg Carbon Isotope Excursion (GICE), the Boda Event, and the influx of nutrient-rich waters into the Sebree Trough of southern Laurentia. BIMEs during this temporal interval include both long-distance dispersal between paleocontinents, such as Baltica and northern Laurentia, and within-craton dispersal occurring between geographically adjacent depocenters, such as the Nashville Dome and Cincinnati Arch. The distance, magnitude, and timing of BIMEs were constrained for a suite of taxa comprising mainly articulated brachiopod and trilobite clades and augmented by other marine invertebrate taxa common in Ordovician seas. Speciation rate and mode were characterized via phylogenetic biogeographic methods, and biodiversity levels were determined from published faunal lists and data extracted from the Paleobiology Database.

Results of speciation mode analyses indicated that two primary macroevolutionary regimes occurred during the study interval: one in which speciation occurred primarily via passive vicariance and the other in which speciation occurred primarily by population range expansion followed by subsequent vicariance (i.e., "dispersal" speciation). These two macroevolutionary regimes alternated through time, and shifts between regimes correlate with changes in tectonic and oceanographic conditions as well as immigration intensity. Vicariance speciation prevailed during intervals of high tectonic activity and increased physical separation between marine basins, which limited the frequency of BIMEs. In contrast, intervals characterized by high levels of BIMEs were associated with mainly speciation by dispersal. Thus, the processes by which diversity accumulated under these two regimes correspond to different macroevolutionary dynamics. During high vicariance/low immigration intervals, diversity was maintained or increased by high speciation rates. If speciation rates were high, as during the GOBE, diversity increased rapidly. Conversely, low vicariance/high immigration intervals were characterized by comparatively low speciation rates. Biodiversity increases during these intervals, such as the Richmondian Invasion, were primarily due to niche partitioning between incumbent and immigrant taxa and greater β-diversity.

The alternation of the vicariance and dispersal-dominated macroevolutionary regimes establishes a "taxon-pulse" for generating diversity. In the first phase, the high frequency of BIMEs increase regional β-diversity via niche partitioning, although this may not substantially increase γ-diversity because speciation rate declines. This high β-diversity is then transformed into higher γ-diversity in the second phase as earth system events facilitate high rates of speciation by vicariance, which may reduce β-diversity as α-diversity increases. The repetition of the two-phase diversification system occurred at least twice during the Middle to Late Ordovician study interval and forms a useful hypothesis against which to examine diversification in other Ordovician clades.

A revised biostratigraphic framework for the near-field Hirnantian deposits of the central Anti-Atlas (southern Morocco) and their correlation to the Wangjiawan GSSP (Yichang, China)

Lorena Tessitore[1], Thijs R. A. Vandenbroucke[1], Jean-François Ghienne[2], Marie-Pierre Dabard[3], Alfredo Loi[4], Florentin Paris[3] and Philippe Razin[5]

[1]UMR 8098 du CNRS: EEP, Université Lille 1, France, lorena.tessitore@ed.univ-lille1.fr.
[2]UMR 7516 du CNRS: Institut de Physique du Globe de Strasbourg, Université de Strasbourg, 1, France.
[3]UMR 6118 du CNRS: Geosciences Rennes, Université de Rennes 1, France.
[4]Dipartimento di Scienze Chimiche e Geologicche, Università di Cagliari, Italia.
[5] Géoressources et Environnement, Université de Bordeaux, France.

The Hirnantian Stage has a short duration, less than 2 My, but it records one of the largest global extinctions in Earth history, and an important glaciation. Evidence for the Hirnantian glaciation is widespread in western Gondwana, and an extensive glacial record exists in several sedimentary basins in Morocco. Our study areas are located in the Central Anti-Atlas, between Zagora and western Maider/Tafilalt region (southern Morocco).

Our methodology consists of sampling sections within a highly resolved sequence stratigraphic framework (Ghienne et al. 2014), and using palynological data (mainly chitinozoans) to correlate these pre-, syn-, and post-glacial deposits across various locations. Moreover, this also identifies and tracks the Katian-Hirnantian limit, which remains obscure in some areas. An additional challenge comprises the palaeogeographical disparity in chitinozoan data, causing difficulties in establishing an efficient global biostratigraphical correlation framework for the Upper Ordovician (Vandenbroucke et al., 2010). In this presentation, we explore two aspects of our research program, which is part of an ANR project (French national research foundation) that re-investigates the sedimentology and sequence stratigraphy of these glacial deposits:

(1) In the Central Anti-Atlas, the Upper Ordovician outcrops between Zagora and western Maider/Tafilalt areas are characterized by sedimentary gaps and large incisions caused by the waxing and

waning of the ice sheets. This complicates long distance correlation, and one of our targets is the biostratigraphic correlation of two key areas; (i) the western Maider/Tafilalt (Clerc et al. 2013) and (ii) the Bou Ingarf section and neighbouring sections around Tazzarine (Loi et al. 2010).

(2) We will also present our preliminary biostratigraphic data from the Wangjiawan River Section (south-eastern China), which is immediately adjacent to the GSSP of the base-Hirnantian (Chen et al., 2006), and how these data can be correlated to the near field sections in southern Morocco.

REFERENCES

CLERC, S., BUONCRISTIANI, J-F., GUIRAUD, M., VENNIN, E., DESAUBLIAUX, G. and PORTIER, E., 2013. Subglacial to proglacial depositional environments in an Ordovician glacial tunnel valley, Alnif, Morocco. *Pal., Pal., Pal.* 370, 127-144.
CHEN, X., RONG, J., FAN, J., ZHAN, R., MITCHELL, C.E., HARPER, D. A. T., MELCHIN, M. J., PENG, P., FINNEY, S. C. and WANG, X., 2006. The Global Boundary Stratotype Section and Point (GSSP) for the base of the Hirnantian Stage (the uppermost of the Ordovician System). *Episodes* Vol. 29, no. 3.
GHIENNE, J. F., DESROCHERS, A., VANDENBROUCKE, T. R. A., ACHAB, A., ASSELIN, E., DABARD, M. P., FARLEY, C., LOI, A., PARIS, F., WICKSON, S. and VEIZER, J., 2014. A Cenozoic-style scenario for the End-Ordovician glaciation. *Nature Communications* 5:4485.
LOI, A., GHIENNE, J.-F., DABARD, M.P., PARIS, F., BOTQUELEN, A., CHRIST, N., ELAOUAD-DEBBAJ, Z., GORINI, A., VIDAL, M., VIDET, B. and DESTOMBES, J., 2010. The Late Ordovician glacio-eustatic ecord from a high-latitude storm-dominated shelf succession: The Bou Ingarf section (Anti-Atlas, southern Morocco). *Pal., Pal., Pal.* 296, 332-358.
VANDENBROUCKE, T. R. A., ARMSTRONG, H., WILLIAMS, M., PARIS, F, SABBE, K., ZALASIEWICZ, J., NOLVAK, J., VERNIERS, J. and SERVAIS, T., 2010. Polar front shift and atmospheric CO2 during the glacial maximum of the Early Paleozoic Icehouse. *PNAS* 107, 14983–14986.

Agglutinated benthic foraminifera in Upper Ordovician black shales from the northern Holy Cross Mountains (Poland)

Wieslaw Trela and Sylwester Salwa

Polish Geological Institute, National Research Institute, Zgoda 21, 25-953 Kielce, wieslaw.trela@pgi.gov.pl.

Black/dark shales reported worldwide in Upper Ordovician sedimentary records provide insight into understanding of climate changes and palaeooceanographic conditions prior to the Hirnantian glaciation. In the northern Holy Cross Mountains black/dark shales of the Jeleniów Formation form as thick as 120 m succession spanning the latest Darriwilian to early Katian time interval. They are subdivided into two horizons by thin interval of bioturbated mudstones corresponding to the upper *foliaceus* graptolite zone. The Jeleniów black shales grade upwards into the upper Katian greenish-grey limy mudstones of the Wólka Formation (up to 70 m), which are intensely bioturbated at the base and homogenous in the upper part of the unit. The Hirnantian strata are represented by sandy mudstones and marls of the Zalesie Formation (up to 6 m), dated by trilobite fauna of *Mucronaspis*.

The characterized mudrock-dominated succession has been studied extensively, including stratigraphic, sedimentologic and geochemical approaches concentrated lately on reconstruction of water column oxygenation level (Trela, 2007; Zhang et al., 2011). Detailed analyses of TOC, S isotopic signature, V/(V + Ni) ratio and pyrite content for the Jeleniów black shales indicate their deposition was beneath anoxic/dysoxic waters (Zhang et al., 2011). A major shift into oxic bottom waters has been reported in the Wólka mudstones, which coincides with the rebound of marine animal diversity during the Late Ordovician (*op. cit.*).

Microscopic examination of the Jeleniów black/dark shales from the Wilków IG 1 and Daromin IG 1 wells revealed lenticular and oval structures composed of cherty rims surrounding residual infill material. The oval bodies are up to 200 µm in diameter, while the lenticular ones are up to 700 µm in length and up to 80 µm thick and show collapse features. The cherty rim is made up of angular and well sorted micron-size quartz grains bounded by cryptocrystalline silica cement. The considered structures strongly resemble remains of benthic agglutinated foraminifera from modern and ancient (Mississippian and

Devonian) muds deposited in oxygen deficient conditions (Pike and Kemp, 1996; Milliken et al., 2007; Schieber, 2009). In the Jeleniów Formation they are common constituents of black shales showing more or less continuous sub-millimetre lamination; however, some examples were also reported in discretely bioturbated dark shale intervals and laminae. Noteworthy, the bioturbated greenish-grey Wólka mudstones are devoid of foraminifera remains.

  The presence of agglutinated benthic foraminifera reported in modern and ancient sediment deposited under suboxic bottom waters indicates that they can thrive in environments affected by short-lived anoxia produced by seasonal thermoclines (Schieber, 2009). Their occurrence in the Jeleniów Formation showing both sub-millimetre lamination and bioturbational mottling suggests that the sedimentary environment was affected by intermittent anoxic and oxic/dysoxic conditions providing a minimum amount of oxygen for the survival of benthic foraminifera.

REFERENCES

MILLIKEN, K.L., CHOH, S.-J., PAPAZIS, P., SCHIEBER, J., 2007. "Cherty" stringers in the Barnett Shale are agglutinated foraminifera. *Sedimentary Geology*, 198: 221–232.
PIKE, J. and KEMP, A.E.S., 1996. Silt aggregates in laminated marine sediment produced by agglutinated Foraminifera. *Journal of Sedimentary Research*, 66: 625–631.
SCHIEBER, J., 2009. Discovery of agglutinated benthic foraminifera in Devonian black shales and their relevance for the redox state of ancient seas. *Palaeogeography, Palaeoclimatology, Palaeoecology*, 271: 292–300.
TRELA, W., 2007. Upper Ordovician mudrock facies and trace fossils in the northern Holy Cross Mountains, Poland, and their relation to oxygen- and sea-level dynamics. *Palaeogeography, Palaeoclimatology, Palaeoecology,* 246, 488–501.
ZANG, T., TRELA, W., JIANG, S-Y., NIELSEN, J.K., SHEN, Y., 2011. Major oceanic redox condition change correlated with the rebound of marine animal diversity during the Late Ordovician. *Geology*, 39: 675–678.

Brachiopod Community Response to the Ordovician Mass Extinction on Anticosti Island

Amelinda E. Webb and Lindsey R. Leighton

Department of Earth and Atmospheric Sciences, University of Alberta, 1-26 Earth Science Building, Edmonton, AB, T6G 2E3 Canada, amelinda.webb@gmail.com; lindseyrleighton@gmail.com.

  The Ordovician Mass Extinction receives much attention because of its taxonomic impact (second largest) contrasted by a lesser ecological impact. To better understand the ecological impact of the Ordovician extinction, we need to examine both local dynamics and global patterns. Here, we investigated brachiopod community response before, during, and after the Ordovician extinction in the Anticosti Basin, Canada. The strata exposed on Anticosti Island are one of the most complete shallow water, fossiliferous records of the Ordovician-Silurian boundary. In addition, the basin deepened towards the west, providing an ideal setting to test community response along a depth gradient during the Ordovician extinction.

  Brachiopod communities, based on material from the Paul Copper collection at the Geological Survey of Canada-Ottawa, were surveyed across the island through the late Ordovician-earliest Silurian. Samples (n = 133) were collected only from limestone surfaces that did not show evidence of taphonomic overprinting; taxa were identified to the species level. Stratigraphic coverage included the Vaureal (5 members of Katian age), Ellis Bay (3 members of Hirnantian age), and Becscie Formations (2 members of Rhuddanian age). The boundaries of the Ellis Bay Formation mark the first and second pulses of the mass extinction, coinciding with the rapid transition from greenhouse to icehouse conditions and back respectively. We used evenness and rank-abundance curve kurtosis (RAC-K) to measure community structure, and ordinations to visualize the changes in community composition. Community metrics were

compared to stratigraphy (time), lithology (Dunham carbonate classification, depositional environment), and geography (depth).

During the late Katian, evenness increased through time while RAC-K decreased. An inverse correlation often occurs between these metrics as both measure community structure; however RAC-K is more sensitive to communities with extremely low evenness. In ecological terms, low evenness and high RAC-K have often been equated with more unstable communities. The high variance observed in RAC-K indicates that Katian community stability was highly variable through time, which may be an ecological warning sign before the first pulse of the extinction. Ordination revealed that community composition changed through time but was only slightly related to depth. Throughout the entire section, community metrics had little association with lithology. Geographically, eastern communities (shallow) showed higher values and variance of RAC-K, suggesting the 'deeper water' communities might have been slightly buffered from the effects of the extinction. After the first extinction pulse and through the Hirnantian, evenness fell as RAC-K increased, suggesting increasing instability. Taxonomic turnover occurred at the start of the Hirnantian linked to the first pulse of extinction, but there was also an increase in diversity (due to expanding ranges of 'cool water taxa'). The high evenness and low RAC-K might indicate that the survivors and invaders formed stable communities. However, there was no pattern in the community ordination, indicating that community composition was in a state of flux during the Hirnantian. In the early Rhuddanian, evenness continued to drop as RAC-K rose, before both reversed. This suggests an initial unstable fauna in the aftermath of the second, final pulse of the mass extinction. However, the communities with high evenness and low RAC-K in the uppermost member may hint at the start of an ecological recovery. The ordination again revealed a weak relationship between community composition and depth, similar to the Katian.

The results of this study reveal distinct trends and changes in brachiopod communities related to the two pulses of the Ordovician Mass Extinction. The Anticosti Basin was greatly impacted during the extinction; this analysis provides a nuanced record of the effect of a global event on a local ecosystem.

Foreland basin formation, environmental change and trilobite paleoecology, Late Ordovician of eastern Laurentia

Stephen R. Westrop[1], Lisa Amati[2], Jesse R. Carlucci[3], Carlton E. Brett[4], and Robert E. Swisher[5]

[1]Oklahoma Museum of Natural History and School of Geology & Geophysics, University of Oklahoma, Norman, OK 73072, swestrop@ou.ed.
[2]Department of Geology, SUNY Potsdam, Potsdam, NY 13676.
[3]Kimbell School of Geosciences, Midwestern State University, Wichita Falls, TX 76308.
[4]Department of Geology, University of Cincinnati, Cincinnati, OH 45221.
[5]Department of Geophysical Sciences, University of Chicago, Chicago, IL 60637.

Trilobite distribution, abundance and diversity in the Late Ordovician of Laurentia are influenced by environmental changes associated with the Taconic Orogeny. Establishment and infilling of the Taconic foreland basin led to profound changes in the distribution of lithofacies and biofacies across the eastern half of the continent. Here we report on trilobite faunas of the late Sandbian to Katian interval. In the late Sandbian, mid-continent regions such as Oklahoma, and foreland basin regions share similar deep-water faunas, dominated by raphiophorid and isoteline trilobites. Later, in the Katian, regions in the mid-continent, such as central Oklahoma, have a relatively continuous record of carbonate deposition, and diverse platformal biofacies that pass down-ramp into deeper subtidal, low-diversity cryptolithine faunas. In the foreland basin, cryptolithine biofacies became widespread in the Katian, and expanded geographically as the clastic wedge prograded westward. Sedimentary evidence indicates that cryptolithines have a broader bathymetric range in the foreland basin and emerged at least locally into shallow subtidal, storm-influenced settings. Up-ramp, around the margins of the basin in such regions as

southern Ontario, more diverse biofacies lack cryptolithines and share taxa with mid-continent faunas. Preliminary data also indicate that the distribution of trilobite biofacies reflects patterns in the carbonate isotope stratigraphy, suggesting a relationship with various water masses recorded by aquafacies. The emerging patterns of biofacies distribution demonstrate the influence of regional processes on trends in diversity, faunal turnover and replacement over a broad area of Laurentia.

The more the merrier? Reconciling sequence stratigraphy, chemostratigraphy and multiple biostratigraphic indices in the correlation of the Katian reference section, central Oklahoma

Stephen R. Westrop[1], Lisa Amati[2], Carlton E. Brett[3], Robert E. Swisher[4], Jesse R. Carlucci[5], Daniel Goldman[6], Stephen A. Leslie[7], Roger Burkhalter[8]

[1]*Sam Noble Museum and School of Geology & Geophysics, University of Oklahoma, Norman, OK 73072, swestrop@ou.edu.*
[2]*Department of Geology, SUNY Potsdam, Potsdam, NY 13676.*
[3]*Department of Geology, University of Cincinnati, Cincinnati, OH 45221.*
[4]*Department of Geophysical Sciences, University of Chicago, Chicago, IL.*
[5]*Kimbell School of Geoscience, Midwestern State University, Wichita Falls, TX 76308.*
[6]*Department of Geology, University of Dayton, Dayton, OH 45469.*
[7]*Department of Geology and Environmental Science, James Madison University, Harrisonburg, VA 22807.*
[8]*Sam Noble Museum, University of Oklahoma, Norman, OK 73072.*

   The auxilliary stratotype section of the Katian Stage (Upper Ordovician) is a roadcut through the Viola Springs Formation near Fittstown, Oklahoma. Work by Bergström and colleagues on condont biostratigraphy and carbon isotope stratigraphy led to the novel interpretation that this section is entirely older (M5 sequence of eastern Laurentia) than the well-known Viola Springs succession of the south flank of the Arbuckle Mountains exposed along I35 (M6 and younger sequences). Studies of the sequence stratigraphy and trilobite biostratigraphy of the Viola Springs and the coeval Kimmswick Limestone of Missouri challenge this view. At the reference section, much of the Viola Springs is composed of shallow subtidal facies with diverse trilobite faunas. At least nine trilobite species are shared with the Kimmswick, which post-dates the GICE excursion in the St. Louis region and represents sequence M6 and possibly younger strata. The lower 0.5 m of the Viola Springs contains graptolites that indicate an uppermost Sandbian age, and a collection at 0.55 yielded graptolites that also occur in Katian strata. The occurrence of *Diplacanthograptus spiniferus* at 35 m and other characteristic *D. spiniferus* Zone graptolites higher up in the carbon isotope excursion interval also seem to indicate that the upper half of the section is no older than M6. Under this new interpretation, the carbon isotope excursion reported from the upper half of the Katian reference section as the GICE may in fact be the same excursion, identified as the Kope Excursion near the base of the Viola in the I-35 section. The GICE may prove to lie within a distinctive, unconformity-bounded, graptolitic interval at the base of the Viola Springs Formation that likely represents sequence M5A. Our interpretation also implies that the conodonts *Plectodina tenuis* and *Belodina confluens* make relatively "late" entries into the succession at the reference section. The base of M6 at this section is marked by a TST of coarse, cross-bedded bioclastic grain- to rudstone facies and appears to correlate with the base of Kimmswick Limestone in the St. Louis area. The apparent presence of Kope in the reference section also implies that it extends into strata correlative with sequence C1 of the Cincinnati region. Although the I35 section overlaps with the Fittstown section, there remains a larger break beneath the Viola in the former, with cut-out of part of M4 and most, if not all, of M5. The differing interpretations of these sections underscore the need to consider all lines of evidence in determining the age and correlation of isotope excursions, using sequence stratigraphy and biostratigraphy, preferably with multiple faunal groups.

Characterization of a platform to basin transistion in a mixed siliclastic-carbonate basin: Upper Ordovician of central, Kentucky and Cincinnati, Ohio

Allison Young[1], C.E Brett[1], and P.I. McLaughlin[2]

[1]*Department of Geology, University of Cincinnati, 500 Geology/Physics Building, Cincinnati, OH 45221-0013, younga9@mail.uc.edu.*
[2]*Wisconsin Geological Survey, University of Wisconsin - Extension, 3817 Mineral Point Rd, Madison, WI 53705.*

Correlation of shallow marine limestones into deeper shale-dominated settings remains a challenge in sedimentary basin analysis. The Upper Ordovician (lower Katian Stage) "Point Pleasant-Utica" interval is a succession of dark shales and fine-grained carbonates, largely restricted to the subsurface. The offshore basinal facies were deposited in the Sebree Trough, a NE-SW trending region of subsidence from central Kentucky through northeastern Ohio. The seemingly monotonous dark shale facies of the trough have prevented detailed correlation and study of its paleoenvironmental history. The Lexington Platform-Sebree Trough crosssection represents a well-preserved Upper Ordovician example of a carbonate ramp to muddy basin transition.

In this study drill cores from Cincinnati, Ohio were logged using facies analysis, and litho- and biostratigraphy to develop detailed profiles and interpretations of packages across a major facies transition from a the carbonate-dominated Lexington Limestone platform succession to the dark, mudrock-dominated deposits at the center of the Sebree trough. A number of facies-crossing markers provide useful, first-order controls on stratigraphy: these include abrupt facies offsets, carbon isotope curves, K-bentonites, fossil epiboles (e.g., *Prasopora* bryozoans), and deformed beds, probably representing regional seismites. This research expands the regional correlation of the Lexington Formation and its members from the outcrop belt of the Cincinnati Arch into the correlative dark shales of more distal settings and provides strong evidence that depositional sequences, and distinctive faunal epiboles are of regional extent.

The development of two transects across the Sebree Trough documenting lithologic gradients, package geometries, and faunal density mapping allows for an integrative approach to sequence stratigraphy providing a high-resolution stratigraphic framework. As predicted by sequence stratigraphic models, highstand systems tracts (HSTs) thicken and become more mud-rich toward the basin and transgressive systems tracts (TSTs) become thinner and more condensed approaching the basin. The degree of facies change across this gradient varies strongly with stratigraphic levels. Thus, lower units (Curdsville, Logana members) persist across most of the profile with relatively little change. In contrast, the upper Lexington units display much more abrupt northward change to shaly facies, suggesting increasing rates of subsidence in the Sebree trough through deposition of the Lexington sediments. In addition, there appears to be a distinct submarine erosion/corrosion surface that crosscuts lower Lexington units and dies out in an upramp direction near Cincinnati. This surface is overlapped by black shale and may record submarine erosion by bottom currents during an interval of sediment starvation and a rising pycnocline/oxycline.

Comparison of stratigraphic sequences in different transects was used to test whether isopach maps for the Point Pleasant-Utica of the Sebree Trough are an accurate predictor of facies belt strike. In general, there appears to be parallelism between isopachs and isoliths (e.g. proportion of limestone vs. shale at particular levels). Thus, it may be possible to map facies belts along strike on the scale of fourth-order sequences (100 to 400 kyr). This will aid in development of a refined three-dimensional model of the Sebree Trough-Lexington Platform and its evolution through the Katian from platform to deep, sediment starved basin to filled trough.

Middle–Late Ordovician (Darriwilian–Sandbian) paired δ^{34}S and δ^{13}C records reveal dynamic cycling through the Great Ordovician Biodiversification Event

Seth A. Young[1], Benjamin C. Gill[2], Cole T. Edwards[3], Matthew R. Saltzman[4], Stephen A. Lesile[5]

[1]*Department of Earth, Ocean & Atmospheric Science, Florida State University, Tallahassee, FL, 32306, sayoung2@fsu.edu.*
[2]*Department of Geosciences, Virginia Polytechnic Institute & University, Blacksburg, VA 24061.*
[3]*Department of Earth and Planetary Sciences, Washington University, Saint Louis, MO 63130.*
[4]*School of Earth Sciences, The Ohio State University, Columbus, OH 43210.*
[5]*Department of Geology and Environmental Science, James Madison University, Harrisonburg, VA 22807.*

Major phases of the Great Ordovician Biodiversification Event (GOBE) occurred during the Darriwilian Stage (468 to 460.5 Ma), and roughly coincided with a globally documented perturbation of the carbon cycle. This unprecedented change in biodiversity and biocomplexity of marine life has been previously linked to an L-chondrite asteroid breakup event in addition to sea surface temperatures that cooled to modern equatorial ranges. Ocean oxygenation events, associated with major perturbation of the carbon and sulfur cycles, have also been linked to large diversification events of marine life, from the Neoproterozoic (Ediacaran) Period to the late Cambrian in which pulses of oxygen progressively ventilated marine environments. Recent sulfur and carbon isotope studies of Early to Middle Ordovician sequences in Newfoundland and the Argentine Precordillera have highlighted evidence for persistent widespread euxinic (anoxic, sulfidic) deep marine waters that were intermittently oxidized. There is, however, very limited amount of sulfur isotope data from the Darriwilian Stage of the Ordovician, even though a positive $\delta^{13}C$ excursion (MDICE) has been recognized globally in the middle Darriwilian Stage. Here we present carbonate-associated sulfate ($\delta^{34}S_{CAS}$) and pyrite ($\delta^{34}S_{pyrite}$) S-isotopic measurements, paired with carbonate ($\delta^{13}C_{carb}$) and organic matter ($\delta^{13}C_{org}$) C-isotopic analyses from expanded Middle to Upper Ordovician sequences from the Appalachian Basin and Arbuckle Mountains regions of North America (Laurentia). Two major negative shifts in $\delta^{34}S_{CAS}$ of 12‰ are documented, the oldest occurring within the *Histiodella holodentata–Phragmodus polonicus* Conodont Zones and the younger drop occurring within the *Cahabagnathus sweeti–Amorphognathus tvaerensis* (*Baltoniodus gerdae* subzone) Conodont Zones. These negative shifts in $\delta^{34}S_{CAS}$ have antithetical relations with positive shifts in $\delta^{34}S_{pyrite}$ (~+10‰) and $\delta^{13}C_{carb}$ (~+3‰) values from the same samples. The older negative $\delta^{34}S_{CAS}$ shift is coincident with the widely documented MDICE, and the younger negative $\delta^{34}S_{CAS}$ shift is coincident with another positive shift in $\delta^{13}C_{carb}$ values in the early Sandbian Stage. Geochemical box modeling of these sulfur isotope shifts suggest that a decrease in the global rate of pyrite burial for approximately a million years would lead to the negative $\delta^{34}S_{CAS}$ trends.

Additionally, a substantial increase in the weathering flux of pyrite to the global oceans could also induce these secular sulfur isotope trends. Increased weathering from exposed terranes is broadly consistent with a sea-level lowstand, and the seawater $^{87}Sr/^{86}Sr$ isotope record of change in continental weathering in the late Darriwilian Stage of the Ordovician. However, there is no geologic evidence for distinct pulses of continental weathering on such rapid time scales required (< 1 million years) to generate the negative shifts in $\delta^{34}S_{CAS}$. Syndepositional sediment reworking could also be an important factor on regional expressions of our documented sulfur and carbon isotopic fractionations as the MDICE and associated negative $\delta^{34}S_{CAS}$ shift coincide with a major Ordovician eustatic sea-level lowstand (Sauk-Tippecanoe sequence boundary). These antithetical isotope trends may be best explained by changes in the marine redox state forcing the chemocline deeper into the sediments and restricting porewater sulfate exchange with overlying water masses. A change to a more oxygenated ocean would have further ventilated marine environments and allowed for the major phases of biodiversification in the Darriwilian Stage of the Ordovician.

Carbonate microfacies analysis of the Middle-Upper Ordovician succession of the Moyero River section, northeast of Siberian Platform

Alexey Zaitsev[1,2], Inna Ziyatdinova[1], Evdokiya Kozhevnikova[1], and Andrei Dronov[2]

[1]*Department of Lithology and Marine geology, Geological Faculty of M.V. Lomonosov Moscow State University, Moscow, Russia, alz@geol.msu.ru.*
[2]*Geological Institute of the Russian Academy of Science, Moscow, Russia.*

Ordovician outcrops along the Moyero River valley compose one of the most complete and best-exposed Ordovician sections on the entire Siberian Platform. In the year 2013, a special expedition was organized in order to re-investigate this key Ordovician section. Here we present a preliminary result of the carbonate microfacies analysis of the upper Volginian, Kirensko-Kudrinian and lowermost Baksian regional stages (uppermost Darriwilian and Sandbian Global Stages) in the outcrops along the Moyero River valley. Using the model introduced by E. Flügel (Flügel, 2004), the following facies zones of the carbonate ramp could be distinguished in the studied interval of the section:

The tidal deposits of the inner ramp are well developed in the Volginian and the lower and middle parts of the Kirensko-Kudrinian regional stage. These rocks are represented by mudstone and bioclastic wackestone and with admixture of algae and tiny quartz grains.

The sand shoals and banks of the inner ramp include two microfacies: 1) oolitic grainstone with concentric ooids and bioclastic packstone. This microfacies could be found in the upper part of Volginian and the lower part of Kirensko-Kudrinian regional stages; 2) fine-grained quartz sandstones with phosphate grains comprise the upper part of the Kirensko-Kudrinian regional stage deposits.

Restricted-marine settings of the inner ramp are represented by the bioclastic packstone with numerous echinoderms and wackestone with ostracods. These facies develop locally and underlie the quartz sandstones of the sand bank in the upper part of the Kirensko-Kudrinian regional stage.

The open-marine settings of the inner ramp (packstone and wackestone with various bioclasts) compose stratigraphic intervals of the Chertovskian and the lower part of the Baksian regional stages. These facies directly overlie the quartz sandstones of the Kirensko-Kudrinian regional stage. The sharp boundary between these two contrasting facies is interpreted as a marine flooding surface and sequence boundary.

The sediments of the mid-ramp settings are represented by intercalation of non-bioturbated mudstones and highly bioturbated bioclastic wackestone with ostracods and trilobites as main components. These facies are typical for the lower part of the Baksian regional stage.

The general distribution of the carbonate ramp facies zones in the studied succession reflects development of marine transgression interrupted at the base of Kirensko-Kudrinian regional stage, at the middle of Kirensko-Kudrinaian regional stage (base of the Kudrinian substage) and at the base of the Chertovskian stage by regressive events.

Geographic differentiation of the Middle and Upper Ordovician strata in South China

Linna Zhang[1,2], Junxuan Fan[1] and Yuandong Zhang[3]

[1]*State Key Laboratory of Palaeobiology and Stratigraphy, Nanjing Institute of Geology and Palaeontology, Chinese Academy of Sciences, Nanjing 210008, China; zhanglinna88@gmail.com ; fanjunxuan@gmail.com*
[2]*University of Chinese Academy of Sciences, Beijing 100049, China*
[3]*Key Laboratory of Economic Stratigraphy and Palaeogeography, Nanjing Institute of Geology and Palaeontology, Chinese Academy of Sciences, Nanjing 210008, China; ydzhang@nigpas.ac.cn*

South China Plate is a key area for studying the evolution of the Earth in the Ordovician. From the Cambrian to the Middle Ordovician, the South China maintained the "Platform - Slope - Basin" geographic pattern (Fig. 1), which was representative by the distribution of the Yangtze Platform, Jiangnan Slope and Zhujiang Basin from northwest to southeast. On the whole, the water depth gradually increased towards the southeast. The platform was mostly deposited with the carbonate rocks, while the slope deposited with clastic rocks interbedded with carbonate rocks, and the basin mainly deposited with the black shales. Meanwhile, it's clear that different regions in South China were deposited with the Middle and Upper Ordovician strata of varying thicknesses, which formed the particular topography of the South China sea floor at that time.

In order to examine the geographic differentiation and depositional history of South China during the Middle - Late Ordovician, the paleogeographic maps and isopach maps of the Ordovician rocks in South

China were reconstructed in successive time intervals by using the Geobiodiversity Database and ArcGIS software. The studying interval, the Middle and Late Ordovician were divided into six time units: 1) Dapingian to early Darriwillian, 2) middle Darriwillian, 3) late Darriwillian to middle Sandbian, 4) late Sandbian to middle Katian, 5) late Katian to early Hirnantian, 6) middle Hirnantian. For each time unit, the paleogeographic distributions of the strata were quantitatively illustrated and the distribution area of each sedimentary belt can be recognized precisely. The present results indicate that the "Platform - Slope - Basin" pattern was maintained until the middle Katian, when the Kwangsian Orogeny originated along the southeastern coast of China and stepwise influenced the South China Plate in a northwestward direction.
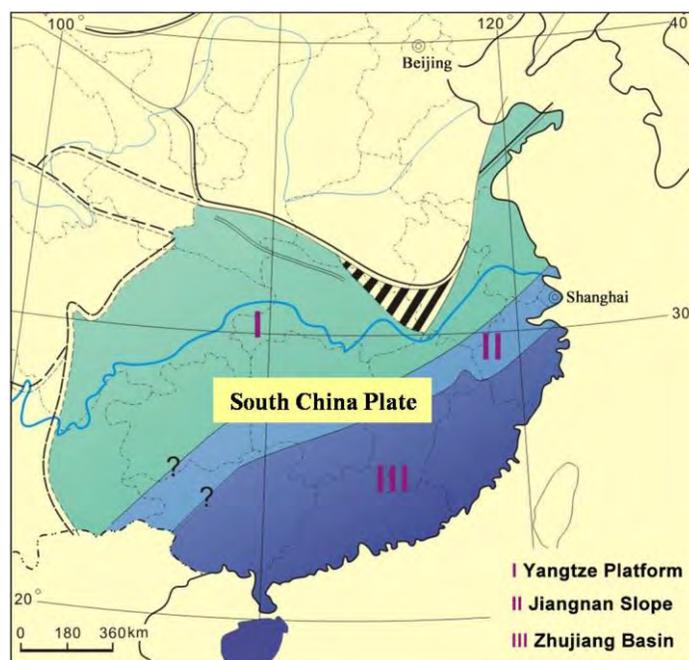
Fig. 1.—The "Platform - Slope - Basin" paleogeographic pattern of South China

Lithofacies differentiation of the Late Ordovician Lianglitag Formation limestones on the central part of the central Tarim Uplift, Tarim Block, northwest China

Yuanyuan Zhang[1], Yue Li[1], Axel Munnecke[2], and Wang Guan[3]

[1]*Nanjing Institute of Geology and Palaeontology Chinese Academy of Science, East Beijing Road, 39, 210008 Nanjing, P R China, yuanyuanzh85@163.com.*
[2]*GeoZentrum Nordbayern, Fachgruppe Palaöumwelt, Loewenichstr. 28, 91054 Erlangen, Germany.*
[3]*South China Sea Institute of Oceanology, Chinese Academy of Sciences, Guangzhou, 510301, P R China.*

Limestone sequences of the Katian (Late Ordovician) Lianglitag Formation are partly composed of sessile biota with a potential for forming of reef complexes, which extend from outcrops of the Bachu area to the Tazhong Oil Field, in the Central Uplift. The fossil components of reefal units are diverse ranging from a microbial-dominated realm in the northwest ramp to a metazoanl-dominated realm in the southeastern margin, respectively. To outline the biogeographical boundary between these reefal facies, six well loggings covering the medial region between Bachu and Tazhong were employed for the litho- and biofacies correlation. Calcimicrobial components are frequently present in the wells of the inner platform part, such as the Fang 1, Badong 2 and He 4 wells. Thus, the benthic biota herein is quite similar to that of the microbial mounds of the Bachu outcrop. However, reefal bindstones formed by coral,

142

stromatoporoid, and sponge taxa are abundant along the platform margin examplified by the He 3, Ma 401 and Ma 5 wells. They are typical frameworks typical of metazoanl reefs. Thus, their biotic compositions are essential analogues of the Tazhong Oil Field. Such a palaeoecological differentiation suggests that the evolutionary pattern of metazoan reef communities was not uniformly developed in the Late Ordovician. More advanced metazoan reefs were concentrated along the platform margin belt; in contrast, more primitive microbial communities inhabited in the inner platform.

Katian GSSP and Carbonates of the Simpson and Arbuckle Groups in Oklahoma

Jesse R. Carlucci[1]
Daniel Goldman[2]
Carlton E. Brett[3]
Stephen R. Westrop[4]
Stephen A. Leslie[5]

[1]*Assistant Professor, Kimbell School of Geosciences, Midwestern State University, Wichita Falls TX, jesse.carlucci@mwsu.edu*

[2]*Professor & Chair, Department of Geology, University of Dayton, Dayton OH, dgoldman1@udayton.edu*

[3]*Professor, Department of Geology, University of Cincinnati, Cincinnati OH, brettce@ucmail.uc.edu*

[4]*Professor & Curator of Invertebrate Paleontology, University of Oklahoma, Sam Noble Oklahoma Museum of Natural History, Norman OK, swestrop@ou.edu*

[5]*Professor & Department Head, Department of Geology and Environmental Science, James Madison University, Harrisonburg VA, lesliesa@jmu.edu*

INTRODUCTION

The Arbuckle Mountains region of Oklahoma is characterized by a large inlier of faulted and folded rocks of Precambrian and Paleozoic age. Precambrian and Cambrian basement rocks and early Paleozoic carbonates are overlain by westward dipping Pennsylvanian and Permian strata and by Cretaceous sediments of the Western Interior Seaway. The Arbuckle Mountain region of Oklahoma contains one of the best and most continuous exposures of late Cambrian to Devonian aged strata in all of the midcontinent (nearly 3350 m or 11,000 feet; Ham 1969), most of which is highly fossiliferous. This incredible sequence of rocks has generated substantial interest within the geologic community, with several books (e.g., Sprinkle 1982; Johnson 1991), field guides (e.g., Ham 1969; Fay et al. 1982a; Johnson et al. 1984; Fay 1989; Ragland and Donovan 1991; Cardott and Chaplin 1993; Suneson 1996), and journal papers (e.g., Goldman et al. 2007; Carlucci et al. 2014) devoted to the geology of the area.

The collision of Gondwana (Yucatan terrane) with Laurentia and the development of the Ouachita Mountains during the Pennsylvanian and Permian uplifted the carbonate strata that are the focus of this trip. Exposure of these subsurface rocks has had not only scientific impact, but economic repercussions as well. The Arbuckle (latest Cambrian; Stage 10 to Floian) and Viola groups (Katian) are mined for cement-producing materials, dolomite, and commercially viable crushed stone. Quartz arenites in the Simpson Group are mined for silica and even the Precambrian basement rock (Tishamingo Granite) is quarried for building materials. The oil and natural gas resources stored in subsurface extensions of the Simpson Group in Arbuckle region strata have long engendered substantial interest. Highly porous sandstones of the Bromide, Tulip Creek, and McLish formations and fractured carbonates of the Viola and Arbuckle Groups are well known petroleum reservoirs.

This guidebook was written for the 2015 International Symposium on the Ordovician System (ISOS) as a synopsis of the recent work (e.g., Goldman et al. 2007; Carlucci et al. 2014, forthcoming work for the ISOS meeting) on Ordovician-Silurian rocks of south-central and south-eastern Oklahoma. This new research and past studies (e.g., Harris 1957; Longman 1976; Longman 1982a, b; Fay et al. 1982a; Fay et al. 1982b) underscore the scientific importance of this region. The global stratotype section and point for the Katian Stage of the Upper Ordovician Series is examined on this trip. The first appearances of important graptolites, conodonts and chitinozoans in that section are crucial for worldwide chronostratigraphic correlation. Vertical and lateral facies changes of the Simpson Group demonstrate the variety and intricacy of sedimentary cycles and the importance of updating depositional models with sequence stratigraphic data. Carbonate facies of the Arbuckle Group are of general interest to all geologists, as they demonstrate a wide variety of sedimentary structures and fabrics that were deposited in tropical epeiric seas. Arbuckle Group carbonates show a variety of peloidal, oolitic, fossiliferous, stromatolitic, and brecciated facies that provide important insights into the depositional history of the "Great American Carbonate Bank" (Taylor et al. 2012). Simply put, these deposits are an exceptional natural laboratory for the sedimentary geologist. Siliciclastic deposits are also common in the Simpson and Arbuckle Groups, with shoreface sands and siltstones forming "bookends" to formation boundaries. The scientific importance of the

Arbuckle region also extends into the realm of structural geology, where geologic cross sections (Fig. 1) of the Ardmore Basin, Arbuckle Anticline, and Washita Valley demonstrate overturned strata, extensive reverse faulting, and a series of major synclines and anticlines at a variety of scales. Pennsylvanian age tectonic features are just another example of why the Arbuckle Mountains is an excellent natural laboratory for field geologists. We hope to convey some of that importance to the attendees of this 2015 ISOS pre-meeting field trip.

Tectonic Setting of the Arbuckle Mountain Region

  The Arbuckle Mountains contain a core of Precambrian and Cambrian basement rocks that are uniquely exposed in the southwest portion of the region. These basement rocks are well-studied and represent some of the same igneous provinces exposed in the Wichita Mountains of Oklahoma. Precambrian basement extends through the subsurface between the Wichita and Arbuckle Mountains (Ham 1969) and underlies much of the deformed area associated with the uplifts. Precambrian basement rocks (approximately 1.3 bya) in the Arbuckles are represented by the Tishamingo and Troy granites, which vary from coarse to fine-grained, and are rich in microcline and biotite (Taylor 1915). These are overlain by the Cambrian Colbert rhyolite group, which consists of extrusive rhyolite flows and tuffs, together with beds of agglomerate and sills of diabase (Finnegan and Hanson 2014; Hanson et al. 2014). Details of the basement rocks of Oklahoma, including their petrology, distribution, and origin were most recently discussed by Pucket et al. (2014).
  The uplift of the Cambrian and Ordovician strata in the Arbuckles is associated with the Ouachita Orogeny (Viele and Thomas 1989), a mountain building event in the Pennsylvanian and Permian caused by collision of the Yucatan terrane, which is part of present day Mexico, but was at that time attached to Gondwana, with the Laurentian craton. The Ouchitan tectonic system is extensive, and ranges from Alabama (Black Warrior Basin) through Arkansas and Oklahoma (Wichitas and Arbuckles), and then southwest into Texas (Llano, Marathon, Solitario Uplifts). As a result of Ouchita tectonics, the Arbuckle mountain region exposes a series of fold and thrust belt structural features, such as the Arbuckle Anticline (Figs. 1, 2), Mills Creek Syncline, Ardmore Basin, and Washita Valley. A detailed analysis of all these structural features is beyond the scope of this field trip, but there are some important details to note.
  The most intensely deformed part of the region is the Arbuckle Anticline (Figs. 1, 2), a faulted anticline that is overturned to the north. The faulted portion of the Arbuckle Anticline contains a graben that is filled with Pennsylvanian synorogenic molasse sediments (Collings Ranch Conglomerate). The Collings Ranch Conglomerate is structurally deformed into a synclinal fold, indicating that deformation continued after deposition. The core of the anticline consists of the Cambrian Colbert Rhyolite Group, with Upper Cambrian and Ordovician carbonates flanking the rhyolites. The fault axis is located near the East Timbered Hills region, offsetting volcanics on either side of the fold. Just south of the Arbuckle Anticline lies the Ardmore Basin, a downwarped remnant of the Southern Oklahoma Aulacogen (Brewer et al.
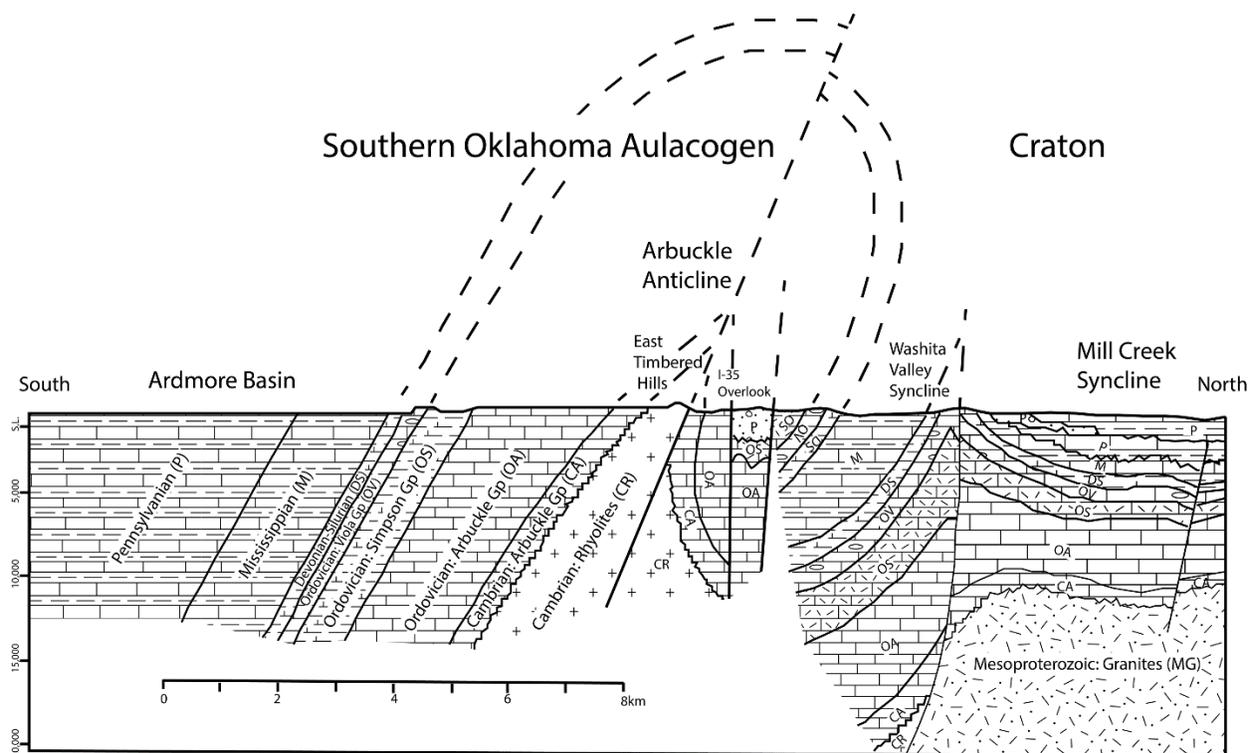
TEXT-FIGURE 1.—Structural cross-section of the Arbuckle Mountains region along I-35, between Davis and Ardmore (modified from Ham 1969). Line of cross section shown in Figure 2.

1989), which includes over 10,000 meters of Cambrian – Pennsylvanian-age strata. The overall structure is of a large, faulted syncline, punctuated by smaller anticlines. Mississippian and Pennsylvanian rocks in the Ardmore Basin dip between 45-90° to the northeast, and include the Hoxbar, Deese, Noble Ranch, and Dornick Hills Groups (Suneson 1996). Much of these deposits consist of conglomerates and shales that record the extensive input from the adjacent Ouchita event. As part of the larger Southern Oklahoma Aulacogen system, the Ardmore Basin is central to our discussion of the Cambrian-Ordovician carbonates in central Oklahoma.

Formation of the Southern Oklahoma Aulacogen

Approximately 550 million years ago, the granitic basement rocks (Tishamingo Granite) of central Oklahoma begun to undergo extensional stress associated with the rifting of Iapetus and development of a failed continental rift (Southern Oklahoma Aulacogen, [SOA], or Anadarko Basin). The faults bounding the SOA were northwest trending, and the structure extended in a zone across south-central Oklahoma, and into the panhandle of Texas. The Washita Valley fault zone, for example, was a rift-forming normal fault that separated the subsiding aulacogen in the south from the craton to the north (Fig. 2). During the Middle Cambrian, continued extension led to the infilling of the SOA with the volcanics of the Colbert Rhyolite Group. Suneson (1996) noted that this igneous activity was concentrated in southern
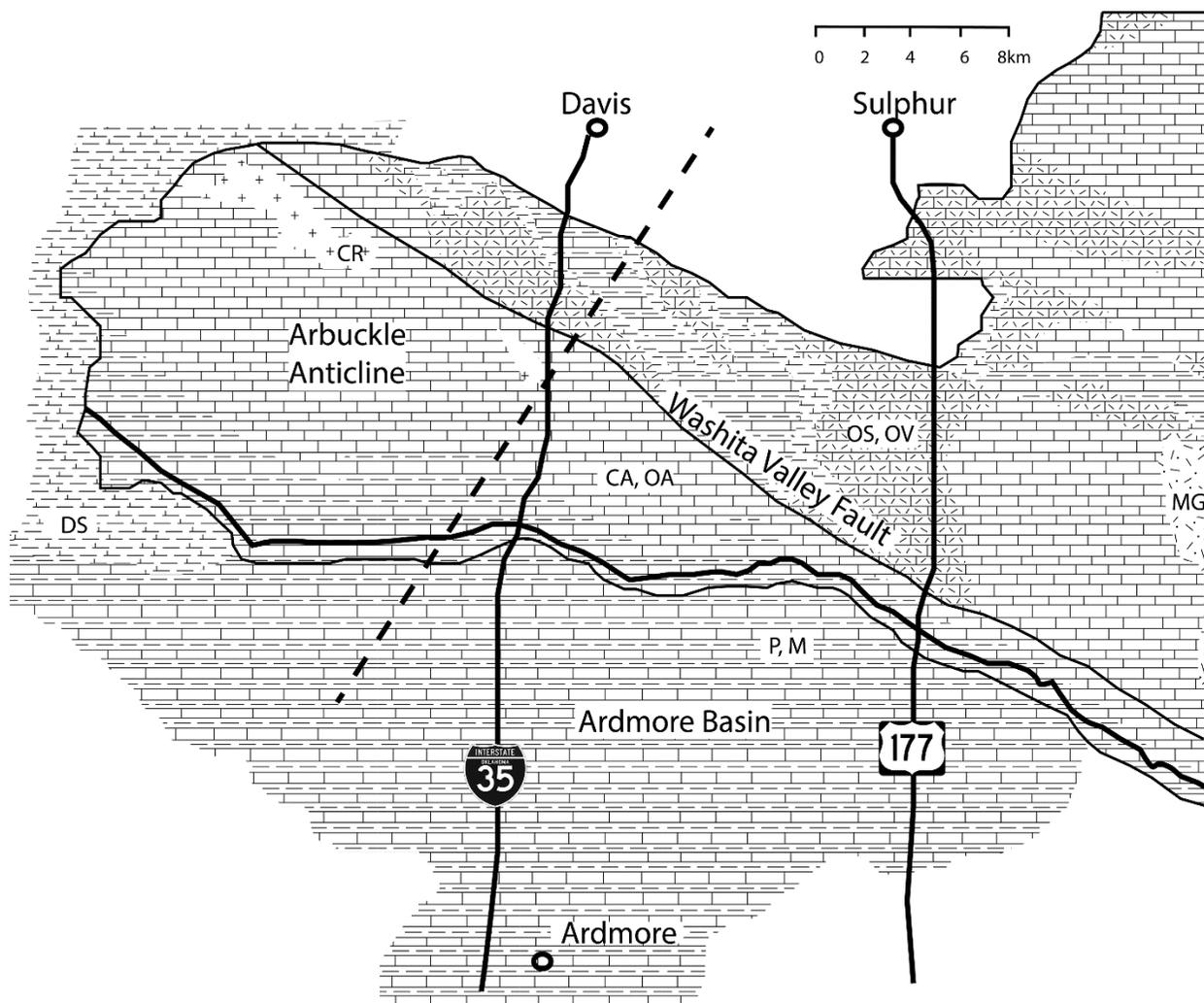
TEXT-FIGURE 2.—Generalized geologic map of the Arbuckle Mountains region between Davis and Ardmore (modified from Ham 1969). Abbreviations correspond to units shown in Figure 1, dotted line is the line of cross section.

Oklahoma because the basement rock had been weakened by faulting associated with the rifting. Cooling and contraction of the Cambrian rhyolites potentially led to additional subsidence that allowed the Southern Oklahoma Aulacogen to be a major depocenter in the Ordovician (Suneson 1996). Between the Late Cambrian and Early Devonian, subsidence of the aulacogen allowed for extensive accumulation of marine limestones, sandstones, and shales (e.g., Arbuckle and Simpson Groups). Cambrian and Ordovician strata of Oklahoma were deposited in a broad epeiric sea (Oklahoma Basin) that extended across most of the state (Johnson 1991; Carlucci et al. 2014). The Oklahoma Basin intersected the margins of the SOA, where deeper water sedimentation was dominated by carbonate interbedded with sandstone and shale. Most authors (e.g., Longman 1982a, b; Johnson 1991) have considered the Southern Oklahoma Aulacogen (SOA) to be the depocenter of the Oklahoma Basin, as subsidence rates and sediment thicknesses are considerably higher than in shallow-ramp to platform environments outside the SOA. To the north, the Oklahoma Basin was bordered by the stable Arbuckle platform (Longman 1982b),

which was a desert region that likely supplied wind-blown sand deposited as sheets into the SOA. In the early to middle Cambrian, the craton was deeply eroded. Input of siliciclastics into the SOA was temporarily suspended during a major transgression in the late Cambrian which established the broad epeiric sea across vast areas of Oklahoma, and facilitated deposition of the Arbuckle Group (St. John and Eby 1978; Johnson et al. 1984). In the lower to middle Whiterockian, Simpson Group deposition began when the carbonate shelf that bordered the SOA was exposed (McPherson et al. 1988). Wind-blown sand was reworked and mantled the carbonate platform (Johnson et al. 1988), and was eventually overlain by marine shale and carbonate.

   After the initial infilling of the aulacogen in the Ordovician, subsidence developed again in the Late Devonian to Mississippian, accumulating thick deposits of marine shale (e.g., Woodford, Delaware Creek, and Goddard shales). In the Pennsylvanian and Permian, uplift of the entire region led to the development of many previously mentioned tectonic features (including the Arbuckle Mountains themselves), and an angular unconformity between Ordovician-Mississippian and Pennsylvanian strata.

Paleozoic Stratigraphy of the Arbuckle Mountains

   The Paleozoic stratigraphic succession of the Arbuckle Mountains (Fig. 3) comprises a thickness of more than 3,000 meters (10,000') of sediments ranging in age from Early Cambrian to Pennsylvanian, recording some 200 million years of geologic time. It is arguably one of the most complete and thickest Cambrian-Ordovician successions in central North America. The following summary provides an overview of stratigraphy and facies of this classic succession and it incorporates the litho- and biostratigraphic research of many previous workers, most notably Taff (1902), Edson (1927), Decker (1931, 1933, 1935, 1941), Decker and Merritt (1931), Hendricks et al. (1937), Wengerd (1948), Cardott and Chaplin (1963), Amsden (1967), Ham (1969), Ham and Amsden (1973), Amsden and Sweet (1983), Sprinkle (1982), Fay et al. (1982a, b), Longman (1982a, b), Finney (1986, 1988), Fay (1989), Ethington et al. (1989), Derby et al. (1991), Wilson et al. (1991), Johnson (1992, 1997), Amati and Westrop (2004, 2006), Goldman et al. (2007), Leslie et al. (2008), Bergström et al. (2010), Rosenau et al. (2012); Carlucci et al. (2012, 2014). Average stratigraphic thicknesses given by Fay (1989) are used in the following descriptions.

   At the base of the succession resting unconformably upon Proterozoic basement is the Colbert Rhyolite, now dated radiometrically as early Cambrian age (525 Ma). This basal igneous rock is nonconformably overlain by the Upper Cambrian Timbered Hills Group; the latter is comprised of about 73 meters (240') of arkosic, glauconite-bearing Reagan Sandstone and 32 m (105') of Honey Creek Limestone. Above is a thick succession (2,073 m; 6800') of predominantly massive, shallow-water, dolomitic and frequently cherty carbonates with a variety of sedimentary structures indicative of peritidal to shallow subtidal deposition. The Arbuckle Group strata are roughly dated on the basis of trilobites and other megafossils as being of Late

Arbuckle Mountains Along I-35N

Global Series	Global Stages	N. American Series	N. American Stages	Group	Formation	Field Trip Stop #
Silurian	Rhuddanian		Richmondian-Gamachian	Lower Hunton Gp	Cochran Limestone	6
Upper Ordovician	Hirnantian	Cincinnatian			Keel Limestone	6
					Sylvan Shale	6
	Katian	Mohawkian	Chatfeldian	Viola Gp	Welling Fm	8
					Viola Springs Fm	4, 7, 11, 12
	Sandbian		Turinian		Bromide Fm	4, 7, 11, 12
Middle Ordovician	Dapingian-Dariwillian	Whiterockian	Rangerian-Chazyan	Simpson Group	Tulip Creek Fm	11
					McLish Fm	
					Oil Creek Fm	9
					Joins Fm	
Lower Ordovician	Tremadocian-Floian	Ibexian	Starsian-Tulean-Black Hillsian	Upper Arbuckle Group	West Spring Creek Fm	2
					Kindblade Fm	2
					Cool Creek Fm	1
Cambrian	Stage 10	Furongian	Skullrockian	Lower Arbuckle Group	Signal Mountain Fm	
			Sunwaptan		Royer Dolomite	
					Fort Sill Limestone	10

Southeast Oklahoma, Atoka County Black Knob Ridge Section

Global Series	Global Stages	N. American Series	N. American Stages	Formation	Field Trip Stop #
Upper Ordovician	Katian	Mohawkian	Chatfeldian	Polk Creek Shale	3
				Bigfork Chert *GSSP*	3
	Sandbian		Turinian	Womble Shale	3

TEXT-FIGURE 3.—Stratigraphic nomenclature of the Paleozoic as exposed in the Arbuckle Mountains and Black Knob Ridge regions. Data compiled from Derby et al. (1991), Stitt (1991), Johnson and Cardott (1992), Bauer (1994), Johnson et al. (1994), Babcock et al. (2005), Goldman et al. (2007), Bergström et al. (2008), Rosenau et al.(2012).

Cambrian (Furongian) and Early Ordovician (Tremadocian-Floian) age. The Cambrian portion of the Arbuckle Group shows a three-fold division with lower and upper dark bluish gray, massive carbonates of the Fort Sill Limestone (47 m; 155') and Signal Mountain Formation (126.5 m; 415'). They are separated by a thick, pinkish to ocherous yellow dolostone of the Royer Formation (219 m; 717'). The Signal Mountain Formation may span the Cambrian-Ordovician boundary.

   The Lower Ordovician portion of the Arbuckle Group itself averages nearly a mile in thickness (1653 m; 5422') and includes in ascending order, the Butterly Dolostone (90 m; 297'), McKenzie

Hill Formation (274m; 900'), Cool Creek Formation (396 m; 1300'), Kindblade Formation (430 m; 1410'), and West Spring Creek Formation (462 m; 1515'). These carbonates are exposed on both the north and south flanks of the Arbuckle Mountains, although they are disturbed by faulting in some areas. The Cool Creek Formation (stop 1) displays excellently preserved peritidal indicators including stromatolites, oncoids, and flat-pebble conglomerates. Large stromatolites are also typical of the upper beds of the West Spring Creek Formation slightly below its contact with the Simpson Group. Overall, the Arbuckle Group is the expression of a long ranging gradually subsiding passive margin of Laurentia, the "Great American carbonate bank".

Simpson Group

The fully exposed Middle-Upper Ordovician strata unconformably overlying the upper part of the Arbuckle Group are assigned to the Simpson Group, Viola Group and Sylvan Shale. These strata are the primary focus of this trip and hence are discussed in somewhat greater detail.

The widespread Simpson Group, named for exposures near the village of Simpson, presently called Pontotoc (Taff 1902), is a highly fossiliferous, mixed carbonate and siliciclastic succession about 732m (2400') thick that ranges in age from Dapingian to Sandbian (Fig. 3). The interval is divided into five formations, each of which, except for the basal Joins, has been defined as starting with a lower submature quartz-rich sandstone, overlain by shales and then limestones (Decker and Merritt 1931). Altogether, this suggests a lower lowstand to early transgressive sand to shale succession with a maximum flooding within the lower shales, and an abruptly upward shallowing and "cleaning" upward succession.

The basal Joins Formation (up to 90 m thick) commences with a thin basal conglomerate that records a transgressive lag of carbonate clasts derived from erosion of the underlying West Spring Creek Formation. This unit marks the overspreading of the Sauk-Tippecanoe megasequence boundary (or Knox unconformity, which is locally of relatively small magnitude). The conglomeratic beds are overlain by thin, micritic limestones and shales with a low diversity fossil fauna, but yielding diagnostic conodonts that are assignable to the *Histiodella altifrons* to lower *H. sinuosa* conodont zones (Bauer 2010). Decker and Merritt (1931) note that these beds also contain common specimens of the graptolite *Didymograptus artus* indicating a Chazyan (late Dapingian- early Darriwillian) age, which is consistent with the conodont biostratigraphy.

The Oil Creek Formation, named for Oil Creek 14 miles SW of Sulfur, Oklahoma, is the thickest unit of the Simpson Group ranging from more than 91 m (300') to over 328 m (1075') near Spring Creek at the Daube Ranch. It comprises a basal sand which thickens eastward from a feather edge in western localities to over 175 m in the eastern Arbuckles. It locally oversteps the truncated Joins Formation to the north and rests directly on the West Spring Creek. This basal sandy interval is overlain by a thick succession of coarse bioclastic limestones (echinoderm pack- and grainstones) and shales. Beds of intraformational conglomerate are numerous as are hardgrounds, many of which show encrusting bryozoans and pelmatozoan holdfasts. A moderately diverse fauna (~35 species) includes ramose trepostome bryozoans, orthid and clitambonitacean brachiopods (*Clitambonites*, *Dinorthis*), gastropods *(Lecanospira*, *Liospira*, *Maclurites*)*, small bivalves, nautiloids, and leperditians. Trilobites (especially *Pliomerops*) and

rhombiferan cystoid plates are also abundant and well preserved. Megafaunas indicate an early Chazyan (Darriwillian) age. Bauer (2010) assigns the Oil Creek Formation to the mid Darriwilian *Histiodella sinuosa* to *H. holodentata* conodont zones.

The McLish Formation named for McLish Ranch near Bromide, Oklahoma is about 102 to 162 m (335 to 533') thick and sharply, locally unconformably, overlies the Oil Creek Formation. The McLish comprises a basal unit (Burgen Member) of up to 12 m (40') of hard to uncemented quartz sand overlain in turn by thin greenish shales (6 m; 20') and earthy brownish limestones that pass upward into dense micritic, fenestral dove gray limestones with minor dolostones and greenish shales. Overall, the unit is not highly fossiliferous, but the lower brown limestones yield sponges, gastropods, a limited diversity of brachiopods (*Rafinesquina*, S*trophomena*, *Zygospira*), small bivalves, and a thin zone of cystoid plates (*Palaeocystites*). Bergström (1971) and Bauer (1987) correlate the McLish formation with the *Cahabagnathus friendsvillensis* conodont Zone indicating a middle Chazyan (Darriwillian) age.

The Tulip Creek Formation (83-120 m; 271-394') is named for Tulip Creek near Springer, Oklahoma, and again comprises a basal sandstone (Wilcox Member), overlain by a poorly exposed interval of soft shales and thin-bedded limestones. A limited fauna of some 20 species includes abundant plates of crinoids and cystoids and the typically Blackriveran brachiopods *Pionodema* and *Dalmanella*, a few gastropods, bivalves and nautiloids. Rare conodonts, assignable to the *Cahabagnathus friendsvillensis* Zone (= *Pygodus serra* North Atlantic conodont Zone), suggest a late Chazyan age (Bergström 1971; Bauer 1987).

The uppermost unit of the Simpson Group is the Bromide Formation named for exposures in quarries near the small town of Bromide, which is itself named for naturally carbonated waters derived from aquifers in the Simpson Group. The Bromide is richly fossiliferous and has been studied in detail from the standpoint of stratigraphy and paleontology (especially its rich echinoderm faunas; see Sprinkle 1982). Decker and Merritt (1931) listed nearly 100 species including diverse brachiopods (28), bryozoans (13 species), trilobites (12), gastropods (11), cephalopods (8), algae, tetradiid corals and echinoderms. The latter have been intensively studied in the interim and now more 61 genera in 13 classes are recognized making the Bromide one of the most diverse Ordovician faunas (Sprinkle 1982). Trilobite diversity in the Bromide has also been refined upwards (e.g., Shaw 1974; Carlucci et al. 2012; Carlucci and Westrop 2014) in recent years. The Bromide Formation is notably cyclic on several scales and the documentation of this cyclicity is a major theme of recent papers (Carlucci et al 2014; Carlucci and Westrop 2014) and of this field excursion.

The Bromide is traditionally divided into two members, the Mountain Lake and Pooleville (Cooper, 1956), both named for exposures along Spring Creek on the Daube Ranch (formerly Johnston Ranch) west of Ardmore. Recent study of the Bromide (Carlucci et al. 2014) has led to recognition of a third, basal sandstone member, redefinition of the other members and interpretation of three depositional sequences probably equivalent to the M2, M3, and M4 of Holland and Patzkowsky (1996). Each commences with coarse sandstone or skeletal grainstone that passes upward into a shaly interval and then into a progradational shale to thinly bedded wacke- and packstone, and in some cases peritidal lime mudstone highstand facies.

As with other Simpson Group formations, the Bromide commences with widespread quartz sandstone which thickens toward the northeast, although originally included in the Mountain Lake Member this sandstone unit is sufficiently distinctive that it warrants separate designation and Carlucci et al. (2014) named this the Pontotoc Member. As is the pattern with the other formations, the sandstone passes upward into a greenish gray, chloritic shale with thin fossiliferous limestones. A ~1m shale thin limestone interval overlying a distinctive thick packstone ledge has yielded a prolific echinoderm fauna. This "Lower Echinoderm Zone" (Fay and Graffham 1969) has been identified in 16 localities in the Arbuckles (Sprinkle 1982) and more tentatively in the Criner Hills. More than 6,000 complete echinoderm thecae have been collected. More than half of those collected are *Hybocrinus*, another quarter the paracrinoid *Platycystites*, and in total some 30 other genera, including paracrinoids, rhombiferans, crinoids, edrioasteroids, asteroids and stylophorans.

This shale and packstone succession passes upward abruptly into an interval of thick grainstones and shales of the upper Mountain Lake Member. To the north, near Fittstown this package of echinoderm skeletal grainstones passes laterally into thicker sandstone and sandy limestone package comparable to the Pontotoc Member, but more restricted in aerial distribution. The overlying thick upper Mountain Lake Member is comprised of thinly bedded limestones and shales that yield additional brachiopods, bryozoans, echinoderms and trilobites, including the isoteline *Vogdesia*. These beds closely resemble a main mass of the interval assigned to the Pooleville to the south in the Criner Hills, which we have inferred, actually to be coextensive with the Mountain Lake Member.

A sharply based package of thick echinoderm grainstones occurring about 75 m above the base of the Bromide is identifiable at all localities and we have used it to redefine the base of the Pooleville Member. It is overlain by a greenish shaly interval identified previously in the Arbuckles as the upper Echinoderm Zone, which has yielded several thousand echinoderms, mostly the paracrinoid *Oklahomacystis*. As with the lower Echinoderm zone this interval has been widely correlated through some 15 locations in the Arbuckles. This interval is overlain by a shallowing upward succession of dense, burrow mottled lime mudstones and wackestones, typical of the Pooleville Member. The lateral continuity of both Lower and Upper Echinoderm Zones, which represent highstand facies of small-scale cycles is simply an example of the overall continuity of many units within the Bromide and strongly suggests an allocyclic (eustatic) influence on their formation.

The upper several meters consist of fenestral, microbially laminated micrites with thin shales and desiccation cracks. This interval, the Corbin Ranch submember contains thin clay beds some of have been shown to be K-bentonites and tentatively identified as the Deicke and Millbrig beds, the most widespread bentonites in the Ordovician. Thus, this interval is identified as equivalent to very similar and extraordinarily widespread micritic facies of the upper "Blackriveran" in the Mississippi Valley (Plattin Fm) Appalachian Basin (Lowville Fm), Kentucky (Tyrone Fm), Tennessee (Carters Fm), and elsewhere. It is clearly of Turinian (upper Sandbian) age based upon conodonts, as well as bentonites.   These indicators also indicate correlation of the Corbin Ranch with the upper portion of the Womble Shale in the allochthonous

deep water facies of the Ouachitas, as at the Katian stratotype section at Black Knob Ridge in Atoka.

A most important new discovery of our research is that the Pooleville Member appears to be truncated progressively southward into the Oklahoma Aulacogen, such that the overlying Viola Group rests on progressive lower Pooleville beds and ultimately on strata of the upper Mountain Lake Member. This pattern suggests, either, that there was a reversal of topography following deposition of the Bromide or that other process of deeper ramp corrosion, erosion and bypass thinned and/or removed upper Bromide strata prior to deposition of the Viola Springs. This pattern requires further study.

Viola Group and Sylvan Shale

Throughout much of the Arbuckles, the Viola Group, named for exposures near Viola, Oklahoma (Taff 1903), is a ~213 m (700') thick succession of resistant, ridge-forming, dark gray, but whitish weathering limestones. The Viola is very widespread with representation as far north as South Dakota and as far west as the subsurface of Colorado (Wengerd, 1948). In places it rests unconformably on strata as old as the Arbuckle Group at a disconformity that may represent the M4-M5 sequence boundary of Holland and Patzkowsky (1996). This unit represents much of the Katian Stage, roughly the Chatfieldian and Cincinnatian of North American terminology. The majority of the Viola Group is assigned to the Viola Springs Formation, thin- to medium-bedded, sparsely fossiliferous, commonly cherty, laminated calcisiltites with thin, dark shaly partings. Bedding can be notably hummocky (HCS?) and nodular in some portions of the formation. Thin shaly beds yield graptolites, cryptolithine trilobites and small brachiopods at many levels. The upper ~25-30 m of medium to thick-bedded packstone and grainstone is assigned to the Welling Member; it yields a diverse benthic fauna of bryozoans, brachiopods and trilobites. The base of the Welling may represent a disconformity, perhaps a mid-Richmondian unconformity.

A rather different facies aspect of the Viola Springs Formation is represented in the northern Arbuckles at Fittstown (also termed Highway 199 or Murray Lane in the literature, stop 4 here). Here, the lowest 80 cm is distinctively set off as a non-cherty interval with shaly wackestone, rich in graptolites of the upper *Climacograptus bicornis* Zone. The next 15 m of the Viola Springs Formation (member 4 of Wengerd 1948) is more typical cherty, thin-bedded, and buff weathering. Higher beds are less cherty and include pelmatozoan rich pack and grainstones (20 m, member 3 of Wengerd) overlain by light gray weathering, slightly argillaceous, highly fossiliferous wacke- and packstones (members 1 and 2). These beds yield graptolites at some levels, indicative of the *Diplacanthograptus spiniferus* Zone as well diverse bryozoan, coral, brachiopod and trilobite faunas. The latter have recently been studied in detail by Amati and Westrop (2006). Amati (2014) recognized two distinctive faunas, separated by a relatively abrupt transition at about 32 meters above the base of the Viola Springs Formation at Fittstown. Wengerd (1948) was able to trace members throughout the Arbuckle Mountains, despite changes in thickness and facies.

The Viola Springs strata yield a succession of graptolites that have permitted a detailed biostratigraphy (e.g., Finney 1986, 1988). Although there is some ambiguity, the Viola Springs at the Fittstown section is dated from the *C. bicornis* Zone (uppermost Sandbian) to the Katian

D. spiniferus Zone (see further discussion of Stop 4). In sections along I-35 the succession ranges upward to the *Amplexograptus manitoulinensis* of the upper Cincinnatian (Richmondian). Recent studies of carbonate carbon isotopes have also revealed a series of positive isotopic excursions that have tentatively been identified as the GICE and Kope Excursion (Bergström et al. 2010). The upper Cincinnatian (Richmondian) Waynesville excursion was tentatively identified in the Welling Formation.

   Based upon graptolite biostratigraphy, the Viola Springs is approximately equivalent to the Bigfork Chert of the allochthonous succession in the Ouachitas as at Black Knob Ridge (see Stop 4). The latter shows facies similarities with the distal Viola Springs, including a succession of thinly bedded chertified limestones and nodular cherts and minor shales. The sparse benthic fauna is typified by cryptolithine trilobites at some levels.

   The Viola Group is conformably overlain by some 180 m (600') of dark fissile mudrock (Wengerd 1948), assigned to the Sylvan Shale (stop 6). The latter has been dated as late Katian on the basis of graptolites of the *Styracograptus tubuliferus* to *Dicellograptus ornatus* zones (Dworian 1990). It is approximately equivalent to the widespread Shale in the Ouachitas and the Mannie Shale of the Appalachian Basin. It is overlain sharply and probably unconformably by thin widespread oolitic limestone of the Keel Formation in Oklahoma and laterally equivalent Noix Oolite in the Misssissippi Valley both of Hirnantian age and probably representing initial transgression following the late Ordovician glacioeustatic lowstand.

Post-Ordovician Strata

   Silurian and Lower Devonian shaly carbonates are assigned to the Hunton Group, which totals 40 to 70 m (130-230'). The Silurian succession in the Arbuckles includes the Llandovery age Cochrane and early Wenlock Clarita carbonates, each about 4 m thick, separated by a thin but widespread shale tongue, and the overlying Henryhouse Formation 58 m (191') of mixed siliciclastics and limestones. Locally, these rocks are highly fossiliferous with well-documented brachiopod, trilobite and echinoderm faunas (Amsden 1975).

   Devonian strata are thin and highly incomplete but include the Lower Devonian (Lochkovian) Harragan Formation,~8 m (25') thick in the southern Arbuckles and the overlying Bois d'Arc, 2.5m (8') thick, both marly, slightly cherty limestones and shales noted for diverse brachiopod and trilobite assemblages. These beds are unconformably overlain by the Upper Devonian (Famennian) Woodford Shale, black shales and cherts, up to 85 m (280') thick. The Lower to Middle Mississipppian consists of a relatively thin carbonate succession (Sycamore Limestone, 67 to 113m m, 380'). It is overlain by thick Middle and Upper Mississippian siliciclastics (the Delaware Creek Shale and the Chesterian Goddard Formation). Both are comprised of shales and sandstones, together totaling more than half a mile in thickness (Fay 1989). This shift toward much thicker siliciclastic sediments records the onset of early phases of reactivation in the Anadarko Basin (Oklahoma Aulacogen) and uplift of the Wichita Mountains to the south. Finally, the Pennsylvanian Collings Ranch Formation consists of more than 900 m (3000') of reddish, coarse polymictic conglomerate, representing Ouachita syntectonic molasse sediments.

FIELD TRIP STOPS

Figure 3 shows the Upper Cambrian to lower Silurian stratigraphy with important global and North American stage and series boundaries. The majority of the field trip stops (3, 4, 7, 8, 11, and 12) focus on deposits that formed during the Sandbian-Katian (Upper Ordovician) stages, including the Global Standard Stratotype and Point (GSSP) and auxillary section for the base of the Katian (Goldman et al. 2007), and a newly established reference section for the Bromide (Carlucci et al. 2014). Other stops expose strata above the Katian (Hirnantian), and below the Sandbian (Dapingian-Dariwillian, Tremadocian-Floian), and even into Stage 10 of the Upper Cambrian. Field trip stops in relation to important city and county boundaries, and major highways are shown in Fig. 4.

DAY 1
Stop 1: Turner Falls Overlook and the Cool Creek Formation

Turner Falls, a well-known attraction for visitors to central Oklahoma, lies just west of US Highway 77 in the East Timbered Hills region (see Fig. 1). Stop 1 is located at an overlook looking back towards the recreational area of Turner Falls. The falls are interesting from a geological perspective because they are building outward along an accreting travertine precipice, rather than eroding inwards like most waterfalls (Ham 1969). In the Pleistocene and continuing into the present day, Honey Creek has been down cutting into Arbuckle Group limestone and storing calcium carbonate in solution that is re-precipitated onto the precipice. The falls are currently in balance between travertine development and mechanical erosion from down cutting, although, during the middle Pleistocene, it appears that Honey Creek cut a deep wedge into its depositional platform (Ham 1969).

In the East Timbered Hills surrounding Turner Falls, exposures of the Colbert Rhyolite Group (see line of cross section on Figure 2) form a scenic vista. The Turner Falls overlook provides a perfect opportunity to see exposures of the some of the early core deposits of the Arbuckles, overlain by younger Cambrian limestone. The overlook is located just south of the
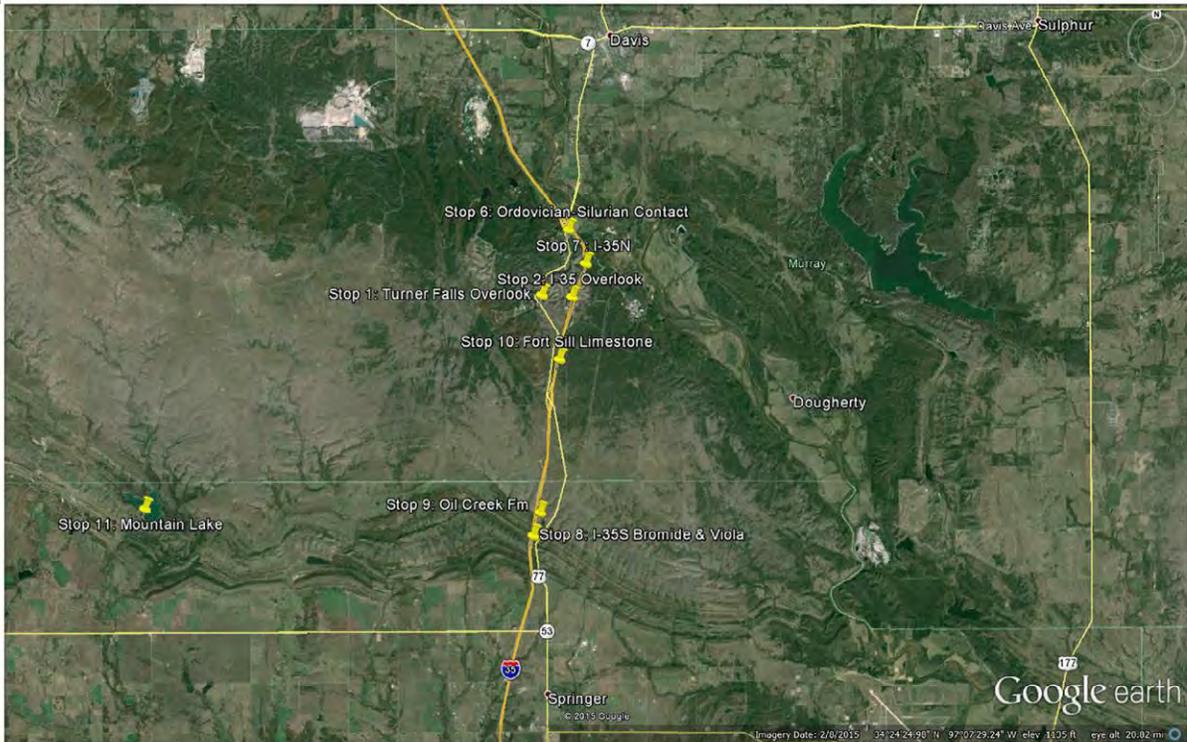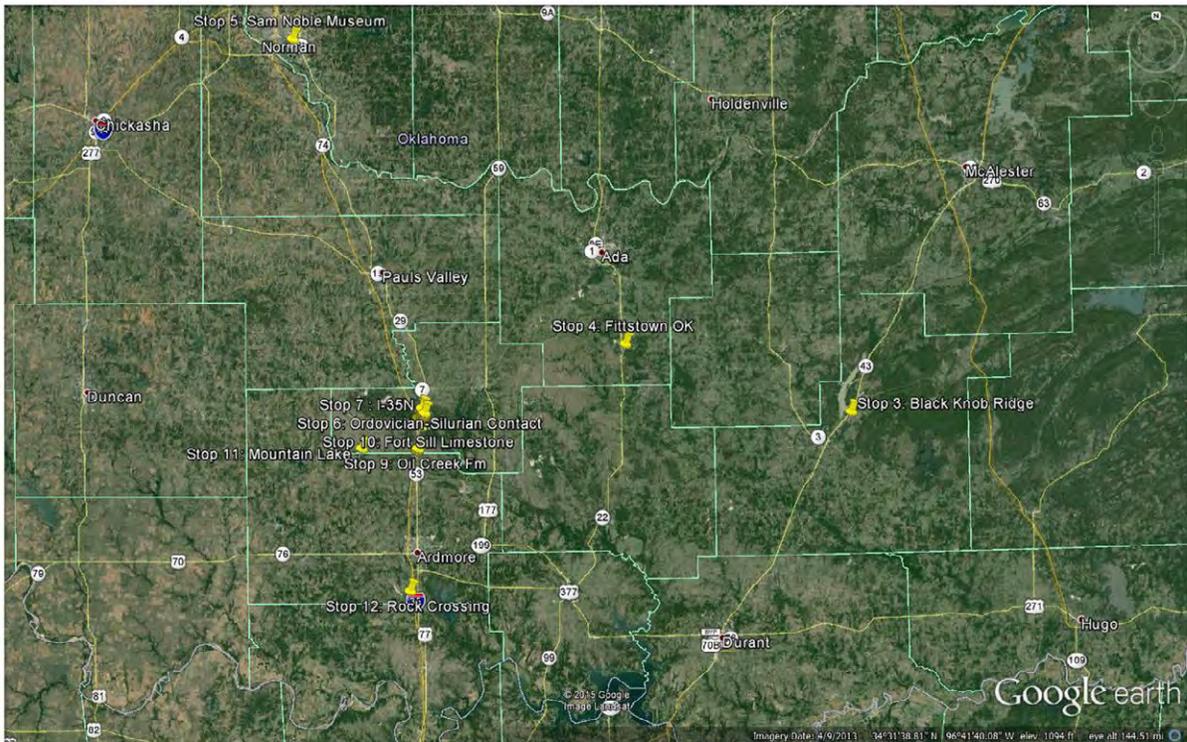
TEXT-FIGURE 4.—Field trip stops (1-12) with county, town, and state boundaries. a, close up view of all localities in the Arbuckle Mountains. b, broad view, including localities outside the Arbuckles.

Washita Valley Fault (Fig. 2), immediately to the southwest is a hill that forms the rhyolitic core of the Arbuckle Anticline. Between the core of the anticline and Turner Falls are folded and faulted strata of the Arbuckle Group. The overlook exposes the Cool Creek Formation of the Arbuckle Group (Fig. 3), which is separated by the Mackenzie Hill Formation (exposed across the valley) by a fault trace that parallels the Honey Creek valley (Cardott and Chaplin 1993). Many of these fault traces are present in the East Timbered Hills, and they represent splays from the Washita Valley or Chapman Ranch fault zones. As noted earlier, the Washita Valley fault zone is a normal fault that likely developed during early rifting and formation of the Southern Oklahoma Aulacogen in the late Precambrian and early Cambrian.

The Lower Ordovician (Tremadocian) Cool Creek Formation is one of the lower units of the Ordovician portion of the Arbuckle Group (Fig. 3). Arbuckle Group deposition varies from subtidal to supratidal, and took place on a low gradient carbonate ramp on the southern edge of the North American craton (Wilson et al. 1991). The Arbuckle Group consists of eight formations (some omitted from Fig. 3) that total nearly 2400 m (8,000 feet) in the SOA, with extensive dolomitization across most of the units. Wilson et al (1991) and Cardott and Chaplin (1993) characterized the shallowing upward cycles (Fig. 5) that are prevalent in much of the Arbuckle Group. They identified common components in the sub- inter- and supratidal environments of individual cycles (idealized succession shown in Figure 6). The top of each cycle is typically disconformable, and overlain by thin transgressive marine beds that represent backstepping prior to successive parasequence development.

Across from the gift shop at stop 1, is a roadcut through the Cool Creek Formation that shows a series of facies and sedimentary structures associated with peritidal cycles. Facies at stop 1 include: stromatolitic and thrombolitic boundstone, intraformational mud-supported breccias, oolitic grainstone, bioturbated mud- wacke- packstone, heterolithically bedded units, and chert-rich mud- and boundstones. Figure 5 shows a series of facies through a portion of a shallowing upward cycle. At the base, is an intraformational breccia of lime mudstone and algal boundstone clasts. This is directly overlain by a thin algal boundstone and then a heterolithically bedded unit of micrite and quartz silt. At the top of the cycle is a micrite with chert nodules and bands, which likely represent evaporative conditions (see explanation below). The boundstone above the chert facies likely represents the start of a new cycle, and a switch to lower intertidal or subtidal conditions.

Bedded and nodular evaporates (anhydrite) have been identified in the Cool Creek Formation in the subsurface (St. John and Eby 1978), although in outcrop these same facies have been extensively replaced by chert. Halley and Eby (1973) and St. John and Eby (1978) both suggested that hypersaline conditions were common during Cool Creek Formation deposition, based on a number of indicators, including: syndepositionally broken ooids, length-slow chalcedony, and high-relief stromatolites that occupy lower intertidal or subtidal conditions devoid of grazers. There is also direct evidence of "vanished evaporites" in the Cool Creek Formation. St. John and Eby (1978) discovered evidence of pseudomorphs and microscopic molds in all chert nodules they thin sectioned. SEM studies also revealed evidence of very small

TEXT-FIGURE 5.—Outcrop photograph from the Cool Creek Formation (stop 1), across from the gift shop at the Turner Falls overlook. See text for explanation of facies. GPS: 34°25'36.44"N, 97° 8'42.32"W.

anhydrite and celestite crystals that escaped silicification (Ragland and Donovan 1986). Macro-scale evidence of replacement of evaporites includes solution-collapse breccias in multiple intervals of the Cool Creek (St. John and Eby 1986).

Stop 2: I-35 Overlook, Kindblade Formation, Collings Ranch Conglomerate

The scenic view at stop 2 shows the Bromide Formation (see Johnson et al. 1984, fig. 8) exposed just to the north along I-35N, in fault contact with exposures of the northward dipping strata of the upper Arbuckle group (Kindblade and West Spring Creek formations) exposed immediately to the south.

Limestone beds of the Kindblade Formation (Arbuckle Group) are exposed at the scenic I-35 overlook at stop 2. The Kindblade is the middle unit of the Upper Arbuckle Group (Fig. 3), and was deposited in supra to subtidal marine environments. Loch (2007, fig 1) identified two separate facies belts: hypersaline supratidal to shallow subtidal marine limestones, and more distal, faunally diverse, open marine limestones. Supratidal to shallow subtidal deposits are

Laminated mudstone
Dessication fabrics
Anhydrite nodules

Laminated mudstone

Stromatolitic bindstone

Intraformational
matrix-supported breccia
Stromatolitic bindstone

Herringbone
crossstratified sandstones

Bioturbated mudstone/
wackestone- thrombolitic

Oolitic, peloidal, intraclastic
shoals (packstone/grainstone)

Thrombolitic, bioturbated
mudstone/wackestone

Nodular lime mudstone

TEXT-FIGURE 6.—Idealized shallowing upward cycle from the Cool Creek Formation (Arbuckle Group) (modified from Wilson et al. 1991; Cardott and Chaplin 1993). Figure 5 shows facies from a portion of this cycle.

dolomitized across much of the state (Ross 1976; Loch 2007). In comparison to the underlying Cool Creek Formation (stop 1), the Kindblade represents a return to more "open" marine conditions, with comparatively fewer sedimentary structures indicative of evaporative conditions (e.g., pseudomorphs and oolites).

TEXT-FIGURE 7.—Limestone dissolution megabreccia in the Kindblade Limestone, stop 2 (GPS: 34°25'34.26"N, 97° 8'4.29"W).

   The outcrop consists of thin- to thick-bedded subtidal marine wackestones, packestones, and locally stromatolitic boundstones. Oolitic and peloidal packstones often form sharp boundaries with silt-laminated, digitate boundstones. Fay (1989) described three distinct facies associations that can be seen in this outcrop, which likely record a larger–scale regressive cycle.
Lower deposits are characterized as thin to medium bedded, bioturbated lime mudstones, with thin skeletal grainstones interpreted as tempestites. The middle association consists of oolitic wackestone and packstones, interbedded with lime mudstone. Fay (1989) and Loch (2007) interpreted this unit as being shallower than the lower unit, possibly representing transport of ooid shoal allochems into a more restricted, lagoonal environment. The absence of oolitic grainstones (expected in a high energy shoal) is consistent with this hypothesis. The uppermost association consists of thick-bedded lime mudstones with dolomitic partings, stromatolitic boundstones, and a decrease in faunal diversity. Most authors (Fay 1989; Osleger and Read 1991: Loch 2007) consider this lithology consistent with restricted circulation. Therefore, lagoonal deposits are a likely explanation, but the Kindblade probably did not reach intertidal conditions.

   Another interesting feature of the Kindblade Limestone at this exposure is a megabreccia (Fig. 7) with a framework of randomly oriented boulders in an otherwise undeformed sequence of strata. Tapp (1978) showed that insoluble clay layers encased the boulders and were nearly

90° to layering. This strongly suggests that the megabreccia formed by dissolution of limestone along joints during the Pennsylvanian, and subsequent collapse of the boulders during Ouchita uplift. Thus, it is interpreted as both a karst and tectonic feature. Stop 2 also exposes one of the best examples of the Pennsylvanian Collings Ranch Conglomerate (CRC) in the Arbuckles. The CRC is an interesting unit because it is a coarse orogenic product that records evidence of the faulting, folding and uplift in the late Pennsylvanian. The CRC is a limestone boulder conglomerate (polymict and grain-supported in most exposures) that was deposited in an area trending from the NW-SE as the Arbuckle Mountains were still rising (Cardott and Chaplin 1993). The unit crops out in the northern portion of the Arbuckle Anticline along the Washita Valley Fault zone. The conglomerate is unconformable with the underlying Bromide and Viola Groups (seen in stop 7 of this trip), and is preserved as a NW-SE trending, fault-bounded graben. Provenance studies (e.g., Nick and Elmore 1990) have shown that the limestone clasts mostly originate from various formations within the upper and lower Arbuckle Group, with sandstone and limestone clasts derived from the Simpson Group present in small quantities. The lack of rhylolitic clasts suggests that the core of the Arbuckles was not exposed during Pennsylvanian erosion, or possibly that the drainage area did not include the Cambrian Colbert Rhyolite (Cardott and Champlin 1993).

  Individual cycles of poorly sorted, graded, and grain-supported clasts are well exposed in outcrop at stop 2. These deposits are considered by most authors to have formed as debris and mud flows in an intermontane alluvial fan complex, with both sheet and channel geometries. Cardott and Champlin (1993) suggested that matrix-starved intervals with lenticular geometries represent a more proximal braided stream environment, suggestive of rapid channel shifting.

DAY 2
Stop 3: Black Knob Ridge, Katian GSSP, Womble Shale, Bigfort Chert, and Polk Creek Shale.

        The Upper Ordovician rocks that crop out in the Ouachita Mountains of west-central Arkansas and southeastern Oklahoma are composed primarily of graptolite-rich shales associated with deep-water limestones and cherts (Ethington et al. 1989). These strata were deposited in the deep marine environment of the Ouachita Foredeep off the southern margin of Laurentia (Finney 1988). The rich graptolite faunas have been used traditionally to correlate these rocks with other Upper Ordovician successions in North America and around the world. A correlation chart for the main lower Upper Ordovician graptolite zonal successions discussed in this field guide is provided below.
In southeastern Oklahoma Upper Ordovician strata are exposed along Black Knob Ridge, a low narrow ridge at the extreme western end of the Ouchita Mountains (Hendricks et al. 1937; Finney 1988). The units exposed along Black Knob Ridge are, in ascending order, the Womble Shale, Bigfork Chert, and Polk Creek Shale. The base of the Ordovician succession is in fault contact with the Pennsylvanian Atoka Formation and the Silurian age Blaylock Sandstone
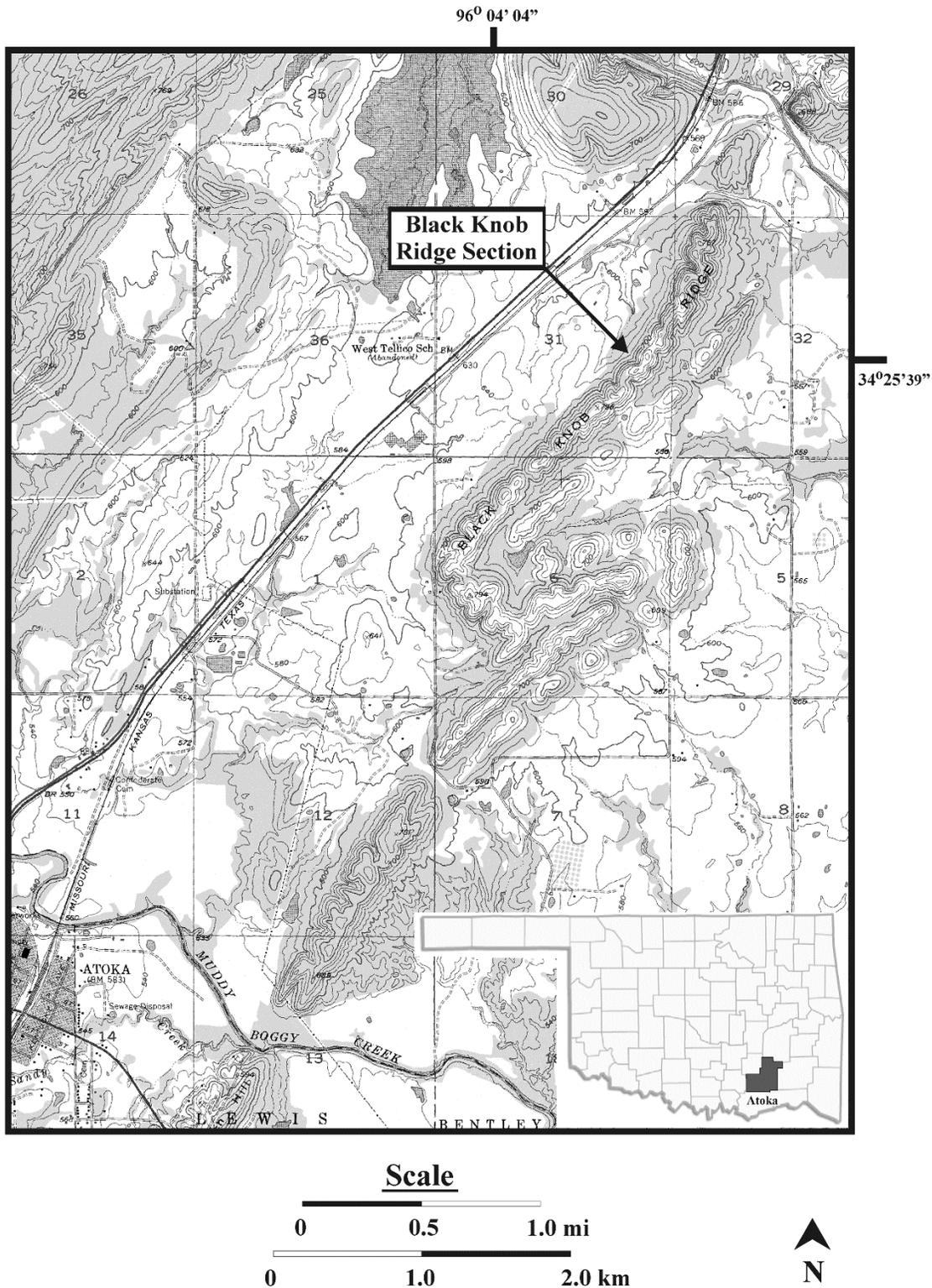
TEXT-FIGURE 8.—Locality map for the Black Knob Ridge Section. The section is located 5 kilometers north of the town of Atoka, SW1/4, Section 31, T. 1S, R. 12E, Atoka County, Oklahoma; 34° 25' 39.08" N, 96° 04' 3.78" W. From Goldman et al., 2007.

disconformably overlies the top of the sequence (Ethington et al. 1989). An excellent exposure of the Womble to Polk Creek succession occurs on a hill slope approximately 5 kilometers north

of the town of Atoka, SW1/4, Section 31, T. 1S, R. 12E, Atoka County, Oklahoma; 27° 25.9' N, 96°04.5' W (Figure 8). This exposure, which we refer to as the Black Knob Ridge (BKR) section (Figure 9A, B), extends along strike for several hundred meters, is readily accessible, contains a continuous graptolite succession across the *Climacograptus bicornis – Diplacanthograptus caudatus* zonal boundary, and yields biostratigraphically important conodonts and chitinozoans.

The International Subcommission on Ordovician Stratigraphy (ISOS) recommended that the first appearance of *Diplacanthograptus caudatus* at the Black Knob Ridge section be used as the GSSP of the middle stage of the Upper Ordovician Series. The ISOS also recommended the

Global Stages	Laurentia (Oklahoma & Eastern USA)		Pacific Faunal Province (General)	Australia	Laurentia (Scotland)
Katian	*Amplexo. manitoulinensis*		*Styraco. tubuliferus*	*Dicello. gravis*	*Pleuro. linearis*
	Geniculo. pygmaeus			*Dicrano. kirki*	
	Diplacantho. spiniferus	*D. spiniferus*	*Diplacantho. caudatus*	*Diplacantho. spiniferus*	*Dicrano. clingani*
		O. rudemanni			
	Diplacantho. caudatus	*Corynoides americanus*		*Diplacantho. lanceolatus*	
Sandbian	*Climaco. bicornis*		*Climaco. bicornis*	*Ortho. calcaratus*	*Climaco. bicornis*

Table 1.—Correlation of Upper Ordovician biozones discussed in this field guidebook. Key references used in constructing this chart are Finney (1986), Goldman et al (2007), Riva (1969, 1974), VandenBerg and Cooper (1992), and Zalasiewicz et al. (1995).

designation Katian Stage for this stage, a name derived from the nearby Katy Lake (now drained) near the southern end of Black Knob Ridge (Bergström et al. 2006). These decisions were ratified by the ICS in 2006 (Bergström et al. 2006).

At the BKR section, approximately 20 meters of dark, graptolite-rich Womble Shale are exposed. The lower 15 meters is composed of blocky, white to chocolate brown weathering mudstone, interbedded with fissile black shale, siliceous limestone, and bedded chert. Within this unit, approximately 15 meters below the base of the Bigfork Chert is a distinct channel-like feature that is filled with 80 cm of soft, fissile, dark gray shale with abundant specimens of *Dicellograptus* sp. (Figure 9C). This feature might be interpreted as the M3-M4 sequence boundary of Holland and Patzkowsky (1996). About five meters below the Bigfork Chert the
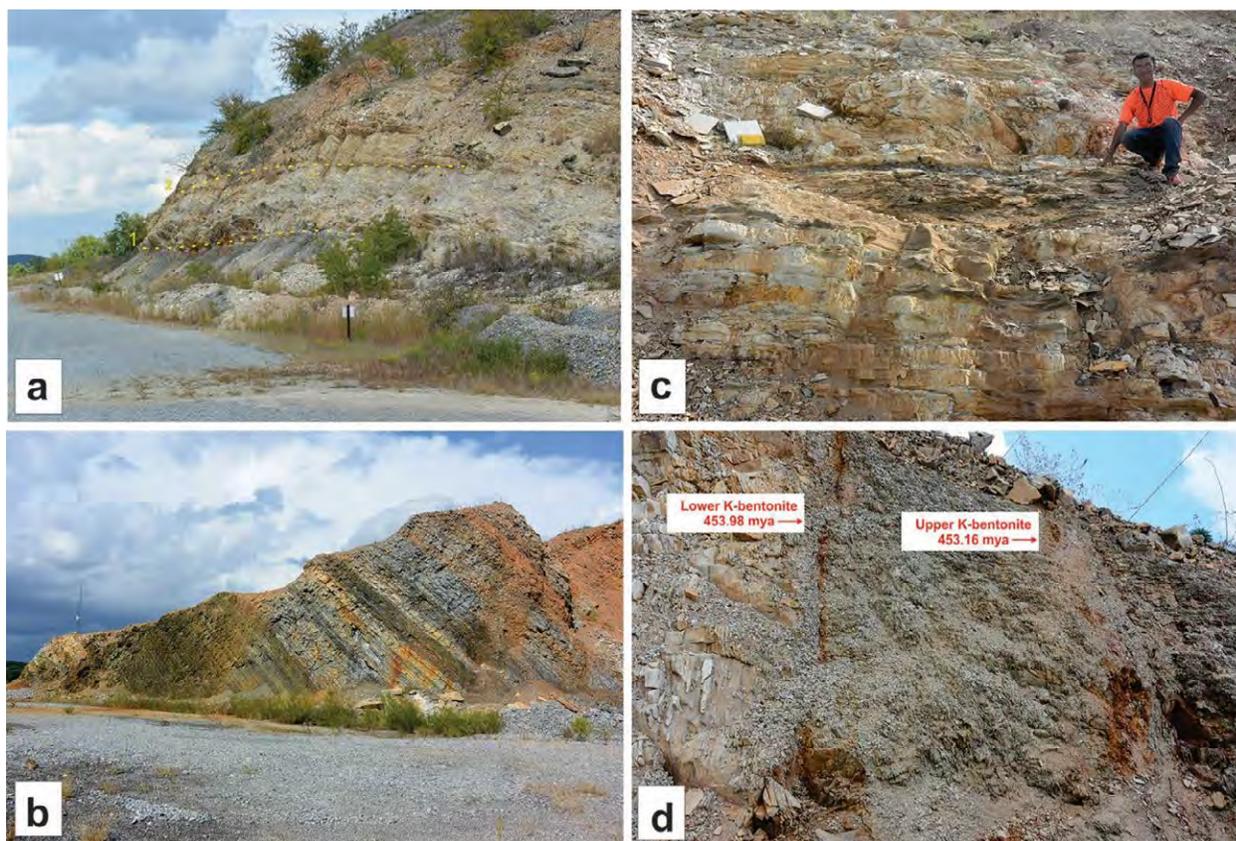
TEXT-FIGURE 9.—The Black Knob Ridge Section. a, The Upper Womble Shale and Bigfork Chert at the Black Knob Ridge Section. 1, The contact between the two units is placed at the first organic-rich, siliceous shale that forms a prominent ledge. This bed is extremely rich in graptolites and conodonts. 2, The base of the *Diplacanthograptus caudatus* Zone. The yellow dashed line is 4.0 meters above the base of the Bigfork Chert and marks the FAD of *D. caudatus*. b, Steeply dipping uppermost Womble Shale and Bigfork Chert. Up-section is to the right. c, Channel in the upper Womble Shale. d, Distinctive shale package at the top of the Womble Shale. This 3.65 meter intervals contains two K-bentonites with ages of 453.98 and 453.16 mya, respectively (Sell et al. 2013).

mudstone becomes more fissile, thinner bedded, and platy. These beds are in turn overlain by a distinct 3.65 meter package of soft, friable shale that has a 4 cm K-bentonite at its base and another 10 cm K-bentonite at 1 meter above the unit base (Leslie et al. 2008; Figure 9D herein). These beds have zircon phenocrysts that yielded U/Pb ages of 453.98 Ma and 453.16 Ma, respectively (Sell et al., 2013). These age data suggest that in addition to their correct biostratigraphic position (upper *C. bicornis* Zone), the Womble K-bentonites at the BKR section are potentially the Deicke and Millbrig K-bentonites (Sell et al. 2013). These dates also fit well with the most recent age of the base of Katian, 453 Ma, the date given in the latest Ordovician time scale by Cooper et al. (2012). It is possible that this shale package correlates either with the upper Pooleville Member of the Bromide Formation at Highway 99, which also contains two K-bentonites (Leslie et al. 2008), or the lowermost 0.8 meters of the Viola Springs Formation at that same section (see below).

Conformably overlying the Womble Shale are approximately 145 meters of Bigfork Chert (Figures 9). The contact between the two units appears gradational. The base of the

Bigfork Chert is a 0.5 meter interval of hard, splintery black shale that contains abundant conodonts and chitinozoans. The Bigfork Chert is composed of nodular and bedded chert, and siliceous mudstone intercalated with black shale and siliceous limestone. Because limestone beds are absent in the shale below and above the Bigfork Chert, its upper boundary is placed at the last limestone bed in the section (Finney 1988). The limestone is medium bedded, siliceous, fine- to coarse-grained skeletal calcarenites. Fossils include graptolites, conodonts, chitinozoans, sponge spicules, inarticulate brachiopods, and radiolarians (Hendricks et al. 1937) with skeletal fragments of pelmatozoans and brachiopods (Finney 1988). Decker (1935) noted an abundance of the trilobite *Cryptolithus* in some beds of the Bigfork Chert at the Stringtown Quarry (BKR); this trilobite is also typical of the correlative Viola Springs Formation. There is no evidence of a depositional break within the lower Bigfork Chert at the study section.

The Polk Creek Shale overlies the Bigfork Chert with an apparently conformable contact. Although the Polk Creek has not been measured at the BKR section, Hendricks et al. (1937) measured 43 meters at the Atoka city trash dump and Dworian (1990) recorded 32 meters from a locality along Black Knob Ridge south of the stratotype section. Decker (1935) correlated the Polk Creek Shale with the Sylvan Shale (see Stop 6) and showed that both had a similar graptolite fauna, including *Dicellograptus complanatus* that indicates a late Katian age.

The upper Womble shale contains an abundant graptolite fauna that is referable to the *Climacograptus bicornis* Zone. Diagnostic elements of this fauna include *C. bicornis*, *C. bicornis tridentatus*, *C. cruciformis*, *Orthograptus whitfieldi*, *O. calcaratus* ssp., *Archiclimacograptus modestus*, *Dicranograptus spinifer*, *D. contortus*, *D. arkansasensis*, *Normalograptus brevis*, and *Nemagraptus gracilis*. The transition between the *C. bicornis* Zone and the underlying *N. gracilis* Zone has not yet been found at Black Knob Ridge.

Climacograptus bicornis, *C. bicornis tridentatus*, *Archiclimacograptus modestus*, and *Dicranograptus arkansasensis* range upward into the lowermost 3.1 meters of the Bigfork Chert. *Orthograptus quadrimucronatus* makes its first appearance 3.2 meters above the base of the Bigfork Chert. The base of the Katian Stage of the Upper Ordovician Series is placed at the FAD of *Diplacanthograptus caudatus*, 4.0 meters above the base of the Bigfork Chert (Figure 10). At this horizon, several taxa diagnostic of the *D. caudatus* Zone first appear. These are, *Orthograptus pageanus*, *Neurograptus margaritatus*, and *Corynoides americanus*. *Dicranograptus hians* was found 2.0 meters higher up. *Diplacanthograptus spiniferus* and *Climacograptus tubuliferus* debut at 9.8 and 52.5 meters, respectively, above the base of the Bigfork Chert (Finney 1986 and personal communication). Characteristic graptolite species from the *Climacograptus bicornis* and *Diplacanthograptus caudatus* zones are illustrated in Figure 11.

Conodonts have been known from the Black Knob Ridge since Hendricks et al.'s (1937) description of the geology at this section. Harlton (1953) also reported the occurrence of conodonts at BKR. However, as Repetski and Ethington (1977), and Ethington et al. (1989) reported, these early studies did not identify the conodonts, and their stratigraphic occurrences
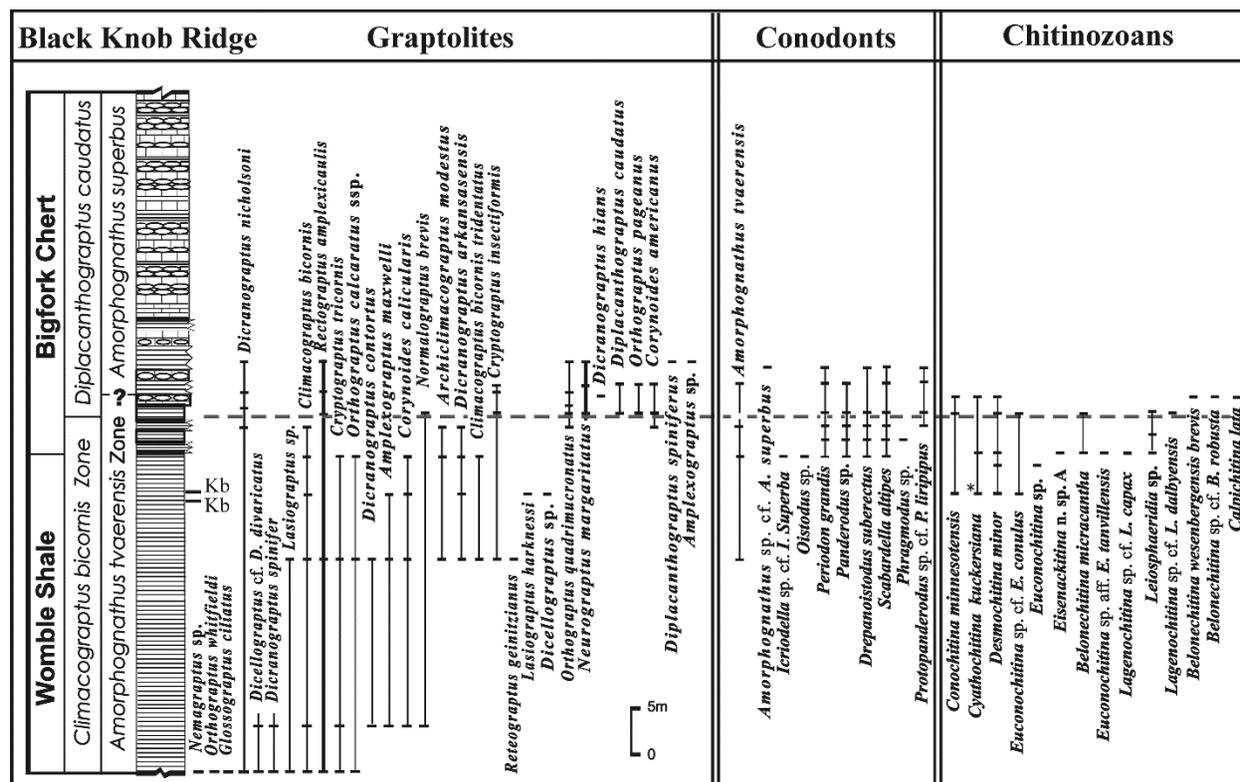
TEXT-FIGURE 10.—Stratigraphic column with a range chart of graptolites, conodonts, and chitinozoans for the Black Knob Ridge section. The GSSP for the base of the Katian Stage is placed at the first appearance of *D. caudatus* four meters above the base of the Bigfork Chert. The *C. bicornis* - *D. caudatus* zonal boundary occurs high in the *Amorphognatus tvaerensis* conodont Zone. From Goldman et al., 2007.

were not documented precisely. Bradshaw (1974) identified a conodont fauna of Midcontinent aspect from the Bigfork Chert at BKR. She reported occurrences to the genus-level, and identified a fauna of *Panderodus*, *Belodina*, *Drepanodus*, *Oistodus*, and *Phragmodus* from siliceous limestone beds. More recently, Krueger (2002) reported on the occurrence of conodonts from the Stringtown Quarry approximately 3 kilometers north of the BKR section. The fauna that Kreuger reported from the limestone beds is also of Midcontinent aspect.

Unfortunately, the former limestone beds in the lower part of the Bigfork at the BKR section are completely silicified and cannot be dissolved for conodonts. There are also well-preserved conodonts on the dark shale bedding planes in both the Womble Shale and Bigfork Chert that are typical of the North Atlantic Fauna. The uppermost Womble Shale contains an abundant, low diversity but biostratigraphically important conodont fauna that includes elements of *Amorphogathus tvaerensis* and *Icriodella* cf. *I. superba* (Figure 10). The presence of these species demonstrates that the uppermost Womble at BKR is within the *B. alobatus* Subzone of the latest *A. tvaerensis* Zone (Bergström 1982). It is younger than the *B. gerdae* Subzone fauna reported elsewhere from the Womble by Repetski and Ethington (1977; Ethington et al. 1989). The uppermost Womble Shale at BKR also contains *Periodon grandis*, *Drepanoistodus*
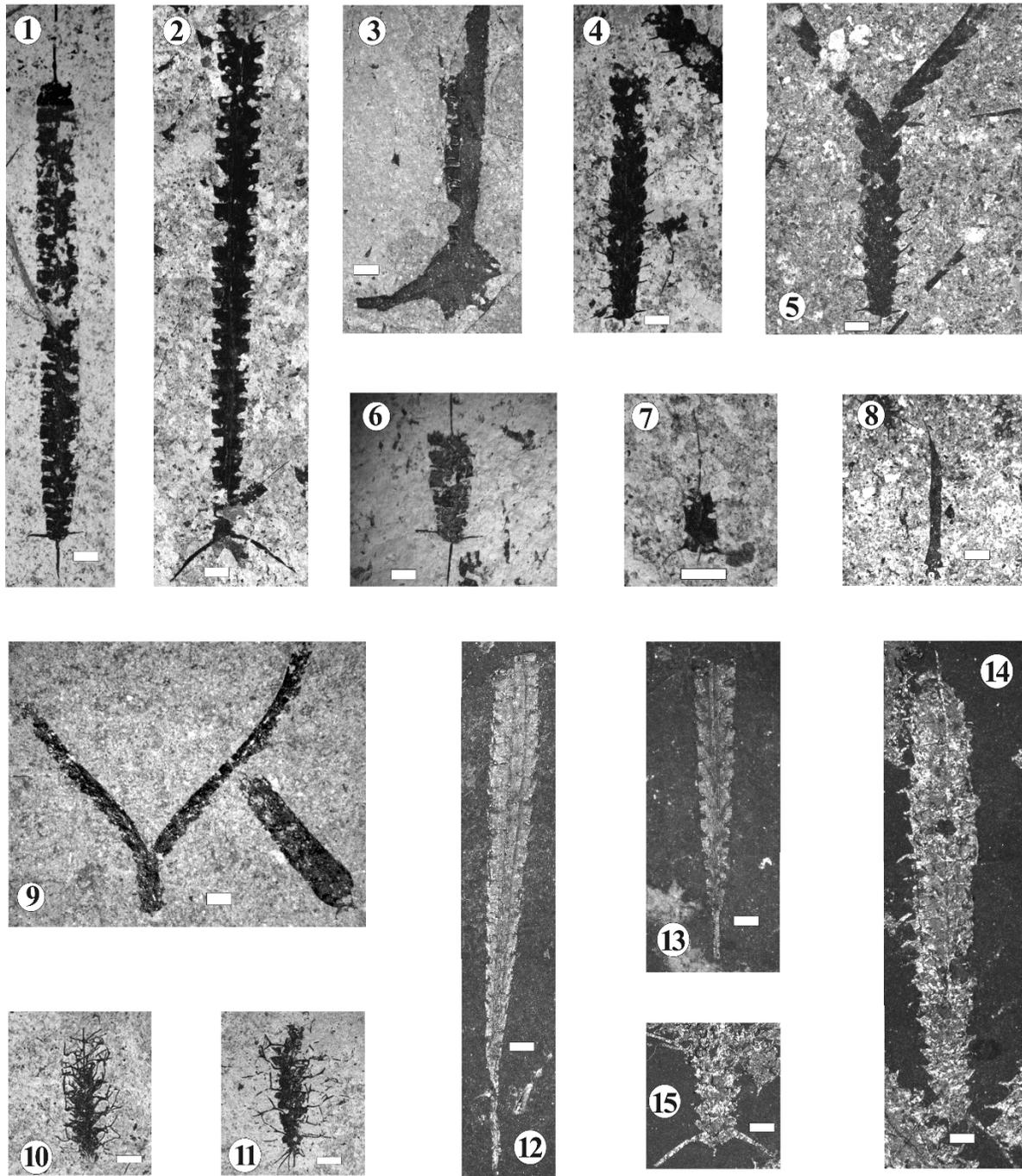
TEXT-FIGURE 11.—Graptolites from Black Knob Ridge. 1–8, graptolites from the *Climacograptus bicornis* Zone. 1, 6, *Archiclimacograptus modestus*; 2, 7, *Climacograptus* bicornis; 3, *Climacograptus bicornis tridentatus*; 4, 5, *Dicranograptus spinifer* (= *D. nicholsoni longibasalis*); 8, *Corynoides calicularis*. 9–15, graptolites from the *Diplacanthograptus caudatus* Zone. 9, *Dicranograptus hians* and *Cryptograptus insectiformis*; 10, 11, *Neurograptus margaritatus*; 12, 13, *Diplacanthograptus caudatus*; 14, 15, *Orthograptus pageanus.* Scale bar on each photograph is 1 mm.

suberectus, *Dapsilodus* sp. aff. *D. mutatus*, *Oistodus* sp., and *Panderodus* sp. (Goldman et al. 2007).

The conodont fauna from lowermost Bigfork Chert at BKR consists of *A. tvaerensis*, *Periodon grandis*, *Protopanderodus* cf. *P. liripipus*, *Drepanoistodus suberectus*, *Dapsilodus* sp.aff. *D. mutatus*, *Phragmodus* sp., and *Panderodus* sp. This fauna is nearly identical to that from the upper Womble, with the exception of relatively abundant specimens of *P*. cf. *P. liripipus*. Of particular interest is the occurrence of two specimens of *Amorphognathus* sp. approximately 5.7 meters above the base of the Bigfork Chert (Goldman et al., 2007). These specimens are morphologically very similar to *A. superbus*, but unquestionable identification is not possible from the material at hand.

The biostratigraphically significant conodonts known from BKR suggest that the *Climacograptus bicornis - Diplacanthograptus caudatus* zonal boundary is located in the *B. alobatus* subzone of the *Amorphognathus tvaerensis* conodont zone (Goldman et al., 2007). This correlation is consistent with the graptolite – conodont zonal relationships described from Europe and eastern North America by Bergström (1971, 1986) and Goldman et al. (1994).

Stop 4: Bromide Formation, Viola Springs Formation, Katian Auxiliary GSSP

The HW 99/377 section has a long history of study (e.g., Decker 1933; Wengerd 1948), and the locality is known in the older literature as "Murray Lane". The section encompasses the upper Sandbian and lower Katian succession, with the boundary lying somewhere within the lower 20 m of the Viola Springs Formation. It was designated as an auxiliary stratotype for the base of the Katian (Goldman et al. 2007) because it yields diverse shelly faunas in addition to graptolites and conodonts. Young et al. (2005) demonstrated the presence of a positive carbon isotope excursion that they equated with the GICE excursion of the Upper Mississippi Valley, although, as discussed below, this correlation has been disputed (Westrop et al. 2012). The underlying Bromide Formation is less fossiliferous, although a recent sequence-stratigraphic framework (Carlucci et al. 2014) facilitates correlation with the classic localities farther to the south (e.g., Sutherland and Amsden 1959; Shaw 1974).

Overview of the succession

Bromide Formation. The HW 99 locality includes the type section of the basal Pontotoc Member of the Bromide Formation (Carlucci et al. 2014), which comprises a succession of cross-bedded to rippled sandstones and siltstones. In platformal sites like HW 99, it represents the TST of the lowest of three depositional sequences identified in the Bromide (Carlucci et al. 2014). The overlying Mountain Lake Member (HST of Sequence 1; Sequence 2) is poorly exposed, but Fay et al. (1982b) provide a detailed description of exposures from an adjacent quarry that is now almost completely covered. Higly fossiliferous, greenish gray shales and thin packstones of the "lower Echinoderm Zone" are still exposed, though largely covered, along the northwest side of the roadcut, southwest of crossing of the gully, which separates the roadcuts into two sectors. These shales yield abundant plates of hybocrinids, rhombiferans and other
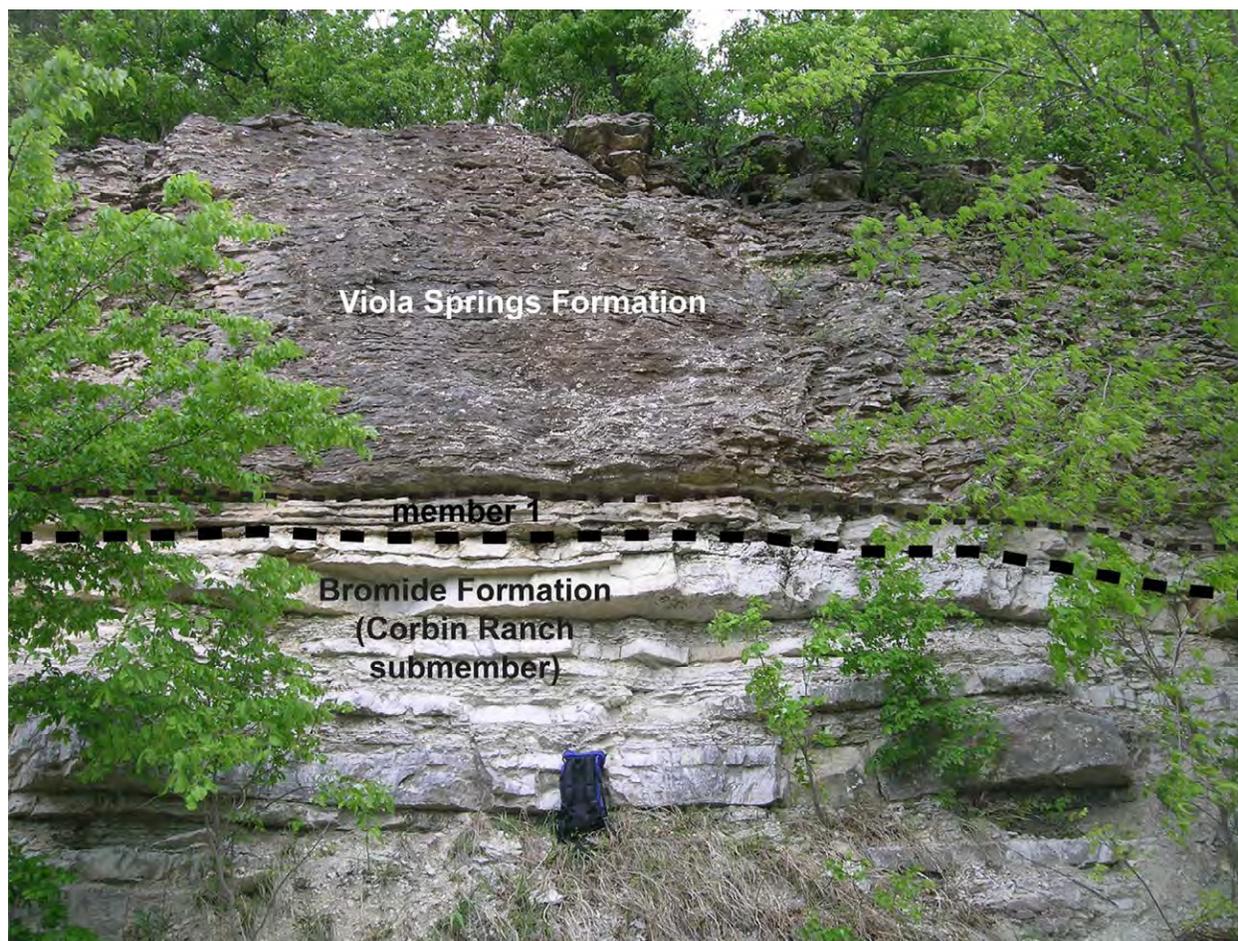
TEXT-FIGURE 12.—Outcrop photograph (stop 4) showing the position of "member 1" of the Viola Formation (to be formally named elsewhere) relative to the peritidal cycles of the Corbin Ranch Submember of the Bromide Formation. GPS: 34°34'11.11"N, 96°37'52.31"W.

echinoderms as well as diverse brachiopods and bryozoans. An overlying bundle of sandstones and sandy limestones crops out along the same cut just SW of the gully and area of covered section.

The youngest strata assigned to the Bromide Formation, fully exposed NE of the gully, represent the Pooleville Member (HST of Sequence 3). The lower Pooleville is for the most part a sparsely fossiliferous succession of wackestone and calcisiltite that is overlain by peritidal carbonates of the Corbin Ranch submember (Amsden, in Amsden and Sweet 1983) (Figure 12). The latter includes the rhynchonelliform brachiopod *Ancistrorhynchia* (Amsden, in Amsden and Sweet 1983), and rare sclerites of the trilobite *Bathyurus* (e.g., Ludvigsen 1978); the latter is indicative of the traditional Blackriveran stage of eastern North America. The Pooleville is also noteworthy because bentonites at 4.1 and 11.3 m below the top of the Corbin Ranch Member have been correlated with the well-known Millbrig and Deicke K-bentonites (Rosenau et al. 2012). However, these bentonites have not yet been geochemically "fingerprinted", and interpretation rests largely upon stratigraphic position.

Viola Springs Formation. The Viola Springs Formation begins with a thin (~ 0.8 m) package of mostly deep subtidal, graptolitic wackestone and shale that has a sequence-like architecture (sequence 4 of Carlucci et al. 2014). It will be named formally elsewhere and is simply designated "member 1" herein (Figure 12). At the base, the TST is recorded by a condensed interval of packstone and grainstone that includes rare sclerites of unnamed species of *Cryptolithus* (Amati 2014) and *Flexicalymene* (Amati 2004) that indicate a "Trentonian" age, and a cm-thick clay (Decker 1933) that may represent a bentonite. The overlying HST comprises about five beds of wackestone and shale that yield an upper Sandbian graptolite fauna. Previous workers (e.g. Young et al. 2005; Leslie et al. 2008) have agreed that the base of the Viola Springs is the M4–M5 sequence boundary that has been correlated widely across eastern North America. Member 1 likely represents the M5A of the Cincinnati region (Carlucci et al. 2014).

Member 1 is truncated by an irregular unconformity surface that is succeeded by about 15 m of cherty, laminated lime mudstone, wackestone and calcisiltite, with a sparse fauna of cryptolithine and isoteline trilobites, and graptolite fragments (Amati 2014, appendix 2). A major lithofacies change to coarse, bryozoan-rich, bioclastic grain- and rudstone (Amati and Westrop 2006) occurs at about 18 m above the base of the Viola Springs, although the contact with the underlying cherty limestone is not exposed. This high-energy bioclastic facies presumably represents the TST of a depositional sequence that we suspect is correlative with sequence M6 of eastern North America.

About 40 m above the base of the Viola Springs, the succession shifts to deeper subtidal, trilobite-brachiopod bioclastic pack- and rudstone interlayered with wackestone (high diversity wackestone–rudstone facies of Amati and Westrop 2006).
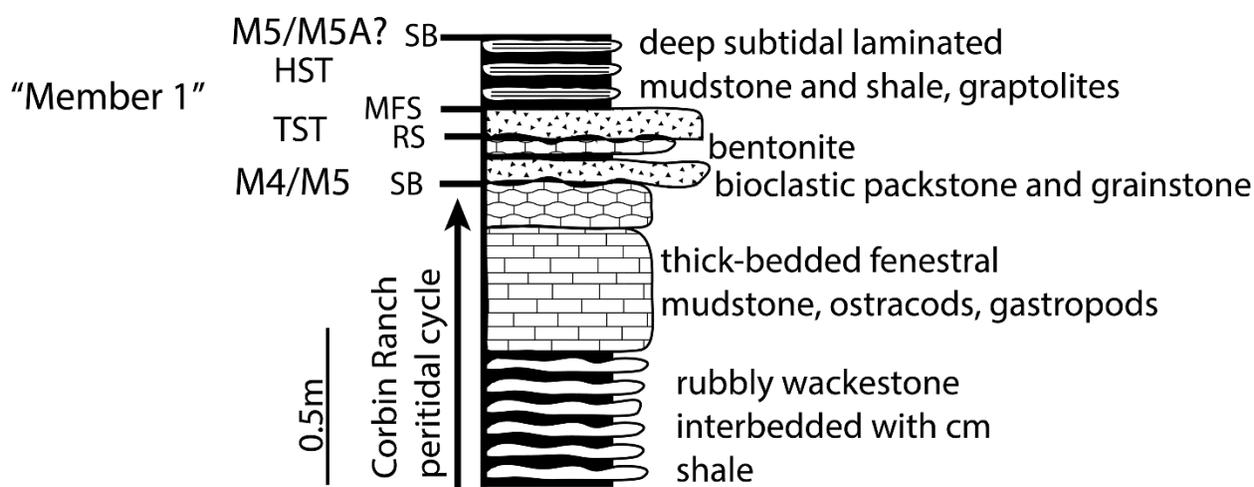
TEXT-FIGURE 13.—Stratigraphic column of "member 1" and inferred position of sequence boundaries, maximum flooding surfaces, ravinement surfaces, and Mohawkian depositional sequences (M4, M5, M5A).

Age and correlation of the HW99 section

Recent assessment of the conodont biostratigraphy of the HW 99 section (Young et al. 2005) follows graphic correlation by Sweet (1983, 1984). The Bromide and lower Viola Springs (including member 1) falls within the *Phragmodus undatus* Zone (Sandbian). The bulk of the Viola Springs has been assigned to the *Plectodina tenuis* Zone, with only the uppermost few meters representing the *Belodina confluens* Zone (Young et al. 2005, fig. 3). Thus, the conodont biostratigraphy is consistent with the interpretation of the unconformable contact of the Bromide and Viola Springs as the base of the M5 depositional sequence. However, the conodont faunas would also suggest that the entire Viola Springs at HW 99 lies within sequence M5, and that the carbon isotope excursion is correlative with the GICE (Bergström et al. 2010, fig. 4). It also implies that the coarse bioclastic TST at about 18 m records a lower rank sequence (4th order?) within M5.

The trilobite and graptolites also support the conclusion that the base of the Viola Springs (member 1) is of late Sandbian age, and correlative with the base of M5. However, in the upper half of the section, the graptolite and trilobite faunas indicate a significantly younger age than is suggested by the conodonts. The trilobites belong to the *Bumastoides* and *Thaleops* biofacies of Amati and Westrop (2006), and include a number of species (e.g., Amati and Westrop 2004; Amati 2014; Swisher et al. 2015) that are known to occur in the Kimmswick Limestone in the St. Louis, Missouri, area. There the Kimmswick rests unconformably on strata, including the Guttenburg Limestone, that surely record the GICE (Metzger and Fike 2013), and the trilobite faunas are no older than M6, and may extend into correlatives of the C1 sequence (Swisher 2015). Elements of the Kimmswick trilobite fauna enter the HW 99 succession in the coarse bioclastic grain- and rudstone facies at about 18 m above the base of the Viola Springs (Amati 2014), and indicate that this is in fact the local expression of a TST at the base of sequence M6. Moreover, if the age of the Viola Springs suggested by the trilobites is correct, then there are obvious implications for the identity of the carbon isotope excursion present in the upper half of the section. It cannot be the GICE, and may in fact the same excursion that Bergström et al. (2010) identified as the "Kope excursion" in the lower part of the Viola Springs at the I35 south section (Westrop et al. 2012). A correlation chart illustrating the Upper Ordovician graptolite zones, conodont zones, and important event and chemostratigraphic marker horizons in the principal localities discussed in the text is shown in Table 2 below.

The differing perspectives on the age of the upper half of the Viola Springs at HW 99 demand that either the conodont or the trilobite faunas have diachronous first appearances. They can be reconciled only if the conodont index species have relatively late (stratigraphically young) first appearances relative to the trilobites or, alternatively, species of the Kimmswick trilobite fauna appear relatively earlier in Oklahoma. This problem is still not fully resolved, but graptolite faunas seem to favor diachroneity of conodont species.

Series	Stage	N. American Sequences and Graptolite Zones			North Atlantic Conodont Zones		N. American Midcontinent Conodont Zones
		Sequences	Pacific Province	Eastern N.A.			
Upper Ordovician	Katian	C5	Dicellograptus complanatus	Dicellograptus complanatus	Amorphognathus ordovicicus		A. grandis
		C4	Styracograptus tubuliferus	Amplexograptus manitoulinensis	Amorphognathus superbus		O. robustus
		C3					O. velicuspis
		C2		G. pygmaeus			
		C1	Kope δ¹³C Excursion	Diplacanthograptus spiniferus			B. confluens
		M6	Diplacanthograptus caudatus	O. ruedemanni			
		M5		Corynoides americanus			
	Sandbian	M4	GICE δ¹³C Excursion		Amorphognathus tvaerensis	B. alobatus	P. tenuis
		M3	Millbrig k-bentonite	Diplograptus foliaceous (= D. multidens)			P. undatus
							B. compressa
		M2	Climacograptus bicornis			B. gerdae	E. quadridactylus
		M1					P. aculeata
			Nemagraptus gracilis	Nemagraptus gracilis		B. variabilis	C. sweeti
						P. anserinus	

Table 2.—Correlation chart illustrating the Upper Ordovician graptolite zones, conodont zones, and important event and chemostratigraphic marker horizons discussed in the text. Key references used in constructing this chart are Finney (1986), Goldman et al (2007), Bergstrom et al. (2010) and Webby (2004).

Graptolites are unevenly distributed through the Viola Springs Formation, and the boundary between the *Climacograptus bicornis* and *Diplacanthograptus caudatus* zones is poorly constrained (Goldman et al. 2007). The lowermost 0.4 meters of the Viola Springs Formation (Member 1) contain *Climacograptus bicornis*, *Dicranograptus semispinifer* (= *D. nicholsoni longibasalis* Ruedemann), *Normalograptus brevis*, *Corynoides calicularis*, and *Hustedograptus* sp., a fauna that that belongs to the Upper Sandbian *C. bicornis* Zone. Interestingly, collections at 0.45 and 0.55 m contain graptolites that indicate the strata are uppermost Sandbian in age. The 0.45 m collection contains the graptolites *Lasiograptus* n.sp. A. and *Rectograptus intermedius*, species that also occur in the 75NY-2 drill core from eastern New York State (Roloson 2010) and outcrops from the Gaspé Peninsula, respectively (Riva, pers. com.). These taxa occur in an interval that postdates the LAD of *C. bicornis*, but just before the FAD of *D. caudatus*. A collection at 0.55 m contains *Orthograptus quadrimucronatus*, a graptolite generally considered to be restricted to Katian age strata. In some Chinese sections this species has been reported in upper Sandbian strata but generally (and in North America) its range is Katian. Hence, the graptolite fauna in Member 1 of the Viola Springs Formation at Highway 99 indicates that these beds belong to the uppermost Sandbian Stage.

The following 20 meters of strata are devoid of graptolites but Finney's (1986) report of *Geniculograptus typicalis* at a horizon 25 m above the base of the Viola Springs and *Diplacanthograptus spiniferus* at 35 m, together with other species of the eastern Laurentian *D.*

spiniferus Zone at higher levels (Goldman et al. 2007), is consistent with the upper half of the section being no older than M6. Graptolites collected in the upper half of the Highway 99 section include:

43 m – *Diplacanthograptus caudatus*, *Corynoides americanus*, *Cryptograptus insectiformis*
44 m – *Diplacanthograptus spiniferus*
45 m – *C. americanus*, *Cryptograptus insectiformis*
51 m – *G. typicalis*, *Orthoretiolites hami*, *D. caudatus*, *D. spiniferus*
65 m – *Orthograptus quadrimucronatus*

Additionally, the collection at 43 m contains the Baltic chitinozoan *Angochitina capillata*, a species restricted to the Nabala through Pirgu regional stages in Estonia (Goldman et al. 2007). If its stratigraphic range in North America is consistent with its range in Baltoscandia, then the occurrence of *A. capillata* at this level implies a correlation with the uppermost *D. spiniferus* Zone. No graptolite species that would indicate this interval should be assigned to the younger *Geniculograptus pygmaeus* Zone have been found at the Highway 99 section. This age interpretation fits with the carbon isotope excursion at Highway 99, previously referred to as GICE actually correlating with the Kope Excursion of Bergström et al. (2010).

DAY 3
Stop 5: Sam Noble Oklahoma Museum of Natural History

The Sam Noble Museum is both a state natural history museum as well as an academic unit of the University of Oklahoma. Established in 1899, the Museum moved to a new building on the university campus in 1999, and this move consolidated the collections under one roof. It is now one of the largest university-based natural history museums in North America. Three paleontological collections house invertebrates, plants and microfossils, and vertebrates, respectively.

Coincident with the move to the new building, the Invertebrate Paleontology Collection expanded significantly with the acquisition of macrofossils from the Amoco Petroleum Company following its merger with BP. This material represents the results of decades of work by the Amoco paleontology and biostratigraphy research group. It includes numerous field samples from measured sections at localities throughout North America, including frontier regions such as Alaska and the Canadian Arctic. The Amoco collection is largely undescribed and represents a significant research resource.

With the incorporation of the Amoco donation and extensive material from the Oklahoma Geological Survey (T.W. Amsden's collections of Ordovician–Devonian brachiopods), the Invertebrate Paleontology Collection now comprises about one million specimens, including about 10,000 type and figured specimens. Particular strengths include Cambrian and Ordovician trilobites and graptolites, Silurian and Devonian brachiopods, and Carboniferous brachiopods, corals, and echinoderms. Much of the collection can be searched via the web at http://samnoblemuseum.ou.edu/collections-and-research/invertebrate-paleontology/integrated-invertebrate-paleontology.

The exhibits at the Museum include an ancient life gallery that spans the Archean to Pleistocene. Highlights include two Ediacaran dioramas, and a diorama based on the Upper

Ordovician (Sandbian) of Oklahoma, as well as a series of dinosaur exhibits that include *Apatosaurus*, *Saurophaganax*, *Deinonychus*, *Tenontosaurus*, and *Pentaceratops*.

Stop 6: Sylvan Shale, Keel and Cochrane limestones, Ordovician-Silurian contact

The outcrop at stop 6 is located along HWY 77 on the west size of the I-35 interchange, across the road from Arbuckle Fried Pies. The base of the section is located to the south, where it exposes the uppermost Ordovician (Hirnantian) rocks in the Arbuckle Mountains, and its contact (Fig. 14) with the lowermost Silurian (Llandovery). Progressively younger strata at this locality include the Sylvan Shale (Ordovician), Keel Formation (Ordovician), Cochrane Formation (Silurian), and Clarita Formation (Silurian). Additional exposed units to the north along HWY 77 are the later Silurian and Devonian strata of the Upper Hunton Group including the Henryhouse Formation, Haragan Formation, and Woodford Formation.

Our focus at stop 6 is the Chimneyhill subgroup of the Hunton (Keel, Cochrane, and Clarita), and the underlying Sylvan Shale. The Sylvan Shale lies conformably on the Welling Formation (stop 7) of the Viola Group, and forms a recessive interval between the weathering resistant carbonates above and below it. It formed as a widespread sheet of anoxic, fine siliciclastic silt and clay that extends westward into north Texas, eastward into the Ouchita Mountains region, and northward into the Mississippi Valley region (Playford and Wicander 2006). The upper portion of the Sylvan (exposed at stop 6) is especially fissile and is lacking in carbonate fines, with the exception of a few marly interbeds and sandy dolomitic stringers. Pyrite clusters are common, and provide further evidence of widespread reducing conditions prior to the deposition of the Chimneyhill subgroup. The Sylvan Shale is generally considered to be of upper Katian (Ashgill or Richmondian) age on the basis of biostratigraphy (Amsden 1975). Graptolites throughout the formation indicate an age no older than the *Dicellograptus complanatus* Zone, while chitinozoans also suggest an "Ashgill" age (Jenkins, 1970, 1971). Some authors (e.g., Ham 1969) have argued that the Sylvan/Chimneyhill contact is disconformable, but Playford and Wicander (2006) stated that there is little biostratigraphic evidence to support that assertion.

The oldest unit of the Chimneyhill subgroup is the Keel Formation, exposed at stop 6 directly above the Sylvan Shale. The Keel is a massive, fossiliferous oolitic packstone that contains both micrite matrix and spar cement, and may show silicified ooliths and flecks of glauconite in the matrix. Brachiopods of the Keel Limestone are Hirnantian in age (Ham 1973), and those of the overlying Cochrane are early Silurian (Llandovery). Much of the Llandovery is apparently missing at the contact, during which time there must have been regional erosion and truncation of the Keel (Amsden 1963; Ham 1973). The Cochrane Limestone is the lowest unit of

TEXT-FIGURE 14.—Ordovician-Silurian contact and formations exposed at stop 6 (GPS: 34°26'44.55"N, 97° 8'7.86"W). Brachiopods of the Keel Limestone are Hirnantian in age (Ham 1973), and those of the Cochrane are early Silurian (Llandoverian).

the Silurian at stop 6, and is a thick-bedded, glauconitic limestone whose brachiopod fossils (*Microcardinalia protoplesiana*) reveal a late Llandovery (Aeronian to early Telychian) age the upper part that allow for correlation with the Silurian Blackgum Formation in eastern Oklahoma (Amsden, 1966; Ham 1973) and probably with the Sexton Creek Formation of Arkansas, Missouri and Illinois. The overlying thin shale above the Cochrane (Fig. 14), termed Prices Fall Member, is possibly a remnant of a widespread shaly interval termed 76 Shale in Arkansas and Illinois; this interval is a feather edge of latest Llandovery to early Wenlock (*Pterospathodus amorphognathoides* Zone) Osgood Shale of Indiana-Kentucky and records a major Telychian transgression. The overlying Clarita grainstones are likewise a local representative of lower Wenlock (Sheinwoodian) transgressive limestones.

Stop 7: I-35N, Bromide Formation Reference Section

  Late Whiterockian through Mohawkian (Fig. 3) deposition in the Arbuckle Mountains and Criner Hills regions of Oklahoma is recorded by the mixed carbonate-siliciclastic Bromide

Formation, the youngest unit of the Simpson Group. Bromide deposition took place during a period of relative stability of the Oklahoma Basin (see Carlucci et al. 2014, fig. 1), where a shallow, tropical, carbonate-dominated sea bordered the SOA. To the north, the Oklahoma Basin was bordered by the Arbuckle platform (Longman 1982b), which was a desert region that likely supplied wind-blown sand deposited as sheets in the basins. As with the majority of Simpson Group formations, carbonate production in the Bromide was periodically interrupted by siliciclastic sediment supply from the north and east.

  The Bromide Formation is subdivided into three members and one submember. The lowest unit is the Pontotoc Member (Carlucci et al. 2014), a massive, thick-bedded or rippled unit of shoreface sandstone. The next unit (Mountain Lake Member) is a succession of quartz sandstone, interbedded sandstone and illitic-chloritic shale, and shale and limestone (mostly pelmatozoan packstone and grainstone). The basal shaly interval above the Pontotoc Member comprises the "Lower Echinoderm" Zone of Sprinkle (1982), which is widely noted for high diversity assemblages of echinoderms, including crinoids, (hybocrinids, camerates, *Cleiocrinus*), paracrinoids, rhombiferan cystoids; these echinoderms have been well documented (Sprinkle, 1982).

  The mixed carbonate-siliciclastic units are overlain by the Pooleville Member, a thick-bedded to massive unit of carbonate mud-, wacke-, and packstone. The basal Pooleville is marked by a thick-bedded echinodermal grainstone, overlain by a shale and packstone rich interval, the "upper Echinoderm Zone" of Sprinkle (1982). The upper Pooleville is set off as a lithologically distinct submember called the Corbin Ranch, which is a fenestral, commonly dolomitic limestone that forms peritidal cycles just below the contact with the Viola Springs Formation. Figure 15 summarizes the range of facies and inferred depositional environments in all units of the Bromide Formation.

Biostratigraphy and Age of the Bromide

  Stop 7 is the newly established standard reference section (Carlucci et al. 2014) for correlation and discussion of depositional sequences in the Bromide Formation. This outcrop is well preserved, nearly complete (except for the Pontotoc Member), and has previously been well-studied biostratigraphically (e.g., Bauer 1994). Bauer (1994) suggested that the Bromide is Sandbian age (Fig. 3, late Whiterockian to Mohawkian of classical North American nomenclature) by comparison of the conodont fauna with the graphic correlation standards of Sweet (1984) and Bergström (1983). In the lower Mountain Lake, *Cahabagnathus sweeti* is indicative of the late Whiterockian, and is replaced by the Mohawkian conodonts *Baltoniodus gerdae* and *Eoplacognathus elongatus* in the Mountain Lake. Bauer (1994) suggested that the conodont fauna of the intertidal Corbin Ranch submember includes forms that range from Blackriveran (Whiterockian) to Mohawkian, and could not constrain the age of the unit. He (1994, table 2) also noted that *C. sweeti* showed a strong proclivity for shallower water environments, while *B. gerdae* apparently favored deeper water environments. Such facies control on distribution has important implications for conodont-based correlation of the sections. Although *B. gerdae* occurs through the entire section down-ramp at RC in the Criner Hills, it is restricted to just four meters of the deepest portion of the upper Mountain Lake up-ramp at I-35N

(Bauer 1994, table 1). The narrower stratigraphic distribution up-ramp is exactly what would be predicted from a hypothesis of facies control, so that differences in the first appearance of *B. gerdae* cannot be used as evidence that the deeper facies are stratigraphically younger down-ramp.

Independent estimates of the age of the upper Bromide strata in the Criner Hills (stop 12) relative to I-35N are inconclusive. Decker (1935, 1941) and Finney (1986) showed that graptolites from the upper Bromide (*Amplexograptus maxwelli*, *Dicellograptus flexuosus*) are diagnostic of the British *D. multidens* Zone. The *D. multidens* zone spans the Deicke, Millbrig, and Kinnekulle bentonites, and consequently, its duration is too long to provide a biostratigraphic test of the absence of Pooleville Member down-ramp (see stops 11 and 12 for more explantion). Interestingly, both Bauer (1994) and Rosenau et al. (2012) found the upper Sandbian condont, *Phragmodus undatus*, in the Pooleville at HWY 99 (far up-ramp, stop 4), but it has not been recorded from the down-ramp "Poolville" of the Criner Hills (stop 12). Although this could be yet another example of facies control, it might instead provide evidence that the "Pooleville" within the SOA has been miscorrelated with the true Pooleville, which is missing down-ramp.

The composite section comprises the north and south sides of I-35, and the median, which together expose a nearly complete succession of Bromide units. The completeness and preservation of the I-35N section allows it to serve as a model to characterize cyclicity at meter and decameter scales (Fig. 15) and correlate with other sections up- and down-ramp (Fig. 17).

Sequence Stratigraphy and Cyclicity

Meter scale cycles in the Bromide Formation (Figs. 16, 18) consist of alternating small-scale or "micro"-TSTs and HSTs (meter-scale analogues of systems tracts) that form packages of condensed and more rapidly accumulated deposits (cf. Brett and Algeo 2001; Brett et al. 2008). In the Mountain Lake Member, micro-TSTs are amalgamated, nodular to tabular beds of poorly sorted bryozoan-echinoderm grainstone. Bases of micro-TSTs are marked by sharp facies offsets and scouring (merged transgressive/high-frequency sequence boundary surfaces), whereas flooding surfaces at their tops commonly include authigenic mineral crusts (iron oxide and pyrite) or a heavily bioturbated firmground (e.g., McLaughlin et al. 2008). HSTs are mostly shale, interbedded with thin nodular bryozoan and echinoderm packstone and grainstone.

TEXT-FIGURE 15.—Facies descriptions, fossil content, and depositional interpretation of Bromide Formation lithologies (modified from Carlucci et al. 2014). ⟶

Facies	Description	Fossil content	Interpretation
Fenestral and Microbial Laminated Mudstone	White to dark grey, dense mudstone with fenestral cavities (Fig. 5d), microbial laminations, desiccation cracks, vertical tubes and oxidation marks. Cycles of well-bedded fenestral mudstone and thinner bedded nubbly wackestone that lack fenestrae are common. Wackestone beds have mm to cm scale shaly interbeds	Ostracods (e.g., *Leperditella*, *Ningulella*, *Ctenobolbina*), corals (e.g., *Tetradium*), conodonts, brachiopods (e.g., *Ancistrorhyncha*), gastropods, and rarely trilobites (e.g., *Bathyurus*)	Low energy intertidal to supratidal tidal flat
Lime Mudstone	Massive, has some small voids filled with calcite cement and contains well-preserved ostracod fossils	Ostracods	Restricted inner-ramp deposit likely from a shallow lagoon or tidal flat environment
Massive to Crossbedded Sandstone Facies	Dental, fine to medium grained, well-sorted, well-rounded, frosted quartz arenite grains, with small percentages of clay minerals, feldspar and other rock fragments. Wave ripples, hummocky cross-beds, minor siltsone	Bryozoan and echinoderm	Upper shoreface to lower shoreface
Massive to Nodular Lime Mudstone	Medium to dark, grey, blue, or tan lime mudstone, massive or nodular bedded, stylolitic, peloidal (Fig. 3c), and heavily bioturbated. Recrystallization to microspar common in burrows and mottled features. Mudstone often interbedded with fossiliferous and thinner bedded wackestone	Ostracods, gastropods, tabulate corals (*Tetradium*, Fig. 5a), receptaculitids, and brachiopods	Shallow subtidal lagoon or protected inner-ramp
Interbedded Sandstone and Shale Facies	Dental, fine grained, well-sorted, well-rounded, frosted quartz arenite grains, with shale interbeds. Abundant silt and bioclasts	Bryozoans and echinoderms	Transitional between shoreface and offshore deposits (inner-ramp), but likely still receiving sand from the lower shoreface
Rippled Calcisiltite and Grainstone	Couples of white, thin-bedded (~2cm) wave rippled calcisiltite and medium bedded packstone or red-hued very coarse grainstone (Fig. 4a).	Crinoids, cystoids (e.g., *Diabolocrinus*, *Okahomacystis*, *Parocystella*), ramose and massive bryozoans (e.g., *Batostoma*, *Diamillus*), brachiopods (e.g., *Sowerbyella*, *Bellimurina*, *Valcourea*), and receptaculitids	High energy, detached shoreface deposited on a wave-dominated inner-ramp, during forced regression
Interbedded Grainstone, Rudstone and Shale	Thin to medium-bedded (cm scale), poorly sorted, lenticular grainstone (Fig. 4e) and mudstone interbedded with green to tan fissile shale. Articulated bryozoan horizons, some minor packstone		At or below fair weather wave base, basinward of the lower shoreface but likely represent a broad bathymetric range, from upper middle-ramp to upper outer-ramp
Thin Phosphatic Grainstone and Packstone	Below-wave base laminated mudstone and shale with a thin packstone unit at the base overlain by fine-grained bioclastic grainstone (Fig. 3f). Multiple irregular surfaces (Fig. 5e)	Packstone: coral, gastropod and echinoderm debris; grainstone: diplograptid graptolites and trilobites (e.g., *Cryptolithus*)	Thin transgressive lag that records the landward shift of the shoreline followed by inner-ramp shoal environments scoured by wave action
Bioclastic Grainstone and Packstone	Medium to dark, blue to grey; medium- bedded to thick-bedded or massive beds of rubbly, fossiliferous, argillaceous limestone. Packstone often interbedded with grainstone (Fig. 4b). Wavy or rubbly grainstone interbedded with planar beds. Authigenic mineral crusts of pyrite and iron oxide; condensation features	Trilobites (*Anataphrus*, *Failleana*), ramose bryozoans, and echinoderm debris (Fig. 3d)	High energy, inner-ramp shoal and mid-ramp packstone, subject to constant wave agitation, or frequent storm reworking (above storm wave base)
Wackestone with Rudstone Pavements	Light blue-grey, medium to thick-bedded, slightly nodular, tan-weathering wackestone. Packstone locally present. Beds are often capped by fossiliferous rudstone pavements (Fig. 5c)	Rudstone: brachiopods (e.g., *Sowerbyella*, *Strophomena*, *Plectoglossa*), trilobites (e.g., *Calyptaulax*, *Bumastoides*, *Thaleops*), ramose bryozoans, and cystoids	Subtidal, moderate energy; mid-ramp environment between storm and fair weather wave base, not subject to regular wave agitation
Packstone and Wackestone	Fossiliferous, amalgamated wackestone or packstone beds that are medium grey, nodular, with shales either absent or highly indurated. Condensed relative to F12.	Trilobites, strophomenid brachiopods, ramose bryozoans, and gastropods	Between fair-weather and storm weather wave base in lower middle-ramp to outer-ramp
Wackestone, Rhythmic Mudstone, Wackestone and Shale	Couples of thin (3-10 cm), tan to grey, planar to nodular bedded mudstone and wackestone (Fig. 4c, d), with argillaceous sublaminated shale of varying thickness. Tempesites and obrution horizons common. Expands into the basin during sequence 2, correlates across study area.	Strophomenid brachiopods, trilobites (e.g., *Isotelus*, *Thaleops*, *Calyptaulax*, *Remopleurides*) straight cephalopods, receptaculitids, echinoderms, gastropods (e.g., *Cyclonema*, *Eotomaria*) and ostracods (e.g., *Anisocyamus*, *Bromidella*).	Between fair-weather and storm weather wave base in lower middle-ramp to outer-ramp
Thin bedded Mudstone and Shale	Thin-bedded (~5cm), fine-grained lime mudstone, with very thin partings of shale and marls	Trilobites (e.g., *Lonchodomas*), straight cephalopods, graptolites and inarticulate brachiopods	Outer-ramp to basin, low energy, dysoxic, and typically below storm level wave base
Fissile Illitic-Chloritic Shale	Dark greenish-grey, fissile, clay-rich, sublaminated green shale that weathers to a tan color. Clay component rich in illite-smectite and chlorite.	Echinoderms	Deltaic-fluvial fines transported onto the ramp and deposited below the action of storm waves. Upper occurrence represents a lowstand package of siliciclastics that directly overlies a major sequence boundary
Laminated Mudstone and Shale	White to light grey lime mudstone interbedded with a fissile to nearly shale. Mudstone fossiliferous, thinly laminated (Fig. 5f) and evenly bedded. Shale interbeds thicken upwards from 1 cm to 5 cm above the base of the Viola contact.	Diplograptid graptolites and trilobites (e.g., *Flexicalymene*, *Cryptolithus*)	Outer-ramp to basin environment below storm level wave base. Marks a major change in the trilobite fauna that characterizes sequence M5 of Holland and Patzkowsky (1996) elsewhere in eastern Laurentia, so that the ravinement surface beneath F8 is likely the M4/M5 sequence boundary

Meter-scale cycles

a = micro-TST
b = micro-HST

TEXT-FIGURE 16.—Example of 5th order meter scale cycles in the Mountain Lake Member of the Bromide Formation. "a" and "b" refer to meter-scale analogues of systems tracts (modified from Carlucci et al. 2014).

In the Pooleville Member, micro-TSTs are indurated wackestone and packstone and are shale-poor, show evidence of condensation upwards, poor sorting, pyritization of bioclasts, and flooding surfaces that are heavily stained with iron-oxide and pyritic or phosphatic mineral crusts. These mineralized surfaces also represent the highest degree of sediment starvation in the micro-sequence (maximum sediment starvation surfaces of Baum and Vail 1988; Brett et al. 2004) and are overlain by thinner, late TST shell hashes and/or micro-HSTs of aggradational to progradational, interbedded shale and limestone rhythms. Micro-HSTs are thinly and planar bedded near their bases, and gradually become more nodular as they decrease in siliciclastic content. Low-rank transgressive surfaces/high-frequency sequence boundaries sharply overlie the micro-HSTs, and are commonly irregular erosive disconformities.

At a larger scale of accommodation space dynamics, Carlucci et al. (2014) documented three distinct, 3rd order depositional sequences that record the transition from siliciclastic to carbonate dominance during Bromide deposition. Portions of sequence 1 and the entirety of sequences 2 and 3 are exposed at stop 7. Sequence 1 is likely the last major depositional sequence of the Whiterockian (Dariwillian), and consists of massive, cross-bedded, and/or rippled sandstones (Pontotoc Member) that grade abruptly upward into sandy limestones, in what Carlucci et al. (2014) considered to be a transition from lowstand (LST) to early transgressive (TST) conditions.
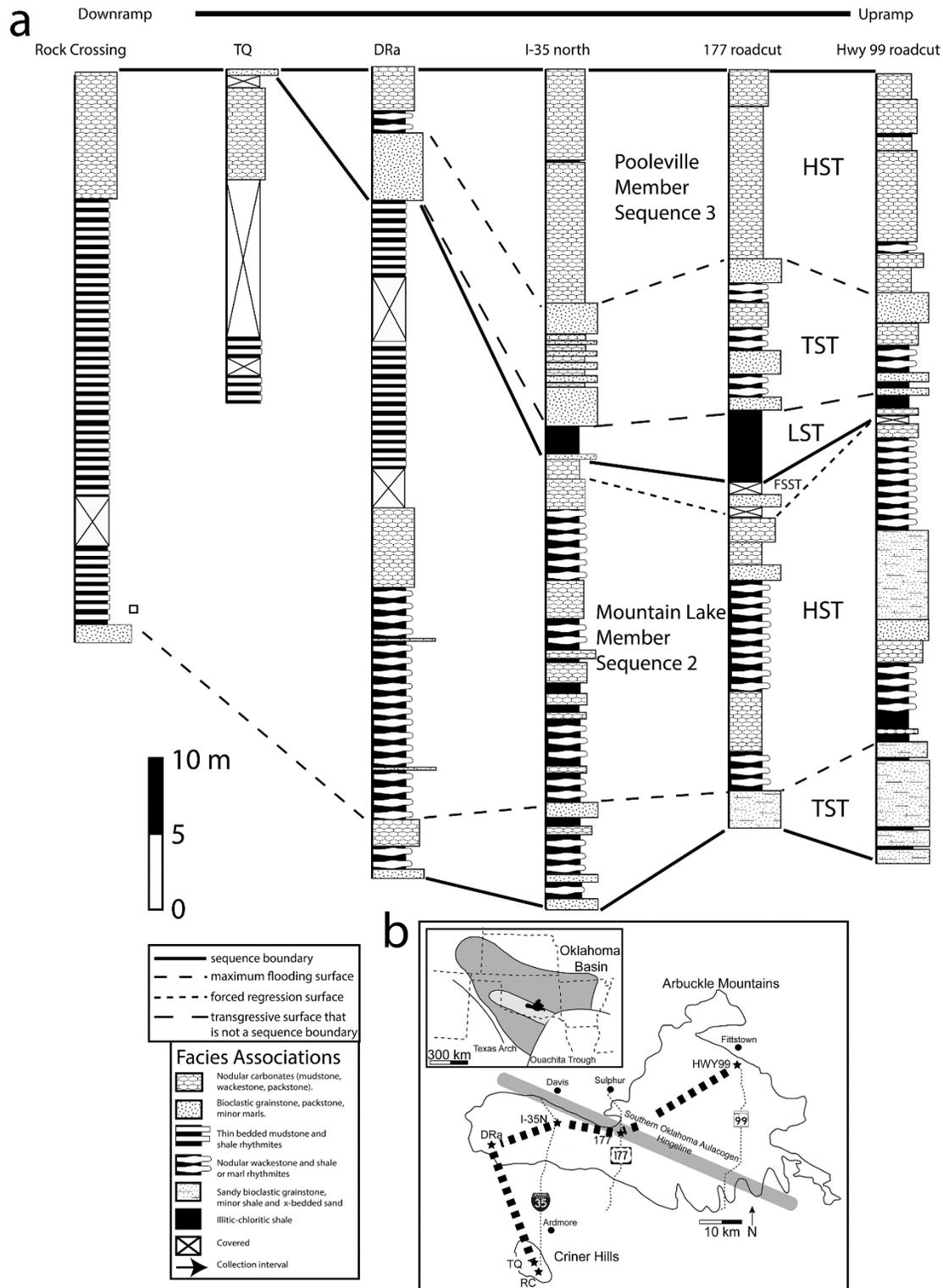
TEXT-FIGURE 17.—Simplified summary of facies associations and depositional sequence architecture of the Bromide Formation (modified from Carlucci et al. 2014: Carlucci and Westrop 2015). a, correlation of stratigraphic columns based on sequence stratigraphic surfaces. b, Arbuckle Mountains map showing line of cross section and localities.

TEXT-FIGURE 18.—Outcrop example (stop 7) of meter scale cycles in the Mountain Lake Member of the Bromide Formation. See Figure 16 for interpretation. GPS: 34°26'9.21"N; 97° 7'46.88"W.

Coarse, sandy bioclastic packstones and grainstones with condensation features represent TST deposition, and these are overlain at a maximum flooding surface by HST units of interbedded green fossiliferous shales ("Lower Echinoderm Zone"), rudstones, and grainstones. The sequence boundary is a sharp contact between the interbedded green shale and marly packstone, and a rippled and crossbedded, sandy crinoidal grainstone.

   Complete description of the depositional architecture of sequences 2 and 3 is beyond the scope of this field guide; however, Figure 17 shows the facies associations contained within depositional sequences 2 and 3. These facies associations and the corresponding bounding surfaces are well exposed at I-35N, and participants can walk south along the highway and study the sequences. In brief, sequence 2 is composed of a basal sandy crinoidal grainstone and trilobite packstone succession interpreted as TST deposits. These are overlain by thick, marly limestone-shale rhythmites (HST) whose component meter scale cycles shallow upwards. Rapid facies change to a rippled calcisiltite and grainstone unit likely represents an interval of forced regression, just prior to a major sequence boundary below the uppermost green shale of the I-35 outcrop. Sequence 3 deposition starts with an input of siliciclastic fines ("the big green shale" or

Upper Echinoderm Zone) that likely formed as the coastline was exposed during sea level lowstand. These are overlain by a fossiliferous unit of rubbly, phosphatic packstones and grainstones with hematite-pyrite mineral crusts. This facies is interpreted as a carbonate shoal deposit that formed during a major marine transgression, and was mapped across the Arbuckles by Carlucci et al. 2014 (Fig. 17). Above the maximum flooding surface of the sequence 3 TST, predominantly carbonate mud- and wackestone deposition show a gradual shallowing upward trend to the fenestral beds of the Corbin Ranch Submember. The sequence boundary with the Viola Springs Formation (Sandbian-Katian boundary) directly overlies the fenestral beds at this locality.

Note that the thin sequence at the base of the Viola Springs Formation ("member 1" of the stop 4 discussion) is not present at the Bromide/Viola contact at stop 7, likely due to erosional truncation at the Bromide/Viola Springs unconformity.

Stop 8: I-35S, Viola Springs and Welling Formation

The I-35 South section comprises a pair of road cuts on the south flank of the Arbuckle Mountains that expose the uppermost Bromide, much of the Viola Springs, and the Welling formations. Amati (2014) recently published locality information, including a lithologic log of this section. The Bromide is represented by only a few meters of subtidal facies that includes massive wackestones with brachiopod and gastropod shell beds that likely record storm-influenced deposition. Cross sections through receptaculitids are commonly encountered in the uppermost beds. The peritidal facies of the Corbin Ranch submember, reduced to only a thin remnant at the I35N section relative to the type area near Fittstown (stop 4), is entirely missing at I-35S.

The Viola Springs Formation is exposed in two segments separated by a covered interval of about 75 m, although it is more complete on the north-bound lane. The base of the formation is a major unconformity marked by an irregular mineralized, rusty weathering surface that cuts out much of HST of Sequence 3 (Corbin Ranch, upper Pooleville Member). The discussion of the stratigraphy and facies follows Amati's (2014) description of the section. The basal two meters of the formation is a white-weathering ostracode-rich wackestone-packstone with interbedded black graptolite-bearing calcareous shale, and capped by another planar, mineralized surface. The succeeding 25 m is mostly thin-bedded, plane-laminated, cherty, lime mudstone with thin, dark gray, marly interlayers; bioturbation is variable, but generally low. Bioturbation increases higher in the section, and the lithology switches to burrow-homogenized wackestone to packstone with marly layers at about 55 m; debris of cryptolithine and isoteline trilobites, as well as graptolites can be seen commonly in the marly layers, although specimens are not easily collected.

Above the covered interval, the upper part of the section includes thicker-beddded limestone that forms meter-scale cycles with intervals of dark, strongly bioturbated lime mudstone alternating with crinoidal grainstone. The section is capped by about 10 m of massive crinoidal grainstone of the Welling Formation. According to Amati (2014), the contact between the Viola Springs and Welling is gradational over about a meter of section.

Biostratigraphy

   Graptolites. Finney (1986, fig. 7) published a range chart (his section U) for graptolites. Most of his collections were made from the lower segment of the section. These show that the lower 20 m is characterized by an assemblage that includes *Diplacanthograptus spiniferus*, *Orthoretiolites hami* and *Geniculograptus typicalis*, taxa that indicate these beds belong to the *D. spiniferus* Zone. However, recent sampling by Goldman (unpublished) of the basal meter of the Viola Springs at this locality yields an assemblage with, among others, *Diplacanthograptus caudatus*, *Neurograptus margaritatus*, *Normalograptus brevis*, and *Dicranograptus hians*, which he interprets as earliest Katian (*D. caudatus* Zone). The presence of *D. caudatus* and *Dicr*anograptus *hians* indicates a correlation with the Australasian Stage Ea1, which is pre- *D. spiniferus* Zone. There is one juvenile specimen in the 3.0 – 6.0 cm collection that resembles *D. spiniferus*, but the identification is uncertain. Hence the lowermost Viola Springs Formation at the I-35 section is similar in age to its base at the Mountain Lake section, which also yields *D. caudatus* Zone graptolites (Finney, 1986).

   The base of the *Geniculograptus pygmaeus* Zone is marked by the appearance of the eponymous species at 32 m above the base of the Viola Springs (Finney, 1986); this boundary correlates into sequence C1 of the Cincinnati region (Brett et al., 2004). Finney (1986, fig. 7) does not record any other species entering the succession above *G. pygmaeus*, although a few species extend from the lower to the upper segment of the section (e.g., *Orthograptus quadrimucronatus*).

   Conodonts. Conodont data are limited for I35 South, but Bergström et al. (2010) recently showed the distribution of zones, albeit without any species range data. They placed the base of the Viola Springs within the *Belodina confluens* Zone, confirming the conclusions of Carlucci et al. (2014) that there is significant unconformity with the underlying Bromide Formation. The upper part of the formation is assigned to the *Amorphognathus superbus* Zone; the Welling Formation apparently lies in the overlying *A. ordovicicus* Zone.

   On the basis of the conodont biostratigraphy, Bergström et al. (2010) concluded that a positive isotope excursion at the base of the Viola Springs at I-35S represented the "Kope excursion" of the Cincinnati region. They interpreted the excursion at the HW 99 section as the GICE, with the implication that this section is entirely older than the I-35S section (Berström et al., 2010, fig. 4). However, the trilobite biostratigraphy of HW 99 indicates that the interval containing the so-called "GICE" is younger than previously thought, and the positive excursion may well be the same excursion identified as the "Kope" at I-35S (Westrop et al., 2012). The graptolite data do not conflict with this hypothesis, which implies an overlap of about 25 m between the sections.

DAY 4
Stop 9: Oil Creek Formation (if time allows)

   This locality is an exposure through the 2nd oldest unit of the Simpson Group, the Oil Creek Formation. The Oil Creek is well known in Oklahoma for its economic impact and industrial importance. The basal unit of the Oil Creek is a thick (~ 350 ft, Ham 1973) sandstone that is comprised of well-sorted and rounded quartz sand. This sand is over 99% pure silica, and companies such as the Pennsylvania Glass Sand Corporation (now known as U.S. Silica Corp)

have been selling it for use in glass-making and as silica flour for over 90 years. Quartz sand in the lower Oil Creek is unique because there are few pressure solution contacts, quartz overgrowths, and only loose illite cement at grain boundaries (Ham 1973). For these reasons, the sand is easily disarticulated in solution and processed into glass. The cleanly washed and high porosity sands of the Oil Creek are also a prolific oil reservoir in southern Oklahoma, and have been extensively mapped into the subsurface.

The exposure of the Oil Creek at stop 9 is from the upper unit, which is primarily composed of sandy packstone, grainstone, and shale. The transition from the lower unit is gradational, with bioclasts gradually becoming a more common framework component. The sandy limestone facies as exposed here is heavily bioturbated and extremely fossiliferous, and contains a number of hardgrounds encrusted by bryozoan and echinoderm holdfasts, which are indicative of slowing rates of deposition relative to the lower sandstone unit. Limestones are exceptionally fossiliferous and contain a diverse fauna of brachiopods, bryozoans, gastropods, nautiloids, and trilobites; cystoid plates are also common on some bedding planes. The lowest beds of the limestone unit contain stromatolitic boundstone and sand filled desiccation cracks (Brown 2003), and may record undocumented bounding surfaces that better document the nature of the transition. Like the Bromide Formation (see stop 7) and other units in the Simpson Group, deposition in the Oil Creek evolves from primarily siliciclastic to mostly carbonate. Ham (1973) stated that ascertaining the depositional environment of the Oil Creek was problematic because of the lack of diagnostic sedimentary structures. One possibility is that the lower unit represents shoreface deposits with input from a regional desert on the Arbuckle Platform (Longman 1982), with limestone clasts becoming incorporated during a large-scale transgression. Carlucci et al. (2014) noted that this type of model might be problematic for some units of the Simpson Group, because many of the sands thicken toward the SOA, as would be expected during lowstand normal regression. The Oil Creek sands are thick and extensive mostly in eastern Oklahoma, though they do form a wedge toward the SOA (Schramm 1964, fig. 8), which might be consist with lowstand progradation. In this scenario, it seems likely that wedge development during lowstand conditions was followed by a transgression at some point that allowed for the preservation of open marine fossils.

Stop 10: Structural Features in the Fort Sill Limestone

The Fort Sill Limestone (Fig. 19) is the lowest unit in the Arbuckle Group (Cambrian; Sunwaptan), primarily distinguished from the underlying Honey Creek Limestone based on the

TEXT-FIGURE 19.—Folding in the Fort Sill Limestone, stop 10 (GPS: 34°24'29.76"N, 97° 8'20.85"W).

prevalence of lime mud deposition in the Arbuckle Group (Ragland and Donovan 1991), and the loss of glauconite and siliciclastic sand. Therefore, the early Arbuckle Group represents a shift in depositional style, where the carbonate platform was able to retain most of the mud that its carbonate factory produced. Similar to other carbonate deposits of the Arbuckle Group, the Fort Sill was deposited in a shallow, low gradient epeiric sea. During the Cambrian and into the Early Ordovician, margins were passive with high rates of post-rift subsidence, and there was little relief in the lowland areas of Laurentia (Ragland and Donovan 1991). This unique setting allowed for accumulation of the incredibly thick deposits of tropical carbonates that characterize the Arbuckle Group.

   The Fort Sill Limestone can be subdivided into three informal lithologic groups: a lower unit of thin bedded stromatolitic mudstones, middle unit of dolomitic siltstone-lime mudstone rhythmites, and an upper unit of massive algal boundstones (Ragland and Donovan 1991). The upper two lithologies are expressed at stop 10, but this locality is much better known for its structural features.

   Along the north and south sides of I-35, the Fort Sill Limestone at stop 10 contains a series of fold sets that are offset by thrust faults. The fold sets take a variety of shapes, most commonly as box or polyclinal (sub-parallel hinge lines but non-parallel axial surfaces) folds (Tapp 1991).

The folds at stop 10 all show a flexural-slip style of folding, where volume accommodation is preserved by layer-parallel slip between layers, rather than layer parallel flow ("flexural flow"). The folds at stop 10 show vergence to the north, and are generally considered to be evidence of compressional forces causing the Arbuckle uplift (Brown 1984: Tapp 1991) rather than strike-slip deformation (Wickham and Denison 1978). The structural features at the outcrop have been interpreted as part of a flower structure associated with the Chapman Ranch Fault (exposed near Turner Falls), part of the larger compressional forces of the Arbuckle Uplift (Brown et al. 1985), or as expression of volume accommodation in a larger-scale flexural-slip fold (Tapp 1991).

Stop 11: Mountain Lake and Daube Ranch (DRa), Tulip Creek, Bromide, and Viola Springs Formation

Ulrich (1911) first used the term "Bromide" for a unit that lay unconformably below the "Viola Limestone", but he did not propose any type locality or section. Edson (1927) proposed that the type locality of the Bromide be placed at the McLish Ranch, in the town of Bromide, Coal County, Oklahoma. The type sections of the Mountain Lake and Pooleville members of the Bromide as proposed by Cooper (1956) were placed at his Johnston Ranch locality, which is now owned by Sam Daube (referred to as DRa by Carlucci et al. 2014). Cooper defined the Mountain Lake to include a basal fine-grained quartz arenite (now called the Pontotoc Member), an overlying interbedded illitic-chloritic shale and sandstone, and an uppermost limestone and shale sequence at the top (Fay et al. 1982b). Cooper confined the Pooleville to the various limestones (occasionally interbedded with calcareous shales and marls) above the Mountain Lake, in particular near the SOA axis. Stop 11 at the DRa location is the type section of the Mountain Lake and Pooleville Members.

The section at stop 11 begins in the Tulip Creek Formation (Fig. 3) of the Simpson Group, exposed down-section from the Upper Humble Lake (a reservoir), with progressively younger strata towards the dam. Thick packages of green shale interbedded with massive limestones near the base of the section record the upper portion of the Tulip Creek, below its contact with the Pontotoc Member of the Bromide. Lower parts of the section may be overgrown during the summer, so visibility of the Pontotoc and lower Mountain Lake Members might be limited.

In the middle Mountain Lake at DRa, there is an obvious expansion of the thickness of sequence 2 (Fig.17), in both the illitic-chloritic green shale, and shale-limestone rhythmite associations. A particularly thick, trench-forming shale interval is prominent at DRa (not shown on Fig. 17), and is interpreted as the lower green shale (lower Echinoderm Zone of Sprinkle 1982) of the Bromide Formation, which correlates up-ramp into the lower Mountain Lake (Carlucci et al. 2014), rather than the Pooleville as done previously. This correlation is not intuitive at first, because there are lower shales at DRa that are poorly exposed (Fay et al. 1982b), but they are likely part of the lower sequence 1, which is dominated by grainstone and shales at all the Bromide sections.

Longman (1982) stated that the putative basinal deposits of the ''lower Pooleville'' within the SOA (e.g., at sections DRa, RC, stops 11 and 12) and those of the upper Mountain Lake along the hingeline (e.g., I-35 N, stop 7) shared the same characteristic bedding (compare Figs. 18 and

20). Evidence discussed by Carlucci et al. 2014 suggests that they are similar because the supposed "lower Pooleville" strata of DRa and RC are, in fact, correlative with the middle to upper Mountain Lake elsewhere. This hypothesis demands that the down-ramp expansion of the Bromide thickness (sequence 2, Fig. 17) applies only to the siliciclastic-rich Mountain Lake Member, whereas the predominantly carbonate Pooleville Member (sequence 3) is largely missing at these sections owing to erosional truncation. Evidence for down-ramp erosion of the Pooleville Member is shown on this field trip at stops 4, 7, 8, 10, and 11. There is an obvious truncation of the facies in our transect (partially shown here in Fig. 17), at the Bromide/Viola unconformity and down into sequence 3. "Member 1" of the Viola is removed from the basin between stop 4 and 7, the Corbin Ranch is removed between 7 and 8, and then the Pooleville is progressively removed into the aulacogen in the Criner Hills, from stops 8 to 10, and 11. The true Pooleville Member at DRa is only preserved on the other side of the Upper Humble Lake, and this correlation is further evidenced by the widespread, mappable grainstone that is always present at the base of sequence 3 (exposed at DRa along the ground in the wooded area by the dam). Indeed, this condensed grainstone unit is so consistently cut out from the basin that a thin wedge of it is preserved at the TQ locality (see Carlucci et al. 2014), just below the Bromide-Viola unconformity. Additional paleontological evidence includes closely comparable strophomenid brachiopod beds, horizons with straight cephalopods, and identical species of trilobites in the rhythmite packages in the I-35 N, DRa and RC sections (Carlucci and Westrop 2014).

Karim and Westrop (2002) described the taphonomy of the well-known '*Homotelus*' beds (*Vogdesia*) from the TQ locality in the Criner Hills. These same beds, previously referred to as belonging to the Pooleville Member in the Criner Hills, are exposed at stop 11 (Fig. 20) in a trench-forming limestone-shale rhythmite that overlies the green shale unit, and which clearly lies low within the Mountain Lake. These assemblages of articulated exoskeletons likely recorded behavioral aggregations that were preserved beneath storm-influenced 'mud dumps' (Karim and Westrop 2002; Brett et al. 2012). These obrution beds occur most commonly in the early HST of sequence 2 across the Bromide Formation. When siliciclastics are no longer sequestered near the coastline during early HST, rapid deposition of mud layers in mixed carbonate– siliciclastic systems leads to exceptional preservation. In the rhythmite-dominated HST deposits, sedimentary structures in the limestone beds include burrow-mottled fabrics, *Chondrites*, disrupted laminae, vertical burrows and strophomenid brachiopods and trilobites (including articulated *Vogdesia*, *Thaleops*, *Calyptaulax*, *Remopleurides*) that formed as obrution

TEXT-FIGURE 20.--Outcrop photograph from the DRa locality, showing limestone-shale rhythmites in the unit that produces the 'Homotelus' (*Vogdesia*) beds, interpreted as a behavioral aggregation smothered during a mud-dump event. GPS: 34°21'56.66"N, 97°17'7.24"W.

horizons below storm wave base (Karim and Westrop 2002). Trilobites in the sequence 2 obrution horizons lack epibionts as noted by Karim and Westrop (2002), whereas disarticulated specimens in shell pavements elsewhere are usually encrusted by various bryozoans and Cornulites tubes. This suggests the obrution-derived HST deposits were not exposed at the surface for long periods of time, and were probably smothered in place by mud blanketing events (Brett et al. 2012).

Stop 12: Rock Crossing, Criner Hills Region, Bromide Formation

In the Criner Hills of southern Oklahoma, cuts along Hickory Creek (stop 12) are well-known for producing important trilobite fossils, including the holotypes of *Lonchodomas mcgeheei* (Decker 1931; Sutherland and Amsden 1953) and *Probolichas kristiae* (Carlucci et al. 2012). Rock Crossing has a long history of study (e.g., Decker 1931; Decker and Merrit 1931; Sutherland and Amsden 1959; Longman 1982a, b; Fay et al. 1982; Carlucci et al. 2014), and

plays a pivotal role in any interpretation of Simpson Group strata because it lies southward of the inferred SOA basin axis.

East of D3265 Road, there is an exposure of rock that forms the creek bed around a meander of the Hickory Creek. The strata are assigned to the lower Bromide Formation (Mountain Lake) and correspond to sequence 1 of Carlucci et al. (2014). There is a hogback along the creek bank, developed in the Pontotoc Sandstone downstream of a waterfall that exposes the overlying sequence of packstone/grainstone, green shales, and bryozoan-rich beds (sequence 1 HST, sequence 2 TST of Carlucci et al. 2014). This succession is similar to that of the reference section at I-35N. Above these units at the top of the waterfall is the same limestone-shale rhythmite package ('*Homotelus* beds') that is exposed at stop 11. Trilobites such as *Vogdesia* are somewhat more difficult to find at this locality, but the unit is rich in large, articulated straight cephalopods, brachiopods, and other trilobites. Note how much thinner the interval between the basal sandstones and *Homotelus* beds is at this locality compared to stop 11.

Up-section towards the bridge, additional rhythmite packages are exposed, including the thin bedded, *Lonchodomas*-rich (Fig. 21) facies that is finely internally laminated and clearly formed below storm wave base (see Fig. 15). Facies form a shallowing succession towards the bridge, becoming more nodular and fossiliferous, before abruptly ending without any evidence of "normal" Pooleville deposition below the Viola contact. Carlucci et al. (2014) took this is as additional evidence for southward truncation of the M4/M5 sequence boundary, which is somewhat counterintuitive as the magnitude of the truncation appears to increase into the SOA basin. However, the pattern is extremely consistent from stops 4-7-8-10-11. First, "member 1" of the Viola is removed, then the Corbin Ranch, then part of the Pooleville, and then all of the Pooleville in the Criner Hills. Down-ramp facies change does not account for this pattern, because the same facies and stacking patterns typical of the Mountain Lake are consistently developed across the sections, with those at the top missing progressively southward, at the unconformity. The Viola Springs was deposited at the onset of a major tectonic phase of the Taconic Orogeny (Pope and Read 1997), and it is possible that far-field tectonics produced an inversion of topography of the SOA after the deposition of the Corbin Ranch submember, when shallowing was apparently still to the north, and prior to the start of Viola Springs deposition. This scenario is similar to the one proposed by Finney (1986, fig. 19) to explain an apparent earlier onset of Viola Springs deposition at the HWY 99 section, and we suggest that the uplifted southern region may have been beveled during a prolonged period of sea-level lowstand associated with the M4–M5 sequence boundary, which is a major break elsewhere in eastern Laurentia (e.g., Holland and Patzkowsky 1996). An alternative model for the removal of an older carbonate unit in a down-ramp direction is rapid subsidence of the Criner Hills region in association with pre-Viola Springs tectonics. Under this scenario, abrupt down warping of the strata into a corrosive environment below the pycnocline could possibly result in dissolution and erosion from internal waves and deep anoxic currents (see Pomar et al. 2012; Baird and Brett 1986).
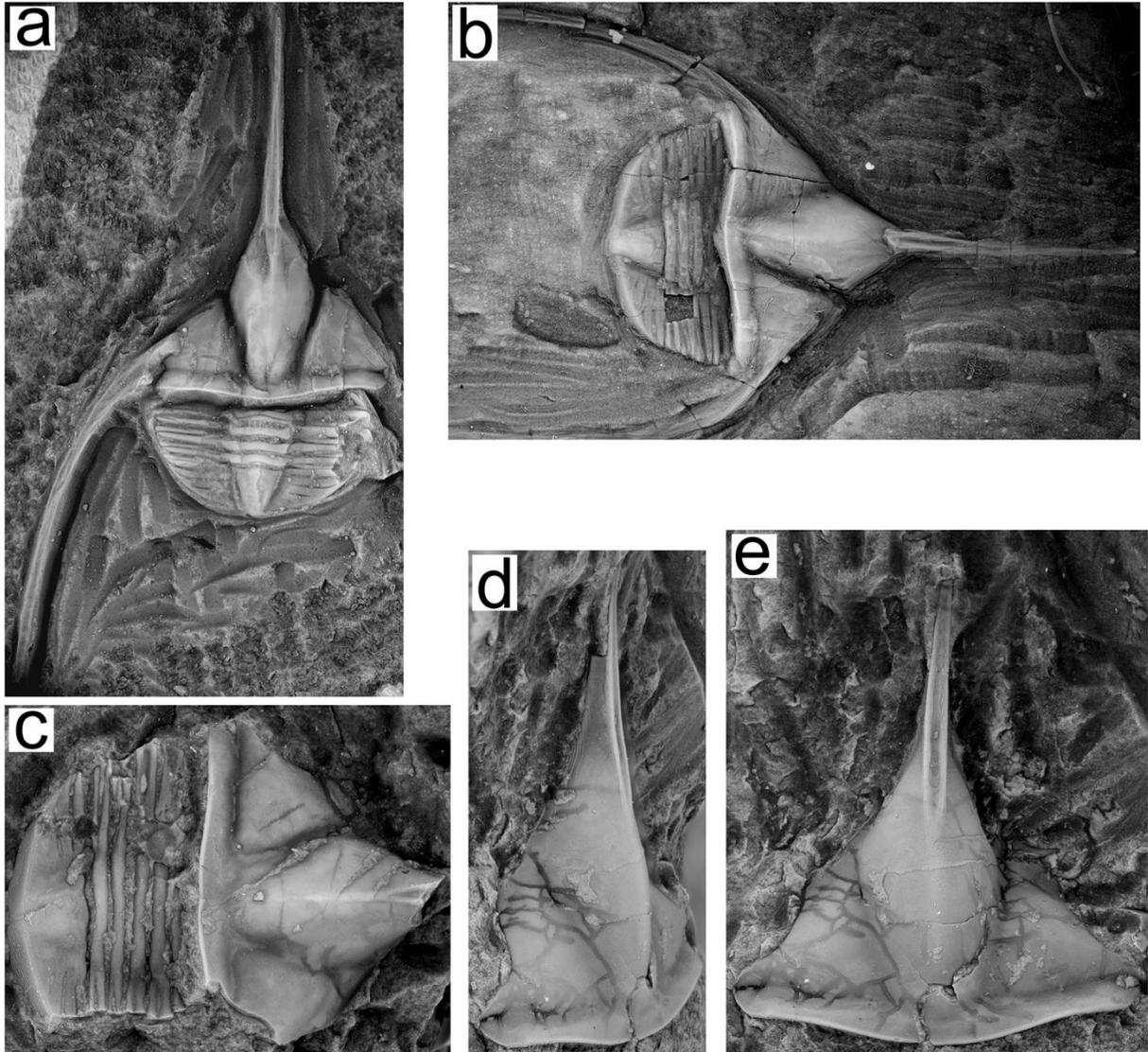
TEXT-FIGURE 21.—*Lonchodomas mcgheei* (Decker 1931), a common fossil at stop 12 (Rock Crossing) approximately 15 meters below the Bromide/Viola contact. a, complete individual (OU 12531), x 4, dorsal view. b, topotype complete individual (OU 3448), x 4.2, dorsal view. c, damaged individual (OU 12533), x 8, dorsal view. d, e, cranidium (OU 12532), d, lateral view, x7 e, dorsal view, x6.7.

The facies spectrum (Fig. 15) across the Bromide Formation suggests a more continuous and less dramatic down-ramp change in facies then expected. One implication is that localities such as Rock Crossing were likely deposited on a southern ramp that shallowed southward towards the Texas Arch. Intuitively, this makes sense because the succession in the lower Bromide on the northern ramp towards the SOA (I-35N, stop 7) is similar to the lower Bromide at Rock Crossing.
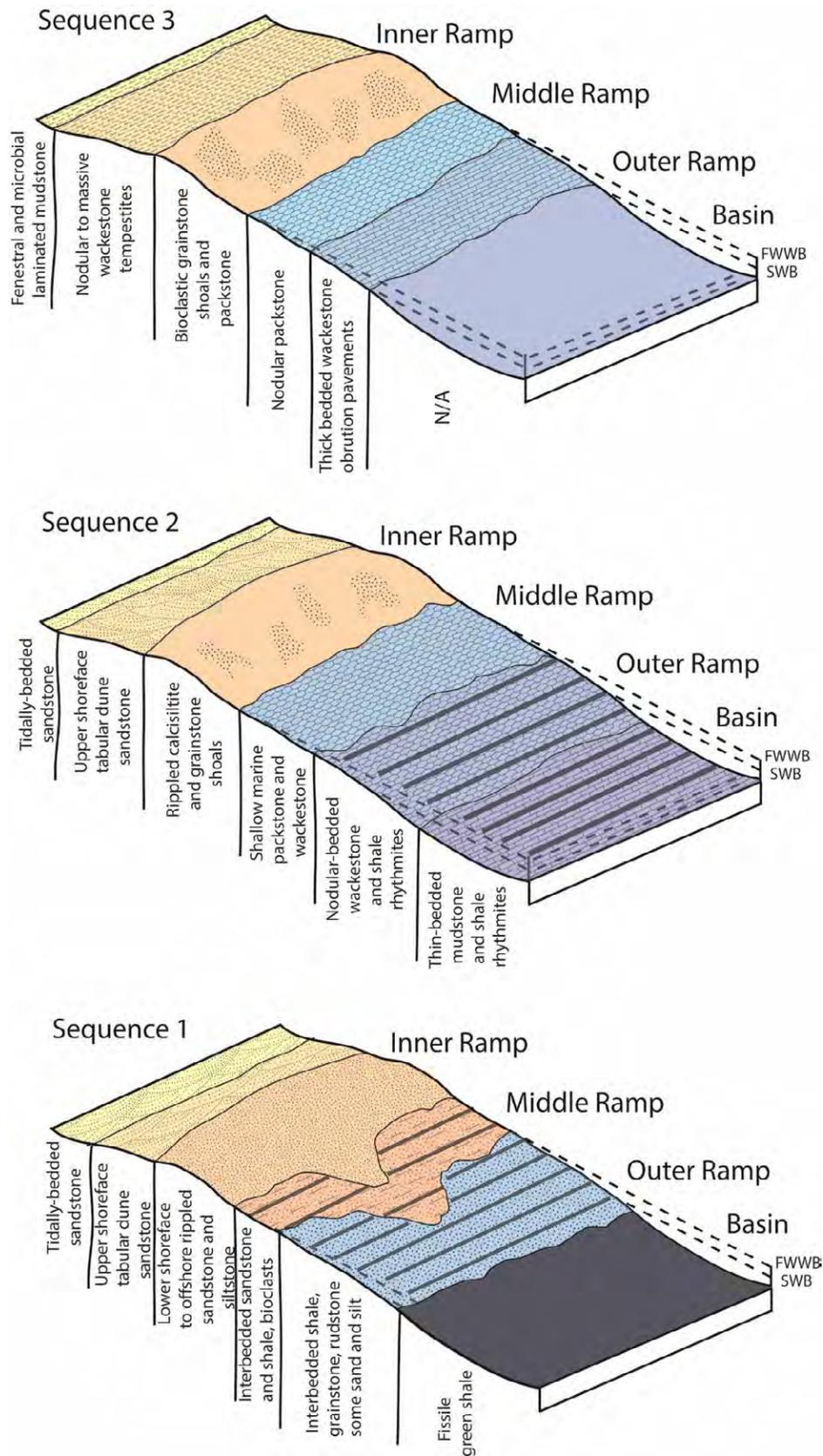
TEXT-FIGURE 22.—Depositional model of sequences 1-3 in the Bromide Formation. FWWB= Fair weather wave base, SWB = Storm wave base (modified from Carlucci et al. 2014).

Rock Crossing was pivotal in developing a depositional model of the Bromide Formation through three third-order depositional sequences (Fig. 22). The model records the gradual transition from a siliciclastic dominated ramp (sequence 1), to a mixed siliciclastic-carbonate ramp (sequence 2), to a warm-water neritic carbonate ramp (sequence 3). The ramp profile in sequence 3 is preserved in most of Oklahoma, but not on the southern ramp of the SOA, and only partially in the center of the aulacogen.

REFERENCES

AMATI, L. 2014. Isoteline Trilobites of the Viola Group (Ordovician: Oklahoma): Systematics and Stratigraphic Occurrence. *Oklahoma Geological Survey Bulletin*, 151:1–131.

AMATI, L., and WESTROP, S.R., 2004. A systematic revision of Thaleops (Trilobita: Illaenidae) with new species from the middle and late Ordovician of Oklahoma and New York. *Journal of Systematic Palaeontology*, 2:207-256.

AMATI, L., and WESTROP, S.R., 2006. Sedimentary facies and trilobite biofacies along an Ordovician shelf to basin gradient, Viola Group, South-Central Oklahoma. *PALAIOS*, 21:516-529.

AMSDEN, T.W., 1963. Silurian Stratigraphic Relations in the Central Part of the Arbuckle Mountains, Oklahoma. *Geological Society of America Bulletin*, 74:631-636.

AMSDEN, T.W., 1966. *Microcardinalia protriplesiana* Amsden, a new species of stricklandiid brachiopod, with a discussion on its phylogenetic position: *Journal of Paleontology*, 40:1009-1016.

AMSDEN, T.W., 1967. Silurian and Devonian strata in Oklahoma. *Tulsa Geological Society Digest*, *35*:25-34.

AMSDEN, T.W. 1975. Hunton Group (Late Ordovician, Silurian, and Devonian) in the Anadarko Basin of Oklahoma. *Oklahoma Geological Survey Bulletin*, 121:1-220.

AMSDEN, T.W., and SWEET, W.C., 1983. Upper Bromide Formation and Viola Group (Middle and Upper Ordovician) in Eastern Oklahoma. *Oklahoma Geological Survey Bulletin*, 132:1-76.

BABCOCK, L.E., PENG, S., GEYEF, G., and SHERGOLD, J.H., 2005. Changing perspectives on Cambrian chronostratigraphy and progress toward subdivision of the Cambrian System. *Geosciences Journal*, 9:101-106.

BAIRD, G.C., and BRETT, C.E., 1986. Erosion on an anaerobic seafloor: signficance of reworked pyrite deposits from the Devonian of New York State. *Palaeogeography, Palaeoclimatology, Palaeoecology*, 57:157-193.

BARRICK, J.E. 1986. Part II--Conodont faunas of the Keel and Cason Formations. Oklahoma Geological Survey. In: Amsden, T.W. and Barrick, J.E., Eds.*, Late Ordovician-Early Silurian Strata of the Central United States and the Hirnantian Stage*, 57-95. Oklahoma Geological Survey Bulletin 139.

BAUER, J. A. 1987. *Conodonts and conodont biostratigraphy of the McLish and Tulip Creek Formations (Middle Ordovician), south-central Oklahoma*. Norman: Oklahoma Geological Survey Bulletin 141, 58 pp.

BAUER, J.A., 1994. Conodonts from the Bromide Formation (Middle Ordovician), south-central Oklahoma. *Journal of Paleontology*, 68:358-376.

BAUER, J. A. 2010. *Conodonts and conodont biostratigraphy of the Joins and Oil Creek Formations, Arbuckle Mountains, south-central Oklahoma.* Norman: Oklahoma Geological Survey Bulletin 150, 44 pp.

BAUM, G.R., and VAIL, P.R., 1988. Sequence stratigraphic concepts applied to Paleogene outcrops, Gulf and Atlantic basins. In: Wilgus, C.K., Hastings, B.K., Posamentier, H., Wagoner, J.V., Ross, C.A., Kendall, C.G.S.C. Eds., *Sea-level changes: An integrated approach*, 309-327. Society of Economic Paleontology and Mineralogy Special Publication 42.

BERGSTRÖM, S. M., 1971. Conodont biostratigraphy of the Middle and Upper Ordovician of Europe and Eastern North America. *Geological Society of America Memoir*, 127:83–157.

BERGSTRÖM, S. M., 1986. Biostratigraphic integration of Ordovician graptolite and conodont zones - a regional review. In: C.P. Hughes and R.B. Rickards, Eds*., Paleoecology and biostratigraphy of graptolites*, 61-78. Geological Society Special Publication No. 20.

BERGSTRÖM, S.M., and LÖFGREN, A., 2008. The base of the global Dapingian Stage (Ordovician) in Baltoscandia: conodonts, graptolites and unconformities. *Earth and Environmental Science Transactions of the Royal Society of Edinburgh*, 99:189-212.

BERGSTRÖM, S.M., SALTZMANN, and M.R. SCHMITZ., B. 2006. First record of Hirnantian (Upper Ordovician) δ13C excursion in the North American Midcontinent and its regional implications. *Geological Magazine*, 143:657-678.

BERGSTRÖM, S. M., FINNEY, S. C., CHEN, XU, GOLDMAN, D., and LESLIE, S. A., 2006. Three new Ordovician global stage names. *Lethaia*, 39:287–288.

BERGSTRÖM, S.M., SCHMITZ, B., SALTZMAN, and M.R., HUFF, W.D., 2010. The Upper Ordovician Guttenberg δ13C excursion (GICE) in North America and Baltoscandia: occurrence, chronostratigraphic significance, and paleoenvironmental relationships. *Geological Society of America Special Papers*, 466:37-67.

BRADSHAW, L.E., 1974. Ordovician conodonts from Black Knob Ridge, Oklahoma: *Geological Society of America Abstracts with Programs*, 6:494.

BRETT, C.E., and ALGEO, T.J., 2001. Sequence stratigraphy of Upper Ordovician and Lower Silurian strata of the Cincinnati Arch region. In: Algeo, T.J., Brett, C.E. Eds., *Sequence, cycle and event stratigraphy of the Upper Ordovician and Silurian Strata of the Cincinnati Arch region*. Cincinnati: Kentucky Geological Survey Field Trip Guidebook 1, series XII.

BRETT, C.E., MCLAUGHLIN, P.I., BAIRD, G.C., and CORNELL, S.R., 2004. Comparative sequence stratigraphy of the Upper Ordovician (Turinian-Edenian) of the Trenton shelf (New York-Ontario) and Lexington Platform (Kentucky, southern Ohio) successions: implications for improved paleogeographic resolution of eastern Laurentia. *Palaeogeography, Palaeoclimatology, Palaeoecology*, 210:295-329.

BRETT, C.E., ALGEO, T.J., and MCLAUGHLIN, P.I., 2008. Use of event beds and sedimentary cycles in high-resolution stratigraphic correlation of lithologicaly repetetive successions: the upper Ordovician Kope Formation of northern Kentucky and southern Ohio. In: Harries, P.J. Ed., High-Resolution Approaches in Stratigraphic Paleontology, 315-350. Springer Science.

BRETT, C.E., ZAMBITO, J.J., HUNDA, B.R., and SCHINDLER, E., 2012. Mid-Paleozoic trilobite lagerstatten: models of diagenetically enhanced obrution horizons. *Palaios*, 27:326-345.

BROWN, W., 1984. Washita Valley fault system—a new look at an old fault. *Technical Proceedings of the 1981 AAPG Mid-Continent Regional meeting*, 68-80.

BROWN, W.G., 1985. *Tectonism and sedimentation in the Arbuckle Mountain region, Southern Oklahoma Aulacogen*. Waco: Baylor University, Unpublished Thesis.

CARDOTT, B.J., and CHAPLIN, J.R., 1993. *Guidebook for selected stops in the western Arbuckle Mountains, southern Oklahoma*. Norman: Oklahoma Geological Survey.

CARLUCCI, J.R., and WESTROP, S.R., 2012. Trilobite biofacies along an Ordovician (Sandbian) carbonate buildup to basin gradient, southwestern Virginia. *Palaios*, 27:19-34.

CARLUCCI, J.R., WESTROP, S.R., AMATI, L., ADRAIN, J.M., and SWISHER, R.E., 2012. A Systematic revision of the Upper Ordovician trilobite genus *Bumastoides* (Trilobita: Illaenidae) with new species from Oklahoma, Virginia, and Missouri. *Journal of Systematic Palaeontology*, 10:679-723.

CARLUCCI, J.R., WESTROP, S.R., BRETT, C.E., and BURKHALTER, R., 2014. Facies architecture and sequence stratigraphy of the Ordovician Bromide Formation (Oklahoma): a new perspective on a mixed carbonate-siliciclastic ramp. *Facies*, 60:987-1012.

Carlucci, J.R., and Westrop, S.R., 2014. Trilobite biofacies and sequence stratigraphy: an example from the Upper Ordovician of Oklahoma. *Lethaia,* DOI 10.1111.

COOPER, G.A., 1956. Early Middle Ordovician of the United States. In: Bassett, M.G. Ed., *The Ordovician System*, 171-194. University of Wales Press and National Museum of Wales.

COOPER, R.A. and SADLER, P.M., 2012. The Ordovician Period. In: F.M. Gradstein, J. Ogg, M. Schmitz, & G. Ogg, Eds., *The geologic time scale 2012*, 489-524. Oxford: Elsevier.

DECKER, C.E., 1931. A new species of *Ampyx*. *Journal of Paleontology*, 5:153-155.

DECKER, C.E., 1933. Viola Limestone, Primarily of Arbuckle and Wichita Mountain Regions, Oklahoma. *AAPG Bulletin*, 17:1405-1435.

DECKER, C.E., 1935. Graptolites of the Sylvan Shale of Oklahoma and the Polk Creek Shale of Arkansas. *Journal of Paleontology*, 9:697-708.

DECKER, C.E., 1941. Simpson Group of Arbuckle and Wichita mountains of Oklahoma. *American Association of Petroleum Geologists Bulletin*, 25:650-667.

DECKER, C.E., and MERRITT, C.A., 1931. The stratigraphy and physical characteristics of the Simpson Group. *Oklahoma Geological Survey Bulletin*, 55.

DERBY, J.R., BAUER, J.A., CREATH, W.B., DRESBACH, R.I., ETHINGTON, R.L., LOCH, J.D., STITT, J.H., MCHARGUE, T.R., MILLER, J.F., MILLER, M.A., REPETSKI, J.E., SWEET, W.C., TAYLOR, J.F., and WILLIAMS, M., 1991. Biostratigraphy of the Timbered Hills, Arbuckle, and Simpson groups, Cambrian and Ordovician, Oklahoma: A review of

correlation tools and techniques available to the explorationist. *Oklahoma Geological Survey Circular*, 92:15-41.

DWORIAN, P.R., 1990. *The biostratigraphy and biogeography of Upper Ordovician graptolites from North America*. Long Beach: California State University, Unpublished M.S. Thesis.

EDSON, F.C., 1927. Ordovician correlations in Oklahoma. *American Association of Petroleum Geologists Bulletin*, 11:967-975.

ETHINGTON, R.L., FINNEY, S.C., AND REPETSKI, J.E., 1989. Biostratigraphy of the Paleozoic rocks of the Ouachita Orogen, Arkansas, Oklahoma, West Texas. In: R.D. Hatcher, Jr., W.A. Thomas, and G.W. Viele, Eds., *The geology of North America, v. F-2, The Appalachian-Ouachita Orogen in the United States*, 563-573. Denver: Geological Society of America.

FAY, R.O. AND GRAFFAM, A.A. 1969. Bromide Formation on Tulip Creek and in the Arbuckle Mountains region. *Oklahoma Geological Survey Guidebook*, 17:37-41.

FAY, R.O., 1989. *Geology of the Arbuckle Mountains along Interstate 35, Carter and Murray Counties, Oklahoma*. Norman: Oklahoma Geological Survey Guidebook 26.

FAY, R.O., GRAFFHAM, A.A., and SPRINKLE., J., 1982a. Stratigraphic studies. In: Sprinkle, J. Ed., *Echinoderm faunas from the Bromide Formation (Middle Ordovician) of Oklahoma*, 195-209. University of Kansas Paleontological Contributions, Monograph 1.

FAY, R.O., GRAFFHAM, A.A., and SPRINKLE, J., 1982b. Appendix: Measured sections and collecting localities. In: Sprinkle, J. Ed., *Echinoderm faunas from the Bromide Formation (Middle Ordovician) of Oklahoma*, 195-209. University of Kansas Paleontological Contributions, Monograph 1.

FINNEY, S.C., 1986. Graptolite biofacies and correlation of eustatic, subsidence, and tectonic events in the Middle to Upper Ordovician of North America: *Palaios*, 1:435–461.

FINNEY, S.C., 1988. Middle Ordovician strata of the Arbuckle and Ouachita Mountains, Oklahoma: Contrasting lithofacies and biofacies deposited in southern Oklahoma Aulacogen and Ouachita Geosyncline. In: O.T. Heyward, Ed., *Geological Society of America centennial field guide - south-central section*, 171–176. Denver: Geological Society of America.

GOLDMAN, D., MITCHELL, C.E., BERGSTRÖM, S.M., DELANO, J.W., and TICE, S., 1994. K-bentonites and graptolite biostratigraphy in the Middle Ordovician of New York State and Quebec: A new chronostratigraphic model: *Palaios*, 9:124–143.

GOLDMAN, D., LESLIE, S.A., NOLVAK, J., YOUNG, S., BERGSTRÖM, S.M., and HUFF, W.D., 2007. The global stratotype section and point (GSSP) for the base of the Katian Stage of the Upper Ordovician Series at Black Knob Ridge, Southeastern Oklahoma, USA. *Episodes*, 30:258-270.

HALLEY, R.B., and EBY, D.E., 1973. Cambro-Ordovician high relief stromatolites: evidence of evolutionary or environmental paucity. *Geological Society of America Abstracts with Programs Northeast*, 5:172-173.

HAM, W.E., 1969. Regional geology of the Arbuckle Mountains, Oklahoma. *Oklahoma Geological Survey Guide Book*, 17:1-54.

HAM, W.E., Amsden, T.W., 1973. *Regional geology of the Arbuckle Mountains*. Norman: Oklahoma Geological Survey, Field Trip Number 5, 55 pp.

HARLTON, B.H., 1953. Ouachita chert facies, southeastern Oklahoma. *Bulletin of the American Association of Petroleum Geologists*, 37:778–796.

HARRIS, R.W., 1957. Ostracoda of the Simpson Group. *Oklahoma Geological Survey Bulletin*, 75:1-333.

HENDRICKS, T.A., KNECHTEL, M.M., and BRIDGE, J., 1937. Geology of Black Knob Ridge, Oklahoma. *Bulletin of the American Association of Petroleum Geologists*, 21:1–29.

HOLLAND, S.M., and PATZKOWSKY, M.E., 1996. Sequence stratigraphy and long-term paleoceanographic changes in the Middle and Upper Ordovician of the eastern United States. In: B.J. Witzke, G.A. Ludvigson, and J.E. Day, Eds., *Paleozoic sequence stratigraphy: Views from the North American craton*, 117-128. Geological Society of America Special Paper 306.

JOHNSON, K.S., BURCHFIELD, M.R., and HARRISON, W.E., 1984. Guidebook for the Arbuckle Mountain field trip, southern Oklahoma. *Oklahoma Geological Survey Special Publication*, 84.

JOHNSON, K.S., AMSDEN, T.W., DENISON, R.E., DUTTON, S.P., GOLDSTEIN, A.G., RASCOE, B., SUTHERLAND, P.K., and THOMPSON, D.M., 1988. Southern midcontinent region. In: Sloss, L.L. Ed., *Sedimentary cover- North American craton,* 307-359. Geological Society of America.

JOHNSON, K.S, 1991. Geologic overview and economic importance of late Cambrian and Ordovician rocks in Oklahoma. In: Johnson, K., Ed*., Late-Cambrian-Ordovician geology of the southern midcontinent 1989 symposium*, 3-14. Norman: Oklahoma Geological Survey Circular 92.

JOHNSON, K., and CARDOTT, B., 1992. Geologic framework and hydrocarbon source rocks of Oklahoma. *Oklahoma Geological Survey Circular*, 93:21-37.

JOHNSON, K.S., 1997. Simpson and Viola Groups in the southern Midcontinent, 1994 Symposium. *Oklahoma Geological Survey Circular*, 99:1-281.

KARIM, T., and WESTROP, S., 2002. Taphonomy and Paleoecology of Ordovician Trilobite Clusters, Bromide Formation, south-central Oklahoma. *Palaios*, 17:394-403.

KRUEGER, D., 2002. *Conodont biostratigraphy of Middle and Upper Ordovician rocks in the Ouachita Mountains of Arkansas and Oklahoma*. Columbia: University of Missouri-Columbia, 279 pp.

MCLAUGHLIN, P.I., BRETT, C., and WILSON, M., 2008. Hierarchy of sedimentary discontinuity surfaces and condensed beds from the Middle Paleozoic of Eastern North America: Implications for cratonic sequence stratigraphy. In: Pratt, B., Holmden, C. Eds., *Dynamics of epeiric seas*. Geological Association of Canada special paper 48.

LESLIE, S.A., BERGSTRÖM, S. M., and HUFF, W.D. 2008. Ordovician K-bentonites discovered in Oklahoma. *Oklahoma Geology Notes*, 68:4-14.

LOCH, J.D., 2007. Trilobite biostratigraphy and correlation of the Lower Ordovician Kindblade Formation of Carter and Kiowa Counties, Oklahoma. *Oklahoma Geological Survey Bulletin*, 149:1-159.

LONGMAN, M.W., 1976. *Depositional history, paleoecology, and diagenesis of the Bromide Formation (Ordovician) Arbuckle Mountains, Oklahoma*. Austin: University of Texas at Austin.

LONGMAN, M.W., 1982a. Depositional environments. In: Sprinkle, J. Ed., *Echinoderm Faunas from the Bromide Formation (Middle Ordovician) of Oklahoma*, 17-29. University of Kansas Paleontological Contributions, Monograph 1.

LONGMAN, M.W., 1982b. Depositional setting and regional characteristics. In: Sprinkle, J. Ed., *Echinoderm Faunas from the Bromide Formation (Middle Ordovician) of Oklahoma,* 6-10. The University of Kansas Paleontological Contributions, Monograph 1.

LUDVIGSEN, R., 1978. The trilobites *Bathyurus* and *Eomorachus* from the Middle Ordovician of Oklahoma and their biofacies significance. *Life Sciences Contributions ROM*, 114:1-17.

MCPHERSON, J.G., DENISON, R.E., KIRKLAND, D.W., and SUMMERS, D.M., 1988. Basal sandstone of the Oil Creek Formation in the quarry of the Pennsylvania Glass Sand Corporation, Johnson County, Oklahoma. In: Hayward, O.T. Ed., *Centennial field guide 4*, 165-170. Geological Society of America, South Central Section.

GARRECHT METZGER, J., and FIKE, D.A., 2013. Techniques for assessing spatial heterogeneity of carbonate δ13C values: Implications for craton-wide isotope gradients. *Sedimentology*, 60:1405-1431.

NICK, K.E., and ELMORE, R.D., 1990. Paleomagnetism of the Cambrian Royer Dolomite and Pennsylvanian Collings Ranch Conglomerate, southern Oklahoma: An early Paleozoic magnetization and nonpervasive remagnetization by weathering. *Geological Society of America Bulletin*, 102:1517-1525.

OSLEGER, D., and READ, J.F., 1991. Relation of eustasy to stacking patterns of meter-scale carbonate cycles, Late Cambrian, USA. *Journal of Sedimentary Research*, 61.

PLAYFORD, G., and WICANDER, R., 2006. Organic-walled microphytoplankton of the Sylvan Shale (Richmondian: Upper Ordovician), Arbuckle Mountains, southern Oklahoma, USA. *Oklahoma Geological Survey*, 148:1-116.

POMAR, L., MORSILLI, M., HALLOCK, P., and BÁDENAS, B., 2012. Internal waves, an under-explored source of turbulence events in the sedimentary record. *Earth-Science Reviews*, 111:56-81.

POPE, M., and READ, J.F., 1997. High-resolution surface and subsurface sequence stratigraphy of Late Middle to Late Ordovician (Late Mohawkian-Cincinnatian) foreland basin rocks, Kentucky and Virginia. *AAPG Bulletin*, 81:1866-1893.

PUCKETT, R. E., JR., HANSON, R.E., ESCHLBERGER, A.M., BRUESEKE, M.E., BULEN, C.L., and PRICE, J. D., 2014. New Insights into the Early Cambrian Igneous and Sedimentary History of the Arbuckle Mountains Area of the Southern Oklahoma Aulacogen from Basement Well Penetrations. In: Suneson, N. H., Ed*., Igneous and tectonic history of the Southern Oklahoma Aulacogen*, 61-94. Oklahoma Geological Survey Guidebook 38.

RAGLAND, D., and DONOVAN, R., 1991. Sedimentology and diagenesis of the Arbuckle Group in outcrops of southern Oklahoma. In: Johnson, K.S., Ed., *Arbuckle Group core workshop and field trip*, 9-30. Oklahoma Geological Survey Special Publication 91-3.

REPETSKI, J.E., and ETHINGTON, R.L., 1977. Conodonts from the graptolite facies in the Ouachita Mountains, Arkansas and Oklahoma. In: C.G. Stone, Ed., *Symposium on the geology of the Ouachita Mountains*, 92-106. Arkansas Geological Commission.

RIVA, J., 1969. Middle and Upper Ordovician graptolite faunas of St. Lawrence Lowlands of Quebec, and of Anticosti Island. In: M. Kay, Ed., *North Atlantic - geology and continental drift. A symposium*, 579-595. American Association of Petroleum Geologists Memoir 112.

RIVA, J. 1974. A revision of some Ordovician graptolites of eastern North America. *Palaeontology*, 17:1-40.

ROLOSON, M., 2011. *Biostratigraphic analysis of core 75 NY-2 from near Ballston Spa, New York.* Amherst: University at Buffalo, 78 pp.

ROSENAU, N.A., HERRMANN, A.D., and LESLIE, S.A., 2012. Conodont apatite del180 values from a platform margin setting, Oklahoma, USA: implications for initiation of late Ordovician icehouse conditions. *Palaeogeography, Palaeoclimatology, Palaeoecology*, 315-316: 172-180.

ROSS JR, R.J., 1976. Ordovician sedimentation in the western United States. In: Hill, G.J. Ed., *Geology of the Corilleran hingeline* 1976, 109-133. Rocky Mountain Association of Geologists 1976 Symposium.

SALTZMAN, M.R. 2001, Silurian 13C stratigraphy: A view from North America. *Geology*, 29:671-674.

SELL, B.K., AINSAAR, L., and LESLIE, S.A., 2013. Precise timing of the Late Ordovician (Sandbian) super-eruptions and associated environmental, biological, and climatological events. *Journal of the Geological Society of London*, 170:711–714.

SCHRAMM, M.W., 1964. Paleogeologic and quantitative lithofacies analysis Simpson Group, Oklahoma. *Bulletin of the American Association of Petroleum Geologists*, 48:1164-1195.

SHAW, F., 1974. Simpson Group (Middle Ordovician) Trilobites of Oklahoma. *Journal of Paleontology Memoir*, 48:1-54.

SPRINKLE, J., 1982. Echinoderm zones and faunas. In: Sprinkle, J. Ed., *Echinoderm faunas from the Bromide Formation (Middle Ordovician) of Oklahoma*, 47-56. University of Kansas Paleontological Contributions, Monograph 1.

ST JOHN JR, J.W., and EBY, D.E., 1978. Peritdal Carbonates and Evidence for Vanished Evaporites in the Lower Ordovician Cool Creek Formation-Arbuckle Mountains, Oklahoma. *Gulf Coast association of Geological Societies Transactions*, 28:589-599.

SUNESON, N., 1996. *The geology of the Ardmore Basin in the Lake Murray Stake Park Area, Oklahoma.* Norman: Spring Field Meeting of the Oklahoma Academy of Science, 44 pp.

SUTHERLAND, P.K., and AMSDEN, T.W., 1959. A re-illustration of the trilobite *Lonchodomas mcgeheei* Decker from the Bromide Formation (Ordovician) of southern Oklahoma. *Oklahoma Geological Notes*, 19:212-218.

SWISHER, R.E. 2015. Trilobite faunas, sedimentary facies and sequence stratigraphy of the Upper Ordovician (Sandbian–Katian) succession of Missouri. Norman: University of Oklahoma, Unpublished Ph.D. dissertation, 305 pp.

SWISHER, R.E., WESTROP, S.R., and AMATI, L. 2015 (in press). Systematics and biogeographic significance of the Upper Ordovician pterygometopine trilobite *Achatella* Delo, 1935. *Journal of Paleontology*.

TAFF, J.A. 1902. Description of the Atoka Quadrangle. *US Geological Survey Folio*, 79: 1-10.

TAPP, J., 1978. Breccias and megabreccias of the Arbuckle Mountains, southern Oklahoma aulacogen. Oklahoma: Norman: University of Oklahoma, Unpublished M.S.thesis.

TAPP, B., 1991. Folding and thrusting in the Lower Arbuckle. In: Johnson, K.S., Ed., *Arbuckle Group core workshop and field trip*, 216-217. Oklahoma Geological Survey Special Publication 91-3.

TAYLOR, J.F., REPETSKI, J.E., LOCH, J.D., and LESLIE, S.A., 2012. Biostratigraphy and chronostratigraphy of the Cambrian–Ordovician great American carbonate bank. In: Derby, J.R., Fritz, R.D., S.A, L., W.A, M., C.A, S. Eds., *The great American carbonate bank: The geology and economic resources of the Cambrian-Ordovician Sauk megasequence of Laurentia*, 15-35. AAPG Memoir 98.

VANDENBERG, A.H.M., and COOPER, R.A., 1992. The Ordovician graptolite sequence of Australasia: *Alcheringa*, 16:33–85.

WEBBY, B.D., COOPER, R.A., BERGSTRÖM, S.M., and PARIS, F., 2004. Stratigraphic Framework and Time Slices. In: B.D. Webby, F. Paris, M.L. Droser, and I.G. Percival, Eds., *The great Ordovician biodiversification event*, 41-47, New York: Columbia University Press.

WENGERD, S.A., 1948. Fernvale and Viola limestones of south-central Oklahoma. *AAPG Bulletin*, 32:2183-2253.

WESTROP, S.R., AMATI, L., BRETT, C.E., SWISHER, R.E., and CARLUCCI, J.R., 2012. When approaches collide: reconciling sequence stratigraphy, chemostratigraphy and biostratigraphy in the correlation of the Katian (Upper Ordovician) reference section, central Oklahoma. *GSA Charlotte Abstracts with Programs*, 44:606.

WICKHAM, J., and DENISON, R., 1978. *Structural style of the Arbuckle region*: Geological Society of America. South Central Section, Guidebook for Field Trip 3, 111 pp.

WILSON, J.L., FRITZ, R., and MEDLOCK, P., 1991. The Arbuckle Group-relationship of core and outcrop analyses to cyclic stratigraphy and correlation. In: Johnson, K. Ed., *Late Cambrian-Ordovician geology of the southern midcontinent, 1989 Symposium*, 133-143. Norman: Oklahoma Geological Survey Circular 92.

YOUNG, S., SALTZMAN, and BERGSTRÖM, S.M., 2005. Upper Ordovician (Mohawkian) carbon isotope stratigraphy in eastern and central North America: Regional expression of a perturbation of the global carbon cycle. *Palaeogeography, Palaeclimatology, Palaecology* 222:53-76.

ZALASIEWICZ, J., RUSHTON, A., and OWEN, A., 1995. Late Caradoc graptolitic faunal gradients across the Iapetus Ocean. *Geological Magazine*, 132:611-617.

12th International Symposium on the Ordovician System

Ordovician of the Southern Appalachians, USA
Pre-Symposium Field Trip

June 3rd – 7th, 2015

Achim Herrmann[1]
John T. Haynes[2]

[1]*Assistant Professor, Department of Geology & Geophysics, Louisiana State University Baton Rouge, LA 70803, aherrmann@lsu.edu*

[2]*Associate Professor, Department of Geology and Environmental Science, James Madison University, Harrisonburg, VA 22807, haynesjx@jmu.edu*

Welcome to the Southern Appalachians pre-meeting field trip that is a part of the 2015 International Symposium on the Ordovician System meeting! This trip is scheduled to consist of three full days of stops at selected locations. Each day will provide you with a west-to-east traverse across the Valley and Ridge province from the predominantly carbonate depositional environments in the western and northwestern strike belts to the predominantly clastic depositional environments in the eastern and southeastern strike belts.

DAY 1. ORDOVICIAN CARBONATE AND CLASTIC DEPOSITS ALONG STRIKE AND ACROSS THE HELENA THRUST FAULT, NORTH CENTRAL ALABAMA

Introduction

At today's stops we will examine three exposures of Ordovician strata in Alabama (Fig. 1). Two of these exposures (Red Mountain Expressway, Stop 1-1, and Tidwell Hollow, Stop 1-2) consist of predominantly carbonate strata originally deposited in platform and shelf margin settings, and the third exposure (Alexander Gap, Stop 1-3) is of siliciclastic strata originally deposited in nearshore marine settings (Fig. 2). At all three locations, the Deicke and Millbrig K-bentonites of Katian and Sandbian age (~452-453 Ma) are present, and they provide chronostratigraphic control for these strata of Katian, Sandbian, and upper Darriwilian age across the region (Fig. 2). They are also important for tying together newly generated carbon and oxygen isotope curves for the Red Mountain Expressway, Tidwell Hollow, and other stratigraphic sections in this area.

The Paleoceanographic conditions across the Turinian/Chatfieldian Boundary, and paleoenvironmental changes

The stops today will mostly span the M4 and M5 sequences of Holland and Patzkowsky (1996), including the GICE interval (Young et al., 2005) (Fig. 4). In Middle and Upper Ordovician strata of the eastern North American mid-continent, 14 sequences are identified (Holland and Patzkowsky, 1996). Of these 14 sequences, 6 are Mohawkian in age (458-453 m.y., Webby et al., 2004) and are designated as M1 through M6. The M4-M5 sequence boundary is a possible climatic turning point (Fig. 4). This boundary coincides with several distinct lithological changes suggesting a transition from warm-water to cool-water conditions within the shallow epicontinental sea of Laurentia during the early Late Ordovician (Brookfield and Brett, 1988; Brookfield and Elgadi, 1998; Holland and Patzkowsky, 1996; Lavoie and Asselin, 1998; Patzkowsky and Holland, 1996; Pope and Read, 1997). In particular, the change to a skeletal association reminiscent of brynoderm and bryomol associations of modern and ancient temperate water settings supports cooling at this time, analogous to other Paleozoic ice-house intervals (Beauchamp and Desrochers, 1997; Samankassou, 2002). The M4-M5 lithologic transition coincides with an extinction event recognized in the eastern United States (Patzkowsky and Holland, 1993; 1996; 1999) that affected articulate brachiopods (Patzkowsky and Holland, 1993;
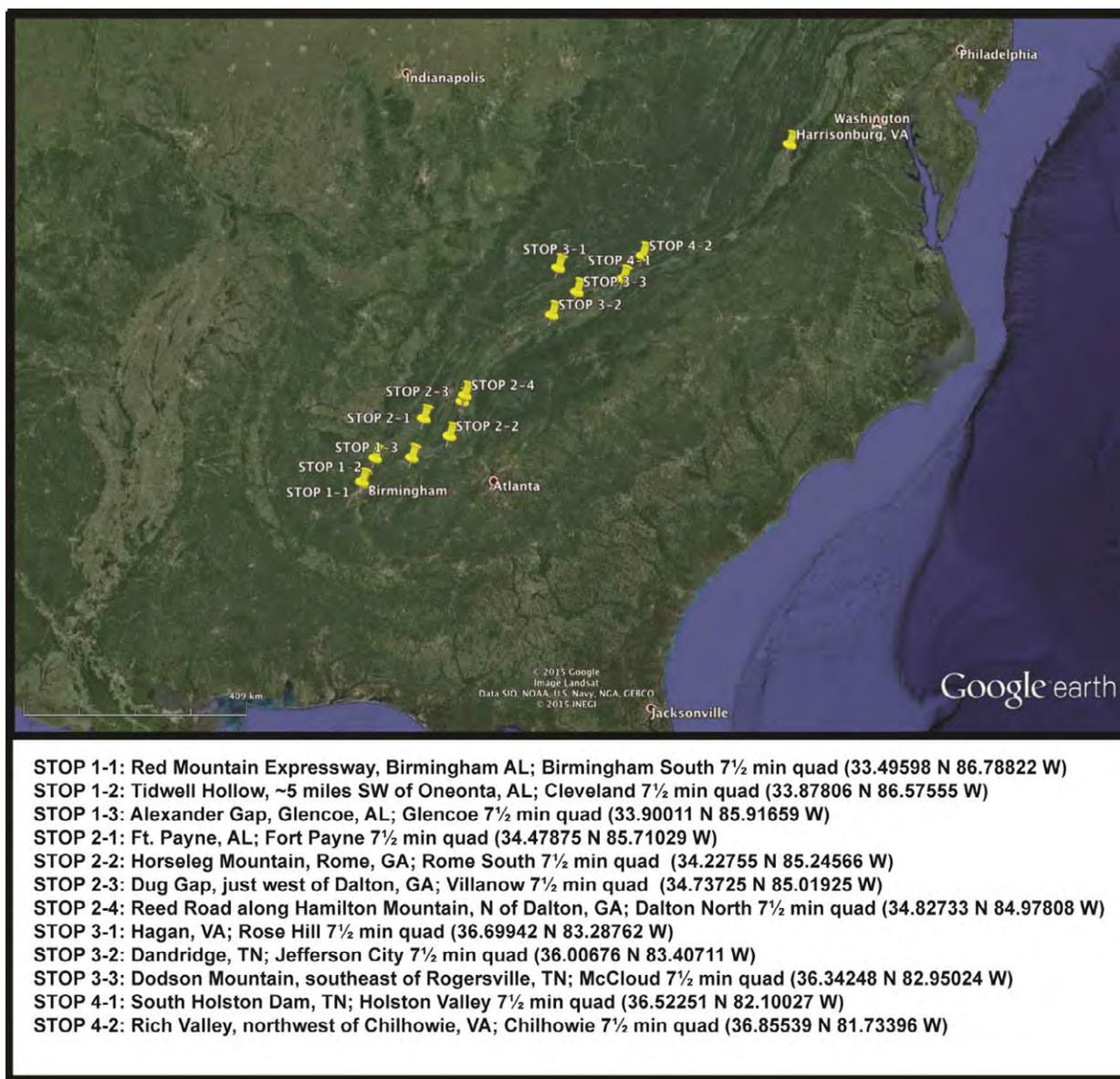
Figure 1.—Location of field trip stops between Birmingham, Alabama, and Harrisonburg, Virginia.

1996; Patzkowsky and Holland, 1997), cephalopods (Frey, 1995), corals (Patzkowsky and Holland, 1996), and crinoids (Eckert, 1988). Onset of late Ordovician glaciation has been advanced as a cause of these changes (Lavoie and Asselin, 1998; Pope and Read, 1997), and, based on sequence stratigraphic evidence and carbon isotope data, Saltzman and Young (2005) suggested that the transition to Late Ordovician ice-house conditions occurred during this time. Nonetheless, significant cooling in the mid-continent epicontinental sea is problematic because eastern North America was then at tropical to subtropical latitudes (Scotese and McKerrow, 1990; 1991). Furthermore, whereas evidence for benthic cooling exists below the Deicke K-bentonite (Herrmann et al., 2010), the best paleotemperature estimates available suggest, if

206
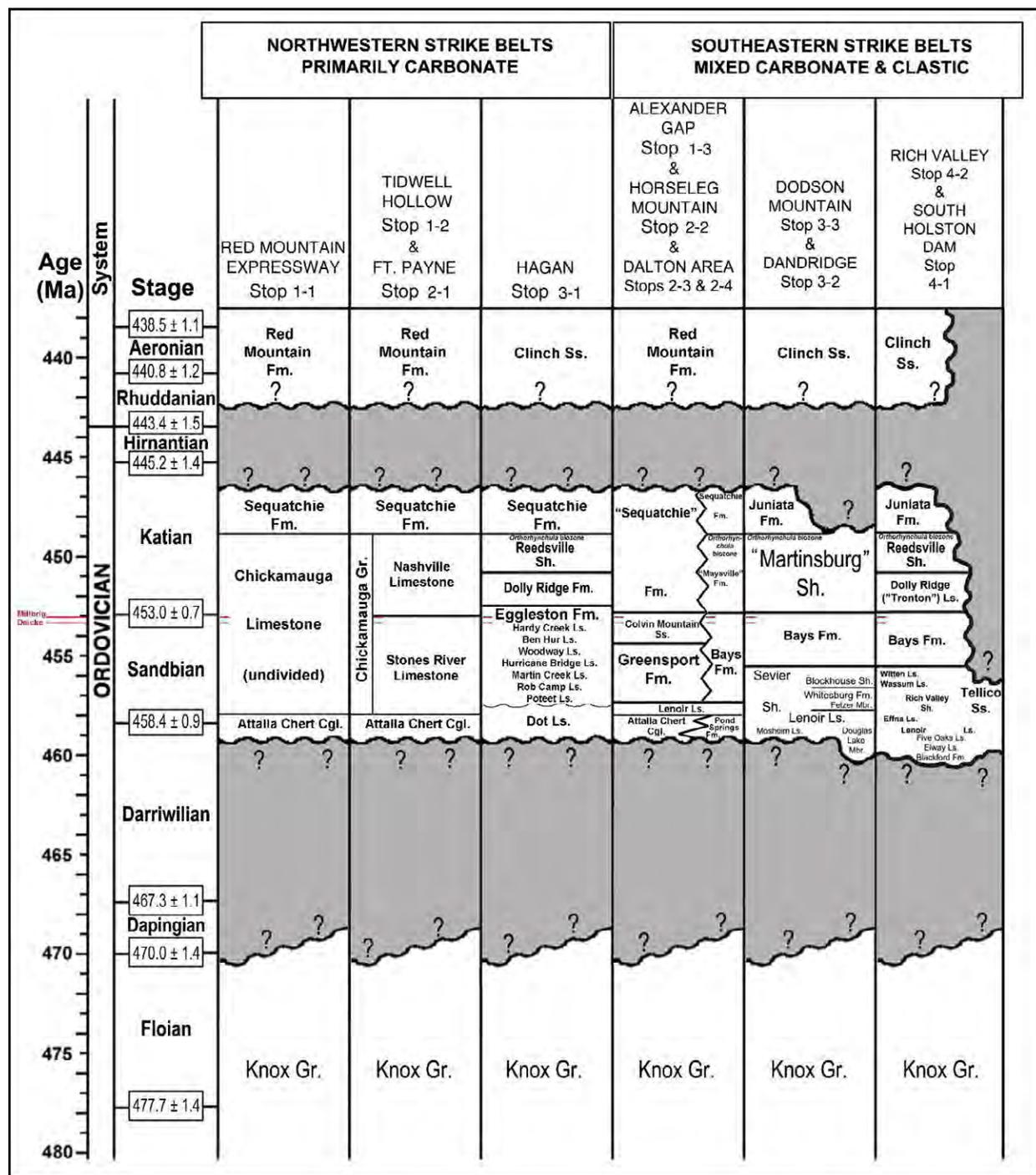
Fig. 2.—Stratigraphic correlation chart of the locations visited.

anything, warming across this interval in Minnesota and Kentucky (Buggisch et al, 2010) and Oklahoma (Rosenau et al., 2012). The leading alternative hypothesis to a shift in climate modes invokes oceanographic and sedimentological responses to the Taconic orogeny (Holland and Patzkowsky, 1996).

One interpretation of the lithologic and faunal changes is that they are a response to initiation of cooling during the later Ordovician, which eventually led to a glaciation in the Hirnantian (Lavoie and Asselin, 1998; Pope and Read, 1997). In response to the global cooling, the tropical belt shrank and cold water was able to penetrate into tropical areas (Lavoie, 1995); the mechanism(s) proposed for cooling vary. Kolata et al. (2001) hypothesized that the Sebree Trough acted as a passage through which cold oceanic waters could reach the Laurentian epeiric sea. Herrmann et al. (2004), using a 3-dimensional global ocean circulation model, demonstrated that changes in paleogeography and atmospheric pCO$_2$, could have led cold water currents from higher southern latitudes to inundate the shallow epeiric ocean of Laurentia. Upwelling of cold, open ocean water was also suggested as an explanation for changes in epicontinental seas by Pope and Steffen (2003), who cited the widespread deposition of phosphatic and cherty carbonates along the southern and western margin of Laurentia as evidence for vigorous thermohaline circulation, and, therefore, the influence of cold deep ocean water as early as the late Middle Ordovician. Finally, Young et al. (2005) concluded that the Chatfieldian Guttenburg δ^{13}C excursion (GICE) (e.g., Hatch et al., 1987; Ludvigson et al., 1996; Ludvigson et al., 2004; Patzkowsky and Holland, 1997) reflected enhanced upwelling along the southern margin of Laurentia during the Chatfieldian. From a conodont perspective, the GICE begins in the upper part of the *P. undatus* Zone, continues through the *P. tenuis* Zone, and ends in the *B. confluens* Zone. That places the GICE within the M5 sequence. Estimates of cooling, where given, are typically a few degrees, but as already noted conodont δ^{18}O analyses do not support cooling across this interval (Buggisch et al., 2010; Rosenau et al., 2012).

  Our stops today will provide a transect from shelf and platform margin carbonate environments to siliciclastics that accumulated atop the nearly filled Blount foredeep that had developed along the southern margin of Laurentia during the early stages of the Taconic orogeny (Fig. 3). The exposures we have selected for examining today will provide us with ample opportunity to discuss different driving mechanisms for environmental change during the middle and later Ordovician.

The Ordovician carbonate succession northwest of the Helena thrust

  From the Cambrian – Ordovician boundary, which in this region occurs in the lower Knox Group, to the Knox unconformity (which is variously Floian, Dapingian, to Darriwilian in its stratigraphic extent; Fig. 2), Ordovician strata are primarily shallow water peritidal and lesser open shelf carbonates, both limestones and dolomites (Read and Repetski, 2012). Immediately above the Knox unconformity in north central Alabama is the Attalla Chert Conglomerate, a deposit of chert-rich karst regolith and rubble that accumulated on and around lows on the Knox unconformity paleokarst during the long periods of subaerial exposure that occurred during Floian to Darriwillian time as the Knox unconformity developed throughout much of eastern North America.
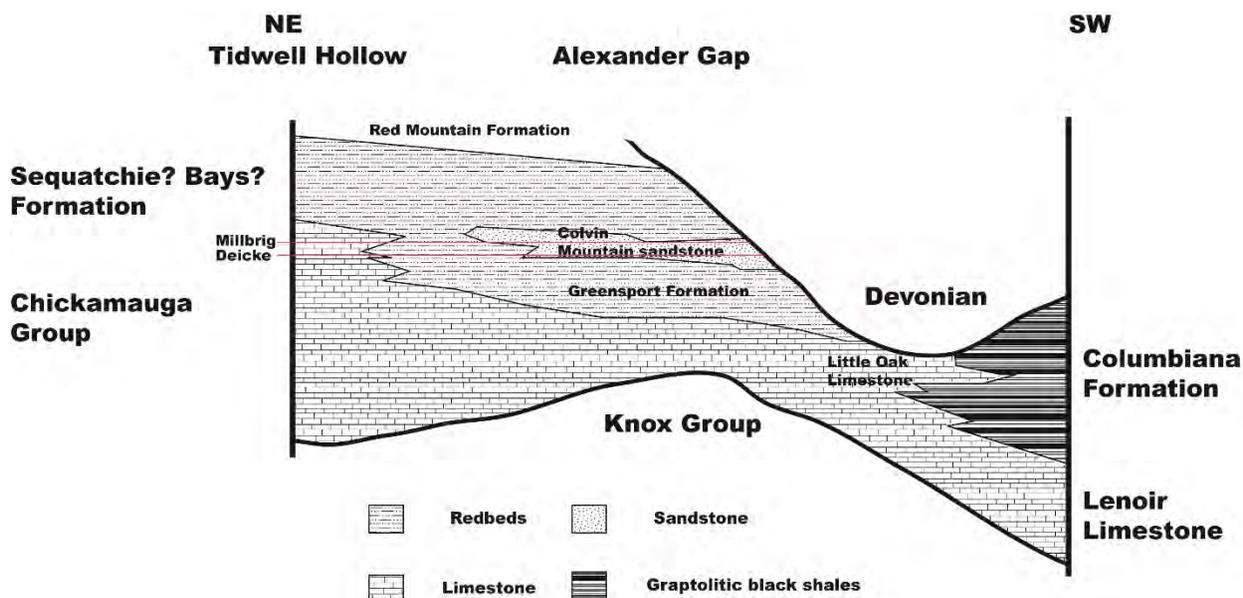
Figure 3.—Stratigraphic cross section across northeastern Alabama showing the stratigraphic and depositional relationship between the second (Tidwell Hollow) and third (Alexander Gap) stops of day 1. Modified from Chowns and McKinney (1980).
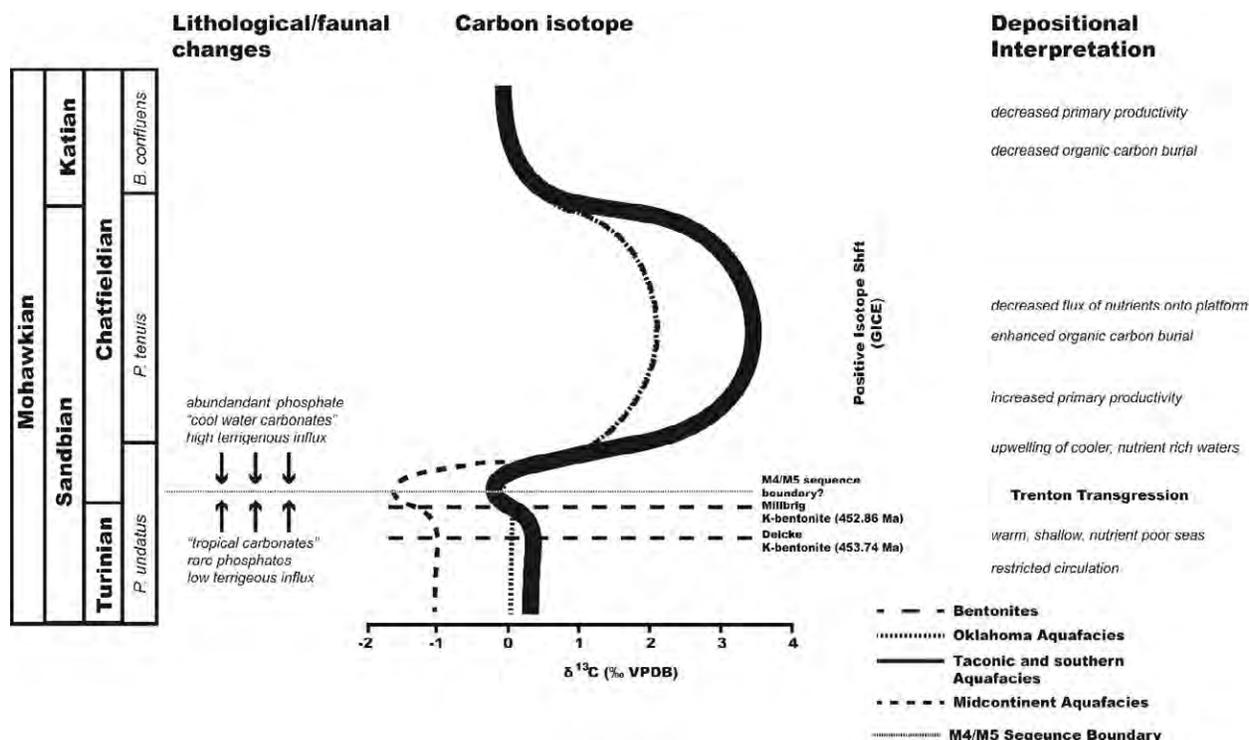
Figure 4.—Paleoceanographic model for the Guttenberg Isotope Carbon Excursion (based on Young et al., 2005). Age of Deicke and Millbrig K-bentonites from Sell et al. (2013, 2015). M4/M5 sequence boundary and lithological changes based on Holland and Patzkowsky (1996).

   Above the Attalla, the character of the strata changes gradually upsection, with the occurrence of more open shelf and slope carbonates, and even some buildups. In the area of today's stops, most of these strata are placed into the Chickamauga Limestone undivided because facies changes and erosional truncation has removed the upper part of the sequence (Red Mountain Expressway) or the Chickamauga Group and its component Stones River and overlying Nashville Limestones (Tidwell Hollow), with the later Katian strata being split out as the Sequatchie Formation (Fig. 2).

   At over 60 m in elevation change from the crest of Red Mountain to the roadbed, the Red Mountain Expressway cut is the deepest highway cut in this region (Fig. 5), and it exposes over 200 meters of section from Upper Cambrian carbonates of the Copper Ridge Formation to Lower Mississippian cherts of the Fort Payne Formation, a stratigraphic thickness that includes the approximately 75 meters of Chickamauga Limestone. The Chickamauga Limestone at the Red Mountain Expressway records deposition in a more open marine and deeper shelf setting, whereas the equivalent but much thicker stratigraphic interval at Tidwell Hollow includes many beds deposited in shallower, peritidal settings. The oldest Chickamauga limestones that overlie the Attalla are now mostly covered by ~45 years of vegetation growth and slope retreat at the northwest end of the deep cut, but they include about 7 m of fenestral lime mudstones and mudcracked algal laminates that were deposited in supratidal and intertidal environments. These are overlain by about 70 m of bioclastic and peloidal wackestones and packstones, with several thin grainstones. Some intervals are noticeably argillaceous, and these tend to be characterized by nodular bedding. Fossil abundance and diversity varies, with some beds containing a restricted fauna of ostracodes and gastropods, whereas many other beds have a diverse open marine fauna that includes crinoids, brachiopods, trilobites, bryozoans, calcareous algae, stromatoporoids, corals, and mollusks.

   The long roadcut at Tidwell Hollow is the most complete and extensive exposure of the limestones of the Chickamauga Group in Alabama. The carbonate lithologies that occur in the almost 200 m thick section of Chickamauga Group limestones include lime mudstones and dolomites, some of which are mudcracked, burrowed, and/or fenestral, with some ostracodes and gastropods, and which alternate with peloidal and bioclastic wackestones, packstones, and some grainstones that have a more diverse assemblage of crinoids, bryozoans, trilobites, tabulate corals, calcareous red algae, and brachiopods. Oolitic, oncoidal, and intraclastic packstones and grainstones are present as well. Low-angle cross-bedding occurs in some of the skeletal grainstones, and other sedimentary structures include nodular bedding, horizontal and wavy lamination, ripples, and thin to thick beds, with some beds having a lenticular to almost wedge-shaped character.

   Of note is that at both the Red Mountain Expressway and Tidwell Hollow sections, small mud-rich bioherms are present, and they consist of a diverse assemblage of bryozoans, sponges, brachiopods, corals and stromatoporoids, and some calcareous algae.

   The Deicke and Millbrig K-bentonites, with their distinctive phenocrystic mineralogical assemblages, are also present at both sections, and provide time lines for correlation (Fig. 5-7).
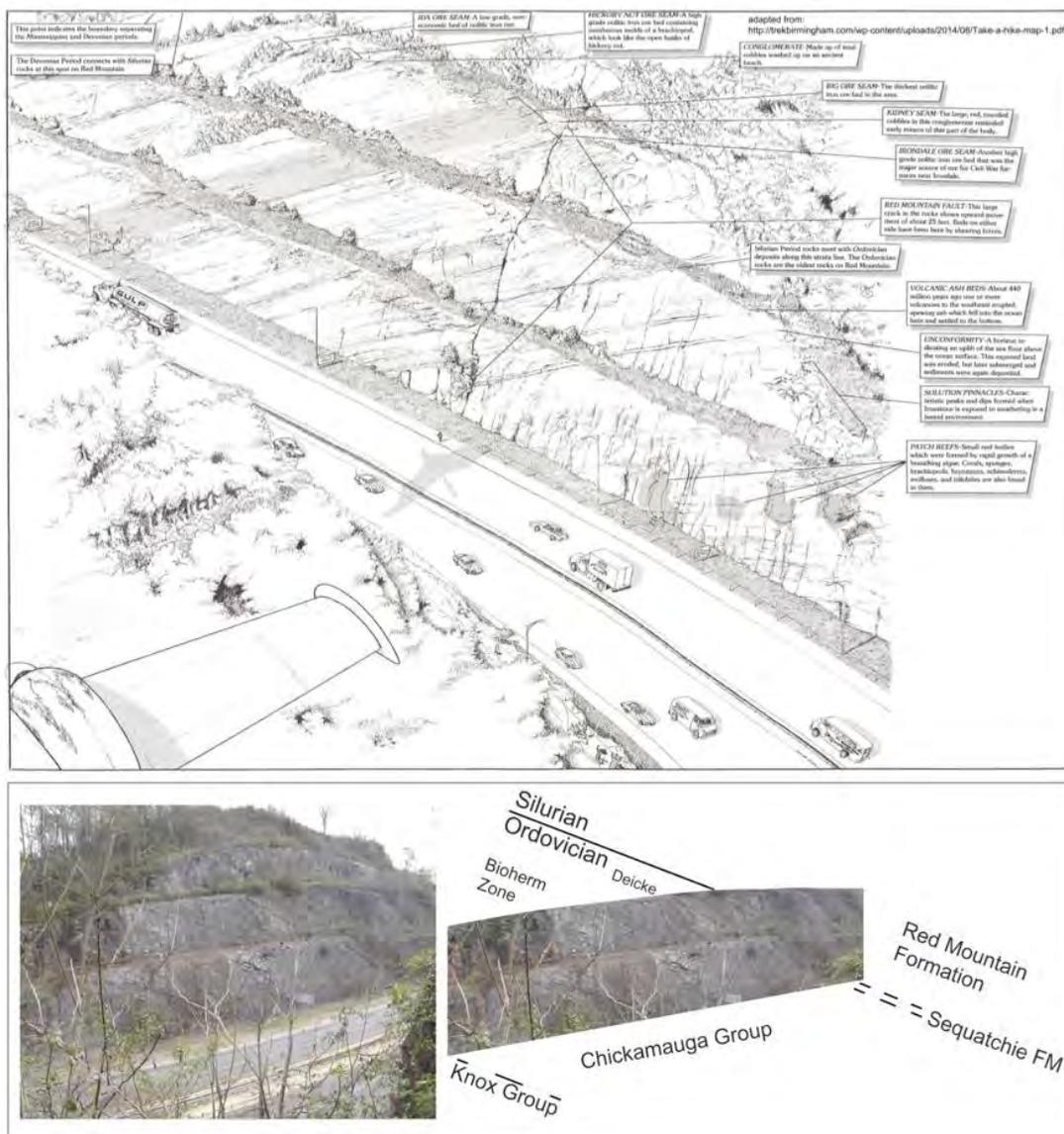
Figure 5.—The Red Mountain Expressway roadcut in Birmingham, Alabama. Top: sketch of major features that can be seen in the south side of the roadcut. Bottom: view of the north side of the cut, which is Stop 1-1, where we will examine Ordovician carbonates and the Deicke and Millbrig K-bentonites. The Ordovician-Silurian boundary at this stop is an angular unconformity with an angle of 1.6° between the Upper Ordovician Sequatchie Formation and the Lower Silurian Red Mountain Formation.

At the Red Mountain Expressway both occur in the nodular bedded argillaceous limestones of the uppermost Chickamauga Limestone. The Deicke is a distinct bed but the Millbrig is a biotite-rich bentonitic zone (Haynes, 1994), suggesting that the Millbrig tephra was either deposited and then reworked, most likely by scouring from the deeper wave base associated with storms on the shelf, or, that the Millbrig is in fact comprised of multiple and separate tephras (Huff et al., 2004). By contrast, both K-bentonites are discrete beds at Tidwell Hollow, where
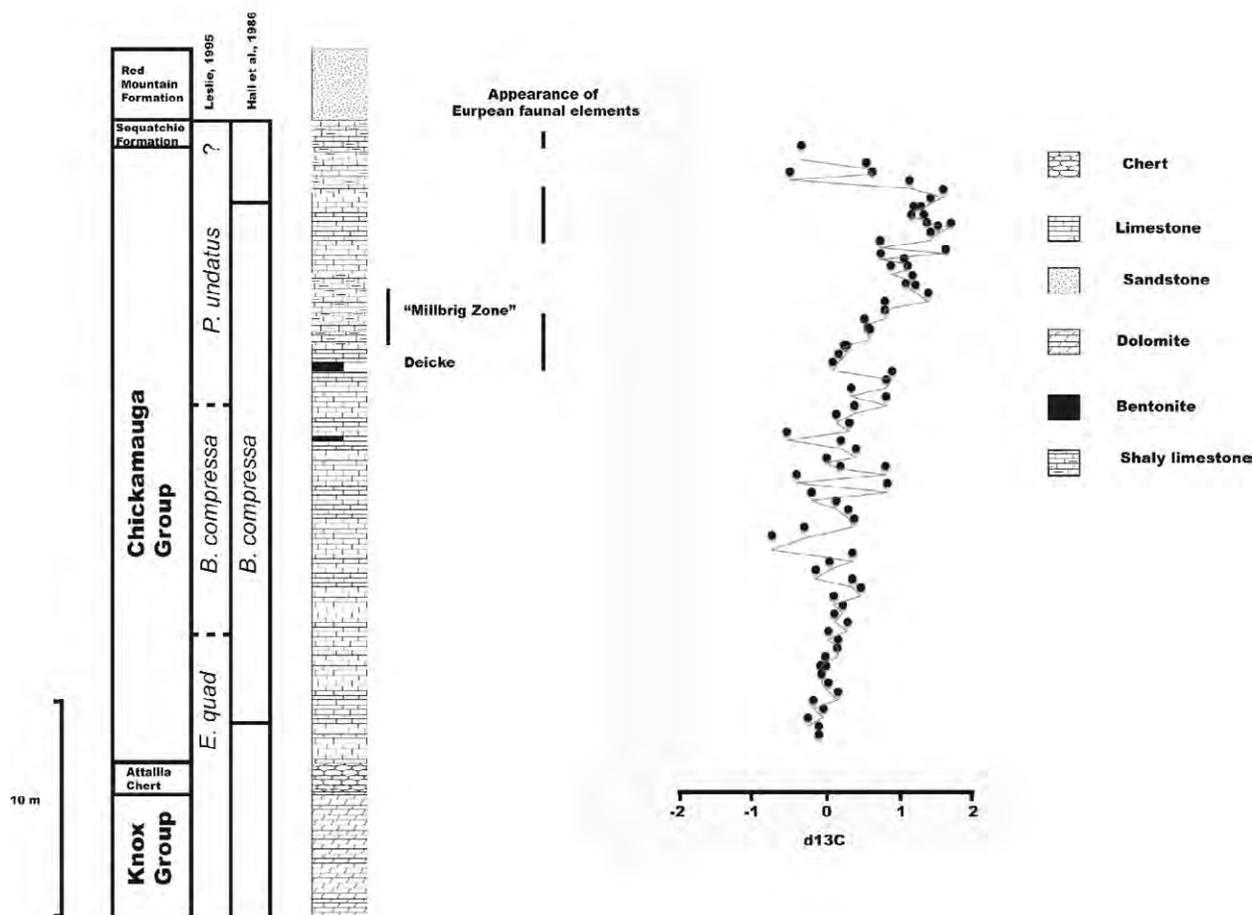
Figure 6.—Lithology, stratigraphy and carbon isotope data at the Red Mountain Expressway. Carbon isotopes from Quinton et al. (in review). 3-point average. Lithology and European faunal data from Raymond et al. (1986).

they occur in the upper few meters of the Stones River Limestone, with the Millbrig occurring right at the contact of the Stones River and Nashville Limestones. This contact would seem to correlate with the M4-M5 sequence boundary of Holland and Patzkowsky (1996) as defined in the cratonic interior sections of the Nashville and Jessamine Domes of Tennessee and Kentucky, respectively. Yet at the Red Mountain Expressway, there is no obvious lithologic break that would likewise seem to correlate with the M4-M5 boundary, nor can an obvious M4-M5 boundary be identified at Alexander Gap. Difficulties associated with identifying sequence boundaries across the midcontinent have been addressed and scrutinized previously by Pope and Read (1997) and Kolata et al. (1998), and the problem of locating any of the sequence boundaries of Holland and Patzkowsky (1996) in the Blount foreland basin sections, when the various boundaries were originally defined at cratonic sections, will be addressed at a number of the stops on this trip. We suggest that perhaps eustatic sealevel changes influenced stratal architecture far less in the flysch and molasse deposits of the Blount foredeep than in the cratonic
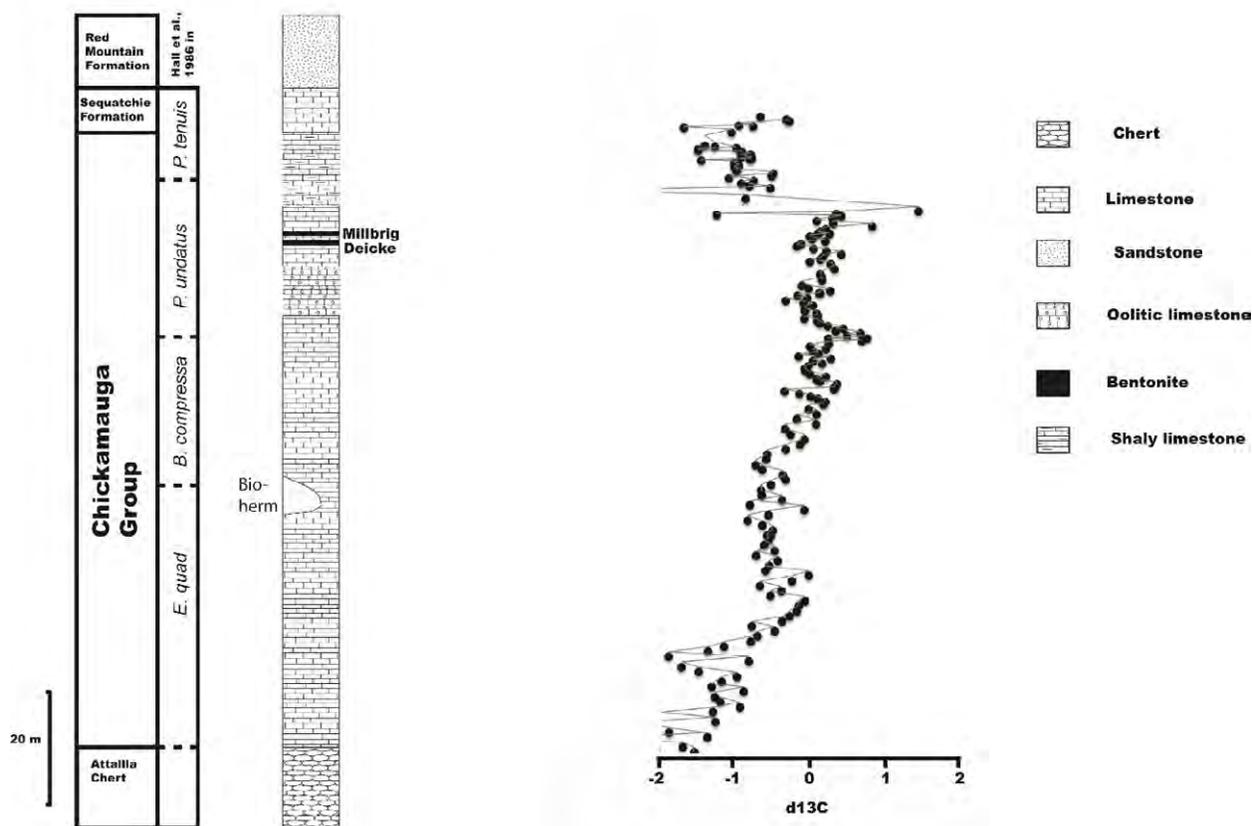
Figure 7.—Lithology, stratigraphy, and carbon isotopes at Tidwell Hollow. Carbon isotopes from Quinton et al. (in review). 3-point average. Location of Millbrig from Haynes (1994). Location of Deicke based on field observations of Haynes and Herrmann.

sequences, because in the depositional environments that were most proximal to the Blount orogenic highlands tectonic influences may have very likely overwhelmed the eustatic signals in the depositional sequence, but in the distal cratonic sequences, the eustatic signals were dominant.

Recently, Quinton et al. (in review) measured bulk carbonate $\delta^{13}C$ and $\delta^{18}O$ as well as organic carbon $\delta^{13}C$ values from four locations in Alabama (in addition to Tidwell Hollow, Red Mountain Expressway, and Fort Payne, samples from an exposure north of Gadsden at Big Ridge were analyzed, but we will not visit that outcrop on this trip). The Deicke and Millbrig K−bentonites have been identified in these sections (Haynes, 1994), and they can be used for precise correlation between sections and to evaluate the exact timing of the isotope curve among the different sites. $\delta^{13}C$ results from Fort Payne and Gadsden record an ~1‰ positive excursion following the Millbrig K−bentonite. The other two sites, Tidwell Hollow and Red Mountain expressway, both located near the continental margin, a ~2‰ negative excursion follows the Millbrig K-bentonite. Currently, the lack of a GICE signature is attributed to a hiatus spanning the GICE interval. The presence of a hiatus is also suggested by the conodont biostratigraphy of the different sites (Table 1 and 2; personal communication S. Leslie, 2015).

	Drepanoistodus suberectus	*Panderodus Gracilis*	*Curtognathus sp.*	*Erismodus sp. cf E. radicans*	*Phragmodus undatus*	*Belodina compressa*	*Dapsilodus aff. D.mutatus*	*Plectodina/Aphelognathus?*	*Aphelognathuss ap. Aff. A. grandis*	*Yaoxianognathus abruptus*	*Apheognathus kimmswickensis*	*Oulodus subundulatus*	*Plectodina sp*	*Oulodus sp.*	*Plectodina tenuis*	*Rhipidognathus symmetricus*	*Oulodus oregonia*	*Apheognathus politis*	Biozone
TH 25m					x						x				x	x	x	x	
TH 22.85											x				x	x	x	x	
TH 20m															x	x	?	?	*P. tenuis or higher*
TH 18.5 m												x			x	?	x	x	
TH 16m		x									x			x		?			
TH 11m	x										x	x	x						
TH 10.5 m		x			x			x	x	x									
TH 8m		x	x	x				x											*P. undatus Zone*
TH 0m	x	x	x	x	x	x	x												

Table 1.—Conodont fauna distributions for Red Mountain Expressway (from Quinton et al., in review).

	Drepanoistodus suberectus	*Panderodus gracilis*	*Phragmodus undatus*	*Belodina compressa*	*Oistodus venustus*	*Dapsilodus aff. D.mutatus*	*Plectodina sp.*	*Yaoxianognthus abruptus*	*Icriodella superba*	BioZone
RM 10.5		x	x						x	
RM 10	x		x							
RM 9.5	x		x						x	
RM 8.97	x	x	x					?	x	
RM 8.5	x		x			x				
RM 8	x	x	x			x		?		
RM 7.5										
RM 7.05			x							
RM 7	x		x					x	x	
RM 6	x		x						x	P. undatus
RM 5.25	x	x	x	x				x	x	
RM 5	x	x	x	x				x	x	
RM 4.55			x							
RM 4	x		x	x					x	
RM 3.55			x	x					x	
RM 3.5			x					x	x	
RM 3.45	x	x	x	x				x	x	
RM 2	x	x	x	x		x		x		
RM 1.5	x	x	x	x				x		
RM 1	x	x	x	x				x		
RM 0.9	x		x	?				x		
RM 0.5				x						
RM 0	x	x	x	x	x	x	x			

Table 2.—Conodont data for Red Mountain Expressway (from Quinton et al., in review).

STOP 1-1: Red Mountain Expressway section, Birmingham AL; 8:30 – 10:30 am (120 mins)

At this stop (Fig. 5), trip participants will be introduced to some of the important ideas regarding Ordovician strata in the Southern Appalachians, with an ~15-20 minute overview of litho-, bio-, chrono-, and sequence stratigraphy, isotope geochemistry, paleoclimate, facies relations, carbonate buildups, K-bentonites, and paleoecology. We will discuss this exposure in particular, as well as regional Ordovician relationships in general. As we walk upsection along the walkway, we will point out the changes in lithology that occur, while also highlighting the ongoing isotopic work to identify isotope excursions (Fig. 6), as well as various aspects of paleoclimate, the Taconic orogeny, Ordovician volcanism and the tephras that have become the Deicke and Millbrig K-bentonites including an overview of their mineralogy and petrology, and then finally, the extreme thinness of the Sequatchie? Fernvale? Formation here. Participants are also encouraged to walk upsection to view and collect the world-famous ironstones of the Silurian Red Mountain Formation, in addition to any Ordovician samples.

STOP 1-2: Tidwell Hollow section along Blount County Highway 15, ~5 miles SW of Oneonta, AL; 12:30 – 2:30 pm (120 mins)

At this exposure, we will focus more provincially on a sequence of primarily platform carbonates that were deposited along the Laurentian margin. The first stop will be at the Attalla Chert Conglomerate, near the base of the section, to see limited exposures of the cherty rubble that accumulated over a wide area of the paleokarst surface of the Knox unconformity. From there we will go upsection into the younger strata that are far more extensively exposed. We will be able to examine small buildups of bryozoans, sponges, corals, and stromatoporoids, along with other facies that accumulated in the shelf and peritidal environments that were prevalent in this area. Discussion will center on the isotopic and paleoclimate work currently being done (Fig. 7), which includes the search for the Guttenberg Isotopic Carbon Excursion (GICE). The importance of the Deicke and Millbrig K-bentonites as reference horizons for that work will be discussed (Fig. 2), and we will see the distinctive biotite-rich middle zone of the Millbrig and discuss how crystal-rich (vs. vitric-rich) the original tephra was as compared to many or most other K-bentonites in this region and elsewhere. We will also discuss the similarities and differences of the Tidwell Hollow section and sections to the north on the Nashville Dome, especially regarding the sequence boundaries of Holland and Patzkowsky (1996), i.e., the M3, M4, M5 etc., and the problems that arise when attempts to extend cratonic sequence architecture into proximal, molasse deposits of the Taconic foredeep, vs. more distal, flysch deposits in the Taconic foredeep, where eustatic signals have been recognized and correlated (Joy et al., 2000; Brett et al., 2004; Mitchell et al., 2004). The Ordovician – Silurian boundary is not exposed here, but we note that the very thick ironstones of the Silurian Red Mountain Formation that we saw at Stop 1-1 are here reduced in thickness to just a 6-8 cm thick ironstone that is exposed to the northwest along the road (Fig. 8).
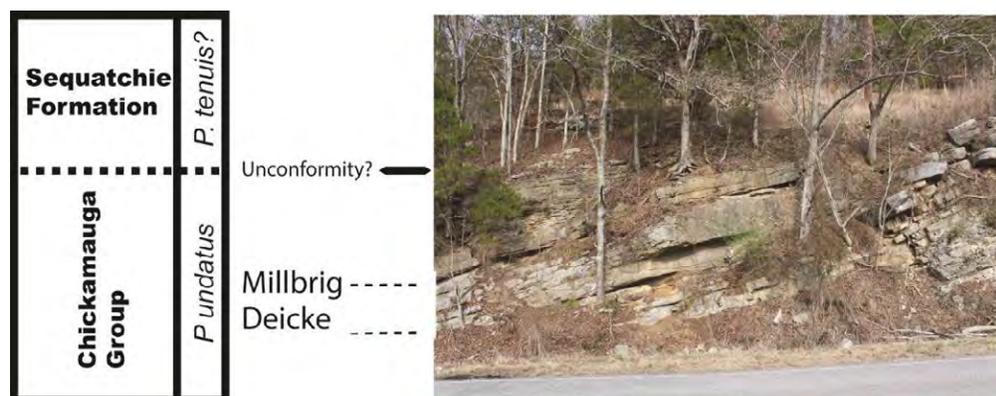
Figure 8.—The stratigraphic interval in which the Deicke and Millbrig K-bentonites occur at Tidwell Hollow. Based on lithologic change and conodont zones, it appears that an previously unidentified unconformity is present, and as a result the GICE interval is missing at the Tidwell Hollow section.

The Ordovician siliciclastic succession southeast of the Helena Thrust

On a regional scale, carbonate sedimentation persisted throughout what is now the southern Appalachians until the onset of tectonic activity associated with the Taconic orogeny (Read and Repetski, 2012), when the southeastern edge of the Laurentian carbonate shelf began to subside and foreland basins developed on what had been shallow continental shelf margin environments. The collision of Laurentia with the Taconic microplates and terranes occurred first in the southern Appalachians from Alabama northeastward to west-central Virginia in what is widely referred to as the Blountian phase of the Taconic orogeny, a deformational event that produced the Blount foredeep (Rodgers, 1971; Drake et al., 1989). In Alabama, development of the Blount foredeep occurred in late Darriwilian to early Sandbian time. The change is evident in sections south and east of Birmingham, where shelf limestones of the Lenoir, Pratt Ferry, and Little Oak Limestones are overlain by black graptolitic mudrocks of the Athens and Columbiana Shales (Fig. 3, not seen on this trip) that were deposited in basinal environments.

When the Blount foredeep filled with these flysch deposits, a molasse sequence of redbeds and quartz arenites prograded west and northwest from the perimeter of the Blount highlands across the now-filled foredeep, and these marginal marine to transitional and non-marine sediments of the Bays Formation and its lateral equivalents extend from north-central Alabama to west-central Virginia. At Alexander Gap, we will see the Colvin Mountain Sandstone, a sequence of mature quartz arenites, some pebbly zones as well as some prominent cross-bedded intervals. These quartz arenites are underlain and overlain by redbeds, which include siltstones and shales, some of which are calcareous.

STOP 1-3: Alexander Gap, and roadcut through Colvin Mountain along the E side of northbound US Highway 431, Glencoe, AL; 3:45– 4:45 pm (60 mins)

This stop will introduce the group to the redbeds and quartz arenites and conglomerates of the molasse that prograded over the now-filled Blount foredeep, and which represent the first pulse of siliciclastic sediments deposited in various fluvial-deltaic-beach-coastal environments. The gradational contact of the upper several meters of Greensport Formation redbeds (primarily mudrocks) with the coarser and more mature quartzose beds of the overlying ~20 m thick Colvin Mountain Sandstone will be observed, as will both the Deicke and Millbrig K-bentonites in the upper several meters of the quartz arenites of the Colvin Mountain Sandstone (Table 3). The presence of quartz sandstones both above and below the Deicke and Millbrig is an important stratigraphic relationship (Fig. 9), and one that will be referred to at other stops in the next couple of days where the two K-bentonites occur in the Blount molasse. Diagenetic alteration of the tephras in the sandstone has occurred along a different pathway than in the carbonate sections to the northwest (Haynes, 1994); the feldspars are extensively kaolinized, and the biotite in the Millbrig is gone, but the ilmenites in the lower Deicke are little altered, and as discussed below in more detail at Stop 2-2, that is the case in the Deicke throughout the region where it occurs in the redbeds and quartz arenites of the Blount molasse (Haynes and Melson, 1997).
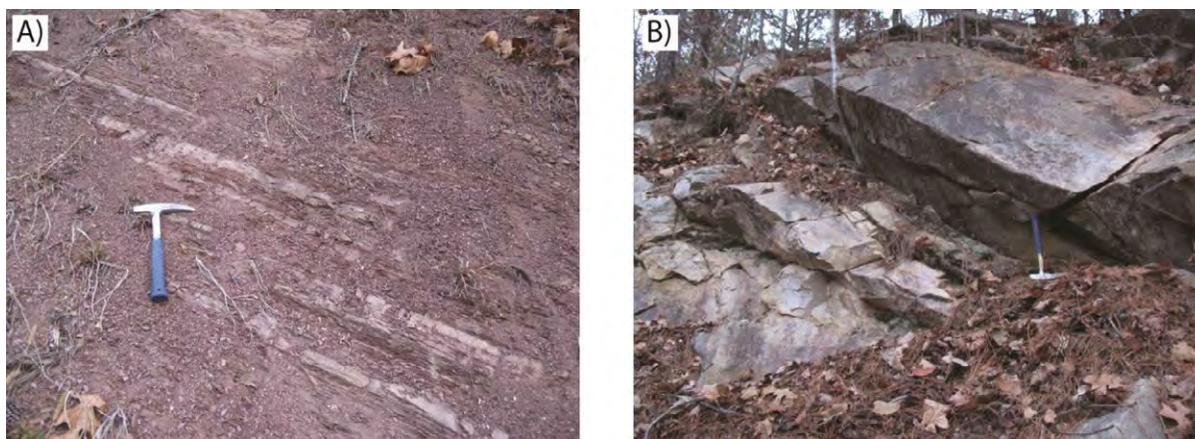
Figure 9.—(A) Redbeds of the Greensport Formation at Alexander Gap. (B) The Deicke K-bentonite as identified by Haynes (1994) in the cross-bedded quartz arenites of the Colvin Mountain Sandstone at Alexander Gap.

Underlying the quartz arenites of the Colvin Mountain Sandstone are several meters of the red mudrocks that comprise the Greensport Formation, which in this region ranges in thickness from 60 to 75 m, with a variety of sedimentary structures (ripple marks, flaser bedding, burrows, desiccation cracks) that point to deposition in peritidal environments ranging from shallow shelf to supratidal mud flats (Benson and Mink, 1983). The sandstones of the Colvin Mountain include planar and trough cross-bedding, planar laminae that are bedding parallel to

Table. 3.—Measured section of Colvin Mountain Sandstone Member at Alexander Gap along the east side of the cut through the gap along northbound U.S. Highway 431, Calhoun Co., Ala. Alexander Gap section: measured top down beginning at uppermost quartz arenite bed "Sequatchie" Formation. 1436 Measurements made by J. Haynes in 2003.

Bed

43   Some redbeds above the uppermost quartz arenites (we agree with the speculation of J. Dennison, which is that this actually not the Sequatchie, but the upper redbeds of the Bays Formation, and that there is no unconformity at the top of the Colvin Mountain: "the redbed sequence may be Middle Ordovician, analogous to the upper redbed sequence of the Bays Mountains of Tennessee, where redbeds underlie the Martinsburg Shale (Reedsville Formation of some authors) and overlie a middle whitish sandstone of the Bays Formation, which in turn overlies a lower redbed sequence of the Bays Formation.") .... .not measured

Colvin Mountain Sandstone Total estimated thickness: 63.25 ft.

Unless noted otherwise, all cross bedding is tangential, S to N paleocurrent direction

42 Med. bedded yellowish med. ss., planar lamination .... .5 in

41 Med. ss., cross beds and some planar lamination ....1 ft 4 in

40 Med. ss, planar lamination .... 7 in

39 Med. ss., planar lamination .... 6 in

38 Med. ss., cross beds... 7 in

37 Med. ss, planar lamination ....1 ft 1 in

36 Med. ss., cross-bedded 5 in. above base ....2 ft

35 Med. ss., cross bedding in lower 6 in., with sharp top to cross beds,

rusty oxidation color to bed (photo # 3243).. 11 in

34 Med. ss., planar lamination .... 6 in

33 Med. ss., planar lamination (photo # 3242) .... 8 in

32 Millbrig K-bentonite ....3 ft 4 in

Pale blue gray coarse tuffaceous zone, but no obvious biotite .... 4 in

Pale blue gray clay, no obvious structure ....3 ft

31 Med. ss., planar lamination .... 8 in

30 Med. ss., cross bedding in 8 in. to 16 in. interval above base...2 ft 1 in

29 Med. ss., planar lamination .... 10 in

28 Med. ss., splits into a 12 in. and 5 in. bed along outcrop ....1 ft 5 in

27 Massive yellowish white med. to crs. ss ....4 ft 4 in

26 Massive yellowish white med. to crs. ss ....1 ft 10 in

25 Massive yellowish white med. to crs. ss ....1 ft 5 in

24 Massive yellowish white med. to crs. ss .... 8 in

23 Massive yellowish white med. to crs. ss ....1 ft 6 in

22 Massive yellowish white med. to crs. ss., rusty oxidation zone at base.............................1 ft 4 in

21 Massive yellowish white med. to crs. ss., lowest sandstone in the exposure

that is not obviously white on the weathered surface ....1 ft 3 in

20 Massive white med. to crs. ss, trough cross bedded... 6 in

19 Deicke K-bentonite ....1 ft 2 in

Pale blue gray clay with small shiny black ilmenite grains and small bright green zones,

medium gray and heavily pyritized at ditch level but not higher up on exposure

18 Massive very hard silicified and rusty oxidized med. ss.. 1-2 in

17 Massive white cross-bedded med. ss. .... 6 in

16 Massive white cross-bedded med. ss., with channel? form .... 1 ft 6 in

15 Massive white med. ss., light gray 13 in. zone 21 in. below top; cross-beds
with microslump? (photo # 3246) in 5 in. oxidized zone 7 in. above base..5 ft 6 in

14 Massive white med. ss ....2 ft

13 Massive white med. ss ....3 ft 4 in

12 Massive white med. ss., cross bedded...2 ft 11 in

11 Massive white med. ss., distinct cross-bedding pattern (photo # 3236)... 3 ft 8 in

10 Blocky white med. ss. with rusty spots... 18 in

9 Thin to medium bedded white med. ss ....1 ft 8 in

8 Massive white med. ss .... 7 in

7 Massive fn. to med. ss., basal 3 in. is remarkably porcelaneous, quartzite-like .... 10 in

6 Massive white crs. ss., less indurated than overlying bed, but still hard... 7 in

5 Massive white med. ss., cross-bedded ....1 ft

4 Massive white v. crs. ss., slightly crumbly, planar lamination .... 7 in

3 Massive white crs. ss., with granules in lenses 5 to 6 in above
base (photo # 3234)... 1 ft 5 in

2 Massive white v. crs. ss., with granules in basal 6 in..2 ft

1 Massive white med. to crs. ss., both planar and cross bedding; some heavy
mineral laminae? outlining laminations..2 ft 4 in

Greensport Formation (or Shale Mbr. of Bays?) .... not measured

[Jenkins (1984) measured the Greensport, which here is/was very well exposed for quite some
distance along the road, and consists of red shale with noticeable yellow laminae and thin
beds throughout (e.g. photo # 1987, 1988, 3250, 3251, 3252, & 3253), but the upper 5+ feet
is noticeably transitional with the Colvin Mountain Sandstone (photo # 3247, 3248, and
3249) and maybe ought to be included in the Colvin Mountain, as it is thin bedded and silty
to fine sandstones, but NOT RED. Low-angle cross-laminated, *Skolithos*, and some ripple marks
including oscillation ripples, leading Benson and Mink (1983), and Bayona and Thomas (2003, 2006) to
interpret the Colvin Mountain as a sequence of shoaling shallow-marine sand bars.]

  Overlying the Colvin Mountain Sandstone is another redbed sequence that we will also
examine because there is yet some controversy as to the stratigraphic assignment (age and
position) of these younger redbeds (Fig. 9a). They have been identified variously as the
Sequatchie Formation (Benson and Mink, 1983; Carter and Chowns, 1989) or as redbeds that are
older than the Sequatchie and which are equivalent to the redbeds of the upper Bays Formation
farther northeast in Tennessee and Virginia (Dennison, 1991). If these redbeds above the Colvin
Mountain Sandstone are the Sequatchie Formation, then an unconformity occurs at the top of the
Colvin Mountain Sandstone that cuts out the intervening pre-Sequatchie age Ordovician strata,
which would include equivalents of the "Trenton" and Reedsville Formations, as well as the
regionally extensive *Orthorhynchula* zone at the Reedsville – Sequatchie contact.

The lack of any obvious unconformable relations between the uppermost bed of the Colvin Mountain Sandstone and the redbeds that overlie it, along with the presence of the Deicke and Millbrig K-bentonites in the upper few meters of the Colvin Mountain Sandstone, suggest to us that these overlying redbeds are in fact NOT the Sequatchie Formation, but are as Dennison (1991) suggested instead, a lateral equivalent of the upper Bays Formation farther north. In the Bays Mountains of Tennessee and farther north along Big Walker Mountain in Virginia, redbeds of the Bays Formation sandwich one or several white quartz arenites of varying thickness, and the upper redbeds are overlain by the bioclastic grainstones and packstones of the "Trenton" Limestone or its equivalents (Haynes, 1994). Fossils are very scarce in these redbeds, but brachiopods of Trenton character occur in similar redbeds along Rocky Face Mountain in Georgia at Stop 2-3 (R. Neuman, pers. comm.), which is about 120 km NNE of Alexander Gap. At this stop, we will also expand on our dialog about the uncertain nature of how the sequence stratigraphic framework from cratonic sections (M4-M5 etc. of the Nashville Dome area; Holland and Patzkowsky, 1996) might be recognized – or not – in the molasse deposits of the Blount foredeep.

DAY 2. ORDOVICIAN CARBONATE AND CLASTIC DEPOSITS ACROSS STRIKE FROM ALABAMA TO GEORGIA

Introduction

At today's stops we will examine four exposures of Ordovician strata, one in Alabama, and three in Georgia. The first stop (Ft. Payne, Stop 2-1) is essentially along strike with the Red Mountain Expressway and Tidwell Hollow stops (Stops 1-1 and 1-2) that we saw yesterday. However, at Ft. Payne we will examine in greater detail a critical stratigraphic interval in the carbonate platform sediments in the several meters below and above the contact of the upper laminated lime mudstones of the Stones River and the overlying fossiliferous grainstones to wackestones of the Nashville Group (Fig. 10). This stratigraphic interval includes the Deicke and Millbrig K-bentonites in the upper Stones River, and our discussion will emphasize new isotopic data obtained from analyses of samples collected across the contact, as well as continued discussion on this contact being equivalent to the M4-M5 sequence boundary in the Nashville area of central Tennessee. This will be a good opportunity to examine and collect some of the corals that thrived in the more open marine environments that characterized the Nashville Limestone (Fig. 10). These fossiliferous beds are in contrast to the underlying more restricted peritidal laminated limestones of the upper Stones River Limestone, which themselves are quite a contrast from the bioclastic grainstones and packstones that occur at the equivalent
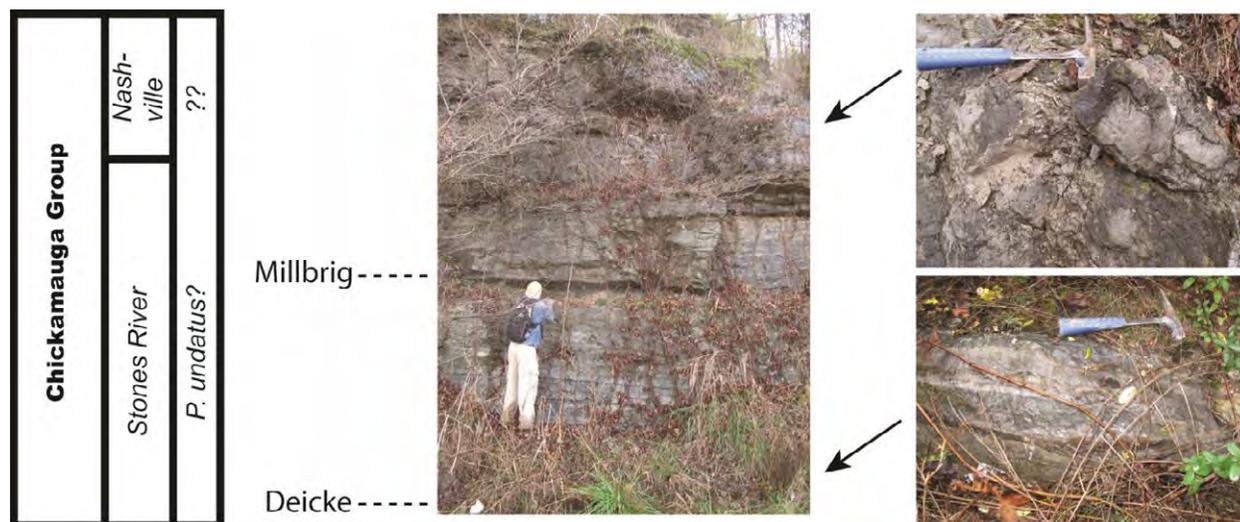
Figure 10.—The Deicke K-bentonite, which here is underlain by black chert up to 8-10 cm thick (lower right), is at the base of this outcrop. At this location, unlike at the Red Mountain Expressway farther south (Stop 1-1), the Chickamauga Group can be subdivided into two distinct formations, the Stones River Formation and the Nashville Formation. The contact between the two is perhaps correlative with the M4-M5 sequence boundary. There is a distinct lithologic change from the underlying laminated lime mudstones of the upper Stones River to the bioclastic packstones, grainstones, and boundstones of the lower Nashville, which here is fossil rich including several corals (*Tetradium? sp.*; upper right).

stratigraphic horizon in the Red Mountain Expressway exposure, as determined by using the Deicke and Millbrig K-bentonite beds as isochrons. The stops at Horseleg Mountain, near Rome, Georgia (Stop 2-2) and along Reed Road north of Dalton (Stop 2-4) are in the redbeds and quartz arenites of the Blount molasse, which we saw at Alexander Gap (Stop 1-3) at the end of the day yesterday. Important differences are the much thinner quartz arenites at both stops, the coarser grain size of the quartz arenites at Reed Road, and perhaps most significantly, the stratigraphic relations of the quartz arenites and the Deicke and Millbrig K-bentonites. At Alexander Gap (Stop 1-3), the K-bentonites were enclosed by thick cross-bedded quartz arenites of the Colvin Mountain Sandstone (Fig. 9), whereas at Horseleg Mountain, the Deicke is immediately beneath the Colvin Mountain Sandstone and it overlies the uppermost redbeds of the Greensport Formation (Fig. 11), and at Reed Road, both the Deicke and Millbrig are in redbeds downsection from the oldest pebbly quartz arenites that are tentatively correlated with the Colvin Mountain Sandstone on the basis of petrographic analysis. The Millbrig has not been definitively identified at Horseleg Mountain, but it may be a very weathered clay-rich zone in the redbeds upsection from the prominent ledge of the Colvin Mountain Sandstone. Again, as at Alexander Gap, the redbeds above the Colvin Mountain Sandstone are questionably correlated with the Sequatchie Formation (Chowns and Carter, 1983), but those redbeds may in fact be correlative instead with the upper redbeds of the Bays Formation farther north, as discussed yesterday at Alexander Gap.
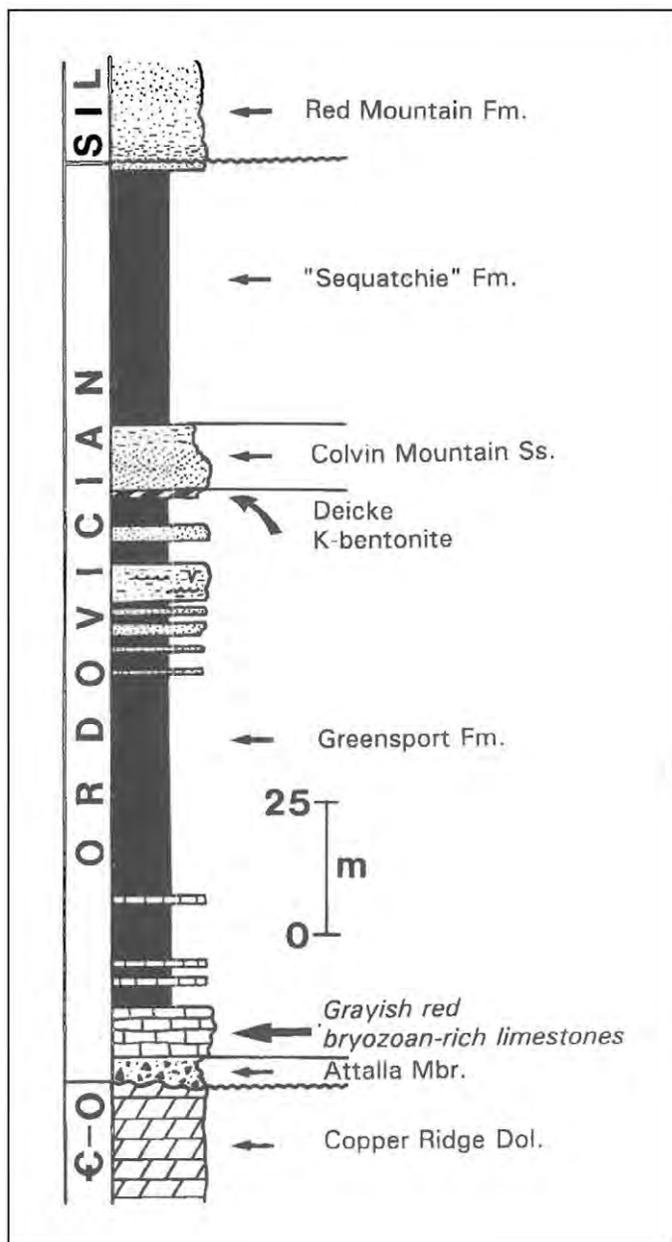
Figure 11.—Composite stratigraphic column of exposures on Horseleg Mountain, Stop 2-3, near Rome, GA.

The section at Horseleg Mountain will be our first look at the thin limestones that underlie the Greensport Formation redbeds and overlie the Attalla Chert Conglomerate. These may be correlative with the Lenoir Limestone, or as shown in Figure 2, they may be limestone beds within the Greensport Formation. The limestones are reddish brown from hematite that coats most of the framework grains and is also pervasive in the patchy micritic matrix. Most samples are skeletal packstones and grainstones that contain an abundance of bryozoans, with lesser calcareous red algae, and some brachiopods and trilobites as well.

The Deicke K-bentonite here at the Horseleg Mountain section yields appreciable quantities of ilmenite phenocrysts that are little altered (Fig. 12). Visually, they are still weakly magnetic, black, and shiny, with a metallic luster (Fig. 12C, D), and thus quite unlike the highly altered (to leucoxene) ilmenites in the Deicke obtained from exposures where that K-bentonite is in a carbonate sequence, such as at Tidwell Hollow and Fort Payne. The leucoxene pseudomorphs of ilmenite from Deicke samples in those and other carbonate sections are various shades of light brown, are non-magnetic, and they exhibit a more dull luster (Fig. 12E, F), but there is a continuum of textures between nearly unaltered ilmenites to the leucoxene pseudomorphs. Data obtained from electron microprobe analysis of several ilmenites from the Deicke here at Horseleg Mountain are compared with ilmenites separated from the Deicke at the Thorn Hill section in Tennessee and the Rockdell (Hayters Gap) section in Virginia (not seen on this trip), and with an ilmenite standard of Jarosewich et al. (1980). Our results (Fig. 13) show that although the ilmenites in the Deicke are compositionally different from the ilmenite standard that
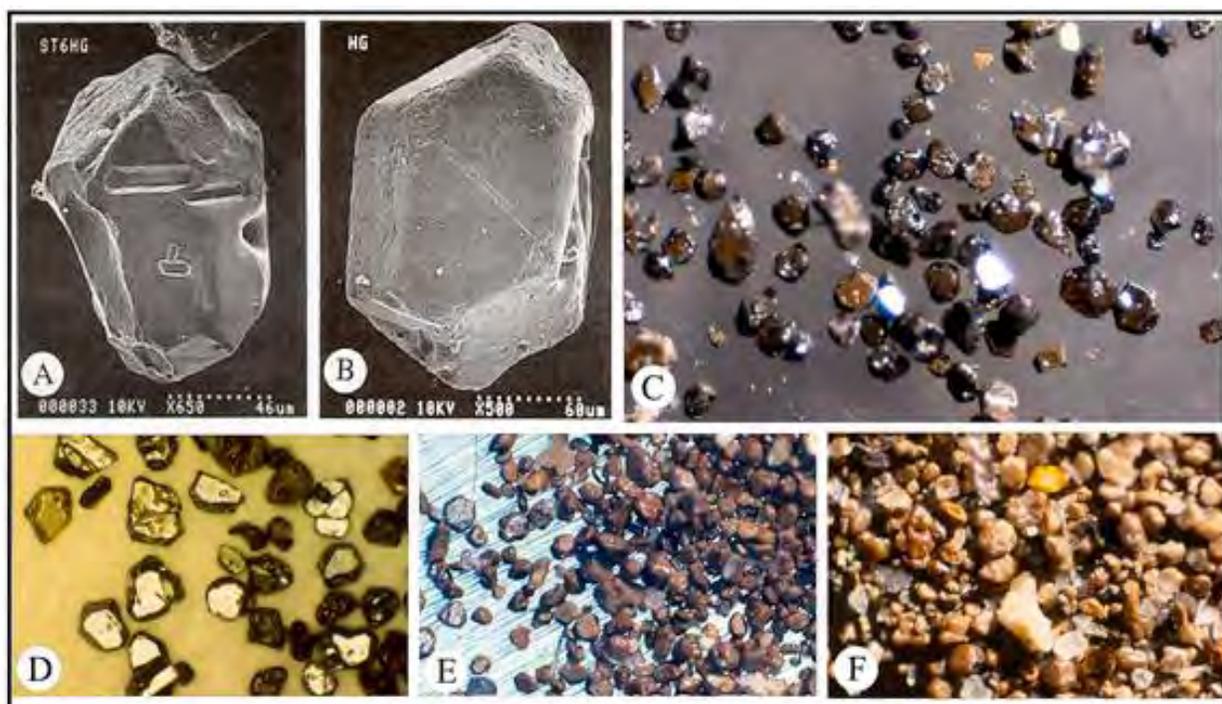
Figure 12.—**Ilmenite grains from the Deicke K-bentonite that exhibit some of the distinguishing textures observed in many samples. (A) Grooves in ilmenite where other mineral crystals, probably apatite, were originally present in the magma chamber and possibly during and after eruption of the tephra as well. Hayters Gap, near Rockdell, Virginia, (B) Euhedral ilmenite that, like the grain in (A), exhibits the hexagonal crystal shape that is common in ilmenite phenocrysts. Hayters Gap. (C) Reddish brown to dark brown to black weakly magnetic ilmenite grains, several of which exhibit a shiny metallic luster on the larger crystal faces. Hayters Gap. (D) Ilmenite grains that are very similar in texture to those from Hayters Gap in (C), with their metallic luster, black color, and weak movement in a magnetic field. Horseleg Mountain, near Rome, Georgia. (E) Ilmenite grains now partly altered to leucoxene. Citico Beach, Tennessee. (F) Ilmenite grains that are entirely altered to leucoxene, as evidenced by their dull luster, light brown color, and lack of response to a magnet. Frankfort, Kentucky.**

was used to monitor analytical precision, the Deicke ilmenites are nonetheless relatively consistent compositionally between this exposure near Rome, Georgia, the Thorn Hill exposure northwest of Knoxville, Tennessee, and the Hayters Gap exposure southeast of Rockdell, Virginia. So within limits, the ilmenite in Deicke samples from the Blount molasse has value as a correlation tool, along with other phenocrysts including feldspar and biotite (Haynes, 1994; Haynes et al., 1995, 1996), and apatite (Samson et al., 1988, 1995; Emerson et al., 2004; Sell and Samson, 2011; Sell et al., 2015).

It is worth noting that either phenocrystic ilmenite, or leucoxene pseudomorphs of original ilmenite phenocrysts, was obtained and analyzed from samples of the Deicke at 29 of the sections that were studied by Haynes (1994) throughout the eastern midcontinent, and in none of those samples was any evidence observed that would support the suggestion of Samson et al. (1988) that leucoxene in the Deicke might be an alteration product of biotite. Rather than invoking a biotite-to-leucoxene alteration process that "must be complex to remove most of the

Al, Si, Fe, and K from the biotite" (Samson et al., 1988), we suggest a simpler explanation, that the leucoxene is the product of an alteration process that starts with phenocrysts of ilmenite in the original Deicke tephra, which are far more abundant, and far larger, than the biotite grains in the Deicke of that region (Haynes, 1994; Haynes et al., 1995; Haynes and Melson, 1997), rather than with phenocrysts of biotite. Diagenetic removal of Fe^{2+} from originally volcanogenic ilmenite is a far less complex chemical process overall (Morad, 1988; Morad and AlDahan, 1986) than any of the alteration pathways suggested by Samson et al. (1988). In many phenocrystic ilmenite and authigenic leucoxene grains that we obtained from samples of the Deicke, embedded apatite crystals or rodlike grooves are present (Fig. 12A; Haynes and Melson, 1997, Fig. 3). These embedded apatites (or the grooves where embedded crystals had been present) are a petrographic characteristic that Samson et al. (1988) referenced as evidence that the authigenic leucoxene in Deicke samples was derived from alteration of biotite grains. Whereas it is true that some biotite grains in the Deicke (and the Millbrig) do contain apatite inclusions, as well as zircon inclusions (Haynes, 1994, Fig. 10), we nevertheless favor the much simpler chemical alteration process of primary ilmenite to authigenic leucoxene. That alteration pathway adequately explains the abundance of leucoxene in Deicke samples from dozens of sections throughout Kentucky, Tennessee, Alabama, Georgia, and Virginia (Haynes, 1994), and it is a pathway that is consistent with the abundance of nearly unaltered ilmenite phenocrysts in Deicke samples from the Blount molasse including samples from Alexander Gap and Horseleg Mountain (Haynes, 1994; Haynes and Melson, 1997).

The stop at Dug Gap (Stop 2-3) will be our first stop that is focused on the youngest Ordovician strata of this region. We will see what may be one of the most, or even the most, southerly occurrences of the regionally widespread *Orthorhynchula* biozone (known informally as just the *Orthorhynchula* zone), which separates the underlying Reedsville? Formation here from the overlying Sequatchie Formation (Fig. 14). This biozone, characterized by many densely clustered molds and casts of brachiopods including the large brachiopod *Orthorhynchula sp.*, especially *Orthorhynchula linneyi*, extends northward to Pennsylvania (Bretsky, 1969, 1970), and is a very useful stratigraphic marker horizon. The measured section of Dug Gap by Zeigler (1988) does not note the presence of any *Orthorhynchula*, and in fact our review of the literature indicates that the only mention of *Orthorhynchula* in Georgia are these two citations:
(1) Butts & Gildersleeve (1948, p. 33), who noted it in the "Maysville Fm" which they describe as a soft, tawny, clayey siliceous rock, and that *Orthorhynchula linneyi* was found on the road east of Trion at Narrows Gap on Taylor Ridge (that location is southwest of Dug Gap); Butts and Gildersleeve also state (p. 34):
"The Sequatchie is known to be present wherever its horizon crops out as far east as the northwest slope of White Oak Mountain, and its southward continuation, Taylor Ridge. It has not been observed, however, in the ridges carrying the Red Mountain formation east and south of Tunnel Hill to and including Lavender Mountain. It may be present in those areas, however, although unobserved."
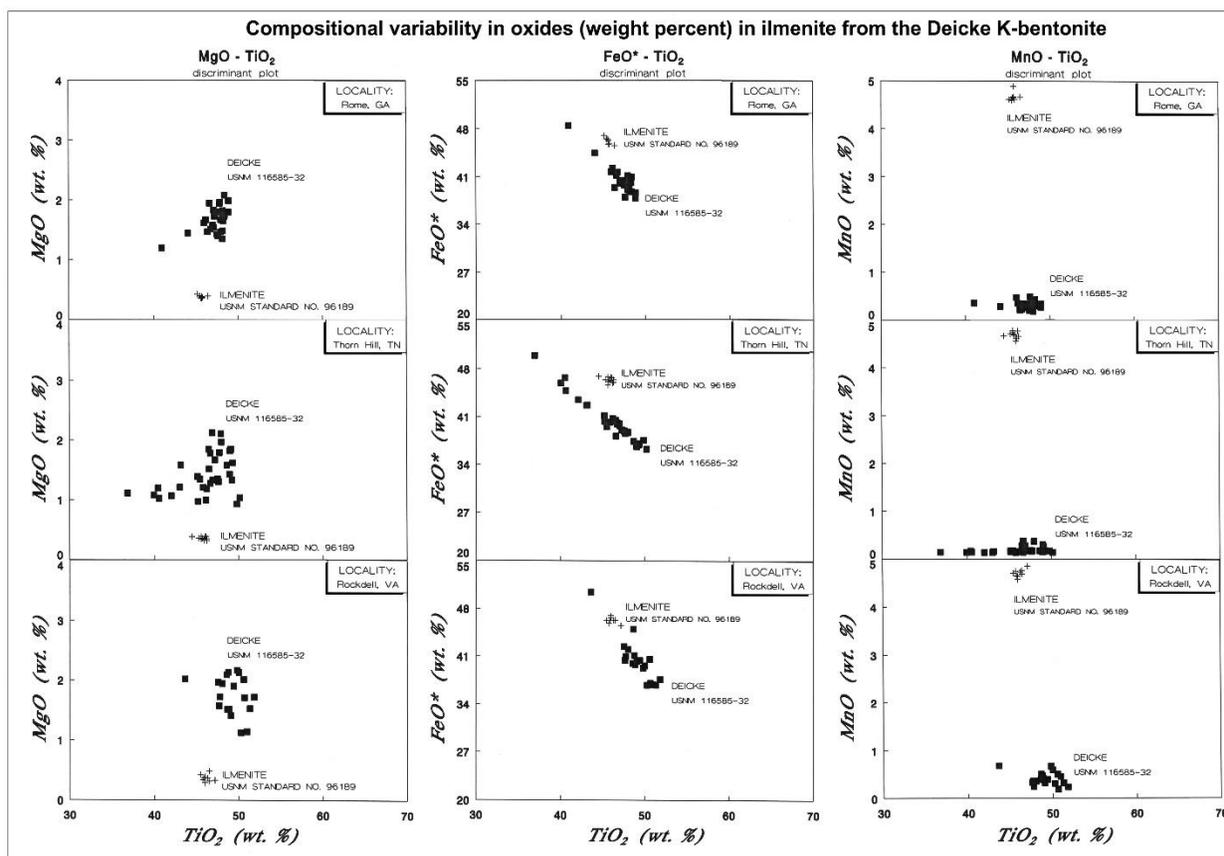
Figure 13.—Electron microprobe analyses of major elements (as oxides) in nearly unaltered ilmenite phenocrysts from samples of the Deicke K-bentonite at 3 localities: Horseleg Mountain, near Rome, Georgia, Thorn Hill, Tennessee, and Hayters Gap, near Rockdell, Virginia. Horseleg Mountain and Hayters Gap are about 420 km apart, and yet the compositional trends in the ilmenites are quite constant over that distance, which represents about ¾ of the along-strike extent of the Blount foredeep.

And this comment suggests to us that the exposure of the *Orthorhynchula* zone here at Dug Gap was not seen by Butts and Gildersleeve:

 (2) Allen and Lester (1957, p. 17, 19, 51), who list *Orthorhynchula* in an exposure at Dunaway Gap on Horn Mountain, to the south of Dug Gap, and in many of the carbonate sections to the northwest. Unfortunately, Allen and Lester (1957) did not list which fossils came from which specific exposures, so their faunal lists are now of somewhat limited value.

  Uphill and upsection from the exposure of the *Orthorhynchula* zone is an exposure of the Sequatchie Formation that we will examine. We will note how the Sequatchie differs from what we saw in the equivalent stratigraphic interval at Stop 1-1 in the Red Mountain Expressway exposure, as well as what we saw above the Colvin Mountain Sandstone at Alexander Gap. In addition, we will discuss the relationship of the Sequatchie to the Juniata and Oswego Formations farther north. This exposure will be our introduction to the significance of these three stratigraphic units in the Ordovician of the Appalachians from New York and Pennsylvania

Figure 14.—The *Orthorhynchula* zone at Dug Gap, with the characteristic dense abundance of brachiopods, both molds and casts, along discrete bedding planes. Inset at upper left shows the exposure at Dug Gap. Inset at lower right shows several brachiopod molds from samples collected at this location, which we will see at Stop 2-3.

southward to right here at Dug Gap, specifically to the importance of those units as principal components of the younger Queenston molasse that prograded over the main Taconic foredeep, which had by that time shoaled to near sea level. The Sequatchie-Oswego-Juniata interval records the second pulse of fluvial-deltaic-coastal molasse clastics associated with the Taconic orogeny, and sediment generated thusly (the aforementioned Queenston molasse) was dispersed over a far larger area than the earlier Blount molasse, which, as we have already seen yesterday at Stops 1-2 and 1-3, did not even reach across the width of the present-day folded Appalachians of the Valley and Ridge province. By contrast, the Sequatchie-Oswego-Juniata sediments extend west of the Valley and Ridge and into the subsurface of the Appalachian basin. We will be highlighting the presence of strata associated with the Blount molasse and of younger strata associated with the Queenston molasse at Dug Gap and the preceding stop at Horseleg Mountain (Stop 2-2) as well as the final stop of the day at Reed Road (Stop 2-4) just north of Dalton (Fig. 15).

STOP 2-1: Ft. Payne, AL, at Exit 222 on I-59; exposures along entrance ramp to northbound I-59 and just to north on E side of I-59 N; 8:30 – 10:00 am (90 mins)

At this stop we will begin with a recap of what we have seen thus far regarding stratigraphy, isotope geochemistry, paleoclimate, facies relations, carbonate buildups, K-bentonites, and paleoecology of the Ordovician carbonates in this region. As we did at Tidwell Hollow (Stop 1-2), this stop will also include discussion of current and ongoing isotopic work on carbon isotope excursions, and on various aspects of climatic changes in the later Ordovician. We will examine excellent exposures of the upper few meters of the Stones River Limestone, and the associated outstanding exposures of relatively thick sections of both the Deicke and Millbrig K-bentonites, as well as one or two thinner K-bentonites, in the Stones River (Fig. 10). The contact of the
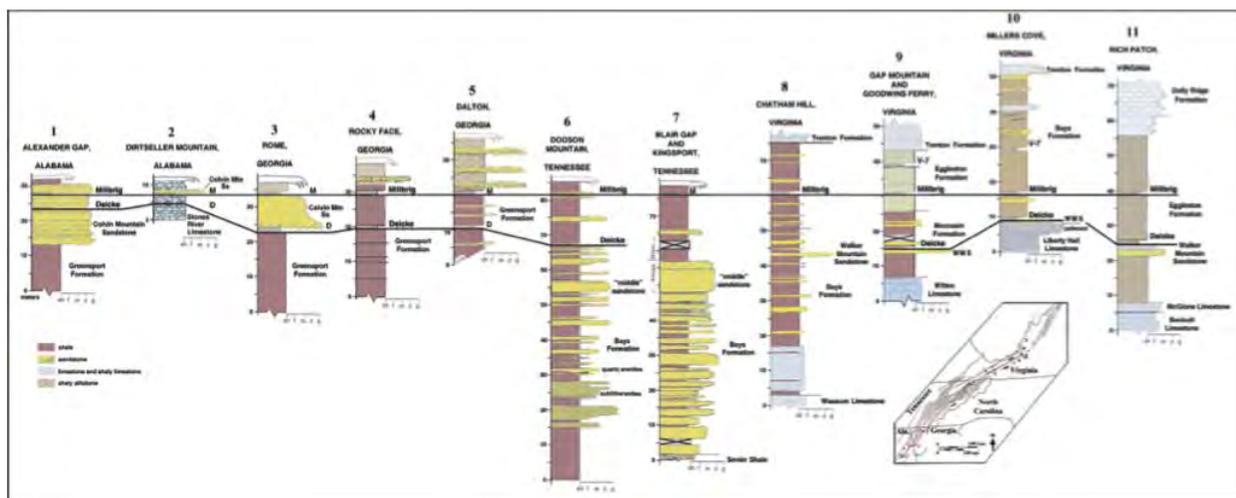
Figure 15.—Correlation of sections in the Blount molasse along depositional strike from Alexander Gap, Alabama to Rich Patch, Virginia. The stratigraphic relationships of the quartz arenites in these sections to the Deicke and Millbrig K-bentonites show that these quartz sands and gravels were being delivered to the depositional basin before (Sections 6 to 11 in Tennessee and Virginia, including Section 6, Dodson Mountain, which is Stop 3-3 of this trip), during (Alexander Gap and Rome, which are Stops 1-3 and 2-2 of this trip, respectively), and after (Sections 2, 4, and 5, including Section 5, Dalton, which is Stop 2-4 of this trip) the times that the Deicke and Millbrig tephras were erupted.

Stones River Limestone and the overlying Nashville Limestone, which is perhaps the M4-M5 sequence boundary? is superbly exposed here, as are the overlying several meters of the Nashville Limestone, which is a sequence of open marine and more extensively fossiliferous carbonate strata. This will be one of the best exposures to collect samples of both K-bentonites, including the ilmenite (now leucoxene) bearing zone of the lower Deicke, and the biotite-rich middle zone of the Millbrig. In addition, we will continue to discuss the sequence stratigraphic framework, and how the M4-M5 sequence boundary is recognized in the carbonate sections like this one throughout the region.

STOP 2-2: Horseleg Mountain, along Radio Springs and Mont Alto Roads, crest of Horseleg Mountain, just south of Rome, GA; 11:15 am – 1:00 pm (105 mins incl. lunch)

The initial parking place at this stop is underlain by float of the Attalla Chert Conglomerate, and as we walk a short distance down the road, we go upsection into an exposure of thin-bedded, reddish brown bioclastic grainstones of the Greensport (or Lenoir?) Formation that is only a few meters thick. After examining these interesting limestones, we will drive a little farther up the road to see the 80-120 cm thick Deicke K-bentonite and the overlying ~6 m thick ledges of Colvin Mountain Sandstone that are cross-bedded, including herringbone cross-bedding (Chowns and Carter, 1983) where we will continue our discussion about the stratigraphic relations of the quartz sandstones, the redbeds both below and above the Colvin Mountain Sandstone, the K-bentonites, and the M4-M5 sequence boundary.

STOP 2-3: Dug Gap, cuts along State Highway 52 across Rocky Face Mountain, just west of Dalton, GA; 2:20 pm – 3:45 pm (85 mins)

We will first examine here what is likely the southernmost described exposure of the *Orthorhynchula* zone in the Appalachians (Fig. 14). This typically 3-4 m thick stratigraphic interval "consists of an irregularly bedded, lumpy, brown sandstone that is almost incredibly filled with fossils which break out and weather out in molds and casts. The rock is gray and solid when fresh, but turns brown and crumbles rapidly on surface exposures. A few zones have become slightly calcareous because of their fossils." (Woodward, 1951). The *Orthorhynchula* zone separates the Reedsville? Formation here (the "Maysville Fm" of Butts and Gildersleeve (1948)) from the overlying Sequatchie Formation, and its distinctive texture looks very much the same here as it does in sections 100s of km to the north, in the Virginias and Pennsylvania, which is worth noting for reference when we see the *Orthorhynchula* zone again during the conference field trip to Germany Valley in West Virginia on June 10th.

Just up the road toward the summit at Dug Gap we will stop to see a second exposure that is stratigraphically upsection in the sequence of exposures along the Dug Gap road. This is an exposure of part of the Sequatchie Formation, and we will note the reddish color of some of the beds, a textural feature that led Chowns (1972) to in fact refer to these strata at this exposure as Juniata rather than Sequatchie, but since then Zeigler (1988) and others have considered these strata to be the Sequatchie Formation. We will also take this opportunity to discuss the weathering profile of this exposure of the Sequatchie vs. the appearance of the Sequatchie? redbeds at the Alexander Gap and Horseleg Mountain sections, where the redbeds above the Colvin Mountain Sandstone may or may not be correlative with the strata here, which by all accounts are indeed unequivocally Sequatchie.

At the summit of Rocky Face Mountain, the Silurian Red Mountain Formation and its characteristic resistant quartz arenites overlie the Sequatchie, in what looks much like the same stratigraphic relationship that exists farther north in Tennessee, Virginia, West Virginia, Maryland, and Pennsylvania, where the Clinch or Tuscarora Sandstone overlies the Juniata Formation.

STOP 2-4: Reed Road, low cut along the east side of the road where it parallels Hamilton Mountain between West Haig Mill/Caprice/Raindance Roads (south of cut) and Battle Way (north of cut), north of Dalton, GA; 4:00 – 4:30 pm (30 mins)

At this exposure, which does not look like much compared to the grand outcrops like those we have seen at the Red Mountain Expressway and Tidwell Hollow, and will see at Hagan and Dodson Mountain, we will examine THE coarsest sandy conglomerates and pebbly sandstones of the Colvin Mountain Sandstone? (or is it the Bays Formation?) that JTH has found to date in the Blount molasse anywhere in the southern Appalachians, AND we will see that both the Deicke and Millbrig K-bentonites are in redbeds of the Greensport Formation? Bays Formation? a few meters ***downsection*** from the stratigraphically oldest of three conglomeratic zones (Fig.

16). This stratigraphic relationship makes for an important contrast with the Alexander Gap and Horseleg Mountain sections that we have already seen, the now inaccessible Dirtseller Mountain quarry section in Alabama (not seen on our trip), and the Dodson Mountain section (Stop 3-3) that we will see tomorrow, where the Deicke and Millbrig are ***upsection*** from all the quartz sandstones and which is stratigraphically representative of all the exposures in northeast Tennessee and southwest Virginia where the Walker Mountain Sandstone occurs downsection from the Deicke and Millbrig. Also at this stop, we will pose these questions again: Where is the M4-M5 boundary? How could we tell it if we saw it in this sedimentary sequence of redbeds, pebbly sandstones, and as yet no known fossils? Why is it so difficult to identify a sequence boundary in these strata that elsewhere is evidently so readily recognized? What is the evidence for the presence of an unconformity beneath many of the quartz arenites in the Blount molasse? as well as other questions related to sequence stratigraphy in the Ordovician of the entire southern Appalachians, not just those exposures comprised of carbonate strata.

DAY 3. ORDOVICIAN CARBONATE AND CLASTIC DEPOSITS ACROSS STRIKE FROM VIRGINIA TO TENNESSEE VIRGINIA TO TENNESSEE

Introduction

At today's stops we will examine three exposures of Ordovician strata, one in Virginia, and two in Tennessee. As we have done on the previous two days, we will be following a route that takes us on an across-strike transect from the carbonate facies in the northwestern Valley and Ridge to the siliciclastic facies in the southeastern Valley and Ridge. This will again allow us to see various aspects of sedimentation in the Ordovician that were governed by the Taconic orogeny in the southern Appalachians. The first stop (Hagan, Stop 3-1; Fig. 17)) is in the westernmost Valley and Ridge, on the west limb of the Powell Valley anticline, and the eastern edge of the Cumberland Plateau rises immediately west of the Hagan section as the prominent escarpment formed by erosion of the nearly horizontal Pennsylvanian sandstones that comprise the caprock of the Plateau. Like the Tidwell Hollow section, which had several features in common with the cratonic exposures around the Nashville Dome in central Tennessee, the Hagan section shares many sedimentologic and stratigraphic features with the time-equivalent carbonate strata in the cratonic exposures around the Jessamine Dome in central Kentucky, as first noted by Huffman (1945). At Hagan we will examine a long section that is over 310 m thick and is mostly continuous from the base of the Hardy Creek Limestone to the contact of the Sequatchie Formation and the overlying Clinch Sandstone, which is the Ordovician – Silurian boundary (see Miller and Brosgé 1954).

Figure 16.—Exposure along Reed Road on the west wide of Hamilton Mountain north of Dalton, in 1994, which we will examine at Stop 2-4. The Deicke and Millbrig K-bentonites are in red mudrocks of the Bays? Greensport? Formation, and just a couple of meters above the Millbrig is the oldest of three polymictic pebble conglomerates (inset, upper right), which share several petrographic features with the other quartz arenites and conglomerates in the Blount molasse, but which are the youngest of those coarse clastics in the southern Appalachians, as shown in Fig. 14.

The second stop (Dandridge, Stop 3-2) will provide us with our first look at the Knox unconformity in this region, and the several meters of strata below and above it. The Douglas Lake Member that discontinuously overlies the unconformity has some features in common with the roughly equivalent Attalla Chert Conglomerate Member in Alabama and Georgia that we saw at Tidwell Hollow. Both units contain cherty regolith and rubble that accumulated in topographic lows on the subaerially exposed karst surface that became the Knox unconformity, and the thickness of both units commonly varies abruptly in all directions. At Dandridge we will in fact see a pinch out of the Douglas Lake Member along strike, such that the overlying Lenoir Limestone overlies the Knox Group carbonates just a short distance from a location where the Douglas Lake Member is approximately 6 m thick.

The third stop (Dodson Mountain, Stop 3-3) will be our introduction to the Bays Formation in its type region of the Bays Mountains (although no type section has yet been described and

formally proposed). The exposure at Dodson Mountain is the best and most complete exposure of the redbeds and the interbedded and prominent quartz arenites of the Bays Formation, which here is over 220 m thick. The Bays Formation is the molasse facies of the Blount phase of the Taconic orogeny in northeast Tennessee and southwest Virginia, and it is equivalent to the Greensport Formation, the Colvin Mountain Sandstone, and quite possibly the redbeds ("Sequatchie"?) that overlie the Colvin Mountain Sandstone at Alexander Gap, Horseleg Mountain, and other exposures in that region. At this stop we will yet again emphasize the stratigraphic position of the quartz arenites relative to the Deicke and Millbrig K-bentonites, which are both present here, and are **_upsection_** from all of the major quartz arenites, in contrast to what we saw in Georgia and Alabama (Fig. 15). We will also discuss Ordovician paleoclimate and the presence of what may be paleosols in the redbeds of the Bays Formation, and we will yet again ponder how the M4-M5 sequence boundary, and other eustatically-driven sequence boundaries, might be recognized in the Bays Formation, and whether or not we would even expect them to be present. The exposure at Dodson Mountain is very accessible because of the near-vertical dip of the beds and the width of shoulder, such that one is easily able to walk the entire length of the exposure and see all beds. There is unfortunately no exposure of the stratigraphic contacts with either the underlying Sevier Shale or the overlying "Martinsburg" or "Trenton" Formation.

STOP 3-1: Hagan, outcrops along railroad at Hagan, VA; 9:30 – 11:30 am (120 mins)

   At this outstanding exposure (Fig. 17) we will examine several hundred meters of, from oldest to youngest, middle and upper Ordovician carbonates of the upper Ben Hur, Hardy Creek, and Eggleston Limestones, the interbedded thick bioclastic limestones and thinner shales of the overlying "Trenton" (Dolly Ridge) Formation, and the shalier strata of the Reedsville and Sequatchie Formations that are themselves separated by the _Orthorhynchula_ zone (Miller and Brosgé, 1954). Being in the far western (Lee confacies) belt of the Valley and Ridge makes this section similar in some ways to Tidwell Hollow, with minimal evidence here for the Blount phase of the Taconic orogeny in such a western location (we are about at the longitude of Detroit, Michigan here). But by contrast, the shales of the Reedsville Formation, and the coarser clastics of the Sequatchie and of the overlying Silurian Clinch Sandstone are evidence for expansive deposition of siliciclastic sediments associated with the Queenston phase of the Taconic orogeny.
   Of particular note at the Hagan section is the overall deepening upward sequence from the ~130 m thick upper Ben Hur, Hardy Creek, and Eggleston Limestones that are variably open shelf to peritidal deposits, upsection into the "Trenton" (Dolly Ridge) Formation that was deposited on a deeper, storm-dominated shelf, and then into the deeper shelf or slope deposits of the Reedsville Formation, which represent the deepest environments of this sequence. The _Orthorhynchula_ zone is interpreted as recording deposition in a nearshore setting (Bretsky, 1969, 1970), which implies regional shallowing from the middle to the uppermost Reedsville to explain the transition from the shales of the lower and middle Reedsville that were deposited in shelf edge to slope settings, to the muddy sandstones of the _Orthorhynchula_ zone with their abundant and diverse

community of robust brachiopods and other marine organisms, which were deposited in shallow shelf to nearshore environments. The Sequatchie Formation here, with its variable but appreciable quantities of siliciclastic muds, silts, and fine sands in addition to beds of fossiliferous limestone (Miller and Brosgé 1954), contrasts with the underlying Reedsville. The Sequatchie overlies the *Orthorhynchula* zone here, as it does at Dug Gap and throughout much of the southern Appalachians. The limestones of the Sequatchie were deposited in shallow marine shelf to nearshore settings, and the siliciclastics were deposited in environments ranging from marine to transitional coastal and supratidal environments that were subaerially exposed at times as evidenced by the desiccation cracks in some beds.
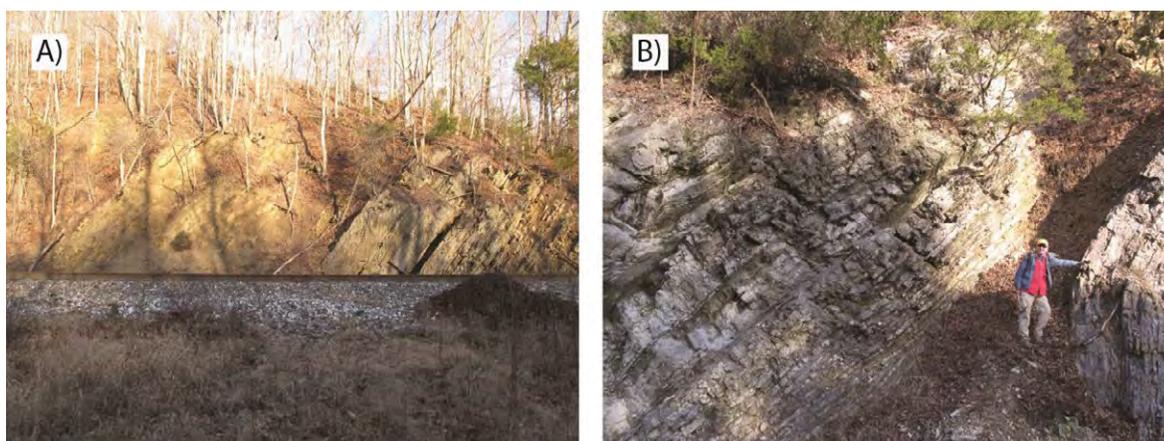
Fig. 17.—STOP 3-1: Hagan, VA. A) Reedsville Shale and Dolly Ridge Limestone (transition about middle of picture) and B) Deicke K-bentonite in the Egglestone Formation. John Haynes for scale.

Another characteristic that the exposure at Hagan shares with the cratonic exposures of central Kentucky is that several of the eustatically-generated sequence boundaries identified and named by Holland and Patzkowsky (1996) in the cratonic exposures (e.g., M2-M3, M3-M4, M4-M5, and M5-M6) can be recognized here at Hagan. Others who have studied the exposures in and around the Hagan area, however, including Pope and Read (1997) and Kolata et al. (1998) have suggested that there is more complexity to the unconformities and the sequence boundaries that may be present here at Hagan. At least some of that complexity seems attributable in part to our previous findings regarding correlations of the Deicke and Millbrig K-bentonites into the Blount molasse, where, as we have seen already on this trip, problems surrounding the identification of unconformities and their correlative conformities occur in not only a Cincinnati Arch-to-eastern Valley and Ridge direction, but in the opposite direction as well. Therefore, as we have been discussing each day thus far, the correlation of sequence stratigraphic boundaries identified from detailed study of cratonic carbonate sections might not be so readily demonstrated with the coarser siliciclastic deposits of molasse in foredeep sections, and unconformities that are

prominent and widespread in the molasse may not persist into the cratonic sections (Haynes, 1994; Haynes and Goggin, 1993, 1994, 2011).

STOP 3-2: Dandridge Municipal Park, sections along shoreline of Douglas Lake just off of Chestnut Hill Road (State Highway 92), at Dandridge, TN; 1:00 – 2:30 pm (90 mins; bathroom stop at park facilities)

Some of the key features of interest at this series of exposures along the lakeshore (Fig. 18) that we will be able to examine in detail are (1) the Knox unconformity (Fig. 19) and associated paleokarst surface; (2) regolith breccias with clasts up to 3.0 m long diameter in the overlying Douglas Lake Member of the Lenoir Limestone, which accumulated in lows on the Knox paleokarst surface; (3) the Lenoir itself, many beds of which are fossiliferous; (4) the overlying condensed section in the Fetzer Member of the Whitesburg Formation, with its phosphatic and metalliferous horizons; and (5) the overlying graptolitic gray to black shales of the main body of the Whitesburg Formation, one of the classic flysch units of the Blountian phase of the Taconic orogeny. This outstanding set of exposures shows evidence for the abrupt and perhaps rapid(?) deepening of the carbonate platform that had been developed and widespread along the Laurentian shelf margin since the Cambrian but which sagged and developed into a foreland basin as a result of Taconic, i.e., Blountian, orogenic activity along the Laurentian continental margin. This abrupt deepening, presumably caused by crustal downwarping much more so than by eustatic sealevel rise, ultimately resulted in drowning of the shallow shelf environments, and subsequent deposition of great thicknesses of graptolitic muds on top of those formerly shallow carbonate sediments. One of the most significant aspects of a visit to these exposures is that the complete depositional sequence from shallow shelf to drowning shelf to deep basin margin is readily seen just by walking upsection through only a few meters of the dipping ledges.

The base of the exposures here consists of about 55 m of the upper Knox Group, and most of that interval consists of peritidal deposits of stromatolitic (planar and wavy laminated to domal) microbial mat carbonates, with some supratidal dolomites, as well as beds of ribbon limestone, all of which are very typical lithologies of the thick Cambro-Ordovician carbonate sequence throughout nearly the entire Appalachian region (Read and Repetski, 2012).

Above the unconformity is the Lenoir Limestone, with its basal Douglas Lake Member, a discontinuous unit that is restricted to topographic lows on the Knox unconformity. This member includes regolithic breccias and conglomerates (Fig. 16), some of which may have been transported short (?) distances, and medium to very coarse lithic sandstones, some with extensive bioturbation. These sandstones contain much chert as framework grains in addition to mono- and polycrystalline quartz, all of which are cemented by a ubiquitous reddish brown and
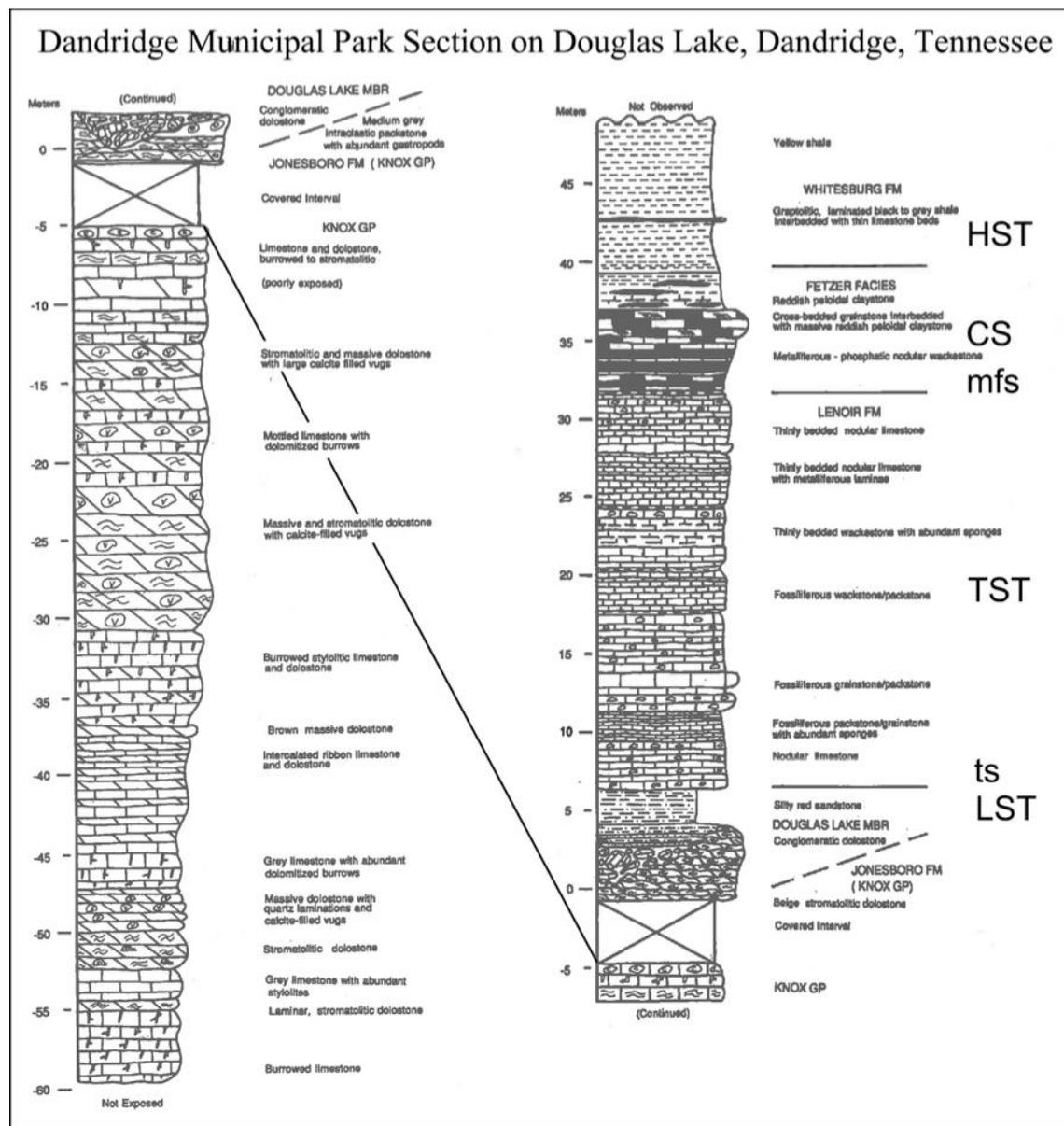
Figure 18.—Stratigraphic section along Douglas Lake at Dandridge, Tennessee, including outstanding exposures of the Knox unconformity and the overlying Douglas Lake Member, an accumulation of regolith that collected in topographic lows on the unconformity surface, and that is now a mixture of lithologies including breccia, lithic sandstones, and argillaceous dolomites. Modified from Steinhauff and Roberson (1989).

presumably hematitic matrix that has nevertheless incompletely reduced the primary interparticle pore spaces, thus the porosity of these sandstones is low to moderate. The overlying main sequence of the Lenoir Limestone varies in thickness here from a thinner western section that is about 12 m thick to a thicker eastern section that is about 24 m thick; this difference over a short distance is attributed to variable topography on the Knox paleokarst surface (Steinhauff and Roberson, 1989). The Lenoir represents a more open marine accumulation that consists

primarily of skeletal grainstones and packstones with an abundant and diverse assemblage of marine fauna, including whole and fragmental bryozoans, brachiopods, trilobites, and crinoids, with some sponges, calcareous algae, and oncoids.

Figure 19.—The Knox unconformity at Dandridge (Stop 3-2), with regolithic breccias of limestone and chert clasts in paleotopographic lows on the paleokarst surface. Ledges in the background are reddish sandstones of the Douglas Lake Member of the Lenoir, and the overlying limestones of the main body of the Lenoir. Staff is marked in decimeters.

The dark colored Fetzer Member of the Whitesburg Formation contrasts markedly with the much lighter colored Lenoir carbonates, and the darker color results from metal oxide staining of the argillaceous matrix in the carbonates and mudrocks of the Fetzer, which are relatively phosphatic and manganiferous (Steinhauff and Roberson, 1989). A more limited fauna of echinoderms, ostracodes, and trilobites has been identified in some of the Fetzer beds here, and the character of the bedding is more nodular and laminated compared to the underlying Lenoir carbonates.

Above the Fetzer Member are monotonous exposures of interbedded fissile graptolitic black shales and silty lime mudstones of the Whitesburg Formation and possibly the Blockhouse Shale above that, which collectively tend to weather into thin shaley plates. These mudrocks are the uppermost unit exposed here, and these shales are at least 40 m thick here, but true thickness is

difficult to determine because of structural complications in these incompetent and ductile strata. Some beds in the Whitesburg/Blockhouse have sole markings on their undersides, suggesting deposition by turbidity currents on a slope.

From a sequence stratigraphic perspective, we interpret the Douglas Lake Member as a Lowstand Systems Tract (LST), the basal bed of the Lenoir Limestone as the transgressive surface (ts), the main body of the Lenoir as a Transgressive Systems Tract (TST), the sharp contact of the uppermost limestone of the Lenoir with the overlying basal bed of the Fetzer Member as a maximum flooding surface (mfs), the main body of the Fetzer Member itself as a Condensed Section (CS, as was likewise suggested by Steinhauff and Roberson, 1989), and then at least the lowest shales of the main body of the Whitesburg/Blockhouse itself as perhaps a Highstand Systems Tract (HST). If these sequence surfaces and systems tracts identifications are correct, this exposure is one of the best, and perhaps THE best, known to us where such an outstanding example of this sequence progression can be seen in the Southern Appalachians in such a relatively thin stratigraphic interval.

There is a chance that the water level in Douglas Lake will be high enough such that some of the exposure along the western part of the section is inaccessible, but we expect that the eastern section (Fetzer Member and Whitesburg) will be exposed and accessible at normal lake level.

STOP 3-3: exposure along north side of State Highway 70 in gap between Dodson and Kite Mountains in the western Bays Mountains synclinorium, southeast of Rogersville, TN; 3:30 – 5:00 pm (90 mins)

This is the best and most complete exposure of the Bays Formation, with its redbeds and associated prominent quartz arenites, in the Bays Mountains (Table 5), which is the type area of the Bays Formation (Fig. 20). At this stop we will emphasize the stratigraphic position of the quartz arenites relative to the Deicke and Millbrig K-bentonites, which here are both upsection from the major quartz arenites, in contrast to what we saw in Georgia and Alabama (Fig. 15). We will discuss the sedimentary structures and burrows that are present in these rocks, paleoclimate and the presence of up to 15? paleosols (as tentatively identified in Table 4), the M4-M5 sequence boundary relative to the Deicke and Millbrig K-bentonites throughout this region, and the difficulty of identifying cratonic sequence boundaries here in the Bays Formation, which comprises the bulk of the Blount molasse in Tennessee and Virginia, and possibly in northern Georgia, as we have discussed at earlier stops.

Because of the near-vertical dip of the beds, and the generous width of the shoulder along SH 70, it is a relatively easy walk along the entire length of exposure to see all the beds, but there is no exposure of stratigraphic contacts with either the underlying (Sevier Shale) or overlying ("Martinsburg" Formation) units.

Table 4.—Measured section of Bays Formation along Tenn. State Hwy. 70 at SW end of Dodson Mountain, Hawkins Co., Tenn. Dodson Mountain section: measured top down, with 15 possible paleosols identified. Measurements made by J. Haynes in 2002.

Trenton Formation
Bed
117 Not exposed here, but the basal several 10s of feet are present at Charles Mtn.
Bays Formation Total estimated thickness: ....730 ft.
116 Estimated distance to base of Trenton ("Martinsburg") based on measurements
at the Charles Mtn. section, along strike to the north of this section, where
the Bays – Trenton contact interval is completely exposed ....~56 ft
115 Red shale/siltstone to covered zone, E. end of exposure along S.H. 70 ....18 ft
114 Red siltstone/v. fn. ss., blocky weathering..2 ft
113 Millbrig K-bentonite ....1 ft 8 in
Red shaly bentonite to bentonitic shale..8-10 in
Biotite zone, red and grayish red to gray bentonitic clay..8-10 in
Red clay ....2 in
112 Red siltstone/v. fn. ss., blocky weathering..9 in
111 Red shale/siltstone ....7 ft 3 in
110 Red siltstone/v. fn. ss., blocky weathering..2 ft
109 Red shale/siltstone ....20 ft
108 **Paleosol**? of red shale; 9 in. blue-gray shale 15 in. above base...3 ft 7 in
107 Sandstone, fn. to med. gr., lt. olive brown, blocky weathering..9 ft 11 in
106 **Paleosol**? of red shale with thin olive drab beds at top..1 ft 11 in
105 Red shale, thin blue-gray beds at base ....13 ft 10 in
104 Siltstone, olive drab, blocky weathering... 4 in
103 Red shale..1 ft 9 in
102 Deicke K-bentonite ....1 ft 3 in
Red and orange-red claystone/shale, bentonitic.. 8 in
White clay with ilmenite as dark specks in red shale.. 7 in
101 Siltstone, red, blocky weathering, top 2-3 in. fractured, top 1/4 in. green, chert-like.................1 ft 5 in
100 **Paleosol**? of red shale, noticeably gullied... 9 in
99 Sandstone, f. to med. gr., lt. olive brown ....2 ft 10 in
98 Red shale/siltstone ....3 ft 3 in
97 Red shale with discontinuous blue-green mudrock interbeds.. 10 in
96 Sandstone, f. to med. gr., lt. olive brown ....2 ft 10 in
95 Red shale/siltstone ....5 ft 5 in
94 Red shale with lenses of blue-green shale ....1 ft 6 in
93 Sandstone, f. to med. gr., lt. olive brown ....5 ft 4 in
92 Red shale/siltstone ....8 ft
91 Sandstone, f. to med.gr., olive brown ....7 ft 2 in
90 Sandstone, v. fn. gr., first noticeably massive bed above bed # 80..8 ft
89 Red shale/siltstone ....5 ft 7 in
88 **Paleosol**? of red shale, gullied, with olive and blue gray layers..21-24 in

87 Red shale/siltstone, rare blue gray blebs = reduction zones? ....6 ft 6 in
86 Red and olive shale/siltstone to red and blue-gray in upper 6 in ....2 ft 8 in
85 **Paleosol**? of red shale ....9 in
84 Red shale/siltstone, blocky weathering, with olive beds...1 ft 1 in
83 **Paleosol**? of red shale with olive beds at top...9 in
82 Olive siltstone, blocky weathering..4 in
81 **Paleosol**? of red shale with olive beds at base and top ....5 in
80 Sandtone, med. gr., lt. olive brown, blocky weathering (bed 31 of Herg)...........................3 ft
79 Red shale/siltstone, 2 beds may be paleosols? ....8 ft
78 Sandstone, med. gr., white to yellow-gray, med. bdd...5 ft
77 **Paleosol**? of red shale ....1 ft 10 in
76 Sandstone, med. gr., white to yellow-gray, med. to thk. bdd, "**middle sandstone member**", poss. equival. to Walker Mtn. Ss. (bed 27 of Herg)....................................26 ft 10 in
75 Red and olive interbeds at top of red shale paleosol? ....4-6 in
74 **Paleosol**? of red shale ....11 in
73 Sandstone, f. gr., x-bdd., current from SE, thickens at road level.................................25-40 in
72 Red and olive interbeds at top of red shale paleosol? ....2-3 in
71 **Paleosol**? of red shale ....1 ft 4 in
70 Red and olive shale/siltstone...9 in
69 Siltstone/v. fn. ss., olive brown..1 ft 2 in
68 **Paleosol**? of red shale ....6 in
67 Red shale and interbdd. olive shale/siltstone ....1 ft 8 in
66 Olive shale/siltstone, blocky weathering ....1 ft 7 in
65 Sandstone, med. gr., white to v. lt. gray, med. to thk. bdd. (bed 25 of Herg).............10 ft 8 in
64 **Paleosol**? of red shale with10 in. of interbdd. olive and red shale at top ....5 ft 7 in
63 Sandstone, med. gr., lt. greenish gray, med. bdd ....3 ft 8 in
62 Olive and red shale/siltstone interbdd... 10 in
61 **Paleosol**? of red shale ....3 ft 8 in
60 Red shale/siltstone ....20 ft
59 Sandstone, v. fn.gr., siltstone at top ....3 ft 1 in
58 **Paleosol**? of red shale ....3 ft 11 in
57 Sandstone, med. gr., v. lt. gray, med. bdd..10 ft 7 in
56 Red shale/siltstone ....27 ft 6 in
55 Sandstone, f. gr., lt. olive brown, thn. to med. bdd, some red shale laminae................8 ft 6 in
54 Red shale/siltstone ....2 ft
53 Siltstone, red and olive, blocky weathering...9 in
52 Red shale/siltstone, with interbdd. olive siltstone..3 ft
51 Sandstone, v. fn. gr., lt. olive brown ....12-15 in
50 Red shale/siltstone ....2 ft 5 in
49 Sandstone, v. fn. gr, olive and blue-gray ....9 in
48 Red shale/siltstone (below ravine that drains into grated culvert) ....15 ft 10 in
47 Sandstone, med. gr., lt. greenish gray (5GY8/1), med. bdd. (first sandstone west of the grated culvert) ....10 ft 2 in
46 **Paleosol**? of red shale with 1 in. olive bed at base and 0-3 in at top ....2 ft 1 in

45 Red shale/siltstone with olive interbdds..3 ft
44 Red shale/siltstone ....5 ft
43 Sandstone, v. fn. gr., lt. olive brown, thin "spine" up the exposure................................... 11 in
42 Red and olive shale/siltstone.. 8 in
41 Siltstone, red and olive... 11 in
40 Red shale/siltstone ....7 ft 9 in
39 Siltstone, red and olive...3 ft 8 in
38 Olive shale/siltstone ....1 ft 1 in
37 Sandstone, v. fn. gr, olive brown ....1 ft 11 in
36 Olive shale .... 5 in
35 Red shale/siltstone ....10 ft 7 in
34 Siltstone, olive...1 ft 8 in
33 Sandstone, v. fn. gr., olive, 1 massive bed at road, splits into two with
bedding plane halfway up cut ....3 ft 4 in
32 Olive yellow-brown siltstone/v.fn. ss ....3 ft 9 in
31 Sandstone, fn. gr., white to pale yellow, channel fill at road, thins up slope................................14-21 in
30 Red shale/siltstone ....4 ft 10 in
29 Siltstone/v. fn. ss., olive to blue-gray, med. bdd..1 ft 2 in
28 Sandstone, v. fn. gr., olive to blue gray, blocky...1 ft 2 in
27 Red shale/siltstone, thin blue-gray interbdds. at base, top, and 8 ft.
above the base ....16 ft 8 in
26 Sandstone, med. gr., greenish gray, med. bdd..7 ft 2 in
25 Olive brown siltstone/shale...5 ft 7 in
24 Sandstone, med. gr., lt. greenish gray, med. bdd ....3 ft 10 in
23 Olive brown siltstone/shale... 10 in
22 Sandstone, med. gr., blueish-gray, med. bdd., superficially like
Oswego at Brocks Gap...5 ft 1 in
21 Sandstone, fn. gr., olive brown, thn. to med. bdd ....11 ft 3 in
20 Olive brown shale ....2 ft 11 in
19 Sandstone, silty to v. fn. gr., olive brown, med. bdd..3 ft 6 in
18 Red shale/siltstone with interbdd. olive and blue-gray shale/siltstone...1 ft 6 in
17 Sandstone, v. fn. gr., olive brown .... 6 in
16 Olive and blue-gray shale/siltstone..1 ft 5 in
15 Sandstone, v. fn. gr., olive brown ....2 ft 2 in
14 Red shale/siltstone with interbdd. olive and gray green shale ....12 ft 5 in
13 Sandstone, fn. gr., olive, notably massive and resistant compar. w.
surrounding mudrocks .... 5 in
12 Red shale/siltstone, interbdd. olive shale in lower 8 in...2 ft
11 Sandstone, fn. gr., olive, resistant like # 13 .... 8 in
10 Red shale/siltstone ....2 ft 3 in
9 Olive siltstone ....2 ft
8 Red shale/siltstone/v. fn. Ss ....1 ft 11 in
7 Sandstone, med. to crs. gr., greenish gray (5GY 7/1), med. bdd ....20 ft
6 Olive siltstone/v. fn. Ss ....10 ft

5 Red shale/siltstone ....8 ft 8 in
4 Sandstone, fn. gr., olive gray, med. bdd...10 ft 11 in
3 Red shale/siltstone ....41 ft
2 Red shale/siltstone/v. fn. ss, to covered zone at W. end of exposure................................90+ ft
Sevier Formation
1 Micrite and calcareous shale, not exposed in July '02,
but observed by Hergenroder in 1964..not measured

Figure 20.—Vertical beds of red mudrocks, including what may be several paleosols, and white quartz arenites in the Bays Formation at Dodson Mountain, Stop 3-3. As seen in the inset (lower right), some of the redbeds are moderately to extensively burrowed, with the burrows being highlighted by the color differences, which are probably the result of oxidation differences.

DAY 4. ORDOVICIAN PROXIMAL CARBONATE AND CLASTIC DEPOSITS OF THE BLOUNT FOREDEEP IN TENNESSEE AND VIRGINIA VIRGINIA TO TENNESSEE

Introduction

At today's stops we will examine our final two exposures of Ordovician strata, one in Tennessee and one in Virginia, and then we will head north along Interstate 81 to Harrisonburg, and James Madison University and the kick-off of the 2015 ISOS meeting.   Our first stop (South Holston Dam, Stop 4-1) will be to see some of the coarsest and most proximal conglomeratic sediments of the Tellico Formation that are a part of the flysch deposits that accumulated as distal to proximal submarine fan deposits along the eastern margin of the Blount foredeep. The exposures below South Holston Dam, which include over 200 m of coarse conglomerates both matrix and clast supported (Fig. 21), pebbly sandstones, turbidite sandstones and shale, should be thought of as being linked to the section we examined yesterday at Dandridge (Stop 3-2) as well as to the shales that we will drive by enroute to the South Holston Dam, because they are stratigraphically upsection from the graptolitic shales of the Whitesburg and Blockhouse Formations that represent the deepest and most distal deposits that accumulated in the nascent Blount foredeep. The Tellico Formation, however, is of course younger and more proximal than the older graptolitic shales, and the clasts in the Tellico provide important information about their provenance in the Taconic orogenic highlands that were sourcing these sediments.

Figure 21.—Cobble and pebble conglomerates in the Tellico Formation at the South Holston Dam (Stop 4-1) deposited in submarine fan channels. These submarine fans were developed along the east margin of the Blount foredeep and were receiving sediment brought into the foredeep from the Blount tectonic highlands along the southeastern margin of Laurentia (Bowlin et al., 1989). Staff is marked in decimeters.

Our second and final stop (Rich Valley, Stop 4-2) will provide us with the opportunity to see a vertical sequence that records initial downwarping of the Laurentian shelf and the subsequent growth and development of a downslope buildups of the Effna Limestone, which has abundant small bryozoan colonies, followed by continued deepening of the shelf, which ultimately led to drowning of the Effna buildup by black graptolitic mudrocks of the Rich Valley Shale. This sequence is yet again similar to the section at Dandridge, where in a few

meters we could see the flooding of the Knox paleokarst, development of the open marine deposits of the Lenoir, and then abrupt drowning and deposition of the metalliferous Fetzer Member and finally by the accumulation of great thicknesses of graptolitic muds that became the Whitesburg and Blockhouse Formations. A main difference at Stop 4-2 is that we will actually be able to see a bioherm that developed during the relative sealevel rise that accompanied the development of the Blount foredeep throughout much of the southern Appalachians.

STOP 4-1: exposures along Holston Dam/Ruthton Roads below South Holston Dam, TN; 8:50 – 9:50 pm (60 mins)

   At these exposures below the dam, we will have the opportunity to look at coarse polymict conglomerates, turbiditic sandstones, and shales of the Tellico Formation that collectively record a prograding submarine fan complex into a more proximal part of the Blount foredeep. The conglomerates we will focus on at this stop have been interpreted as an incised channel-fill deposit on a prograding submarine fan (Bowlin et al., 1989), and it should be possible to see a variety of textures and fabrics including clast-supported conglomerates with no visible grading or imbrication, clast-supported conglomerates with inverse to normal grading and distinct imbrication, and even some indistinct cross-bedding, as well as matrix-supported conglomerates with only very few areas where imbrication, or bedding, either normal or inverse, is evident. Clasts were derived from Precambrian, Cambrian, and older Ordovician units, and it should be possible to find clasts of quartzose and arkosic sandstone, chert of various colors, vein quartz, and maybe some rhyolites from the late Precambrian Mt. Rogers Formation to the east-northeast of us, along with abundant clasts of limestone and dolomite. Bowlin et al. (1989) speculate that perhaps an 8-10 km thick sequence of Precambrian to Lower Paleozoic strata was present in the Taconic highlands and was being eroded during the later Ordovician to provide the polymictic population of clasts that are present here.

STOP 4-2: Cuts along State Highway 107 in Rich Valley northwest of Chilhowie, VA; 10:45 am – 12 Noon (75 mins), lunch following the stop in Marion at the Black Rooster Restaurant in the General Francis Marion Hotel.

   Here we will walk along exposures of the deep ramp downslope buildup of the Effna Formation with its bryozoan thickets, and the overlying Rich Valley Shale that is a sequence of graptolitic black shales and limestones which record the relative sealevel rise that ultimately resulted in drowning of the buildup. The work of Read (1980, 1982) elucidated the stratigraphic and paleogeographic relations of the shelf margin and downslope buildups in the Ordovician of Virginia, and their diversity relative to each other. These deeper water buildups are part of a larger trend of buildups that includes the Holston buildups in the Knoxville area of Tennessee and elsewhere in that region to the south (Walker and Ferrigno, 1973), possibly extending as far south as the Pratt Ferry Beds in Alabama, as well as the Murat buildups to the north of here near Lexington and Stuarts Draft, Virginia. In addition, there were generally contemporaneous

buildups along the shelf edge that developed in the Rockdell and Ward Cove Limestones (Read, 1980, 1982).

Read (1982) notes that these downslope buildups of the Effna share some similarities with the Waulsortian-type buildups of the later Paleozoic, but because the buildups in Virginia have calcareous algae throughout them, Read (1982) suggests that buildups like this one we will see developed in deeper water, but water that was still in the lower reaches of the photic zone. The core of the Effna buildups is a massive lime wackestone to lesser lime mudstone, and it is enclosed by flanking deposits of crinoid-bryozoan sands and coarser gravels of bioclastic debris, with some thickets of bryozoan bafflestones (Read, 1982). The drowning of the buildups evidently occurred rather abruptly, and there may be some hardgrounds, with metalliferous crusts discontinuously present, similar to the beds of the Fetzer Member at Dandridge (Stop 3-2).

From here we will go into Marion for lunch, and then we will drive to Harrisonburg, the end point of our field trip.

ACKNOWLEDGEMENTS

REFERENCES

ALLEN, A.T., and LESTER, J.G., 1957, Zonation of the Middle and Upper Ordovician strata in northwestern Georgia: *Georgia Geological Survey Bulletin* 66, 110 p.

BAYONA, G., and THOMAS, W.A., 2003, Distinguishing fault reactivation from flexural deformation in the distal stratigraphy of the Peripheral Blountian Foreland Basin, southern Appalachians, USA: *Basin Research*, v. 15, p. 503-526.

BAYONA, G., and THOMAS, W.A., 2006, Influence of pre-existing plate-margin structures on foredeep filling: Insights from the Taconian (Blountian) clastic wedge, Southeastern USA: *Sedimentary Geology*, v. 191, p. 115-133.

BEAUCHAMP, B., and DESROCHERS, A., 1997, Permian warm- to very cold-water carbonates and cherts in northwest Pangea, in James, N.P., and Clarke, J.A.D., eds., Cool-Water Carbonates: Tulsa, SEPM (Society for Sedimentary Geology), p. 327–347.

BENSON, D.J., and MINK, R.M., 1983, Depositional history and petroleum potential of the Middle and Upper Ordovician of the Alabama Appalachians: *Transactions Gulf Coast Association of Geological Societies*, v. 33, p. 13-21.

BOWLIN, B.K., KELLER, F.B., and WALKER, K.R., 1989, Stop 9 – Incised submarine channel-fan deposits in the Tellico Formation, South Holston Dam, Tennessee, in Walker, K.R., Read, J.F., and Hardie, L.A., (leaders), Cambro-Ordovician carbonate banks and siliciclastic

basins of the United States Appalachians: Washington DC, *28th International Geological Congress, Field Trip Guidebook T161*, p. 28-33.

BRETSKY, P. W., 1969, Ordovician benthic marine communities in the central Appalachians: *Geological Society of America Bulletin*, v. 80, p. 193-212.

BRETSKY, P. W. 1970: Upper Ordovician Ecology of the Central Appalachians: *Yale University Peabody Museum of Natural History Bulletin* 34, p. 1-150.

BRETT, C.E., MCLAUGHLIN, P.I., CORNELL, S.R., and BAIRD, G.C., 2004, Comparative sequence stratigraphy of two classic Upper Ordovician successions, Trenton Shelf (New York–Ontario) and Lexington Platform (Kentucky-Ohio): Implications for eustasy and local tectonism in eastern Laurentia: *Palaeogeography, Palaeoclimatology, Palaeoecology*, v. 210, p. 295–329.

BROOKFIELD, M.E., and BRETT, C.E., 1988, Paleoenvironments of the Mid-Ordovician (Upper Caradocian) Trenton limestones of southern Ontario, Canada: Storm sedimentation on a shoal-basin shelf model: Sedimentary Geology, v. 57.

BROOKFIELD, M.E., and ELGADI, M., 1998, Sedimentology and paleocommunities of the Black River and Trenton Limestone groups (Ordovician), Lake Simcoe area, Ontario, p. 35.

BUGGISCH, W., JOACHIMSKI, M.M., LEHNERT, O., BERGSTRÖM, S.M., REPETSKI, J.E., and WEBERS, G.F., 2010, Did intense volcanism trigger the first Late Ordovician icehouse?: Geology, v. 38, p. 327–330, doi:10.1130/G30577.1.

BUTTS, C., and GILDERSLEEVE, B., 1948, Geology and mineral resources of the Paleozoic area in northwest Georgia: *Georgia Geological Survey Bulletin* 54, 176 p.

CARTER, B.D., and CHOWNS, T.M., 1989, Stratigraphic and environmental relationships of Middle and Upper Ordovician rocks in northwest Georgia and northeast Alabama, in KEITH, B.D., ed., The Trenton Group (Upper Ordovician Series) of eastern North America: *American Association of Petroleum Geologists Bulletin Studies in Geology* no. 29, p. 17-26.

CHOWNS, T.M., 1972, Depositional environments in the Upper Ordovician of northwest Georgia and southeast Tennessee, in CHOWNS, T.M., ed., Sedimentary environments in the Paleozoic rocks of northwest Georgia: *Georgia Geological Society*, 11th Annual Field Trip Guidebook, p. 3-12.

CHOWNS, T.M., and CARTER, B.D., 1983, Stratigraphy of Middle and Upper Ordovician redbeds in Georgia, in Chowns, T.M., ed., Geology of Paleozoic rocks in the vicinity of Rome, Georgia: *Georgia Geological Society*, 18th Annual Field Trip Guidebook, p. 1-15.

DENNISON, J.M., 1991, Sea level drop contrasted with peripheral bulge model for Appalachian basin during Mid-Ordovician: *Geological Society of America Abstracts with Programs*, Northeast and Southeast Sections, v. 23, p. 21.

DRAKE, A.A. JR., SINHA, A.K., LAIRD, J., and GUY, R.E., 1989, The Taconic orogen, in Hatcher, R.D. Jr., Thomas, W.A., and Viele, G.W., eds., The Appalachian – Ouachita orogen in the United States: Boulder, *Geological Society of America, The Geology of North America*, v. F-2, p. 101-177

ECKERT, J.D., 1988, Late Ordovician extinction of North American and British crinoids: Lethaia, v. 21, p. 147-167.

EMERSON, N.R., SIMO, J.A., BYERS, C.W., and FOURNELLE, J., 2004, Correlation of (Ordovician, Mohawkian) K-bentonites in the upper Mississippi Valley using apatite chemistry:

implications for stratigraphic interpretation of the mixed carbonate-siliciclastic Decorah Formation: *Palaeogeography, Palaeoclimatology, Palaeoecology*, v. 210, p. 215-233.

FREY, R.C., 1995, Middle and Upper Ordovician nautiloid cephalopods of the Cincinnati Arch region of Kentucky, Indiana, and Ohio, 1-126 p.

HATCH, J.R., JACOBSON, S.R., WITZKE, B.J., RISATTI, J.B., ANDERS, D.E., WATNEY, W.L., NEWWLL, K.D., and VULETICH, A.K., 1987, Possible late Middle Ordovician carbon isotope excursion: evidence from Ordovician oils and hydrocarbon source rocks, Mid-Continent and East-Central United States: AAPG Bulletin, v. 71, p. 1342-1354.

HAYNES, J.T., 1994, The Ordovician Deicke and Millbrig K-bentonite beds of the Cincinnati Arch and the southern Valley and Ridge province: *Geological Society of America Special Paper* 290, 80 p.

HAYNES, J.T., and GOGGIN, K.E., 1993, Field guide to the Ordovician Walker Mountain Sandstone Member: Proposed type section and other exposures: *Virginia Minerals*, v. 39, p. 25-36.

HAYNES, J.T., and GOGGIN, K.E., 1994, K-bentonites, conglomerates, and unconformities in the Ordovician of southwestern Virginia, in Schultz, A., and Henika, W., eds., *Field guides to southern Appalachian structure, stratigraphy, and engineering geology*, Virginia Tech Department of Geological Sciences Guidebook Number 10: Blacksburg, Virginia Tech, p. 65-93.

HAYNES, J.T., and GOGGIN, K.E., 2011, Stratigraphic relations of quartz arenites and K-bentonites in the Ordovician Blount molasse, Alabama to Virginia, southern Appalachians, USA, in GUTIERRIEZ-MARCO, J.C., RABANO, I., and GARCIA-BELLIDO, D. (eds.), *Ordovician of the World*: Cuadernos del Museo Geominero, 14, p. 221-228.

HAYNES, J.T., and MELSON, W.G., 1997, SEM and EMX study of titaniferous minerals in the Ordovician Deicke K-bentonite of southwestern Virginia: *Virginia Minerals*, v. 43, p. 1-7.

HAYNES, J.T., MELSON, W.G., and GOGGIN, K.E., 1996, Biotite phenocryst composition shows that the two K-bentonites in the Little Oak Limestone (Ordovician) at the Old North Ragland Quarry, Alabama, are the same structurally repeated tephra layer: *Southeastern Geology*, v. 36, p. 85-98.

HAYNES, J.T., MELSON, W.G., and KUNK, M.J., 1995, Composition of biotite phenocrysts in Ordovician tephras casts doubt on the proposed trans-Atlantic correlation of the Millbrig K-bentonite (United States) and the Kinnekulle K-bentonite (Sweden): *Geology*, v. 23, p. 847-850.

HERRMANN, A.D., HAUPT, B.J., PATZKOWSKY, M.E., SEIDOV, D., and SLINGERLAND, R.L., 2004, Response of Late Ordovician paleoceanography to changes in sea level, continental drift, and atmospheric pCO2: potential causes for long-term cooling and glaciation: Palaeogeography, Palaeoclimatology, Palaeoecology, v. 210, p. 385-410.

HERRMANN, A.D., MACLEOD, K.G., and LESLIE, S.A., 2010, Did a volcanic mega-eruption cause global cooling and a regional extinction during the Late Ordovician?: Palaios, v. 25, p. 831-836, doi: 10.2110/palo.2010.p10069r.

HOLLAND, S.M., and PATZKOWSKY, M.E., 1996, Sequence stratigraphy and long-term paleoceanographic change in the Middle and Upper Ordovician of the eastern United States, in WITZKE, B.J., LUDVIGSON, G.A., and DAY, J., eds., Paleozoic sequence stratigraphy: Views from the North American craton: *Geological Society of America Special Paper* 306, p. 117-129.

HOWE, H. J., 1979. Middle and Upper Ordovician plectambonitacean, rhynchonellacean, syntrophiacean, trimerellacean, and atrypacean brachiopods. *United States Geological Survey Professional Paper* 1066-C, p. C1-C18.

HUFF, W.D., MUFTUOGLU, E., BERGSTROM, S.M., and KOLATA, D.R., 2004, Comparative biotite compositions in the Late Ordovician Deicke, Millbrig and Kinnekulle K-bentonites: a test of consanguinity, <u>in</u> Hints, O., and Ainsaar, L. (eds): *WOGOGOB-2004 Conference Materials*, Tartu University Press, Tartu, p. 47-48.

HUFFMAN, G.G., 1945, Middle Ordovician limestones from Lee County Virginia to central Kentucky: *Journal of Geology*, v. 53, p. 145-174.

JAROSEWICH, E., NELEN, J.A., and NORBERG, J.A., 1980, Reference samples for electron microprobe analyses: *Geostandards Newsletter*, v. 4, p. 43-47.

JENKINS, C.M., 1984, Depositional environments of the Middle Ordovician Greensport Formation and Colvin Mountain Sandstone in Calhoun, Etowah, and St. Clair Counties, Alabama [M.S. thesis]: Tuscaloosa, Univ. Alabama, 156 p.

JOY, M.P., MITCHELL, C.E., and ADHYA, S., 2000, Evidence of a tectonically driven sequence succession in the Middle Ordovician Taconic foredeep: *Geology*, v. 28, p. 727–730.

KOLATA, D.R., HUFF, W.D., and BERGSTRÖM, S.M., 1998, Nature and regional significance of unconformities associated with the Middle Ordovician Hagan K-bentonite complex in the North America midcontinent: *Geological Society of America Bulletin*, v. 110, p. 723-739.

KOLATA, D.R., HUFF, W.D., and BERGSTRÖM, S.M, 2001, The Ordovician Sebree Trough: An oceanic passage to the Midcontinent United States: Geological Society of America Bulletin, v. 113, p. 1067-1078.

LAVOIE, D., and ASSELIN, E., 1998, Upper Ordovician facies in the Lac Saint-Jean outlier, Québec (eastern Canada): palaeoenvironmental significance for Late Ordovician oceanography: Sedimentology, v. 45, p. 817-832.

LAVOIE, D., 1995, A Late Ordovician high-energy temperate-water carbonate ramp, southern Quebec, Canada: implications for Late Ordovician oceanography: Sedimentology, v. 42, p. 95 - 116.

LUDVIGSON, G.A., JACOBSON, S.R., WITZKE, B.J., and GONZÁLEZ, L.A., 1996, Carbonate component chemostratigraphy and depositional history of the Ordovician Decorah Formation, Upper Mississippi Valley, in WITZKE, B.J., LUDVIGSON, G.A., and DAY, J., eds., Paleozoic Sequence Stratigraphy: Views from the North American Craton, Volume Geological Society of America Special Paper 306, p. 67-86.

LUDVIGSON, G.A., WITZKE, B.J., GONZÁLEZ, L.A., CARPENTER, S.J., SCHNEIDER, C.L., and HASIUK, F., 2004, Late Ordovician (Turinian-Chatfieldian) carbon isotope excursions and their stratigraphic and paleoceanographic significance: Palaeogeography, Palaeoclimatology, Palaeoecology, v. 210, p. 187-214.

MILLER, R. L., and BROSGÉ, W.P., 1954, Geology and oil resources of the Jonesville district, Lee County, Virginia: *United States Geological Survey Bulletin* 990, 240 p.

MITCHELL, C.E., ADHYA, S., BERGSTRÖM, S.M., JOY, M.P., and DELANO, J.W., 2004, Discovery of the Ordovician Millbrig K-bentonite bed in the Trenton Group of New York State:

Implications for regional correlation and sequence stratigraphy in eastern North America: *Palaeogeography, Palaeoclimatology, Palaeoecology*, v. 210, p. 331–346.

MORAD, S., 1988, Diagenesis of titaniferous minerals in Jurassic sandstones from the Norwegian Sea: *Sedimentary Geology*, v. 57, p. 17-40.

MORAD, S., and ALDAHAN, A.A., 1986, Alteration of detrital Fe-Ti oxides in sedimentary rocks: *Geological Society of America Bulletin*, v. 97, p. 567-578.

PATZKOWSKY, M.E., and HOLLAND, S.M., 1993, Biotic response to a Middle Ordovician paleoceanographic event in eastern North America: Geology, v. 21, p. 619-622.

PATZKOWSKY, M.E., and HOLLAND, S.M., 1996, Extinction, invasion and sequence stratigraphy: Patterns of faunal change in the Middle and Upper Ordovician of the eastern United States, in WITZKE, B.J., LUDVIGSON, G.A., and DAY, J., eds., Paleozoic Sequence Stratigraphy: Views from the North American craton: Boulder, CO, Geological Society of America Special Paper 306, p. 131-142.

PATZKOWSKY, M.E., and HOLLAND, S.M., 1999, Biofacies Replacement in a Sequence Stratigraphic Framework: Middle and Upper Ordovician of the Nashville Dome, Tennessee, USA: Palaios, v. 14, p. 301-323.

POPE, M., and READ, J.F., 1997, High-resolution surface and subsurface sequence stratigraphy of late Middle to Late Ordovician (Late Mohawkian – Cincinnatian) foreland basin rocks, Kentucky and Virginia: *American Association of Petroleum Geologists Bulletin*, v. 81, p. 1866-1893.

POPE, M.C., and READ, J.F., 1997, High-resolution stratigraphy of the Lexington limestone (Late Middle Ordovician), Kentucky, U.S.A.: A cool-water carbonate-clastic ramp in a tectonically active foreland basin, in Noel, P., and Clarke, J.A.D., ed., Cool-water carbonates, Volume 56: Special Publication - SEPM, p. 410-429.

READ, J.F., 1980, Carbonate ramp-to-basin transitions and foreland basin evolution, Middle Ordovician, Virginia Appalachians: *American Association of Petroleum Geologists Bulletin*, v. 64, p. 1575-1612.

READ, J.F., 1982, Geometry, facies, and development of Middle Ordovician carbonate buildups, Virginia Appalachians: *American Association of Petroleum Geologists Bulletin*, v. 66, p. 189-209.

READ, J.F., and REPETSKI, J.E., 2012, Cambrian – lower Middle Ordovician passive carbonate margin, southern Appalachians, in J. R. DERBY, R. D. FRITZ, S. A. LONGACRE, W. A. MORGAN, and C. A. STERNBACH, eds., The great American carbonate bank: The geology and economic resources of the Cambrian – Ordovician Sauk megasequence of Laurentia: *American Association of Petroleum Geologists Memoir* 98, p. 357 – 382.

RODGERS, J., 1971, The Taconic Orogeny: *Geological Society of America Bulletin*, v. 82, p. 1141-1178.

ROSENAU, N., HERRMANN, A.D., and LESLIE, S., 2012, Conodont apatite δ18O values from a platform margin setting, Oklahoma, USA: Implications for initiation of Late Ordovician icehouse conditions, Palaeogeography, Palaeoclimatology, Palaeoecology. doi:10.1016/j.palaeo.2011.12.003

SAMANKASSOU, E., 2002, Cool-water carbonates in a paleoequatorial shallow-water environment: The paradox of the Auernig cyclic sediments (Upper Pennsylvanian, Carnic Alps, Austria-Italy) and its implications: Geology, v. 30, p. 655-658.

SAMSON, S.D., KYLE, P.R., and ALEXANDER, E.C. Jr., 1988, Correlation of North American Ordovician bentonites by using apatite chemistry: *Geology*, v. 16, p. 444-447.

SAMSON, S.D., MATTHEWS, S., MITCHELL, C.E., and GOLDMAN, D., 1995, Tephrochronology of highly altered ash beds: The use of trace element and strontium isotope geochemistry of apatite phenocrysts to correlate K-bentonites: *Geochimica et Cosmochimica Acta*, v. 59, p. 2527-2536.

SCOTESE, C.R., and MCKERROW, W.S., 1990, Revised world maps and introduction, in MCKERROW, W.S., and SCOTESE, C.R., eds., Palaeozoic palaeogeography and biogeography: Oxford, United Kingdom, p. 1-21.

SCOTESE, C.R., and MCKERROW, W.S., 1991, Ordovician plate tectonic reconstructions, in Barnes, C.R., and Williams, S.H., eds., Advances in Ordovician geology: Geological Survey of Canada Paper 90-9, p. 225-234.

SELL, B.K., and SAMSON, S.D., 2011, Apatite phenocryst compositions demonstrate a miscorrelation between the Millbrig and Kinnekulle K-bentonites of North America and Scandinavia: *Geology*, v. 39, p. 303-306, doi: 10 .1130 /G31425 .1.

SELL, B.K., SAMSON, S.D., MITCHELL, C.E., MCLAUGHLIN, P.I., KOENIG, A.E., and LESLIE, S.A., 2015, Stratigraphic correlations using trace elements in apatite from Late Ordovican (Sandbian-Katian) K-bentonites of eastern North America: *Geological Society of America Bulletin*, v. 127, in press, doi: 10.1130/B31194.1.

STEINHAUFF, D.M., and Roberson, K.E., 1989, Stop 7 – Uppermost Knox Group, the Knox unconformity, and the Middle Ordovician transition between shallow shelf and deeper basin near Dandridge, Tennessee, in WALKER, K.R., READ, J.F., and HARDIE, L.A., (leaders), Cambro-Ordovician carbonate banks and siliciclastic basins of the United States Appalachians: Washington DC, *28th International Geological Congress, Field Trip Guidebook T161*, p. 24-27.

WALKER, K.R., AND FERRIGNO, K.F., 1973, Major Middle Ordovician reef tract in east Tennessee: *American Journal of Science*, v. 273-A, p. 294-325.

WEBBY, B.D., COOPER, R.A., BERGSTROM, S.M., and PARIS, F., 2004, Stratigraphic framework and time slices, in Webby, B.D., Paris, F., Droser, M.L., and Parcival, I.G., eds., The Great Ordovician Biodiversification Event: New York, Columbia University Press, p. 41-47.

WOODWARD, H. P., 1951, The Ordovician System of West Virginia: W. Va. Geol. Survey, v. 21, 627 p.

YOUNG, S.A., SALTZMAN, M.R., and BERGSTRÖM, S.M., 2005, Upper Ordovicain (Mohawkian) carbon isotope (d13C) stratigraphy in eastern and central North America: Regional expression of a perturbation of the global carbon cycle: Palaeogeography, Palaeoclimatology, Palaeoecology, v. 222, p. 53-76.

ZEIGLER, E.L., 1988, Sedimentary petrology and depositional environments of the Upper Ordovician Sequatchie and Lower Silurian Red Mountain Formations, northwestern Georgia [Ph.D. dissertation]: Atlanta, Emory University, 288 p.

Ordovician of Germany Valley, West Virginia

MID-CONFERENCE FIELD TRIP

June 10th, 2015

John T. Haynes[1]

Keith E. Goggin[2]

Randall C. Orndorff[3]

[1]*Associate Professor, Department of Geology and Environmental Science, James Madison University, Harrisonburg, VA 22807,* *haynesjx@jmu.edu*

[2]*Senior Geologist and Sedimentology Manager, Weatherford Laboratories, Houston, TX 77086,* *keith.goggin@weatherford.com*

[3]*Director, Eastern Geology and Paleoclimate Science Center, United States Geological Survey, MS926A National Center, 12201 Sunrise Valley Drive, Reston, VA 20192,* *rorndorf@usgs.gov*

Contributors:
Richard Diecchio, George Mason University
Del Martin, Germany Valley Karst Survey
Rick Lambert, Germany Valley Karst Survey
Steve Leslie, James Madison University

TABLE OF CONTENTS .... **pg. #**

INTRODUCTION

   Welcome to the Conference field trip that is a part of the 2015 International Symposium on the Ordovician System meeting! This trip will consist of stops at five locations (Fig. 1) that will provide us with a detailed look at a major part of the Ordovician section in Germany Valley, West Virginia. We will be highlighting a varied sequence of carbonate and siliciclastic strata that accumulated from Middle to Late Ordovician time, and which record changes in the depositional regime of the region that came about as a result of Taconic tectonic activity in this region.

   The older carbonate strata (New Market, Lincolnshire, Big Valley, McGlone, and McGraw Limestones) record the final stages of deposition in the widespread epeiric sea that existed across much of the Laurentian craton and shelf margin from the Middle Cambrian into the Middle Ordovician. We will see how the depositional environments change upsection from peritidal and shallow shelf setting, to deeper shelf settings (Nealmont Limestone, Dolly Ridge Formation, and lower part of the Reedsville Shale) with a gradually but steadily increasing amount of mud coming into the depositional basin, to deeper slope or basin margin settings where dark gray muds accumulated as accommodation space developed in the Taconic foredeep. Maximum flooding in this sequence occurred at the base of the Reedsville, and it was followed by a gradual shallowing back to shelf and nearshore environments (upper part of Reedsville Shale, *Orthorhynchula* biozone, Oswego Sandstone, and Juniata Formation) that were dominated by siliciclastic rather than carbonate sedimentation.

BACKGROUND AND GEOLOGIC SETTING

   In the Germany Valley area of West Virginia, an estimated 1200 m (4,500 feet) of Ordovician strata are exposed, and a brief description of these stratigraphic units follows Table 1.

NAME	THICKNESS IN METERS (FT)	REFERENCES
Juniata Fm	224 m (736 ft)	Diecchio, 1985
Oswego Ss	56 m (182 (ft)	Diecchio, 1985
Reedsville Sh	605 m (2000 ft)	Ryder, 1992
Dolly Ridge Fm	123 m (405 ft)	Perry, 1972
Nealmont Ls	80 m (265 ft)	Kay, 1956; Perry, 1972; Martin et al., 2014
McGraw Ls	9.5 m (31 ft)	Kay, 1956; Perry, 1972; Martin et al., 2014
McGlone Ls	18 m (60 ft)	Kay, 1956; Perry, 1972; Martin et al., 2014
Big Valley Ls	36.5 m (121 ft)	Kay, 1956; Perry, 1972; Martin et al., 2014
Lincolnshire Ls	10 m (33 ft)	Kay, 1956; Perry, 1972; Martin et al., 2014
New Market Ls	10.5 m (35 ft)	Kay, 1956; Perry, 1972; Martin et al., 2014

TABLE 1.—Ordovician stratigraphic units exposed in Germany Valley, and their approximate thickness in the vicinity of today's stops.
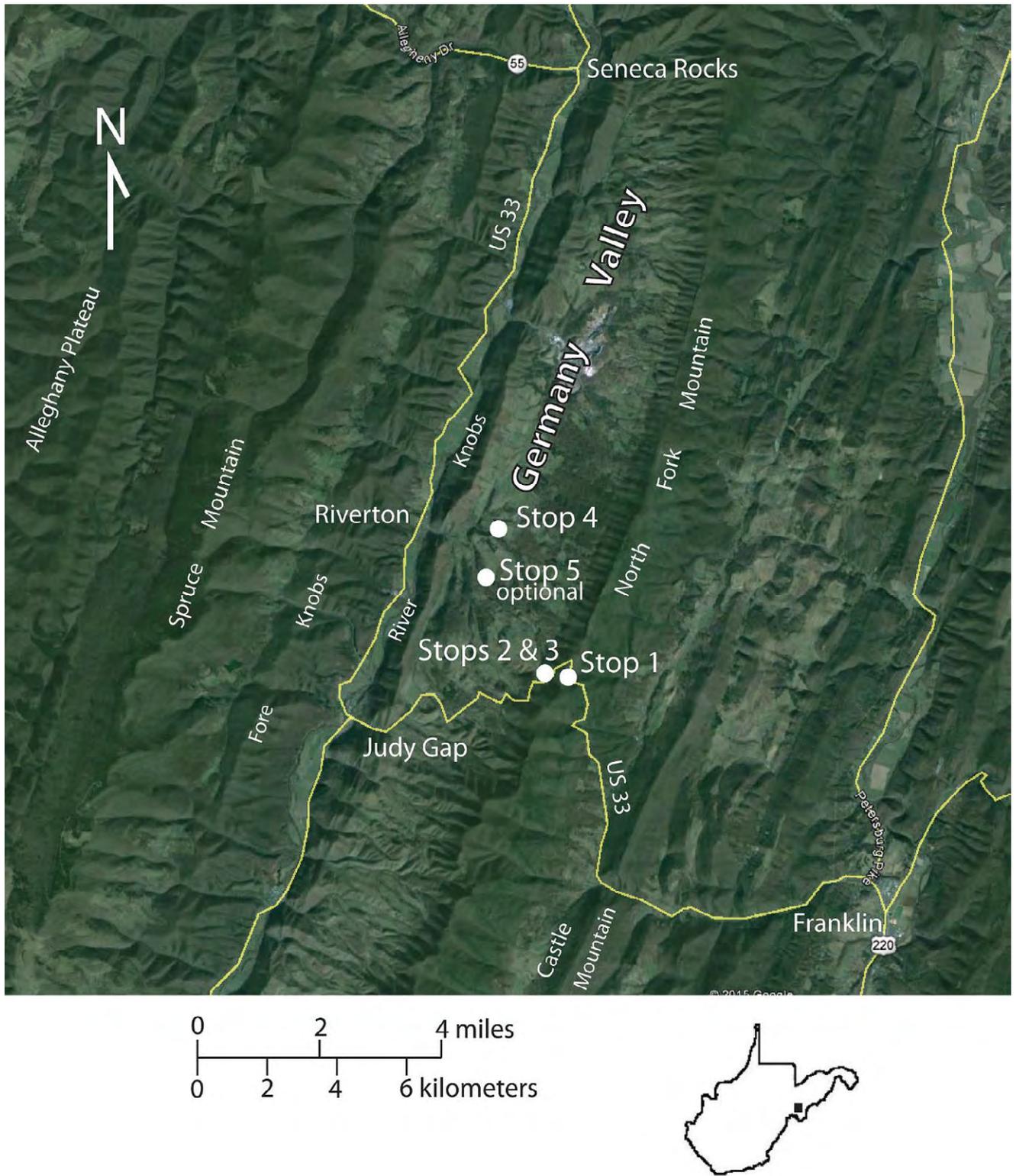
Figure 1.—Location of field trip stops and selected features in and around Germany Valley, in west-central Pendleton County, West Virginia.
New Market Limestone

  Most of the New Market Limestone (Cooper and Cooper, 1946) is typically a light to medium gray fenestral ("birds eye") lime mudstone that commonly breaks with a conchoidal fracture. At some exposures a few fossil gastropods, ostracodes, and corals have been reported, although our scrutiny of New Market samples from many localities suggests that numerous examples of what have long been thought to be *Tetradium syringoporoides* are in fact just fenestral pore spaces ("birdseyes"), or burrows, that have subsequently been reduced with sparry calcite. If coral fossils are as abundant as Butts (1940) and Kay (1956) suggested, then we might expect the presence of coral in the New Market to be accompanied by other marine organisms that were common at this time and that thrived in open marine environments, perhaps especially brachiopods, bryozoans, trilobites, and crinoids. But, when compared to the younger Lincolnshire and Big Valley Limestones, with their small reefs and buildups in this region (Kay, 1956; Cuffey, 2003; Cuffey et al., 2000),the overall lack of a diverse and open marine fauna in most exposures of the New Market seems problematic. This further supports our observations which suggest that much "*Tetradium*" in the New Market Limestone is actually just fenestrae. The fenestral lime mudstones of the New Market accumulated in a quiet muddy environment, probably shallow subtidal to high intertidal to supratidal, with the abundant fenestrae originally being gas bubbles from decaying organic matter that were trapped in the sediment and preserved as fenestral porosity (Grover and Read, 1978).

  In the Arc Hollow section, the upper meter or two of the New Market is exposed in the bed of several of the tributary streams that have cut into the core of the Germany Valley anticline along its axis (Fig. 2), but those exposures are not part of today's stops because of the relatively strenuous effort required to get there. Because of its compositional purity and homogeneity, the New Market is valued for cement manufacturing operations, and is the main rock being obtained in the large quarrying operation to the north of Arc Hollow, in the center of Germany Valley.

Lincolnshire Limestone

  The Lincolnshire Limestone (Cooper and Prouty, 1943) is characteristically a dark gray bioclastic packstone to grainstone to patches of boundstone, with an abundant and diverse assemblage of marine fossils including brachiopods, bryozoans, echinoderms including crinoids and cystoids, trilobites, corals, sponges, cephalopods, and pelecypods (Butts, 1941; Woodward, 1951; Kay, 1956), and in the Arc Hollow section in particular, small 4-6 cm high domal stromatolites in the lowest Lincolnshire immediately above the uppermost New Market (Fig. 3).

  Common to abundant lenses, nodules, and discontinuous beds of hackly and variably fractured black chert are typically observed in the Lincolnshire throughout its extent from southwest Virginia to this region, although Kay (1956) noted, as we have, that the exposures in Germany Valley are less cherty than elsewhere. Also of importance is that the presence of black chert is not unique to the Lincolnshire in the Ordovician limestones of this region, and in fact Kay (1956) described up to six (6) intervals in the Ordovician limestone sequence he was reporting on in which black chert is present. In the Arc Hollow section, we have observed black

Figure 2.—Rick Lambert on the upper beds of the New Market Limestone in a tributary to the main stream valley in Arc Hollow, near Stop 4. Photo by J.T. Haynes.

Figure 3.—Eroded tops of several domal stromatolites on the upper bedding plane surface of the lowest bed in the Lincolnshire Limestone, which directly overlies the New Market Limestone. Exposure in stream valley in Arc Hollow, near Stop 4. Photo by J.T. Haynes.

chert lenses and nodules in two (2) beds of the Big Valley Limestone, and in one (1) bed of the Nealmont Limestone.

The Lincolnshire is the initial unit in a deepening-upward sequence that was deposited in an open shelf to ramp setting during initial stages of a regionally widespread transgression (Read, 1980). The basal layer of domal stromatolites in the Arc Hollow section likely records initial flooding of the uppermost New Market Limestone and subsequent colonization of the surface by microbial communities including domal stromatolites. Because the New Market – Lincolnshire contact in this region is a disconformity, with relief up to 30 cm and has been interpreted as a paleoepikarst and/or a wave-cut platform surface (Kay, 1956; Read and Grover, 1977), we conclude that the thin stromatolite community (Fig. 3) developed in the initially very shallow waters that were transgressing across the now-inundated disconformity that developed on the uppermost bed of the New Market.

Big Valley Limestone

The Big Valley Limestone (Bick, 1962) was named because three units in southwest Virginia, when traced into Bath, Highland, and Pendleton Counties, could not be stratigraphically separated by Bick for mapping purposes in these areas, which includes Germany Valley, the focus of today's field trip. The three units are the Ward Cove Limestone (oldest), the Peery Limestone, and the Benbolt Limestone (youngest) (Cooper and Prouty, 1943). Kay (1956) had earlier recognized the problem of using these names in this area, and he suggested that the Pennsylvania name Hatter Formation (Kay, 1944) might be used in Germany Valley. He did not do so, however, and Bick (1962) opted for the new name Big Valley rather than Hatter (which has not been used subsequently). Perry (1972) also used Big Valley Limestone, and he included the thin Lincolnshire Limestone in it as well. The detailed geologic map of Martin et al. (2014) mapped most of this same stratigraphic interval of shaly and nodular-bedded limestone as the Benbolt Limestone, and that map did not recognize either the older Ward Cove or Peery Limestones. Use of Big Valley Limestone vs. Benbolt Limestone seems warranted to us because of the same uncertainties encountered during field mapping as were encountered by Kay (1956), Bick (1962), and Perry (1972) in this area, and we also agree with Martin et al. (2014) that most of the Big Valley Limestone in Germany Valley is what Kay (1956) recognized and described as the Benbolt Limestone.

The Big Valley of the Germany Valley area is a heterogeneous unit of shaly weathering, argillaceous, nodular bedded lime mudstones, sparsely to moderately fossiliferous wackestones and packstones, and lesser grainstones, a few with sparse lenses and nodules of black chert (Fig. 4). The Big Valley has common to abundant thin argillaceous partings some or all of which might be bentonitic in character and possibly correlative with the K-bentonite zone in the lower Edinburg Limestone of the Shenandoah Valley to the east, a zone that is well-exposed along Tumbling Run in Shenandoah County (Haynes et al., 1998) where it will be seen on the post-meeting field trip.

Although no biohermal or biostromal layers have been observed to date in the Big Valley exposures of Germany Valley, Kay (1956) and Cuffey et al. (2000) describe some thickets or small buildups in correlative exposures of the Ward Cove and the Benbolt Limestones to the south in Virginia.

Regionally, the Benbolt Limestone (and by extension its equivalent stratigraphic interval in Germany Valley that comprises most of the Big Valley Limestone) is recognized as having been deposited in a deeper slope or ramp environment that developed in the middle and late Ordovician along the margin of the Taconic foredeep, during maximum transgression of the Laurentian margin (Read, 1980). In Arc Hollow, that paleoenvironmental interpretation fits the observed stratigraphic sequence, with shallow peritidal to open shelf carbonates both downsection stratigraphically (the New Market and Lincolnshire Limestones) and upsection stratigraphically (the McGlone and McGraw Limestones) from the Big Valley Limestone.

Figure 4.—Rick Lambert at a low bluff of the Big Valley Limestone in Arc Hollow near Stop 4 pointing to black chert nodules along a bedding plane (inset, upper left). Del Martin (left) and Rick Diecchio are in the streambed. Photo by J.T. Haynes.

McGlone Limestone

Above the Big Valley Limestone is the McGlone Limestone (Kay, 1956), which is a heterogeneous unit of light gray fenestral lime mudstones, darker gray peloidal and bioclastic grainstones and packstones and laminated lime mudstones, in places burrowed and with possible desiccation cracks; some wackestone is also present (Fig. 5). Identification of the contact between the Big Valley and the overlying McGlone is based on the same criteria of Kay (1956) and Bick (1962), which is the change from a regionally extensive 3-4 m thick interval of cross-laminated silty to fine-sandy to dolomitic packstones and wackestones in the uppermost Big Valley (Benbolt of Kay, 1956), to interbedded fenestral and laminated lime mudstones and peloidal and bioclastic grainstones of the lower part of the McGlone. At the old North Fork

258

Figure 5.—Rick Lambert in the North Fork quarry looking at shallowing upward cycles in the McGlone Limestone, which will be seen at Stop 4. Photo by J.T. Haynes.

quarry (part of Stop 4), the Big Valley – McGlone contact is at the eastern end of the quarry, around 49 -50 m above the base of the Arc Hollow section, as marked by the tags in the quarry wall.

The McGlone and its stratigraphic equivalents in sections farther south and southwest (Gratton, Wardell, Bowen, and Witten Limestones of Cooper and Prouty, 1943) are part of an overall shallowing-upward sequence that accompanied a regional regression (Read, 1980) associated with the Blountian phase of the Taconic orogeny in the southern Appalachians, a time that flysch and molasse sediments filled the Blount foredeep in parts of Alabama, Georgia, Tennessee, and Virginia south of Roanoke. The McGlone, with its interbedded peloidal grainstones and fenestral and laminated lime mudstones, likely represents alternation of higher energy skeletal shoal and channel deposits and lower energy, peritidal mudflats that at times were overlain by rippled peloidal sands transported from shallow subtidal or intertidal environments. Deposition of the more massive fenestral lime mudstones also occurred in lower energy peritidal mudflats subsequent to shallowing of channeled sand flats (Read, 1980).

McGraw Limestone

The thick-bedded McGraw Limestone (Kay, 1956) overlies the McGlone, and the most distinctive lithology in the McGraw is massive black lime mudstone with abundant tubular burrows that were identified by Kay (1956) as *Camarocladia sp.,* and which are commonly seen to be filled with less resistant sediment that weathers more readily, leaving behind burrow moldic porosity (Fig. 6). Even in the quarry at Stop 4, where the surface of the rock is still relatively unweathered, the compositional difference between the burrows and the sediment that fills them, and the surrounding black micrite, is readily seen on close inspection. Other than these burrows, the McGraw is sparsely fossiliferous. Kay's comment (Kay, 1956, p. 83) that the McGraw Limestone's "uniformity of lithology is paralleled by a persistence of small thickness" seems more true today based on our qualitative observations of similar lithologies at this approximate stratigraphic horizon in exposures from Alabama to Pennsylvania. The McGraw was deposited in a muddy, restricted marine environment where few shelly organisms were living, but evidently there was an abundance of soft-bodied organisms that were actively burrowing into the lime mud. The McGraw of Germany Valley is the uppermost unit of the shallowing upward sequence that began with the upper Big Valley Limestone, so the lack of a diverse fauna is perhaps expected in these shallow peritidal limestones, as deeper water conditions did not return until the transgressive surface that separates the McGraw and the overlying fossiliferous beds of the Nealmont Limestone.

The contact of the McGlone and the McGraw Limestones is one of the key topics that we intend to discuss at Stop 4 on today's trip. Kay (1956) used the presence of *Cryptophragmus antiquatuus* Raymond in the uppermost beds of the McGlone to guide his placement of the contact, and he stated "The basal contact of the McGraw with the McGlone is invariably sharp, as the McGlone commonly has *Cryptophragmus*-bearing calcarenite, particularly in more southerly sections, or plane-bedded calcilutite." The use of a fossil's appearance or disappearance is no longer considered acceptable for determining a stratigraphic contact as per the North American Stratigraphic Code and its restrictions on the use of "biological sequence" in setting lithostratigraphic formation boundaries vs. biozones (North American Commission on Stratigraphic Nomenclature, 2005), so an obvious alternate possibility is the "invariably sharp" basal contact mentioned above by Kay (1956). In the quarry wall at the southwest end of the exposure, we will point to two possible such sharp contacts (Fig. 7), and ask for thoughts and discussion on which contact might best be chosen as the McGlone – McGraw contact here.

Nealmont Limestone

The McGraw Limestone is succeeded upsection by the shaly and thinner-bedded limestones of the Nealmont Limestone (Kay, 1944), which Kay (1956) noted is correlative with the upper part of the "*Camarocladia*" zone of Cooper and Prouty (1943), and indeed, several of the limestone beds in the Nealmont at the Arc Hollow section contain abundant burrows of "*Camarocladia*". Otherwise, the presence of these burrows in both the McGraw and the

Figure 6.—Recessively weathered burrows in the McGraw Limestone, in Arc Hollow, near Stop 4. These trace fossils are "Camarocladia" of Kay (1956). Photo by J.T. Haynes

Nealmont is one of the few characteristics shared by these two stratigraphic units, as overall they are distinctly different.

The McGraw – Nealmont contact is a transgressive surface that is identified by an increase in partings and thin beds of shale that occur upsection with increasing frequency, and by the relatively abrupt appearance of abundant brachiopods in thin beds and on bedding planes. The contrast in both bedding thickness and the limestone:shale ratio between the underlying McGraw and the overlying Nealmont is striking, even though the contact is transitional over a 2-3 m interval. Like the Lincolnshire Limestone downsection, the Nealmont is the oldest unit in a deepening-upward sequence that continues upsection through the entire Dolly Ridge Formation, and ends at the maximum flooding surface in the lower part of the Reedsville Shale.

Kay (1956) notes that the McGraw to Nealmont transition is characterized in particular with the appearance of densely populated beds of argillaceous limestone that have abundant *Pionodema* and *Doleroides*, and lesser *Sowerbyella*, *Resserella*, and *Hesperorthis*, and that throughout the region, these brachiopod grainstones and packstones are invariably within a meter

Figure 7.—John Haynes pointing to the light gray laminated fenestral lime mudstone beds in the upper part of the McGlone Limestone, and the sharp contact with overlying darker gray beds of wavy laminated bioclastic wackestones and packstones. This contact, which we will see at Stop 4, is one of the two "candidates" for the McGlone – McGraw contact. Photo by R.C. Orndorff.

of the base of the Nealmont. This is the case at the Arc Hollow section, as we will see at Stop 4. The Katian – Sandbian contact is probably in the Nealmont Limestone as well, but detailed biostratigraphic work has not yet been done at the Arc Hollow section.

   The medium to thin-bedded, light to medium gray limestones of the Nealmont include laminated lime mudstones, moderately to intensely bioturbated beds (with "*Camarocladia*" burrows), bioclastic wackestones and packstones, with lesser grainstones, which collectively include beds with many intact or nearly intact fossils, especially gastropods and brachiopods, to beds that consist of comminuted skeletal debris of varying sizes and shape (Fig. 8). Kay (1956) describes some of these fossiliferous beds as "coquinal," which is apt. The shales also tend to be light gray, and beds of K-bentonite are also present in the Nealmont, but these have not yet been positively correlated with any regional extensive beds such as the Deicke or Millbrig. The abundant, but only moderately diverse fauna of the Nealmont Limestone, together with the shaly
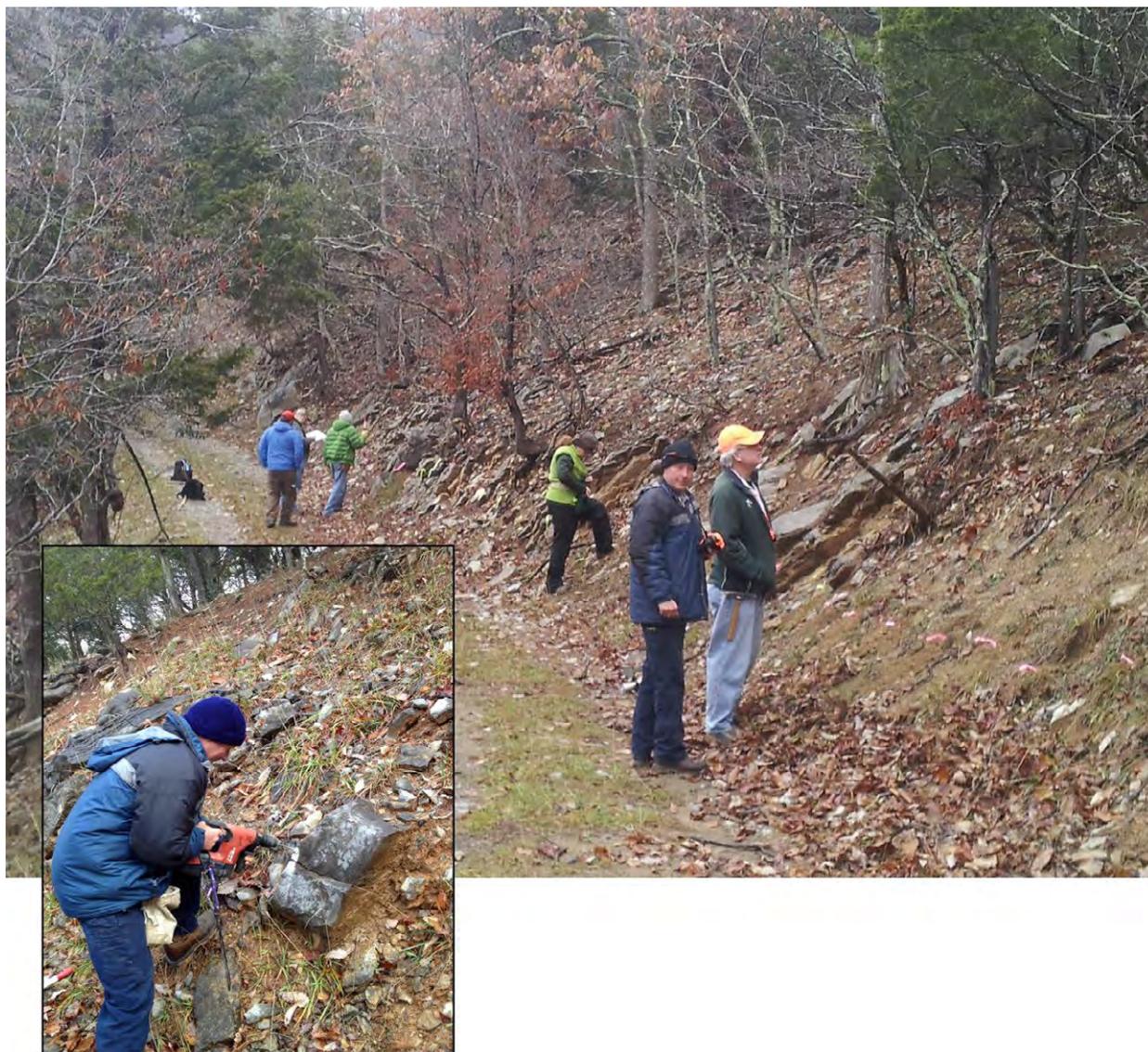
Figure 8—From right to left in main photo: John Haynes, Rick Lambert, Lisa Goggin, Rick Diecchio, Keith Goggin, and Alan Pitts collectively working to measure and describe the Nealmont Limestone at the Arc Hollow section, Stop 4. Subsequent to completion of the measurements and descriptions, Rick Lambert and John Haynes placed labels at regular intervals with the measurement in meters (inset at lower left). Photo by R.C. Orndorff, inset photo by J.T. Haynes.

partings and beds, suggests deposition in a higher-energy, open shelf setting, where mud entered at times, perhaps in association with storms (Carter et al., 1988). Burrows are common in only some thin beds, in contrast to the thick beds of extensively bioturbated limestones in the underlying McGraw, and this may be a result of more extensive predation, higher energy conditions that disrupted the previously quieter muds of the McGraw or some other degree of restriction.

Dolly Ridge Formation

As we will see at Stops 4 and 5, the contact of the Nealmont and the overlying Dolly Ridge Formation (Perry, 1972) is placed at the first prominent greenish gray shale between the ledges of light gray limestone that are distinctly of Nealmont character, and the ledges of black micrite that weather almost white and which are distinctly of Dolly Ridge character (Fig. 9). This shale contrasts with the light gray shales downsection that are typical Nealmont shales. The lower part of the Dolly Ridge Formation is a sequence of interbedded shales and cobbly weathering lime mudstones that are black on a fresh surface but which weather almost white, as compared to the lighter gray limestones of the Nealmont on both fresh and weathered surfaces. Overlying those beds is the main body of the Dolly Ridge, which consists of interbedded argillaceous limestone, much of which is cobbly weathering (Fig. 10), thin to medium dark gray to olive gray shales, and several K-bentonites (Perry, 1972). The Dolly Ridge records continued relative deepening of the water column and a slowly but steadily increasing influx of mud into the depositional basin, as a result of increasing tectonic activity and uplift associated with the Taconic orogeny that was ongoing far to the east. Nonetheless, carbonate sedimentation continued throughout the Dolly Ridge, but it became evermore disrupted as the volume of mud increased, along with the volume of volcanic ash as evidenced by the numerous tephras that have altered to become K-bentonite beds, of which there are several in the type section of the Dolly Ridge Formation (Perry, 1964, 1972), as will be seen at Stop 5.

Perry (1972) reports scattered occurrences of *Cryptolithus* and *Isotelus* in the Dolly Ridge, along with *Sowerbyella* and *Dalmanella*, as well as several thin fossiliferous beds in which unidentified fragments of brachiopods, crinoids, and other bioclasts occur. The Dolly Ridge was deposited on a deep shelf or ramp setting, with many of the limestones probably consisting of sediment that originally accumulated in shallower shelf settings, but which was later remobilized and transported down the ramp into deeper environments. These may or may not have been below the photic zone, but it was evidently deep enough for appreciable volumes of mud to accumulate in a quieter, low-energy setting. In the upper few meters of the Dolly Ridge, the limestones abruptly become thinner and thinner, until the entire sequence becomes the dark gray shales that comprise the basal beds of the Reedsville Shale.

Reedsville Shale

Above the Dolly Ridge is the thick Reedsville Shale, the basal beds of which we will see at Stops 4 and 5, and the uppermost beds we will see at Stops 2 and 3. The Reedsville is a heterogeneous formation, with dark gray shales many of which are calcareous at its base that transition upward to repetitively interbedded shales, siltstones, fine-grained sandstones, and bioclastic grainstones and packstones. Maximum flooding of the shelf occurred in the lower part of the Reedsville, when a sequence of dark muds accumulated and became the gray shales of the basal, lowermost Reedsville, which are mostly covered along the higher slopes of Germany Valley. This continued deepening of the water column was evidently a result of the combined eustatic sealevel rise (the "Trenton transgression"; Leslie and Bergstrom, 1995) that was

Figure 9.—Steve Leslie at the Nealmont – Dolly Ridge contact in the Arc Hollow section, Stop 4. Steve Leslie is standing next to the uppermost ledges of bioclastic grainstones, packstones, and wackestones that are characteristic of the Nealmont; those ledges are overlain by greenish gray shale that is the basal bed of the Dolly Ridge Formation. Photo by R.C. Orndorff.

occurring during the later Ordovician, and the buckling and downdropping of the Laurentian shelf edge that occurred as continent-microcontinent collision was producing the Taconic orogeny outboard of the Laurentian margin.

  The middle and upper parts of the Reedsville are the basal units of a second shallowing upward sequence, but unlike the older carbonate sequence (Big Valley, McGlone, and McGraw), this younger sequence is characterized by a transition from mostly carbonate and lesser mud, to mostly siliciclastics, with a few shelly beds of grainstone and packstone. With gradual shallowing of the water column, storm influenced and storm generated sedimentary structures become more common in the Reedsville throughout this region, which on the outcrop include hummocky cross-bedding, gutter casts, undulatory scoured-bases, and sandy whole-fossil packstones (Kreisa, 1981; Lehman and Pope, 1989), and in thin section include preferred shell orientation, various infiltration fabrics, abraded bioclasts of diverse types (Fig. 11), and shells with mud coatings (Kreisa and Bambach, 1982).

Figure 10.—Del Martin looking at cobbly weathering lime mudstone beds in the Dolly Ridge Formation, a characteristic of these limestones in outcrop. At the Dolly Ridge type section, Stop 5. Photo by J.T. Haynes.

Efforts to refine and improve our understanding of the conodont biostratigraphy of the upper part of the Reedsville from analysis of samples collected at Stop 2, have thus far met with limited success (S. Leslie, personal communication to JTH, 2015). This is because the definitive M element needed for identification of species in the genus *Oulodus* (thus far the only genus recovered), has not yet been recovered from any samples. As a result, the conodonts recovered from the Reedsville at Stop 2 (Fig. 12) are currently assigned only to *Oulodus sp.*

The uppermost several meters of the Reedsville are widely known as the *Orthorhynchula* biozone, or more commonly just the *Orthorhynchula* zone (Butts, 1940; Woodward, 1951; Bretsky, 1969, 1970). This typically 3-4 m thick stratigraphic interval "consists of an irregularly bedded, lumpy, brown sandstone that is almost incredibly filled with fossils which break out and weather out in molds and casts. The rock is gray and solid when fresh, but turns brown and crumbles rapidly on surface exposures. A few zones have become slightly calcareous because of their fossils." (Woodward, 1951). Large and numerous specimens of *Orthorhynchula sp.*, notably *Orthorhynchula linneyi*, and other brachiopods including *Lingula*, can be found with little effort at most exposures of the *Orthorhynchula* zone, including the exposure we will
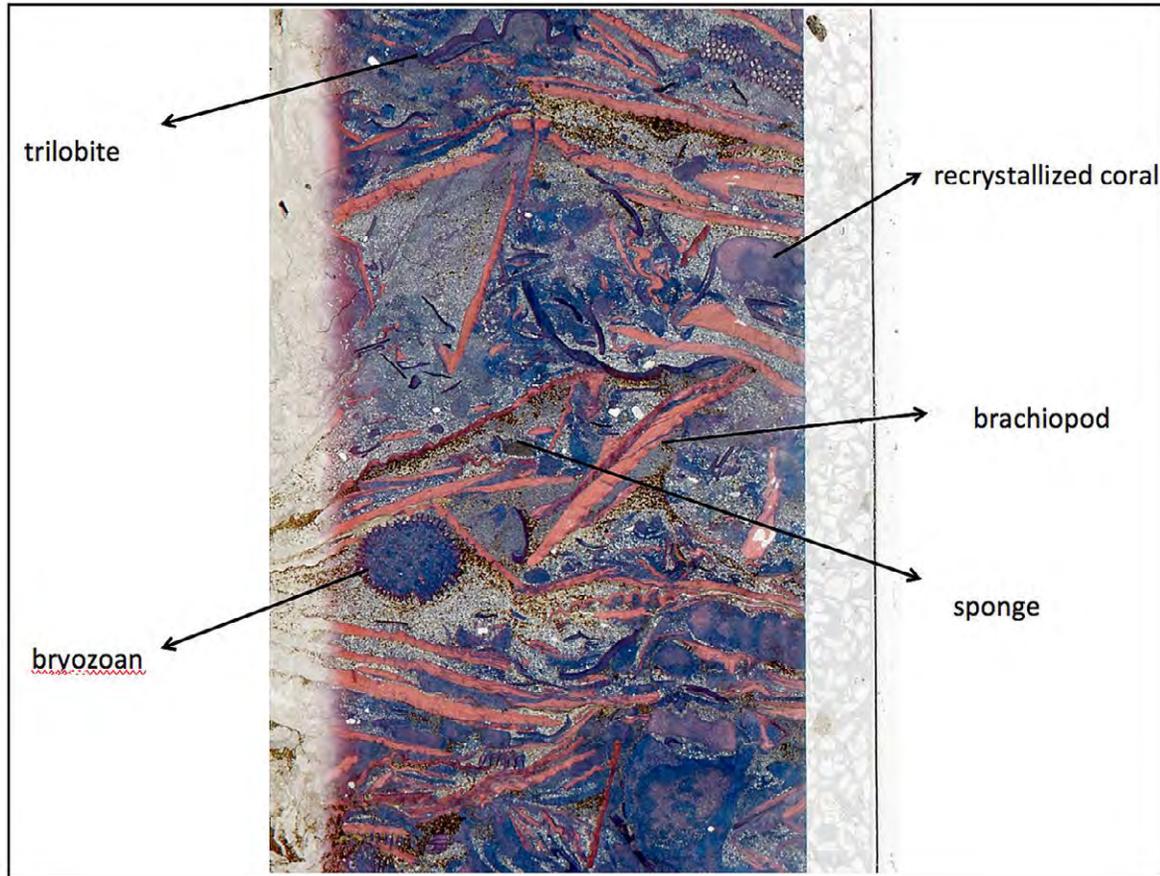
Figure 11. Stained thin section of a bioclastic packstone in the upper part of the Reedsville Shale, collected at Stop 3, with selected skeletal components identified. The packing arrangement of this shelly debris is typical of the storm beds in the Reedsville throughout this area of the Appalachians (Kreisa, 1981; Kreisa and Bambach, 1982). Staining with standard Dickson method by J.T. Haynes, with photo by JMU geology student H. Doherty.

examine at Stop 2. This stratigraphic interval represents shallowing of the basin to nearshore conditions that were favorable for these communities of large brachiopods, and the *Orthorhynchula* zone also represents essentially the last occurrence of marine shelly faunas in the Ordovician of this region. The overlying Oswego Sandstone and Juniata Formation are non-marine to marginal marine, with a few trace fossils including *Skolithos*, but the next marine flooding surface and regional transgression that was accompanied by radiation and colonization of marine organisms into newly marine habitat over a widespread area did not occur until deposition of the Silurian (Telychian) Rose Hill Formation (Woodward, 1941).

Oswego Sandstone
   Above the *Orthorhynchula* zone is the Oswego Sandstone, which in this region is a light brown to gray, medium to fine-grained sublitharenite and lesser lithic wacke, with interbedded siltstone and shale (Fig. 13). The Oswego is almost devoid of fossils, with eurypterid

Figure 12.—Steve Leslie on interbedded shales, siltstones, and bioclastic limestones in the upper part of the Reedsville Shale that we will see at Stop 2. Photo by J.T. Haynes

Figure 13.—R ick Lambert at the exposure of the Oswego Sandstone along US 33 on the east side of Germany Valley, which we will see at Stop 2. Photo by J.T. Haynes.

impressions in the Oswego in Berkeley County, West Virginia (about 145 km NNE of Germany Valley) being the only reported fossils of which we are aware (Diecchio, 1985). Yellow orange flecks of limonite are common in some of the Oswego sandstone beds, and these are the weathering product of iron-bearing lithic framework grains and of the ankerite cement that occurs in minor amounts throughout both the Oswego and the Juniata (Horowitz, 1971). The Oswego represents the culmination of the shallowing upward sequence that was initiated with the maximum flooding surface in the lower part of the Reedsville (Diecchio, 1985; 1986). The sands and muds of the Oswego were derived from weathering and erosion of the Taconic highlands to the east, and dispersal of these siliciclastics toward the west was facilitated by transport in rivers and streams into a shallow nearshore deltaic complex (Bretsky, 1970; Diecchio, 1985), but one that was evidently almost inhospitable to life in much of the region.

Juniata Formation

Above the Oswego Sandstone is the Juniata Formation, the youngest Ordovician unit in the central Appalachians. The transition from the Oswego to the Juniata is first and foremost one of color, as the Juniata is characterized by red shales, siltstones, and sandstones (Fig. 14), in

contrast to the greenish gray siliciclastics of the Oswego. To a far lesser extent, the transition is also one of overall grain size, as the Oswego contains more sandstone and less mudrock overall than the Juniata in most exposures (Diecchio, 1985). The green-to-red transition does not correlate with any lithologic grain size boundaries related to primary depositional settings (Thompson, 1970), but is thought instead (Thompson, 1970; Horowitz, 1971) to be the result of diagenetic changes, specifically from variation in the vertical chemical gradient caused by change in oxidation potential as reducing fluids expelled from the underlying dark organic marine muds of the Reedsville migrated through the overlying sands and muds of the Oswego and Juniata.

The Juniata has a low diversity assemblage of trace fossils, including *Skolithos, Cruziana,* and *Rusophycus*, and the likely environment of deposition is a tidal flat that was intermittently inundated with sea water (Diecchio, personal communication). Cyclic sedimentation characterizes the Juniata. The base of each cycle is thought to be a transgressive surface above which the regressive tidal para sequences were deposited.

Figure 14.—Rick Lambert looking at the cycles in redbeds of the Juniata Formation along US 33 on the east side of Germany Valley. We will see the upper Juniata at Stop 1. Photo by J.T. Haynes

DESCRIPTION OF STOPS

Stop 1: US 33, North Fork Mountain - east, Pendleton County, WV
38.698350 N, 79.403169 W; Circleville 7½ minute quadrangle

  At this stop, we will examine the upper several meters of the Juniata Formation, which in this region is the youngest Ordovician unit, and we will also have the opportunity to discuss the Ordovician – Silurian boundary, which here as in most of eastern North America, is an unconformity.   The boundary here is a lithostratigraphic one that occurs between the red mudrocks and sandstones in the Ordovician Juniata Formation, and the silica-cemented white quartz arenites of the overlying Silurian Tuscarora Formation.
  The upper part of the Juniata Formation here consists of about 48 meters of interbedded grayish-red arenite to sublitharenite interbedded with grayish-red mudstone and mud-shale. For most of this interval, these strata are organized into cycles (Fig. 15) that are interpreted as regressive tidal parasequences.
  Spectral analysis of the thicknesses of the sandstone-mudstone couplets suggests that these meter-scale parasequences have Milankovich periods, and are probably associated with either orbital obliquity or precession (Hinnov and Diecchio, 2015, abstract for this symposium). Further analyses are in progress.

The figure labeled with "CYCLE" on the left side contains the following annotations:
bioturbated mudstone with occasional pedogenic structures near the top
arenite to wacke with vertical burrows (Skolithos) and interbedded mudstone (not well developed at this outcrop)
cross-bedded arenite
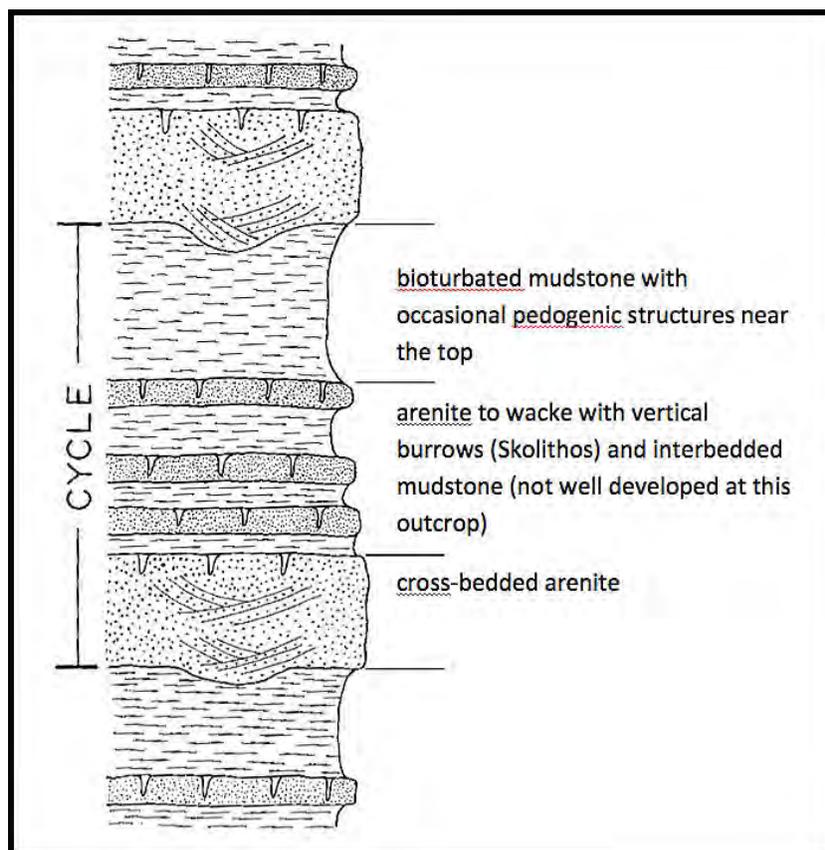
Figure 15.—Generalized cycle in the Juniata Formation (Diecchio, 1985).

  The Juniata Formation is overlain by the Tuscarora Formation, which is primarily a white to light gray quartz arenite (Fig. 16). The lower 2.5 meters of the Tuscarora is light olive gray, brown weathering sandstone that is capped by a 0.3 meter bed of very fine, red sandstone with vertical burrows (*Skolithos*). These beds correspond to the "Lower Tuscarora Sandstone" of Dorsch et al. (1994).
   Above the red sandstone, the majority of the Tuscarora

Figure 16.—John Haynes at the approximate position of the Ordovician – Silurian boundary, which is placed at the contact of the Juniata Formation (redbeds to left) and the Tuscarora Formation (quartz arenites to the right), which we will see at Stop 1 along US 33. Inset at lower left shows Rick Lambert at the reddish sandstone that has numerous Skolithos throughout it, and which is either uppermost Juniata or lowest Tuscarora. Photo by R.A. Lambert, inset photo by J.T. Haynes.

Formation here is 50 meters of very light gray quartzarenite, which corresponds to the "Upper Tuscarora Sandstone" of Dorsch et al. (1994). The lower 20 meters of the "Upper Tuscarora" is medium- to very coarse-grained, well-indurated, and cross-bedded, with occasional interbeds of friable sandstone. The upper 30 meters is very fine- to medium-grained, occasionally cross-bedded, with horizontal burrows (*Arthrophycus*) and interbeds of dark gray shale, especially in the upper portion. The sands of the Tuscarora were deposited in a mosaic of depositional environments including fluvial systems, braided alluvial fan and fan delta systems, high energy foreshore and shoreface zones of a beach or barrier island system, and sand-wave complexes on a shallow marine shelf (Folk, 1960; Yeakel, 1962; Cotter, 1983).

Owing to the lack of fossils, the Ordovician-Silurian boundary in the central Appalachians is not known with certainty. Traditionally, this boundary has been placed at the Juniata-Tuscarora contact (Butts, 1940; Woodward, 1941, 1951; Diecchio 1985), based on an extensive regional unconformity that corresponds to the global Ordovician-Silurian unconformity. Dorsch et al.

(1994) place this unconformity at the "Lower Tuscarora" – "Upper Tuscarora" boundary, and relate it to post-Taconic orogeny basin-rebound uplift. The exact position of, and basis for determining, the Ordovician-Silurian boundary in these strata is still a matter of discussion, and we will discuss it at this stop, including the hypothesis that the ~2.5 m of the lower part of the Tuscarora including the reddish bed with abundant *Skolithos* might represent the Hirnantian in this section.

 Stop 2: US 33, North Fork Mountain - west, Pendleton County, WV
38.708090 N, 79.410665 W; Circleville 7½ minute quadrangle

Figure 17.—Steve Leslie (left) and Randy Orndorff examining fossiliferous beds in exposure of the *Orthorhynchula* biozone along US 33 on the east side of Germany Valley, which we will see at Stop 2. Photo by J.T. Haynes.

   At this stop we will start with scrutiny of the regionally extensive *Orthorhynchula* zone, an assemblage biozone described by Bretsky (1969, 1970), at the contact of the Reedsville Formation and the overlying Oswego Sandstone (Fig. 17). This zone, which participants on the pre-meeting southern Appalachian trip saw at Dug Gap near Dalton, Georgia and in southwestern Virginia at Hagan, is a useful stratigraphic marker from Pennsylvania south to

Georgia. Here, it consists of about 10 m of gray to olive-gray mudstones that weather into distinctive blocky shale, with interbedded siltstones and thinly bedded sandstones exhibiting abundant *Orthorhynchula* molds, and less abundant *Lingula* within discrete beds. Above the *Orthorhynchula* biozone are 20 meters of the Oswego Sandstone, which here is a fine- to very fine-grained, cross-bedded sublitharenite to quartzarenite, commonly with a greenish gray color and common limonite flecks. Below the *Orthorhynchula* biozone is the Reedsville Shale, and at these exposures we will see about 25 m of the upper part of the Reedsville and its heterogeneous lithologies of mudrocks, fine-grained sandstones, and fossiliferous grainstones to wackestones, including the limestone bed that was processed for conodonts (Figs. 11, 12) and the bed from which a large *Isotelus* was obtained (Fig. 18).

Stop 3: US 33, Germany Valley overlook, Pendleton County, WV
38.708133 N, 79.413188 W; Circleville 7½ minute quadrangle

At this stop, we will present an overview of the stratigraphic (Fig. 19) and structural (Fig. 20) setting of Germany Valley, which as seen here, is an anticlinal valley that developed as erosion cut into the Wills Mountain anticline, a culmination on the more regionally extensive Nittany anticlinorium. A cross-section through this region (Fig. 20) shows that the Wills Mountain anticline is the westernmost major fold of the Valley and Ridge province of the Appalachian mountains in this region. Detailed bedrock mapping by Del Martin and Rick Lambert has resulted in a new geologic map and cross-sections of Germany Valley (Martin et al. (2014), included herein as a scaled-down version (Fig. 21) and as an overlay on the GoogleEarth TM landscape (Fig. 22). As a result of that mapping, in combination with the newly generated and still ongoing detailed measurements of the section in Arc Hollow (Plates 1, 2, and 3, included herein as scaled-down versions) that is the focus of Stop 4, we have a far more detailed understanding of the stratigraphy of the Ordovician carbonate sequence from the New Market Limestone upsection to the Reedsville Shale that comprises the several outcrops along US 33 including the exposure just behind us at the overlook.

Stop 4: North Fork quarry area and Arc Hollow, at the Germany Valley Karst Survey Fieldhouse, Riverton, WV, *38.742399 N, 79.423907 W; Circleville 7½ minute quadrangle*

At this stop, the principal stop of the field trip, we will have ample time to examine in detail the Ordovician limestone sequence from the upper part of the Big Valley Limestone upsection to the lower part of the Dolly Ridge Formation. The oldest strata in the part of the Arc Hollow section that we will see are the upper part of a regionally widespread shallowing upward sequence, from the middle of the Big Valley Limestone through the McGlone and into the McGraw. This is followed by a regionally widespread deepening upward sequence that we will

Figure 18.—*Isotelus* sp. in a siltstone bed of the Reedsville Shale at Stop 2. Photo by R.C. Orndorff.

also see, from the base of the Nealmont Limestone through the base of the Dolly Ridge Formation, which we will see more of at Stop 5. These sea-level changes are inferred from the changes that we will see in depositional environments. We will also discuss the detailed geologic map of this location (Fig. 23), and the detailed measured section that is being constructed from composite sections in Arc Hollow and adjacent ravines. This and other research efforts that collectively have been completed to date will be the focus at this stop as we
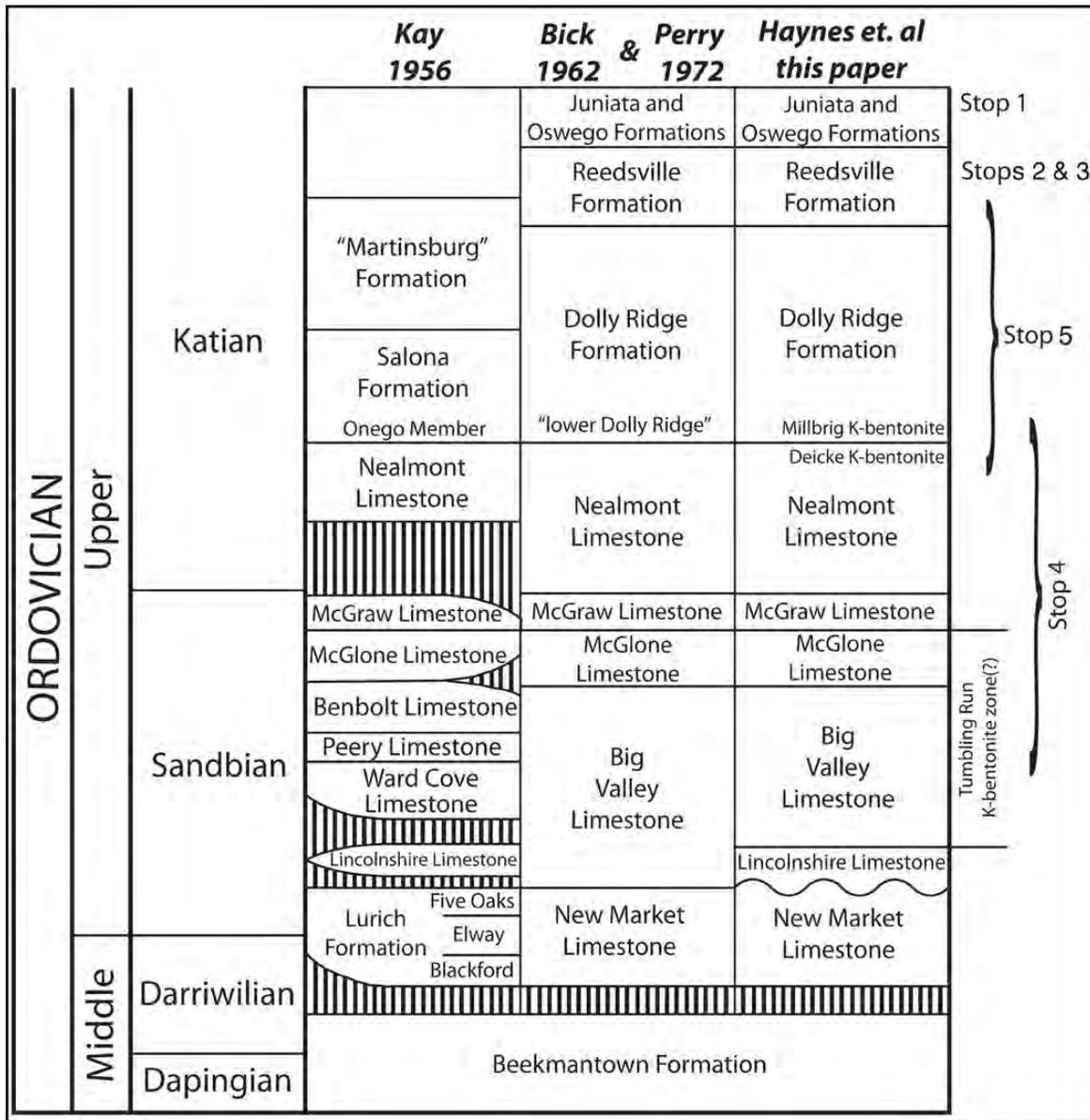
Figure 19.—Comparison of stratigraphic names used by geologists who have worked in the Germany Valley area.

walk from the Field House to the old North Fork Quarry. The section has been marked with aluminum tags at approximately 2 m intervals, and these measurements correspond to the measured section that comprises Plates 1, 2, and 3.
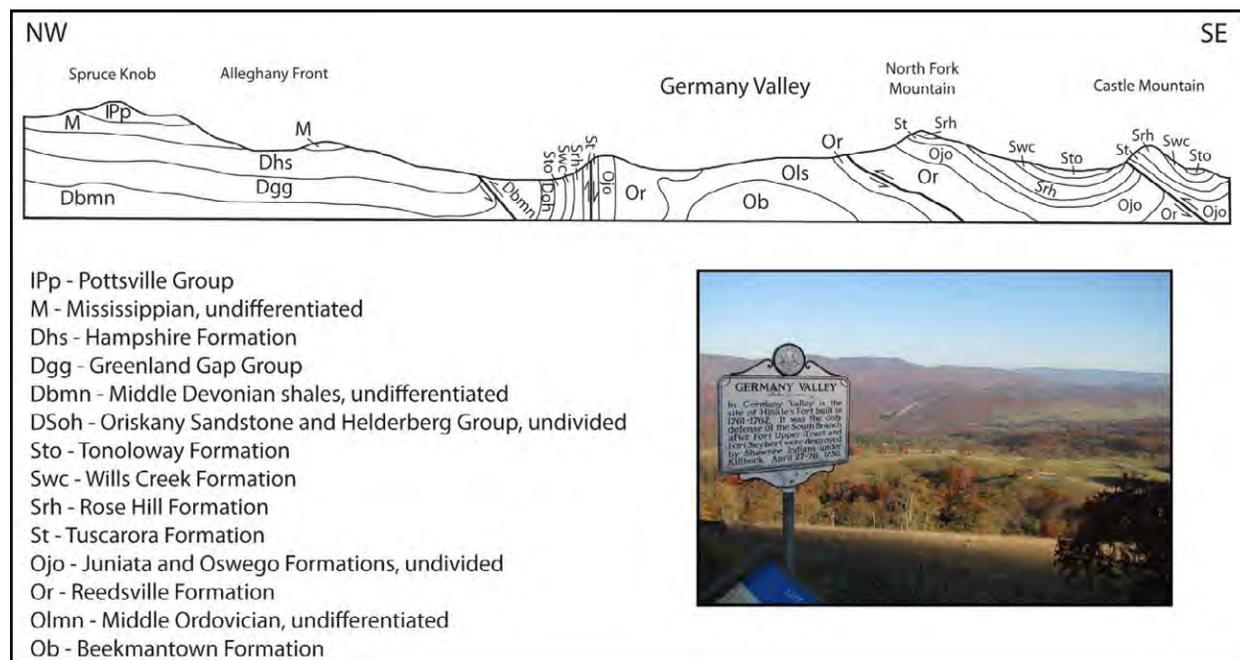
Figure 20.—Structural cross section across the Germany Valley area, which we will discuss at the Germany Valley overlook at Stop 3.

Stop 5 (optional): Dolly Ridge Formation type section, Riverton, WV
38.738466 N, 79.424618 W; Circleville 7½ minute quadrangle

There will probably be an opportunity in mid-afternoon for those who are interested to walk over to the Dolly Ridge road and examine the type section of the Dolly Ridge Formation (Fig. 22) of Perry (1972). The Arc Hollow section and the type Dolly Ridge section are correlated at the ~ 3 m thick olive gray shale that is the lowest bed in the Dolly Ridge Formation. It is at the top of the Arc Hollow section, and near the base of the type Dolly Ridge section, so with that bed to tie both sections together, our goal is to construct a composite stratigraphic section from the New Market Limestone to the base of the Reedsville Shale.

Figure 21.—Bedrock geologic map of Germany Valley from field mapping by Del Martin and Rick Lambert of the Germany Valley Karst Survey (Martin et al., 2014). Ordovician carbonates were folded under brittle conditions across the northwest verging, overturned Wills Mountain anticline, with the carbonates experience only minor additional flexing. Tighter folds are recognized above the carbonates, especially in the Reedsville Shale, and these, along with the overall fissile nature of the Reedsville suggests significant shearing across its entire thickness. Thus, we hypothesize that the Reedsville absorbed the majority of the regional deformation, and may even have acted as a decollement between the underlying carbonates and the overlying sandstones. Further field work is needed on each these specific areas.
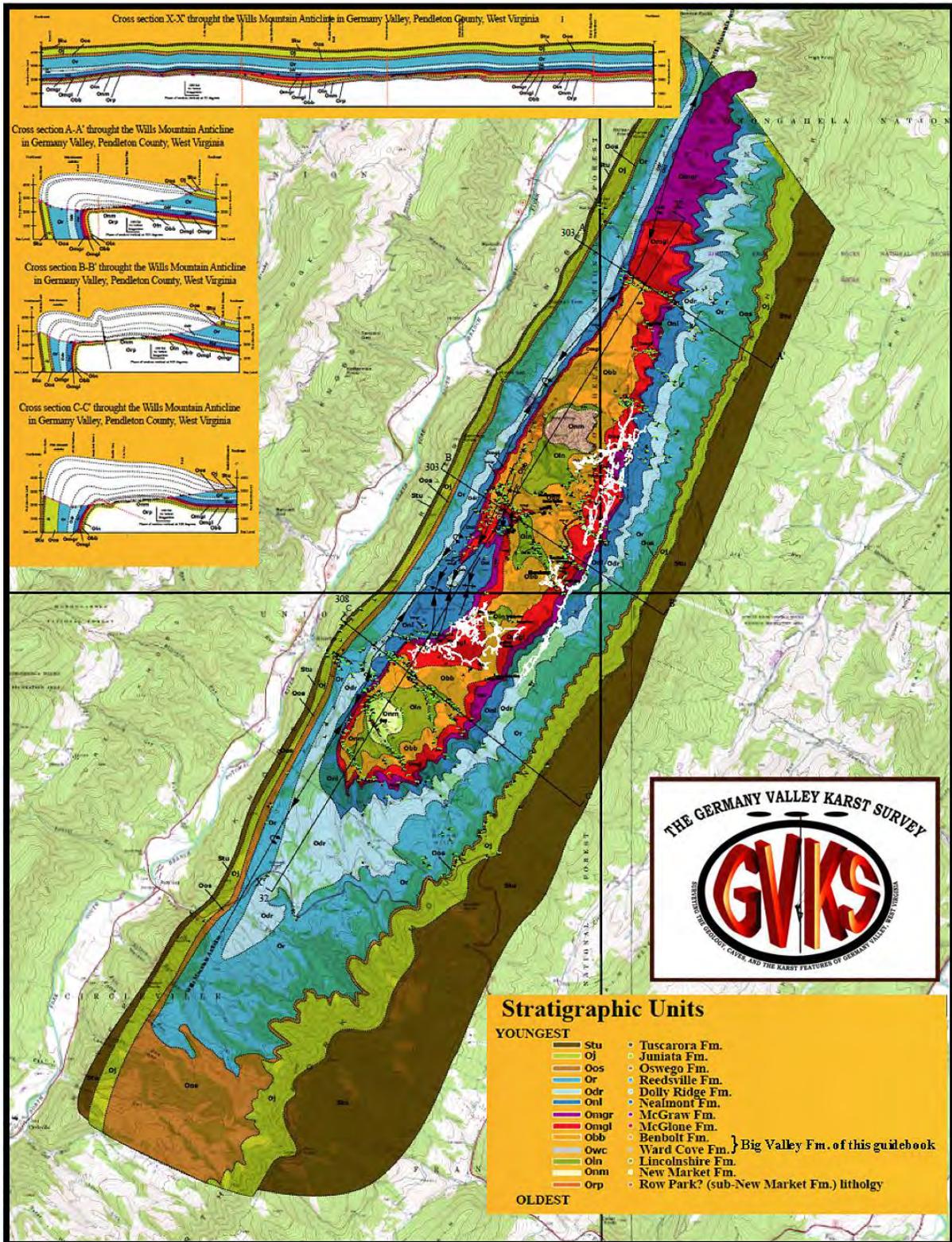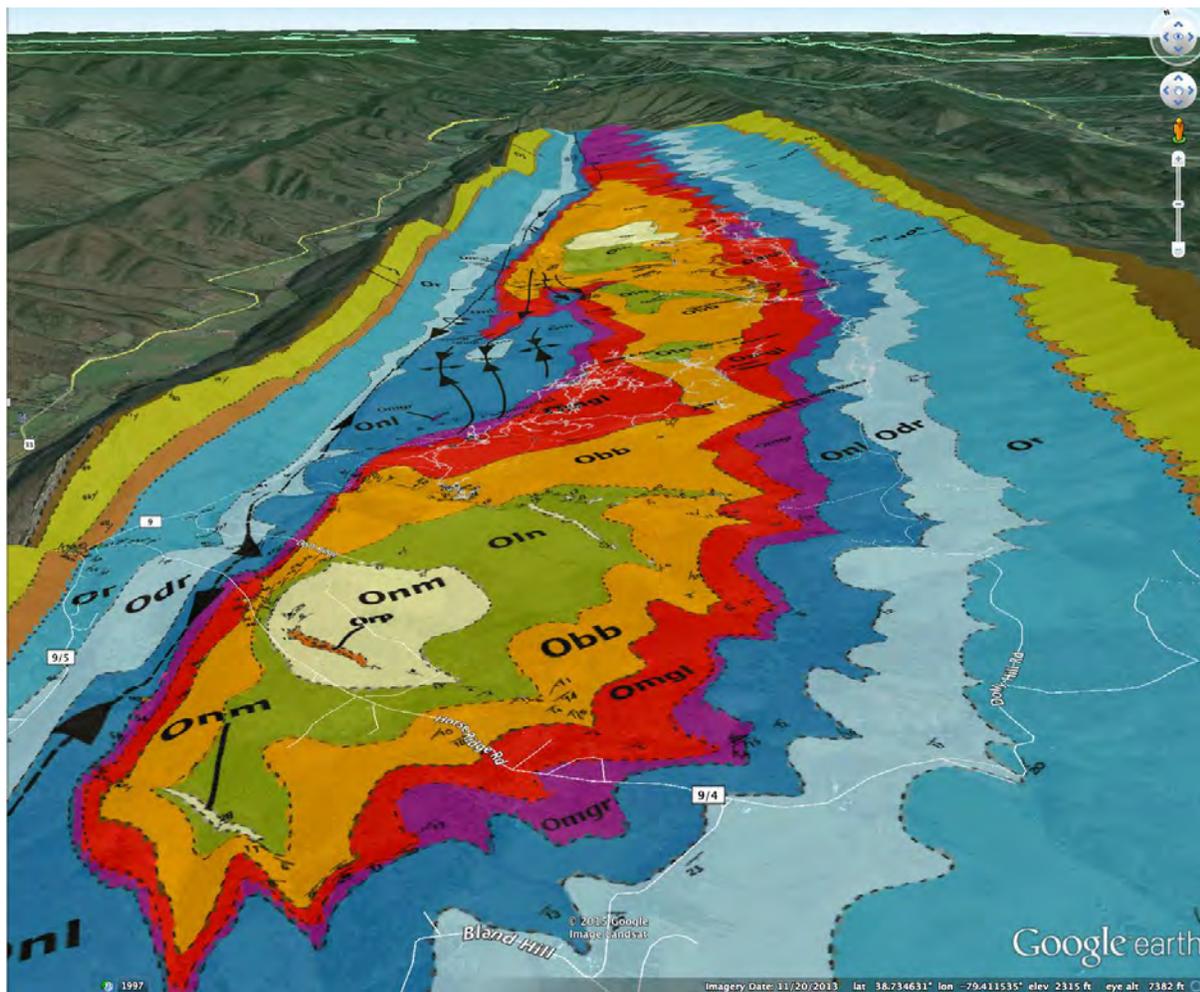
Figure 22.—Geologic map of Germany Valley (Martin et al., 2014) overlain on GoogleEarth terrain, which shows the breached anticlinal structure of the valley, with its two structural culminations where New Market Limestone (Onm) is exposed. This is the view we will have from the Germany Valley overlook at Stop 3. Geospatial processing done by Steve Whitmeyer.
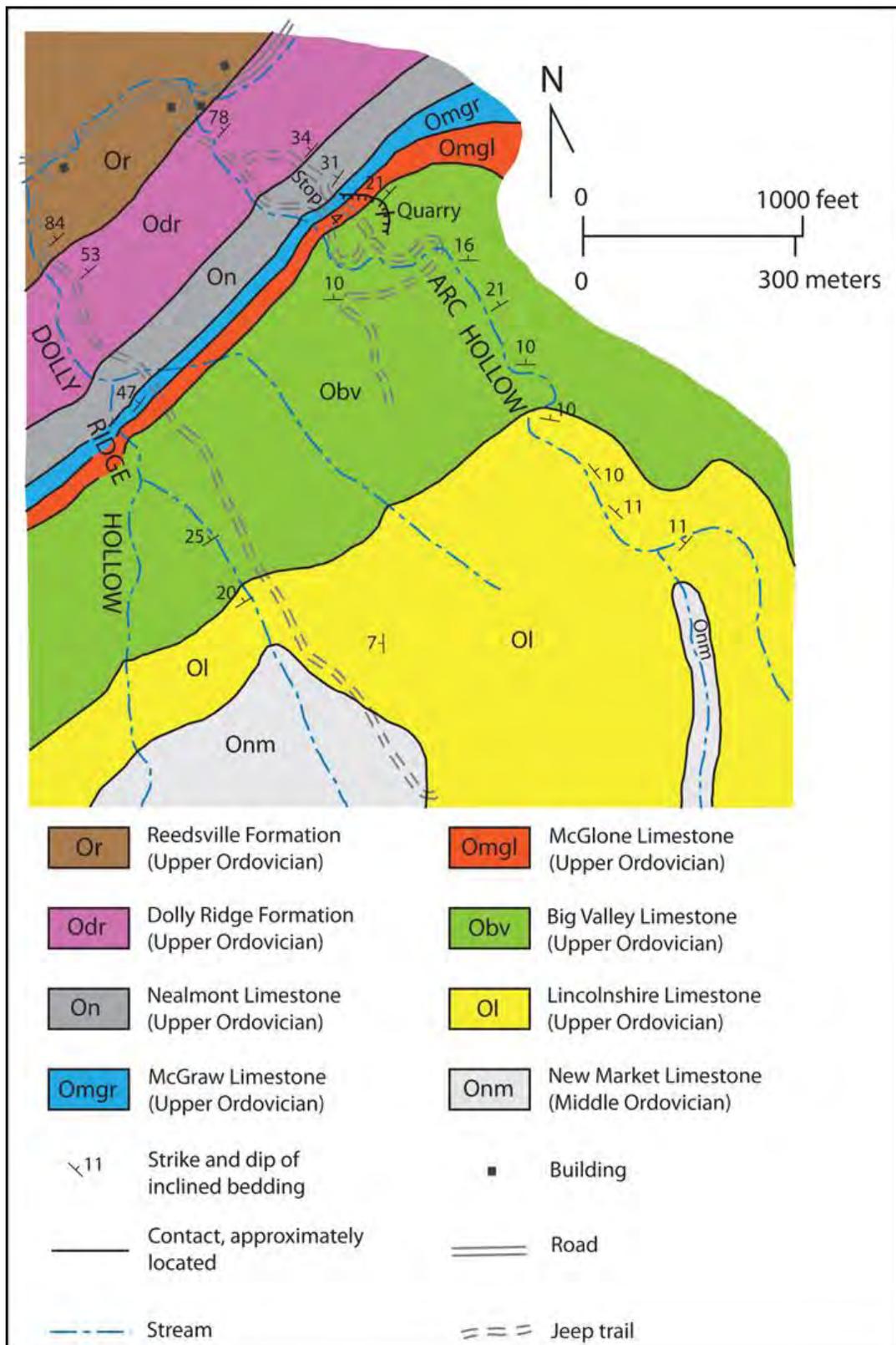
Figure 23.—Detailed geologic map of the Arc Hollow and Dolly Ridge areas that are the focus of Stops 4 and 5. Adapted and modified by R.C. Orndorff from the map of Martin et al. (2014).

Plate 1.—Arc Hollow measured section, Dolly Ridge Formation and Nealmont Limestone.

Plate 2.—Arc Hollow measured section, Nealmont Limestone, McGraw Limestone, and McGlone Limestone.

Plate 3. Arc Hollow measured section, McGlone, Big Valley, Lincolnshire, and New Market limestones.

ACKNOWLEDGEMENTS

REFERENCES

BICK, K.F., 1962, Geology of the Williamsville Quadrangle: *Virginia Division of Mineral Resources Report of Investigations* 2, 40 p.

BRETSKY, P. W., 1969, Ordovician benthic marine communities in the central Appalachians: *Geological Society of America Bulletin*, v. 80, p. 193-212.

BRETSKY, P. W. 1970: Upper Ordovician Ecology of the Central Appalachians: *Yale University Peabody Museum of Natural History Bulletin* 34, p. 1-150.

BUTTS, C., 1940, Geology of the Appalachian Valley in Virginia – Part 1: Geologic Text and Illustrations: *Virginia Geological Survey Bulletin* 52, 568 pp.

CARTER, B., Miller, P, and Smosna, R., 1988, Environmental aspects of Middle Ordovician limestones in the central Appalachians: *Sedimentary Geology*, v. 58, p. 23-36

COOPER, B.N., and COOPER, G.A., 1946, Lower Middle Ordovician stratigraphy of the Shenandoah Valley, Virginia: *Geological Society of America Bulletin*, v. 57, p. 35-114.

COOPER, B.N., and PROUTY, C.E., 1943, Stratigraphy of the lower Middle Ordovician of Tazewell County, Virginia: *Geological Society of America Bulletin*, v. 54, p. 819-886.

COTTER, E., 1983, Shelf, paralic, and fluvial environments and eustatic sea-level fluctuations in the origin of the Tuscarora Formation (Lower Silurian) of central Pennsylvania: *Journal of Sedimentary Petrology*, v. 53, p. 25-49.

CUFFEY, R.J., 2003, Bryozoan species, diversity, and constructional roles in early mid-Ordovician bryozoan reefs of eastern and central North America, in Viskova, L.A., Mezentseva, O.P., Morozova, I.P., and Udodov, V.P., eds., Bryozoans of the Globe: *Kuzbass State Pedagogical Academy, and Paleontological Institute of the Russian Academy of Science*: v. 1, p. 20-26.

CUFFEY, R.J., CAWLEY, J.C., LANE, J.A., BERNARSKY-REMINGTON, S.M., ANSARI, S.L, MCCLAIN, M.D., ROSS-PHILLIPS, T.L., and SAVILL, A.C., 2000, Bryozoan reefs and bryozoan-rich limestones in the Ordovician of Virginia, in Moosa, M.K. and 6 others, eds., *Proceedings of the 9th Int'l Coral Reef Symposium, Bali, Indonesia*: Ministry of Environment; Indonesian Institute of Sciences; International Society for Reef Studies: v. 1., p. 205-210.

DIECCHIO, R.J., 1985, Post-Martinsburg Ordovician stratigraphy of Virginia and West Virginia: *Virginia Division of Mineral Resources Publication* 57, 77p.

DIECCHIO, R.J., 1986, Taconian clastic sequence and general geology in the vicinity of the Allegheny Front in Pendleton County, West Virginia, in Neathery, T.L., ed., *Centennial Field Guide – Southeastern Section*: Boulder, Geological Society of America, p. 85-90.

DORSCH, J., BAMBACH, R.K., and DRIESE, S.G., 1994, Basin-rebound origin for the "Tuscarora Unconformity" in southwestern Virginia and its bearing on the nature of the Taconic Orogeny: *American Journal of Science*, v. 294, p. 237-255.

FOLK, R.L., 1960, Petrography and origin of the Tuscarora, Rose Hill, and Keefer Formations, Lower and Middle Silurian of eastern West Virginia: *Journal of Sedimentary Petrology*, v. 30, p. 1-58.

GROVER, G. Jr., and READ, J.F., 1978, Fenestral and associated vadose diagenetic fabrics of tidal flat carbonates, Middle Ordovician New Market Limestone, southwestern Virginia: *Journal of Sedimentary Petrology*, v. 48, p. 453-473.

HAYNES, J.T., MELSON, W.G., O'HEARN, T., GOGGIN, K.E., and HUBBELL, R., 1998, A high potassium mid-Ordovician shale of the central Appalachian foredeep: Implications for reconstructing Taconian explosive volcanism, in Schieber, J., ed., *Shales and Mudstones*, Vol. 2: Stuttgart, E. Schweizerbart'sche, p. 129-141.

HOROWITZ, D.H., 1971, Diagenetic significance of color boundary between Juniata and Bald Eagle Formations, Pennsylvania: *Journal of Sedimentary Petrology*, v. 41, p. 1134-1136.

KAY, G.M., 1944, Middle Ordovician of central Pennsylvania, Part II: Later Mohawkian (Trenton) formations: *Journal of Geology*, v. 52, p. 97-116

KAY, G.M., 1956, Ordovician limestones in the western anticlines of the Appalachians in West Virginia and Virginia northeast of the New River: *Geological Society of America Bulletin*, v. 67, p. 55-106.

KREISA, R.D., 1981, Storm-generated sedimentary structures in subtidal marine facies with examples from the Middle and Upper Ordovician of southwestern Virginia: *Journal of Sedimentary Petrology*, v. 51, p. 823-848.

KREISA, R.D., and BAMBACH, R.K.,1982, The role of storm processes in generating shell beds in Paleozoic shelf environments, in Einsele, G., and Seilacher, A., eds., *Cyclic and event stratification*: Berlin, Springer, p. 200-207.

LEHMAN, D., and POPE, J.K., 1989, Upper Ordovician tempestites from Swatara Gap, Pennsylvania: Depositional processes affecting the sediments and paleoecology of the fossil faunas: Palaios, v. 4, p. 553-564.

LESLIE, S. A., and BERGSTRÖM, S. M., 1995. Revision of the North American late Middle Ordovician standard stage classification and timing of the Trenton transgression based on K-bentonite bed correlation, *in* Cooper, J. D. et al., eds., *Ordovician odyssey: Short papers for the Seventh International Symposium on the Ordovician System*, Pacific Section of the Society for Sedimentary Geologists (SEPM), Book 77, p. 49–54.

MARTIN, D.C., HAYNES, J.T., LAMBERT, R.A., and DIECCHIO, R.J., 2014, A new geologic map of Germany Valley, Pendleton County, West Virginia, with cross sections and revised structural and stratigraphic interpretations: Geological Society of America *Abstracts with Programs,* v. 46, no. 3, p. 14.

NORTH AMERICAN COMMISSION ON STRATIGRAPHIC NOMENCLATURE, 2005, North American Stratigraphic Code: *American Association of Petroleum Geologists Bulletin*, v. 89, p. 1547-1591.

PERRY, W.J. Jr, 1964, Geology of Ray Sponaugle well, Pendleton County, West Virginia:

American Association of Petroleum Geologists Bulletin, v. 48, p. 659-669.

PERRY, W.J. Jr., 1972, The Trenton Group of Nittany Anticlinorium, eastern West Virginia: *West Virginia Geologic and Economic Survey Circular Series* No. 13, 30 p.

READ, J.F., 1980, Carbonate ramp-to-basin transitions and foreland basin evolution, Middle Ordovician, Virginia Appalachians: *American Association of Petroleum Geologists Bulletin*, v. 64, p. 1575-1612.

READ, J.F., and GROVER, 1977, Scalloped and planar erosion surfaces, Middle Ordovician limestones, Virginia: Analogues of Holocene exposed karst or tidal rock platforms: *Journal of Sedimentary Petrology*, v. 47, p. 956-972.

RYDER, R.T., 1992, Stratigraphic framework of Cambrian and Ordovician rocks in the central Appalachian basin from Morrow County, Ohio, to Pendleton County, West Virginia: *United States Geological Survey Bulletin* 1939-G, p. G1-G25.

THOMPSON, A. M., 1970, Geochemistry and color genesis in redbed sequence, Juniata and Bald Eagle formations, Pennsylvania: *Journal of Sedimentary Petrology*, v. 40, p. 599-615.

WOODWARD, H.P., 1941, Silurian of West Virginia: West Virginia Geological Survey, v. XIV, 325 p.

WOODWARD, H.P., 1951, Ordovician system of West Virginia: West Virginia Geological Survey, v. XXI, 627 p.

YEAKEL, L.S., Jr., 1962, Tuscarora, Juniata, and Bald Eagle paleocurrents and paleogeography in the central Appalachians: *Geological Society of America Bulletin*, v. 73, p. 1515-1540.